Analyse du modèle d'Ising planaire au-delà du cadre critique Z-invariant

Rémy Mahfouf

université
PARIS-SACLAY

Analyse du modèle d'Ising planaire au-delà du cadre critique Z-invariant

Analysis of the planar Ising model beyond the critical Z-invariant setup

Thèse de doctorat de l'université Paris-Saclay

École doctorale de mathématiques Hadamard $n°574$
Spécialité de doctorat : Mathématiques fondamentales
Graduate School : Mathématiques
Référent : Faculté des sciences d'Orsay

Thèse préparée au **Département des Mathématiques et Applications (École Normale Supérieure de Paris, CNRS)** sous la direction de **Dmitry CHELKAK**, Professeur.

Thèse soutenue à Paris, le 30 Août 2022, par

Rémy MAHFOUF

Composition du jury

Giambattista GIACOMIN Professeur, Université de Paris	Président
Cédric BOUTILLIER Maître de conférences, HDR, Sorbonne Université	Rapporteur & Examinateur
Ioan MANOLESCU Professeur, Université de Fribourg	Rapporteur & Examinateur
Michel BAUER Directeur de recherche, CEA Saclay	Examinateur
Béatrice DE TILIÈRE Professeure, Université Paris Dauphine	Examinatrice
Vincent VARGAS Professeur associé, Université de Genève	Examinateur
Dmitry CHELKAK Professeur, École Normale Supérieure de Paris	Directeur de thèse

THESE DE DOCTORAT
NNT : 2022UPASM016

université PARIS-SACLAY | ÉCOLE DOCTORALE de mathématiques Hadamard (EDMH)

Titre : Analyse du modèle d'Ising planaire au-délà du cadre critique Z-invariant
Mots clés : Ising, Isoradial, Universalité

Résumé : Dans cette thèse on explore l'existence et l'universalité du modèle d'Ising planaire, dans un cadre critique et presque-critique. En utilisant le formalisme de Kadanoff et Ceva, on étudie grâce à des méthodes d'analyse complexe discrète les limites d'échelles et les propriétés à grandes distance du modèle d'Ising sur les grilles isoradiales ainsi que leur généralisations au modèle d'Ising quantique et aux les s-plongements introduit récemment.

Title : Analysis of the planar Ising model beyond the critical Z-invariant setup
Keywords : Ising, Isoradial, Universality

Abstract : In this thesis we explore the existence and the universality of the planar Ising model, at and near criticality. Basing upon the formalism of Kadanoff and Ceva, we study by discrete complex analysis means the scaling limit and large scale properties of the Ising model on isoradial grids, as well as its generalizations to the quantum Ising model and the recently introduced s-embeddings.

Table des matières

«La plupart du temps, quand tu réchauffes de 2 degrés en p-adique, t'as pas changé la température en valeur absolue.»

Seginus Mowlavi, luttant contre le réchauffement climatique.

Remerciements

À bien des égards, ces remerciements représentent infiniment plus pour moi que la production mathématique qui les suit.

Il est d'usage de commencer ses remerciements par son directeur de thèse. Comme nous n'avons jamais suivi les usages, cette discussion-là aura lieu plus tard. Je commence donc par remercier les membres de mon jury. Je dois dire l'immense privilège que je ressens face à ces scientifiques de très haut niveau, qui ont montré tant de bienveillance à mon égard au long de ma jeune carrière. Je tiens à remercier mes rapporteurs d'avoir accepté la tâche ingrate de lire mon manuscrit. Leurs commentaires et questions en ont grandement amélioré la qualité. Merci à Cédric de m'avoir si souvent encouragé, d'avoir porté de l'intérêt à mes travaux et de m'avoir permis de faire mon premier exposé (même si le résultat était catastrophique). Merci à Ioan pour sa bienveillance à chacune de nos rencontres et pour m'avoir proposé plusieurs opportunités au cours des dernières années. Je voudrais chaleureusement remercier Béatrice pour m'avoir encouragé avec beaucoup de gentillesse depuis maintenant plus de 4 ans et d'avoir regardé mes idées infructueuses sur les exponentielles discrètes. Enfin merci de m'avoir aidé à trouver mon prochain poste.
Merci à Michel pour son enthousiasme à l'idée de faire partie de ce jury. Tout l'honneur est pour moi. Que dire sur Vincent, mon tuteur au DMA et grand conseiller scientifique depuis maintenant plus de 6 ans. C'est Vincent qui m'a introduit au modèle d'Ising via un groupe de travail, puis poussé à faire une thèse avec Dmitry. Malgré nos désaccords politiques profonds (puisque Ronaldo est meilleur que Messi) il a toujours su m'aiguiller, que ce soit dans la recherche, mais aussi dans la vie. J'éprouve beaucoup de gratitude envers toi et suis très heureux de venir à Genève. Je tiens enfin à remercier Giambattista pour m'avoir tant appris durant ces trois dernières années. Au-delà de nos discussions scientifiques, Giambattista a fait de moi un bien meilleur enseignant, tout en me laissant le choix des sujets à traiter avec les élèves. Il a même réussi à me faire aimer l'exercice 'ABRACADABRA', que je détestais en tant qu'étudiant. Venir te déranger dans ton bureau a toujours été un plaisir, que ce soit pour me plaindre de ma vie, raconter des ragots ou bien mettre à l'épreuve mes qualités d'organisation souterraines. Du fond du cœur, merci pour tout !

Je voudrais remercier mes collaborateurs scientifiques et co-auteurs, sans qui ma production scientifique ne se résumerait probablement qu'à ces remerciements. Je voudrais remercier Clément Hongler pour notre collaboration (bien que décalée dans le temps) sur le modèle en zig-zag, et pour avoir généreusement proposé ton aide à diverses étapes cruciales de ma carrière balbutiante. I also wish to thank Konstantin Izyurov for our work on the universality of correlations, for bringing many great ideas to the table and for kindly explaining how you made it to compute those massive asymptotics. This thesis contains many ideas of both Clément and Konstantin and I'm very grateful for the opportunity of collaborations. J'ai beaucoup aimé travailler avec Jhih-Huang, pour son esprit aiguisé, ses connaissances sur la physique, mais aussi nos discussions culturelles où j'ai appris beaucoup. I wish to warmly thank the Team, for being such a positive research environment. First Yijun, for sharing office and learning not to be freaked out by my crazy ideas. Even if we are very different from each other, I'm really happy that we are real friends. What to say about Micha. Thanks for kindly investing some time in this weird Beltrami business, and showing that, despite majoring in algebraic geometry, he is stronger in analysis than I will ever be. I also want to thank him for our funny daily life discussion, and for quite often helping me cool down. I wish to thank

Niklas for teaching me there are so many different geometries. I hope that you will find the one that fits the embedding formalism. Finalmente, quiero sinceramente agradecer a Sung Chul por sus habilidades en el idioma de Cervantes, solo superado por su conocimiento de los spinores masivos holomorfos. Trabajar y discutir con él, aun a las dos de la mañana, es siempre un gran placer y espero que siga así en el futuro.

Je voudrais remercier mes aînés, qui m'ont inspiré et poussé à faire de la recherche. Merci à Stéphane Boucheron et Robin Rider, pour m'avoir introduit aux statistiques. Many thanks to Luke Bornn for giving me a glimpse of what the life of an NBA statistician looked like. Merci à Mathieu Merle, pour son cours sur les temps de mélanges et son mentorat, toujours plein de bon sens. Merci à Nicolas Curien pour ses cours à Orsay, ses conseils sur l'enseignement, et ses légendaires remerciements de thèse. Merci à Hugo Duminil-Copin pour son cours sur la percolation, véritable déclic dans mon choix de faire de la mécanique statistique. Merci pour cette formidable opportunité de venir à Genève, dont j'espère tirer le meilleur. Merci à Hubert Lacoin de m'avoir si bien accueilli à Rio, encadré avec beaucoup de gentillesse durant le stage, et permis de découvrir cet endroit fabuleux qu'est l'IMPA. Merci à Étienne Ghys, pour ses conseils sur la carrière d'un mathématicien, ton humilité contagieuse, et pour tous ces déjeuners en face des montagnes cariocas. Merci à Christophe Garban pour tes encouragements durant nos rencontres en conférences, qui ont été une excellente source de motivation. Enfin merci à Sanjay Ramassamy pour m'avoir expliqué ses perspectives et sa vision sur le formalisme que j'utilise tous les jours.

Je tiens à remercier Mendes, mon futur Premier ministre. Malgré de nombreuses tentatives, nous n'avons jamais réussi à travailler sérieusement. Car le moindre début de commencement d'un bout de lemme suffisait à aller se reposer et surtout commencer à discuter. Les s-embeddings sont bien moins intéressant que le FLN, la JSK, le RND, le Hirak, la démocratie, l'idiocratie, la plomberie, Numérobis, le jardinage, les carrelages, les boutiques qui ne vendent rien, les phacochères de l'IHES, ou bien ma dernière complainte du jour. J'admire tes savoirs et ton humilité. On travaillera ensemble sérieusement à l'avenir. Mais dans une supérette à Bab Ezzouar.

Je voudrais remercier les jeunes mathématiciens pour tous les moments que j'ai eu le plaisir de partager avec eux. À Thomas et Michel, mes prédécesseurs du bureau V2, pour vos recommandations que je m'efforce de suivre. À Francois, pour toutes tes explications en analyse, et pour être le plus Algérien des Suisses. À Paul, mon premier co-bureau, pour nos séances d'épluchage de CV se terminant souvent par un "Solide". À Baptiste, pour connaître ma limite dans la vie. À Maxime et Wei pour nos soirées chez Golosino, à ressasser le même sujet. À Daniel tes questions sur le Brownien (auquel je ne comprends rien) et nos après-midi gossip. À Arnaud, pour nos discussions tardives au DMA, et notre entente cordiale avec les vigiles de l'entrée. À Nathaniel, pour danser presque aussi bien que tu fais des maths. À Emmanuel, pour m'avoir aidé avec Paris Maths, pour ta relecture de mon introduction, et pour être au fond mon premier vrai étudiant. Ton avenir me semble radieux. Finalement, à Barbara, Benoît, Dima (my new favorite one), Franco et Trishen, pour ces moments échangés en conférence.

Un grand merci à la direction du DMA, en particulier à Nicolas Bergeron, de m'avoir donné l'opportunité de devenir caïman et laissé une grande liberté afin de m'épanouir à ce poste, toujours au service de mes élèves. Merci d'avoir soutenu les activités de Paris Maths. Merci à tous mes élèves, dont j'ai beaucoup appris. Je tiens aussi à remercier Fabienne pour ses encouragements constants, sa bonne humeur, et sa joie de vivre communicative. Passer la voir est toujours un plaisir.

Je voudrais remercier du fond du cœur Laure-Helène Bize-Reydellet et Hervé Gianella d'avoir cru en moi à une époque où je ne le faisais plus moi-même. Mon parcours universitaire vous doit beaucoup. Je voudrais aussi remercier Zahir Malou pour m'avoir tout appris de la mécanique, soutenu et suivi durant toutes ces années. Je garde de lui le souvenir d'un superbe enseignant.

Depuis 2015, j'ai eu la chance de rencontrer mes deux mamans du DMA. Je les remercie d'avoir fait semblant que j'étais normal. Mon tout premier contact avec le DMA a eu lieu avec Son Excellence Albane-Kanika Norodom-Trémeau, héritière du trône du Cambodge, et je me suis littéralement vautré en entrant dans son bureau. J'ai ensuite trouvé beaucoup d'excuses pour y retourner et discuter avec Albane, qui a toujours réponse à tout. Merci de m'avoir enlevé de la tête l'envie de devenir médecin et motivée à continuer la recherche. Merci de toujours faire preuve d'humanité. Et merci d'avoir accepté avec un immense enthousiasme (et gardé pendant plus d'un an) ma couronne de la galette des rois. Puis un jour, je me suis devenu un «adulte» au DMA. J'avais dramatiquement besoin d'un bureau, et Zaïna m'en a proposé un, au détour d'un couloir, sans vraiment savoir qui j'étais. C'était tellement important à ce moment-là. Merci de m'avoir appris comment fonctionne un labo, raconté tous les gossips et histoires du DMA, merci de répéter "Rémy" 20 fois par conversation, merci pour ton soutien à mon style claquette-chaussettes, pour tes encouragements et pour l'exégèse du couloir. Je n'ai toujours pas compris ta comparaison entre moi et un de mes illustres prédécesseurs. Enfin, merci de si bien raconter la fameuse histoire des chiens, j'en pleure de rire à chaque fois que j'y repense.

Ces dernières années, j'ai eu la chance de rire et d'apprendre de mes amis. Je commencerai par l'époque où cuisiner était mon métier à plein temps. Merci à Alexane, juge en chef de l'équipe CAP, pour connaître les vraies leçons de piano vicinoises, pour m'avoir expliqué le sens de l'hymne britannique et pour avoir su rester exigeante avec mes plats, tout en pardonnant mon premier raté. À Chloé M.O.V. Du Laurent De la Barre, pour tes passions du chocolat chocolaté et du bleu, pour m'avoir fait imprimer tout et n'importe quoi, pour ta nullité derrière une agrafeuse, et pour me faire rire comme personne. Ta bonne humeur m'a été contagieuse. À Benjamin, pour nos tentatives de se lancer dans la culture, parce que je ne savais pas qu'il faut payer l'ouvreur, parce que tu anticipes ce que je vais dire après la pièce, et pour nos déjeuners au Jardin des Plantes. À Pierre, digne héritier de la Riola corp, pour m'avoir fait découvrir les comédies musicales de Cocody, pour ton étonnement face aux idées de l'Animal, parce qu'on est trop souvent d'accord sur tout, et parce que le poulet sans tête nous a bien bluffé. A Rayane, pour ton intêret irrationnel pour le championnat d'Algérie et l'OL, pour me faire briller en société par ta seule présence, et parce qu'en cas de doute, شربة فوق نار ٤.

Je voudrais remercier Auriane, pour cette discussion qui m'a permis de mesurer l'état réel de ma vie, à un moment où je n'avais pas les idées très claires. J'espère aussi que tu en as oublié tous les détails. Tomber sur Auriane, que ce soit au milieu du 5ème ou en plein Manhattan est toujours un grand plaisir, et mène à des conversations aussi improbables qu'enrichissantes.

Qu'aurait été ma vie sans les habitants de Voisins Beach. À Arthur pour nos inoubliables (mais dangereuses) balades cariocas, notre passion pour le pire club de toute la Belgique (et son milieu de terrain liquide), pour tes remarquables talents culinaires, et pour m'apprendre toujours des nouvelles choses. À Paul-Antoine, pour avoir découvert Roland-Garros et les films en classe 10 ans avant tout le monde, parce qu'une bonne journée commence au cri d'un "Bolkov", pour avoir été mon premier fan durant mes années de businessman (vive la location de blouses), et parce que le lien entre binômes de TP est éternel. À Philippine, parce que la vie est trop courte pour utiliser un shampoing bas de gamme, parce qu'une longue balade commence à l'Occitane et fini toujours

par une magnifique vue de Paris depuis le Sacré-Cœur, parce qu'il est vraiment possible de naître avant la honte, pour le parfum à la rhubarbe et pour la lettre de recommandation que j'attends avec impatience. À Ludal, le pire lodgmatee qu'on puisse imaginer, parce qu'on peut devenir ministre du cinéma en passant le concours de professeur d'espagnol, parce qu'on est encore en vie (cette phrase m'étonne vraiment), pour avoir tort 49 fois sur 50, pour les potes au second degré, et pour le troisième étage de la fusée. Merci, à Émeline d'avoir assumé la garde partagée de l'Animal, je te le laisse à plein temps et attends avec impatience ta réaction en découvrant un snowboard sous ton lit. Enfin, à Victor, parce qu'on peut tout résumer à un réservoir de mobylette, un burin, une fourchette, du nettoyeur à fosse septique, un contrat de vente écrit sur une lettre usagée et suffisamment d'espoir pour penser qu'on peut faire tourner un moteur cassé à la main. Je voudrais aussi remercier Anne-Laure et Philippe de m'avoir toujours chaleureusement accueilli chez eux depuis bientôt 15 ans.

J'ai partagé ces années de thèse avec les membres du Filtre. Un premier constat, nous sommes tous rentrés en vie de l'ascension du Ventoux, ce dont j'ai fortement douté pendant 6 km après le chalet Reynard. Ensuite, il me faut avouer que l'objectif initial de cette conversation est bel est bien atteint, puisque je suis maintenant devenu présentable, consensuel, et même corporate. Mon mariage à Tallinn sera ma dernière folie. À Cyril, mon compère d'attaque du FC Caïman (malgré nos défaites contre des illettrés de 10 ans), pour tes cyrillisme qui me poussent à l'UCPA, parce que les intégrales se calculent maintenant sur Instagram, pour notre journée au Parc Astérix, pour ta nullité technologique et ta croyance ingénue que j'y comprends plus que toi. À David, parce que je ne sais toujours pas si tu supportes ou non le PSG, pour nos interminables débats NBA, pour tes 1000 et 1 questions sur l'inégalité de Markov, et pour m'avoir, bien malgré moi, rendu bien plus écolo. À Jean, pour toutes ces sociétés qu'on avait prévu de créer et dont l'existence n'a dépassé 3 jours (même si j'aime beaucoup la dernière idée de production d'olives), pour nos marches aléatoires sur le réseau New-yorkais, pour toutes nos photos Blanc-Barthez et pour avoir assisté avec moi au grand vent de l'histoire (merci Vivien pour ce moment). À Marc, pour avoir eu l'indécence de me donner une manette cassée et d'en profiter lors d'une soirée honteuse où FIFA buggait, pour notre passion commune pour les crédences, pour raconter si bien les aventures du cousin albanais de Numérobis, et pour être le meilleur fond d'écran du monde. À Seginus, pour toutes nos discussions maraboutage qui durent des heures, parce qu'après tout il est sain et rationnel d'en choisir 400 parmi les plus beaux, pour tous nos plats ratés (la sauce burger industrielle est plus simple à réaliser que la mayonnaise maison) et pour nos interminables soirées autour du jus le moins cher du monde. À Simon, parce que les Parisiens habitant rive droite sont clairement plus beaux que ceux de la rive gauche, pour m'avoir fait découvrir les oranges, pour nos voyages qui ne se passent jamais comme prévu, parce que le couscous se mange à la cuillère, pour former la pire paire possible au badminton et parce que sans toi, essentiellement, je ne saurais pas faire les éclairs. À Thibaut, parce que les peintres et le FC Chômage font partie de ton vocabulaire, pour ton arabe à couper au couteau, pour tes ondulations parfaites au rythme de Jul, pour nos discussions à l'heure où Cyril se lève, et pour notre compétition continue consistant à trouver la cour des miracles sur le net. À Ulysse, pour ce Game 7 dont je n'ai toujours pas compris les 5 dernières minutes, pour tes capacités à t'asseoir dans toutes les positions, pour ton immense culture qui m'épate à chaque fois (surtout sur les sujets sans aucun intérêt), pour ta vision presque romantique de la NBA, et pour cet inoubliable réveil New-yorkais où le spectre de John et Jane Doe nous a plongé dans une scène de film. J'ai partagé avec vous cette expérience de thèse comme avec personne d'autre, et j'en garderai un souvenir magnifique. L'ère des Birkenstock-chaussettes Adidas dépareillées ne fait que commencer. Cette thèse vous doit énormément.

Et
merci
d'avoir
appris
à
me
lire.

Je veux aussi remercier ce que j'appellerai simplement la composante connexe du Filtre, que j'ai eu le plaisir de fréquenter très souvent ces dernières années. À Arielle, pour ta culture incroyable, nos discussions sur les mondanités, et tes conseils toujours très précieux (parfois via un téléphone fixe, et oui cela existe encore). À Claire, pour ton enthousiasme débordant, pour avoir transmis ton accent breton à Cyril, pour tes prises de notes, et tes capacités d'entremetteuse qui dépassent les meilleurs sites de rencontres. À Juliette, pour ton accueil toujours chaleureux et bienveillant. I wish to thank Fenella for acknowledging my algerian-russian accent. À Souraya, pour avoir initié Thibaut aux gossips à la méditerranéenne, et car comme dirait l'autre أنا حمار.

Merci à Hacène, pour tes talents de chirurgiens dont je me rappelle tous les jours, à Saliha pour ta patience face aux théories hasardeuses des deux jumeaux, à Samira pour m'avoir fait visiter toute l'Île-de-France avant mes 6 ans, à Elliott pour m'avoir appris les échecs, et même laissé gagner une fois, et à Sofiane, parce que tu détestes Numérobis autant que moi.

J'en viens maintenant à ma famille. Il faut rire dans la vie. Et rien de mieux pour cela que de débarquer dans ce monde avec mon arbre généalogique. Je tiens à remercier Djoudi (PDG) et Nadia pour avoir fait de moi un meuble chez eux. Votre maison est pour moi l'endroit le plus paisible au monde. À Racha, pour l'agence d'espions, les coups de tête sur les murs créponnés, pour le bonbon, et pour Betetra Pimpimpula. À Asma, ma soeur de lait, parce qu'on a découvert le cinema ensemble, pour toujours faire attention à moi, et parce qu'on est encore des enfants à 27 ans. À Chérif, pour les 100$ de Babana, pour Georges V, pour la vue sur mur, pour le chapati, et pour la clim à 16 degrès en décembre. On n'en dira pas plus ici. À Mounir, pour le remake de Peter Pan et les recherches du professeur Jamelski. À Marwa, حبيبتي, parce que manifestement, ils ont un plan pour nous, et qu'il va donc falloir trouver une solution pour la chambre à coucher. À Djamila, pour m'avoir appris à amadouer la sécurité civile, et pour ta cuisine inégalable. À Toufik, pour ta classe vestimentaire, pour les tee-shirts Lexmark et pour me pousser à toujours faire mieux. À Fawzi, car dans la vie, ce sont souvent 30 métiers et 30 misères. À Zineb, pour m'avoir éduqué. Ton influence reste présente tous les jours. À Nadjette, pour nos parties de tennis, nos sorties à vélo, et parce qu'Ocean 11 est le meilleur des films. À Hacène Babana 100$, pour m'avoir donné le goût des sciences, pour être le seul propriétaire en Amérique d'un téléphone Condor, pour ton humilité, pour les mille-feuilles, et pour m'avoir offert mon premier télescope professionnel (avec lequel je regardais chez les voisins). À Farouk, pour m'avoir arnaqué comme personne, pour nos allers-retours à Fleurial, et pour m'avoir donné le goût de la science. À Claire, pour être LA seule personne normale de cette famille. Merci pour les Kickers, pour tes combats syndicalistes perdus d'avance, et pour faire semblant de ne plus être surprise par nos coutumes. Ton avis comptera toujours à mes yeux. À Seddik, pour le chat piou-piou, pour avoir été mon premier client des calendriers, de la

Rémy Banque, et du carwash. À Lilia, pour aimer autant que moi la mafia familiale. À Yacout, pour représenter la droiture et le sérieux dans ce monde de fous, mais aussi ta vision très actuelle du Prince de Machiavel. À Amine, Lord Aït War, pour me faire rire tous les jours, avec la CNEP, les inventions de l'Artiste, et pour tes fractures quotidiennes du cerveau face à la société algérienne. À Dalia, qui s'en sort toujours bien mieux que je ne veux bien l'avouer, même si tout n'est pas facile à porter. À Nana, pour être sur toutes les photos, de tous les voyages, de toutes les aventures depuis bientôt 28 ans, sans jamais se plaindre ni même me contredire. J'espère que la soutenance te plaira. Je voudrais remercier mes parents. Leur parcours de vie force le respect. Quitter une vie confortable pour en reconstruire une ailleurs, à partir de rien, n'est pas donné à tout le monde. Comme beaucoup de parents, ils ne se plaignent jamais, ne sont jamais fatigués, ne sont jamais malades et répondent présent tous les jours (parfois un peu trop, surtout quand il faut choisir MON carrelage). Mais ils ne ratent jamais un seul jour dans le rôle de parents. Et cela force l'admiration. Je tiens donc à les en remercier. À mon père, pour ses connaissances en médecine (sans rire), pour son efficacité légendaire au travail, pour son altruisme, pour la chaîne de 7.2km devant la meilleure crémerie du monde, pour ses connaissances sur la cadastre bônoises, pour le parking H23, et pour m'avoir fait découvrir les mathématiques à l'âge de 3 ans. À ma mère, docteure en informatique, pour m'avoir appris à être économe (le terme approprié est plutôt مشحاح), parce qu'on juge la qualité d'un plat au nombre de casseroles utilisées, et pour me demander mon avis sur tous les sujets où je suis un incompétent notoire. Merci de continuer à te préoccuper de mes tracas comme si j'avais 3 ans, sinon je n'en réglerais probablement aucun. Je tiens enfin à remercier mes grands-parents, mes modèles dans la vie. Leurs vies ont été remplies de joies et de peines, de guerres et de paix, de réussites et d'échecs, mais ils ont toujours traité chaque personne, quelle que soit sa condition, dans le respect, la dignité et avec une bienveillance sans faille. J'espère, être digne de cet héritage.

Une journée dans cette famille ressemble souvent à une version Bollywood de Tenet. Quasiment tous sont des personnages de sitcom, chacun méritant un spin-off d'au moins 5 saisons. Mais, pour rien au monde, je n'en changerai un seul.

It's now time to thank, wholeheartedly, the architect of many things I am today, including the mathematician who wrote this thesis.

I wouldn't be a doctor if not for Professor Dmitry Sergeevich Chelkak. As insane as this quote might look, it is he most accurate statement of the entire manuscript. I almost left academia few years ago. Not that I particularly wanted to, but I was dumb enough dive into whatever insane Паноптикум you can imagine (nothing to do with scholarship issues). As there is some fun in every story, it is Dmitry himself who once explained me that very Russian concept that you won't find in a french dictionary. At the same time, without even searching for one, I was offered one of the few jobs that I've always considered impossible to refuse. I was going to take that job, for a very wrong reason, but cancelled it at the very last minute, simply because I wanted to be Dmitry's student. That was the right choice.

I could have written an entire thesis on what it looks like to work with someone having such a powerful mind, full of amazing insights, with a gargantuan culture and a remarkable ability to see analysis in probability. It it quite depressing when Dmitry shows up clueless of what I've been doing, and has better ideas in 10 minutes than I will ever have in months. The most impressive is that Dmitry never hides in front of tricky questions, and always tries to level-up to tough problems, no matter what they are. His computational abilities are simply not human. But this is not what

comes first to my mind when thinking about Dmitry.

Dmitry is kind. The local combinatorics might require a deeper branching structure time to time. But Dmitry is really kind. On the contrary, the world around is harsh. And I'm now convinced that it is way better to look like an idiot in front of your advisor, behind closed doors, than in front of the world (in my case it was pretty easy to adapt as we both know I'm not the brightest in town). Dmitry kept showing me, starting with himself, that one should behave properly, and work on evenly proper questions. He sat very high standards, that I was never able to achieve. But this exigence he instilled in me became my safe spot, something I can always rely on. It even transpired in my personal life, as I learned to be ready for anything, and understood that unfortunate events are simply a matter of life. My personal journey became way smoother, and wild times are easier to handle following his guidelines. This will be my main memory. I had the chance to work alongside someone I admire, who saw me laughing, crying, mocking and being mocked, trying many stupid ideas and even looking smart on rare occasions. And that person actually improved me, both as mathematician and as a person.

Now, as you can read in all acknowledgements, Dmitry is indeed a great advisor, he kindly shared his ideas with me, he invested the time he had to introduce me to this rich and rather magical field of discrete complex analysis (no need to be a probabilist to prove cool probabilistic statements). I loved being his student. And I'm forever thankful for that. I simply view the maths as pretty small in the global picture.

Rémy Youssef Mahfouf,
Août 2022

1 - Introduction

1.1 . Histoire du modèle

Le modèle d'Ising a été introduit par Wilhem Lenz en 1920 et été proposé comme sujet de thèse à son étudiant Ernst Ising à l'université d'Hambourg en 1924. On commence par rappeler brièvement quelques points importants de sa riche histoire [29, 133, 131, 132, 91]. Ce modèle est encore aujourd'hui l'un des plus étudiés en physique statistique, avec une production totale de plusieurs dizaines milliers d'articles, aussi bien publiés dans des journaux de mathématiques que de physique. Au début du $\mathrm{XX}^{\mathrm{ème}}$ siècle, les connaissances de la physique sur les phénomènes de magnétisation des matériaux ferromagnétiques étaient encore balbutiantes. Une des premières découvertes majeures dans ce domaine est attribuée à Pierre Curie [53], qui a remarqué expérimentalement que les aimants *perdent* leur aimantation au dessus d'une température critique T_C, appelée température de Curie. Les travaux de Niels Bohr [23] ont mis en avant le caractère aléatoire du phénomène de magnétisme, c'est à dire que la répartition des aimants élémentaires dont l'orientation est donnée par une loi de probabilité. Selon le postulat de Bohr, ces aimants élémentaires pouvaient prendre à priori toute les directions de l'espace. C'est cette assertion que Lenz a remis en cause dans son article fondateur [150], prédisant qu'en réalité les micro-aimants ne peuvent prendre que deux directions opposées de 180 degrés, et proposant un modèle à deux états pour expliquer la magnétisation spontanée en-dessous de la température critique T_C. C'est ainsi que Lenz donna l'opportunité à Ising de construire un modèle tri-dimensionnel. La tâche d'Ising se répartissait entre les deux objectifs suivants :

1. Proposer une modélisation des interactions entre les micro-aimants élémentaires qui favorise les configurations alignées.
2. Prouver *analytiquement* l'existence d'une magnétisation non nulle en dessous d'une certaine température.

Pour répondre à la première question, Ising [150] (se basant sur des travaux d'Ewing [69]) supposa que les interactions entre aimants élémentaires "décroissent rapidement avec leur distance", travaillant donc avec un modèle simplifié d'interaction au plus proche voisin. Cette hypothèse était selon lui en "contradiction grossière" avec l'approximation en champs moyen (dont on sait aujourd'hui qu'elle n'est valable pour le modèle d'Ising qu'en grande dimension [152]). Pour répondre à la seconde question, Ising choisit de restreindre son étude au modèle uni-dimensionnel, que l'on peut voir comme une chaine de spins sur $\mathbb{Z}$. Il calcula alors la magnétisation moyenne $\mathcal{J}$ [90, eq (8)] d'une chaine de $n \gg 1$ spins, qui est donnée par

$$\mathcal{J} = m \times n \times \frac{\sinh(\alpha)}{\sqrt{\sinh^2(\alpha) + e^{-\frac{2\varepsilon}{kT}}}}, \quad \alpha = \frac{mH}{kT}, \tag{1.1.1}$$

avec m le moment magnétique élémentaire, H le champ magnétique extérieur, T la température, k la constante de Boltzmann et ε l'énergie interne du système. Lorsque $H = 0$, c'est à dire sans champ extérieur, il n'y a pas de transition de phase à température finie. Dans ce même article [90] (dans la section "le modèle spatial") Ising propose une description du phénomène en dimension supérieure, affirmant qu'il est "imaginable qu'un modèle spatial, où tous les éléments interagissent les uns avec les autres, apporte suffisamment de stabilité évitant que la magnétisation ne disparaisse avec H", tout en admettant ne pas être en mesure de fournir de preuve. Il conclut à impossibilité d'expliquer le ferromagnétisme en utilisant sa modélisation. Il est à noter qu'avec les connaissances d'aujourd'hui, le modèle d'Ising avec des interactions entre particules décroissant suffisamment lentement admet tout de même une transition de phase [112].

La question de prouver l'existence d'une magnétisation spontanée en dimensions supérieures resta ouverte pour les physiciens de l'époque. Le très renommé Heisenberg soutient dans une lettre à Pauli une réponse affirmative, au moins en dimension suffisamment grande [82]. Pauli fut aussi le premier à introduire dans [147] la notation Hamiltonienne moderne

$$H = -A \sum_k (\sigma_k, \sigma_{k+1}), \tag{1.1.2}$$

où le paramètre A mesure l'intensité de l'interaction entre voisins. La formulation de Pauli met en avant le caractère unifié d'un système contenant beaucoup de particules, et dont les interactions locales produisent un effet global.

C'est en 1936 que Peierls a montré [139] que le modèle homogène sur $\mathbb{Z}^2$ fait apparaitre du *ferromagnétisme*, via un argument de comptage de circuits. Ce résultat a poussé Kramers et Wannier à développer l'usage des matrices de transfert [104, 105] pour calculer la fonction de partition du modèle unidimensionnel via la plus grande valeur propre d'une matrice 2×2. En dimension 2, cette matrice de transfert devient infini-dimensionnelle et un calcul similaire leur permit de prouver l'existence d'une transition de phase à une certaine température finie T_c. Ils ont aussi découvert une *symétrie* entre le modèle *sous-critique* et le modèle *sur-critique* que l'on appelle aujourd'hui la dualité de Kramers Wannier (voir la section 1.2.4 pour une description détaillée). C'est en février 1942 qu'Onsager, à la fin d'un exposé de Wannier, annonça avoir déterminé la température critique pour le modèle homogène, donnée par $kT_c/J = 2/\log(1+\sqrt{2})$. Le calcul d'Onsager [135] pour des constantes de couplages horizontale et verticale qui valent respectivement J_1 et J_2, montre que l'énergie libre f du modèle sans champ magnétique extérieur est donnée par l'expression

$$\begin{aligned} -\beta f = \ln(2) + \frac{1}{8\pi^2} \int_0^{2\pi} d\theta_1 \int_0^{2\pi} d\theta_2 \ln[\cosh(2\beta J_1)\cosh(2\beta J_2) \\ - \sinh(2\beta J_1)\cos(\theta_1) - \sinh(2\beta J_2)\cos(\theta_2)] \end{aligned}$$

Ce résultat majeur lui permit aussi d'établir que la transition de phase est *du second ordre* (c'est donc la dérivée seconde de l'énergie libre qui diverge). La valeur de la magnétisation sous-critique fut déterminée tout d'abord par Onsager et Kaufman en 1949. Cependant, cette preuve ne fut pas publiée et c'est Yang qui en 1952 [167] publia une première preuve rigoureuse du fait que la magnétisation se comporte voisinage de T_c est de la forme $(T - T_c)^{\frac{1}{8}}$ uniquement *d'un seul côté de la criticalité*, lorsque $T < T_c$. Ce résultat de Yang justifie la notion de transition de phase du modèle. Dans son article, Yang mentionne explicitement avoir eu accès aux notes d'Onsager et Kauffman mais propose une dérivation alternative du résultat (voir [11, Section 5] pour plus de détails). Les travaux d'Onsager et Kaufman [95] permettent aussi de déduire que la corrélation du modèle critique entre deux points à distance r décroit comme $r^{-\frac{1}{4}}$. Ces relations font déjà apparaitre la notion *d'exposants critiques*, que les travaux de Essam, Fisher et Widom (voir [70] pour une formulation en des termes modernes) tentent de relier entre eux. À cette époque Kadanoff prédit de son côté un phénomène dit *d'universalité*, qui suppose que les exposants critiques ne dépendent pas de la géométrie locale des graphes, mais plutôt de la dimension du modèle ainsi que de l'intensité des interactions à longue portée. Dès lors, une école très productive à travaillé sous l'impulsion de McCoy, Wu [122] ou bien encore de Perk (e.g. [142]) et a permis de réaliser des calculs *exacts* de corrélations en volume infini (voir e.g. [122, 136] pour une exposition complète) utilisant des représentations déterminantales de Toeplitz ainsi que des méthodes d'isomonodromies, qui consistent à déplacer infinitésimalement l'un des spins pour obtenir une équation sur la limite d'échelle des corrélations (comme par exemple dans [166], dont il existe une traduction dans un langage actuel dans [137, Section 4]). Une des raisons expliquant l'existence de formules exactes (en concomitance avec l'utilisation de techniques de calcul très élégantes) est le caractère exactement soluble du modèle sans champ magnétique extérieur, dont la fonction de partition est le pfaffien d'une certaine matrice d'adjacence [37, Theorème 1.1]. Cette même matrice d'adjacence fait aussi apparaitre la notion *d'observable fermionique* (qui est cruciale dans l'étude que l'on fait du modèle d'Ising dans ce manuscrit) et fait du modèle d'Ising un modèle de *fermion libre* (e.g. [155]).

D'un autre côté, la théorie du groupe de renormalisation introduite en premier lieu par Wilson [165] postule qu'il existe des transformations du modèle qui ne modifient pas son Hamiltonien. Cette méthode de renormalisation affirme qu'il est possible d'agréger les spins d'un même bloc et les remplacer par un seul spin, et permet de jouer sur les différents facteurs d'échelle pour tenter de déterminer les exposants critiques d'un modèle. Une des conséquences des articles fondateurs Belavin Polyakov et Zamolodchikov [16, 17] qui ont par ailleurs mené à l'expansion rapide de l'étude de la Théorie Conforme des Champs (CFT) est l'affirmation que la limite d'échelle du modèle critique est *invariante conforme* (les applications conformes étant localement la composition d'une rotation et d'une homothétie, qui

apparaissent comme des propriété naturelle de la limite d'échelle si cette dernière est bien un point fixe du groupe de renormalisation). Cette invariance conforme a été ensuite explorée numériquement [108, 106, 107], par exemple pour les probabilité de croisement du modèle critique sur les rectangles topologiques.

En 2000, l'introduction par Schramm [154] des processus SLE (Stochastic Loewener Evolution) pour décrire la limite d'échelle des marches à boucles effacées et des arbres couvrant uniformes a revivifié l'activité scientifique visant à prouver l'invariance conforme des modèles de physique statistique planaires. Comme l'explique Schramm dans l'introduction de cet article révolutionnaire, l'objectif originel de sa construction est de fournir un processus continu étant un candidat solide pour décrire la limite d'échelle des interfaces associées au modèle de percolation. Son approche s'est avérée très rapidement être fructueuse, avec une première preuve de la convergence des interfaces de percolation critique sur le réseau triangulaire par Smirnov [161] (voir aussi [163]). Cette construction de limite d'échelle pour les interfaces est complétée par l'introduction des processus CLE (Conformal Loop Ensembles) par Sheffield [156] qui ont largement été développés depuis (voir par exemple [157] où une caractérisation très utile du CLE est donnée par Sheffield et Werner), afin de décrire non seulement les interfaces mais aussi les ensembles de boucles issus de modèles discrets (un des premiers exemples effectifs est la percolation critique dans le travail de Camia et Newman [30]). En parallèle, les travaux de Kenyon sur les modèles de dimères et du Laplacien discret [101, 98, 100] ainsi que les travaux de Smirnov [161] sur la percolation prouvant la formule de Cardy [31], ont montré l'intérêt de considérer des fonctions holomorphes discrètes afin prouver la convergence de modèles planaires. Pour le modèle d'Ising, l'utilisation de l'holomorphie discrète des observables fermioniques pour prouver l'existence d'une limite d'échelle apparait pour la première fois dans les travaux fondateurs de Smirnov [160]. Les questions autour de l'existence d'une forme d'holomorphie discrète pour le modèle d'Ising font naturellement suite aux travaux de Kenyon, étant donnés les nombreux liens combinatoires entre le modèle de dimères et le modèle d'Ising. Il est à noter qu'une formulation alternative de l'holomorphie discrète est apparue dans les travaux de Mercat [129] (mais sans leur complexification ni technique permettant de déduire leur convergence), et était, selon Barry McCoy [129, Remerciements], une notion déjà connue de manière plus ou moins formelle. Le travail pionnier de Smirnov [160] lui a permis de prouver la convergence de l'interface FK vers le processus SLE(16/3) et crée par la suite une école très productive dédiée à l'invariance conforme sur les domaines bornés du plan (ces résultats sont detaillés dans la section 1.8). Cela a permis de prouver la convergence des interfaces, ensembles de boucles et corrélations du modèle critique sur les graphes isoradiaux, ainsi qu'une généralisation aux modèles massifs mais aussi en dehors du cadre isoradial (voir par exemple [34] pour un récapitulatif complet des résultats connus).

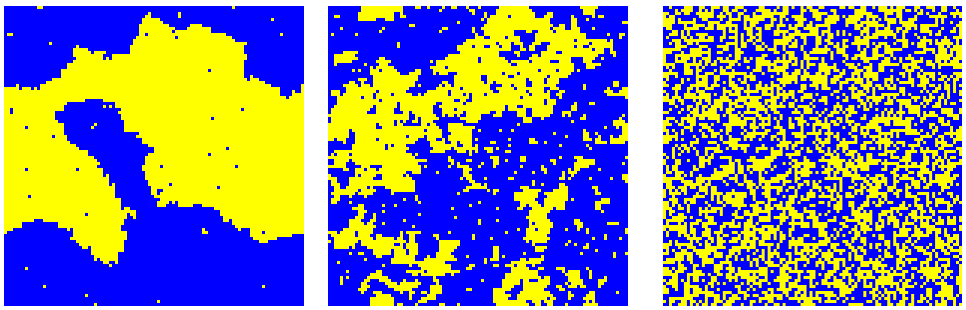

FIGURE 1.1.1 – Simulation du modèle d'Ising sur le réseau carré avec conditions de bord libres, avec une température (de gauche à droite) sous-critique, critique, et sur-critique. La simulation provient de la page internet *https ://physics.weber.edu/schroeder/software/demos/isingmodel.html*.

1.2 . Notations de graphe et définitions combinatoire

1.2.1 . Notations

Dans ce manuscrit, on travaille avec un graphe planaire G (plongé dans le plan ou dans la sphère et considéré à homéomorphisme près préservant l'orientation). On autorise la présence d'arêtes doubles entre sommets mais interdit la présence de boucles autour d'un même sommet. On définit alors les ensembles suivants :

- $G^\bullet$ le graphe primal, constitué de l'ensemble des sommets de G, ainsi que $E(G)$ l'ensemble des arêtes de G, reliant deux à deux des sommets voisins de G. Typiquement, les sommets de G sont notés $v^\bullet$.
- G° le graphe dual, constitué de l'ensemble des faces de G, vu comme le dual du graphe $G^\bullet$. Typiquement, les faces de G sont notées v°. On note $e^\star$ l'arête duale de e, qui relie les deux faces séparées e.
- $\Lambda(G) := G^\circ \cup G^\bullet$, vu comme un graphe bipartite, i.e. chaque arête de $\Lambda(G)$ est composée d'un sommet de $G^\bullet$ et d'une face G° où le sommet de $G^\bullet$ appartient à la face G° dans G.
- $\Upsilon(G)$ l'ensemble des arêtes de $\Lambda(G)$, dont les sommets sont appelés *coins* et sont typiquement notés c. Chaque arête $[v^\bullet v^\circ]$ de $\Lambda(G)$ s'identifie à un coin $c = (v_c^\bullet v_c^\circ)$ de $\Upsilon(G)$, où $v_c^\bullet$ est le sommet appartenant à $G^\bullet$ incident à c et v_c° est la face appartenant à G° incidente à c. Deux coins sont voisins s'ils appartiennent à deux arêtes de $\Lambda(G)$ qui ont un sommet de $\Lambda(G)$ en commun.
- le graphe des diamants $\diamondsuit(G)$, dual de $\Lambda(G)$, appelé graphe des quadrilatères, dont les sommets (qui correspondent aux faces de $\Lambda(G)$) sont typiquement notés z. Les faces du graphe $\diamondsuit(G)$ sont en bijection naturelle avec $E(G)$.

Dans le cas où le graphe est plongé dans la sphère, on fixe une face dite extérieure v_{ext}° et les définitions présentées au-dessus sont adaptées. En particulier,

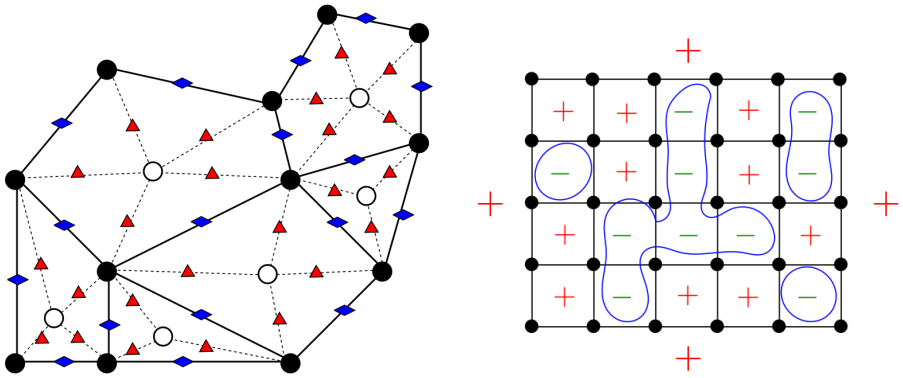

FIGURE 1.2.1 – Gauche :Notations de graphe utilisées dans ce manuscrit. Les arêtes pleines correspondent aux arêtes du graphe $G^\bullet$, les arêtes pointillées correspondent aux arêtes de $\Lambda(G)$, qui est lui-même en bijection avec l'ensemble $\Upsilon(G)$ des coins. Les coins sont marqués par des triangles rouges, les sommets du graphe des diamants sont marqués par des losanges bleus. Droite : Représentation par les contours de l'expansion à basse température, séparant (en bleu) les spins opposés avec des conditions branchées, où le spin extérieur vaut ici $+1$.

elles restent les mêmes pour $G^\circ \backslash \{v^\circ_{ext}\}$ et sont modifiées en considérant la face v°_{ext} comme une *unique* face, adjacente à toutes les faces de bord.

Contrairement aux conventions usuelles et à la formulation historique du modèle d'Ising, on travaille majoritairement dans ce manuscrit avec le modèle d'Ising défini sur l'ensemble des *faces* de G (i.e. les spins sont assignés à G°). On fixe G un sous-graphe connexe fini, ainsi qu'un nombre réel strictement positif $\beta^\circ = 1/kT$, dont l'interprétation physique est celle de l'inverse d'une température. On associe à chaque arête $e \in E(G)$ séparant les faces $v^\circ_\pm(e) \in G^\circ$ une constante de couplage $J^\circ_e > 0$. On peut alors définir une loi de probabilité assignant une configuration de spins $\sigma \in \{\pm 1\}^{G^\circ}$ aux faces de G selon la loi de probabilité

$$\mathbb{P}^\circ[\sigma] := \frac{1}{\mathcal{Z}(G^\circ, (J^\circ_e)_{e\in G}, \beta^\circ)} \exp\big[\,\beta^\circ \sum_{e\in E(G)} J^\circ_e \sigma_{v^\circ_-(e)}\sigma_{v^\circ_+(e)}\,\big] \tag{1.2.1}$$

Le facteur de normalisation

$$\mathcal{Z}^\circ(G^\circ, (J^\circ_e)_{e\in G}, \beta^\circ) \;:=\; \textstyle\sum_{\sigma: G^\circ \to \{\pm 1\}} \exp\big[\,\beta^\circ \sum_{e\in E(G)} J^\circ_e \sigma_{v^\circ_-(e)}\sigma_{v^\circ_+(e)}\,\big], \tag{1.2.2}$$

appelé la *fonction de partition* du modèle est choisi pour que la somme des probabilités sur les configurations élémentaires soit 1. Cette mesure de probabilité est une mesure de Boltzmann, de la forme $\exp(-\beta \mathbf{H}(\sigma))$ où le Hamiltonien $\mathbf{H}(\sigma)$ représente l'énergie de la configuration σ. On peut voir dans la définition de (1.2.1) que cette distribution de probabilité *favorise* les configurations de spins où les voisins

sont alignés (c'est à dire que les spins prennent la même valeur), ce qui produit un modèle *ferromagnétique* (dont l'exemple physique le plus simple est celui de l'aimant). La constante de couplage J_e° quantifie le coût probabiliste nécessaire pour casser l'alignement entre deux spins voisins séparés par l'arête e. Le modèle que l'on vient d'introduire correspond à des conditions de bord *branchées* : à chaque arête e au bord de G se trouve assigné une constante de couplage J_e°, et le tirage d'une configuration aléatoire correspond à assigner un spin ± 1 à toutes les faces de G°, et en particulier à v_{ext}°, qui est considéré comme un *unique* spin. Ainsi l'impact de v_{ext}° dans le coût probabiliste d'une configuration prend en compte le poids de toutes les arêtes de bord adjacentes à v_{ext}°.

Dans ce manuscrit, on ne s'intéresse qu'au cas du modèle d'Ising *sans champ magnétique extérieur* (ce qui correspondrait à ajouter des termes dans le hamiltonien $\mathbf{H}$ mentionné ci-dessus). Dans le cadre de l'introduction d'un champ extérieur h non nul, c'est le plus souvent le signe de h qui gouverne la magénétisation globale du modèle, les interactions entre voisins devenant secondaires [72, Chapitre 3].

1.2.2 . Expansion à basse température

On présente maintenant *l'expansion à basse température* du modèle, aussi appelée représentation de contours. Pour cela, on note $\mathcal{E}(G)$ l'ensemble des sous-graphes *pairs* de G, dont les sommets sont tous de degré pair.

Une fois fixée la valeur du spin de la face extérieure, il existe une bijection simple (voir 1.2.1) entre une configuration de spins $\sigma : G^\circ \to \{\pm 1\}$ et un sous-graphe pair C de G. Entant donné une configuration σ, on lui associe le sous-ensemble C des arêtes du graphe G séparant des spins voisins opposés, comme le montre la figure 1.2.1 (droite). On peut donc associer exactement *deux* configurations de spins $\sigma, -\sigma$ sur G° (dont la probabilité d'apparition est la même) à un unique sous-graphe pair de G. Dans ce qui suit, on pose pour une arête e de G la quantité $x_e^\circ := \exp(-2\beta^\circ J_e^\circ)$, qui permet de définir pour une collection $\mathcal{C}$ de sous-graphes pairs $C \in \mathcal{C}$ les quantités

$$x^\circ(C) := \prod_{e \in C} x_e^\circ, \text{ et } x^\circ(\mathcal{C}) := \sum_{C \in \mathcal{C}} x^\circ(C). \tag{1.2.3}$$

En utilisant la représentation de contours expliqué ci-dessus, on peut réécrire (e.g. [37, eq (1.3)])

$$\mathcal{Z}^\circ(G^\circ, (J_e^\circ)_{e\in G}, \beta^\circ) \ = 2 \prod_{e \in E(G)} \exp(\beta^\circ J_e^\circ) \times x^\circ(\mathcal{E}(G)), \tag{1.2.4}$$

où le facteur 2 provient de l'association de deux configurations de spins à une unique représentation de contour. Cette représentation de contours permet en particulier d'exprimer de manière compacte les corrélations entre spins.

En effet, fixons un entier pair n, des sommets $v_1^\circ, \dots, v_n^\circ \in G^\circ$, ainsi qu'un sous-graphe arbitraire $\gamma^\circ = \gamma_{[v_1^\circ, \dots, v_n^\circ]} \subset G^\circ$ de G dont tous les sommets sont de degré

pair, mis à part ceux de $v_1^\circ, \dots, v_n^\circ$. Une manière de représenter graphiquement une telle configuration consiste à se donner collection de boucles de G, auxquelles on a ajouté des chemins reliant deux à deux les $v_1^\circ, \dots, v_n^\circ$. On peut alors définir pour une arête e de G

En utilisant cette représentation, on voit que (e.g. [37, Proposition 1.3])

$$\mathbb{E}_{G^\circ}\left[\sigma_{v_1^\circ} \dots \sigma_{v_n^\circ}\right] \;=\; x^\circ_{[\gamma]}(\mathcal{E}(G))/x^\circ(\mathcal{E}(G)). \tag{1.2.5}$$

En suivant la représentation à basse température, le signe de $x^\circ_{[v_1^\circ,\dots,v_n^\circ]}(C)$ compte la parité du nombre de boucles contenant un nombre *impair* des $2n$ spins, ce qui correspond exactement au produit $\sigma_{v_1^\circ} \cdots \sigma_{v_n^\circ}$. De plus, l'expression précédente assure que $x^\circ_{[\gamma]}(\mathcal{E}(G))$ ne dépend pas du choix de γ.

On rappelle qu'il est naturel d'identifier un arête e de G et une face $z(e)$ de $\Lambda(G)$. Cela permet de définir une paramétrisation alternative par un *angle abstrait* $\theta_{z(e)}$ en posant

$$\theta_{z(e)} \;:=\; 2\arctan x^\circ(e) \;\in\; (0, \tfrac{1}{2}\pi). \tag{1.2.6}$$

Ici l'angle $\theta_{z(e)}$ n'a pas spécialement d'interprétation géométrique. Cette paramétrisation sera utilisée à plusieurs reprise dans la suite de cette introduction.

1.2.3 . Expansion à haute température

On présente maintenant *l'expansion à haute température* du modèle d'Ising. Pour cela, on considère un modèle d'Ising assignant des spins ± 1 aux *sommets* $G^\bullet$ de G. Comme précédemment, on se donne $(J_e^\bullet)_{e\in E(G)}$ une suite de constantes de couplages associées aux arêtes $(e)_{e\in E(G)} = ((v_-^\bullet(e)v_+^\bullet(e))_{e\in E(G)}$ ainsi qu'une température inverse $\beta^\bullet$. On définit alors la distribution de probabilités pour une configuration $\sigma \in \{\pm\}^{G^\bullet}$ par

$$\mathbb{P}^\bullet[\sigma] := \frac{1}{\mathcal{Z}^\bullet(G^\bullet, (J_e^\bullet)_{e\in G}, \beta^\bullet)} \exp\big[\,\beta^\bullet \sum_{e\in E(G)} J_e^\bullet \sigma_{v_-^\bullet(e)}\sigma_{v_+^\bullet(e)}\,\big]). \tag{1.2.7}$$

Le modèle est à présent avec condition de bord *libre*, c'est à dire que les spins sont portés par les sommets de $G^\bullet$ et qu'il n'est plus nécessaire de traiter (comme précédemment) le cas particulier du spin assigné à la face extérieure. Cette fois-ci la fonction de partition du modèle est donnée par

$$\mathcal{Z}^\bullet(G^\bullet, (J_e^\bullet)_{e\in G}, \beta^\bullet) \;:=\; \textstyle\sum_{\sigma: G^\bullet\to\{\pm1\}} \exp\big[\,\beta^\bullet \sum_{e\in E(G)} J_e^\bullet \sigma_{v^\bullet-(e)}\sigma_{v_+^\bullet(e)}\,\big]. \tag{1.2.8}$$

Pour $e = (uv)$, on pose cette fois $x_e^\bullet := \tanh[\beta^\bullet J_e^\bullet]$ et utilise l'identité élémentaire pour tout $\sigma_u, \sigma_v \in \pm 1$

$$\exp[2\beta^\bullet J_{uv}^\bullet \sigma_u\sigma_v] = \cosh[\beta^\bullet J_e^\bullet](1 + \sigma_u\sigma_v \tanh[\beta^\bullet J_e^\bullet]), \tag{1.2.9}$$

on peut voir que [37, eq (1.2)]

$$\mathcal{Z}^\bullet(G^\bullet, (J_e^\bullet)_{e\in G}, \beta^\bullet) \;= 2^{|G^\bullet|} \textstyle\prod_{e\in E(G)} \cosh[\beta^\bullet J_e^\bullet] \times x^\bullet(\mathcal{E}(G)). \tag{1.2.10}$$

En effet, on rappelle que la fonction de partition $\mathcal{Z}^\bullet(G^\bullet, (J_e^\bullet)_{e\in G}, \beta^\bullet)$ est une somme sur l'ensemble des configurations $\sigma \in \{\pm 1\}^{G^\bullet}$ des poids élémentaires naturellement associés à chaque configuration. On réinjecte ensuite $(1.2.9)$ dans le membre de gauche de $(1.2.10)$, ce qui permet d'écrire $\mathcal{Z}^\bullet(G^\bullet, (J_e^\bullet)_{e\in G}, \beta^\bullet)$ comme polynômes pondéré en les variables variables σ_v parcourant $|G^\bullet|$. Chaque produit de monômes contenant au moins une puissance impaire de l'un des σ_v se retrouve exactement compensé (avec un signe opposé) en passant à la sommation lorsque l'on considère l'ensemble des configurations qui coïncident en dehors du spin σ_v. Après sommation, il reste ainsi seulement les polynômes pour lesquels *toutes* les variables σ_v sont exprimées en des puissance paires. Il y a $2^{|G^\bullet|}$ polynômes de ce type (selon la présence ou non de la variable σ_v associée à chaque spin) et la contribution de chacun de ces polynômes est la même (car $\sigma_v^{2p} = 1$).

Fixons à présent m un entier pair et $v_1^\bullet, \dots, v_m^\bullet$ des sommets distincts de $G^\bullet$. En utilisant les mêmes arguments que précédemment (et en remarquant que le facteur $\sigma_{v_1^\bullet} \dots \sigma_{v_m^\bullet}$ est cette fois ci déjà présent dans le développement de $(1.2.10)$) on a directement [37, Section 1.2]

$$\mathbb{E}_{G^\bullet}[\sigma_{v_1^\bullet} \dots \sigma_{v_m^\bullet}] = x^\bullet(\mathcal{E}^{[v_1^\bullet,\dots,v_m^\bullet]})/x^\bullet(\mathcal{E}(G)), \tag{1.2.11}$$

où $\mathcal{E}^{[v_1^\bullet,\dots,v_m^\bullet]}$ représente l'ensemble des sous graphes de $E(G)$ qui ont degré pair partout excepté en les sommets $v_1^\bullet, \dots, v_m^\bullet$.

1.2.4 . Dualité de Kramers-Wannier

On remarque que si on a l'égalité

$$x_e = x_e^\circ = x_e^\bullet = \exp[-2\beta^\circ J_e^\circ] = \tanh[\beta^\bullet J_e^\bullet], \tag{1.2.12}$$

les fonctions de partition des modèles défini sur G° et $G^\bullet$ par $(1.2.4)$ et $(1.2.8)$ ont alors la même forme, ce qui est un signe usuel en mécanique statistique que les deux modèles sont reliés. L'identité $(1.2.12)$ se réécrit sous une forme beaucoup plus invariante $\sinh[2\beta^\circ J_e^\circ]\sinh[2\beta^\bullet J_e^\bullet] = 1$ [37, Section 1.2]. Cela permet en particulier de définir le poids dual associé à l'arête e en posant

$$x_e^\star := (1 - x_e)(1 + x_e)^{-1} = \tanh[\beta^\circ J_e^\circ] = \exp[-2\beta^\bullet J_e^\bullet]. \tag{1.2.13}$$

Remplacer x_e par $x_e^\star$ revient ainsi à échanger le rôle des modèles d'Ising sur les graphes $G^\bullet$ et G° (on ne détaille pas ici les subtilités au niveau de la face extérieure). Cette égalité est appelée la *dualité de Kramers-Wannier*, et relie un modèle d'Ising sur $G^\bullet$ à un modèle d'Ising sur son dual G° tant que leur constantes de couplages satisfont l'égalité $\sinh[2\beta^\circ J_e^\circ]\sinh[2\beta^\bullet J_e^\bullet] = 1$.

C'est cette observation qui a permis à Kramers et Wannier de prédire la valeur du point critique du modèle homogène sur le réseau carré. En effet, ils considèrent le modèle homogène $J_e^\bullet = 1$ sur $\mathbb{Z}^2$ et $J_e^\circ = 1$ sur son dual $(\mathbb{Z}^2)^\star = \mathbb{Z}^2 + (\frac{1}{2}; \frac{1}{2})$ qui est lui-même isomorphe à $\mathbb{Z}^2$. Selon eux, le modèle critique (dont le paramètre critique est le même pour $\mathbb{Z}^2$ et son dual), doit l'être exactement au point de

symétrie entre son paramètre primal et son paramètre dual, et doit donc vérifier $x = x^\star = (1-x)(1+x)^{-1}$, ce qui donne la valeur critique $x_c = \sqrt{2}-1$ et la température critique $\beta_c^\bullet = \frac{1}{2}\log(\sqrt{2}+1)$. C'est en se basant sur cette dualité de Kramers et Wannier [104] qu'Onsager a déterminé dans [135] la valeur du paramètre critique (en calculant explicitement l'énergie libre du système homogène).

1.2.5 . Représentation Fortuin-Kasteleyn du modèle

Parmi les multiples représentations du modèle d'Ising, il en existe une faisant partie d'un modèle plus général de clusters aléatoires, introduit par Fortuin et Kasteleyn [71]. Ce lien se fait via le couplage d'Edwards-Sokal [68]. Fixons une configuration de spins $\sigma = (\sigma_v)_{v\in G^\bullet}$ sur $G^\bullet$. Cette configuration est dite *compatible* avec un ensemble d'arêtes $C \subseteq E(G)$ si les spins d'une même composante connexe C (que l'on appelle aussi clusters de C) prennent tous la même valeur. Pour le modèle d'Ising sur $G^\bullet$ dont les poids duaux sont $x_e^\star = \exp(-2\beta^\bullet J_e^\bullet)$, la fonction de partition du modèle d'Ising se réécrit (à un facteur global près) par [60, Proposition 7.7]

$$\prod_{e\in E(G)} (x_e^\star)^{\frac{1}{2}} \mathcal{Z}^\bullet(G^\bullet, (J_e^\bullet)_{e\in G}, \beta^\bullet) = \sum_{C\subset E(G)} 2^{\#clusters(C)} \prod_{e\notin C}(1-x_e^\star) \prod_{e\in C} x_e^\star. \tag{1.2.14}$$

En particulier, cela permet de retrouver (et inversement) un modèle de clusters aléatoires à partir d'une configuration d'Ising via le couplage d'Edwards-Sokal via la procédure suivante

- Ising $\to$ modèle FK : à partir d'une configuration $\sigma \in \{\pm 1\}^{G^\bullet}$, on tire (indépendamment les unes des autres) une variable de Bernoulli de paramètre $x_e^\star$ pour chaque arête reliant des spins voisins et alignés. On ne garde alors que les arêtes pour lesquelles la variable de Bernoulli vaut 1. Cela construit la configuration C du modèle FK.
- Modèle FK $\to$ Ising : Pour chaque cluster de C la configuration FK, on tire (indépendamment des autres clusters de C) une variable centrée à valeur dans $\{\pm 1\}$ et assigne le spin tiré à *tous* les sommets du cluster.

On note $\mathbb{P}_{G^\bullet}^{FK}$ la mesure de probabilités associée. Ce lien entre les modèles d'Ising et FK, qui traduit en particulier entre par une interprétation des corrélations d'Ising via les probabilités de connexions du modèle FK, est crucial pour énoncer le résultat principal du chapitre 5. On note $u \leftrightarrow v$ l'évènement où les deux sommets sont connectés dans le modèle FK (i.e. ils appartiennent au même cluster). On a alors [60, Proposition 7.9]

$$\mathbb{P}_{G^\bullet}^{FK}(u \leftrightarrow v) = \mathbb{E}_{G^\bullet}[\sigma_u \sigma_v]. \tag{1.2.15}$$

Ce résultat se démontre directement en remarquant qu'avec le couplage d'Edwards-Sokal, conditionnellement au fait que les deux spins soient dans le même cluster, leur produit vaut toujours 1 alors que si les deux spins se trouvent dans deux cluster différents, la moyenne conditionnelle de leur produit est nulle (car les spins associés à leurs clusters respectifs sont tirés indépendamment).

1.2.6 . Passage en volume infini

On explique à présent comment définir le modèle d'Ising en *volume infini*, ce qui correspond à créer un modèle de spins sur toutes les faces de $\mathbb{Z}^2$. La mesure de probabilité associée sur le plan n'est pas triviale à construire, et on détaille à présent sa construction. On commence par se donner une suite croissante $(G_n)_{n\geqslant 0}$ de sous-graphes de $\mathbb{Z}^2$ qui le recouvrent à la limite.

Une des premières observations est la *monotonicité vis à vis des conditions de bord* [72, Lemme 3.12], c'est à dire qu'avec des conditions de bord $+$ sur les graphes $G_n \subseteq G_{n+1}$ et pour un spin $u^\circ \in G_n$, alors $\mathbb{E}^+_{G_n}[\sigma_{u^\circ}] \geqslant \mathbb{E}^+_{G_{n+1}}[\sigma_{u^\circ}]$. Autrement dit la magnétisation décroit lorsque l'on *repousse* les conditions de bord. L'égalité inverse est vraie pour des conditions de bord $-$. De même il existe une monotonicité vis-à-vis des constantes de couplages qui se démontre grâce à l'inégalité GKS (Griffiths,Kelly et Sherman) rappelée dans [72, Théorème 3.20]. Si les constantes de coupage $(J^\circ_{1,e})_{e\in\mathbb{E}(G)}$ sont *toutes* inférieures ou égales au constantes de couplages $(J^\circ_{2,e})_{e\in\mathbb{E}(G)}$, alors on a

$$\mathbb{E}^+_{G_n,(J^\circ_{1,e})_{e\in\mathbb{E}(G)},\beta^\circ}[\sigma_{u^\circ}] \geqslant \mathbb{E}^+_{G_n,(J^\circ_{2,e})_{e\in\mathbb{E}(G)},\beta^\circ}[\sigma_{u^\circ}]$$

Une généralisation de cette dernière inégalité permet de définir [72, Théorème 3.17] au moins deux mesures en volume infini avec conditions de bord à l'infini $\pm$ via la limite faible

$$\mathbb{P}^{\circ,\pm}_{\mathbb{Z}^2}[\cdot] := \lim_{n\to\infty} \mathbb{P}^{\circ,\pm}_{G_n}[\cdot]. \tag{1.2.16}$$

Pour le modèle homogène avec $\beta^\circ = 1$ et $J^\circ_e = J$ sur toutes les arêtes e de $\mathbb{Z}^2$, la valeur de J influe sur l'unicité de la mesure en volume infini. Dans ce même cadre, on remarque que les deux mesures construites ci-dessus sont *invariantes par translation*. Pour ce qui est de l'unicité on a

1. Si $J \geqslant \frac{1}{2}\log(1+\sqrt{2})$ alors $\mathbb{P}^{\circ,+}_{\mathbb{Z}^2} = \mathbb{P}^{\circ,-}_{\mathbb{Z}^2}$ et il n'existe qu'une seule mesure de Gibbs (au sens de [72, Section 3.4]) en volume infini.
2. Si $J < \frac{1}{2}\log(1+\sqrt{2})$ alors les mesures de Gibbs $\mathbb{P}^{\circ,+}_{\mathbb{Z}^2}$ et $\mathbb{P}^{\circ,-}_{\mathbb{Z}^2}$ sont les deux seules mesures de Gibbs *extrémales* (i.e. qui ne sont pas une combinaison convexe non-triviale d'autre mesures de Gibbs). Il est possible de voir (comme redémontré récemment dans un cadre plus général par Raoufi [149]) que toute mesure de Gibbs invariante pas translation est une combinaison convexe de $\mathbb{P}^{\circ,\pm}_{\mathbb{Z}^2}$.

Il est par ailleurs possible de définir ces mesures en volume infini en utilisant la représentation FK du modèle (e.g. [60, Proposition 7.12]). On note que lorsque $J \geqslant \frac{1}{2}\log(1+\sqrt{2})$, l'égalité entre les deux mesures extrémales en volume infini, l'invariance par retournement des spins ainsi que l'invariance par translation implique que $\mathbb{E}_{\mathbb{Z}^2}[\sigma_{u^\circ}] = 0$ pour tout $u \in (\mathbb{Z}^2)^\star$. Pour ce qui est du sens physique, cela indique que si les constantes de couplages ont une valeur trop grande, le coût pour transporter la magnétisation positive de l'infini à l'origine est trop important.

Au contraire si les constantes de couplages sont suffisamment petites, alors les conditions de bord à l'infini se propagent jusqu'à l'origine et $\mathbb{E}^+_{\mathbb{Z}^2}[\sigma^\circ_u] > 0$ (e.g. [60, Théorème 7.13]).

Il est aussi possible de calculer la magnétisation d'un produit de deux spins $\mathbb{E}^+[\sigma_{u^\circ}\sigma_{v^\circ}] = \mathbb{E}^-[\sigma_{u^\circ}\sigma_{v^\circ}]$ (cette égalité étant vraie par invariance par retournement des spins). On déduit du caractère extrémal des deux mesures avec conditions de bord $\pm$ à l'infini que la quantité $\mathbb{E}[\sigma_{u^\circ}\sigma_{v^\circ}]$ est toujours bien définie et à nouveau invariante par translation. En particulier, un calcul explicite du à Yang [167] (alors que le résultat avait été annoncé en amont par Kaufman et Onsager mais sans publier de preuve) fournit la dichotomie du théorème suivant.

Theorème 1.2.1 (**Onsager-Kauffman-Yang**). Pour le modèle d'Ising ur $\mathbb{Z}^2$ avec des constantes de couplages homogènes $J = 1$ on a les deux alternatives suivantes

— Si $\beta < \frac{1}{2}\log(1+\sqrt{2})$, alors $\lim_{v^\circ\to\infty} \mathbb{E}[\sigma_{u^\circ}\sigma_{v^\circ}] = (1-\sinh^{-4}[2\beta])^{\frac{1}{4}}$.

— Si $\beta \geqslant \frac{1}{2}\log(1+\sqrt{2})$, alors $\lim_{v^\circ\to\infty} \mathbb{E}[\sigma_{u^\circ}\sigma_{v^\circ}] = 0$.

Il est possible d'en déduire de l'inégalité GKS [72, Théorème 3.20] et de l'invariance par translation que pour $\beta < \frac{1}{2}\log(1+\sqrt{2})$, on a $\mathbb{E}^+_{\mathbb{Z}^2}[\sigma_{u^\circ}] = (1-\sinh^{-4}[2\beta])^{\frac{1}{8}}$. Plus d'une décennie après ce premier calcul analytique de la magnétisation spontanée, un calcul explicite de la corrélation à deux points sur la diagonale du réseau carré critique a été trouvé par Wu. Lorsque $\beta^\circ = \frac{1}{2}\log(1+\sqrt{2})$ et $J = 1$, on a alors

$$\mathbb{E}_{\mathbb{Z}^2}[\sigma^\circ_{(\frac{1}{2};\frac{1}{2})}\sigma^\circ_{(n+\frac{1}{2};n+\frac{1}{2})}] = \Big(\frac{2}{\pi}\Big)^n \prod_{k=1}^{n-1}(1-\frac{1}{4k^2})^{k-n} \underset{n\to\infty}{\sim} \mathcal{C}^2_\sigma (2n)^{-\frac{1}{4}}, \qquad (1.2.17)$$

avec $\mathcal{C}_\sigma = 2^{\frac{1}{6}} e^{\frac{3}{2}\zeta'(-1)}$. Ce calcul ainsi qu'une multitude d'autres sont consignés dans le livre de McCoy et Wu [123], qui ont développés intensivement la représentation des corrélations via des déterminants de Toeplitz pour en trouver des expressions exactes.

Il est important de noter que la transition de phase du modèle d'Ising est *abrupte* sur le réseau carré. En dessous de la température critique, la magnétisation en volume infinie est strictement positive. A la température critique, la corrélation entre spins décroit polynômialement en leur distance. Au dessus de la température critique, il s'avère que la corrélation entre spins décroit exponentiellement avec leur distance comme le montre à nouveau le formalisme développé par McCoy et Wu [123] (on notera par ailleurs les travaux de Aizenman, Barsky et Fernández [1] qui généralisent ce résultat en dimension supérieure). Des travaux récents de Beffara et Duminil-Copin identifient le point critique et généralisent ensuite cette dichotomie de comportement des corrélations à tous les modèles FK (pour $q \geqslant 1$) dans [15, Théorème 1.2].

1.3 . Invariance triangle étoile sur les grilles isoradiales

Il est possible de réaliser des transformations locales du modèle d'Ising qui préservent la loi de probabilité des configurations concernant les spins distants du lieu de cette modification de graphe. Une des transformations les plus connues est la transformation *triangle-étoile*, dont il existe un analogue dans le cadre des fonctions harmoniques sur les réseaux électriques [115] ainsi que les modèles de dimères (e.g. [164]). Cette transformation a été largement étudiée pour les graphes planaires généraux (sans plongement particulier) par Baxter dans [12] et admet une interprétation géométrique naturelle dans le cadre des grilles isoradiales, dont les propriétés élémentaires seront rappelées dans la section 1.3.2.

1.3.1 . Les poids Z-invariants de Baxter

Dans ce qui suit on utilise les notations de la figure 1.3.2 et travaille avec un graphe planaire *abstrait* G (et ne considère donc pas pour l'instant un éventuel plongement isoradial) contenant un sommet $v^\bullet$ de degré 3, dont les trois voisins sont notés $u^\bullet_{1,2,3}$. On note $u^\circ_{1,2,3}$ les trois faces adjacentes à $v^\bullet$ (à gauche dans la figure 1.3.2). Considérons à présent le graphe $\tilde{G}^\bullet$ (à droite dans la figure 1.3.2), qui coïncide avec G en dehors de $u^\bullet_{1,2,3}$ et où

— Le sommet $v^\bullet$ est remplacé par une face u°,

— Les arêtes $e_i = (v^\bullet v_i)$ sont remplacées par les arêtes $e_{12,13,23}$.

On utilise à présent la paramétrisation $x_e \in]0;1[\leftrightarrow \theta_e := 2\arctan(x_e)$ [37, Section 3.5], rappelée dans $(1.2.6)$, pour laquelle la dualité de Kramers-Wannier rappellée dans la section 1.2.4 se traduit par l'égalité $\theta_e + \theta^\star_e = \frac{\pi}{2}$.

Les travaux de Baxter [12, equations (6.4.8)-(6.4.16)] impliquent que si pour tout $\{p,q,r\} \in \{1,2,3\}$ on a l'identité sur les poids d'Ising (appelée équations de Yang-Baxter)

$$x_p x_q = \frac{x_{pq} + x_{pr}x_{qr}}{1 + x_{pq}x_{pr}x_{qr}} \iff \frac{x^\star_p + x^\star_q}{1 + x^\star_p x^\star_q} = \frac{x^\star_{pq}(x^\star_{pr} + x^\star_{qr})}{1 + x^\star_{pr}} x^\star_{qr} \tag{1.3.1}$$

$$\iff x^\star_{pq} x^\star_{rr} = \frac{x^\star_p + x^\star_q x^\star_r}{1 + x^\star_p x^\star_q x^\star_r}, \tag{1.3.2}$$

alors

— les lois de probabilités $\mathbb{P}_{\tilde{G}^\bullet}$ et $\mathbb{P}_{G^\bullet \setminus \{v^\bullet\}}$ sont identiques.

— les lois de probabilités $\mathbb{P}_{\tilde{G}^\circ \setminus \{v^\circ\}}$ et $\mathbb{P}_{G^\circ}$ sont identiques.

On peut noter par ailleurs que $(1.3.1)$ est une bijection entre les triplets de la forme (x_1, x_2, x_3) et ceux de la forme (x_{12}, x_{23}, x_{13})..

On présente maintenant *une solution* à ces équation découverte par Baxter. La version que l'on montre ici est une version légèrement modifiée de sa résolution originale et correspond à la paramétrisation qui sera utilisée dans le chapitre 3. Les lignes qui suivent échangent le rôle des paramètres elliptiques k et $k^\star$ par rapport

au travail original [12], comme rappelé dans [28, Section 2.2.2]. Baxter commence par se donner trois angles *abstraits* $\overline{\theta}_1, \overline{\theta}_2, \overline{\theta}_3$ dans $]0; \frac{\pi}{2}[$ vérifiant $\overline{\theta}_1 + \overline{\theta}_2 + \overline{\theta}_3 = \pi$ et pose [12, equations (6.4.8)-(6.4.16)]

$$\overline{\theta}_{12} := \frac{\pi}{2} - \overline{\theta_3}, \quad , \overline{\theta}_{13} := \frac{\pi}{2} - \overline{\theta_2} \text{ et } \overline{\theta}_{23} := \frac{\pi}{2} - \overline{\theta_1}. \tag{1.3.3}$$

Il fixe ensuite un paramètre elliptique $k \in [0; 1[\cup i\mathbb{R}_+$ (i.e. $k^2 \leqslant 1$) et définit les modèle d'Ising pour lesquel les constantes de couplage vérifient

$$x_p := \tan(\frac{\theta_p}{2}) \ , \ \tan(\theta_p) := \mathsf{sc}(\frac{2\pi\overline{\theta}_p}{K(k)}|k) \ , \ \tan(\theta_{qr}) := \mathsf{sc}(\frac{2\pi\overline{\theta}_{qr}}{K(k)}|k), \text{ où } (1.3.4)$$

— $\mathsf{sc}(\cdot|k)$ est la fonction elliptique de Jacobi associé au paramètre elliptique k (voir e.g. [27, Appendix A]).

— $K(k)$ l'intégrale elliptique de première forme (voir e.g. [27, Appendix A]).

On a alors la proposition suivante

Proposition 1.3.1 (Baxter). *La paramétrisation* (1.3.4) *fournit* une solution *au système* (1.3.1) *d'équations de Yang-Baxter.*

On rappelle qu'avec les notations précédentes, $\theta_p^\star = \frac{\pi}{2} - \theta_p$ et $\overline{\theta_p^\star} = \frac{\pi}{2} - \overline{\theta_p}$. Ainsi, avec le choix des poids de Baxter donné par (1.3.4), la dualité de Kramers-Wannier se traduit par $x_e^\star = \tan(\frac{1}{2}\theta_e^\star)$, où $\tan(\theta_e^\star) = \mathsf{sc}(\frac{2K\overline{\theta}_e^\star}{K(k^\star)}|k^\star)$ et $k^\star := ik(1-k^2)^{-\frac{1}{2}}$ est le paramètre elliptique dual à k. Autrement dit avec le choix des poids de Baxter, la dualité de Kramers-Wannier correspond à

— Remplacer θ_e par $\theta_e^\star$,

— Remplacer k par $k^\star$.

On notera une paramétrisation qu'il existe alternative du modèle [28, Section 4.3] par un réel appelé le *nome*, noté $q \in \mathbb{R}$ et qui lui est relié par la relation $q := \exp(-\pi\frac{K'(k)}{K(k)})$ (où $K'(k)$ est l'intégrale elliptique de la seconde forme). Avec cette paramétrisation, la dualité de Kramers-Wannier se traduit en posant paramètre $q^\star := -q$.

1.3.2 . Les grilles isoradiales

On rappelle ici la notion de graphe isoradial, dont le nom a été fixé dans [99] (et dont il existe aussi des traces précédentes dans la littérature [129, 59]), et qui est un des objets d'étude centraux dans ce manuscrit. Sur cette classe de graphes, l'analyse complexe discrète est relativement bien comprise [47, 99, 36], dans des proportions comparables à celles sur le réseau carré.

Definition 1.3.1. On dit qu'un graphe G admet un *plongement isoradial propre* $\Gamma^\delta(G) \to \mathbb{C}$ de pas δ si chaque face de Γ^δ est inscrite dans un cercle de rayon δ, chaque centre de cercle inscrit se trouve à l'intérieur de la face associée, et que les différentes faces ne se recouvrent pas en dehors des segments qui les relient.

On confondra très souvent dans la suite un graphe isoradial G et son plongement isoradial $\Gamma^\delta(G)$. En particulier, lorsque l'on considère un plongement isoradial de G, chaque face du graphe plongé $\Gamma^\delta(\Lambda(G))$ se trouve être un *losange*, dont les côtés sont des segments parallèles et de longueur δ. On associe à ce losange l'angle $\bar{\theta}_e$ formé entre la diagonale des sommets de $G^\bullet$ et l'une des arêtes adjacentes à cette diagonale.

Le plongement isoradial crée un système de *lignes de chemin de fer* (aussi appelées *lignes de rapidité d'un système intégrable* dans [12]), vu comme une chaine bi-infinie d'arêtes de losanges voisins dans $\diamondsuit(G)$, tel que si la chaine entre dans un losange par une arête, elle en sort par l'arrête qui lui est opposée (et donc ici parallèle). Il est aussi possible de définir de la même manière ces lignes de chemin de fer sur un graphe planaire abstrait. Dans ce cas là, un théorème de Kenyon et Schlenker [102] assure qu'un graphe G admet un plongement isoradial si et seulement si

1. Aucune des lignes de chemin de fer ne se repasse par elle même ou bien n'est périodique.
2. Deux lignes de chemin de fer distinctes ne se coupent au plus qu'une seule fois.

La classe des grilles isoradiales contient par exemple les réseaux carrés, rectangulaires, hexagonaux, triangulaires, leurs mélanges, mais aussi des grilles sans symétrie apparente.

Il est possible de réaliser une modification *locale* du graphe isoradial en restant dans le cadre isoradial. Cette transformation s'appelle le *retournement de cube*, le nom provenant d'une interprétation de graphe isoradial comme une surface dans $\mathbb{R}^3$ (voir par exemple [127, Figure I.12]). Plus précisément, soit G un graphe isoradial, $v^\bullet$ un sommet de degré 3 dont les trois voisins sont notés $u^\bullet_{1,2,3}$. On peut remplacer les trois losanges de $\Lambda(G)$ adjacents à $v^\bullet$ par trois losanges de même bord extérieur, mais avec un sommet v° à la place. Cette opération revient à échanger deux lignes de chemin de fer qui se croisent en un losange (e.g. [27, Fig.1]).

Comme cela est démontré dans le chapitre 3, il est possible d'étendre une partie finie d'un graphe isoradial en une grille isoradiale infinie, dont une partie de la grille correspond à un réseau rectangulaire. Cette chirurgie est un des ingrédients cruciaux pour prouver la non-dépendance en la géométrie locale de certains observables associées au modèle d'Ising sur les graphes isoradiaux. Pour appliquer ces idées, on commence par prouver (en utilisant par exemple des méthodes d'analyse complexe discrète) une non-dépendance en la géométrie locale *sur un graphe isoradial donné*, approxime la mesure de probabilité en volume infini par une mesure en volume fini sur un (grand) sous-graphe $\mathcal{B}$, puis conclut en utilisant la non-dépendance en la géométrie locale *sur l'extension du graphe contenant* $\mathcal{B}$ ainsi qu'une partie d'un réseau rectangulaire (où des calculs explicites sont possibles). Il est utile de remarquer que cette opération est réalisée sans utiliser de *retournement de cube*, mais simplement par une extension des lignes de chemin de fer.

On présente maintenant le lien entre la paramétrisation abstraite de Baxter et le modèle d'Ising sur les graphes isoradiaux. Dans le cadre isoradial, les travaux de Boutillier, de Tilière et Raschel [28] prouvent qu'en choisissant les angles *abstraits* $\overline{\theta}$ dans $(1.3.3)$ égaux aux angles *géométriques* des losanges du plongement isoradial (définis à gauche dans la figure 5.3.1), la paramétrisation devient *Z-invariante* (c'est à dire invariante par *retournement de cube* et par transformation *triangle-étoile*).

Dans cette série d'articles, la définition des poids est locale et ne dépend que de la géométrie du losange z_e associé à une arête e dans le graphe isoradial. Le paramètre elliptique k (ou alternativement le nome q) joue le rôle d'une température, le modèle est critique au poids auto-duaux qui correspondent à $k = 0$ [28, Théorème 3] (dans ce cas là les angles géométriques $\overline{\theta}_e$ et abstraits θ_e coïncident). C'est la dérivée seconde de l'énergie libre qui diverge logarithmiquement, fournissant une transition de phase du second ordre. Lorsque $k = 0$, les poids deviennent des fonctions trigonométriques usuelles des θ_e, avec par exemple $x_e = \frac{\overline{\tan(\theta_e)}}{2}$.

Toujours pour les poids Z-invariants, les travaux de Lis [114] assurent que lorsque $k^2 > 0$, le modèle est sur-critique (les corrélations décroissent exponentiellement vite avec la distance entre les spins) alors que pour $k^2 < 0$ la magnétisation en volume infini est strictement positive.

Le chapitre 3 est centré sur l'étude du modèle dit *massif* sur les graphes isoradiaux, suivant les récents travaux de Park [137, 138]. En des termes plus précis, on commence par se fixer un paramètre réel m. On considère alors un graphe isoradial Γ^δ de pas δ équipé du modèle d'Ising aux poids de Baxter Z-invariants avec un nome qui vaut $q = \frac{1}{2}m\delta$. L'objet de notre étude est alors la limite d'échelle (proprement normalisée) du modèle lorsque l'on fait tendre le pas δ du réseau vers 0 en même temps que l'on fait tendre la température vers la température critique. Dans la formulation usuelle du modèle d'Ising sur le réseau carré avec des constantes de couplages unitaires, notre travail revient à étudier la limite d'échelle du modèle sur $\sqrt{2}\delta\mathbb{Z}^2$ à la température $\beta^\delta := \beta_c + \frac{m\delta}{2}$ (où β_c est la température critique du réseau carré rappelée dans la section 1.2.6).

1.4 . Motivations et perspectives sur les résultats présentés dans ce manuscrit

Avant de rentrer dans les détails les plus techniques de cette introduction et d'énoncer les résultats de notre travail, il nous semble important d'essayer de donner au lecteur quelques perspectives et motivations sur les nombreux travaux passés et futurs concernant la limite d'échelle du modèle d'Ising planaire critique et presque-critique. Nous expliquons aussi en quoi les connaissances actuelles nous ont poussé à explorer certains résultats et quelles sont les conjectures que l'on souhaite traiter (à long terme) avec le formalisme et les outils présentés dans ce manuscrit. Nous écrivons cette section sous forme de liste, afin d'en simplifier la lecture et d'en assurer la clarté.

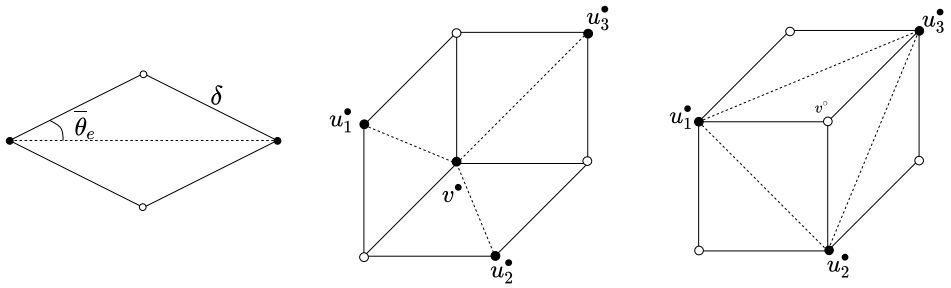

FIGURE 1.3.1 – (Gauche) Paramétrisation géométrique de l'angle $\overline{\theta}_e$ pour le losange $z(e)$ pour le plongement isoradial de pas δ. (Centre et droite) Retournement de cube, passant d'une configuration *triangle* à une configuration *étoile*. Le reste du graphe isoradial n'est pas modifié. On fera dans ce manuscrit souvent l'hypothèse dite des *angle bornées* sur les graphes isoradiaux, qui suppose que les angles géométriques $\overline{\theta}_e$ des losanges sont tous bornés inférieurement par une constante universelle η_0.

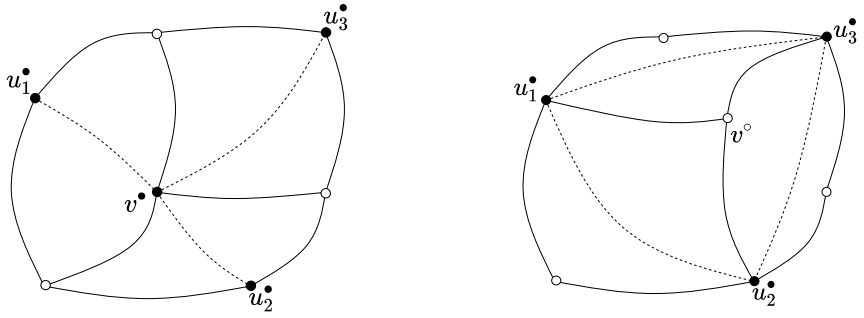

FIGURE 1.3.2 – Transformation abstraite passante d'une configuration *triangle* à une configuration *étoile*. Les arêtes du graphe bipartite $\Lambda(G)$ sont dessinées cette fois-ci en traits pleins alors que les arêtes de G sont dessinées en pointillées. (Gauche) Configuration étoile dans G avec le sommet $v^\bullet \in G^\bullet$ qui possède 3 voisins. (Droite) Configuration triangle dans G avec la face $u_1^\bullet, u_2^\bullet, u_3^\bullet$ dont le centre est v°. En choisissant des poids d'Ising correspondant à ceux de Baxter (1.3.4), les lois de probabilités concernant les événements en dehors de cette modification locale sont les mêmes sur le graphe contenant le triangle et celui contenant l'étoile.

1. Dans les travaux fondateurs des physiciens de la théorie conforme des champs (notamment via articles de Belavin Polyakov et Zamolodchikov [16, 17]), il a été conjecturé que le modèle d'Ising critique admet une *limite d'échelle invariante conforme*. Les développements (rappelés dans la section 1.8) suivant les travaux de Smirnov [160] permettent de justifier cette prédiction en lui donnant une formulation simple dans les domaines simplement connexes (où il la notion d'application conforme prend tout son sens). Ces résultats, proposant une description extrêmement précise de la limite d'échelle, ont tous été originellement prouvés sur le réseau carré. Dès lors, un des objectifs naturels a été de justifier la prédiction originale de Kadanoff, qui postule que la limite d'échelle du modèle d'Ising critique ne dépend pas de la géométrie locale du graphe. On appelle ce phénomène *l'universalité vis-à-vis de la géométrie locale*. La classe de graphes sur laquelle il a longtemps semblé raisonnable de prouver une forme d'universalité est celle des graphes isoradiaux équipé de leur poids Z-invariants critiques (dont les caratéristiques sont détaillées dans la section 1.3.1). Pour les grilles isoradiales critiques, le seul résultat qui n'avait pas encore été étendu au-delà de la grille carré critique concernait les corrélations de spins, pour lequel la preuve mais aussi les facteurs de normalisations n'étaient pas connus. Le chapitre 3 répond à cette question (généralisant aussi des travaux de Park sur le modèle Z-invariant massif [137]).
2. La seconde motivation est celle de traiter le cas des graphes généraux équipés d'un modèle d'Ising critique et presque critique, là où la notion de criticalité n'admet que rarement (pour l'instant) de formulation claire. On peut tout de même considérer deux problèmes suivants suivants
   — Les grilles doublement périodiques équipées de leur poids critiques (la condition de criticalité a été prouvée par Cimasoni et Duminil-Copin dans [52]). Trouver un plongement, prouver l'invariance conforme du modèle et une forme d'universalité sur ces graphes doublement périodiques correspond à une question posée par Duminil-Copin et Smirnov dans [65]
   — Les cartes aléatoires équipées d'un modèle d'Ising critique, dont les physiciens conjecturent (voir e.g. [67]) qu'elles convergent vers un objet appelé la *Gravité Quantitque de Liouville*.

   Pour répondre à ces questions, Chelkak a introduit une procédure de plongement explicite (décrite dans la section 1.7), prouvant déjà la convergence des interfaces vers FK vers le processus SLE(16/3) sur les grilles doublement périodiques critiques. Au-delà du traitement de ce cas précis, les conséquences principales de la construction de Chelkak sont les suivantes :
   — Le formalisme des s-plongements unifie le traitement des graphes doublement périodiques critiques, isoradiales critiques et Z-invariantes massives. Cependant ce formalisme dépasse les cadres que l'on vient de

mentionner. Il est possible de construire un s-plongement propre pour tout les graphes finis, ce qui fait espérer qu'on puisse l'utiliser (dans très longtemps) pour prouver des résultats de convergence sur des grandes cartes aléatoires critiques et se rapprocher des prédictions des physiciens. On peut aussi envisager d'utiliser le formalisme sur des grilles dont la combinatoire est déterministe mais les poids sont choisis aléatoirement.

— Le formalisme des s-plongements fait un lien surprenant entre le modèle d'Ising et certaines surfaces dans l'espace de Minkowski $\mathbb{R}^{2,1}$, indiquant qu'il existe une description naturelle de la limite d'échelle du modèle d'Ising planaire utilisant la géométrie Lorentzienne.

Si l'on devait formuler ainsi quelques conjectures et perspectives, auxquelles on espère apporter une (très modeste) contribution à l'avenir, les plus importantes seraient les suivantes :

1. Prouver complètement l'invariance conforme du modèle d'Ising sur les graphes critiques doublement périodiques (c'est à dire traiter les corrélations de spins et le champ d'énergie).
2. Développer et illustrer le lien découvert par Chelkak entre le modèle d'Ising planaire et les fonctions massives holomorphes sur des surfaces plongées dans $\mathbb{R}^{2,1}$.
3. Construire une classe de quadrangulations aléatoires (équipées par exemple des poids critiques uniformes du réseau carré) et développer une théorie de convergence pour faire le lien avec la Gravité Quantique de Liouville. La première étape semble être d'essayer d'appliquer les résultats du chapitre 5 pour prouver une résultat du type Russo-Seymour-Welsh sur les grandes cartes aléatoires.
4. Prouver (en appliquant à nouveau les résultats du chapitre 5) un résultat du type Russo-Seymour-Welsh sur la grille $\mathbb{Z}^2$ équipée de poids aléatoires i.i.d. centrés autour de température critique du réseau carré homogène, et étendre à ce cadre là des résultats de convergence concernant les observables du modèle.

1.5 . Le formalisme de Kadanoff et Ceva

On présente dans cette section le formalisme de Kadanoff et Ceva introduit dans [93], qui explique de manière claire le lien entre le modèle d'Ising présenté plus haut et l'analyse complexe discrète. *Ce formalisme unifie la quasi-intégralité des approches utilisées jusqu'ici (et rappelées dans la section 1.8) sur les grilles isoradiales Z-invariantes équipés de poids critiques et massifs, ainsi que sur les graphes doublement périodiques.* Comme développé dans la section suivante, ce

formalisme permet de créer à partir du modèle de physique statistique des fonctions dont les relations locales s'interprètent (après complexification) comme une forme d'holomorphie discrète. On commence par ajouter quelques notations de graphes. On rappelle que $\Upsilon(G)$ correspond aux arêtes de $\Lambda(G)$ et que ses sommets sont appelés *coins* et sont notés typiquement par $c \in \Upsilon(G)$. Dans ce qui suit, on considère des *revêtements ramifiés à deux feuillets*, dont on précise la structure locale de branchement selon les contexte. La ramification à deux feuillets autour d'un point correspond à la ramification de la surface de Riemann définie par $z \mapsto \sqrt{z}$ autour de l'origine. Le lecteur est invité à consulter la figure 3.2.1 pour suivre les définitions qui suivent.

— On note $\Upsilon^{\times}(G)$ le revêtement ramifié à deux feuillets qui branche autour de *toutes* les faces de $\Upsilon(G)$, c'est à dire autour de chaque $v^{\bullet} \in G^{\bullet}$, $v^{\circ} \in G^{\circ}$ et $z \in \diamondsuit(G)$. Cette notion reste bien définie pour un graphe fini, le théorème d'Euler assurant que $\#(G^{\bullet})+\#(G^{\circ})+\#(\diamondsuit(G))$ est pair, ce qui assure que la ramification autour de la face extérieure est une notion bien définie.

— On se donne $\varpi = \{v_1^{\bullet}, \dots, v_m^{\bullet}, v_1^{\circ}, \dots, v_n^{\circ}\} \subset \Lambda(G)$ avec n et m deux entiers pairs. On note $\Upsilon_{\varpi}^{\times}(G)$ le revêtement ramifié à deux feuillets de $\Upsilon(G)$ branchant autour de toutes ses faces (c'est à dire à nouveau tous les sommets de $v^{\bullet} \in G^{\bullet}$, $v^{\circ} \in G^{\circ}$ et $z \in \diamondsuit(G)$) *hormis* les sommets de ϖ.

— On note $\Upsilon_{\varpi}(G)$ le revêtement ramifié à deux feuillets de $\Upsilon(G)$ branchant *uniquement* autour des points de ϖ.

On notera $c, c^{\#}$ les deux coins différents d'un revêtement provenant du relèvement d'un même coin $c \in \Upsilon(G)$.

On définit maintenant les *spineurs*, qui représentent une une classe de fonction importante dans le formalisme de Kadanoff et Ceva. Soit F une fonction définie sur un sous-ensemble de $\Upsilon_{\varpi}^{\times}(G)$ ou bien de $\Upsilon_{\varpi}(G)$ pour ϖ fixé. On dit que F est un *spineur* si pour toute paire de coins $c, c^{\#}$ correspondant au relèvement du même coin dans G, on a

$$F(c) = -F(c^{\#}).$$

Avec des mots, cela veux dire que les valeurs de F en deux relèvements différents d'un même coin ne diffèrent que d'un facteur multiplicatif -1. Cette propriété correspond à une caractéristique de la fonction $z \mapsto \sqrt{z}$ lorsqu'on la définit sur la surface de Riemann naturelle associée.

1.5.1 . Introduction du désordre

On invite dans cette section le lecteur à se référer à la figure 1.5.2 pour une illustration des objets utilisés. Pour m un entier pair et $v_1^{\bullet}, \dots, v_m^{\bullet} \in G^{\bullet}$, fixons comme précédement un sous graphe arbitraire $\gamma^{\bullet} = \gamma^{[v_1^{\bullet}, \dots, v_m^{\bullet}]} \subset G^{\bullet}$ dont tous les sommets sont de degré pair, excepté ceux de $\{v_1^{\bullet}, \dots, v_m^{\bullet}\}$ (représenté en rouge dans la figure 1.5.2). L'idée de Kadanoff et Ceva, introduite dans [93] commence

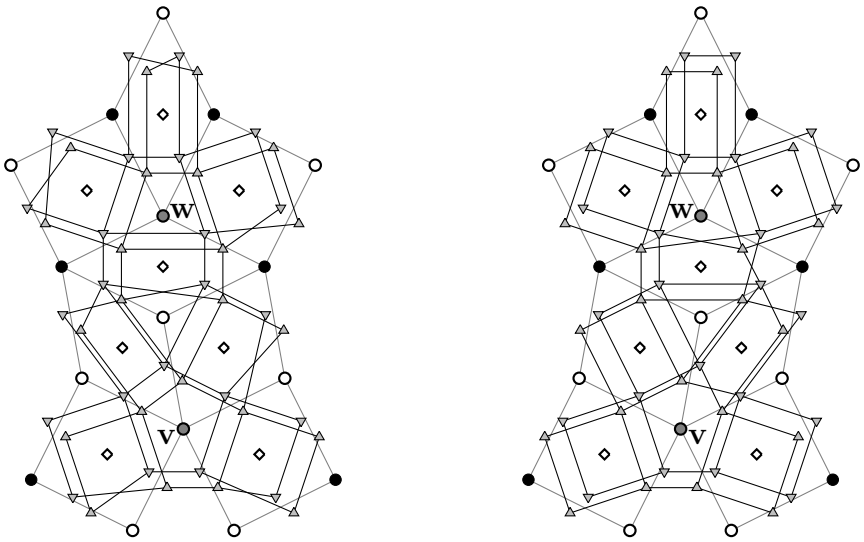

FIGURE 1.5.1 – Exemples de représentation graphique de différents revêtements ramifiés annoncés au-dessus. Les coins $c, c^{\#}$ correspondant au relevement du même coin de G sont représentés par deux triangles, la pointe de l'un étant orientée vers le haut et celle de l'autre vers le bas. Deux coins sont voisins dans le revêtement associé s'il sont reliés par un trait plein épais. (Gauche) Structure locale du revêtement ramifié $\Upsilon^{\times}_{[v,w]}$ du graphe médial de Υ ; les sommets $v \in \Gamma^{\bullet}$ et $w \in \Gamma^{\circ}$ sont coloriés en gris. (Droite) Structure locale correspondante du revêtement ramifié $\Upsilon_{[v,w]}$. Le revêtement de gauche branche *partout* hormis autour v et w alors que celui de droite ne branche qu'autour de v et w.

par modifier le modèle d'Ising, en remplaçant les constantes de couplages J_e° (qui sont jusqu'ici toujours positives) par $-J_e^\circ$ le long des arêtes de $\gamma^\bullet$. Ceci revient à rendre le modèle *anti-ferromagnétique* au long de $\gamma^\bullet$, en favorisant les configurations de spins opposés autour de $\gamma^\bullet$ (comme cela apparaitra pour le calcul des corrélations mixtes définies dans $(1.5.2)$). D'un point de vue des notations introduites précédemment, cela revient à remplacer $x^\circ(e)$ par $x^\circ(e)^{-1}$ le long de γ lorsque l'on calcule les corrélations mixtes définies ci-dessous. Une manière *formelle* de préciser cette anti-ferromagnétisation du modèle est de considérer la variable aléatoire *de désordre* (qui dépend à priori de $\gamma^\bullet$) définie par

$$\mu_{v_1^\bullet} \dots \mu_{v_m^\bullet} \;:=\; \exp\big[-2\beta \textstyle\sum_{e\in\gamma^{[v_1^\bullet,\dots,v_m^\bullet]}} J_e^\circ \sigma_{v_-^\circ(e)}\sigma_{v_+^\circ(e)}\big]\,.$$

En utilisant l'expansion à basse température de la section 1.2.2, on voit que ([37, Section 3.3])

$$\mathbb{E}_{G^\circ}\big[\mu_{v_1^\bullet}\dots\mu_{v_m^\bullet}\big] \;=\; x^\circ(\mathcal{E}^{[v_1^\bullet,\dots,v_m^\bullet]}(G))/x^\circ(\mathcal{E}(G)), \qquad (1.5.1)$$

Une remarque importante est que l'expression $(1.5.2)$ ne dépend *pas* du choix de $\gamma^\bullet$. En effet, pour $\gamma_1^\bullet$ et $\gamma_2^\bullet$ définis comme ci-dessus, il existe une bijection naturelle (préservant le poids des configurations) entre configurations de spins pour lesquelles on a inversé le poids des arêtes $x^\circ(e)$ le long de $\gamma_{1,2}^\bullet$. Il suffit alors de concaténer $\gamma_{1,2}^\bullet$ pour former une configuration de boucles, puis inverser la valeur des spins à l'intérieur des boucles de $\gamma_1^\bullet \oplus \gamma_2^\bullet$.

On peut alors généraliser les formules $(1.2.5)$ and $(1.5.1)$ aux *corrélations mixtes* (qui correspondent à la corrélation entre spins multiplié par une variable de désordre $\mu_{v_1^\bullet}\dots\mu_{v_m^\bullet}$ définie comme ci-dessus). C'est ici que la caractère anti-ferromagnétique apparait, puisque lorsque l'on calcule cette corrélation mixte entre spins et désordres, cela revient à calculer la corrélation entre spins en ayant inversé les constantes de couplage le long des lignes de désordre. Plus formellement, on pose (voir e.g. [37, eq (3.4)]) pour $v_1^\circ,\dots,v_n^\circ \in G^\circ$

$$\mathbb{E}_{G^\circ}\big[\mu_{v_1^\bullet}\dots\mu_{v_m^\bullet}\sigma_{v_1^\circ}\dots\sigma_{v_n^\circ}\big] \;=\; x^\circ_{[v_1^\circ,\dots,v_n^\circ]}(\mathcal{E}^{[v_1^\bullet,\dots,v_m^\bullet]}(G))/x^\circ(\mathcal{E}(G)), \qquad (1.5.2)$$

où l'on rappelle que $x^\circ(C) := \prod_{e\in C} x_e^\circ$, $\mathcal{E}^{[v_1^\bullet,\dots,v_m^\bullet]}$ représente l'ensemble des sous graphes de $E(G)$ qui ont degré pair partout excepté en les sommets $v_1^\bullet,\dots,v_m^\bullet$ et

$$x^\circ_{[\gamma]}(e) := \begin{cases} x_e^\circ & \text{si } e \neq \gamma \\ -x_e^\circ & \text{sinon.} \end{cases}$$

comme cela a été défini dans les sections 1.2.2 et 1.2.3. L'expression $(1.5.2)$ est à priori définie au signe près (i.e. elle dépend du choix joint des ensembles γ° and $\gamma^\bullet$) puisque dans la définition de $x^\circ_{[v_1^\circ,\dots,v_n^\circ]}(\mathcal{E}^{[v_1^\bullet,\dots,v_m^\bullet]}(G))$, la parité du nombre d'intersections entre γ° and $\gamma^\bullet$ rentre en compte. Il n'est pas possible de fixer de manière canonique l'ambiguïté de signe dans $(1.5.2)$ si on se limite au produit cartésien $(G^\bullet)^{\times m}\times(G^\circ)^{\times n}$.

On va maintenant considérer l'expression (1.5.2) comme une *fonction* des sommets $v_1^\bullet, \dots, v_m^\bullet, u_1^\circ, \dots u_n^\circ$. Il faut en particulier outrepasser l'ambiguïté de signe que l'on vient d'expliquer (ce qui passe par considérer la fonction comme étant définie sur un ensemble plus grand). Pour cela, on commence par fixer un plongement *arbitraire* $\mathcal{S}$ de G dans le plan, et considérer le revêtement ramifié à deux feuillets de $(G^\bullet)^{\times m} \times (G^\circ)^{\times n}$ dont la structure de branchement est celle de $[\prod_{p=1}^m \prod_{q=1}^n (\mathcal{S}(v_p^\bullet) - \mathcal{S}(v_q^\circ))]^{1/2}$. Dans ce cas là, les quantités de la forme (1.5.2) sont toujours vues comme fonction de $v_1^\bullet, \dots, v_m^\bullet, u_1^\circ, \dots u_n^\circ$, mais il est en plus possible de fixer l'ambiguïté de signe de manière consistante lorsque l'on modifie les positions respectives de $v_1^\bullet, \dots, v_m^\bullet, u_1^\circ, \dots u_n^\circ$. Cette discussion est très délicate (y compris pour les spécialistes) et est réalisé de manière remarquable et complète dans dans [39, Section 2.2]. En quelques mots, l'idée est de fixer un signe arbitraire pour *une* configuration $v_1^\bullet, \dots, v_m^\bullet, u_1^\circ, \dots u_n^\circ$ puis de le faire évoluer le choix de de signe de manière *canonique* lorsque l'on passe d'un revêtement dont la structure de branchement est celle de $[\prod_{p=1}^m \prod_{q=1}^n (\mathcal{S}(v_p^\bullet) - \mathcal{S}(v_q^\circ))]^{1/2}$ au revêtement $[\prod_{p=1}^m \prod_{q=1}^n (\mathcal{S}(v_p'^\bullet) - \mathcal{S}(v_q'^\circ))]^{1/2}$, lorsque les $v_1^\bullet, \dots, v_m^\bullet, u_1^\circ, \dots u_n^\circ$ et $v_1'^\bullet, \dots, v_m'^\bullet, u_1'^\circ, \dots u_n'^\circ$ ne diffèrent que d'un élément.

Un calcul similaire à celui de la dualité de Kramers-Wannier introduite dans la section 1.2.4 permet de vérifier que (e.g. [37, Proposition 3.3])

$$\mathbb{E}_{G^\circ}\left[\mu_{v_1^\bullet} \dots \mu_{v_m^\bullet} \sigma_{v_1^\circ} \dots \sigma_{v_n^\circ}\right] \;=\; \mathbb{E}_{G^\bullet}\left[\mu_{v_1^\circ} \dots \mu_{v_n^\circ} \sigma_{v_1^\bullet} \dots \sigma_{v_n^\bullet}\right] \tag{1.5.3}$$

ce qui signifie que dans la définition des *corrélations mixtes*, les roles joués par les graphes $G^\bullet$ et G° sont équivalents.

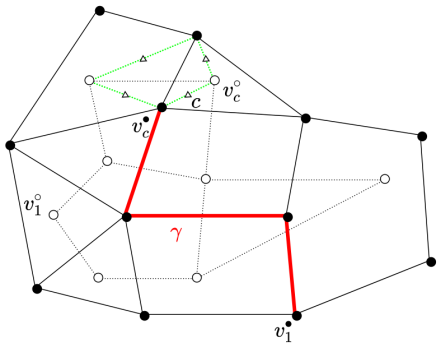

FIGURE 1.5.2 – Configuration correspondant à l'insertion du désordre le long de l'interface γ (déssinée en rouge), reliant $v_1^\bullet$ à $v_c^\bullet$. On peut calculer alors la corrélation mixte $\mathbb{E}_{G^\circ}[v_1^\circ v_c^\circ v_1^\bullet v_c^\bullet]$, où les sommets $v_c^\bullet$ et v_c° sont adjacents au même coin $c \in \Upsilon$. Cette quantité dépend (au signe près) du nombre d'intersection entre γ et de chemin (entre arêtes duales) reliant v_1° à v_c°.

1.5.2 . Construction des corrélateurs

On va a présent utiliser le formalisme du désordre introduit précédemment, mais pour construire une fonction définie sur l'ensemble des coins de G. On appelera ces fonctions des *corrélateurs de Kadanoff-Ceva*. Avant cela, on commence par rappeler une paramétrisation *abstraite* des poids d'Ising déjà mentionnée dans les paragraphes précédents. On rappelle qu'il existe une identification naturelle entre une arête e de G et une face $z(e)$ de $\Lambda(G)$. On définit le paramètre abstrait $\theta_{z(e)}$ par

$$\theta_{z(e)} \;:=\; 2\arctan x^\circ(e) \;\in\; (0, \tfrac{1}{2}\pi). \tag{1.5.4}$$

Ici $\theta_{z(e)}$ n'a pas spécialement d'interprétation géométrique.

En utilisant les formules de trigonométrie usuelles, on remarque directement que $\cos(\theta_{z(e)}) = (1 - x^\circ(e)^2)(1 + x^\circ(e)^2)^{-1}$ ainsi que $\sin(\theta_{z(e)}) = 2x^\circ(e)^2(1 + x^\circ(e)^2)^{-1}$. Pour m et n deux entiers pairs, on considère une expression de *correlation mixte* où l'un des spins et l'un des désordres sont choisis comme étant voisins dans $\Lambda(G)$. Pour un coin $c \in \Upsilon(G)$, soient $v^\bullet(c) \in G^\bullet$ et $v^\circ(c) \in G^\circ$ les deux sommets de $\Lambda(G)$ reliés via c. On définit *de manière purement formelle le fermion* au coin c par

$$\chi_c := \mu_{v^\bullet(c)}\sigma_{v^\circ(c)}. \tag{1.5.5}$$

Plus précisément, on définit *le corrélateur fermionique de Kadanoff-Ceva* (1.5.2) en posant (voir e.g. [37, Proposition 3.3]) pour un coin c de $\Upsilon^\times_\varpi(G)$

$$X_\varpi(c) := \mathbb{E}_{G^\circ}[\,\chi_c \mu_{v_1^\bullet} \dots \mu_{v_{m-1}^\bullet}\sigma_{v_1^\circ} \dots \sigma_{v_{n-1}^\circ}]. \tag{1.5.6}$$

Ainsi, lorsque les points de ϖ sont fixés, la quantité $X_\varpi(c)$ est bien définie au signe près, dont on peut à nouveau lever l'ambiguïté lorsqu'on la définit sur le revêtement $\Upsilon^\times_\varpi(G)$. Ainsi, on va considérer les corrélation mixtes comme une fonction de la variable c.

L'objectif final de notre utilisation des corrélateurs de Kadanoff-Ceva est d'étudier leur limite d'échelle, dans un sens que l'on précisera par la suite. Pour cela, ce sont des fonctions remarquables puisqu'elles vérifient une relation locale très simple, qui s'interprétera ensuite comme une forme d'holomorphie discrète. On détaille à présent cette relation locale, qui est purement abstraite et ne requiert pas de plongement particulier.

Les notations des lignes suivantes correspondent à la figure ci-dessous. On considère le quadrilatère $z = (v_0^\bullet v_1^\circ v_1^\bullet v_0^\circ)$ dont les sommets sont donnés dans l'ordre trigonométrique et pour lesquels on choisit trois relèvements de c_{pq}, $c_{p,1-q}$ et $c_{1-p,q}$ consécutifs dans $\Upsilon^\times_\varpi(G)$ (en notant $c_{pq} = (v_p^\bullet v_q^\circ)$). Dans ce cas là, le corrélateur fermionique de Kadanoff-Ceva satisfait une equation linéaire de propagation locale très simple autour de $z(e)$, dont les coefficients dépendent uniquement de la constante de couplage J_e° du modèle via la paramétrisation (1.5.4) . On a alors (e.g. [37, eq (3.11)])

$$X_\varpi(c_{pq}) = X_\varpi(c_{p,1-q})\cos\theta_{z(e)} + X_\varpi(c_{1-p,q})\sin\theta_{z(e)}. \tag{1.5.7}$$

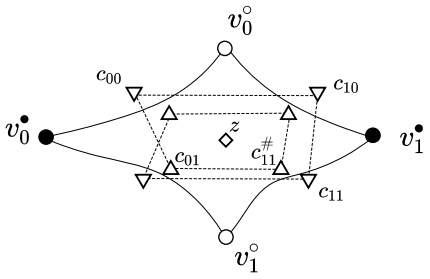

FIGURE 1.5.3 – Notations utilisées pour la relation de propagation à trois termes (1.5.7). Les coins sont représentés par des triangles, avec deux relèvements du même coin dans le revêtement représentés par des triangles orientés à l'opposé l'un de l'autre. Les coins voisins dans le revêtement sont reliés par les traits pointillés. Le graphe des coins branche localement autour de $z \in \diamondsuit(G)$.

Cette relation locale a été introduite sous cette forme par Mercat (voir e.g. [129, Section 4.3] mais celle-ci a été mentionée par Dosentko [56] et apparaît aussi dans les travaux de Perk [142, 141]) et se démontre de manière formelle (e.g. [37, Remarque 3.12]) en remarquant (via (1.2.9)) que $\mu_{v_0^\bullet}\mu_{v_1^\bullet}\sin(\theta_z) = 1-\cos(\theta_z)\sigma_{v_0^\circ}\sigma_{v_1^\circ}$, ce qui revient à considérer de manière combinatoire les configurations contenant ou non l'arête $e = (v_0^\bullet v_1^\bullet)$ dans le calcul de la corrélation (1.5.2). En particulier, toute solution de (1.5.7) est automatiquement un spineur (c'est une conséquence algébrique très simple de la relation (1.5.7)). C'est cette relation (1.5.7) qui explique la possiblité de construire des observables holomorphes discrètes. Il est crucial de noter que cette relation est *abstraite* et ne nécessite pas de fixer d'un plongement de G dans le plan.

On fixe à présent un plongement $\mathcal{S} : \Lambda(G) \to \mathbb{C}$ de $\Lambda(G)$ dans le plan et on définit

$$\eta_c := \varsigma \cdot \exp\big[-\tfrac{i}{2}\arg(\mathcal{S}(v^\bullet(c)) - \mathcal{S}(v^\circ(c)))\big], \qquad \varsigma := e^{i\frac{\pi}{4}}, \tag{1.5.8}$$

où le pré-facteur ς est choisi pour être consistant avec les notations de [48, 33]. L'ambiguïté de signe dans la définition de η_c peut être a nouveau évitée en travaillant sur $\Upsilon^\times(G)$. Dans le cas ou $\mathcal{S}$ est un plongement isoradial, $z = (v_0^\bullet v_0^\circ v_1^\bullet v_1^\circ)$ est un losange et on peut voir directement que η_c est une solution de (1.5.7). Plus généralement, les produits de la forme

$$\eta_c X_\varpi(c) : \Upsilon_\varpi(G) \to \mathbb{C} \tag{1.5.9}$$

sont des spineurs sur le revêtement $\Upsilon_\varpi(G)$, branchant uniquement autour des sommets de l'ensemble $\varpi = \{v_1^\bullet, \dots v_{m-1}^\bullet, v_1^\circ, \dots v_{n-1}^\circ$ utilisés pour la construction des corrélateurs réalisée via (1.5.6).

Un ingrédient essentiel pour l'analyse des spineurs est l'introduction de la fonction *abstraite* H_{X_ϖ} associée au corrélateur X_ϖ. Cette fonction est une forme quadratique du spineur X qui s'avère fort utile pour étudier la limite d'échelle des observables complexifiées mais aussi de construire les s-plongements 1.7. Il est à noter que la présence des branchements n'influe pas sur la définition de H_{X_ϖ} et on ne mentionnera pas l'indice ϖ dans la définition qui suit (ici seule la relation locale (1.5.7) importe pour la consistance de la définition). La définition suivante, a été introduite dans une forme équivalente par Smirnov dans [162], mais son extension à $\diamondsuit(G)$ a été faite pour la premiere fois dans [33]

Definition 1.5.1. Soit X un spineur sur $\Upsilon^\times(G)$ satisfaisant l'équation(1.5.7). On peut alors définir à une constante additive près la fonction H_X sur $\Lambda(G) \cup \diamondsuit(G)$ via ses incréments pour $p, q = 0, 1$

$$\begin{array}{rcl} H_X(v_p^\bullet(z)) - H_X(z) & := & X(c_{p0}(z))X(c_{p1}(z))\cos\theta_z, \\ H_X(v_q^\circ(z)) - H_X(z) & := & -X(c_{0q}(z))X(c_{1q}(z))\sin\theta_z, \\ H_X(v_p^\bullet(z)) - H_X(v_q^\circ(z)) & := & (X(c_{pq}(z)))^2, \end{array} \tag{1.5.10}$$

où les coins sont choisis comme étant consécutifs sur $\Upsilon^\times(G)$. Cette définition est purement combinatoire, et sa consistance provient directement de l'équation de propagation (1.5.7).

1.5.3 . L'observable de Smirnov sur les graphes isoradiaux

On explique à présent l'étape décisive faisant le lien entre le modèle d'Ising et sa limite d'échelle dans le continu. Cette percée majeure est due à Smirnov [162, 160] dans ses travaux fondateurs sur le modèle critique sur le réseau carré et a été développée par la suite sur les grilles isoradiales. En des mots très simples, l'idée de Smirnov consiste à construire des fonctions discrètes holomorphes définies uniquement par leur conditions de bord et singularités, et qui composent bien avec les interfaces et corrélations du modèle d'Ising. Il s'agit alors de prouver l'existence et l'invariance conforme d'une limite d'échelle pour ces observables discrètes afin de prouver l'existence et l'invariance conforme d'une limite d'échelle du modèle d'Ising. On présente ici la première observable introduite par Smirnov, c'est à dire l'observable FK-Ising avec condition de bord *Dobrushin*, qui a mené ensuite à une activité très importante autour de l'invariance conforme comme le montrent les nombreux résultats rappelés dans la section 1.8.

On utilise dans ce qui suit les notations de la figure 1.5.4 (qui utilise des notations semblables à [33, Figure 2]). On fixe un domaine fini Ω d'une grille isoradiale avec des conditions de bord dites Dobrushin, c'est à dire que son bord $\partial\Omega$ (toujours avec les notations de la figure 1.5.4) se divise en

— Un arc $(ab)^\bullet$ de sommets du graphe primal (en pointillés rouges).

— Un arc $(ba)^\circ$ de sommets du graphe dual (en pointillés bleus).

— Les deux arêtes de $\Lambda(G)$ qui passent par les coins a et b (pointillés violets).

Tous les sommets de $(ba)^\circ$ sont *branchés* ensembles (représenté par l'arc bleu) et tous les sommets de $(ab)^\bullet$ sont *branchés* ensembles (représenté par l'arc rouge). Le bord du graphe $\Lambda(G)$ est représenté en pointillés verts. Il s'agit donc, si on considère le point de vue du modèle sur G° comme des conditions branchées sur $(ba)^\circ$ et*libres* sur $(ab)^\bullet$. On considère alors le modèle FK-Ising sur Ω avec les conditions de bord ci-dessus, et définit grâce à cela

— $\gamma_{a,b}$ l'interface la plus à gauche reliant a à b et séparant le cluster primal attaché au spin de bord $(ba)^\circ$ du cluster dual attaché au désordre de bord $(ab)^\bullet$. L'interface séparant des éléments de $G^\bullet$ et de G°, elle s'interprète directement comme une suite de coins voisins dans Υ qui débute en a et termine en b. Cette interface est representée en orange.

— Pour un coin c appartenant à $\gamma_{a,b}$, on définit $\mathsf{wind}(\gamma_{a,b}, a \to c)$ l'incrément de l'argument (compté algébriquement) le long du chemin $\gamma_{a,b}$ entre a et c. Si c n'appartient pas à $\gamma_{a,b}$, on pose $\mathsf{wind}(\gamma_{a,b}, a \to c) := 0$.

C'est avec ces objets que Smirnov définit pour $c \in \Upsilon(G)$ la fonction [160, eq (19)]

$$F(c) := \eta_a \mathbb{E}_\Omega^{\mathsf{FK}}\big[\mathbb{1}[c \in \gamma_{a,b}] \exp\big(-\frac{i}{2}\mathsf{wind}(\gamma_{a,b}, a \to c)\big)\big], \tag{1.5.11}$$

où la mesure de probabilité $\mathbb{E}_\Omega^{\mathsf{FK}}$ est rappelée dans la section 1.2.5. Cette formule semble à priori étrange, ésotérique et difficile à exploiter. En réalité, *cette fonction qui a été introduite de manière purement combinatoire par Smirnov sans utiliser de lien avec formalisme de Kadanoff et Ceva* s'avère être une complexification du formalisme de Kadanoff et Ceva i.e. la fonction F de $(1.5.4)$ coïncide exactement avec $\eta_c \mathbb{E}_\Omega^{\mathsf{w/f}}[\chi_c \mu_{(ab)^\bullet} \sigma_{(ba)^\circ}]$ (voir e.g. [35, Remarque 3.2]).

1.5.4 . S-holomorphie des observables et étude de leur limite d'échelle

La construction des observables fermioniques présentées ci-dessus ne permet pas pour l'instant de faire quelconque passage à la limite d'échelle et construire de lien avec l'analyse complexe. En effet, ces observables sont a priori pour l'instant des fonctions réelles ou bien avec une phase complexe prescrite par le réseau (sur la grille carrée, il n'y a que 4 directions possibles pour η_c). Pour les étudier, Smirnov prend une combinaison linéaire [160, Section 2] de la fonction sur les coins d'un même losange de $\diamondsuit(G)$ pour en faire une fonction holomorphe discrète sur $\diamondsuit(G)$. Il lui reste alors à prouver que ces observables holomorphes discrètes convergent bien pour en extraire de l'information reliant discret et continu. La définition cruciale est celle de la s-holomorphie que l'on présente maintenant, introduite dans [160, Définition 3.1] et dont le nom a été fixé dans [48, Définition 3.1]. On note $\mathsf{Pr}[\cdot, \alpha\mathbb{R}]$ l'opérateur de projection orthogonale usuel, qui a un nombre complexe $\tilde{z} \in \mathbb{C}$ associe $\mathsf{Pr}[z, \alpha\mathbb{R}]$ son projeté orthogonal sur la droite $\alpha\mathbb{R} \subset \mathbb{C}$.

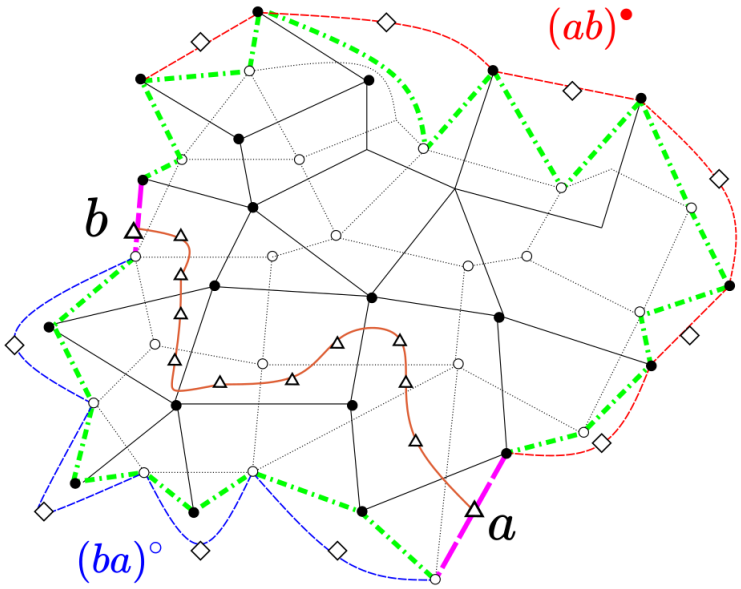

FIGURE 1.5.4 – Exemple d'un domaine avec *des conditions de bord Dobrushin*. Toutes les faces de l'arc $(ba)^\circ$ constituent *un unique spin* alors que tous les sommets de l'arc $(ab)^\bullet$ constituent *un unique désordre*. Les quadrilatères de bord sont notés par des losanges. Les coins a et b font la jonction entre les deux arcs de bord. L'interface reliant a à b en séparant les clusters primaux et duaux pour le modèle FK est matérialisée, en orange, par la suite des coins qu'elle traverse.

Definition 1.5.2. On dit qu'une fonction F définie sur un sous-ensemble de $\diamondsuit(G)$ est *s-holomorphe* si pour chaque paire $z, z' \in \diamondsuit(G)$ de faces adjacentes de $\Lambda(G)$, dont l'arête commune est $(v^\circ(c)v^\bullet(c))$ (avec $c \in \Upsilon(G)$), on a

$$\Pr[F(z)\,;\eta_c\mathbb{R}] \;=\; \Pr[F(z')\,;\eta_c\mathbb{R}] \tag{1.5.12}$$

Dans le cadre critique isoradial sur une grille de pas δ, la notion de s-holomorphie est complètement équivalent à l'existence au fait que la relation de propagation (1.5.7) soit vraie. Plus précisément, un spineur $X^\delta_\varpi : \Upsilon^\times_\varpi(G) \to \mathbb{R}$ satisfait l'équation de propagation (1.5.7) autour d'un quadrilatère $z \in \diamondsuit(G)$ si et seulement si il existe un nombre complexe $F^\delta_\varpi(z)$ tel que (e.g. [37, Section 3.6])

$$X^\delta_\varpi(c) = \overline{\eta}_c \delta^{\frac{1}{2}} \Pr[F^\delta_\varpi(z); \eta_c\mathbb{R}], \tag{1.5.13}$$

pour tous les coins c du losange z. On peut donc construire à partir de chaque spineur X^δ_ϖ une fonction s-holomorphe F^δ_ϖ sur le revêtement de $\diamondsuit$ qui branche autour des points de $\varpi = \{v^\bullet_1, \dots, v^\bullet_{m-1-}, v^\circ_1, \dots v^\circ_{n-1}\}$, et inversement on peut reconstruire chaque spineur X^δ_ϖ à partid=r d'une fonction s-holomorphe F^δ_ϖ. La fonction F_ϖ est discrète holomorphe au sens où l'intégrale discrète vérifie $\oint F^\delta_\varpi(z)dz = 0$ [48, Lemme 3.3], ce qui assure en particulier (modulo la pré-compacité des fonctions F^δ sur des grilles des pas $\delta \to 0$) que la limite des F^δ est bien une fonction holomorphe.

1.5.5 . Le problème de Riemann-Hilbert et détermination de la limite d'échelle

On vient de voir que les observables de Smirnov correspondent sur les graphes isoradiaux à des fonctions discrètes holomorphes construites à partir du modèle d'Ising. Pour prouver l'existence d'une limite d'échelle, Smirnov montre que pour une suite de grilles isoradiales Γ^δ de paramètre $\delta \to 0$, la suite des observables $(F^\delta)_{\delta>0}$ est pré-compacte [160, Lemma 5.3] (ainsi on peut en extraire des sous-suites convergentes) et caractérise la limite f [160, Lemma 4.11]. Pour cela, l'ingrédient crucial est l'utilisation de la partie imaginaire de la primitive du carré d'une fonction s-holomorphe. Cette primitive permet de prouver non-seulement la pré-compacité des $(F^\delta)_{\delta>0}$ mais aussi caractériser la limite d'échelle. On commence par définir cette fonction en des termes plus précis, suivant la définition originale donnée dans [162, eq (20)] et [160, Lemme 3.6].

Definition 1.5.3. Soit F^δ une fonction s-holomorphe sur une grille isoradiale et $z = (v^\bullet_0 v^\circ_0 v^\bullet_1 v^\circ_1) \in \diamondsuit(G)$. On peut alors définir (à une constante additive près) la fonction $H_{F^\delta} : \Lambda(G) \mapsto \mathbb{R}$ *simultanément* sur $G^\bullet$ et sur G° et dont les incréments sont donnés par

$$H_{F^\delta}(v^\circ_1) - H_{F^\delta}(v^\circ_0) := (v^\circ_1 - v^\circ_0)F^\delta(z)^2 \tag{1.5.14}$$

$$H_{F^\delta}(v^\bullet_1) - H_{F^\delta}(v^\bullet_0) := (v^\bullet_1 - v^\bullet_0)F^\delta(z)^2 \tag{1.5.15}$$

Alors la fonction H_{F^δ} définie sur $\Lambda(G)$ par. De plus si X^δ et F^δ sont reliées par la relation $X(c) = \delta^{\frac{1}{2}}\overline{\eta_c}\mathrm{Proj}[F(z); \eta_c\mathbb{R}]$, alors H_{F^δ} et H_{X^δ} coïncident à une constante additive près (voir par exemple [48, Proposition 3.6]).

Pour l'observable FK-Dobrushin (mais de manière plus générale lorsqu'un des spins de ϖ est attaché au bord du domaine), H_{X^δ} est constante sur l'arc $(ba)^\circ$ ainsi que sur l'arc $(ab)^\bullet$. Traduit pour l'observable F^δ, cela implique que pour $z \in \partial\Omega_\delta$ un losange de bord, on a $(F^\delta)^2(z) \in \tau\mathbb{R}$ où τ est la normale dirigée vers l'extérieur du domaine discret [48, eq (3.16)]. Cette condition de bord est relativement instable vis à vis de la géométrie locale fine d'une approximation d'un domaine, au contraire de la fonction $H^\delta = H_{F^\delta} = H_{X^\delta}$ (dans le cadre de l'observable Dobrushin mais aussi dans un cadre plus général après adaptation au contexte). La fonction H^δ permet de

— Prouver la pré-compacité des fonctions F^δ [48, Section 3.5]. Si les oscillations de H^δ sont bornées, alors la famille des F^δ est pré-compacte. En particulier on peut supposer en passant à une sous-suite que $F^\delta \to f$ et $H^\delta \to h = \frac{1}{2}\int \mathrm{Im}[f^2 dz]$ uniformément sur les compacts de Ω. De plus comme dans le discret les intégrales de contour sont nulles, le théorème de Morera assurant que f est holomorphe (et ainsi que h est harmonique).

— Prouver que les conditions de Dirichlet de H^δ passent à la limite continue [48, Section 5] i.e. h hérite des conditions de bord discrète de H^δ. Dans le cadre de l'observable FK Dobrushin, au coins de ramification on a $|X^\delta| = 1$, alors on peut choisir la constante additive telle que H^δ ait des conditions de bord 0 sur l'arc $(ba)^\circ$ et 1 sur l'arc $(ab)^\bullet$ [160, Lemme 4.11]. La preuve de la survie des condition de bord n'est pas aisée et se base sur le fait que H^δ (pour le Laplacien naturel défini e.g. [47, Section 1.2]) est une fonction sous-harmonique sur $G^\bullet$ et sur-harmonique sur G°. Autrement dit, H^δ est déjà *presque* une fonction harmonique dans le discret et cela est suffisant pour prouver que les conditions de bord de h correspondent à celles de H^δ. A la limite on a donc $h = \mathrm{hm}_\Omega(\cdot, (ab)^\bullet)$, la mesure harmonique de l'arc $(ab)^\bullet$ sur dans le domaine Ω, ce qui prouve l'unicité des limites de sous-suites et donc la convergence de f.

L'invariance conforme des mesures harmoniques prouve l'invariance conforme de $f = \sqrt{i\partial_z h}$ d'un domaine à l'autre. Pour prouver l'invariance conforme d'autres observables fermioniques (les résultats sont rappelées dans la section 1.8), les mêmes méthodes s'appliquent en prouvant l'invariance conforme de la limite d'échelle d'observables via l'invariance conforme de la solution au problème de Riemann-Hilbert associé, qui se résume en général à des conditions de bord, de l'harmonicité et l'identification de singularités. Il est à noter que la comparaison entre H^δ et les fonctions harmoniques discrètes sur les grilles isoradiales est cruciale pour prouver toutes ces convergences, et n'admet encore aujourd'hui pas d'explication conceptuelle allant au-delà de la vérification d'une positivité d'une certaine forme quadratique.

Ces dernières années, une approche remarquable a été développée par Park [138, 137], qui a adapté la notion de fonctions s-holomorphes au modèle *massif* Z-invariant (avec un nome $q = \frac{1}{2}m\delta$ sur la grille de pas δ, c'est à dire dans le cadre *presque critique*), en utilisant la même complexification que Smirnov mais avec des projections sur des directions modifiées correspondant à un *losange virtuel* critique [137, Proposition 4]. Park prouve dans ce cadre-là les limites f de sous-suites de fonctions s-holomorphes ne sont plus holomorphes mais deviennent des solutions de l'équation de Dirac $\overline{\partial} f + im\overline{f} = 0$ [138, Section 1.2]. Le passage à la limite pour la fonction H^δ s'avère aussi être plus difficile. Surtout l'étude de la limite d'échelle dans le continu (en particulier lorsque les bords des domaines ne sont pas lisses) est beaucoup plus élaborée et fait appel à un principe de similarité de Bers [138, Théorème 3.2], qui réécrit les solutions de $\overline{\partial} f + im\overline{f} = 0$ comme ressemblant à des fonctions holomorphes, et permet d'étudier de manière précise leur comportement.

Malgré divers efforts et un travail en cours de Chelkak, Park et Wan [46], il n'est pas suffisant de prouver la convergence de l'observable FK pour déterminer la limite d'échelle des interfaces FK séparant les clusters primaux et duaux pour le modèle massif sur $\mathbb{Z}^2$ vers une famille de courbes qui serait une *modification massive du SLE*. Le problème persistant semble être l'identification de la loi limite de l'interface aléatoire associée au modèle massif.

1.6 . Du classique au quantique

Le modèle d'Ising quantique uni-dimensionnel est une chaine de spins définie sur $\mathbb{Z}$ introduite par Pfeuty dans [145]. Pour le construire, on commence par se donner deux paramètres positifs θ et τ qui représentent respectivement l'intensité de l'interaction entre voisins et l'intensité de l'interaction avec le champ transverse. Comme d'usage en mécanique quantique, on note $\sigma^{(1)}$ and $\sigma^{(3)}$ les matrices de spin $\frac{1}{2}$ de Pauli données par

$$\sigma^{(1)} := \begin{pmatrix} 0 & 1 \\ 1 & 0 \end{pmatrix}, \quad \sigma^{(3)} := \begin{pmatrix} 1 & 0 \\ 0 & -1 \end{pmatrix}.$$

Ces matrices agissent sur un espace d'état des spins $\mathbb{C}^2 \cong \mathrm{Vect}(|+\rangle, |-\rangle)$, où l'on a fait l'identification entre $|+\rangle$ avec $(1,0)$ et $|-\rangle$ avec $(0,1)$. On peut alors définir l'opérateur $\sigma_x^{(1)}$ (par produit tensoriel) qui correspond à la matrice de Pauli $\sigma^{(1)}$ sur la cordonnée x de $\bigotimes_{\mathbb{Z}} \mathbb{C}^2$ et qui vaut l'identité partout ailleurs (et on fait de même pour $\sigma_x^{(3)}$). Le Hamiltonien du système quantique est alors l'opérateur

$$\mathbf{H} = -\theta \sum_{x \sim y} \sigma_x^{(3)} \sigma_y^{(3)} - \tau \sum_{x \in V} \sigma_x^{(1)},$$

agissant sur l'espace de Hilbert $\bigotimes_{\mathbb{Z}} \mathbb{C}^2$.

Ce modèle est lui aussi exactement soluble [145], et l'opérateur $e^{-\beta H}$, qui peut être vu comme un quantification de la mesure de Gibbs du modèle classique [89, eq

(2.11)]. Comme remarqué par Aizenmann, Klein et Newman [2], ce modèle quantique peut s'interpréter comme une évolution spatio-temporelle d'une configuration de spins sur $\mathbb{Z}$ via un méthode d'intégrale de chemin, où la variable β représente le temps. Il existe plusieurs expansions formelles de l'opérateur $e^{-\beta H}$ basées sur l'identité [89, eq (2.12)], qui mènent aux diverses représentations (spatio-temporelle, FK, courants aléatoires) et donnent une interprétation des résultats du modèle quantique via leur analogue classique en dimension 2 ([81, 20, 22, 109]). Ces différentes représentations ont permis en particulier de prouver l'existence d'une transition de phase continue et abrupte (voir par exemple deux approches différentes données dans [20, 62]) du modèle au point critique $\frac{\theta}{\tau} = 2$.

1.6.1 . Combinatoire du modèle

On présente maintenant la combinatoire et la définition du modèle quantique via sa représentation spatio-temporelle en dimension 2 sur le réseau demi-discret, utilisée en ces termes par Li [109]. *Contrairement aux autres chapitres de ce manuscrit et pour préserver le sens physique, les spins sont assignés ici au graphe primal et les opérateurs de désordres (défini comme dans* $(1.5.1)$*) sont assignés au graphe dual.* Les définitions utilisées correspondent à celles données par Li dans [109, Section 3.1]. On se donne un domaine simplement connexe $\Omega \subseteq \mathbb{C}$ et $\delta > 0$ et définit par analogie avec le modèle classique :

— $\Omega_\delta^\bullet = \Omega \cap \delta(2\mathbb{Z} \times \mathbb{R})$ le domaine primal, où sont assignés les spins.

— $\Omega_\delta^\circ = \Omega \cap \delta(2\mathbb{Z}+1) \times \mathbb{R})$ le domaine dual, où sont assignés les désordres.

— On définit par analogie le graphe $\Lambda(\Omega_\delta) := \Omega_\delta^\bullet \cup \Omega_\delta^\circ$ que l'on appelle le graphe médial. Les voisins d'un sommet $(x,t) \in \delta(2\mathbb{Z} \times \mathbb{R}) \in \Omega_\delta^\bullet$ dans $\Lambda(\Omega_\delta)$ sont les faces $(x \pm \delta, t) \in \delta(2\mathbb{Z}+1 \times \mathbb{R}) \in \Omega_\delta^\circ$.

— Les arêtes du graphe bipartite $\Lambda(\Omega_\delta)$ sont comme pour le modèle classique en bijection avec $\Upsilon(\Omega_\delta)$, l'ensemble des demi-arêtes, dont les sommets sont appelés les coins.

Les sommets du graphe primal sont typiquement notés par u alors que les sommets du graphe dual sont typiquement notés par v et les coins par c. On dit que u et v sont voisins dans $\Lambda(\Omega_\delta)$ s'ils ont la même coordonnée verticale et que leur coordonnées horizontales respectives diffèrent de $\pm\delta$. Lorsque $\Omega_\delta^\bullet$ et Ω_δ° approximent un domaine simplement connexe Ω borné du plan, la définition du modèle primal avec condition de bord $+$ est faite via deux aléas successifs, dont le premier est un processus de Poisson ponctuel. En suivant le formalisme introduit par Aizenman Klein et Newman dans [2], on commence par se donner deux paramètres positifs τ, θ et on définit $\eta_\tau^\bullet$ un processus de Poisson ponctuel de paramètre τ sur les lignes de $\Omega_\delta^\bullet$. L'ensemble dénombrable des points de $\eta_\tau^\bullet$ est noté D, dont les éléments sont appelés *points de décès*. Une fonction $\sigma : \Omega_\delta^\bullet \to \{+1, -1\}$ est dite être une *configuration de spins compatible* avec D si elle est constante sur chaque composante connexe de $\Omega_\delta^\bullet \backslash D$. On note alors $\bigcup \Sigma(D)$ l'ensemble des configurations

σ compatibles avec D, et définit la mesure ces configurations pour une fonction mesurable $F : \bigcup \Sigma(D) \to \mathbb{R}$ par la formule

$$\mathbb{E}^{\mathsf{spin}}_{\tau,\theta}[F(\sigma)] := \frac{\eta^\bullet_\tau \left[\sum_{\sigma\in\Sigma(D)} F(\sigma) \exp\left(-\frac{\theta}{2}\mathcal{H}(\sigma)\right)\right]}{\eta^\bullet_\tau \left[\sum_{\sigma\in\Sigma(D)} \exp\left(-\frac{\theta}{2}\mathcal{H}(\sigma)\right)\right]}, \tag{1.6.1}$$

où $\theta > 0$, $\mathcal{H}$ est le Hamiltonien $\mathcal{H}(\sigma) := -\mathsf{Leb}^\circ(\varepsilon_v)$, avec Leb° la mesure de Lebesgue sur le graphe dual (c'est à dire la somme des intégrales de Lebesgue sur *toutes* sur les lignes duales) et $\varepsilon_v = \sigma_{v^+}\sigma_{v^-} \in \pm 1$ la *densité d'énergie au point* $v \in$, c'est à dire le produit des spins voisins de v dans $\Lambda(\Omega_\delta)$. La fonction de partition devient alors

$$Z(\tau,\theta) := \eta^\bullet_\tau \left[\sum_{\sigma\in\Sigma(D)} \exp\left(-\frac{\theta}{2}\mathcal{H}(\sigma)\right)\right] = \eta^\bullet_\tau \left[\sum_{\sigma\in\Sigma(D)} \exp\left(\frac{\theta}{2}\cdot \mathsf{Leb}^\circ(\varepsilon_v)\right)\right]. \tag{1.6.2}$$

Le modèle est donc une généralisation du modèle classique avec une interaction entre voisins horizontaux et admet lui aussi une transition de phase lorsque le ratio $\rho = \frac{\theta}{\tau} = 2$ [62]. Lorsque ce ratio est supérieur à 2, la magnétisation en volume infini est strictement positive [62, Théorème 1.5], on se trouve dans le *régime sous-critique*. Lorsque ce ratio est inférieur que 2, la corrélation entre spins décroit exponentiellement vite avec leur distance [62, Théorème 1.5], c'est le *régime sur-critique*. Enfin lorsque ce ratio vaut 2, cette corrélation décroit polynômialement avec leur distance [62, Théorème 1.5], c'est le *régime critique*.

Une des manières de prouver cette transition de phase est d'utiliser le modèle classique sur les graphes isoradiaux rappelé dans la section 1.3.1, en remarquant que la loi du modèle spatio-temporel présenté ci-dessus sur le réseau semi-discret est la limite faible des lois du modèle classique sur une suite de grilles isoradiales de plus en plus aplaties [62, Proposition 5.1]. Considérons comme dans la figure 1.6.1 le réseau $\mathcal{G}^\varepsilon$ constitué d'arêtes horizontales 'longues' de longueur $\delta\cos\frac{\varepsilon}{2}$ et d'arêtes verticales 'courtes' de longueur $\delta\sin\frac{\varepsilon}{2}$. Lorsque $\varepsilon \to 0$ tend vers 0, le réseau isoradial "converge" vers le réseau semi-discret. En choisissant des constantes de couplage horizontale $J^\bullet_h$ et verticale $J^\bullet_v$ vérifiant $\tanh(J^\bullet_h) \sim \frac{\theta}{2}\varepsilon$ et $1-\tanh(J^\bullet_v) \sim 2\tau\varepsilon$ (ici $\beta^\bullet = 1$), la loi de la collection des contours donnée par 1.2.2 sur $\mathcal{G}^\varepsilon$ converge faiblement vers $\eta^\bullet_\tau$ [62, Proposition 5.1].

Il est donc naturel de chercher à obtenir les résultats de convergence des corrélations du régime critiques comme des analogues du cas classique, établis pour les grilles isoradiales avec des angles bornés avant le passage $\varepsilon \to 0$. Cependant il n'est pas aisé d'échanger les limites $\varepsilon \to 0$ et $\delta \to 0$, c'est pourquoi notre travail avec Li introduit dans le chapitre 4 le formalisme de Kadanoff et Ceva dans le domaine semi-discret afin de construire des preuves dans ce cadre là.

1.7 . Les s-plongements

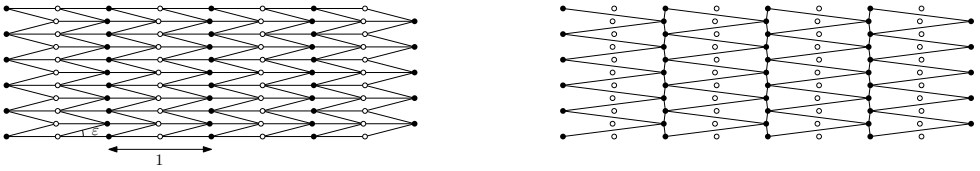

FIGURE 1.6.1 – Le domaine aplatit $\mathcal{G}^\varepsilon$ qui 'converge' vers le réseau semi-discret à la limite. (Gauche) Représentation isoradiale de $\Lambda(\mathcal{G}^\varepsilon)$ lorsque $\delta = \frac{1}{2}$. (Droite) Domaine primal avec les sommets duaux.

Les paragraphes précédents présentent les outils servant de base pour prouver l'existence et décrire la limite d'échelle des modèles d'Ising critiques et presque critiques sur les grilles isoradiales. Le cadre isoradial ne couvrant pas l'intégralité des *graphes pondérés* et en particulier ne permet déjà pas de traiter tous les modèles critiques sur les graphes doublement périodiques, pour lesquels la condition de criticalité a été prouvée par Cimasoni et Duminil-Copin [52, Théorème 1.1]. Ces dernières années, Chelkak a proposé et implémenté dans [33, 34] une procédure partant d'un graphe *abstrait* et fournissant un dessin *explicite* de son plongement dans le plan. Ce plongement est adapté aux méthodes d'analyse complexe discrète et permet déjà de prouver dans certains cas des résultats de convergence.

On suit dans cette section les notations de [33] pour rester consistant avec l'article fondateur de cette approche du modèle d'Ising. La première observation de Chelkak provient de la fonction H introduite par Smirnov dans le cadre isoradial et définie par (1.5.14). On rappelle en premier lieu que la fonction $c \mapsto \delta^{\frac{1}{2}}\eta_c$ est solution de l'équation de propagation (1.5.7). Il est remarquable de noter que si Γ^δ est le plongement isoradial de pas δ, alors

$$\Gamma^\delta(v^\bullet(c)) - \Gamma^\delta((v^\circ(c)) = H^\delta(v^\bullet(c)) - H^\delta((v^\circ(c)) = -i[\delta^{\frac{1}{2}}\overline{\eta_c}]^2 \qquad (1.7.1)$$

Cela a poussé Chelkak à proposer la définition suivante dans [34, Section 6] et [33, Definition 2.1]. **Il est crucial dans toute la suite de remarque que l'idée de Chelkak s'applique à n'importe quel graphe abstrait pondéré (qu'il soit fini ou infini) et décrit une procédure pour lui associer un dessin dans le plan.**

Definition 1.7.1. Soit (G, x) un graphe planaire pondéré et $\mathcal{X} : \Upsilon^\times(G) \to \mathbb{C}$ une solution à l'équation de propagation (1.5.7). On dit que $\mathcal{S} = \mathcal{S}_\mathcal{X} : \Lambda(G) \to \mathbb{C}$ est un s-plongement de (G, x) associé à $\mathcal{X}$ si pour tout $c \in \Upsilon^\times(G)$ on a

$$\mathcal{S}(v^\bullet(c)) - \mathcal{S}(v^\circ(c)) = (\mathcal{X}(c))^2. \qquad (1.7.2)$$

On note $\mathcal{S}^\diamond(z) \subset \mathbb{C}$ le quadrilatère formé des sommets $\mathcal{S}(v_0^\bullet(z))$, $\mathcal{S}(v_0^\circ(z))$, $\mathcal{S}(v_1^\bullet(z))$, $\mathcal{S}(v_1^\circ(z))$, qui est l'image du quadrilatère $z = (v_0^\bullet(z)v_0^\circ(z)v_1^\bullet(z)v_1^\circ(z))$ par $\mathcal{S}$. On dit que le s-plongement est *propre* si les quadrilatères $\mathcal{S}^\diamond(z)$ ne se recouvrent pas mutuellement et non dégénéré si aucun des quadrilatères $\mathcal{S}^\diamond(z)$

n'est réduit à un segment. En particulier, on ne requiert pas de convexité pour $\mathcal{S}^\diamond(z)$.

Plusieurs faits sont à souligner dans la definition précédente

— La définition dépend d'un graphe *pondéré* (G, x) ainsi que *d'une* solution $\mathcal{X}$ fixée de $(1.5.7)$ sur G. Une fois $\mathcal{X}$ fixé, on considère le plongement et ne mentionne plus la dépendance en $\mathcal{X}$.

— Tout graphe, qu'il soit fini (avec une face extérieure fixée) ou bien infini admet une solution non triviale de $(1.5.7)$, ainsi il existe toujours un s-plongement (pas forcement propre).

— Le s-plongement n'est absolument pas unique, puisqu'on peut déjà voir qu'avec une solution complexe (non réelle) non triviale $\mathcal{X}$ de $(1.5.7)$ sur G, alors $\overline{\mathcal{X}}$ permet de construire un *autre* s-plongement.

— Tout graphe fini (avec une face extérieure fixée) admet un s-plongement *propre* (ce résultat ne semble pas avoir de référence publiée est dû à Chelkak).

— Les translations, rotations, homothéties et conjugaisons de s-plongements sont encore des s-plongements.

Il est aussi possible d'étendre cette définition à $\diamondsuit(G)$ en posant comme dans [33, eq (2.5)]. En effet considérons comme dans la section 1.5.2 une arête e de G dont le poids est $x_e = \tan(\frac{\theta_e}{2})$. En suivant à nouveau les notations de la figure **??**, on définit le quadrilatère $z = z_e = z(v_0^\bullet v_1^\circ v_1^\bullet v_0^\circ) \in \diamondsuit(G)$ qui est naturellement associé à l'arête e, et labellise les sommets de $\Lambda(G)$ appartenant à z dans l'ordre trigonométrique. On pose aussi $\theta_z = \theta_e$. Pour des relèvements des coins c_{p0} et c_{p1} (respectivement, c_{0q} et c_{1q}) choisis comme voisins dans $\Upsilon^\times(G)$ (en rappelant que $c_{pq} = (v_p^\bullet v_q^\circ)$) on définit le point $\mathcal{S}(z)$ par

$$\begin{aligned} \mathcal{S}(v_p^\bullet(z)) - \mathcal{S}(z) &:= \mathcal{X}(c_{p0})\mathcal{X}(c_{p1})\cos\theta_z, \\ \mathcal{S}(v_q^\circ(z)) - \mathcal{S}(z) &:= -\mathcal{X}(c_{0q})\mathcal{X}(c_{1q})\sin\theta_z, \end{aligned} \tag{1.7.3}$$

La définition de $\mathcal{S}$ est consistante grâce à l'équation de propagation $(1.5.7)$ et ne nécessite pas que le s-plongement soit propre ou non-dégénéré.

D'un point de vue géométrique (voir e.g. [33, Section 2.2]) une face $\mathcal{S}^\diamond(z)$ dans un s-plongement est un quadrilatère *tangent* dont le centre (qui correspond à l'intersection des quatre bissectrices) est le point $\mathcal{S}(z)$ défini par $(1.7.3)$. Une illustration est donnée dans la figure 1.7.1. Ce point est aussi le *centre du cercle inscrit* dont le rayon est noté r_z. Ici la tangence à un cercle est comprise (dans le cas d'un quadrilatère non-convexe) comme la tangence *aux lignes* contenant les arêtes de $\mathcal{S}^\diamond(z)$. On peut voir de manière élémentaire qu'un quadrilatère est tangent à un cercle si et seulement si *la somme alternée des longueurs de ses côtés est nulle*. Il est en particulier possible de retrouver le rayon r_z et le paramètre d'Ising

θ_z grâce aux propriétés géométriques de $\mathcal{S}^\diamond(z)$. En notant φ_{vz} le demi-angle du quadrilatère tangent $\mathcal{S}^\diamond(z)$ en $\mathcal{S}(v)$, on a alors [33, eq (2.7)-(2.8)]

$$\tan\theta_z \;=\; \left(\frac{\sin\varphi_{v_0^\bullet z}\sin\varphi_{v_1^\bullet z}}{\sin\varphi_{v_0^\circ z}\sin\varphi_{v_1^\circ z}}\right)^{1/2} \text{ et} \tag{1.7.4}$$

$$r_z = \mathrm{Im}[\,\mathcal{X}(c_{01}(z))\overline{\mathcal{X}(c_{00}(z))}\,]\cos\theta_z = \mathrm{Im}[\,\mathcal{X}(c_{00}(z))\overline{\mathcal{X}(c_{10}(z))}\,]\sin\theta_z. \tag{1.7.5}$$

Certaines des propriétés géométriques des s-plongements ont aussi étudiées par Melotti, Ramassamy et Thevenin dans [128] (voir aussi une étude sur les t-plongements dans [103]).

Il est crucial de comprendre qu'il est toujours possible de construire un s-plongement d'un graphe (fini ou infini) à partir d'une solution de $(1.5.7)$. Cependant, pour appliquer la théorie développée ci-dessous et prouver des résultats concernant le modèle d'Ising associé, il est nécessaire de vérifier que le s-plongement sur lequel on travaille (qui dépend du choix de la solution de $(1.5.7)$ utilisée) est *propre*, c'est à dire que les faces distinctes ne se recouvrent pas en dehors des arêtes qui les séparent.

Le second objet d'importance pour réaliser de l'analyse complexe discrète sur les s-plongements est la fonction dite d'*origami*, dont on rappelle la définition maintenant, introduite dans [33, Définition 2.2]. On se donne $v^\bullet(c) \sim v^\circ(c)$ deux sommets de $\Lambda(G)$ adjacents au même coin $c \in \Upsilon(G)$.

Definition 1.7.2. Soit $\mathcal{S} = \mathcal{S}_\mathcal{X}$ un s-plongement. Il est possible de définir (à une constante additive près) la fonction d'origami $\mathcal{Q} = \mathcal{Q}_\mathcal{X} : \Lambda(G) \to \mathbb{R}$ par ses incréments

$$\mathcal{Q}(v^\bullet(c)) - \mathcal{Q}(v^\circ(c)) \;:=\; |\mathcal{X}(c)|^2 \;=\; |\mathcal{S}(v^\bullet(c)) - \mathcal{S}(v^\circ(c))|\,. \tag{1.7.6}$$

Le nom de la fonction $\mathcal{Q}$ provient de l'art japonais consistant à plier replier un papier sur lui même, ce qui est de manière pratique une preuve de la consistance de la définition de $\mathcal{Q}$. La fonction $\mathcal{Q}$ est 1-lipschitzienne, car elle n'augmente pas les distances. La consistance de cette définition provient à nouveau de $(1.5.7)$ et se traduit géométriquement sur la somme alternée nulle des longueurs du quadrilatère. L'exemple le plus simple de calcul d'une fonction d'origami est sur une grille isoradiale Γ^δ de pas δ. En choisissant correctement la constante additive dans la définition de $\mathcal{Q}$, alors $\mathcal{Q} = \delta$ pour tous les sommets de $\Gamma^\delta(G^\bullet)$ et $\mathcal{Q} = 0$ pour tous les sommets de $\Gamma^\delta(G^\circ)$. La fonction d'origami est cruciale car c'est elle qui dicte l'équation locale vérifiée par la limite d'échelle des observables fermionique lorsque l'on passant à la limite continue.

Comme on le précisera dans les paragraphes suivants, lorsque $\mathcal{S}$ est propre et non dégénéré, le plongement $\mathcal{S} : \Lambda(G) \cup \diamondsuit(G) \to \mathbb{C}$ peut être vu comme un t-plongement $\mathcal{T}$ (dont la définition issue de [45] est rappelée dans les prochaine lignes), ce qui permet d'étendre $\mathcal{Q}$ linéairement par morceau sur *tout* le plan (et non uniquement aux arêtes de $\Lambda(G)$).

Quelques exemples de graphes pondérés que l'on peut étudier en utilisant le formalisme des s-plongements, c'est à dire qui admettent un s-plongement propre Le formalisme des s-plongements est dans la présentation que l'on en a fait jusqu'ici relativement aride. On explique maintenant que ce formalisme est suffisamment général pour pouvoir étudier les différentes classes de graphes pondérés suivantes qui ont déjà étudiées auparavant, lorsque l'on les équipe des poids d'Ising appropriés

— Les graphes finis

— Les grilles isoradiales équipées de leur poids Z-invariants critiques introduit dans la section 1.3.1, avec un générateur $\mathcal{X} = \eta_c$.

— Les grilles isoradiales avec angles bornés équipées de leur poids Z-invariants *massifs* i.e. on prend $q = \frac{1}{2}m\delta$ sur la grille de pas δ, via la procédure de re-plongement introduite dans le chapitre 3. Ici le générateur $\mathcal{X}$ correspond aux exponentielles discrètes massives introduite par Boutillier de Tilière et Raschel dans [27, 28].

— Les grilles doublement périodiques critiques (pour lesquels la condition de criticalité a été déterminée par Cimasoni et Duminil-Copin dans [52]). Dans ce cadre là, le s-plongement associé est unique à rotation, conjugasion et translation près comme démontré dans [33, Lemma 2.3], où le choix du générateur est fait à partir de deux solutions linéairement indépendantes bi-périodiques de $(1.5.7)$.

— Le modèle d'Ising sur les *circle patterns* introduit par Lis dans [114] avec des poids correspondant à la température $\beta = 1$. Cela se voit assez simplement via les faces de $\Lambda(G)$ se trouvent être des kites, qui correspondent bien à un des quadrilatères tangents.

1.7.1 . Définition du pas du plongement

On donne à présent une définition du *pas* δ d'un s-plongement $\mathcal{S}$, en utilisant la fonction d'origami $\mathcal{Q}$ rappelée dans la définition 1.7.2. Cette définition correspond à celle donnée par Chelkak Laslier et Russkikh dans [45, Section 1], se base sur l'hypothèse $\textsc{Lip}(\kappa,\delta)$ que l'on rappelle maintenant (voir [45, Hypothèse 1.1] pour sa définition originale)

Hypothèse 1.7.1 $(\textsc{Lip}(\kappa,\delta))$**.** On dit que le s-plongement $\mathcal{S}^\delta$ satisfait l'hypothèse $\textsc{Lip}(\kappa,\delta)$ pour $\kappa < 1$ si on a

$$|\mathcal{Q}^\delta(v') - \mathcal{Q}^\delta(v)| \leq \kappa \cdot |\mathcal{S}^\delta(v') - \mathcal{S}^\delta(v)| \quad \text{si} \quad |\mathcal{S}^\delta(v') - \mathcal{S}^\delta(v)| \geq \delta. \qquad (1.7.7)$$

En particulier cela permet de construire une *définition* du pas δ du $\mathcal{S}^\delta$ grâce à $\textsc{Lip}(\kappa,\delta)$ comme nous le voyons maintenant.

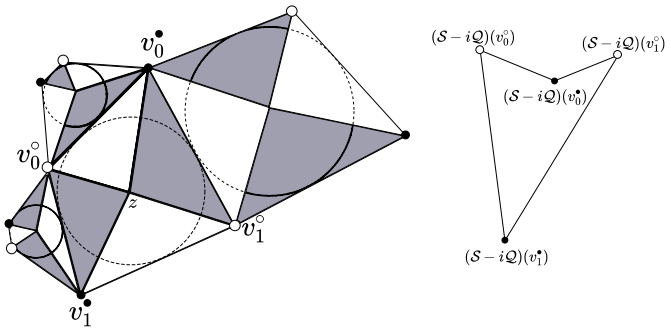

FIGURE 1.7.1 – (Gauche) Quadrilatère tangent d'un s-plongement $\mathcal{S}$. Le cercle inscrit est tracé en pointillés. Le coloriage des faces correspond au coloriage bipartite du t-plongement $\mathcal{T}$ associé. (Droite) Image de ce même quadrilatère tangent dans le S-graphe $\mathcal{S} - i\mathcal{Q}$.

Definition 1.7.3. Soit $\mathcal{S} = \mathcal{S}_\mathcal{X}$ un s-plongement propre, $\kappa < 1$ et U un ouvert du plan. On dit que $\mathcal{S}$ est de pas δ sur U pour la constante κ si

$$\delta := \inf\{\delta', \mathrm{Lip}(\kappa, \delta') \text{ est vraie. }\}$$

En particulier, toutes les arêtes de $\mathcal{S}$ sont de longueur δ.

Cette définition a été proposée dans [45, Section 1] pour traiter le cas de grilles très irrégulières, où les faces sont de taille très différentes et où n'y a pas de définition immédiate qui correspondrait à une certaine taille typique. En particulier, avec cette définition (à κ fixé), les différentes marches aléatoires associées au s-plongement (qui seront détaillées dans la section 1.7.2) sont elliptiques au-delà d'une distante $r \geqslant \mathrm{cst}(\kappa) \cdot \delta$, c'est à dire que pour r supérieur à une distance comparable avec δ, les marches aléatoires qui apparaissent naturellement dans la théorie ont une probabilité bornée inférieurement de sortir d'une boule de rayon par n'importe quel arc de dimension macroscopique comparable avec r.

Lorsque les angles géométriques de $\mathcal{S}^\delta$ sont bornés inférieurement et que toutes les arêtes sont de longueurs comparables entre elles (ce qui correspond à l'hypothèse UNIF(δ) dans [33, Section 1.3]), la définition abstraite via LIP(κ,δ) coïncide (à un facteur multiplicatif près) avec la longueur commune des arêtes. En particulier lorsque l'on parle d'une limite d'échelle de s-plongements $(\mathcal{S}^\delta)_{\delta>0}$, cette limite est prise pour une sous-suite $(\mathcal{S}^{\delta_n})_{\delta_n}$ avec $\delta_n \to 0$ lorsque $n \to \infty$ et *tous* les graphes $\mathcal{S}^{\delta_n}$ vérifient $\mathrm{Lip}(\kappa, \delta_n)$ pour le *même* paramètre $\kappa < 1$.

Lorsque l'on étudie la limite d'échelle de fonctions s-holomorphes sur des s-plongements (dont la définition est rappelée ci-dessous), on le fera toujours

sous l'hypothèse $\textsc{Lip}(\kappa,\delta)$, qui permet de prouver la régularité des fonctions s-holomorphes dans le discret ainsi que de leur analogue continu (qui s'expriment comme nous le verrons dans les paragraphes suivants via des solutions d'équations de Beltrami conjuguées). A l'heure actuelle, il est malheureusement encore nécessaire d'ajouter une hypothèse supplémentaire à $\textsc{Lip}(\kappa,\delta)$ sur les dégénérescences autorisées de la géométrie locale des graphes sur lesquels on travaille. Cette seconde hypothèse assure la pré-compacité des fonctions s-holomorphes tant que les faces exponentiellement petites (en δ^{-1}) ne forment pas de cluster de taille macroscopique. Cette idée est précisée par l'hypothèse $\textsc{Exp-Fat}(\delta)$, introduite dans [45, Section 6]. Une famille de s-plongements $(\mathcal{S}^\delta)_{\delta>0}$ vérifie l'hypothèse $\textsc{Exp-Fat}(\delta)$ sur un ouvert $U \subset \mathbb{C}$ si pour tout $\gamma > 0$:

en enlevant de U tous les quadrilatères $(\mathcal{S}^\delta)^\diamond(z)$ dont le rayon vérifie $r_z \geq \exp(-\gamma\delta^{-1})$, le diamètre de la plus grande des composantes connexes restantes tend vers 0 lorsque $\delta \to 0$.

En particulier ces hypothèses n'utilisent pas de notion *d'angles bornés ou de comparabilité entre la longueur des arêtes*, mais plutôt que la fonction d'origami n'est pas dégénérée à partir d'un certaine échelle δ et que les faces de taille exponentiellement petite en δ^{-1} n'envahissent pas macroscopiquement le graphe.

1.7.2 . Lien avec le modèle de dimères : t-plongements et S-graphes

Il existe une multitude de liens entre le modèle d'Ising et les modèles de dimères (on peut consulter par exemple [164, Section 2.3] ou bien encore [37, Section 3.1] pour un rappel très complet). On présente ici en détails un de ces liens permettant de construire un modèle de dimères à partir d'un graphe planaire équipé du modèle d'Ising. Ceci correspond à la *bosonisation* du modèle d'Ising, étudiée par Dubédat dans [58]. Dans cette section, on ne présente le formalisme et les liens entre modèle d'Ising et dimères que le cas des graphes *sans face extérieure* (i.e. des graphes infinis ou bien des graphes finis mais loin de la face extérieure). Une discussion sur les traitements possibles du cas de la face extérieure est donnée dans [103, Section 3].

Soit (G,x) un graphe planaire équipé du modèle d'Ising sur ses faces, dont on se donne un plongement $\mathcal{S}$ dans le plan (qui n'est pas nécessairement un s-plongement). On garde en particulier la paramétrisation des poids d'Ising par la relation $(1.5.4)$. On suit à présent les notations de la figure 1.7.2 Il est possible de construire (sans préciser ici les modifications au bord de G) un modèle de dimères à partir de ce modèle d'Ising. On commence par diviser en 4 triangles chaque quadrilatère $z \in \diamondsuit(G)$. Chaque face est à présent un triangle dont deux sommets sont des voisins dans $\Lambda(G)$ et le troisième sommet est le centre de z (ici le centre n'admet pas de position naturelle en dehors du cadre des s/t-plongements). On rappelle que chaque quadrilatère $z \in \diamondsuit(G)$ s'associe à une arrête e de G dont le poids est $x_e = \tan(\frac{\theta_e}{2})$. On note $\theta = \theta_z = \theta_e$ l'angle associé à x_e via $(1.5.4)$.

On considère alors le modèle de dimères [101] sur le graphe bipartite des *faces* que l'on vient de former (et dont les sommets sont notés par 'W' et 'B' en référence à leur coloriage bi-chromatique), avec les poids [37, Section 3.1] :

— 1 entre les faces appartenant à deux quadrilatères différents,

— $\cos(\theta)$ si les deux faces du même quadrilatère (d'angle θ) ont un sommet de $G^\bullet$ en commun,

— $\sin(\theta)$ si les deux faces du même quadrilatère (d'angle θ) ont un sommet de G° en commun.

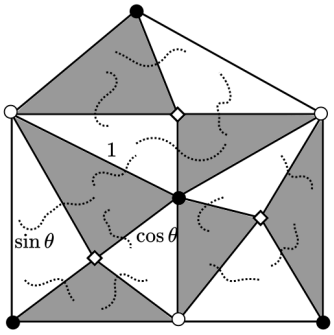

FIGURE 1.7.2 – Configuration de dimères associée au modèle d'Ising. Le poids d'une arête entre deux faces adjacentes du graphe bipartite W/B (qui correspond ici aux faces claires ou foncées). L'angle θ associé au poids est l'angle $\theta_z = \theta_e$ associé au quadrilatère $z \in \diamondsuit(G)$, lui-même associé à l'arrête e dont le poids est $x_e = \tan(\frac{\theta_e}{2})$.

Pour le modèle de dimères, il existe une notion de *t-plongement* introduite dans [45], qui est analogue à celle des s-plongements. Le formalisme des t-plongements est par ailleurs équivalent à celui des *jauges de Coulomb* introduit dans [103] (les liens entre les deux formalismes sont précisés dans [45, Appendix]). En quelques mots, un t-plongement $\mathcal{T}$ d'un graphe planaire abstrait dont le dual est bipartite équipé d'un modèle de dimères (sur ses faces) est le plongement de son dual dans le plan, tel que [45, Definition 2.1 et Figure 1]

— Les arêtes sont des segments non dégénérés, les faces sont convexes et ne se recouvrent pas.

— Pour tout sommet v du plongement, la somme des angles attachés aux faces noires incidentes à v est égale à π.

— Pour tout sommet v du plongement, la somme des angles attachés aux faces blanches incidentes à v est égale à π.

Les poids du modèle de dimères associé sont *équivalents par jauge* [103, Section 2] aux longueurs des arêtes dans $\mathcal{T}$.

Lorsque $\mathcal{S}$ est un s-plongement propre et non dégénéré de (G, x), on peut voir l'application $\mathcal{S} : \Lambda(G) \cup \diamondsuit(G) \to \mathbb{C}$ comme un t-plongement de $(\Upsilon^\circ(G) \cup$

$\Upsilon^\bullet(G))^*$ [33, Section 2.6]. Il est aisé de vérifier la propriété sur la somme des angles grâce aux propriétés géométriques des quadrilatères tangents. Une notion cruciale pour l'étude d'un t-plongement est celle des *racines d'origami* (au sens de [45, Definition 2.4]) associées aux faces de $\mathcal{T}$. Il est possible [33, Section 2.3] de construire un racine d'origami η sur $\mathcal{T} = \mathcal{S}$ en posant pour les faces $c^\bullet \in B$ et $c^\circ \in W$ adjacentes au coin $c \in \Upsilon$ la fonction $\eta_{c^\bullet} = \eta_{c^\circ} := \overline{\varsigma}\eta_c$ (où η_c est donnée par $(1.5.8)$). Avec la convention précédente, la fonction d'origami $\mathcal{Q} : \Lambda(G) \to \mathbb{R}$ de la Définition 1.7.2 pour le s-plongement est la restriction de la fonction d'origami $\mathcal{O} : \Lambda(G) \cup \diamondsuit(G) \to \mathbb{C}$ [45, Section 2.2] associée au t-plongement $\mathcal{T}$. En particulier, cela permet d'étendre $\mathcal{Q}$ (dans le contexte d'Ising) de manière linéaire par morceaux sur l'intégralité du plan.

On présente maintenant de manière rapide la notion de *S-graphes*, introduite dans [33, Section 2.5] et associée aux s-plongements, qui correspondent à un cas particulier des *T-graphes* associés aux t-plongements (voir [45, Section 4.1] pour une définition précise). On garde ici les notations de [33, Section 2.3].

Definition 1.7.4. Soit $\mathcal{S} : \Lambda(G) \to \mathbb{C}$ un s-plongement non dégénéré, $\mathcal{Q} : \Lambda(G) \to \mathbb{R}$ la fonction d'origami associée et α un nombre unimodulaire. On appelle le plongement $\mathcal{S} + \alpha^2\mathcal{Q} : \Lambda(G) \to \mathbb{C}$ un S-graphe associé à $\mathcal{S}$. On dit que le S-graphe est non dégénéré si pour tout $v \neq v'$, alors $(\mathcal{S} + \alpha^2\mathcal{Q})(v) \neq (\mathcal{S} + \alpha^2\mathcal{Q})(v')$.

Les arêtes de $\mathcal{S} + \alpha^2\mathcal{Q}$ sont automatiquement des segments (car $\mathcal{Q}$ est localement linéaire) qui ne s'intersectent pas en dehors de leurs extrémités (on rappelle que $\mathcal{T}$ est supposé être propre). Les dégénérescences de $\mathcal{S}+\alpha^2\mathcal{Q}$ apparaissent pour les arêtes $(v^\circ v^\bullet) \in \Lambda(G)$ telles que $\mathcal{S}(v^\bullet) - \mathcal{S}(v^\circ) \in -\alpha^2\mathbb{R}_+$, c'est à dire lorsque l'image de $(v^\circ v^\bullet)$ dans $\mathcal{S} + \alpha^2\mathcal{Q}$ est réduite à un point (la dégénéressence dans les S-graphes n'est qu'une subtilité qui n'importe quasiment pas dans la théorie). En particulier, pour prouver les résultats de régularité des fonctions s-holomorphes, il est suffisant de travailler avec des S-graphes non-dégénérés puis utiliser un argument de continuité vis à vis de α. Géométriquement, l'image $(\mathcal{S} + \alpha^2\mathcal{Q})^\diamond(z)$ du quadrilatère $\mathcal{S}^\diamond(z)$ dans un S-graphe non-dégénéré est un quadrilatère *non-convexe* [33, Figure 4]. De plus pour $z = (\mathcal{S}(v_0^\bullet)\mathcal{S}(v_0^\circ)\mathcal{S}(v_1^\bullet)\mathcal{S}(v_1^\circ)) \in \diamondsuit(G)$ and $p, q \in \{0, 1\}$, on a alors [33, eq (2.13)]

$$\mathrm{Re}[\,\overline{\alpha}^2(\mathcal{S} + \alpha^2\mathcal{Q})(v_p^\bullet(z))\,] \;\geq\; \mathrm{Re}[\,\overline{\alpha}^2(\mathcal{S} + \alpha^2\mathcal{Q})(v_q^\circ)(z)\,], \tag{1.7.8}$$

l'égalité étant possible si et seulement si l'arête $(\mathcal{S}(v_p^\bullet(z))\mathcal{S}(v_q^\circ(z)))$ est dégénérée dans $\mathcal{S} + \alpha^2\mathcal{Q}$. Les S-graphes sont très utiles car ils permettent (comme nous le verrons dans le prochain paragraphe) d'interpréter les projections d'une fonction s-holomorphe comme des fonctions harmoniques. On remarque tout de même une incompatibilité de notations dans la phrase précédente. En effet, $\mathrm{Pr}[F\,;\alpha\mathbb{R}]$ est une fonction définie sur $\diamondsuit(G)$ tandis que les fonctions harmoniques sur les S-graphes sont définies sur $\Lambda(G)$. Il est possible de régler cette inconsistance de

notations en remarquant (e.g. [33, Definition 2.13]) que l'application (dépendant de α) $\diamondsuit(G) \ni z \mapsto v^{(\alpha)}(z) \in \Lambda(G)$, qui associe à un quadrilatère $z \in \mathcal{S}$ le sommet de $\Lambda(G)$ dont l'image par $\mathcal{S} + \alpha^2\mathcal{Q}$ est *non-convexe* dans $(\mathcal{S} + \alpha^2\mathcal{Q})^\diamond(z)$, est une bijection.

1.7.3 . Analyse complexe discrète sur les s-plongements

Les s-plongements sont par définition construits à partir d'observables satisfaisant la relation locale $(1.5.7)$. Ceci en fait de bons candidats pour admettre une généralisation naturelle de l'analyse complexe discrète, basée sur l'étude des corrélateurs de Kadanoff et Ceva. On explique dans ce paragraphe que c'est bien le cas, comme le montre le formalisme introduit dans [33], dont on conserve les notations. Soit $\mathcal{S} = \mathcal{S}_\mathcal{X}$ un s-plongement propre et non-dégénéré. Il est possible de généraliser l'analyse complexe discrète sur les graphes isoradiaux comme il suit :

— On conserve *à l'identique* la notion de fonction s-holomorphe de la Définition 5.2.3. C'est à dire que F définie sur un sous-ensemble de $\diamondsuit(G)$ est *s-holomorphe* $z, z' \in \diamondsuit(G)$ deux faces adjacentes de $\Lambda(G)$, dont l'arête commune est $(v^\circ(c)v^\bullet(c))$ (avec $c \in \Upsilon(G)$), on a

$$\Pr[F(z)\,;\eta_c\mathbb{R}] \;=\; \Pr[F(z')\,;\eta_c\mathbb{R}]. \tag{1.7.9}$$

— Le lien entre les fonctions s-holomorphes et les solutions de $(1.5.7)$ est à présent modifié. Plus précisément pour une fonction F s-holomorphe sur un sous-ensemble de $\diamondsuit(G)$, le spineur X défini pour un coin $c \in \Upsilon^\times(G)$ de la face $z \in \diamondsuit(G)$ par [33, Proposition 2.5]

$$\begin{aligned} X(c) \;&:=\; |\mathcal{S}(v^\bullet(c)) - \mathcal{S}(v^\circ(c))|^{\frac{1}{2}} \cdot \mathrm{Re}[\overline{\eta}_c F(z)] \\ &=\; \mathrm{Re}[\overline{\varsigma}\mathcal{X}(c)\cdot F(z)] \;=\; \overline{\varsigma}\mathcal{X}(c)\cdot \Pr[F(z)\,;\eta_c\mathbb{R}] \end{aligned} \tag{1.7.10}$$

satisfait l'équation$(1.5.7)$ autour de z. Réciproquement, pour $X : \Upsilon^\times(G) \to \mathbb{R}$ une solution réelle de $(1.5.7)$, il existe une unique fonction s-holomorphe F telle que $(1.7.10)$ soit vérifiée.

— Il est encore possible de reconstruire explicitement la valeur de F via X et $\mathcal{X}$, par exemple [33, Corollaire 2.6] via les coins c_{01} et c_{10}, voisins dans $\Upsilon^\times(G)$

$$F(z) \;=\; -i\varsigma \cdot \frac{\overline{\mathcal{X}(c_{01}(z))}\, X(c_{10}(z)) - \overline{\mathcal{X}(c_{10}(z))}\, X(c_{01}(z))}{\mathrm{Im}[\,\overline{\mathcal{X}(c_{01}(z))}\,\mathcal{X}(c_{10}(z))]}. \tag{1.7.11}$$

— La fonction F n'est à présent plus holomorphe discrète (au sens où les intégrales usuelles de contour s'annulent), mais satisfait une relation locale modifiée, mettant en jeu la fonction d'origami. Grâce à l'extension linéaire par morceaux de la fonction $\mathcal{Q}$ au plan tout entier, il est possible de définir sur $\mathbb{C}$ la fonction [33, Proposition 2.21]

$$I_\mathbb{C}[F] := \int \overline{\varsigma} F d\mathcal{S} + \varsigma\overline{F} d\mathcal{Q}. \tag{1.7.12}$$

De manière concrète sur $\Lambda(G)$, pour $v_1^\circ \sim v_1^\bullet \sim v_2^\circ \in z \in \diamondsuit$ on a

$$I_{\mathbb{C}}[F](v_1^\circ) - I_{\mathbb{C}}[F](v_1^\bullet) = \frac{X(c_{11})}{\mathcal{X}(c_{11})}[\mathcal{S}(v_1^\circ) - \mathcal{S}(v_1^\bullet)]. \tag{1.7.13}$$

$$I_{\mathbb{C}}[F](v_2^\circ) - I_{\mathbb{C}}[F](v_1^\circ) = \bar{\varsigma}F(z)[\mathcal{S}(v_2^\circ) - \mathcal{S}(v_1^\bullet)] + \varsigma\overline{F(z)}[\mathcal{Q}(v_2^\circ) - \mathcal{Q}(v_1^\bullet)]. \tag{1.7.14}$$

— La fonction H_F définie sur les grilles isoradiales $(1.5.14)$ est à présent modifiée et devient [33, eq (2.17)]

$$H_F := \int \tfrac{1}{2}\,\mathrm{Re}(\bar{\varsigma}^2 F^2 d\mathcal{S} + |F|^2 d\mathcal{Q}) = \int \tfrac{1}{2}(\mathrm{Im}(F^2 d\mathcal{S}) + \mathrm{Re}(|F|^2 d\mathcal{Q})), \tag{1.7.15}$$

sur $\Lambda(G) \cup \diamondsuit(G)$. Cette fonction H_F s'étend de manière linéaire par morceaux sur les faces du t-plongement $\mathcal{T} = \mathcal{S}$, mais pas sur les faces de $\diamondsuit(G)$, car chacune des quatre faces de $\mathcal{T}$ associées à $\mathcal{S}^\diamond(z)$ a sa propre racine d'origami $d\mathcal{Q}$. Avec le nouveaux lien entre X et F, l'égalité $H_F = H_X$ reste vraie (voir [33, Lemme 2.9]). Ceci induit par exemple les conditions de bord de type Dirichlet pour H_F associée à l'observable FK.

Au dela de ces définitions, la régularité aux fonctions t-holomophores développée dans [45] (et traduite dans le contexte d'Ising dans [33]) permet de vérifier leur pré-compacité sous les hypothèses $\textsc{Lip}(\kappa,\delta)$ et $\textsc{Exp-Fat}(\delta)$, que l'on supposera toujours vérifiées dans la suite. Il est possible de voir que

— Pour $\alpha \in \mathbb{T}$ un nombre de module 1 et F une fonction s-holomorphe au sens de 5.2.3 (et via à la bijection $z \mapsto v^{(\alpha)}(z)$), la fonction $\mathrm{Proj}[F; \alpha\mathbb{R}]$ est une fonction *harmonique* sur le S-graphe $\mathcal{S} - i\overline{\alpha^2}\mathcal{Q}$ [33, Proposition 2.16], pour la marche aléatoire *renversée* associée à la marche naturelle [33, Définition 2.14 et 2.15] sur $\mathcal{S} - i\overline{\alpha^2}\mathcal{Q}$. En particulier, $\mathrm{Re}[F]$ s'identifie comme une fonction harmonique sur $\mathcal{S} - i\mathcal{Q}$ alors que $\mathrm{Im}[F]$ s'identifie à une *autre* une fonction harmonique sur un autre S-graphe $\mathcal{S} + i\mathcal{Q}$. Dans ces deux exemples, les marches sous-jacentes sont complètement différentes.

— Il est possible de contrôler les oscillations de F sur des disques de tailles différentes [33, Théorème 2.17], ce qui implique concrètement un contrôle de type Harnack du maximum F^δ via les oscillations de H_{F^δ}. En supposant que pour les fonctions s-holomorphes F^δ sur $U = B(u,r)$ admettent une borne $\max_{v:\mathcal{S}(v)\in U} |H_{F^\delta}(v)| \leq M$ uniforme en δ, il est possible de montrer que [33, Théorème 2.18]

$$|F^\delta(z)|^2 = O(r^{-1}M) \quad \text{si} \quad \mathcal{S}^\delta(z) \in B(u, \tfrac{1}{2}r). \tag{1.7.16}$$

Cela permet de déduire [33, Corrolaire 2.18] qu'un contrôle uniforme des oscillations de H^δ implique la pré-compacité de la suite des fonctions $(F^\delta)_{\delta>0}$, qui sont aussi β-Hölder à partir d'une distance comparable à δ. Cela assure par exemple trivialement la pré-compacité des observables FK [33, Remarque 2.11], pour lesquelles les fonctions H^δ associées sont bornées.

1.7.4 . Limites d'échelles sur les s-plongements

Comme expliqué dans la section 1.4, l'objectif original de Chelkak lorsqu'il a introduit les s-plongements était de proposer une procédure de dessin pour plonger des graphes abstraits critiques et presques critiques, avec deux cibles principales : les modèles critiques sur les graphes doublement périodiques, ainsi que les cartes aléatoires équipées du modèle d'Ising (les termes exacts en lesquels cette seconde question restent encore aujourd'hui flous, mais, nous l'espérons, seront clarifiés à l'avenir). Ainsi, Chelkak a développé le formalisme de plongement présenté dans la partie précédente de la section 1.7, et, comme cela arrive fréquement en mathématiques, son formalisme a fait apparaitre des perspectives d'une portée bien plus large. En particulier, en étendant le formalisme des observables fermioniques aux s-plongements, la description naturelle de leur limite d'échelle s'avère aller bien au-delà de l'holomorphie et de l'holomorphie massive. En particulier, une des conséquence des travaux de Chelkak (voir [33, Section 2]) est l'apparition des liens suivants, qui sont gouvernés par le comportement de la limite des fonctions d'origami (cette dernière existant toujours après passage à une sous-suite) :

— La limite d'échelle continue du modèle d'Ising sur les s-plongements est reliée à la géométrie de Lorentz dans l'espace $\mathbb{R}^{2,1}$ (que l'on note ainsi pour différentier l'utilisation de la métrique de Minkowski à l'utilisation de la métrique euclidienne usuelle dans $\mathbb{R}^3$). En particulier, les *surfaces minimales pour la métrique de Minkowski* (c'est à dire avec une courbure moyenne nulle en chaque point) semblent jouer un rôle très particulier pour le modèle puisqu'elles font apparaître des limites holomorphes (dans une autre paramétrisation que le plan) et semblent traîter des systèmes critiques.

— La limite d'échelle continue du modèle d'Ising sur les s-plongements peut aussi s'interpréter via des solutions d'équations de Beltrami conjuguées.

Le paragraphe qui suit peut sembler relativement technique pour le lecteur n'utilisant pas l'analyse fréquemment dans ses recherches. On essaye cependant de rendre le plus pédagogique possible la discussion qui suit, en donnant au moins un avant-goût de la nature des résultats. Une discussion détaillée et précise sur la structure des limite d'échelle sur les s-plongement généraux est réalisée dans le chapitre 5, où le lecteur intéressé pourra trouver plus de détails.

On décrit à présent le comportement potentiel des limites de sous-suites de fonctions s-holomorphes sur les s-plongements. La nature de ces limites continues provenant de s-plongements généraux est plus élaborée que pour les système critiques et massifs Z-invariants sur les grilles isoradiales, puisqu'en toute généralité ce ne sont plus des fonctions holomorphes mais des solutions d'équations de Beltrami conjuguées qui apparaissent. Ce paragraphe rappelle les faits décrits dans [33, Section 2.7].

On commence par se donner une suite de s-plongements $\mathcal{S}^\delta$ qui vérifient $\textsc{Lip}(\kappa,\delta)$ lorsque $\delta \to 0$ pour le *même* paramètre $\kappa < 1$ et dont les images couvrent $U = B(u,r) \subset \mathbb{C}$. Comme les fonctions $\mathcal{Q}^\delta$ sont 1-Lipschitz et définies à constante additive près, on peut trouver une sous-suite $\delta_k \to 0$ telle que $\mathcal{Q}^{\delta_k}$ converge vers une fonction κ-lipschitzienne $\vartheta : U \to \mathbb{R}$, c'est à dire

$$\mathcal{Q}^{\delta_k} \circ (\mathcal{S}^{\delta_k})^{-1} \xrightarrow{||\ ||_\infty} \vartheta : U \to \mathbb{R}. \tag{1.7.17}$$

Parmi les conséquence du formalisme directes du formalisme développé dans le discret (qui est détaillé dans le chapitre 5) on a les faits suivants :

— Pour $f : U \to \mathbb{C}$ une limite de sous-suite de fonctions s-holomorphes F^δ sur $\mathcal{S}^\delta$, alors (voir e.g. [33, Proposition 2.21]) la forme différentielle $\frac{1}{2}(\overline{\varsigma} f dz + \varsigma \overline{f} d\vartheta)$ est fermée sur U, avec un pré-facteur $\varsigma = e^{i\frac{\pi}{4}}$ choisi comme dans $(1.5.8)$. C'est à dire que pour tout contour orienté lisse $\mathcal{C} \subset U$, on a

$$\oint_{\mathcal{C}} \tfrac{1}{2}(\overline{\varsigma} f dz + \varsigma \overline{f} d\vartheta) = 0. \tag{1.7.18}$$

Lorsque la fonction ϑ n'est pas une fonction lisse, la définition de cette intégrale est faite via les sommes Riemann sur les contours réguliers (i.e. les intégrales sont des intégrales de Riemann-Stieltjes).

— En choisissant correctement les constantes additives dans leur définitions, les fonctions H_{F^δ} convergent uniformément [33, Proposition 2.21] sur les compacts de U vers $h := \frac{1}{2}\int \mathrm{Im}(f^2 dz) + |f|^2 d\vartheta$. En particulier, il apparait que h n'est plus une fonction harmonique.

La condition sur la forme différentielle $\frac{1}{2}(\overline{\varsigma} f dz + \varsigma \overline{f} d\vartheta)$ est difficile à interpréter et utiliser pour déterminer la nature de l'équation vérifiée localement par la fonction f. En effet lorsque $d\vartheta = 0$ (ce qui est un cas particulier des grilles isoradiales critiques), on avait directement que $\oint_{\mathcal{C}} \frac{1}{2}\overline{\varsigma} f dz = 0$ sur chaque contour lisse $\mathcal{C} \subset U$, ce qui implique (en utilisant le théorème de Morera) que f est une fonction holomorphe. Ce raisonnement ne s'applique plus lorsque $d\vartheta \neq 0$.

On va décrire à présent l'idée remarquable de Dmitry Chelkak, présentée tout d'abord dans dans [33, Sec 2.7], qui consiste à changer la paramétrisation de l'espace ambiant pour pouvoir interpréter la condition sur la forme différentielle $\frac{1}{2}(\overline{\varsigma} f dz + \varsigma \overline{f} d\vartheta)$ en utilisant l'espace $\mathbb{R}^{2,1}$ équipé de la métrique de Minkowski, mais aussi en utilisant des équations de Beltrami.

Le paragraphe qui suit est dû aux explications de Dmitry Chelkak et Mikahil Basok, pour la partie qui n'est pas déjà présente dans [33, Sec 2.7], et l'auteur leur en est immensément reconnaissant. Chelkak propose deux approches différentes pour traiter la nature locale des limite d'échelle.

Première approche : Paramétrisation conforme dans l'espace de Minkowski

Dans son article, Chelkak commence par se donner [33, eq (2.26)]

$$\mathbb{D} \ni \zeta \ \mapsto \ (z, \vartheta) \in \mathbb{C} \times \mathbb{R} \cong \mathbb{R}^{2+1} \tag{1.7.19}$$

une *paramétrisation conforme* de la surface $(z, \vartheta(z))_{z\in U}$ (qui est ici dans le cône spatio-temporel de $\mathbb{R}^{2,1}$ dû à l'hypothèse $\kappa < 1$), que l'on équipe d'une métrique positive provenant de l'espace de Minkowski ambiant. Il considère ensuite les incréments infinitésimaux associé à la paramétrisation $(1.7.19)$ de la surface $(z, \vartheta(z))_{z\in U}$. Une paramétrisation conforme est une paramétrisation qui préserve exactement les angles entre $\mathbb{D}$ et (z, ϑ) via l'application de $(1.7.19)$. Un calcul (quelque peu désagréable) montre que la paramétrisation préserve les angles (c'est-à-dire qu'il s'agit bien d'une paramétrisation conforme) si et seulement si *presque partout pour la mesure de Lebesgue* on a l'égalité [33, eq (2.27)]

$$z_\zeta \overline{z}_\zeta \ = \ (\vartheta_\zeta)^2 \quad \text{et} \quad |z_\zeta| > |\vartheta_\zeta| \geq |\overline{z}_\zeta| \, . \tag{1.7.20}$$

Ici on note comme d'usage en analyse $z_\zeta := \partial z/\partial\zeta$, $\overline{z}_\zeta$ et ϑ_ζ les dérivées de Wirtinger dans la paramétrisation ζ. L'équivalence entre la paramétrisation conforme et $(1.7.20)$ est expliquée dans [33, Section 2.7] lorsque la fonction ϑ est lisse puis étendu dans le chapitre 5 sans conditions sur ϑ.

Seconde approche : Paramétrisation quasi-conforme dans le plan

Chelkak a aussi découvert une paramétrisation alternative du plan z par la même variable $\zeta \in \mathbb{D}$, qui reste reliée à la paramétrisation $(1.7.20)$. L'utilisation de cette paramétrisation alternative possède l'avantage de pouvoir interpréter de manière efficace la condition sur la forme différentielle $\frac{1}{2}(\overline{\varsigma} f dz + \varsigma \overline{f} d\vartheta)$ même lorsque la fonction ϑ n'est pas régulière.

Dans ce second cas, l'idée de Chelkak consiste à remarquer que dans le cas où ϑ est une fonction $\kappa < 1$-lipschitz, il est possible de réécrire la paramétrisation conforme de la surface $(z, \vartheta(z))$ via une paramétrisation *quasi-conforme* du plan z. Une paramétrisation quasi-conforme est une paramétrisation vérifiant une équation de Beltrami du type $(1.7.21)$, et qui au lieu de préserver les angles limite leur distorsion (d'un facteur ne dépendant que de κ). Chelkak donne ainsi une paramétrisation *quasi-conforme* du plan z par la variable $\zeta \in \mathbb{D}$, qui correspond à une *paramétrisation conforme* de la surface (z, ϑ). La paramétrisation quasi-conforme $z \mapsto \zeta(z)$ (ou de manière équivalente $\zeta \mapsto z(\zeta)$) est alors solution de l'équation de Beltrami suivante, avec un coefficient de Beltrami noté μ :

$$\zeta_{\bar{z}} = \mu(z)\zeta_z. \tag{1.7.21}$$

Le travail de Chelkak assure que $(1.7.20)$ est vérifiée si et seulement si le coefficient μ défini par $(1.7.21)$ est solution de l'équation

$$\frac{\bar{\mu}}{1+|\mu|^2} = -\frac{\vartheta_z^2}{1-2|\vartheta_z|^2}. \tag{1.7.22}$$

Maintenant que l'on a présenté les changement de variables réalisés par Chelkak avec l'introduction de la variable ζ, il est possible, pour une fonction f vérifiant que la forme différentielle $\frac{1}{2}(\overline{\varsigma} f dz + \varsigma \overline{f} d\vartheta)$ est fermée, de réécrire l'équation locale qui régit le comportement des fonctions $f, I_{\mathbb{C}}[f]$ et $h[f]$. Avant cela, on réalise un dernier changement de variable, cette fois-ci de la fonction f vers une fonction φ, dont la définition est plus symétrique dans sa dépendance vis-à-vis de la variable ϑ. On pose alors comme dans [33, eq (2.28)], et *dans la paramétrisation* ζ

$$\varphi(\zeta) := \overline{\varsigma} f(z(\zeta)) \cdot (z_\zeta)^{1/2} + \varsigma \overline{f(z(\zeta))} \cdot (\overline{z}_\zeta)^{1/2} \tag{1.7.23}$$

Ce changement de variable permet les réécritures suivantes

$$g(\zeta) = I_{\mathbb{C}}[f](\zeta) \int \overline{\varsigma} \varphi(\zeta) \cdot z_\zeta^{\frac{1}{2}} d\zeta + \varsigma \overline{\varphi(\zeta)} \cdot (z_{\bar{\zeta}})^{\frac{1}{2}} d\bar{\zeta} \qquad \text{et} \tag{1.7.24}$$

$$h(\zeta) = \int \mathrm{Im}[\varphi(\zeta)^2 d\zeta]. \tag{1.7.25}$$

Comme expliqué dans [33, Section 2.7] et détaillé le chapitre 5, lorsque la fonction ϑ est lisse, alors

— La fonction φ vérifie une équation de *Dirac massif* [33, eq (2.28)]

$$\varphi_{\bar{\zeta}} \; = \; im \cdot \overline{\varphi}\,, \quad \text{avec} \quad m = \frac{z_{\zeta\bar{\zeta}}}{2(z_\zeta z_{\bar{\zeta}})^{1/2}} = \frac{(|\vartheta_{\zeta\bar{\zeta}}|^2 - |z_{\zeta\bar{\zeta}}|^2)^{1/2}}{2(|z_\zeta| - |z_{\bar{\zeta}}|)},$$

où le paramètre de masse $m = \frac{1}{2} H \ell$ est le produit de l'élément de longueur $\ell = |z_\zeta| - |\overline{z}_\zeta| = (|z_\zeta|^2 + |\overline{z}_\zeta|^2 - 2|\vartheta_\zeta|^2)^{1/2}$ au point $z(\zeta)$ dans la paramétrisation $(1.7.19)$ par la *courbure moyenne* de la surface $(z, \vartheta(z))$ au point $z(\zeta)$ donnée par $H = \pm \|(z_{\zeta\bar{\zeta}}; \vartheta_{\zeta\bar{\zeta}})\|_{\mathbb{R}^{2+1}} \cdot \ell^{-2}$. Ainsi, lorsque ϑ est lisse, la limite d'échelle du modèle peut alors s'exprimer somme solution d'équation de Dirac massive dont la masse admet une interprétation complètement géométrique vis-à-vis de la surface $(z, \vartheta) \subset \mathbb{R}^{2,1}$ dans l'espace de Minkowski.

— Sans hypothèse de régularité supplémentaire sur la limite des fonctions d'origami ϑ, il n'est pas possible de définir de dérivées secondes de la fonction ϑ et ainsi de notion de courbure moyenne. Cependant, la fonction $f(\zeta)$ satisfait tout de même l'équation de Beltrami conjuguée

$$\overline{f}_\zeta = \frac{\overline{\vartheta_\zeta}}{z_\zeta} f_\zeta. \tag{1.7.26}$$

— Sans hypothèse de régularité sur la limite des fonctions d'origami ϑ, la fonction $g(\zeta)$ satisfait de son côté l'équation de Beltrami conjuguée

$$g_{\bar{\zeta}} = -\frac{\overline{\vartheta_\zeta}}{z_\zeta} \overline{g_\zeta}. \tag{1.7.27}$$

Comme g est la primitive d'une forme différentielle continue, elle hérite d'une certaine régularité et on peut en particulier conclure que g ressemble a une fonction holomorphe, via le théorème de factorisation de Stoïlow (voir par exemple [3, eq.(2.27)]). L'existence d'une factorisation de ce type n'est pas automatique pour f, puisqu'il est nécessaire d'avoir un contrôle a priori sur le comportement des dérivées de f.

Une des conséquences de ces remarques sur la description de la limite d'échelle dans le continu est qu'il devient plus naturel de plonger le graphe $\mathcal{S}^\delta$ dans l'espace $\mathbb{R}^{2,1}$ sous forme d'une surface linéaire par morceaux $(\mathcal{S}^\delta, \mathcal{Q}^\delta) \subset \mathbb{R}^{2,1}$, qui correspond au relèvement de $\mathcal{S}^\delta$ dans l'espace avec pour troisième coordonnée la fonction d'origami $\mathcal{Q}^\delta$. La convergence de $\mathcal{Q}^\delta$ vers ϑ revient à la convergence des surfaces discrètes $(\mathcal{S}^\delta, \mathcal{Q}^\delta)$ vers $(z, \vartheta(z))$.

1.8 . Résultats de convergence déjà connus

On rappelle à présent l'ensemble des résultats de convergence sur le modèle d'Ising critique et presque critique utilisant le formalisme des observables fermioniques sur les domaines bornés. Comme rappelé au début de la section 1.5.1, le formalisme de Kadanoff et Ceva permet d'unifier la construction de toutes les observables utilisées jusqu'aujourd'hui pour prouver des résultats de convergence sur les grilles isoradiales équipées de leurs poids Z-invariants critiques et massifs, ainsi que sur les grilles doublement périodique. On liste à présent tous ces résultats de manière détaillée, en précisant lorsque cela est possible à quel corrélateur de Kadanoff-Ceva correspond l'observable utilisée (observable qui est par ailleurs très souvent écrite dans les articles en question sous forme purement combinatoire).

1. Convergence et invariance conforme sur le réseau carré critique de l'observable FK et de l'interface FK-Ising vers SLE(16/3) par Smirnov dans [162, 160]. Il s'agit de la première preuve rigoureuse d'invariance conforme du modèle d'Ising, dans un article fondateur qui a poussé à utilisation extensive des observables. C'est dans cet article que la fonction H^δ définie dans $(1.5.14)$ est introduite pour passer à la limite d'échelle. L'observable utilisée correspond au corrélateur $\mathbb{E}[\chi_c \sigma_{(ba)^\circ} \mu_{(ab)^\bullet}]$, qui est une fonction du coin c et les coins a et b sont fixés au bord du domaine comme dans la figure 1.5.4. Cette preuve a ensuite été étendue pour l'interface Spin-Ising convergeant vers SLE(3) dans [49], en utilisant une partie de la technologie développée par Kemppainen et Smirnov sur le comportement de l'interface au voisinage de sa trace [97, 96]. Pour ce second résultat, l'observable utilisée est de la forme $\mathbb{E}[\chi_c \chi_b]\mathbb{E}[\chi_a \chi_b]^{-1}$ où a est le point source et b la cible.
2. Convergence, invariance conforme et universalité de l'observable FK sur les grilles isoradiales par Chelkak et Smirnov [48]. Dans cet article, les méthodes d'analyse complexe discrète développées dans [47] sont appliquées au modèle d'Ising, avec une étude détaillée du comportement de la fonction H^δ au

bord du domaine. Il est aussi démontré la convergence des probabilités de connexion [48, Section 6] vers une limite invariante conforme, dont il existe un expression exacte sur le disque. L'observable utilisée correspond à nouveau au corrélateur $\mathbb{E}[\chi_c \sigma_{(ba)^\circ} \mu_{(ab)^\bullet}]$.

3. Convergence et covariance conforme de la densité d'énergie normalisée $\delta^{-1}\mathbb{E}_\Omega[\sigma_{e^+}\sigma_{e^-} - 2^{-\frac{1}{2}}]$ sur le réseau carré critique par Smirnov et Hongler dans [87], avec identification de sa limite via la métrique hyperbolique. Ce papier est complété par la thèse d'Hongler [83] où est prouvée la convergence du produit d'un nombre arbitraire de densités d'énergie grâce aux règles de Pfaffien (voir e.g. [37, Proposition 1.3]). L'observable utilisée correspond au corrélateur $\mathbb{E}[\chi_c \chi_a]$ dont la singularité est identifiée grâce à la fonction de couplage de Kenyon introduite dans [98]. Cette preuve s'étend directement aux grilles isoradiales avec angles bornés.

4. Convergence des spineurs-holomorphes sur des revêtement à deux feuillets de domaines simplement et multiplement connectés par Chelkak et Izyurov [41]. La normalisation des spineurs est faite par un facteur inconnu $\beta(\delta)$ (Thm 1) et permet de prouver la convergence du ratio entre corrélations avec des conditions de bord différentes (Corollaire B). L'observable introduite dans ce papier correspond à un corrélateur de la forme $\mathbb{E}_\Omega[\chi_c \mu_{v^\bullet} \sigma_{u_2^\circ} \dots \sigma_{u_p^\circ}]\mathbb{E}_\Omega[\mu_{v^\bullet} \sigma_{u_2^\circ} \dots \sigma_{u_p^\circ}]^{-1}$ et a aussi permis à Izyurov de prouver dans [92] que les interfaces multiples d'Ising convergent vers un processus invariant conforme.

5. Convergence et covariance conforme des corrélations $\delta^{-\frac{n}{8}}\mathbb{E}_\Omega[\sigma_{u_1} \dots \sigma_{u_n}]$ sur le réseau carré critique par Chelkak Hongler et Izyurov approximant un domaine simplement connexe du plan dans [38]. La normalisation explicite en volume infini [38, Theorème 1.2] est calculée grâce à l'asymptotique de la corrélation à deux points de McCoy et Wu rappelée dans $(1.2.17)$. Une des étapes cruciales dans cet article est la définition des corrélations continues, identifiées grâce à un contrôle très précis de la dérivée logarithmique des corrélations discrètes [38, Théorème 1.5]. Une formule explicite de la limite d'échelle sur $\mathbb{H}$ y est donnée [38, Remarque 1.4], confirmant les résultats prédits par la théorie conforme des champs. L'observable introduite dans ce papier correspond à un corrélateur de la forme $\mathbb{E}[\chi_c \mu_{v^\bullet} \sigma_{u_2^\circ} \dots \sigma_{u_n^\circ}]$.

6. Convergence et invariance conforme de la loi de l'ensemble des boucles macroscopiques séparant les clusters de spins opposés vers le processus CLE(3) par Benoist et Hongler [18] pour le modèle critique sur $\delta\mathbb{Z}^2$. Cet article utilise la caractérisation markovienne des CLE donnée par Werner et Sheffield [157], ainsi que la convergence d'un processus d'exploration nommé "Ensemble libre d'arcs", prouvée par Benoist, Duminil-Copin et Hongler [19]. Cette preuve donnée sur le réseau carré reste valide sur les grilles isoradiales avec des angles bornés.

7. Convergence des corrélations de spins $\delta^{-\frac{n}{8}}\mathbb{E}_\Omega[\sigma_{u_1}\dots\sigma_{u_n}]$ pour le réseau carré *massif* ($q=\frac{1}{2}m\delta$ sur $\sqrt{2}\delta\mathbb{Z}^2$) par Park [137], pour les domaines à bord lisse avec conditions de bord appropriées selon le signe de m. Cet article utilise un corrélateur de la forme $\mathbb{E}[\chi_c\mu_v\bullet\sigma_{u_2^\circ}\dots\sigma_{u_n^\circ}]$ en ajoutant une méthode de complexification des observables s-holomorphes massives via un losange virtuel. Park y définit et analyse aussi la limite d'échelle dans le continu des observables fermioniques (qui sont solutions de l'équation de Dirac $\overline{\partial}f+imf=0$) via le principe de similarité de Bers [138, Theorème 3.2] reliant les observables massives à leur analogues critiques.
8. Convergence de l'observable FK-Dobrushin avec des poids Z-invariants massifs *sans restriction sur le signe de la masse* m (à nouveau $q=\frac{1}{2}m\delta$ sur la grille de pas δ) sur les graphes isoradiaux avec des angles bornés approximant *les domaines aux bords arbitrairement irréguliers* par Park [138]. Ici la définition et l'unicité des observables dans le continu est un obstacle majeur, qui est contourné en utilisant un tiré en arrière vers un domaine lisse puis étudié en grâce à une invariance dans L^2 [138, Définition 3.10]. Les deux observables de cet article correspondant au corrélateurs $\mathbb{E}[\chi_c\sigma_{(ba)^\circ}\mu_{(ab)\bullet}]$ et $\mathbb{E}[\chi_c\sigma_{(ab)^\circ}\mu_{(bc)\bullet}]$ permettent aussi de prouver convergence des probabilités de connexion, qui dégénèrent vers le système hors-critique lorsque $|m|$ tend vers l'infini [138, Section 6].
9. Convergence de l'observable FK et de l'interface FK-Dobrushin vers SLE(16/3) sur les s-plongements qui vérifient $\textsc{Unif}(\delta)$ et $\mathcal{Q}^\delta=O(\delta)$ par Chelkak dans [33]. Cette preuve est la première preuve d'invariance conforme en dehors du cadre isoradial et prouve en particulier l'invariance conforme du modèle critique doublement périodique. La convergence de l'observable FK est quantitative en δ et permet de donner la vitesse de convergence de l'interface vers SLE(16/3) en utilisant les travaux de Binder et Richards [151]. L'observable utilisée correspond au corrélateur $\mathbb{E}[\chi_c\sigma_{(ba)^\circ}\mu_{(ab)\bullet}]$.
10. Calcul explicite de la longueur de corrélation par Beffara et Duminil-Copin [14, Théorème 2], en approximant le comportement des observables de Smirnov hors criticalité par des fonctions de Green massives [14, Proposition 4.1]. L'approximation utilisée peut d'ailleurs être remplacée par une égalité grâce aux travaux récents de de Tilière [164, Corollaire 4.16] pour en retrouver une preuve plus courte. L'observable utilisée correspond à un corrélateur de la forme $\mathbb{E}[\chi_c\sigma_{(ba)^\circ}\mu_{(ab)\bullet}]$ sur une bande infinie.
11. Convergence des corrélations mixtes sur le réseau carré (produits arbitraires de spins, désordres, densité d'énergies (produit de spins voisins) proprement normalisés) par Chelkak Hongler et Izyurov dans [39]. Cet article donne une exposition complète des méthodes de convergence des corrélations et interfaces vers leur limite continue, et développe de manière détaillée les propriétés des corrélations dans le continu. Une des nouveautés importante de cet article est la preuve des règles de fusion, lorsque deux éléments se

rapprochent l'un de l'autre [39, Section 6].

12. Convergence et invariance conforme de l'interface FK quantique par Li dans [109]. Cet article introduit les observables pour le modèle quantique et prouve la convergence d'un analogue quantique du corrélateur $\mathbb{E}[\chi_c \sigma_{(ba)^\circ} \mu_{(ab)^\bullet}]$.

1.9 . Résultats obtenus dans cette thèse

On résume à présent de manière très brève les résultats obtenus dans cette thèse. Chaque sous-section correspondant ici à l'un des chapitres de cette thèse.

1.9.1 . Magnétisation du modèle d'Ising par tranche et polynômes orthogonaux

Dans cet article écrit en collaboration avec **Dmitry Chelkak** et **Clément Hongler**, on explore les liens entre les corrélations du modèles d'Ising, la théorie des polynômes orthogonaux, et la représentation des corrélation sous forme de déterminants Toeplitz+Hankel. En particulier, on fournit une approche moderne, simplifiée et alignée avec les méthodes actuelles de calcul de corrélations du modèle d'Ising.

On considère le modèle d'Ising sur le demi-plan gauche du réseau carré tourné de $\frac{\pi}{4}$ noté par $\mathbb{H}^\diamond$ (voire la figure 1.9.1). La mesure de probabilité en volume infinie sur $\mathbb{H}^\diamond$ est définie via une suite croissante de domaines recouvrant $\mathbb{H}^\diamond$, en imposant des conditions de bord $+$ à l'infini ainsi qu'à la colonne la plus à droite C_0. Toutes les constantes de couplage entre les colonnes C_{p-1} et C_p sont identiques et valent $x_p = \exp[-2J_p] = \tan\frac{1}{2}\theta_p$, avec $\theta_p \in (0, \frac{1}{2}\pi)$. On définit alors la magnétisation de la $(2m)^{\text{ème}}$ colonne par

$$M_m = M_m(\theta_1, \theta_2, \dots) \;:=\; \mathbb{E}^+_{\mathbb{H}^\diamond}[\,\sigma_{(-2m-\frac{1}{2},0)}\,], \tag{1.9.1}$$

ainsi que la matrice J (avec $\theta_0 := 0$ et $b_1 = \cos^2\theta_1 \cos^2\theta_2$) donnée par

$$J = \begin{bmatrix} b_1 & -a_1 & 0 & \dots \\ -a_1 & b_2 & -a_2 & \dots \\ 0 & -a_2 & b_3 & \dots \\ \dots & \dots & \dots & \dots \end{bmatrix} \qquad \begin{aligned} b_k &= \cos^2\theta_{2k-1}\cos^2\theta_{2k} \\ &\quad + \sin^2\theta_{2k-2}\sin^2\theta_{2k-1}\,, \\ a_k &= \cos\theta_{2k-1}\cos\theta_{2k}\sin\theta_{2k}\sin\theta_{2k+1}\,, \end{aligned} \tag{1.9.2}$$

dont la mesure spectrale est notée ν_J. On pose aussi $\mathrm{H}_m[\,\nu_J\,] := \det[\,\int_0^1 \lambda^{p+q}\nu_J(d\lambda)\,]_{p,q=0}^{m-1}$ le $m^{\text{ème}}$ déterminant de Hankel des moments de ν_J et P_m le projecteur orthogonal sur les m premières coordonnées de ℓ^2. On a alors le théorème suivant :

Theorème 1.9.1. Pour tout $\theta_1, \theta_2, \dots \in (0, \frac{\pi}{2})$ et $m \geq 1$,

$$M_m \;=\; \frac{\det P_m J^{1/2} P_m}{\prod_{k=1}^{2m}\cos\theta_k} \;=\; \frac{\mathrm{H}_m[\lambda^{1/2}\nu_J]}{(\,\mathrm{H}_m[\nu_J]\cdot\mathrm{H}_m[\lambda\nu_J]\,)^{1/2}}\,. \tag{1.9.3}$$

Le théorème précédent ainsi que sa preuvent permettent de décrire plusieurs faits remarquables à propos des liens profonds entre le modèle d'Ising et la théorie spectrale, dont on détaille maintenant plusieurs exemples :

1. Pour le modèle homogène $\theta_k = \theta$ pour tout $k \geqslant 1$, on voit que $\mathrm{supp}\nu_J = [\cos^2(2\theta), 1]$ si $\theta \leq \frac{\pi}{4}$ et $\mathrm{supp}\nu_J = \{0\} \cup [\cos^2(2\theta), 1]$ si $\theta > \frac{\pi}{4}$, ce qui pousse fortement à penser (même si cela ne suffit pas de manière stricto sensus pour en faire une preuve) que la valeur critique du modèle correspond à $\theta = \frac{\pi}{4}$, comme le montrent les résultats rappelés dans la section 1.1. Le modèle homogène est sur-critique lorsque $\theta > \frac{\pi}{4}$. En effet, dans ce cas là, on peut voir que M_m décroit exponentiellement en m en identifiant des vecteurs propres de racine carré de l'opérateur J qui décroissant exponentiellement vite vers le vecteur nul.

2. Pour le modèle doublement périodique équipé de poids critiques, la condition de criticalité (provenant de [52]) pour un système périodique de taille $2n$ se réécrit de manière très simple comme étant la condition $\prod_{k=1}^{2n} \tan\theta_k = 1$. Dans ce cadre là, on peut définir *la densité intégrée des états* de J, c'est à dire pour chaque $\lambda > 0$ (lorsque $N \to \infty$), le nombre de valeurs propres comprises entre 0 et λ pour la troncature de J à ses nN premières colonnes. On peut alors cacluler l'asymptotique lorsque $\lambda \to 0$ de la densité densité intégrée des états de J (au voisinage du bas du spectre admet) qui est de la forme $C_J \cdot \pi^{-1}\sqrt{\lambda}$, où C_J est *la longueur moyenne d'une période horizontale* du s-plongement canonique associé au modèle doublement périodique (et dont la construction est rappelée dans la section 1.7). Cela fait donc un lien entre la géométrie du s-plongement le spectre de l'opérateur J permettant d'exprimer la magnétisation.

3. On peut aussi appliquer le théorème 2.1.1 pour étudier un modèle homogène sous-critique à partir de la seconde colonne ($\theta_k = \theta < \frac{\pi}{4}$ pour tout $k \geq 2$) mais en autorisant la constante de couplage de la première colonne à être différente. Ceci se reformule directement comme traiter le cas d'un modèle homogène avec un *champ magnétique extérieur additionnel* $h = 2J_1$ (où $x_1 = \tan(\frac{\theta_1}{2}) = \exp[-2J_1]$) à la première colonne (qui interagit à sa gauche avec les conditions de bord $+$ de la colonne C_0). On peut alors traduire le résultat abstrait de $(2.1.1)$ de manière explicite des déterminants Toeplitz+Hankel. On commence par définir pour $z \in \mathbb{C}$

$$q := \tan\theta < 1\,, \qquad r := 1 - \frac{\cos^2\theta_1}{\cos^2\theta} \in (-q^2; 1)\,,$$
$$w(z) := |1 - q^2 z|\,, \qquad \xi(z) := \frac{(rz - q^2)(q^2 z - 1)}{(z - q^2)(q^2 z - r)}\,. \tag{1.9.4}$$

On a alors le théorème suivant.

Theorème 1.9.2. Pour le modèle avec un champ magnétique extérieur introduit précédemment, on a

$$M_m \;=\; (1-r)^{-3/2} \det\left[\,\alpha_{k-n} - \beta_{k+n} + (1-r)^{3/2}\gamma_{k+n}\,\right]_{k,n=0}^{m-1}, \text{avec} \tag{1.9.5}$$

$$\alpha_s := \frac{1}{2\pi}\int_{-\pi}^{\pi} e^{-is\theta} w(e^{i\theta})d\theta\,, \qquad \beta_s := \frac{1}{2\pi}\int_{-\pi}^{\pi} e^{-is\theta}\xi(e^{i\theta})w(e^{i\theta})d\theta,$$

et $\gamma_s := c\cdot(q^2/r)^s$, $c = (r^2-q^4)r^{-3/2}(r-q^4)^{-1/2}$, si $r > q^2$ et $\gamma_s := 0$ sinon.

4. Il est alors possible de passer à la limite $r \to 1^-$, ce qui correspond à choisir un champ magnétique extérieur $J_1 \to 0^+$ et donne un modèle avec conditions de bord *libres* (c'est à dire que la constante de couplage choisie à la première colonne découple l'intérieur des conditions de bord $+$ à la conne C_0. La magnétisation de la première colonne devient alors

$$\mathbb{E}^{+,0}_{\mathbb{H}^\diamond}[\sigma_{(-\frac{5}{2},0)}] \;=\; (1-q^4)^{1/2}.$$

   Cette formule peut paraître surprenante lorsque $h = 0$, puisqu'avec des conditions de bord *libres* à la colonne C_0, on a toujours une magnétisation strictement positive à la première colonne, et n'est pas invariante par inversion des spins (sinon la magnétisation serait nulle). Cette absence de symétrie s'explique par le fait les conditions de bord à *l'infini* se transportent jusqu'à l'origine en cassant la symétrie du modèle.

5. Il est aussi possible, en suivant les travaux de [146], d'étendre analytiquement la formule $(1.9.5)$ aux valeurs *négatives* de $(1-r)^{1/2}$, faisant apparaître un *effet de mouillage* pour les valeurs négatives suffisamment petites de champ extérieur $-h$. L'intuition physique derrière le fait que la magnétisation reste positive pour des petites valeurs du champ extérieur $-h$ est que l'interface des $+$ à l'infini touche infiniment souvent l'axe vertical $i\mathbb{R}$ dont les spins sont ultra-majoritairement négatifs à cause du champ extérieur et la magnétisation positive du modèle provenant de l'infini reste dominante. L'étude mathématique complète et rigoureuse de cet effet de mouillage reste une question ouverte.

On détaille à présent la méthode utilisée pour prouver ces résultats. L'idée principale pour prouver ces résultats est *d'interpréter* sur le réseau en zig-zag les relations locales des corrélateurs Kadanoff-Ceva données par $(1.5.6)$ sous la forme d'équations de *Cauchy-Riemann discrètes*, qui se traduisent directement dans les entrées d'un opérateur en dimension infinie. La méthode utilisée est la suivante :

1. On identifie les relations locales d'une observable de Kadanoff-Ceva bien choisie afin que sa valeur au voisinage de son branchement soit exactement la magnétisation M_m.
2. On traduit ces relations locales dans le langage des transformations de Hilbert discrètes et prouve qu'un seul opérateur non-trivial vérifie toutes ces relations.
3. On reconstruit *à la main* cet opérateur via des techniques de transformées de Hilbert.

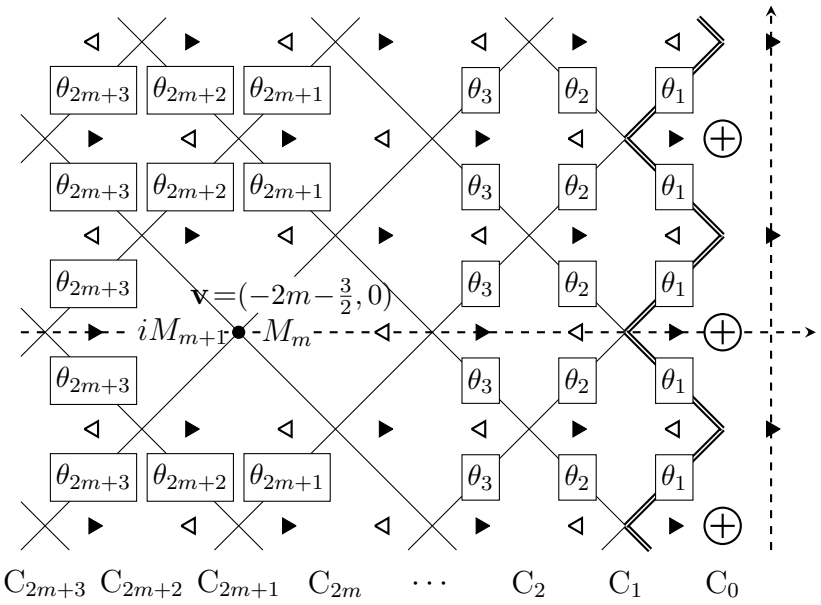

FIGURE 1.9.1 – Le modèle par couches en zig-zag sur le demi-plan gauche $\mathbb{H}^\diamond$. Toutes les interactions entre colonnes voisines sont les mêmes et la condition de bord + est imposée à la colonne C_0.

Il est remarquable de voir que la méthode générale utilisée (reconstruction explicite de corrélateurs de Kadanoff-Ceva à travers leurs relations locales) s'avère fonctionner non seulement sur le demi-plan mais fournit aussi des idées pour calculer la magnétisation sous-critique et la corrélation horizontale à deux points du modèle homogène $\mathbb{Z}^2$ (avec pour constante de couplage θ^v pour les arêtes verticales et θ^h les arêtes horizontales). Bien que les deux théorèmes suivants n'ait pas de lien avec le théorème , il est possible de réaliser à nouveau une réécriture des relations locales de corrélateurs de Kadanoff-Ceva, cette fois via des méthodes de transformée de Fourier, pour déduire deux preuves alternatives des résultats classiques suivants :

Theorème 1.9.3 (**Kauffman–Onsager–Yang**). Lorsque $\theta^{\mathrm{h}}+\theta^{\mathrm{v}} < \frac{\pi}{2}$, la magnétisation spontanée $\mathcal{M}(\theta^{\mathrm{h}},\theta^{\mathrm{v}})$ du modèle homogène sous-critique est donnée par

$$\mathcal{M}(\theta^{\mathrm{h}},\theta^{\mathrm{v}}) \ := \lim_{n\to\infty} D_n^{1/2} \ = \ \left[1-(\tan\theta^{\mathrm{h}}\tan\theta^{\mathrm{v}})^2\right]^{1/8}. \tag{1.9.6}$$

Theorème 1.9.4 (**McCoy–Wu**). Lorsque $\theta^{\mathrm{h}}+\theta^{\mathrm{v}}=\frac{\pi}{2}$, la corrélation D_m du modèle critique entre deux spins à une distance horizontale $2m$ l'un de l'autre a pour asymptotique

$$D_m \underset{m\to\infty}{\sim} \mathcal{C}_\sigma^2\cdot(2m\cos\theta)^{-1/4}, \text{ avec } \mathcal{C}_\sigma := 2^{\frac{1}{6}}e^{\frac{3}{2}\zeta'(-1)}. \tag{1.9.7}$$

1.9.2 . Universalité du modèle d'Ising sur les graphes isoradiaux

Dans cet article écrit en collaboration avec **Dmitry Chelkak** et **Konstantin Izyurov**, on prouve l'existence d'une limite d'échelle pour les corrélations de spins critiques et massives sur *toutes* les grilles isoradiales satisfaisant la propriété d'angles bornés. Ce résultat est en accord avec la prédiction de Kadanoff et termine de prouver *l'universalité* du modèle sur les graphes isoradiaux, c'est à dire que la limite d'échelle ne dépend pas de la géométrie locale du graphe. Comme rappelé dans la section 1.8, cette universalité était déjà connue dans le cadre critique pour les interfaces, ensembles de boucles, probabilités de croisement, convergence de l'observables FK ainsi que celle de la densité d'énergie. Dans les résultats mentionnés dans la phrase précédente, ce sont *les preuves* qui assuraient l'universalité du modèle, puisqu'elles s'appliquent exactement comme sur le réseau carré. La situation pour les corrélations critiques et massives entre spins (traitées sur le réseau carré par Chelkak Hongler Izyurov puis Park [38, 137]) est bien différente et deux obstacles importants subsistent :

1. Les méthodes utilisées sont intimement reliées aux symétries du réseau carré, en particulier la construction des analogues discrets s-holomorphes de $z^{\pm\frac{1}{2}}$ [38, Section 3.2].
2. La normalisation en volume infinie $\delta^{\frac{n}{8}} C_\sigma^n$ provient du calcul explicite de McCoy et Wu $(4.3.8)$ de la corrélation à deux points sur le réseau carré en volume infini. Ce calcul ne peut être répété pour un réseau irrégulier.

Notre article répond à ces deux questions et conclut à l'universalité du modèle d'Ising critique et presque critique sur les graphes isoradiaux. Étant donné une suite $(\Gamma^\delta)_{\delta>0}$ de grilles isoradiales de pas respectifs δ satisfaisant l'hypothèse des angles bornés pour un certain θ_0, on s'intéresse à la *limite d'échelle massive* du modèle d'Ising Z-invariant (défini dans la section 1.3.1), assignant des spins aux faces de $\Gamma^{\circ,\delta}$ avec un *nome* $q = \frac{1}{2}m\delta$ qui tend linéairement vers 0 lorsque δ tend vers 0. Le paramètre $m \in \mathbb{R}$ est appelé la *masse* du modèle, le modèle critique correspondant au cas $m = 0$. Pour le modèle en volume infini, il existe alors une limite d'échelle pour les corrélations à deux points. Plus précisément on a le théorème suivant :

Theorème 1.9.5. Pour chaque $m \in \mathbb{R}$, il existe une fonction $\Xi(\cdot, m) : \mathbb{R}_+ \to \mathbb{R}_+$ telle que dans le régime $q = \frac{1}{2}m\delta \to 0$ on a

$$\delta^{-\frac{1}{4}} \mathbb{E}^{(m)}_{\Gamma^{\circ,\delta}}[\sigma_{u_1}\sigma_{u_2}] \;\to\; \mathcal{C}_\sigma^2 \cdot \Xi(|u_2 - u_1|, m) \;\text{ lorsque }\; \delta \to 0\,, \tag{1.9.8}$$

où la constante $\mathcal{C}_\sigma = 2^{\frac{1}{6}} e^{\frac{3}{2}\zeta'(-1)}$ est indépendante de la géométrie locale de Λ^δ et de la masse m. Pour le régime critique $m = 0$, on a $\Xi(r, 0) \equiv r^{-\frac{1}{4}}$ et plus généralement on a l'asymptotique $\Xi(r, m) \sim r^{-\frac{1}{4}}$ lorsque $r \to 0$, indépendamment de la valeur de la masse m.

Cela prouve en particulier *l'invariance par rotation du modèle*, des deux côtés de la criticalité (i.e. indépendamment du signe de m), ainsi qu'à petite distance

entre les spins, le système presque-critique se comporte comme le système critique. Il existe une expression explicite de $\Xi(r,m)$ en fonction de solutions aux équations de Painlevé III [166, 153, 94], dont une exposition moderne est rappelée par Park dans [137, Corollaire 1.2 et Section 4.2]. Afin de prouver le résultat sur la limite d'échelle dans le plan tout entier (ce résultat est mis en avant le premier ici car il nous semble être le résultat le plus conceptuel du chapitre 3, étant valide quelque soit le signe de la masse m), on commence par prouver l'universalité des corrélations sur les domaines simplement connexes bornés (à bord lisse) du plan.

On commence par se donner un domaine simplement connexe Ω dont le bord est $\mathcal{C}^1$, que l'on approxime au sens de Carathéodory (voir e.g. [47, Définition 3.4]) par un domaine discret Ω^δ. On définit alors le modèle d'Ising *massif* avec des poids Z-invariant de Baxter avec un nome $q = \frac{1}{2}m\delta$ sur Ω^δ, dont les conditions de bord sont branchées. Notre résultat généralise aux grilles isoradiales la convergence des corrélations prouvée dans [38, Théorème 1.2] lorsque $m = 0$ et dans [137, Théorème 1.1] lorsque $m < 0$.

Theorème 1.9.6. En travaillant sur le modèle Z-invariant sur les grilles isoradiales de nome $q = \frac{1}{2}m\delta$ et en fixant n spins approximant respectivement n points de Ω (supposé à bord lisse), on a alors pour $m \leqslant 0$ la convergence des corrélations entre les n spins qui est donnée par

$$\delta^{-\frac{n}{8}}\mathbb{E}^{(m),\mathrm{w}}_{\Omega^\delta}[\sigma_{u_1}\sigma_{u_2}\dots\sigma_{u_n}] \;\to\; \mathcal{C}^n_\sigma\cdot\langle\sigma_{u_1}\sigma_{u_2}\dots\sigma_{u_n}\rangle^{(m),\mathrm{w}}_{\Omega} \quad \text{lorsque} \quad \delta\to 0$$

avec des fonctions de corrélation continues $\langle\sigma_{u_1}\sigma_{u_2}\dots\sigma_{u_n}\rangle^{(m),\mathrm{w}}_{\Omega}$ qui sont définies exactement comme dans [38, 137]. Cette convergence est *universelle* vis-à-vis de la géométrie locale des graphes isoradiaux.

L'idée principale pour prouver le Théorème 1.9.6 a été introduite dans [38, Théorème 1.5 et Corollaire 1.6] consiste à obtenir un contrôle très précis de la dérivée logarithmique des corrélations, c'est à dire de déterminer une asymptotique de la forme

$$\log\frac{\mathbb{E}^{(m),\mathrm{w}}_{\Omega^\delta}[\sigma_{u_1'}\cdots\sigma_{u_n}]}{\mathbb{E}^{(m),\mathrm{w}}_{\Omega^\delta}[\sigma_{u_1}\cdots\sigma_{u_n}]} \;=\; \mathrm{Re}\left[(u_1'-u_1)\mathcal{A}^{(m)}_{\Omega}(u_1,\dots,u_n)\right]+o(\delta), \qquad (1.9.9)$$

et pousse à définir la corrélation continue par

$$\langle\sigma_{u_1}\sigma_{u_2}\dots\sigma_{u_n}\rangle^{(m),\mathrm{w}}_{\Omega} \;:=\; \exp\int \mathrm{Re}\left[\textstyle\sum_{s=1}^n \mathcal{A}^{(m)}_{\Omega}(u_s,u_1,\dots,u_{s-1},u_{s+1},\dots,u_n)du_s\right],$$

avec un coefficient $\mathcal{A}^{(m)}_{\Omega}$ provenant de l'expansion de la limite d'échelle des observables fermionique au voisinage de l'un de leurs branchements [38, eq (2.13)]. Pour obtenir $(1.9.9)$, on introduit une méthode conceptuelle et abstraite, qui reconstruit la valeur du corrélateur $c\mapsto\mathbb{E}^{\mathrm{w}}[\chi_c\mu_v\sigma_{u_2}\dots\sigma_{u_n}]$ via son intégrale discrète contre un noyau de Cauchy discret (construit à la main en utilisant les *exponentielles discrètes* introduites par Boutillier, deTilière et Raschel dans [27, 28]). En particulier

cette méthode brise la nécessité de symétrie et s'applique en théorie à un cadre plus général.

Reste pour conclure à résoudre l'épineuse question de la normalisation en volume infini et montrer son universalité. Cela est fait en remarquant qu'il est possible d'étendre une partie finie d'une grille isoradiale en lui recollant une partie d'un réseau rectangulaire (où les résultats sont obtenus par des calculs explicites) et que sur cette grille mixte, les corrélations sont (au moins asymptotiquement) identiques. En particulier, ces méthodes utilisées s'appliquent aussi au modèle sous-critique. En utilisant une formule de Cauchy analogue ainsi que les résultats exacts sur les grilles rectangulaires (qui sont redémontrés dans le chapitre 2), nous donnons une preuve complète de la formule de Baxter sur les graphes isoradiaux.

Proposition 1.9.1 (Formule de Baxter)**.** Pour $q < 0$, la magnétisation en volume infini du modèle Z-invariant sous-critique est donnée par

$$\mathbb{E}^{+}_{\Omega_n}[\sigma_u] \to (k^\star)^{\frac{1}{4}} \text{ lorsque } \Omega_n \uparrow \Gamma^\circ \quad \text{et} \quad \mathbb{E}_{\Gamma^\circ}[\sigma_{u_1}\sigma_{u_2}] \to (k^\star)^{\frac{1}{2}} \text{ lorsque } |u_1 - u_2| \to \infty,$$

où le lien entre les paramètres elliptiques q et k est rappelé dans la section 1.3.1.

Le modèle massif Z-invariant peut aussi être encapsulé dans la théorie des s-plongements rappelée dans la section 1.7. En effet, il est possible de construire à partir des exponentielles discrètes associées au modèle massif Z-invariant un s-plongement $\mathcal{S}^\delta$ *propre* du plan (au moins sur les compacts lorsque $\delta \to 0$). Dans le régime $q = \frac{1}{2}m\delta$, la surface $(\mathcal{S}^\delta, \mathcal{Q}^\delta) \subseteq \mathbb{R}^{2,1}$ *converge* vers une surface de *courbure moyenne* proportionelle à la masse m. Autrement dit, cela fournit *une interprétation géométrique de la longueur de corrélation* du modèle massif comme la courbure moyenne d'une surface dans $\mathbb{R}^3$. Une explication détaillée de ce phénomène est faire dans la section 3.3 du chapitre 3.

1.9.3 . Invariance conforme du modèle d'Ising quantique

Dans cet article écrit en collaboration avec **Jhih-Huang Li**, on prouve l'invariance conforme du modèle d'Ising quantique critique introduit dans la section 1.6. Comme précisé à la fin des rappels sur le modèle quantique, la loi de la représentation spatio-temporelle du modèle quantique est la limite des lois sur des grilles isoradiales de plus en plus aplaties, pour lesquelles la propriété des angles bornés n'est alors plus vérifiée. Il est donc vraisemblable de penser que les résultats de convergence des corrélations du modèle survivent à l'échange de limite entre angles bornés et le passage à la limite $\delta \to 0$. Un premier résultat dans cette direction a été prouvé par Jhih-Huang Li dans [109] et concerne la convergence de l'interface du modèle FK quantique vers SLE(16/3)

On se donne à nouveau un domaine simplement connexe Ω du plan approximé par $\Omega^\bullet_\delta$ et on considère la représentation spatio-temporelle du modèle *critique* avec paramètres $\theta = \theta^\star = 2\tau = \frac{1}{2\delta}$. Le premier résultat de notre article généralise la

convergence de la densité d'énergie horizontale traitée par Hongler et Smirnov [87, 83] sur les grilles isoradiales. On a alors le théorème suivant.

Theorème 1.9.7. Soit $a \in \Omega$ un point intérieur approximé par $a^\delta \in \Omega^\bullet_\delta$. On définit alors la variable aléatoire de *densité d'énergie normalisée* par la formule
$\varepsilon_{a^\delta} := \sigma_{a^\delta}\sigma_{a^\delta+2\delta} - \mathbb{E}^+_{\mathbb{C}_\delta}[\sigma_{a^\delta}\sigma_{a^\delta+2\delta}] = \sigma_{a^\delta}\sigma_{a^\delta+2\delta} - \frac{2}{\pi}$. Pour la représentation spatio-temporelle du modèle d'Ising quantique, on a alors la convergence

$$\tfrac{1}{\delta}\,\mathbb{E}^+_{\Omega^\bullet_\delta}[\varepsilon_{a^\delta}] \underset{\delta\to 0}{\longrightarrow} \tfrac{1}{\pi}\ell_\Omega(a), \tag{1.9.10}$$

où $\ell_\Omega(a)$ est la métrique hyperbolique de Ω en a (i.e. $\ell_\Omega(a)$ est *le double* du module de la dérivée en a de n'importe quelle uniformisation de Ω vers $\mathbb{D}$ s'annulant en a). Plus généralement pour des points intérieurs $a_1, \dots, a_n \in \Omega$ de Ω respectivement approximés par $a_1^\delta, \dots, a_n^\delta$, on a la convergence

$$\tfrac{1}{\delta^n}\,\mathbb{E}^+_{\Omega^\bullet_\delta}[\varepsilon_{a_1^\delta}\dots\varepsilon_{a_n^\delta}] \underset{\delta\to 0}{\longrightarrow} \langle\varepsilon_{a_1}\dots\varepsilon_{a_n}\rangle^+_\Omega, \tag{1.9.11}$$

où une corrélation continue $\langle\varepsilon_{a_1}\dots\varepsilon_{a_n}\rangle^+_\Omega$, définie dans [32, Théorème 4.4], est covariante conforme (voir e.g. [39, Section 5]).

La valeur $\frac{2}{\pi}$ de la densité d'énergie horizontale du modèle quantique en volume infini correspond bien à la limite de la densité d'énergie horizontale sur les grilles isoradiales avec un angle $\theta_e = \frac{\pi}{2} - \varepsilon$, qui vaut $\frac{2\varepsilon}{\pi\cos(\frac{\pi}{2}-\varepsilon)}$ [24, Corollaire 11]. Comme pour le cas classique, il suffit de prouver le résultat pour une seule variable d'énergie en a^δ et propager le résultats en utilisant les règles de Pfaffien du modèle d'Ising (voir e.g. [39, Section 2.4] pour une présentation complète). Notre second résultat prouve la convergence des corrélations (pour le modèle critique) entre un nombre arbitraire de spins fixés dans un domaine simplement connexe, généralisant le travail réalisé sur le réseau carré par Chelkak Hongler et Izyurov dans [38] (mais aussi le théorème 1.9.6). Dans ce cadre-là on a alors

Theorème 1.9.8. Soient $a_1, \dots, a_n$ des points intérieurs de Ω approximés par $a_1^\delta, \dots, a_n^\delta$ dans $\Omega^\bullet_\delta$. Pour le modèle avec conditions de bord $+$, on a alors

$$\delta^{-\frac{n}{8}}\,\mathbb{E}^+_{\Omega^\bullet_\delta}[\sigma_{a_1^\delta}\dots\sigma_{a_n^\delta}] \underset{\delta\to 0}{\longrightarrow} \mathcal{C}^n\langle\sigma_{a_1}\dots\sigma_{a_n}\rangle^+_\Omega, \tag{1.9.12}$$

où la fonction de corrélation $\langle\sigma_{a_1}\dots\sigma_{a_n}\rangle^+_\Omega$ est covariante conforme et correspond exactement à la corrélation critique pour $m = 0$ dans le Théorème 1.9.6.

Ce résultat prouve directement *l'invariance par rotation* du modèle quantique critique. Il est possible de généraliser ces convergences à d'autres conditions de bord. Dans notre article, la méthode choisie consiste à travailler directement avec une version quantique des corrélateurs de Kadanoff et Ceva pour prouver les résultats de convergence directement sur le réseau semi-discret. En particulier, la

structure de branchement devient un problème très sensible, car les corrélateurs naturellement définis branchent *partout*. Ainsi la preuve de convergence peut s'apparenter à une généralisation standard des arguments sur les grilles isoradiales une fois que le formalisme de Kadanoff et Ceva a été correctement introduit. La situation est en revanche bien plus délicate pour la convergence des corrélations entre spins. Le contrôle de la dérivée logarithmique des corrélations discrètes, comme dans nos travaux avec Chelkak et Izyurov, ne s'applique que dans la direction *horizontale*. Pour obtenir la dérivée dans la direction verticale, on utilise cette fois-ci la structure locale du branchement autour de chaque point du réseau semi-discret ainsi qu'une *généralisation au modèle quantique de la relation à trois termes* (1.5.7), sous forme d'intégrale. L'intérêt principal des théorèmes 1.9.7 et 4.3.7 va au-delà de la simple généralisation de la convergence des corrélations à un modèle associé du modèle d'Ising. En effet, comme expliqué dans la section 1.6, la représentation spatio-temporelle du modèle d'Ising quantique correspond à l'évolution spatio-temporelle d'une chaîne de spins sur $\mathbb{Z}$, dont le Hamiltonien quantique est donné par $\mathbf{H} = -\theta \sum_{x\sim y} \sigma_x^{(3)}\sigma_y^{(3)} - \tau \sum_{x\in V} \sigma_x^{(1)}$. On peut donc utiliser les résultats des théorèmes 1.9.7 et 4.3.7 pour déterminer *des formules explicites des corrélations spatio-temporelles* lorsque $\Omega = \mathbb{H}$. On note $\mathbb{E}_{\mathsf{QI}_\delta}$ la mesure de probabilité associée au modèle quantique critique sur $2\delta\mathbb{Z}$. On note $\sigma_{x^\delta}^{(t)}$ la variable du spin ± 1 au site x^δ au temps t dans la représentation graphique en dimension 2 de la chaîne d'Aizenmann, Klein et Newman [2]. On a alors les formules suivantes :

Theorème 1.9.9. Pour la chaine quantique unidimensionnelle sur $2\delta\mathbb{Z}$, on note $x_1, \dots, x_n$ des coordonnées horizontales approximées dans $2\delta\mathbb{Z}$ par $x_1^\delta, \dots, x_n^\delta$ ainsi que $t_1, \dots, t_n$ des temps positifs. Soit $\varepsilon_{x^\delta}^{(t)} := \sigma_{x^\delta}^{(t)}\sigma_{x^\delta+2\delta}^{(t)} - \frac{2}{\pi}$ la densité d'énergie horizontale au site x^δ au temps t. Si tous les spins sont alignés à la valeur $+1$ au temps $t = 0$, on a

$$\delta^{-\frac{n}{8}}\, \mathbb{E}^+_{\mathsf{QI}_\delta}[\sigma_{x_1^\delta}^{(t_1)} \dots \sigma_{x_n^\delta}^{(t_n)}] \underset{\delta\to 0}{\longrightarrow} \mathcal{C}^n \prod_{r=1}^n (\tfrac{2}{t_r})^{\frac{1}{8}} \Big(2^{-\frac{n}{2}} \sum_{\mu\in\{\pm1\}^n} \prod_{1\leqslant r<m\leqslant n} \Big|\tfrac{(x_r-x_m)^2+(t_r-t_m)^2}{(x_r-x_m)^2+(t_r+t_m)^2}\Big|^{\frac{\mu_r\mu_m}{4}}\Big)^{\frac{1}{2}}, \tag{1.9.13}$$

$$\tfrac{1}{\delta^n}\, \mathbb{E}^+_{\mathsf{QI}_\delta}[\varepsilon_{x_1^\delta}^{(t_1)} \dots \varepsilon_{x_n^\delta}^{(t_n)}] \underset{\delta\to 0}{\longrightarrow} (\tfrac{2}{i\pi})^n \mathrm{Pfaff}[\mathbb{K}(x_1+\mathrm{i}\,t_1, \dots, x_n+\mathrm{i}\,t_n, x_1-\mathrm{i}\,t_1, \dots, x_n-\mathrm{i}\,t_n)],$$

où Pfaff représente l'opérateur de Pfaffien usuel et $\mathbb{K}(a_1, \dots, a_r)$ est la matrice $r \times r$ définie par $\mathbb{K}_{i,j} := \mathbf{1}_{i\neq j}(a_i - a_j)^{-1}$.

La normalisation des corrélations est à nouveau reliée à l'asymptotique de la corrélation à deux points en volume infini, que l'on retrouve *directement sur le réseau semi-discret*, en adaptant le formalisme du chapitre 2 au modèle quantique. On peut alors calculer pour la magnétisation sous-critique ainsi que la longueur de corrélation sur-critique. Ce second résultat, correspondant à un cas particulier traité par Beffara et Duminil-Copin dans [14] concernant la direction horizontale, et utilise des méthodes supplémentaires comparé à celles utilisées dans le chapitre 2. On a alors les théorèmes suivants :

Theorème 1.9.10. Pour la représentation spatio-temporelle du modèle d'Ising quantique sur $\mathbb{C}$ avec un jeu de paramètres sous-critique ($\theta < \theta^\star$) et des conditions de bord + à l'infini, la magnétisation spontanée est donnée par

$$\mathcal{M}(\theta, \theta^\star) \ := \lim_{n\to\infty} \mathbb{E}^+_{\mathbb{C}}[\sigma_0\sigma_n]^{1/2} \ = \ (\theta^2 + \theta^{\star 2})^{-\frac{1}{2}}(1 - (\tfrac{\theta}{\theta^\star})^2)^{\frac{1}{8}}. \qquad (1.9.14)$$

Theorème 1.9.11. Pour la représentation spatio-temporelle du modèle d'Ising quantique sur $\mathbb{C}$ avec un jeu de paramètres sur-critique ($\theta > \theta^\star$) la longueur de corrélation horizontale ξ est donnée par

$$\xi := \lim_{n\to\infty} -\tfrac{1}{n} \log \mathbb{E}^+_{\mathbb{C}_1}[\sigma_0\sigma_n] = \tfrac{1}{2}\log(\tfrac{\theta}{\theta^\star}). \qquad (1.9.15)$$

1.9.4 . Estimées de croisement sur les s-plongement généraux

Dans cet article, écrit seul, on prouve que la représentation FK du modèle d'Ising sur un s-plongement général et dont les poids sont donnés par (1.7.4) satisfait la propriété croisement usuelle sur les rectangles, comme pour le réseau carré critique (voir e.g. [60, Section 5]). Ce résultat montre que les s-plongements non-dégénérés à grande échelle et équipés de leur poids naturels correspondent à des systèmes 'critiques' et 'presque critiques', y compris lorsque leur géométrie locale est très irrégulière.

On commence ici par clarifier le cadre dans lequel on travaille. Soient $x_1 < x_2$, $y_1 < y_2$, $\mathcal{R} := (x_1, x_2) \times (y_1, y_2) \subset \mathbb{C}$ le rectangle associé, ainsi que U un ouvert contenant strictement $\mathcal{R}$. On se donne une suite $(\mathcal{S}^\delta)_{\delta>0}$ de une suite de s-plongements propres recouvrant U et vérifiant les hypothèses suivantes :

1. On suppose que tous les plongements $(\mathcal{S}^\delta)_{\delta>0}$ satisfont l'hypothèse $\textsc{Lip}(\kappa,\delta)$ pour un certain fixé $\kappa < 1$. En particulier, le pas δ de chacun des plongements est fixé grâce à la définition (1.7.3). Autrement dit, la de toutes les arêtes de $\mathcal{S}^\delta$ est plus petite que δ, et la fonction d'origami $\mathcal{Q}^\delta$ associée à $\mathcal{S}^\delta$ est κ-lipchitz au-delà de la distance δ.
2. On suppose que les plongements $(\mathcal{S}^\delta)_{\delta>0}$ satisfont l'hypothèse de non-dégénérescence que l'on nomme $\textsc{Lenght-Exp-Fat}(\delta)$,qui suppose que pour chaque boule $B \subset U$ et pour $\gamma > 0$:

$$\lim_{\delta\to 0} \sum_{z\in\diamondsuit\cap B, r_z\leqslant \exp(-\gamma\delta^{-1})} \mathsf{diam}(z) = 0.$$

   Autrement dit, une fois que le pas de chacun des plongements a été fixé, on demande que la mesure $\mathcal{H}^1$ de l'ensemble des faces exponentiellement petites en (en la variable δ^{-1}) tende vers 0 lorsque δ tend vers 0.

Pour utiliser ces hypothèses, il n'est plus nécessaire d'utiliser de notion *d'angles bornés* (qui implique que les constantes de couplages sont bornées) ou bien encore de comparabilité entre la taille des arêtes, mais plutôt nécessaire de vérifier si le

plongement admet un pas δ (défini dans la section 1.7.1 comme la distance à partir de laquelle fonction d'origami $\mathcal{Q}^\delta$ admet une constante de Lipchitz strictement meilleure que 1) puis qu'il n'y a qu'une proportion négligeable de faces du graphe pour lesquels le rayon r_z du cercle inscrit est exponentiellement petit en δ^{-1}. Les deux hypothèses précédentes sont vérifiées avec une marge énorme pour les graphes doublement périodiques critiques, ainsi que sur les graphes isoradiaux équipés de leurs poids critiques et massifs.

Pour se rapprocher de la formulation usuelle des estimées de croisement, reformulons les deux hypothèses précédentes dans le cadre classique d'un graphe infini. On se donne une $\mathcal{S}$ un s-plongement propre, dont on assume (quitte à renormaliser la taille du dessin dans le plan) qu'il est de pas $\delta = 1$. Toutes les arêtes de $\mathcal{S}(\Lambda(G))$ sont de longueur inférieure à 1. L'hypothèse $\textsc{Lip}(\kappa,\delta)$ se traduit le fait que $|\mathcal{Q}(z)-\mathcal{Q}(z')| \leqslant \kappa|z-z'|$ dès lors que $|z-z'| \geqslant 1$. Pour le seconde hypothèse, considérerons $\mathcal{B}_n$ l'approximation du carré centré en l'origine et de côté $2n$. Pour cela, l'hypothèse $\textsc{Lenght-Exp-Fat}(\delta)$ se traduit par le fait que pour tout $\gamma > 0$

$$\lim_{n\to\infty} \sum_{z\in\diamondsuit\cap\mathcal{B}_n, r_z\leqslant \exp(-\gamma n)} \mathsf{diam}(z) = o(n),$$

c'est à dire que les faces dont le centre cercle inscrit est de taille exponentiellement petite en n ne contribuent qu'à une partie négligeable de la boite.

Comme cela sera détaillé dans la preuve, il est possible d'affaiblir cette hypothèse en la remplacant par une condition demandant que les faces exponentiellement petites n'envahissent pas complètement toutes les zones de la boite de taille n. Dans les termes originaux, cela revient à relaxer l'hypothèse $\textsc{Lenght-Exp-Fat}(\delta)$ dans le théorème en ne demandant qu'elle ne soit vérifiée que sur portion (macrsocopique mais arbitrairement petite) du graphe.

On a alors les théorèmes suivants, que l'on peut voir comme des meta-théorèmes, c'est à dire une boîte à outils que l'on espère appliquer à une très grande variété de situations. Ces théorèmes sont *uniformes en* δ suffisament petit, et fournissent une borne inférieure à la magnétisation du modèle spin-Ising sur les rectangles avec conditions de bord alternées, ainsi qu'une borne inférieure sur la probabilité de croisement dans le modèle FK d'un anneau de ratio fixé avec condition de bord libre.

Theorème 1.9.12. Soient $x_1 < x_2$, $y_1 < y_2$, $\mathcal{R} := (x_1,x_2)\times(y_1,y_2) \subset \mathbb{C}$, et $(\mathcal{S}^\delta)_{\delta>0}$ une suite de s-plongements propres satisfaisant les hypothèses $\textsc{Lip}(\kappa,\delta)$ et $\textsc{Lenght-Exp-Fat}(\delta)$. On se donne alors $\mathcal{R}^\delta = [\mathcal{R}(x_1,x_2;y_1,y_2)]^{\circ\bullet\circ\bullet}_{\mathcal{S}^\delta}$ une discrétisation quelconque de $\mathcal{R}$ à une distance $o_{\delta\to0}(1)$ du bord de $\mathcal{R}$. Pour le modèle d'Ising sur $\mathcal{R}^\delta$ dont les poids sont donnés par (1.7.4), avec conditions de bord *branchées* sur les arcs 'horizontaux' $(b^\delta c^\delta)^\circ$ et $(d^\delta a^\delta)^\circ$ de $\mathcal{R}^\delta$ ainsi que des conditions de bord *libres* sur les arcs 'verticaux' $(a^\delta b^\delta)^\bullet$ et l'arc droit $(c^\delta d^\delta)^\bullet$, on a

$$\liminf_{\delta\to0} \mathbb{E}^{\circ\bullet\circ\bullet}_{\mathcal{R}^\delta}[\sigma_{(b^\delta c^\delta)^\circ}\sigma_{(d^\delta a^\delta)^\circ}] \;\geq\; \mathrm{cst} \;>\; 0,$$

où la constante $\mathrm{cst} > 0$ ne dépend que de κ et du ratio $|x_2 - x_1| \cdot |y_2 - y_1|^{-1}$.

Une estimée similaire existe pour le modèle dual. Comme rappelé dans la section 1.2.5, il existe une multitude de liens entre les corrélations des spins de modèle d'Ising et les probabilités de connexion dans le modèle FK. Un de ces liens s'avère être ici très utile. Pour $u \in \mathbb{C}$ et $d > 0$, on définit l'anneau

$$\square(u,d) \;:=\; ([\mathrm{Re}\, u - 3d, \mathrm{Re}\, u + 3d] \times [\mathrm{Im}\, u - 3d, \mathrm{Im}\, u + 3d]) \\ \smallsetminus ((\mathrm{Re}\, u - d, \mathrm{Re}\, u + d) \times (\mathrm{Im}\, u - d, \mathrm{Im}\, u + d))$$

et on pose $\mathbb{P}^{\mathrm{libre}}_{\square^\delta(u,d)}$ la mesure de probabilité associée au modèle FK rappelée dans la section 1.2.5 avec conditions de bord libre sur les frontières intérieures et extérieures de $\square^\delta(u,d)$, qui approxime à une distance $o_{\delta\to 0}(1)$ l'anneau $\square(u,d)$. On a alors le théorème suivant.

Theorème 1.9.13. Il existe une constante $p_0 > 0$ ne dépendant que de κ telle que pour tout $u \in \mathbb{C}$, $d > 0$, et toute suite de s-plongements $\mathcal{S}^\delta$ couvrant $B(u,5d)$ et vérifiant $\textsc{Lip}(\kappa,\delta)$ et $\textsc{Lenght-Exp-Fat}(\delta)$, on a

$$\liminf_{\delta\to 0} \mathbb{P}^{\mathrm{libre}}_{\square^\delta(u,d)}\big[\,\text{il existe un circuit ouvert dans } \square^\delta(u,d)\,\big] \;\geq\; p_0.$$

Une estimée similaire existe pour le modèle dual. De plus on peut remplacer la $\liminf$ par l'$\inf$ lorsque les s-plongements satisfont l'hypothèse $\textsc{Unif}(\delta)$. Dans la formulation classique des estimées de croisement pour le modèle FK sur une grille infinie (c'est à dire en considérant une grille infinie avec un pas $\delta = 1$ et les boites $\mathcal{B}_n$ lorsque $n \to \infty$), le théorème 1.9.13 implique que, la probabilité qu'il existe un circuit ouvert du modèle FK dans l'anneau bordé par les boites $\mathcal{B}_n$ et $\mathcal{B}_{3n}$ (avec des conditions de bord libres), est bornée inférieurement, lorsque $n \to \infty$, par une constante ne dépendant que de κ.

Ce second théorème est une conséquence du Théorème 1.9.12 en appliquant la stratégie développée dans [61, Proposition 2.10]. Une version simplifiée de ces résultats a été démontrée par Chelkak dans [33, Théorème 1.3 et Corollaire 1.4], avec des hypothèses beaucoup plus restrictives sur la géométrie locale (la preuve était limitée aux grilles satisfaisant l'hypothèse $\textsc{Unif}(\delta)$, ce qui limite les dégénérescences locales) mais surtout sous l'hypothèse $\textsc{Flat}(\delta)$ qui correspond à imposer $\mathcal{Q}^\delta = O(\delta)$, qui contraint la limite de la fonction d'origami à $\vartheta \equiv 0$ et limite les comportements potentiels des limites d'échelles. En particulier, il est à présent possible d'imaginer appliquer ces deux théorèmes aux grilles tirées aléatoirement, que ce soit dans leur combinatoire ou bien encore dans leur poids. Une des conséquences directe du Théorème 1.9.13 est la *tension* des interfaces FK-Ising sur les graphes satisfaisant $\textsc{Lip}(\kappa,\delta)$ et $\textsc{Lenght-Exp-Fat}(\delta)$ (voir e.g. [97] pour plus de détails). Parmi les conséquences directes de ce théorème 1.9.13, on trouve des preuves alternatives ainsi que l'extension des résultats suivants :

— Borne inférieure sur les estimées sur les probabilités de croisement sur les grilles isoradiales critiques (voir section 1.3.1) comme dans [48, Preuve du Théorème 6.1], en remplaçant la propriété d'angles bornés par l'hypothèse $\textsc{Lenght-Exp-Fat}(\delta)$. En particulier permet de déduire directement la propriété de croisement dans les rectangles pour le modèle FK quantique [62, Theorème 1.5 et Proposition 5.1].

— Borne inférieure sur les estimées sur les probabilités de croisement sur les grilles isoradiales *massives* (voir section 1.3.1) comme dans [138, Théorème 1.3] avec la propriété d'angles bornés, que l'on peut re-plonger comme un s-plongement *propre* en utilisant les méthodes de [43, eq (3.11)].

On peut aussi voir que la magnétisation du modèle d'Ising sur les *kites* introduit par Lis dans [114, Section 6] décroit polynômialement vite grâce au Théorème 1.9.13 et qu'à la température $\beta = 1$, la magnétisation du modèle primal et dual est simultanément nulle. Cela prouve en particulier la criticalité du modèle.

On rappelle qu'il est possible de construire un s-plongement propre pour chaque graphe pondéré fini, en particulier pour réseaux usuels non-critiques, ce qui indique que le théorème 1.9.13 n'est doit pas être valide pour tous les graphes pondérés. On explique maintenant celle phénomènologie, et spécifie (en utilisant deux exemples) ce qui nous semble classifier si le système est d'un côté presque-critique ou critique ou d'un autre côté hors critique.

L'exemple le plus simple est le réseau carré (tourné d'un angle $\frac{\pi}{4}$ pour coller au formalisme du chapitre 2) équipé de ses poids non-critiques. En utilisant les travaux détaillés dans la section 2.5 du chapitre 2, (particulièrement les formules en dessous de l'équation $(2.5.5)$ ainsi que la figure $2.5.1$), on peut voir qu'il est possible d'associer au réseau carré équippé de ses poids non-critiques un s-plongement propre dans le plan, tels que les quadrilatères tangeants (qui sont les faces de $\Lambda(G)$ ont un cercle inscrit de rayon $r = 1$). Dans ce cas précis, un calcul similaire à celui de l'équation $(2.5.8)$ assure que pour $z_1 = x_1 + iy$ et $z_2 = x_2 + iy$ aligné horizontalement, on a

$$\lim_{|x_1 - x_2| \to \infty} \frac{|\mathcal{Q}(z_1) - \mathcal{Q}(z_2)|}{|z_1 - z_2|} = 1,$$

autrement dit c'est la fonction d'origami qui asymptotiquement est 1-lipchitz mais n'est pas κ-lipchitz pour tout $\kappa < 1$.

Pour le modèle *massif*, les travaux de Park [138, Section 6] assurent que lorsque $|m|$ tend vers l'infini, le système se rapproche du système hors critique (c'est à dire que les probabilités de croisement primales et duales dans les rectangles convergent vers 0 et 1, selon le côté de la criticalité où l'on se trouve). En appliquant la procédure de *replongement des grilles Z-invariantes massives comme des s-plongements* de section 3.3 du chapitre 3 ainsi que la valeur explicite des asymptotiques de la fonction d'origami dans ce cadre précis (calculées dans $(3.3.12)$), on voit que

lorsque $|m|$ tend vers l'infini, la constante d'origami optimale à grande distance se rapproche de 1.

En utilisant les deux exemples précédents, on ainsi penser que les systèmes hors-critiques s'identifient à une fonction d'origami dont la constante de Lipchitz optimale est 1.

D'un point de vue conceptuel, l'hypothèse $\textsc{Lenght-Exp-Fat}(\delta)$ (tout comme sa grande soeur $\textsc{Exp-Fat}(\delta)$) nous semble être un choix de confort, qui reste tout de même suffisament souple pour envisager de travailler dans une multitude de cadres, y compris des graphes pondérés aléatoires. Avec ce choix, on peut utiliser des méthodes analytiques pour prouver des estimées de croisement, ce qui semble être la seule méthode aujourd'hui disponible pour traiter des graphes sans symétries. Il est envisageable qu'un jour on puisse se passer des hypothèses du type $\textsc{Exp-Fat}(\delta)$ avec une meilleure compréhension des comportements pathologiques des fonctions harmoniques associées aux fonctions s-holomorphes.

De notre point de vue, le plus grand intérêt du Théorème 1.9.13 est qu'il permet de traiter la question des probabilités de croisement sur des graphes très irréguliers, dont les poids ou la géométrie locale est tirée aléatoirement. La propriété $\textsc{Lenght-Exp-Fat}(\delta)$ semble pouvoir être accessible via des raisonnement du type Borel-Cantelli (prédisant qu'il ne peut y avoir qu'un nombre fini de faces trop petites, qui correspondrait sinon a un nombre exponentiel de faces avec un $r_z \leqslant \exp(\delta^{-1})$ dans une région de taille δ). Dans le cadre des grands graphes finis abstraits, il faut tout d'abord effectuer un re-plongement via un s-plongement propre et étudier les propriétés géométriques de ce plongement, en particulier vérifier qu'en s'éloignant de la face extérieure v_{ext}°, la taille des faces diminue, puis que le graphe vérifie localement le graphe satisfait $\textsc{Lip}(\kappa,\delta)$. Une des premières cible (ambitieuse mais réaliste) de ces théorèmes est de traiter le cas de grilles $\mathbb{Z}^2$ avec des constantes de couplage aléatoires centrées en la valeur critique.

1.9.5 . Convergence de l'observable FK pour les s-plongements à limite lisse

Ce chapitre a été écrit seul et correspond à un article en préparation. Ce projet n'était pas supervisé par Dmitry Chelkak, et j'en assume seul la responsabilité. L'objectif principal de ce chapitre est de montrer que la conjecture de Chelkak (originellement faite dans [33, Section 2.7] et rappelée dans la section 1.7.4) reliant le modèle d'Ising et les solutions de Dirac massives sur une surface dans l'espace de Minkowski. *Ce chapitre fait état d'un travail en cours, et a donc été volontairement écrit de manière sous-optimale, puisque les méthodes présentées ainsi que leur généralisations simples permettraient de traiter un cadre vraiment plus large. Étant donné qu'une partie du puzzle manquant pour obtenir une théorie complète réside dans des considérations purement dans le continu, ce travail nous semble être d'un intérêt non-trivial pour la théorie puisqu'il résout plusieurs questions cruciales sur le comportement des observables discrètes. C'est pourquoi nous avons choisi de*

l'inclure dans ce manuscrit.

Ici, on prouve la convergence des fonctions s-holomorphes associées à l'observable FK-Ising, lorsque la limite des fonctions d'origami $(\mathcal{Q}^\delta)_{\delta>0}$ est une fonction régulière et que les domaines discrets approximent un domaine simplement connexe du plan dont le bord est lisse. Ce travail généralise partiellement les travaux de Chelkak et Smirnov [48] mais ce restreint au-cadre où les domaines ainsi que la limite des fonctions d'origami sont lisses. Il s'agit de la première preuve de convergence des observables sur des s-plongements lorsque la limite d'échelle des fonctions d'origami n'est pas triviale, et pave la voie à de nombreuses généralisations. Comme pour les observables critiques et massives déjà mentionnées précédemment, on se donne un domaine simplement connexe Ω dont le bord est de classe $\mathcal{C}^1$, et on fixe deux points distincts $a, b \in \partial\Omega$, vus comme des extrémités. Lorsqu'on approxime (Ω, a, b) (au sens de Carathéodory) par des domaines discrets $(\Omega^\delta, a^\delta, b^\delta)$ avec des conditions de bord *branchées* sur l'arc $(b^\delta a^\delta)^\circ$ et *libres* sur l'arc $(a^\delta b^\delta)^\bullet$. Les conditions de bord sont donc exactement celles de l'observable utilisée dans la section 1.5.5 et en particulier de la figure 1.5.4. Il est alors possible de définir comme dans $(1.5.4)$ l'observable FK-Dobrushin sur $(\Omega^\delta, a^\delta, b^\delta)$ en posant

$$X^\delta(c) := \mathbb{E}^{\mathsf{w},\mathsf{f}}_{(\Omega^\delta, a^\delta, b^\delta)}[\chi_c \sigma_{(b^\delta a^\delta)^\circ} \mu_{(a^\delta b^\delta)^\bullet}]. \tag{1.9.16}$$

Le corrélateur X^δ induit une fonction s-holomorphe F^δ via $(1.7.11)$ ainsi que la fonction $H^\delta = H_{F^\delta}$ via $(1.7.15)$. Dans notre travail, on se restreint au cadre suivant :

— Chaque s-plongement $\mathcal{S}^\delta$ satisfait l'hypothèse $\textsc{Unif}(\delta)$ (voir e.g. [33, Section 1.3]) pour les mêmes constantes $r_0, \theta_0 > 0$.

— La suite des fonctions d'origami $(\mathcal{S}^\delta)_{\delta>0}$ converge (uniformément sur les compacts du plan) vers une fonction ϑ de classe $\mathcal{C}^2$. On notera que la précompacité des fonctions $(\mathcal{Q}^\delta)_{\delta>0}$ est toujours vraie et donc on peut toujours supposer que la fonction ϑ converge.

On énonce à présent le résultat principal de ce chapitre, qui prouve l'existence d'une limite d'échelle pour les fonctions F^δ lorsque δ tend vers 0.

Theorème 1.9.14. Soit $((\Omega^\delta, a^\delta, b^\delta))_{\delta>0}$ une suite de domaines discrets qui convergent (au sens de Carathéodory) vers un domaine borné (Ω, a, b), dont le bord est de classe $\mathcal{C}^1$ où l'on a fixé deux points distincts a, b. Alors la suite des fonctions $(F^\delta)_{\delta>0}$ associées au corrélateur FK-Dobrushin dans $(\Omega^\delta, a^\delta, b^\delta)$ converge uniformément sur les compacts de Ω vers l'unique fonction f vérifiant

— $(f dz + i\overline{f} d\vartheta)$ est une forme différentielle fermée sur Ω,

— $h := \frac{1}{2}\int \mathrm{Im}[f^2 dz] + |f|^2 d\vartheta$ s'étend de manière continue avec la valeur 0 sur l'arc (ba) et la valeur 1 sur l'arc (ab).

En particulier, la limite d'échelle f des fonctions s-holomorphes n'est ni holomorphe (comme dans le cadre Z-invariant critique), ni massive holomorphe (comme dans le cadre Z-invariant massif) avec une masse constante. En réalisant le changement de variable $\varphi := \overline{\varsigma} f \cdot (z_\zeta)^{1/2} + \varsigma \overline{f} \cdot (\overline{z}_\zeta)^{1/2}$ de $(1.7.23)$ avec la paramétrisation conforme $(1.7.20)$ de la surface (z, ϑ), alors la fonction φ est solution de l'équation Dirac massif (annoncée en premier lieu dans [33, eq (2.28)])

$$\overline{\partial_\zeta} \varphi = im(\zeta) \cdot \overline{\varphi}, \text{ où}$$

— Le paramètre de masse $m(\zeta) \in \mathbb{R}$ vaut la moitié le produit entre *l'élément de longueur* et *la courbure moyenne* de la surface (z, ϑ) au point $(z(\zeta), \vartheta(z(\zeta)) \subset \mathbb{R}^{2,1}$, pour la métrique de Minkowski de $\mathbb{R}^{2,1}$. Ainsi, le paramètre de masse admet une interprétation purement géométrique.

— Le fait que la limite d'échelle admette une telle description naturelle dans $\mathbb{R}^{2,1}$ justifie par ailleurs l'idée de replonger $\mathcal{S}^\delta$ comme une surface discrète $(\mathcal{S}^\delta, \mathcal{Q}^\delta) \subset \mathbb{R}^{2,1}$ dont la troisième coordonnée est la fonction d'origami $\mathcal{Q}^\delta$.

— L'hypothèse faite sur la régularité de la limite ϑ est principalement pour faite pour pouvoir *définir la notion de courbure moyenne*, qui est une fonction des dérivées secondes de ϑ. Une description similaire semble possible à partir du moment où l'on peut définir d'une manière ou d'une autre une notion de courbure moyenne. En particulier, lorsque les dérivées seconde de ϑ se trouvent dans un espace L^p, les méthodes utilisées dans la preuve donnée ici sont très proche de permettre de conclure (l'ingrédient qui diffère sera soulignée dans quelques lignes).

— La description de la limite d'échelle devient explicite lorsque la surface (z, ϑ) est *minimale pour la métrique de Lorentz*, c'est à dire lorsque sa courbure moyenne H (toujours calculée dans l'espace $\mathbb{R}^{2,1}$) est *nulle partout*. Dans ce cadre là, on a un résultat analogue à [48, Theorème A]. En notant Φ l'uniformisation du relèvement $\hat{\Omega}$ de Ω qui envoie $\hat{a}, \hat{b}$ vers $\pm\infty$, alors $\varphi = \sqrt{\Phi'}$.

Le théorème 1.9.14 confirme, en partie, la prédiction faite par Chelkak dans [33, Section 2.7] sur l'existence de limites d'échelles dont la description se fait naturellement dans l'espace $\mathbb{R}^{2,1}$. De notre point de vue, pour compléter ce travail en cours, il faudrait réaliser les avancées suivantes :

— Retirer toute hypothèse de régularité sur la fonction ϑ lorsque le bord du domaine est lisse. Comparé aux méthodes présentées dans le chapitre, cela nécessite majoritairement de prouver des résultats d'unicité dans le continu. Afin d'y arriver, il semble nécessaire de gagner de l'information supplémentaire (en particulier de la régularité) au niveau discret sur les limites de fonctions s-holomorphes, ce qui permettrait de conclure avec un principe de comparaison général. Cette approche suit son cours dans un travail réalisé en ce moment avec Sung-Chul Park et semble prometteuse.

— Retirer toute hypothèse de régularité sur le bord du domaine *lorsque la surface* (z, ϑ) est minimale pour la métrique de Minkowski. Cela permettrait d'annoncer la convergence des interfaces discrètes sur les graphes $(\mathcal{S}^\delta, \mathcal{Q}^\delta)$ vers le processus SLE sur (z, ϑ). La méthode utilisée ici approximant le bord du domaine par sa tangente est cruciale pour réaliser le passage du discret vers le continu. Pour traiter des bords arbitrairements rugueux, cela ne peut être utilisé et requiert d'utiliser une approche alternative, ce que nous explorons aussi actuellement avec Sung-Chul Park. On rappelle tout de même qu'il existe une méthode developpée par Chelkak sur les graphes vérifiants $\mathcal{Q}^\delta = O(\delta)$ (qui permet de traiter les domaines arbitrairement rugueux) mais dont nous ne sommes pour l'instant pas capables de généraliser.

L'une des principales innovations de ce travail est technique, et répond à la problématique de la survie des conditions de bord de Dirichlet pour les fonctions H^δ sur des s-plongements généraux. Cette question est particulièrement délicate en dehors du cadre isoradial critique et massif, car il n'est à présent plus possible de comparer H^δ avec une fonction harmonique dans le discret.

Notons tout de même le cadre (restreint) où $\mathcal{Q}^\delta = O(\delta)$ (qui contient par exemple l'ensemble des graphes doublement périodiques critiques via leur plongement canonique), pour lequel une méthode alternative a été développée dans [33, Section 4], en approximant au niveau discret (de manière moyennée) le Laplacien usuel dans le continu. La preuve donnée dans [33, Section 4] s'applique sans restrictions sur la régularité du bord et permet donc de prouver la convergence des interfaces FK vers le processus SLE(16/3), prouvant au passage l'invariance conforme du modèle critique doublement périodique. Cependant une telle preuve semble être difficile à généraliser, en raison de son utilisation extensive d'opérateurs différentiels discrets (voir [33, Section 3]) qui ne s'interprètent pas aisément en dehors du cadre $\mathcal{Q}^\delta = O(\delta)$.

Pour outrepasser ce problème, on propose une approche complètement différente, qui consiste (après une chirurgie locale du graphe) à comparer localement H^δ avec une observable définie sur un petit rectangle topologique au voisinage d'un des points de bord, et dont la frontière discrète est plus simple à étudier. On peut alors conclure via le principe de comparaison introduit par Park (voir [33, Proposition 2.11]). Le choix des bords du rectangle topologique est réalisé soigneusement (en particulier l'un des arcs discrets est formé, après chirurgie, de kites, ce qui simplifie grandement l'analyse). Une autre innovation est l'utilisation du principe de comparaison avec des primitives de fonctions holomorphes constantes, qui prouve que H^δ ne croit au plus vite que linéairement au voisinage de certains arcs bien choisis, et simplifie grandement l'analyse. *Il est notable de remarquer que le contrôle des conditions de bord ne requiert l'utilisation de dérivée seconde et semble déjà s'appliquer -avec des adaptations très mineures- à toutes les fonctions ϑ définies sur les domaines à bord lisse.*

Notre approche semble suffisamment solide pour être généralisée rapidement (avec des modifications mineures) au delà de l'hypothèse $\textsc{Unif}(\delta)$ (par exemple avec une hypothèse du type $\textsc{Lenght-Exp-Fat}(\delta)$), mais aussi aux fonctions ϑ dont les dérivées secondes existent dans un certain espace L^p (ce qui implique un contrôle sur courbure moyenne de (z, ϑ)). Pour prouver ce second résultat, il est plausible de généraliser le principe de comparaison dans le continu (voir e.g. [138, Lemma 3.1]) aux espaces L^p, en remplacant les estimées ponctuelles par des estimées intégrées.

2 - Magnetization in the Zig-Zag Layered Ising model and orthogonal polynomials

This chapter corresponds to the article [40], written with **Dmitry Chelkak** and **Clément Hongler**, and is currently submited to a scientifical journal.

Abstract : We discuss the magnetization M_m in the m-th column of the zig-zag layered 2D Ising model on a half-plane using Kadanoff–Ceva fermions and orthogonal polynomials techniques. Our main result gives an explicit representation of M_m via $m \times m$ Hankel determinants constructed from the spectral measure of a certain Jacobi matrix which encodes the interaction parameters between the columns. We also illustrate our approach by giving short proofs of the classical Kaufman–Onsager–Yang and McCoy–Wu theorems in the homogeneous setup and expressing M_m as a Toeplitz+Hankel determinant for the homogeneous sub-critical model in presence of a boundary magnetic field.

2.1 . Introduction

The planar Ising (or Lenz–Ising) model, introduced by Lenz almost a century ago, has an extremely rich history which is impossible to overview in a short introduction, instead we refer the interested reader to the monographs [123, 12, 136, 65] as well as the papers [133, 131, 132, 120, 37] and references therein for more information on various facets of this history. From the 'classical analysis' viewpoint, one of the particularly remarkable aspects is a very fruitful interplay between the explicit computations for the planar Ising model and the theory of Toeplitz determinants. This interplay originated in the groundbreaking work of Kaufman and Onsager in late 1940s (see [9]) and, in particular, lead Szegö to the strong form of his famous theorem on asymptotics of Toeplitz determinants ; we refer the interested reader to the recent survey [55] due to Deift, Its and Krasovsky for more information on the developments of this link since then. It is nevertheless worth noting that this research direction mostly originated in questions related to the homogeneous model in the infinite-volume limit – a well-understood case from the physical perspective. At the same time, it seems that the much richer setup of the *layered model* – first considered by McCoy–Wu and Au-Yang–McCoy in [125, 126, 119, 5, 4], see also [118, Sections 3.1,3.2] and [140] for historical comments – did not attract much attention of mathematicians. Unfortunately, *tour de force* computations summarized in the monograph [123], are nowadays often considered (at least, in several mathematical sub-communities interested in 2D statistical mechanics) as being too technically involved to develop their analysis further. Certainly, this is an abnormal situation and by writing this paper we hope to bring the attention to this 'layered' setup, targeting not only probabilists but also the orthogonal

polynomials community. In the mathematical physics literature, the interest to the layered Ising model also reappeared recently ; e.g. see [75] and references therein.

Our paper should not be considered as a '39999th solution of the Ising model'. On the contrary, the methods we use can be viewed as a simplification of the classical ones in presence of the translation and reflection symmetry in the direction orthogonal to the line connecting spins under consideration. Comparing to [123], this simplification comes from the fact that we use the Kadanoff–Ceva lattice instead of the Onsager (or Fisher) one and, more importantly, work directly with *orthogonal polynomials* instead of Toeplitz determinants. Though such details are not vital in the homogeneous case, this allows us to perform computations for a general *'zig-zag layered'* model in a transparent way (see Theorem 2.1.1) ; in the latter case, the polynomials are orthogonal with respect to a certain measure on the segment $[0,1]$ constructed out of a given sequence of interaction constants.

It is worth mentioning that the simplification discussed above manifests itself even in the homogeneous setup since we always deal with *real weights*, the simplest possible framework of the OPUC/OPRL theory. From the perspective of the 'free fermion algebra' solution [155] of the planar Ising model, our derivations can be viewed as its translation to the language of discrete fermionic observables, see [86] for a discussion of such a correspondence. The latter viewpoint was advertised by Smirnov in his celebrated work on the critical Ising model (e.g., see [65] and references therein). We refer the interested reader to [37, Section 3] for a discussion of equivalences between various combinatorial formalisms used to study the planar Ising model, see also [129] and [48, Section 3.2]. In this paper we also want to make a link between discrete complex analysis techniques and classical computations more transparent ; similar ideas are applied to the quantum 1d Ising model in [110].

Before formulating our main result – Theorem 2.1.1 – for the layered Ising model, let us briefly mention the list of questions that we discuss along the way in the homogeneous setup:

— Kaufman–Onsager–Yang theorem on the spontaneous magnetization below criticality: Theorem 2.3.1, cf. [123, Section X.4] ;

— McCoy–Wu theorem on the asymptotic behavior of the horizontal spin-spin correlations at criticality: Theorem 4.7.9, cf. [123, Section XI.5] ;

— the wetting phase transition in the subcritical model caused by a boundary magnetic field [73, 146] (which was interpreted as a hysteresis effect in the earlier work [123]): we discuss a setup similar to [123, Section XIII] in Section 2.4.3 and reduce the problem to the analysis of explicit Toeplitz+Hankel determinants, see Theorem 2.4.2 ;

— Wu's explicit formula for diagonal spin-spin correlations in the fully homogeneous critical Ising model (see [123, Section XI.4]) and magnetization in the zig-zag half-plane: we provide a very short computation via Legendre polynomials in the Appendix, note that we were unable to find neither Theorem A.3 nor the identity $(\mathrm{A}.8)$ in the literature.

We now move on to the layered Ising model in a half-plane. Instead of working in the original framework of Au-Yang, McCoy and Wu, we slightly simplify the setup by considering the Ising model in the (left) half-plane on the $\frac{\pi}{4}$-rotated square grid which we call the *zig-zag half-plane* and denote by $\mathbb{H}^\diamond$, see Fig. 2.4.1 for the notation. We believe that such a simplification does not change key features of the problem, at the same it allows us to obtain more transparent results in full generality. We are mostly interested in making our main result – Theorem 2.1.1 – easily accessible to the *mathematical* community interested in orthogonal polynomials rather than in discussing the *physics* behind the problem. It is worth emphasizing that Theorem 2.1.1 does *not* express M_m as a Toeplitz determinant. Nevertheless, we believe that the formula $(2.1.5)$ is amenable for the asymptotic analysis and is of interest from the mathematical perspective.

The (half-)infinite volume limit of the Ising model on $\mathbb{H}^\diamond$ is defined as a limit of probability measures on an increasing sequence of finite domains exhausting $\mathbb{H}^\diamond$, with '+' boundary conditions at the right-most column C_0 and at infinity. All interaction parameters between the columns C_{p-1} and C_p are assumed to be the same and equal to $x_p = \exp[-2\beta J_p] = \tan\frac{1}{2}\theta_p$, where $\theta_p \in (0, \frac{1}{2}\pi)$ can be viewed as a convenient parametrization of βJ_p, see Section 2.2.1 for more details. Let

$$M_m = M_m(\theta_1, \theta_2, \dots) \;:=\; \mathbb{E}^+_{\mathbb{H}^\diamond}[\,\sigma_{(-2m-\frac{1}{2},0)}\,] \tag{2.1.1}$$

be the magnetization in the $(2m)$-th column (the analysis for odd columns can be done similarly). Denote

$$D_{\mathrm{even}} := i\begin{bmatrix} \cos\theta_1\cos\theta_2 & 0 & 0 & \dots \\ -\sin\theta_2\sin\theta_3 & \cos\theta_3\cos\theta_4 & 0 & \dots \\ 0 & -\sin\theta_4\sin\theta_5 & \cos\theta_5\cos\theta_6 & \dots \\ \dots & \dots & \dots & \dots \end{bmatrix} \tag{2.1.2}$$

and let

$$D^*_{\mathrm{even}} \;=\; U_{\mathrm{even}} S_{\mathrm{even}}, \qquad S_{\mathrm{even}} = (D_{\mathrm{even}} D^*_{\mathrm{even}})^{1/2} \tag{2.1.3}$$

be the polar decomposition of the operator D^*_{even}, see also Remark 2.4.1 for another interpretation of the (partial) isometry U_{even}. Further, denote $J := D_{\mathrm{even}} D^*_{\mathrm{even}}$. A straightforward computation shows that

$$J = \begin{bmatrix} b_1 & -a_1 & 0 & \dots \\ -a_1 & b_2 & -a_2 & \dots \\ 0 & -a_2 & b_3 & \dots \\ \dots & \dots & \dots & \dots \end{bmatrix} \qquad \begin{aligned} b_k \;&=\; \cos^2\theta_{2k-1}\cos^2\theta_{2k} \\ &\quad + \sin^2\theta_{2k-2}\sin^2\theta_{2k-1}\,, \\ a_k \;&=\; \cos\theta_{2k-1}\cos\theta_{2k}\sin\theta_{2k}\sin\theta_{2k+1}\,, \end{aligned} \tag{2.1.4}$$

where $\theta_0 := 0$ and $b_1 = \cos^2\theta_1\cos^2\theta_2$. Let ν_J be the spectral measure of J associated with the first basis vector. It is easy to see that $0 \le J \le 1$ and thus $\operatorname{Supp}\nu_J \in [0,1]$. Given a measure μ on $[0,1]$, let $\mathrm{H}_m[\,\mu\,] := \det[\,\int_0^1 \lambda^{p+q}\mu(d\lambda)\,]_{p,q=0}^{m-1}$ be the m-th Hankel determinant composed from the moments of this measure. Denote by P_m the orthogonal projector on the space of first m coordinates of ℓ^2.

Theorem 2.1.1. For all $\theta_1, \theta_2, \ldots \in (0, \frac{\pi}{2})$ and $m \geq 1$, we have

$$M_m \;=\; |\det P_m U_{\text{even}} P_m| \;=\; \frac{\det P_m J^{1/2} P_m}{\prod_{k=1}^{2m} \cos\theta_k} \;=\; \frac{\mathrm{H}_m[\lambda^{1/2}\nu_J]}{(\,\mathrm{H}_m[\nu_J]\cdot \mathrm{H}_m[\lambda\nu_J]\,)^{1/2}}\,, \tag{2.1.5}$$

where U_{even} is the (partial) isometry factor in the polar decomposition (2.1.3), the Jacobi matrix $J = D_{\text{even}} D^*_{\text{even}}$ is given by (2.1.4), and ν_J is the spectral measure of J.

Remark 2.1.2. Assume that $\theta_k = \theta$ for all $k \geq 1$, i.e., that we work with the fully homogeneous model. One can easily see that

$$\operatorname{supp}\nu_J \;=\; [\cos^2(2\theta)\,,1] \text{ if } \theta \leq \tfrac{\pi}{4} \quad \text{while} \quad \operatorname{supp}\nu_J \;=\; \{0\}\cup[\cos^2(2\theta)\,,1] \text{ if } \theta > \tfrac{\pi}{4}.$$

In particular, this clearly marks the critical value $\theta_{\text{crit}} = \frac{\pi}{4}$ of the interaction parameter. Moreover, in the supercritical regime $\theta > \theta_{\text{crit}}$, the existence of an exponentially decaying eigenfunction $\psi^\circ_k = (\cot\theta)^{2k}$, $\psi^\circ \in \operatorname{Ker} D^*_{\text{even}}$, directly leads to the exponential decay of the truncated determinants $|\det P_m U_{\text{even}} P_m|$.

Remark 2.1.3. Assume now that $\theta_{k+2n} = \theta_k$ for all $k \geq 1$ and some $n \geq 1$. In this case, the criticality condition reads as $\prod_{k=1}^{2n} \tan\theta_k = 1$, see Lemma 2.5.1 below. This condition is equivalent to the fact that the continuous spectrum of J begins at 0. Moreover (see Section 2.5.3), in this setup the integrated density of states of the periodic Jacobi matrix J behaves like $C_J \cdot \pi^{-1}\sqrt{\lambda}$ as $\lambda \to 0$, where

$$C_J \;=\; \Big[\, n^{-2} \textstyle\sum_{k=1}^{n} (\psi^\circ_k)^2 \cdot \sum_{k=1}^{n} (a_k \psi^\circ_k \psi^\circ_{k+1})^{-1} \,\Big]^{1/2} \tag{2.1.6}$$

and ψ°_k denotes the periodic vector solving the equation $J\psi^\circ = 0$. In Section 2.5.2 we show that the quantity (2.1.6) also admits a clear geometric interpretation in the context of the so-called *s-embeddings* of planar Ising models, see (2.5.8) and a discussion following that identity.

It is clear that the spectral properties of the matrix J (which can be viewed as an effective propagator in the direction orthogonal to the boundary of $\mathbb{H}^\diamond$) are directly related to the behavior of the magnetization M_m as $m \to \infty$. Nevertheless, we are not aware of asymptotical results for (2.1.5) in the general case, especially when J has a *singular continuous spectrum*. This leads to the following question:

— to find necessary and sufficient conditions on the measure ν_J that imply the asymptotics (a) $\liminf_{m\to\infty} M_m = 0$ (b) $\limsup_{m\to\infty} M_m = 0$ in (2.1.5).

We believe that an answer to this question should shed more light, in particular, on the *random* layered 2D Ising model. Moreover, it would be very interesting

— to understand the dynamics of the measure ν_J when the inverse temperature β varies from ∞ to 0 and hence all $\theta_p = 2\arctan\exp[-2\beta J_p]$ increase from 0 to 1 in a coherent way.

Classically, this dynamics should lead to the Griffiths–McCoy phase transition for i.i.d. interaction parameters between the columns and also could give rise to less known effects in the dependent case. As already mentioned above, one of the goals of this paper is to bring the attention of the probability and orthogonal polynomials communities to these questions.

The rest of the paper is organized as follows. In Section 2.2 we review the Kadanoff–Ceva formalism of spin-disorder operators in the planar Ising model. In Section 2.3 we illustrate our approach by giving streamlined proofs of two classical results due to Kaufman–Onsager–Yang and McCoy–Wu, respectively: Theorem 2.3.1 and Theorem 4.7.9 ; we believe that this material should help the reader to position this proof into the classical Ising model landscape. We prove our main result – Theorem 2.1.1 – in Section 2.4. In Section 2.5 we briefly discuss the geometric interpretation of our results via s-embeddings of planar Ising models, a generalization of isoradial embeddings of the critical Baxter's Z-invariant model introduced in [34, 33]. The appendix is devoted to the explicit analysis of diagonal correlations (Wu's formula) and of the zig-zag half-plane magnetization at criticality via Legendre polynomials.

Acknowledgements

We are grateful to Yvan Velenik for bringing our attention to the papers [73, 146] on the wetting phase transition in the subcritical model, which was mentioned under the name hysteresis effect in the first version of our paper following the interpretation given in [123, Section XIII]. We also thank Jacques H.H. Perk for useful comments on the immense literature on the Ising model correlations. Several parts of this paper were known and reported since 2012/2013 but caused a very limited interest, we are grateful to colleagues who encouraged us to carry this project out. Dmitry Chelkak would like to thank Alexander Its, Igor Krasovsky, Leonid Parnovski and Alexander Pushnitski for helpful discussions. The research of Dmitry Chelkak and Rémy Mahfouf was partially supported by the ANR-18-CE40-0033 project DIMERS. Clément Hongler would like to acknowledge the support of the ERC SG CONSTAMIS, the NCCR SwissMAP, the Blavatnik Family Foundation and the Latsis Foundation. We also thank Jhih-Huang Li and anonymous referees for carefully reading an earlier version of this manuscript.

2.2 . Combinatorics of the planar Ising model

In order to keep the presentation self-contained, in this section we collect basic definitions and properties of the planar Ising model observables. Below we adopt the notation from [34, 33, 39], the interested reader is also referred to [37] or [88]

for more details (note however that these papers use slightly different definitions). Even though we discuss the spin-disorder observables in the full generality (m spins and n disorders), below we are interested in the situations $m = n = 2$ (Section 2.3 and Appendix) and $m = 1$, $n = 2$ (Section 2.4 and Appendix) only.

2.2.1 . Definition and domain wall representation

Let G be a finite connected *planar* graph embedded into the plane such that all its edges are straight segments. We denote by $G^\bullet$ the set of its vertices and by G° the set of its faces (identified with their centers). The (ferromagnetic) *nearest-neighbor* Lenz-Ising model on the graph *dual* to G is a random assignment of spins $\sigma_u \in \{\pm 1\}$ to the *faces* $u \in G^\circ$ such that the probability of a spin configuration $\sigma = (\sigma_u)$ is proportional to

$$\mathbb{P}_G[\,\sigma\,] \propto \exp\left[\,\beta \textstyle\sum_{u\sim w} J_e \sigma_u \sigma_w\,\right], \qquad e = (uw)^*, \tag{2.2.1}$$

where a positive parameter $\beta = 1/kT$ is called the *inverse temperature*, the sum is taken over all pairs of adjacent faces u, w (equivalently, edges e) of G, and $J = (J_e)$ is a collection of positive *interaction constants*, indexed by the edges of G. Below we use the following *parametrization* of J_e:

$$x_e = \tan \tfrac{1}{2}\theta_e := \exp[-2\beta J_e]. \tag{2.2.2}$$

Note that the quantities $x_e \in (0,1)$ and $\theta_e := 2\arctan x_e \in (0, \frac{1}{2}\pi)$ have the same monotonicity as the temperature β^{-1}.

We let the spin σ_{out} of the outermost face of G be fixed to $+1$, in other words we impose *'+' boundary conditions*. In this case, the *domain wall representation* (also known as the *low-temperature expansion*) of the Ising model is a 1-to-1 correspondence between spin configurations and even subgraphs P of G: given a spin configuration, P consists of all edges that separate pairs of disaligned spins. One can consider a decomposition (not unique in general) of P into a collection of *non-intersecting and non-self-intersecting loops*. The above correspondence implies that

$$\mathbb{E}_G[\sigma_{u_1} \dots \sigma_{u_m}] \;=\; \mathcal{Z}_G^{-1} \textstyle\sum_{P\in\mathcal{E}_G} x(P) (-1)^{\mathrm{loops}_{[u_1,\dots,u_m]}(P)} \tag{2.2.3}$$

for $u_1, \dots, u_m \in G^\circ$, where $\mathcal{E}_G$ denotes the set of all even subgraphs of G,

$$\mathcal{Z}_G := \textstyle\sum_{P\in\mathcal{E}_G} x(P), \qquad x(P) := \prod_{e\in P} x_e, \tag{2.2.4}$$

and $\mathrm{loops}_{[u_1,\dots,u_m]}(P)$ is the number (always well defined modulo 2) of loops in P surrounding an odd number of faces $u_1, \dots, u_m$. Up to a factor $\exp[\beta \sum_{e\in\mathcal{E}_G} J_e]$, the quantity $\mathcal{Z}_G$ is the *partition function* of the Ising model on G°.

2.2.2 . Disorder insertions

Following Kadanoff and Ceva [93], given an even number of vertices $v_1, \dots, v_n \in G^\bullet$ we define the correlation of *disorders* $\mu_{v_1}, \dots, \mu_{v_n}$

$$\langle \mu_{v_1} \dots \mu_{v_n} \rangle_G := \mathcal{Z}_G^{-1} \cdot \mathcal{Z}_G^{[v_1,\dots,v_n]}, \quad \mathcal{Z}_G^{[v_1,\dots,v_n]} := \textstyle\sum_{P \in \mathcal{E}_G(v_1,\dots,v_n)} x(P), \quad (2.2.5)$$

where $\mathcal{E}_G(v_1, ..., v_n)$ denotes the set of subgraphs P of G such that each of the vertices $v_1, \dots, v_n$ has an odd degree in P while all other vertices have an even degree. Probabilistically, one can easily see that

$$\langle \mu_{v_1} \dots \mu_{v_n} \rangle_G = \mathbb{E}_G\big[\exp[-2\beta \textstyle\sum_{(uw)^* \in P_0(v_1,\dots,v_n)} J_e \sigma_u \sigma_w]\big], \quad (2.2.6)$$

where $P_0(v_1, \dots, v_n)$ is a fixed collection of edge-disjoint paths matching in pairs the vertices $v_1, \dots, v_n$; note that the right-hand side does not depend on the choice of these paths. The *Kramers–Wannier duality* implies (e.g., see [93]) that

$$\langle \mu_{v_1} \dots \mu_{v_n} \rangle_G = \mathbb{E}^\star_{G^\bullet}[\sigma^\bullet_{v_1} \dots \sigma^\bullet_{v_n}], \quad (2.2.7)$$

where the expectation in the right-hand side is taken with respect to the Ising model on *vertices* of G, with dual weights $x_{e^*} := \tan\frac{1}{2}(\frac{\pi}{2} - \theta_e)$ and free boundary conditions. Indeed, $(2.2.5)$ is nothing but the *high-temperature expansion* of $(2.2.7)$.

Similarly to $\mathcal{Z}_G$, one can interpret $\mathcal{Z}_G^{[v_1,\dots,v_n]}$ as the low-temperature (domain walls) expansion of the partition function of the Ising model defined on the faces of a *double cover* $G^{[v_1,\dots,v_n]}$ of the graph G that branches over $v_1, \dots, v_n$, with the following *spin-flip symmetry constraint*: we require $\sigma_u \sigma_{u^\star} = -1$ for any pair of faces of the double cover such that u and $u^\star$ lie over the same face in G. Using this interpretation, we introduce mixed correlations

$$\langle \mu_{v_1} \dots \mu_{v_n} \sigma_{u_1} \dots \sigma_{u_m} \rangle_G := \langle \mu_{v_1} \dots \mu_{v_n} \rangle_G \cdot \mathbb{E}_{G^{[v_1,\dots,v_n]}}[\sigma_{u_1} \dots \sigma_{u_m}], \quad (2.2.8)$$

where $u_1, \dots, u_m$ should be understood as faces of the double cover $G^{[v_1,\dots,v_n]}$. Similarly to $(2.2.6)$ one can easily give a probabilistic interpretation of these quantities in terms of the original Ising model on G. Nevertheless, we prefer to speak about the Ising model on $G^{[v_1,\dots,v_n]}$ as this approach is more invariant and does not require to fix an arbitrary choice of the disorder lines $P_0(v_1, \dots, v_n)$.

By definition of the Ising model on $G^{[v_1,\dots,v_n]}$, the correlation $(2.2.8)$ fulfills the sign-flip symmetry constraint between the sheets of the double cover. When considered as a function of both vertices v_p and faces u_q, this correlation is defined on a double cover of $(G^\bullet)^n \times (G^\circ)^m$ and changes sign each time one of the vertices $v_p \in G^\bullet$ turns around one of the vertices $u_q \in G^\circ$ (or vice versa). We call *spinors* functions defined on double covers that obey such a sign-flip property.

2.2.3 . Fermions and the propagation equation

We need an additional notation. Let $\Lambda(G) := G^\bullet \cup G^\circ$ be the planar bipartite graph (a so-called *quad-graph*) whose set of (degree four) faces $\diamondsuit(G)$ is in a 1-to-1 correspondence with the set of edges of G. Let $\Upsilon(G)$ denote the *medial* graph

of $\Lambda(G)$, whose vertices are in a 1-to-1 correspondence with edges (vu) of $\Lambda(G)$ and are also called *corners* of G, while the faces of $\Upsilon(G)$ correspond either to vertices of $G^\bullet$ or to vertices of G° or to quads from $\diamondsuit(G)$. We denote by $\Upsilon^\times(G)$ a double cover of the graph $\Upsilon(G)$ that branches around each of its faces (e.g., see [33, Fig. 3A] or [129, Fig. 27], [48, Fig. 6]). For a corner $c = (v(c)u(c)) \in \Upsilon^\times(G)$ (with $u(c) \in G^\circ$ and $v(c) \in G^\bullet$), let

$$\eta_c := i \cdot \exp[-\tfrac{i}{2} \arg(v(c) - u(c))], \tag{2.2.9}$$

where the global prefactor i is chosen for later convenience. Though a priori the sign in the expression $(2.2.9)$ is ambiguous, it can be fixed so that η_c is a spinor on $\Upsilon^\times(G)$, called the *Dirac spinor*, by requiring that the values of η_c at corners c surrounding each face of $\Upsilon(G)$ are defined in a 'continuous' way. (In particular, this local definition implies the spinor property of η_c on $\Upsilon^\times(G)$.)

Given $c \in \Upsilon^\times(G)$, one defines the *Kadanoff–Ceva fermion* as $\chi_c := \mu_{v(c)}\sigma_{u(c)}$. More accurately, we set

$$X_\varpi(c) := \langle \mu_{v(c)}\mu_{v_1} \dots \mu_{v_{n-1}}\sigma_{u(c)}\sigma_{u_1} \dots \sigma_{u_{m-1}} \rangle_G, \tag{2.2.10}$$

for $\varpi := (v_1, \dots, v_{n-1}, u_1, \dots, u_{m-1}) \in (G^\bullet)^{n-1} \times (G^\circ)^{m-1}$. Let $\Upsilon^\times_\varpi(G)$ denote a double cover of $\Upsilon(G)$ that branches over each of the faces of $\Upsilon(G)$ *except* those corresponding to the points from ϖ. The preceding discussion of mixed spin-disorder correlations ensures that X_ϖ is a spinor on $\Upsilon^\times_\varpi(G)$. Finally, let

$$\Psi_\varpi(c) := \eta_c X_\varpi(c) \tag{2.2.11}$$

where η_c is defined by $(2.2.9)$. The function Ψ_ϖ locally does *not* branch (the signs changes of χ_c and η_c cancel each other). More precisely, Ψ_ϖ is a spinor on the double cover $\Upsilon_\varpi(G)$ of $\Upsilon(G)$ that branches *only* over points from ϖ: it changes the sign only when c turns around one of the vertices v_p or the faces u_q.

We now move on to the crucial three-term equation for the correlations $(2.2.10)$, called the *propagation equation* for Kadanoff–Ceva fermions on $\Upsilon^\times(G)$, see [141, 56, 129] or [37, Section 3.5] for more details. For a quad $z_e \in \diamondsuit(G)$ corresponding to an edge e of G, we denote its vertices by $v_0(z_e) \in G^\bullet$, $u_0(z_e) \in G^\circ$, $v_1(z_e) \in G^\bullet$, and $u_1(z_e) \in G^\circ$, listed in the counterclockwise order. Further, for $p, q \in \{0, 1\}$, let $c_{p,q}(z_e) := (v_p(z_e)u_q(z_e))$. The following identity holds for all triples of consecutive (on $\Upsilon^\times_\varpi(G)$) corners $c_{p,1-q}(z_e)$, $c_{p,q}(z_e)$ and $c_{1-p,q}(z_e)$ surrounding the edge e:

$$X_\varpi(c_{p,q}) = X_\varpi(c_{p,1-q}) \cos\theta_e + X_\varpi(c_{1-p,q}) \sin\theta_e\,, \tag{2.2.12}$$

where θ_e stands for the parametrization $(3.2.3)$ of the Ising model weight x_e of e. In recent papers, the equation $(2.2.12)$ is often used in the context of rhombic lattices, in which case the parameter θ_e admits a geometric interpretation (see Section 2.5.1), but in fact it does not rely upon a particular choice of an embedding (up to a homotopy) of $\diamondsuit(G)$ into $\mathbb{C}$ provided that θ_e is *defined* by $(3.2.3)$.

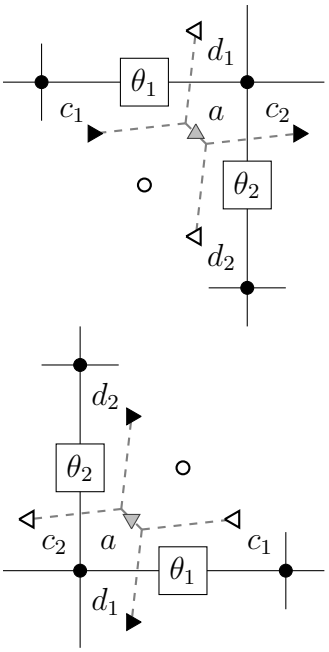

(A) The notation used in Proposition 2.2.1 (Cauchy–Riemann equations (2.2.13)).

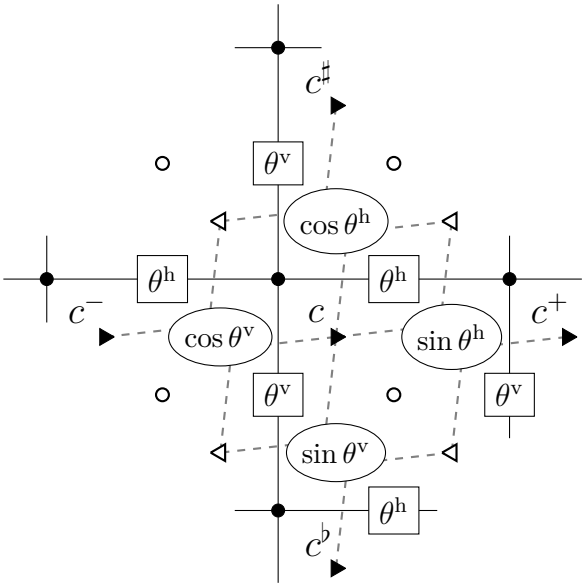

(B) The notation used in Proposition 2.2.2 (massive harmonicity of fermionic observables in the homogeneous model away from the branchings).

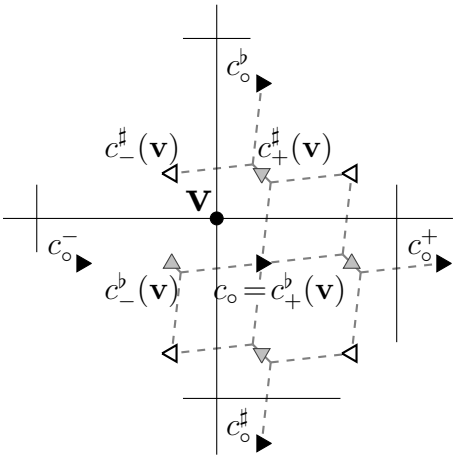

(C) The notation used in the proof of Lemma 4.7.2 (the value $[\Delta^{(m)} X^{\mathrm{sym}}_{[\mathbf{v},\mathbf{u}]}]$ near the branching point $\mathbf{v} = (0, \frac{1}{4})$).

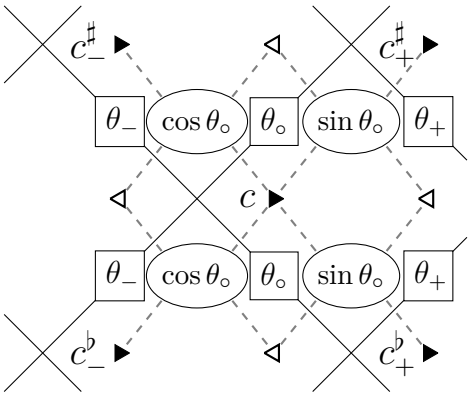

(D) The notation used in Proposition 2.2.3 (harmonicity-type identities in the zig-zag layered model).

FIGURE 2.2.1 – Local relations for Kadanoff–Ceva fermionic observables. We indicate the four 'types' of corners of (subgraphs of) the square grid by orienting and coloring the triangles depicting them.

2.2.4 . Cauchy–Riemann and Laplacian-type identities on the square grid

From now on we assume that G is a subgraph of the regular square grid $\mathbb{Z}^2 \subset \mathbb{C}$. In this situation one can use (2.2.12) to derive a version of discrete Cauchy–Riemann equations for the complex-valued observable Ψ_ϖ defined by (2.2.11).

Proposition 2.2.1. *Let c_1, d_1, c_2, d_2 be corners of G located as in Fig. 2.2.1A (and located on the same sheet of the double cover $\Upsilon_\varpi(G)$). Let θ_1, θ_2 be the interaction parameters assigned via (3.2.3) to the edges e_1, e_2. Then, the following identity holds:*

$$[\Psi_\varpi(c_2)\cos\theta_2 - \Psi_\varpi(c_1)\sin\theta_1] \;=\; \pm i\cdot[\Psi_\varpi(d_2)\sin\theta_2 - \Psi_\varpi(d_1)\cos\theta_1]\,, \quad (2.2.13)$$

where the '$\pm$' sign is '$+$' if the square $(c_1d_2c_2d_1)$ is oriented counterclockwise (top picture in Fig. 2.2.1A) and '$-$' otherwise (bottom picture in Fig. 2.2.1A).

Proof. Let $a \in \Upsilon^\times_\varpi(G)$ be the center of the square $(c_1d_2c_2d_2)$ and let c_1, d_2, c_2, d_1 be the neighbors of a on $\Upsilon^\times_\varpi(G)$. Writing two propagation equations (2.2.12) at a one gets the identity

$$X_\varpi(c_2)\cos\theta_2 + X_\varpi(d_2)\sin\theta_2 \;=\; X_\varpi(a) \;=\; X_\varpi(c_1)\sin\theta_1 + X_\varpi(d_1)\cos\theta_1.$$

Since $\eta_{d_1} = \eta_{d_2} = e^{\pm i\frac{\pi}{4}}\eta_a$ (with the same choice of the sign: '$+$' for the left picture, '$-$' for the right one) and $\eta_{c_1} = \eta_{c_2} = e^{\mp i\frac{\pi}{4}}\eta_a$, the result immediately follows. □

Below we often focus on the values of observables Ψ_ϖ or X_ϖ at corners $c \in \Upsilon(G)$ of one of four 'types'; by a type of c we mean its geometric position inside the face of $G \subset \mathbb{Z}^2$ to which c belongs, see Fig. 2.2.1. For each type of corners, the values η_c are all the same and, moreover, the branching structure of $\Upsilon^\times_\varpi(G)$ restricted to this type of corners coincides with the one of $\Upsilon_\varpi(G)$. In other words, Ψ_ϖ and X_ϖ differ only by a global multiplicative constant on each of the four types of corners.

In this paper, we are interested in the following two setups:

– *homogeneous* model, in which all the parameters θ_e corresponding to horizontal edges of $\mathbb{Z}^2$ have the common value θ^{h} (resp., θ^{v} for vertical edges);

– *zig-zag layered* model on the $\frac{\pi}{4}$-rotated grid, in which all interaction constants between each pair of adjacent columns have the same value (see Fig. 2.4.1).

In both situations, one can use (2.2.13) to derive a harmonicity-type identity for the values of X_ϖ (note however that this is not possible in the general case).

Proposition 2.2.2. *In the homogeneous setup, assume that a corner $c \in \Upsilon_\varpi(G)$ is not located near the branching, i.e., that neither $v(c)$ nor $u(c)$ are in ϖ. Then, the observable X_ϖ satisfies the following equation at c:*

$$X_\varpi(c) \;=\; \tfrac{1}{2}\sin\theta^{\mathrm{h}}\cos\theta^{\mathrm{v}}\cdot[X_\varpi(c^+) + X_\varpi(c^-)] + \tfrac{1}{2}\cos\theta^{\mathrm{h}}\sin\theta^{\mathrm{v}}\cdot[X_\varpi(c^\sharp) + X_\varpi(c^\flat)],$$

where $c^+, c^\sharp, c^-, c^\flat$ are the four nearby corners having the same type as c, located at the east, north, west and south direction from c, respectively (see Fig. 2.2.1B).

Proof. Recall that, at corners of a given type, the values X_ϖ and Ψ_ϖ differ only by a multiplicative constant. Due to the symmetry of the homogeneous model, we can assume that $c, c^+, c^\sharp, c^-, c^\flat$ are located as in Fig. 2.2.1B. Let us write four Cauchy–Riemann equations (2.2.13) between c and c^+, c and $c^\sharp$, c and c^-, c and $c^\flat$. Multiplying the first equation by $\sin\theta^{\mathrm{h}}$, the second by $\cos\theta^{\mathrm{h}}$, the third by $\cos\theta^{\mathrm{v}}$, the fourth by $\sin\theta^{\mathrm{v}}$, and taking the sum with appropriate signs we get the result. □

Remark 2.2.1. (i) Proposition 2.2.2 can be reformulated as the massive harmonicity condition $[\Delta^{(m)}X_\varpi](c) = 0$, where the *massive Laplacian* $\Delta^{(m)}$ is defined as

$$[\Delta^{(m)}F](c) := -F(c)+\tfrac{1}{2}\sin\theta^{\mathrm{h}}\cos\theta^{\mathrm{v}}\cdot[F(c^+)+F(c^-)]+\tfrac{1}{2}\cos\theta^{\mathrm{h}}\sin\theta^{\mathrm{v}}\cdot[F(c^\sharp)+F(c^\flat)].$$

It is worth noting that $\Delta^{(m)}$ is a generator of a (continuous time) random walk on $\mathbb{Z}^2$ with killing rate $1-\sin(\theta^{\mathrm{h}}+\theta^{\mathrm{v}})$; in particular, one can easily guess from Proposition 2.2.2 the classical criticality condition

$$\theta^{\mathrm{h}}+\theta^{\mathrm{v}} = \tfrac{\pi}{2} \quad \Leftrightarrow \quad \sinh[2\beta J^{\mathrm{h}}]\cdot\sinh[2\beta J^{\mathrm{v}}] = 1.$$

(ii) The fact that the near-critical homogeneous Ising model on $\mathbb{Z}^2$ admits a description via massive holomorphic fermions is a commonplace in the theoretical physics literature. In the probabilistic community, an explicit link between formulas for spin-spin correlations derived in [123] and the partition functions of killed random walks was pointed out in [130]. We refer the interested reader to the paper [14], in which the massive holomorphicity property of fermionic observables was used for the analysis of the exponential decay rate of spin-spin correlations $\mathbb{E}[\sigma_0\sigma_{na}]$, $n\to\infty$, and of its dependence on the direction a in the *super*-critical model on $\mathbb{Z}^2$.

A similar identity holds in the layered setup (see Fig. 2.2.1D for the notation). Assume that c is a west corner of a face on the $\frac{\pi}{4}$-rotated square grid. Denote by $c^\sharp_\pm$, $c^\flat_\pm$ the four nearby corners of the same type as c and let θ_-, $\theta_\circ$ and θ_+ be the parameters assigned via (3.2.3) to the edges to the left of $c^{\sharp,\flat}_-$, to the left of c, and to the left of $c^{\sharp,\flat}_+$, respectively.

Proposition 2.2.3. *In the setup described above (see also Fig. 2.2.1D), assume that neither $v(c)$ nor $u(c)$ are in ϖ. Then, the following identity holds:*

$$X_\varpi(c) = \tfrac{1}{2}\sin\theta_-\cos\theta_\circ\cdot[X_\varpi(c^\sharp_-)+X_\varpi(c^\flat_-)]+\tfrac{1}{2}\sin\theta_\circ\cos\theta_+\cdot[X_\varpi(c^\sharp_+)+X_\varpi(c^\flat_+)].$$

Proof. The result follows by summing four Cauchy–Riemann equations (2.2.13) with coefficients $\pm\cos\theta_\circ$, $\pm\sin\theta_\circ$ similarly to the proof of Proposition 2.2.2. □

Remark 2.2.2. It is worth emphasizing that the harmonicity-type identities discussed in Propositions 2.2.2 and 2.2.3 fail when c is located near the branching. The reason is that applying (2.2.13) four times and summing the results as in the proofs of Proposition 2.2.2 and Proposition 2.2.3 one gets the difference $X_\varpi(d^*) - X_\varpi(d)$ with d^*, d located over the same point on the *different sheets* of the double cover $\Upsilon_\varpi(G)$.

2.3 . Homogeneous model

In this section we discuss classical results on the horizontal spin-spin correlations in the infinite volume for the homogeneous model. Namely, we assume that all horizontal edges have a weight $\exp[-2\beta J^{\mathrm{h}}] = \tan\frac{1}{2}\theta^{\mathrm{h}}$ while all vertical edges have a weight $\exp[-2\beta J^{\mathrm{v}}] = \tan\frac{1}{2}\theta^{\mathrm{v}}$, see also Appendix in which the diagonal spin-spin correlations are treated in the fully homogeneous critical case $\theta^{\mathrm{h}} = \theta^{\mathrm{v}} = \frac{\pi}{4}$. Though these results and even a roadmap of the proofs are well-known (e.g., see the classical treatment by McCoy and Wu [123]), we use this setup to illustrate a simplification that comes from working directly with *real-valued* orthogonal polynomials instead of Toeplitz determinants, an approach that we apply to the layered model.

2.3.1 . Full-plane observable with two branchings

Assume that the square grid on which the Ising model lives is shifted so that its vertices coincide with $\mathbb{Z}\times(\mathbb{Z}+\frac{1}{4})$ and the centers of faces are $(\mathbb{Z}+\frac{1}{2})\times(\mathbb{Z}-\frac{1}{4})$, see Fig. 2.3.1A. It is well known (e.g., see [72]) that there are no more than two extremal Gibbs measures (coming from '+' and '−' boundary conditions at infinity) and that the spin correlations in the infinite volume limit are translationally invariant. Given $n \geq 0$, we define the horizontal and next-to-horizontal correlations

$$\begin{aligned} D_n &:= \mathbb{E}_{\mathbb{Z}^2}\big[\sigma_{(\frac{1}{2},-\frac{1}{4})}\sigma_{(n+\frac{1}{2},-\frac{1}{4})}\big], & D^\star_n &:= \mathbb{E}^\star_{(\mathbb{Z}^2)^\bullet}\big[\sigma^\bullet_{(0,\frac{1}{4})}\sigma^\bullet_{(n,\frac{1}{4})}\big], \\ D_{n+1} &:= \mathbb{E}_{\mathbb{Z}^2}\big[\sigma_{(-\frac{1}{2},-\frac{1}{4})}\sigma_{(n+\frac{1}{2},-\frac{1}{4})}\big], & D^\star_{n+1} &:= \mathbb{E}^\star_{(\mathbb{Z}^2)^\bullet}\big[\sigma^\bullet_{(0,\frac{1}{4})}\sigma^\bullet_{(n+1,\frac{1}{4})}\big], \\ \widetilde{D}_{n+1} &:= \mathbb{E}_{\mathbb{Z}^2}\big[\sigma_{(-\frac{1}{2},\frac{3}{4})}\sigma_{(n+\frac{1}{2},-\frac{1}{4})}\big], & \widetilde{D}^\star_{n+1} &:= \mathbb{E}^\star_{(\mathbb{Z}^2)^\bullet}\big[\sigma^\bullet_{(0,\frac{1}{4})}\sigma^\bullet_{(n+1,-\frac{3}{4})}\big], \end{aligned} \tag{2.3.1}$$

where the expectations in the second column are taken for the *dual* Ising model with interaction parameters $\tan\frac{1}{2}(\frac{\pi}{2}-\theta^{\mathrm{v}})$ and $\tan\frac{1}{2}(\frac{\pi}{2}-\theta^{\mathrm{h}})$ assigned to horizontal and vertical edges of the dual square grid $(\mathbb{Z}^2)^\bullet$, respectively. Due to (2.2.7) one can view these quantities as disorder-disorder correlations in the original model.

Let $\mathbf{v} = (0,\frac{1}{4})$ and $\mathbf{u} = (n+\frac{1}{2},-\frac{1}{4})$. Below we rely upon the *full-plane* observable $X_{[\mathbf{v},\mathbf{u}]}$ which can be thought of as a (subsequential) limit of the similar observables defined on finite graphs G exhausting the square grid. Indeed, since

$$\big|\langle\mu_{v(c)}\mu_{\mathbf{v}}\sigma_{u(c)}\sigma_{\mathbf{u}}\rangle_G\big| \;\leq\; \langle\mu_{v(c)}\mu_{\mathbf{v}}\rangle_G \;=\; \mathbb{E}^\star_{G^\bullet}[\sigma^\bullet_{v(c)}\sigma^\bullet_{\mathbf{v}}] \;\leq\; 1, \tag{2.3.2}$$

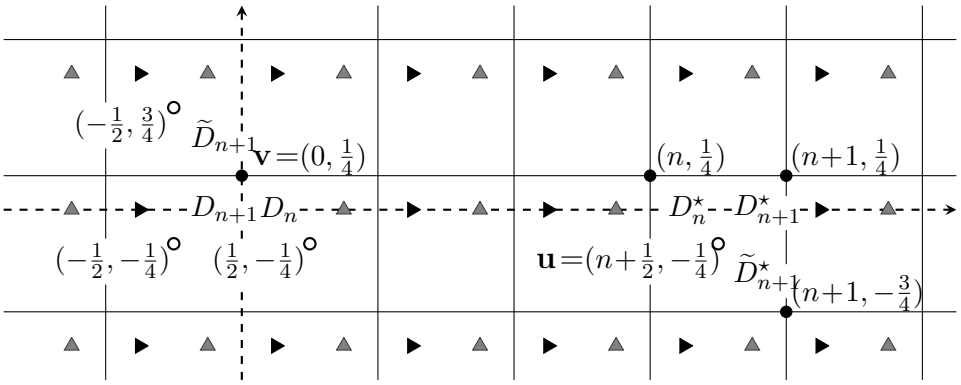

(A) Particular values, considered *up to the sign*, of the Kadanoff–Ceva fermionic observable $X_{[\mathbf{v},\mathbf{u}]}$ near its branching points $\mathbf{v}, \mathbf{u}$; see (2.3.1).

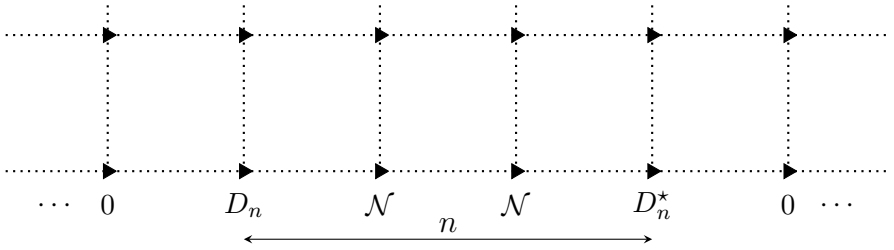

(B) Boundary value problem $[\mathrm{P}_{\mathrm{n}}^{\mathrm{sym}}]$ for the symmetrized observable $X_{[\mathbf{v},\mathbf{u}]}^{\mathrm{sym}}$.

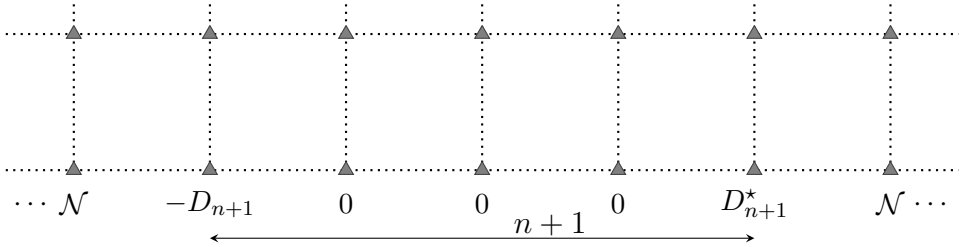

(C) Boundary value problem $[\mathrm{P}_{\mathrm{n+1}}^{\mathrm{anti}}]$ for the anti-symmetrized observable $X_{[\mathbf{v},\mathbf{u}]}^{\mathrm{anti}}$.

FIGURE 2.3.1 – To derive recurrence relations on horizontal spin-spin correlations, we consider the Kadanoff–Ceva fermionic observable $X_{[\mathbf{v},\mathbf{u}]}$ with two branchings at $\mathbf{v} = (0, \frac{1}{4})$ and $\mathbf{u} = (n+\frac{1}{2}, -\frac{1}{4})$. The symmetrized observable $X_{[\mathbf{v},\mathbf{u}]}^{\mathrm{sym}}$ is defined on north-west corners (marked as $\triangleright$ in the figure) and the anti-symmetrized observable $X_{[\mathbf{v},\mathbf{u}]}^{\mathrm{anti}}$ is defined on north-east corners (marked as $\triangle$). Both $X_{[\mathbf{v},\mathbf{u}]}^{\mathrm{sym}}$ and $X_{[\mathbf{v},\mathbf{u}]}^{\mathrm{anti}}$ are massive harmonic in the upper half-plane $\mathbb{Z}\times\mathbb{N}_0$ and solve boundary value problems $[\mathrm{P}_{\mathrm{n}}^{\mathrm{sym}}]$, $[\mathrm{P}_{\mathrm{n+1}}^{\mathrm{anti}}]$, respectively ; the sign $\mathcal{N}$ denotes Neumann boudary conditions.

a point-wise subsequential limit exists; its uniqueness (and hence the existence of the true limit) follows from Lemma 4.7.1 given below. Moreover, in Section 4.7.2, we provide an explicit construction of functions satisfying the conditions listed in Lemma 4.7.1, which allows us to identify $X_{[\mathbf{v},\mathbf{u}]}$ with these explicit functions.

Let $[(\mathbb{Z}\pm\frac{1}{4})\times\mathbb{Z};\mathbf{v},\mathbf{u}]$ denote the double cover of the lattice $(\mathbb{Z}\pm\frac{1}{4})\times\mathbb{Z}$ branching over $\mathbf{v}$ and $\mathbf{u}$. We now introduce the following *symmetrized* and *anti-symmetrized* versions of the observable $X_{[\mathbf{v},\mathbf{u}]}(\cdot)$ on north-west and north-east corners, respectively (see Fig. 2.3.1):

$$X^{\mathrm{sym}}_{[\mathbf{v},\mathbf{u}]}(c) := \tfrac{1}{2}[X_{[\mathbf{v},\mathbf{u}]}(c) + X_{[\mathbf{v},\mathbf{u}]}(\bar{c})], \quad c\in[(\mathbb{Z}+\tfrac{1}{4})\times\mathbb{Z};\mathbf{v},\mathbf{u}], \tag{2.3.3}$$

$$X^{\mathrm{anti}}_{[\mathbf{v},\mathbf{u}]}(c) := \tfrac{1}{2}[X_{[\mathbf{v},\mathbf{u}]}(c) - X_{[\mathbf{v},\mathbf{u}]}(\bar{c})], \quad c\in[(\mathbb{Z}-\tfrac{1}{4})\times\mathbb{Z};\mathbf{v},\mathbf{u}], \tag{2.3.4}$$

where the continuous conjugation $z\mapsto\bar{z}$ on $[(\mathbb{Z}\pm\frac{1}{4})\times\mathbb{Z};\mathbf{v},\mathbf{u}]$ is defined so that it maps the segment $[\frac{1}{4},n+\frac{1}{4}]\times\{0\}$ to itself (i.e., the conjugate of each point located over this segment is chosen to be on the *same* sheet of the double cover). Once $z\mapsto\bar{z}$ is specified in between the branching points, it can be 'continuously' extended to the entire double cover $[(\mathbb{Z}\pm\frac{1}{4})\times\mathbb{Z};\mathbf{v},\mathbf{u}]$. In particular, the points c located over the real line outside of the segment $[\frac{1}{4},n+\frac{1}{4}]$ are mapped by $z\mapsto\overline{z}$ to their counterparts c^* on the *other* sheet of the double cover.

Let us list basic properties of the observables $X^{\mathrm{sym}}_{[\mathbf{v},\mathbf{u}]}$ and $X^{\mathrm{anti}}_{[\mathbf{v},\mathbf{u}]}$ and show that they characterize these observables uniquely. Due to $(4.7.1)$ we have

$$\bigl|X^{\mathrm{sym}}_{[\mathbf{v},\mathbf{u}]}(k+\tfrac{1}{4},s)\bigr|\le 1 \quad\text{and}\quad \bigl|X^{\mathrm{anti}}_{[\mathbf{v},\mathbf{u}]}(k-\tfrac{1}{4},s)\bigr|\le 1 \quad\text{for all}\ \ k,s\in\mathbb{Z}.$$

Proposition 2.2.2 (see also Remark 2.2.1) ensures that the observables $X^{\mathrm{sym}}_{[\mathbf{v},\mathbf{u}]}$ and $X^{\mathrm{anti}}_{[\mathbf{v},\mathbf{u}]}$ are massive harmonic away from the branching points $\mathbf{v},\mathbf{u}$. In particular, one has

$$[\Delta^{(m)}X^{\mathrm{sym}}_{[\mathbf{v},\mathbf{u}]}]((k+\tfrac{1}{4},s))=0 \quad\text{and}\quad [\Delta^{(m)}X^{\mathrm{anti}}_{[\mathbf{v},\mathbf{u}]}]((k-\tfrac{1}{4},s))=0 \quad\text{if}\ \ s\neq 0. \tag{2.3.5}$$

Further, the spinor property of the observable $X_{[\mathbf{v},\mathbf{u}]}$ together with the choice of the conjugation described above gives

$$X^{\mathrm{sym}}_{[\mathbf{v},\mathbf{u}]}((k+\tfrac{1}{4},0))=0,\ \ k\notin[0,n],\quad [\Delta^{(m)}X^{\mathrm{sym}}_{[\mathbf{v},\mathbf{u}]}]((k+\tfrac{1}{4},0))=0,\ \ k\in[1,n-1]; \tag{2.3.6}$$

$$X^{\mathrm{anti}}_{[\mathbf{v},\mathbf{u}]}((k-\tfrac{1}{4},0))=0,\ \ k\in[1,n],\quad [\Delta^{(m)}X^{\mathrm{anti}}_{[\mathbf{v},\mathbf{u}]}]((k-\tfrac{1}{4},0))=0,\ \ k\notin[0,n+1]. \tag{2.3.7}$$

Finally, the definition of $X_{[\mathbf{v},\mathbf{u}]}$ implies

$$X^{\mathrm{sym}}_{[\mathbf{v},\mathbf{u}]}((\tfrac{1}{4},0))=D_n, \qquad X^{\mathrm{sym}}_{[\mathbf{v},\mathbf{u}]}((n+\tfrac{1}{4},0))=D^\star_n; \tag{2.3.8}$$

$$X^{\mathrm{anti}}_{[\mathbf{v},\mathbf{u}]}((-\tfrac{1}{4},0))=-D_{n+1}, \qquad X^{\mathrm{anti}}_{[\mathbf{v},\mathbf{u}]}((n+\tfrac{3}{4},0))=D^\star_{n+1}, \tag{2.3.9}$$

where we assume that these pairs of corners are located on the *same sheet* of the double cover $[(\mathbb{Z}\pm\frac{1}{4})\times\mathbb{Z};\mathbf{v},\mathbf{u}]$ *as viewed from the upper half-plane*; this is why the value D_{n+1} at $(-\frac{1}{4},0)$ appears with the different sign.

Lemma 2.3.1. *(i) The uniformly bounded observable* $X^{\mathrm{sym}}_{[\mathbf{v},\mathbf{u}]}$ *given by* (4.7.2) *is uniquely characterized by the properties* (4.7.4), (4.7.5) *and its values* (4.7.7) *near* $\mathbf{v}$ *and* $\mathbf{u}$.

(ii) Similarly, the uniformly bounded observable $X^{\mathrm{anti}}_{[\mathbf{v},\mathbf{u}]}$ *given by* (4.7.3) *is uniquely characterized by the properties* (4.7.4), (4.7.6) *and its values* (4.7.8) *near* $\mathbf{v}$ *and* $\mathbf{u}$.

Proof. (i) Let X_1 and X_2 be two bounded spinors satisfying (4.7.4),(4.7.5) and (4.7.7). Let $(Z_k)_{k\geqslant 0}$ be the random walk (with killing) started at $c \in [(\mathbb{Z}+\frac{1}{4})\times\mathbb{Z}; \mathbf{u}, \mathbf{v}]$ that corresponds to the massive Laplacian $\Delta^{(m)}$. This random walk almost surely hits the points located over the set $\{(k+\frac{1}{4}, 0), k \notin [1, n-1]\}\}$ or dies. Since the process $(X_1 - X_2)(Z_k)$ is a bounded martingale with respect to the canonical filtration, the optional stopping theorem yields $X_1(c)$–$X_2(c) = 0$. The proof of (ii) is similar. □

The next lemma allows one to use an explicit construction of functions $X_{[\mathbf{v},\mathbf{u}]}$ given in Section 4.7.2 in order to get a recurrence relation for the spin-spin correlations. For $n \geq 1$, denote

$$L_n := \tfrac{1}{2}\cos\theta^{\mathrm{v}}\cdot[D_n + \cos\theta^{\mathrm{h}}\cdot\widetilde{D}_n], \qquad L^\star_n := \tfrac{1}{2}\sin\theta^{\mathrm{h}}\cdot[D^\star_n + \sin\theta^{\mathrm{v}}\cdot\widetilde{D}^\star_n]. \quad (2.3.10)$$

Lemma 2.3.2. *For each* $n \geq 1$, *the following identities are fulfilled:*

$$-[\Delta^{(m)} X^{\mathrm{sym}}_{[\mathbf{v},\mathbf{u}]}]((\tfrac{1}{4}, 0)) = L_{n+1}, \qquad -[\Delta^{(m)} X^{\mathrm{sym}}_{[\mathbf{v},\mathbf{u}]}]((n+\tfrac{1}{4}, 0)) = L^\star_{n+1}; \quad (2.3.11)$$

$$-[\Delta^{(m)} X^{\mathrm{anti}}_{[\mathbf{v},\mathbf{u}]}]((-\tfrac{1}{4}, 0)) = -L_n, \qquad -[\Delta^{(m)} X^{\mathrm{anti}}_{[\mathbf{v},\mathbf{u}]}]((n+\tfrac{3}{4}, 0)) = L^\star_n, \quad (2.3.12)$$

with the same choice of points on the double covers $[(\mathbb{Z}\pm\frac{1}{4})\times\mathbb{Z}; \mathbf{v}, \mathbf{u}]$ *as above. If* $n = 0$, *the identities* (4.7.10) *should be replaced by* $-[\Delta^{(m)} X^{\mathrm{sym}}_{[\mathbf{v},\mathbf{u}]}]((\frac{1}{4}, 0)) = L_1 + L^\star_1$ *while* (4.7.11) *hold with* $L_0 := \cos\theta^{\mathrm{v}}$ *and* $L^\star_0 := \sin\theta^{\mathrm{h}}$.

Proof. We focus on the first identity in (4.7.10). Let $c_\circ = c^\flat_+(\mathbf{v}) := (\frac{1}{4}, 0)$, see Fig. 2.2.1C for the notation. First, note that $X^{\mathrm{sym}}_{[\mathbf{v},\mathbf{u}]}(c^-_\circ) = 0$ and hence

$$-[\Delta^{(m)} X^{\mathrm{sym}}_{[\mathbf{v},\mathbf{u}]}](c_\circ) = X_{[\mathbf{v},\mathbf{u}]}(c_\circ) - \tfrac{1}{2}\sin\theta^{\mathrm{h}}\cos\theta^{\mathrm{v}}\cdot X_{[\mathbf{v},\mathbf{u}]}(c^+_\circ) - \tfrac{1}{2}\cos\theta^{\mathrm{h}}\sin\theta^{\mathrm{v}}\cdot[X_{[\mathbf{v},\mathbf{u}]}(c^\sharp_\circ) + X_{[\mathbf{v},\mathbf{u}]}(c^\flat_\circ)]\,.$$

Recall that we deduced the massive harmonicity property of the observables $X_{[\mathbf{v},\mathbf{u}]}$ away from the branchings from four Cauchy–Riemann identities (2.2.13), each of them based upon two propagation equations (2.2.12); see Fig. 2.2.1B. We now repeat the same proof but with *seven* three-terms identities (2.2.12) instead of eight ones required to prove Proposition 2.2.2, the one involving the

values of $X_{[\mathbf{v},\mathbf{u}]}$ at $c_\circ^- = (-\frac{3}{4}, 0)$, $c_-^\flat(\mathbf{v}) = (-\frac{1}{4}, 0)$ and $c_-^\sharp(\mathbf{v}) = (-\frac{1}{4}, \frac{1}{2})$ missing; see Fig. 2.2.1C. As a result, one sees that the value $[\Delta^{(m)} X^{\mathrm{sym}}_{[\mathbf{v},\mathbf{u}]}](c_+^\flat(\mathbf{v}))$ is $\frac{1}{2}\cos\theta^{\mathrm{v}}$ times the missing linear combination of the values

$$X_{[\mathbf{v},\mathbf{u}]}(c_-^\flat(\mathbf{v})) = D_{n+1} \quad \text{and} \quad X_{[\mathbf{v},\mathbf{u}]}(c_-^\sharp(\mathbf{v})) \cdot \cos\theta^{\mathrm{h}} = \widetilde{D}_{n+1} \cdot \cos\theta^{\mathrm{h}},$$

which leads to the first identity in (4.7.10) (we let the reader to check the signs obtained along the computation). The proofs of the other three identities for $n \geq 1$ are similar. If $n = 0$, one should sum *six* three-term identities (2.2.12) when dealing with $X^{\mathrm{sym}}_{[\mathbf{v},\mathbf{u}]}$ and *eight* ones when dealing with $X^{\mathrm{anti}}_{[\mathbf{v},\mathbf{u}]}$. In the latter case, the values L_0 and $L_0^\star$ appear due to the presence of the branchings $\mathbf{v}, \mathbf{u}$ near the points at which $\Delta^{(m)} X^{\mathrm{anti}}_{[\mathbf{v},\mathbf{u}]}$ is computed (and due to the fact that $D_0 = D_0^\star = 1$). □

2.3.2 . Construction via the Fourier transform and orthogonal polynomials

In this section we construct two bounded functions satisfying the properties (4.7.4)–(4.7.8) using Fourier transform and orthogonal polynomials techniques, the explicit formulas are given in Lemma 4.7.4 and Lemma 4.7.5. Recall that these explicit solutions must coincide with $X^{\mathrm{sym}}_{[\mathbf{v},\mathbf{u}]}$ and $X^{\mathrm{anti}}_{[\mathbf{v},\mathbf{u}]}$ due to Lemma 4.7.1. Instead of the double covers $[(\mathbb{Z} \pm \frac{1}{4}) \times \mathbb{Z}; \mathbf{u}, \mathbf{v}]$, we work in the upper half-plane $\mathbb{Z} \times \mathbb{N}_0$ only (see Lemma 4.7.3 for the link between the two setups).

For a function $V : \mathbb{Z} \times \mathbb{N}_0 \to \mathbb{R}$ we use the same definition of the massive Laplacian $[\Delta^{(m)} V](k, s)$ as above for $s \geq 1$ and introduce the values

$$\begin{aligned}[\mathcal{N}V](k,0) := V(k,0) &- \cos\theta^{\mathrm{h}} \sin\theta^{\mathrm{v}} \cdot V(k,1) \\ &- \tfrac{1}{2} \sin\theta^{\mathrm{h}} \cos\theta^{\mathrm{v}} \cdot [V(k-1,0) + V(k+1,0)] \end{aligned} \qquad (2.3.13)$$

which might be viewed as a version of the normal derivative of V at the point $(k, 0)$. We now formulate two problems $[\mathbf{P}^{\mathbf{sym}}_{\mathbf{n}}]$ and $[\mathbf{P}^{\mathbf{anti}}_{\mathbf{n}}]$ to solve. Due to Lemma 4.7.1, these problems are equivalent to constructing explicitly the functions $X^{\mathrm{sym}}_{[\mathbf{v},\mathbf{u}]}$ and $X^{\mathrm{anti}}_{[\mathbf{v},\mathbf{u}]}$, respectively; see also Fig. 4.7.2B and Fig. 4.7.2C.

— $[\mathbf{P}^{\mathbf{sym}}_{\mathbf{n}}]$: given $n \geq 1$, to construct a bounded function $V : \mathbb{Z} \times \mathbb{N}_0 \to \mathbb{R}$ such that the following conditions are fulfilled:

$$\begin{aligned} &[\Delta^{(m)} V](k,s) = 0 \text{ if } s \geq 1; \qquad [\mathcal{N}V](k,0) = 0 \text{ for } k \in [1, n-1]; \\ &V(k,0) = 0 \text{ for } k \notin [0,n]; \qquad V(0,0) = D_n \text{ and } V(n,0) = D_n^\star . \end{aligned}$$

— $[\mathbf{P}^{\mathbf{anti}}_{\mathbf{n+1}}]$: given $n \geq 0$, to construct a bounded function $V : \mathbb{Z} \times \mathbb{N}_0 \to \mathbb{R}$ such that the following conditions are fulfilled:

$$\begin{aligned} &[\Delta^{(m)} V](k,s) = 0 \text{ if } s \geq 1; \qquad [\mathcal{N}V](k,0) = 0 \text{ for } k \notin [0, n+1]; \\ &V(k,0) = 0 \text{ for } k \in [1,n]; \qquad V(0,0) = -D_{n+1}; \quad V(n+1,0) = D_{n+1}^\star . \end{aligned}$$

Lemma 2.3.3. *Assume that a function $V_n^{\rm sym}$ (resp., $V_{n+1}^{\rm anti}$) solves the problem $[{\rm P}_{\rm n}^{\rm sym}]$ (resp., $[{\rm P}_{\rm n+1}^{\rm anti}]$). Then, the following identities hold:*

$$[\mathcal{N}V_n^{\rm sym}](0,0) = L_{n+1}, \qquad [\mathcal{N}V_n^{\rm sym}](n,0) = L_{n+1}^\star; \tag{2.3.14}$$

$$[\mathcal{N}V_{n+1}^{\rm anti}](0,0) = -L_n, \qquad [\mathcal{N}V_{n+1}^{\rm anti}](n+1,0) = L_n^\star. \tag{2.3.15}$$

Proof. Consider a section of the double cover $[(\mathbb{Z}\pm\frac{1}{4})\times\mathbb{Z};\mathbf{v},\mathbf{u}]$ with a cut going along the horizontal axis outside the segment $[0,n+\frac{1}{2}]$ for the problem $[{\rm P}_{\rm n}^{\rm sym}]$ and along $[0,n+\frac{1}{2}]$ for the problem $[{\rm P}_{\rm n+1}^{\rm anti}]$. Define two functions on north-west and north-east, respectively, corners of the grid by

$$V_{[\mathbf{v},\mathbf{u}]}^{\rm sym}((\pm k+\tfrac{1}{4},s)) := V_n^{\rm sym}(k,s) \qquad V_{[\mathbf{v},\mathbf{u}]}^{\rm anti}((\pm k-\tfrac{1}{4},s)) := \pm V_{n+1}^{\rm anti}(k,s).$$

These functions vanish on the cuts and thus can be viewed as bounded spinors on the double covers $[(\mathbb{Z}\pm\frac{1}{4})\times\mathbb{Z};\mathbf{v},\mathbf{u}]$, which satisfy all the conditions (4.7.4)–(4.7.8). Due to the uniqueness result provided by Lemma 4.7.1, this implies $X_{[\mathbf{v},\mathbf{u}]}^{\rm sym} = V_{[\mathbf{v},\mathbf{u}]}^{\rm sym}$ and $X_{[\mathbf{v},\mathbf{u}]}^{\rm anti} = V_{[\mathbf{v},\mathbf{u}]}^{\rm anti}$. The identities (4.7.13), (4.7.14) now easily follow from (4.7.10), (4.7.11) and the definition (4.7.12). □

Let V be a solution to the problem $[{\rm P}_{\rm n}^{\rm sym}]$, recall that this solution is unique due to Lemma 4.7.1. To construct it explicitly, we start with a heuristic argument. Assume for a moment that the Fourier series

$$\widehat{V}_s(e^{it}) := \textstyle\sum_{k\in\mathbb{Z}} V(k,s)e^{ikt}, \quad s\geq 0, \quad t\in[0,2\pi],$$

are well-defined. The massive harmonicity property $[\Delta^{(m)}V](k,s)=0$ for $s\geq 1$ can be rewritten as the recurrence relation

$$[1-\sin\theta^{\rm h}\cos\theta^{\rm v}\cos t]\cdot\widehat{V}_s(e^{it}) \;=\; \tfrac{1}{2}\cos\theta^{\rm h}\sin\theta^{\rm v}\cdot[\widehat{V}_{s-1}(e^{it})+\widehat{V}_{s+1}(e^{it})]. \tag{2.3.16}$$

A general solution to the recurrence relation (4.7.15) is a linear combination of the functions $(y_-(t;\theta^{\rm h},\theta^{\rm v}))^s$ and $(y_+(t;\theta^{\rm h},\theta^{\rm v}))^s$, where $0\leq y_-\leq 1\leq y_+$ solve the quadratic equation

$$[1-\sin\theta^{\rm h}\cos\theta^{\rm v}\cos t]\cdot y(t) \;=\; \tfrac{1}{2}\cos\theta^{\rm h}\sin\theta^{\rm v}\cdot[(y(t))^2+1].$$

At level $s=0$ we have $\widehat{V}_0(e^{it}) = Q_n(e^{it})$, an unknown trigonometric polynomial of degree n. Since we are looking for bounded Fourier coefficients of $\widehat{V}_s$, we are tempted to say that $\widehat{V}_s(e^{it}) = Q_n(e^{it})\cdot(y_-(t;\theta^{\rm h},\theta^{\rm v}))^s$ for $s\geq 1$. A straightforward computation shows that

$$\textstyle\sum_{k\in\mathbb{Z}}[\mathcal{N}V](k,0)e^{ikt} \;=\; w(t;\theta^{\rm h},\theta^{\rm v})Q_n(e^{it}), \tag{2.3.17}$$

$$w(t;\theta^{\rm h},\theta^{\rm v}) \;:=\; [(1-\sin\theta^{\rm h}\cos\theta^{\rm v}\cos t)^2-(\cos\theta^{\rm h}\sin\theta^{\rm v})^2]^{1/2}. \tag{2.3.18}$$

The key observation of this section is that the left-hand side of (4.7.16) should not contain monomials $e^{it}, \dots, e^{i(n-1)t}$, which is a simple orthogonality condition for the polynomial $Q_n(e^{it})$.

We now use the heuristics developed in the previous paragraph to rigorously identify the unique solution to $[\mathrm{P}_{\mathrm{n}}^{\mathrm{sym}}]$.

Lemma 2.3.4. *Let $n \geq 1$. If a trigonometric polynomial $Q_n(e^{it}) = D_n + \ldots + D_n^\star e^{int}$ of degree n with prescribed free and leading coefficients is orthogonal to the family $\{e^{it}, \dots, e^{i(n-1)t}\}$ with respect to the measure $w(t;\theta^{\mathrm{h}},\theta^{\mathrm{v}})\frac{dt}{2\pi}$, then the function*

$$V(k,s) := \tfrac{1}{2\pi}\int_{-\pi}^{\pi} e^{-ikt} Q_n(e^{it})(y_-(t;\theta^{\mathrm{h}},\theta^{\mathrm{v}}))^s dt$$

is uniformly bounded and solves the problem $[\mathrm{P}_{\mathrm{n}}^{\mathrm{sym}}]$. Moreover,

$$\langle Q_n, 1\rangle_{\frac{w}{2\pi}dt} = L_{n+1} \quad \textit{and} \quad \langle Q_n, e^{int}\rangle_{\frac{w}{2\pi}dt} = L_{n+1}^\star, \tag{2.3.19}$$

where the scalar product is taken with respect to the same measure on the unit circle.

Proof. The values $V(k,s)$ are uniformly bounded as $0 \leq y_- \leq 1$, the massive harmonicity property $[\Delta^{(m)}V](k,s) = 0$ for $s \geq 1$ is straightforward and the required properties of the values $V(k,0)$ and $[\mathcal{N}F](k,0)$ follow from the assumptions made on the polynomial Q_n. The identities (4.7.13) give (4.7.17). □

A similar construction can be done for the problem $[\mathrm{P}_{\mathrm{n+1}}^{\mathrm{anti}}]$, see Fig. 4.7.2C. The only difference is that at level $s = 0$ we now require that $\widehat{V}_0(e^{it})$ does not contain monomials $e^{it}, \dots, e^{i(n+1)t}$ while

$$\textstyle\sum_{k\in\mathbb{Z}}[\mathcal{N}V](k,0)e^{ikt} \;=\; w(t;\theta^{\mathrm{h}},\theta^{\mathrm{v}})\widehat{V}_0(e^{it}) \;=\; -L_n + \ldots + L_n^\star e^{i(n+1)t} \tag{2.3.20}$$

is a trigonometric polynomial of degree $n+1$. In other words, this polynomial is orthogonal to $\{e^{it}, \dots, e^{int}\}$ with respect to the weight

$$w^{\#}(t;\theta^{\mathrm{h}},\theta^{\mathrm{v}}) \;:=\; (w(t;\theta^{\mathrm{h}},\theta^{\mathrm{v}}))^{-1}, \qquad t \in [0, 2\pi]. \tag{2.3.21}$$

provided that $w^{\#}$ is integrable on the unit circle. One can easily see from (2.3.18) that this is true if and only if $\theta^{\mathrm{h}} + \theta^{\mathrm{v}} \neq \frac{\pi}{2}$. We discuss a modification of the next claim required for the analysis of the critical case $\theta^{\mathrm{h}} + \theta^{\mathrm{v}} = \frac{\pi}{2}$ in Section 4.7.4.

Lemma 2.3.5. *Let $n \geq 0$ and assume that $\theta^{\mathrm{h}} + \theta^{\mathrm{v}} \neq \frac{\pi}{2}$. If a trigonometric polynomial $Q_{n+1}^{\#}(e^{it}) = -L_n + \ldots + L_n^\star e^{i(n+1)t}$ is orthogonal to the family $\{e^{it}, \dots, e^{int}\}$ with respect to the measure $w^{\#}(t;\theta^{\mathrm{h}},\theta^{\mathrm{v}})\frac{dt}{2\pi}$, then the function*

$$V(k,s) := \tfrac{1}{2\pi}\int_{-\pi}^{\pi} e^{-ikt} Q_{n+1}^{\#}(e^{it})(y_-(t;\theta^{\mathrm{h}},\theta^{\mathrm{v}}))^s w^{\#}(t;\theta^{\mathrm{h}},\theta^{\mathrm{v}}) dt \tag{2.3.22}$$

is uniformly bounded and solves the problem $[\mathrm{P}_{\mathrm{n+1}}^{\mathrm{anti}}]$. Moreover,

$$\langle Q_{n+1}^{\#}, 1\rangle_{\frac{w^{\#}}{2\pi}dt} = -D_{n+1} \quad \textit{and} \quad \langle Q_{n+1}^{\#}, e^{i(n+1)t}\rangle_{\frac{w^{\#}}{2\pi}dt} = D_{n+1}^\star, \tag{2.3.23}$$

where the scalar product is taken with respect to the same measure on the unit circle.

Proof. The proof repeats the arguments used in the proof of Lemma 4.7.4. □

2.3.3 . Horizontal spin-spin correlations below criticality

In this section we combine the results of Lemmas 4.7.4 and 4.7.5 into a single result on asymptotics of the horizontal spin-spin correlations D_n as $n \to \infty$. We assume that $\theta^{\mathrm{h}} + \theta^{\mathrm{v}} < \frac{\pi}{2}$ and rely upon the fact that $D_n^\star \to 0$ as $n \to \infty$. This can be easily derived from the monotonicity of D_n with respect to the temperature and the fact that $D_n = D_n^\star \to 0$ as $n \to \infty$ in the critical regime $\theta^{\mathrm{h}} + \theta^{\mathrm{v}} = \frac{\pi}{2}$ which is discussed in the next section.

Theorem 2.3.1 (**Kauffman–Onsager–Yang**). Let $\theta^{\mathrm{h}} + \theta^{\mathrm{v}} < \frac{\pi}{2}$. Then, the spontaneous magnetization $\mathcal{M}(\theta^{\mathrm{h}}, \theta^{\mathrm{v}})$ of the homogeneous Ising model is given by

$$\mathcal{M}(\theta^{\mathrm{h}}, \theta^{\mathrm{v}}) \ := \lim_{n\to\infty} D_n^{1/2} \ = \ \left[1 - (\tan\theta^{\mathrm{h}} \tan\theta^{\mathrm{v}})^2\right]^{1/8}. \tag{2.3.24}$$

(Note that under the parametrization (3.2.3) one has $\tan\theta_e = (\sinh(2\beta J_e))^{-1}$.)

Remark 2.3.2. It is worth mentioning that the value $\tan\theta^{\mathrm{h}} \tan\theta^{\mathrm{v}}$ also admits a fully *geometric* interpretation as Baxter's elliptic parameter of the Z-invariant Ising model on isoradial graphs [12, Eq. (7.10.50)], see Section 2.5.1 for details.

Proof. Classically, the computation given below is based upon the strong Szegö theorem on the asymptotics of the norms of orthogonal polynomials on the unit circle. Note however that we use this result in its simplest form, for *real* weights w and $w^\#$ given by (2.3.18) and (4.7.19).

Let $\Phi_n(z) = z^n + \ldots - \alpha_{n-1}$ be the n-th monic orthogonal polynomial on the unit circle with respect to the measure $w(t; \theta^{\mathrm{h}}, \theta^{\mathrm{v}})\frac{dt}{2\pi}$, the real number α_{n-1} is called the *Verblunsky coefficient*, recall that $|\alpha_{n-1}| < 1$ for all $n \geq 1$. Denote by $\Phi_n^* := z^n \Phi_n(z^{-1}) = -\alpha_{n-1} z^n + \ldots + 1$ the reciprocal polynomial. Matching the free and the leading coefficients, it is easy to see that the polynomial Q_n from Lemma 4.7.4 can be written as

$$Q_n(e^{it}) = c_n \Phi_n(e^{it}) + c_n^* \Phi_n^*(e^{it}), \ \text{ where } \ \begin{bmatrix} c_n^* \\ c_n \end{bmatrix} = \begin{bmatrix} 1 & -\alpha_{n-1} \\ -\alpha_{n-1} & 1 \end{bmatrix}^{-1} \begin{bmatrix} D_n^\star \\ D_n \end{bmatrix}.$$

Moreover, one has $\langle \Phi_n, e^{int} \rangle = \langle \Phi_n^*, 1 \rangle = \|\Phi_n\|^2 =: \beta_n = \beta_0 \prod_{k=1}^n (1 - \alpha_{k-1}^2)$ (e.g., see [158, Theorem 2.1]) and $\langle \Phi_n, 1 \rangle = \langle \Phi_n^*, e^{int} \rangle = 0$, here and below we drop the measure $w\frac{dt}{2\pi}$ from the notation for shortness. Therefore, the identities (4.7.13) imply that

$$\begin{bmatrix} L_{n+1}^\star \\ L_{n+1} \end{bmatrix} = \beta_n \begin{bmatrix} c_n^* \\ c_n \end{bmatrix} = \beta_{n-1} \begin{bmatrix} 1 & \alpha_{n-1} \\ \alpha_{n-1} & 1 \end{bmatrix} \begin{bmatrix} D_n^\star \\ D_n \end{bmatrix}, \tag{2.3.25}$$

and hence

$$L_{n+1}^2 - (L_{n+1}^\star)^2 \ = \ \beta_n \beta_{n-1} \cdot (D_n^2 - (D_n^\star)^2) \quad \text{for} \ \ n \geq 1. \tag{2.3.26}$$

Similarly, it follows from Lemma 4.7.5 that

$$\begin{bmatrix} D^\star_{n+1} \\ -D_{n+1} \end{bmatrix} \;=\; \beta^\#_n \begin{bmatrix} 1 & \alpha^\#_n \\ \alpha^\#_n & 1 \end{bmatrix} \begin{bmatrix} L^\star_n \\ -L_n \end{bmatrix}, \tag{2.3.27}$$

where $\alpha^\#_n$ and $\beta^\#_n$ stand for the Verblunsky coefficients and squared norms of monic orthogonal polynomials corresponding to the weight (4.7.19). In particular, we have

$$D^2_{n+1} - (D^\star_{n+1})^2 \;=\; \beta^\#_{n+1}\beta^\#_n \cdot (L_n^2 - (L^\star_n)^2) \quad \text{for} \;\; n \geq 0. \tag{2.3.28}$$

The recurrence relations (2.3.28), (2.3.26) applied for even and odd indices n, respectively, lead to the formula

$$\begin{aligned} D^2_{2m+1} - (D^\star_{2m+1})^2 \;&=\; \beta^\#_{2m+1}\beta^\#_{2m} \cdot \beta_{2m-1}\beta_{2m-2} \cdot (D^2_{2m-1} - (D^\star_{2m-1})^2) \\ &=\; \ldots \;=\; \textstyle\prod_{k=0}^{2m+1} \beta^\#_k \cdot \prod_{k=0}^{2m-1} \beta_k \cdot (L_0^2 - (L_0^*)^2)\,, \end{aligned}$$

note that $L_0^2 - (L_0^*)^2 = (\cos\theta^{\mathrm{v}})^2 - (\sin\theta^{\mathrm{h}})^2 = \cos(\theta^{\mathrm{h}}+\theta^{\mathrm{v}})\cos(\theta^{\mathrm{h}}-\theta^{\mathrm{v}})$.

Recall that $D^\star_{2m+1} \to 0$ as $m \to \infty$. It remains to apply the Szegö theory (e.g., see [78, Section 5.5] or [158, Theorems 8.1 and 8.5]) to the weights (2.3.18) and (4.7.19). A straightforward computation shows that

$$\begin{aligned} w(t;\theta^{\mathrm{h}},\theta^{\mathrm{v}}) \;&=\; C w_{q_-}(t) w_{q_+}(t), \qquad \text{where} \;\; C = (\cos\tfrac{1}{2}\theta^{\mathrm{h}})^2 \cos\theta^{\mathrm{v}}, \\ w_q(t) := \big[(1+q^2)^2 - (2q\cos\tfrac{t}{2})^2\big]^{1/2} &= |1-q^2e^{it}|, \qquad q_\pm^2 = \tan(\tfrac{1}{2}\theta^{\mathrm{h}})\tan(\tfrac{\pi}{4} \mp \tfrac{1}{2}\theta^{\mathrm{v}})\,. \end{aligned}$$

Since $w^\#(t;\theta^{\mathrm{h}},\theta^{\mathrm{v}}) = (w(t;\theta^{\mathrm{h}},\theta^{\mathrm{v}}))^{-1}$, we have

$$\lim_{m\to\infty} \textstyle\prod_{k=0}^{2m+1} \beta^\#_k \cdot \prod_{k=0}^{2m-1} \beta_k \;=\; C^{-2} \cdot G^2,$$

where

$$\begin{aligned} G \;&=\; \exp\Big[\frac{1}{4\pi}\iint_{\mathbb{D}} \Big|\frac{d}{dz}\big(\log(1-q_-^2 z) + \log(1-q_+^2 z)\big)\Big|^2 dA(z)\Big] \\ &=\; \exp\big[-\textstyle\sum_{k\geqslant 1} \frac{1}{4k}(q_-^{2k}+q_+^{2k})^2\big] \;=\; \big[(1-q_-^4)(1-q_+^4)(1-q_-^2q_+^2)^2\big]^{-1/4} \\ &=\; (\cos\tfrac{1}{2}\theta^{\mathrm{h}})^2(\cos\theta^{\mathrm{v}})^{1/2}(\cos\theta^{\mathrm{h}})^{-1/2}(\cos(\theta^{\mathrm{h}}+\theta^{\mathrm{v}})\cos(\theta^{\mathrm{h}}-\theta^{\mathrm{v}}))^{-1/4}\,. \end{aligned}$$

Putting all the factors together, one gets (4.3.8). □

Remark 2.3.3. The identity (4.7.26) with $n = 0$ also provides a formula

$$D_1 = \beta^\#_0 \cdot [\cos\theta^{\mathrm{v}} - \alpha^\#_0 \sin\theta^{\mathrm{h}}]$$

for the *energy density* (on a vertical edge) of the homogeneous Ising model.

2.3.4 . Asymptotics of horizontal correlations D_n as $n \to \infty$ at criticality

Assume now that $\theta^{\mathrm{h}} + \theta^{\mathrm{v}} = \frac{\pi}{2}$. Another classical result that we discuss in this section is that spin-spin correlations D_m decay like $m^{-1/4}$ at large distances.

Theorem 2.3.4 (McCoy–Wu). Let $\mathcal{C}_\sigma := 2^{\frac{1}{6}} e^{\frac{3}{2}\zeta'(-1)}$, $\theta^{\mathrm{h}} = \theta$ and $\theta^{\mathrm{v}} = \frac{\pi}{2} - \theta$. Then,

$$D_m \;\sim\; \mathcal{C}_\sigma^2 \cdot (2m\cos\theta)^{-1/4} \quad \text{as} \quad m \to \infty. \tag{2.3.29}$$

Proof. A straightforward computation shows that

$$w(t;\theta,\tfrac{\pi}{2}-\theta) = 2\sin\theta \cdot [1 - (\sin\theta\cos\tfrac{1}{2}t)^2]^{1/2} \cdot |\sin\tfrac{1}{2}t|\,.$$

In particular, the weight $w^{\#} := w^{-1}$ is not integrable and the arguments used in the proof of Theorem 2.3.1 require a modification. Also, the Kramers–Wannier duality ensures that $D_n = D_n^\star$, $L_n = L_n^\star$ and hence the identities (2.3.26), (2.3.28) become useless (though one still could use (4.7.25)). In this situation we prefer to switch to the framework of orthogonal polynomials on the *real line* (more precisely, on the segment $[-1,1]$) for computations. Let

$$\overline{w}(x;\theta) \;:=\; [\,1 - (\sin\theta\cdot x)^2\,]^{1/2}\,, \quad x \in [-1;1], \tag{2.3.30}$$

and let $P_n(x) = x^n + \dots$ be the monic orthogonal polynomial of degree n on $[-1,1]$ with respect to the weight $\overline{w}(x,\theta)$. It is easy to check that the trigonometric polynomial

$$Q_n(e^{it}) \;:=\; D_n \cdot e^{\frac{1}{2}int} \cdot 2^n P_n(\cos\tfrac{1}{2}t)$$

fits the construction given in Lemma 4.7.4 to solve the problem [$\mathrm{P}_{\mathrm{n}}^{\mathrm{sym}}$]. The formula (4.7.17) gives

$$\begin{aligned} L_{n+1} \;&=\; \frac{1}{2\pi}\int_{-\pi}^{\pi} Q_n(e^{it}) w(t;\theta,\tfrac{\pi}{2}-\theta)dt \\ &=\; \frac{D_n 2^{n-1}}{\pi}\int_{-\pi}^{\pi} \cos(\tfrac{1}{2}nt) P_n(\cos\tfrac{1}{2}t) w(t;\theta,\tfrac{\pi}{2}-\theta)dt \\ &=\; \frac{D_n 2^{n+1}\sin\theta}{\pi}\int_{-1}^{1} (2^{n-1}x^n + \dots) P_n(x)\overline{w}(x;\theta)dx \\ &=\; \pi^{-1}2^{2n}\sin\theta \cdot \|P_n\|^2_{\overline{w}dx} \cdot D_n, \qquad n \geq 1. \end{aligned} \tag{2.3.31}$$

Moreover, a similar computation for $n = 0$ implies that

$$2L_1 \;=\; 2\pi^{-1}\sin\theta \textstyle\int_{-1}^{1} P_0(x)\overline{w}(x;\theta)dx = 2\pi^{-1}\sin\theta \cdot \|P_0\|^2_{\overline{w}dx} \tag{2.3.32}$$

since $D_0 = 1$ and due to the modification required in Lemma 4.7.2 in the case $n = 0$.

We can use the same line of reasoning to construct a solution of the problem $[\mathrm{P}^{\mathrm{anti}}_{\mathrm{n+1}}]$ treated in Lemma 4.7.5 in the non-critical regime. Namely, let $P^{\#}_n(x)$ be the monic orthogonal polynomial of degree n on $[-1,1]$ with respect to the weight

$$\overline{w}^{\#}(x) \;:=\; [\,1-(\sin\theta\cdot x)^2\,]^{-1/2}\,, \quad x\in[-1,1], \tag{2.3.33}$$

and

$$Q^{\#}_{n+1}(e^{it}) \;:=\; L_n\cdot(e^{it}-1)e^{\frac{1}{2}int}\cdot 2^n P^{\#}_n(\cos\tfrac{1}{2}t).$$

It is straightforward to check that the formula (4.7.20) gives a solution to the boundary value problem $[\mathrm{P}^{\mathrm{anti}}_{\mathrm{n+1}}]$, note that the product $(e^{it}-1)w^{\#}(t;\theta,\frac{\pi}{2}-\theta)$ is integrable on the unit circle as the first factor kills the singularity of $w^{\#}$ at $t=0$. Moreover, the computation (4.7.21) remains valid and reads as

$$\begin{aligned} D_{n+1} \;&=\; -\frac{1}{2\pi}\int_{-\pi}^{\pi} Q^{\#}_{n+1}(e^{it})w^{\#}(t;\theta,\tfrac{\pi}{2}-\theta)^{-1}dt \\ &=\; \frac{L_n 2^n}{\pi}\int_{-\pi}^{\pi}\frac{\sin(\frac{1}{2}(n+1)t)}{\sin\frac{1}{2}t}P^{\#}_n(\cos\tfrac{1}{2}t)\frac{(\sin\frac{1}{2}t)^2dt}{w(t;\theta,\frac{\pi}{2}-\theta)} \\ &=\; \frac{L_n 2^n}{\pi\sin\theta}\int_{-1}^{1}(2^n x^n+\dots)P^{\#}_n(x)\overline{w}^{\#}(x)dx \\ &=\; \pi^{-1}2^{2n}(\sin\theta)^{-1}\cdot\|P^{\#}_n\|^2_{\overline{w}^{\#}dx}\cdot L_n, \quad n\geq 0. \end{aligned} \tag{2.3.34}$$

Recall that $L_0=\sin\theta$ (see Lemma 4.7.2). Taking a product of the recurrence relations (4.7.30), (4.7.29) for $n=1,\dots,m-1$, and (4.7.32) for $n=0,\dots,m$, one obtains the identity

$$D_{m+1}D_m \;=\; \pi^{-2m-1}2^{2m^2}\prod\nolimits_{k=0}^{m-1}\|P_k\|^2_{\overline{w}dx}\cdot\prod\nolimits_{k=0}^{m}\|P^{\#}_k\|^2_{\overline{w}^{\#}dx}\,, \tag{2.3.35}$$

where the weights $w(x;\theta)$ and $w^{\#}(x;\theta)$ on $[-1,1]$ are given by (4.7.28) and (4.7.31).

This is again a classical setup of the orthogonal polynomials theory, note that if one now passes back to the unit circle than the $|t|$-type singularity of the weights appear at the point $e^{it}=1$. One might now use the general results (summarized, e.g., in [54]) but we prefer to refer to a specific treatment [7]. Applying [7, Theorem 1.7] with parameters $\alpha=0,\beta=\pm\frac{1}{2}$ and $k=\sin\theta$ one obtains the asymptotics

$$D_{m+1}D_m \;\sim\; \pi[G(\tfrac{1}{2})]^4(1-k^2)^{-1/4}m^{-1/2} \;\sim\; 2^{2/3}e^{6\zeta'(-1)}(2m\cos\theta)^{-1/2}, \quad m\to\infty,$$

where G denotes the Barnes G-function. (Note that [7] also provides subleading terms of this asymptotics.) The proof of (4.7.27) is complete modulo the fact that $D_{m+1}\sim D_m$ as $m\to\infty$. This statement can be proved by the arguments given in the next remark (or, alternatively, using probabilistic estimates). $\square$

Remark 2.3.5. Due to the famous quadratic identities [141, 121] for the spin-spin correlations (recall also the definition (4.7.9) of L_n), one can write (4.7.29) and (4.7.32) as

$$A_n \;:=\; \pi^{-1}2^{2n}\|P_n\|^2_{\overline{w}dx} = \frac{D_{n+1}+\cos\theta\cdot\widetilde{D}_{n+1}}{D_n} = \frac{D_{n+2}}{D_{n+1}-\cos\theta\cdot\widetilde{D}_{n+1}},$$
$$B_{n+1} \;:=\; \pi^{-1}2^{2n+2}\|P^{\#}_{n+1}\|^2_{\overline{w}^{\#}dx} = \frac{D_{n+2}}{D_{n+1}+\cos\theta\cdot\widetilde{D}_{n+1}} = \frac{D_{n+1}-\cos\theta\cdot\widetilde{D}_{n+1}}{D_n}.$$

In fact, one can also prove these identities by considering the anti-symmetrization (resp., symmetrization) of the observable $X_{[\mathbf{u},\mathbf{v}]}$ on the north-west (resp., north-east) corners of the lattice and noticing that, up to a multiplicative constant, it solves the problem $[\mathrm{P}^{\mathrm{anti}}_{\mathrm{n+2}}]$ (resp., $[\mathrm{P}^{\mathrm{sym}}_{\mathrm{n-1}}]$). In particular, we have

$$D_{m+1}/D_m \;=\; \tfrac{1}{2}(A_m + B_{m+1}) \;=\; 2(A^{-1}_{m-1} + B^{-1}_m)^{-1}$$

so one can see that $D_{m+1} \sim D_m$ and find sub-leading corrections to the asymptotics of D_m (and $\widetilde{D}_m$) using the analysis of orthogonal polynomials performed in [7].

2.4 . Layered model in the zig-zag half-plane

In this section we work with the (half-)infinite volume limit of the Ising model on the zig-zag half-plane $\mathbb{H}^{\diamond}$ (see Fig. 2.4.1 for the notation), which is defined as a limit of probability measures on an increasing sequence of finite domains exhausting $\mathbb{H}^{\diamond}$, with '+' boundary conditions at the right-most column C_0 and at infinity. All interaction parameters between the columns C_{p-1} and C_p are assumed to be the same and equal to $x_p = \exp[-2\beta J_p] = \tan\frac{1}{2}\theta_p$. The goal is to find a representation for the magnetization M_m at the column C_{2m}, see (2.1.1). The uniqueness of the relevant half-plane fermionic observable is discussed in Section 2.4.1 and our main result – Theorem 2.1.1 – is proved in Section 2.4.2. In Section 2.4.3 we use Theorem 2.1.1 to discuss the *wetting phase transition* [73, 146] caused by a boundary magnetic field. In this case the Jacobi matrix J can be explicitly diagonalized and the final answer can be written in terms of the so-called Toeplitz+Hankel determinants.

2.4.1 . Half-plane fermionic observable

Let $\mathbf{v} = (-2m-\frac{3}{2}, 0)$. Below we work with the fermionic observable $X_{[\mathbf{v}]}$ defined by (2.2.10); comparing with Section 2.3 one can think about the spin $\sigma_{\mathbf{u}} := \sigma_{\mathrm{out}}$ as being attached to the vertical boundary. We are mostly interested in the values of $X_{[\mathbf{v}]}$ at west corners (see Fig. 2.4.1)

$$H(-k,s) \;:=\; \Psi_{[\mathbf{v}]}((-k,s)) = X_{[\mathbf{v}]}((-k,s)), \quad k\in\mathbb{N}_0,\; s\in\mathbb{Z},\; k+s\notin 2\mathbb{Z},$$

note the convention on η_c chosen in (2.2.9). By definition, one has

$$H(-2m-1,0) \;=\; \mathbb{E}^+_{\mathbb{H}^\diamond}[\sigma_{(-2m-\frac{1}{2},0)}] \;=\; M_m. \tag{2.4.1}$$

We also need the values of $X_{[\mathbf{v}]}$ at east corners:

$$H^\circ(-k,s) \;:=\; \Psi_{[\mathbf{v}]}((-k,s)) = iX_{[\mathbf{v}]}((-k,s)), \quad k\in\mathbb{N},\; s\in\mathbb{Z},\; k+s\in 2\mathbb{Z}.$$

It is convenient to set $\theta_0 := 0$ and $H^\circ(0,s) := 0$ for all $s \in 2\mathbb{Z}$.

The infinite-volume observable $X_{[\mathbf{v}]}$ is defined as a (subsequential) limit of the same observables constructed in finite regions. Subsequential limits exist due to the uniform bound (4.7.1) while the uniqueness of $X_{[\mathbf{v}]}$ is given by Lemma 2.4.1. The discrete Cauchy–Riemann identities (2.2.13) can be written as

$$\begin{aligned} &H(-k-1,s\pm 1)\sin\theta_{k+1} - H(-k,s)\cos\theta_k \\ &= \pm i\cdot[\,H^\circ(-k,s\pm 1)\sin\theta_k - H^\circ(-k-1,s)\cos\theta_{k+1}\,], \quad k\geq 1,\; k+s\notin 2\mathbb{Z}. \end{aligned} \tag{2.4.2}$$

Near the vertical boundary, these equations should be modified as follows:

$$H(-1,s\pm 1)\sin\theta_1 - H(0,s) \;=\; \mp i\cdot H^\circ(-1,s)\cos\theta_1, \quad s\notin 2\mathbb{Z}. \tag{2.4.3}$$

Indeed, $X_{[\mathbf{v}]}((-\frac{1}{2},s\pm\frac{1}{2})) = X_{[\mathbf{v}]}(0,s)) = H(0,s)$ and hence (2.4.3) are nothing but the three-term identities (2.2.12).

Lemma 2.4.1. *The spinors H, H° defined in $\mathbb{H}^\diamond$ and branching over $\mathbf{v}$ are uniquely determined by the following conditions: uniform boundedness, Cauchy–Riemann identities* (2.4.2)*, boundary relations* (2.4.3)*, and the value* (2.4.1) *of H near $\mathbf{v}$.*

Proof. Taking the difference of two solutions, assume that H, H° are uniformly bounded, satisfy (2.4.2), (2.4.3) and that $H(-2m-1,0) = 0$. Recall that Proposition 2.2.3 gives the harmonicity-type identity

$$\begin{aligned} H(-k,s) \;&=\; \tfrac{1}{2}\sin\theta_{k+1}\cos\theta_k\cdot[H(-k-1,s+1)+H(-k-1,s-1)] \\ &+\; \tfrac{1}{2}\sin\theta_k\cos\theta_{k-1}\cdot[H(-k+1,s+1)+H(-k+1,s-1)] \end{aligned} \tag{2.4.4}$$

at all west corners $c = (-k+\frac{1}{2},s)$ with $k\geq 2$ except in the case $k=-2m-1$, $s=0$ (i.e., at the west corner located near the branching $\mathbf{v}$). Moreover, due to the boundary relations (2.4.3), exactly the same identity holds for $k=0,1$ (recall that we formally set $\theta_0 := 0$). In its turn, the function H° satisfies the identities

$$\begin{aligned} H^\circ(-k,s) \;&=\; \tfrac{1}{2}\cos\theta_{k+1}\sin\theta_k\cdot[H^\circ(-k-1,s+1)+H^\circ(-k-1,s-1)] \\ &+\; \tfrac{1}{2}\cos\theta_k\sin\theta_{k-1}\cdot[H^\circ(-k+1,s+1)+H^\circ(-k+1,s-1)] \end{aligned} \tag{2.4.5}$$

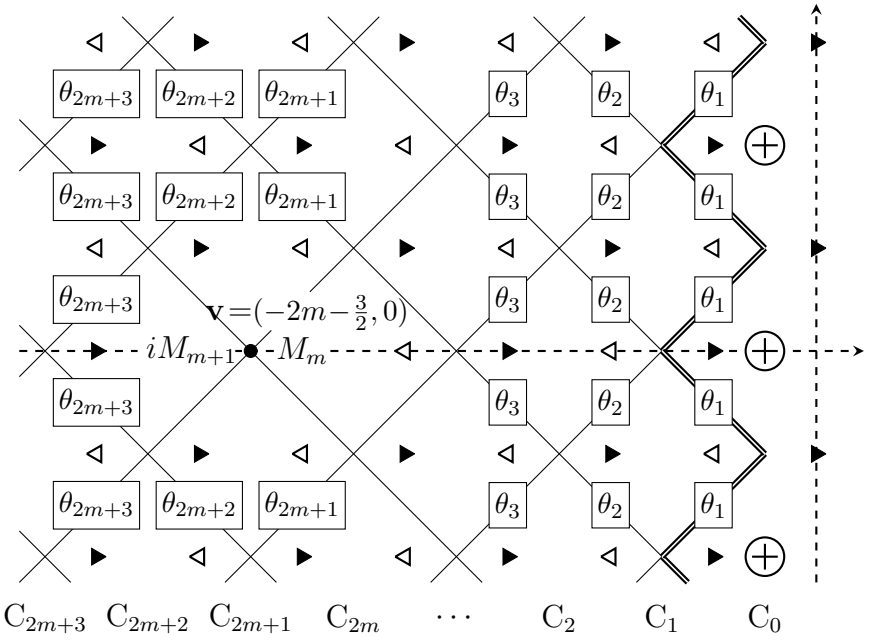

FIGURE 2.4.1 – The zig-zag layered model in the left half-plane $\mathbb{H}^\diamond$. All the interaction parameters between two adjacent columns are assumed to be the same. The '+' boundary conditions are imposed at the column C_0. To analyze the ratio M_{m+1}/M_m we consider the Kadanoff–Ceva fermionic observable branching at $\mathbf{v}=(-2m-\frac{3}{2},0)$.

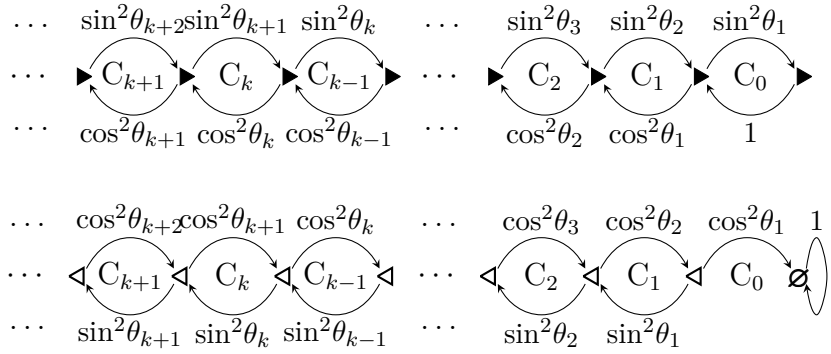

FIGURE 2.4.2 – For appropriately chosen prefactors ϱ_k and ϱ_k°, the identities (2.4.4), (2.4.5) (coming from Proposition 2.2.3) can be written as the discrete harmonicity property of functions $\varrho_k H(-k,s)$ and $\varrho_k^\circ H^\circ(-k,s)$ with respect to random walks having the indicated transition probabilities in the horizontal direction (and $\frac{1}{2}$ in the vertical one). The first random walk (on $\triangleright$) is reflected from the imaginary axis while the second (on $\triangleleft$) is absorbed there.

at *all* east corners $d = (-k + \frac{1}{2}, s)$, including the one located near the branching $\mathbf{v}$ (in the latter case the proof of Proposition 2.2.3 works verbatim due to the fact that $H(-2m-1, 0) = 0$). Both (2.4.4) and (2.4.5) can be rewritten as *true* discrete harmonicity properties if one passes from H and H° to the functions

$$\widetilde{H}(-k, s) := \varrho_k \cdot H(-k, s), \qquad \widetilde{H}^\circ := \varrho_k^\circ \cdot H^\circ(-k, s),$$
$$\varrho_k := \prod_{j=1}^{k} (\sin\theta_j \,/\, \cos\theta_{j-1}), \qquad \varrho_k^\circ := \prod_{j=2}^{k} (\cos\theta_j \,/\, \sin\theta_{j-1}),$$

recall that we set $\widetilde{H}^\circ(0, s) = H^\circ(0, s) := 0$ on the vertical axes.

Let $Z_n = (K_n, S_n)$ (resp., $Z_n^\circ = (K_n^\circ, S_n)$) be the nearest-neighbor random walk on west (resp., east) corners, with jump probabilities $(\frac{1}{2}, \frac{1}{2})$ for the process S_n and $(\cos^2\theta_k, \sin^2\theta_k)$ for the process K_n (resp., $(\sin^2\theta_k, \cos^2\theta_k)$ for the process K_n°), see Fig. 2.4.2. Note that the walk Z_n on west corners is *reflected* from the vertical axes while the walk Z_n° on east corners is *absorbed* there.

It follows from (2.4.4) that the stochastic process $\widetilde{H}(Z_n)$ is a martingale, when equipped with the canonical filtration, until the first time when Z_n hits the west corner $(-2m\text{–}1, 0)$ located near the branching, recall that $\widetilde{H}(-2m-1, 0) = 0$. Similarly, (2.4.5) implies that the process $\widetilde{H}^\circ(Z_n^\circ)$ is a martingale until the first time when Z_n° hits the imaginary axis, recall that $\widetilde{H}^\circ = 0$ there. As we show below, depending on the behavior of ϱ_k and ϱ_k° as $k \to \infty$, the optional stopping theorem allows to conclude that either $\widetilde{H}$ or $\widetilde{H}^\circ$ vanishes identically. Once the identity $\widetilde{H} \equiv 0$ (resp., $\widetilde{H}^\circ \equiv 0$) is proven, the equations (2.4.2), (2.4.3) and the fact that $\widetilde{H}^\circ$ vanishes on the imaginary axis (resp., $\widetilde{H}$ vanishes at the point $(-2m-1, 0)$) imply that $\widetilde{H}^\circ \equiv 0$ (resp., $\widetilde{H} \equiv 0$) too. Recall that the functions H and H° are uniformly bounded and note that $\varrho_k \varrho_k^\circ = (\cos\theta_1)^{-1} \sin\theta_k \cos\theta_k = O(1)$ as $k \to \infty$. It follows from the maximum principle that

— the function $\widetilde{H}$ is uniformly bounded unless $\varrho_k \to \infty$ as $k \to \infty$;

— the function $\widetilde{H}^\circ$ is uniformly bounded unless $\varrho_k^\circ \to \infty$ as $k \to \infty$.

We have three cases to consider separately.

— Let $\liminf_{k\to\infty} \varrho_k = 0$, in particular this implies that $\widetilde{H}$ is uniformly bounded. The optional stopping theorem applied to the martingale $\widetilde{H}(Z_n)$ and the fact that a one-dimensional random walk on $-\mathbb{N}_0$ reflected at 0 almost surely takes arbitrary large (negative) values imply that $H \equiv 0$.

— Let $\liminf_{k\to\infty} \varrho_k^\circ = 0$. A similar argument applied to the martingale $\widetilde{H}^\circ(Z_n^\circ)$ (recall that $\widetilde{H}^\circ$ vanishes on the imaginary axis) shows that $\widetilde{H}^\circ \equiv 0$.

— Let both sequences ϱ_k and ϱ_k° be uniformly bounded from below as $k \to \infty$. Since $\varrho_k \varrho_k^\circ = (\cos\theta_1)^{-1} \sin\theta_k \cos\theta_k$, these sequences are also uniformly bounded from above and the parameters θ_k, $k \geq 1$, stay away from 0. In

this case it is easy to see that the process K_n° hits 0 almost surely (i.e., that the random walk Z_n° hits the imaginary axis almost surely). Indeed, the probability p_k° to hit 0 starting from $-k$ satisfies the recurrence

$$p_k^\circ - p_{k+1}^\circ = \cot^2\theta_k \cdot (p_{k-1}^\circ - p_k^\circ) = \ldots = \varrho_{k+1}^{-2} \sin^2\theta_{k+1} \cdot (1 - p_1^\circ),$$

which is only possible if $p_1^\circ = 1$ since the factors $\varrho_{k+1}/\sin\theta_{k+1}$ are uniformly bounded. We conclude as before by applying the optional stopping theorem to the uniformly bounded martingale $\widetilde{H}(Z_n^\circ)$.

The proof is complete. □

2.4.2 . Magnetization M_m in the $(2m)$-th column

Similarly to Section 4.7.2, below we rely upon the uniqueness Lemma 2.4.1 and aim to construct the values of $X_{[\mathbf{v}]}$ on west and east corners (i.e., the pair of spinors H, H°) as explicitly as possible. Note that we have

$$H(-2p-1,0) = 0 \ \text{ for } \ p \geq m+1, \qquad H^\circ(-2p,0) \ = \ 0 \ \text{ for } \ p \leq m. \quad (2.4.6)$$

since the spinors defined (on the double cover branching over $\mathbf{v}$) by the symmetry $H_1(-k,-s) := H(-k,s)$, $H_1^\circ(-k,-s) := -H^\circ(-k,s)$ also satisfy the Cauchy–Riemann equations (2.4.2), (2.4.3) and thus must coincide with H, H°.

Given $s \geq 0$, let H_s denote the semi-infinite vector of the (real) values $H(-k,s)$, $k \in \mathbb{N}_0$, where we assign zero values to the indices s such that $s+k \in 2\mathbb{Z}$. Similarly, let H_s° be the vector of the (purely imaginary) values $H^\circ(-k,s)$, $k \in \mathbb{N}$, where we assign zero values to the indices s such that $s+k \notin 2\mathbb{Z}$. We can write the harmonicity-type equations (2.4.4) and (2.4.5) as

$$H_s = \tfrac{1}{2} C[H_{s-1} + H_{s+1}], \qquad H_s^\circ = \tfrac{1}{2} C^\circ[H_{s-1}^\circ + H_{s+1}^\circ], \qquad s \geq 1, \quad (2.4.7)$$

where the self-adjoint operators C and C° are given by

$$C \ := \ \begin{bmatrix} 0 & \sin\theta_1 & 0 & 0 & \ldots \\ \sin\theta_1 & 0 & \sin\theta_2\cos\theta_1 & 0 & \ldots \\ 0 & \sin\theta_2\cos\theta_1 & 0 & \sin\theta_3\cos\theta_2 & \ldots \\ 0 & 0 & \sin\theta_3\cos\theta_2 & 0 & \ldots \\ \ldots & \ldots & \ldots & \ldots & \ldots \end{bmatrix},$$

$$C^\circ \ := \ \begin{bmatrix} 0 & \cos\theta_2\sin\theta_1 & 0 & 0 & \ldots \\ \cos\theta_2\sin\theta_1 & 0 & \cos\theta_3\sin\theta_2 & 0 & \ldots \\ 0 & \cos\theta_3\sin\theta_2 & 0 & \cos\theta_4\sin\theta_3 & \ldots \\ 0 & 0 & \cos\theta_4\sin\theta_3 & 0 & \ldots \\ \ldots & \ldots & \ldots & \ldots & \ldots \end{bmatrix}.$$

Let $T(\lambda) := \lambda^{-1} \cdot (1 - \sqrt{1-\lambda^2})$. Similarly to Section 4.7.2, in order to satisfy the recurrences (2.4.7) we intend to write

$$H_s \ := \ [T(C)]^s H_0, \qquad H_s^\circ \ := \ [T(C)]^s H_0^\circ, \qquad s \geq 1. \quad (2.4.8)$$

We now introduce an operator D, which plays the key role in the rest of the analysis:

$$D \;:=\; i\begin{bmatrix} \cos\theta_1 & 0 & 0 & 0 & \dots \\ 0 & \cos\theta_1\cos\theta_2 & 0 & 0 & \dots \\ -\sin\theta_1\sin\theta_2 & 0 & \cos\theta_2\cos\theta_3 & 0 & \dots \\ 0 & -\sin\theta_2\sin\theta_3 & 0 & \cos\theta_3\cos\theta_4 & \dots \\ \dots & \dots & \dots & \dots & \dots \end{bmatrix}.$$

A straightforward computation gives

$$CD = DC^\circ, \qquad DD^* = I - C^2 \quad \text{and} \quad D^*D = I - (C^\circ)^2. \tag{2.4.9}$$

In particular, this implies that $-I \le C, C^\circ \le I$. Therefore, the operators $T(C)$ and $T(C^\circ)$ in (2.4.8) are well-defined and the vectors H_s and H_s° defined by (2.4.8) are uniformly bounded as $s \to \infty$. Still, we need to find the vectors H_0 and H_0° so that not only the harmonicity-type identities (2.4.7) for H and H° but also the Cauchy–Riemann equations (2.4.2), (2.4.3) relating H_s and H_s° are satisfied.

Note that $\operatorname{Ker} D = \{0\}$ while the kernel of D^* might be two-dimensional. Let $D^* = U(DD^*)^{1/2}$ be the *polar decomposition* of D^*, where

$$U \;:=\; (D^*D)^{-1/2}D^* \;=\; D^*(DD^*)^{-1/2} \tag{2.4.10}$$

is a *(partial) isometry*. We are now able to formulate the key proposition on the construction of solutions to (2.4.2), (2.4.3) in the upper quadrant.

Proposition 2.4.2. *Given $H_0 \in \ell^2$, let $H_0^\circ := UH_0$. Then, $H_s := [T(C)]^s H_0$ and $H_s^\circ := [T(C^\circ)]^s H_0^\circ$ are uniformly bounded in ℓ^2 and provide a solution to the Cauchy–Riemann equations* (2.4.2), (2.4.3) *in the upper quadrant.*

Proof. Since $-I \le C, C^\circ \le I$, we have $0 \le T(C), T(C^\circ) \le I$. Therefore, H_s and H_s° are uniformly bounded in ℓ^2. Moreover, (2.4.9) and (2.4.10) imply that $UC = C^\circ U$ and hence $H_s^\circ = [T(C^\circ)]^s UH_0 = U[T(C)]^s H_0 = UH_s$ for all $s \ge 0$. This allows one to write

$$CH_{s+1} - H_s \;=\; -(I-C^2)^{1/2}H_s \;=\; -DUH_s \;=\; -DH_s^\circ\,, \tag{2.4.11}$$

$$H_{s+1} - CH_s \;=\; -(I-C^2)^{1/2}H_{s+1} \;=\; -DH_{s+1}^\circ\,. \tag{2.4.12}$$

It is not hard to see that these equations are equivalent to the Cauchy–Riemann identities (2.4.2), (2.4.3). Indeed, the first entry of the vector-valued equation (2.4.11) or (2.4.12) (depending on the parity of s) gives the relation (2.4.3) while the first entry of the other equation gives a linear combination of (2.4.3) and (2.4.2) with $k = 1$. Further, each of the next entries of (2.4.11) and (2.4.12) gives a linear combination of two identities (2.4.2) with two consecutive k's. Therefore, for each $s \ge 0$ one can inductively (in k) recover all the identities (2.4.3), (2.4.2) from (2.4.11) and (2.4.12). □

Clearly, the operators D and U can be split into independent components indexed by odd/even indices, only one of which is relevant for the value of the magnetization M_m in the *even* columns C_{2m}, the other component is responsible for the magnetization in odd columns. In particular, the relevant block D_{even} of the operator D is given by (2.1.2).

Remark 2.4.1. In view of the result provided by Proposition 2.4.2, the (partial) isometry U_{even} can be thought of as a *discrete Hilbert transform* associated with the Cauchy–Riemann equations (2.4.2), (2.4.3) in the upper quadrant: given the values H_0 of the real part of a 'discrete holomorphic' function (H, H°) on the real line, it returns the boundary values $H_0^\circ = U_{\mathrm{even}} H_0$ of its imaginary part.

We are now able to prove the main result of this section.

Proof of Theorem 2.1.1. Let H and H° be the values of the half-plane observable $X_{[\mathbf{v}]}$ on west and east corners, respectively. Since H_0 is a finite vector (see (2.4.6)), it belongs to ℓ^2. Therefore, Lemma 2.4.1 and Proposition 2.4.2 imply that

$$D_{\mathrm{even}} H_0^\circ \;=\; D_{\mathrm{even}} U_{\mathrm{even}} H_0 \;=\; J^{1/2} \,[\, *\;\ldots\;*\;\; M_m\;0\;0\;\ldots\,]^\top,$$

where we use the symbol $*$ to denote unknown entries of the vector $D_{\mathrm{even}} H_0$ and M_m is its $(m+1)$-th coordinate. On the other hand, note that

$$-iH^\circ(-2m-2,0) = X_{[\mathbf{v}]}((-2m-2,0)) = -\mathbb{E}^+_{\mathbb{H}^\diamond}[\sigma_{-2m-\frac{5}{2}}] = M_{m+1}.$$

By definition of the operator D and due to (2.4.6) one sees that

$$D_{\mathrm{even}} H_0^\circ \;=\; \cos\theta_{2m+1} \cos\theta_{2m+2} \cdot [\,0\;\ldots\;0\;\, M_{m+1}\;\, *\;\, *\;\ldots]^\top.$$

Recall that we denote by P_{m+1} the orthogonal projection from ℓ^2 onto the subspace generated by the first basis vectors $e_1, \ldots, e_{m+1}$ of ℓ^2. It follows from the considerations given above that

$$\begin{aligned} P_{m+1} J^{1/2} P_{m+1} :\; f_{m+1} = [\,*\;\ldots\;*\;\,1\,]^\top \;&\mapsto \beta_m \cdot [\,0\;\ldots\;0\;1\,]^\top = \beta_m e_{m+1}\,, \\ \beta_m \;&:=\; \cos\theta_{2m+1} \cos\theta_{2m+2} \cdot M_{m+1}/M_m\,, \end{aligned}$$

for a certain vector $f_{m+1} = P_{m+1} f_{m+1}$ such that $\langle f_{m+1}, e_{m+1}\rangle = 1$. In particular, if we denote by $e'_1, e'_2, \ldots$ the orthogonalization of the vectors $e_1, e_2, \ldots$ with respect to the scalar product $\langle\,\cdot\,, J^{1/2}\cdot\,\rangle$, then $\langle e'_{m+1}, J^{1/2} e'_{m+1}\rangle = \langle e_{m+1}, J^{1/2} f_{m+1}\rangle = \beta_m$ and hence

$$\det P_{m+1} J^{1/2} P_{m+1} \;=\; \det[\,\langle e'_p, J^{1/2} e'_q\rangle\,]_{p,q=1}^{m+1} \;=\; \prod_{k=0}^{m} \beta_k \;=\; M_{m+1} \cdot \prod_{k=1}^{2m+2} \cos\theta_k\,,$$

where we also used the fact that $M_0 = 1$; note that this computations does *not* require any modification in the case $m = 0$ (when dealing with the magnetization in even columns). This gives the second formula for M_m in (2.1.5).

To prove that M_m also equals to $|\det P_m U_{\rm even} P_m|$, note that

$$(D_{\rm even} D_{\rm even}^*)^{1/2} \;=\; D_{\rm even} U_{\rm even} \quad \text{and} \quad P_m D_{\rm even} \;=\; P_m D_{\rm even} P_m \,,$$

which implies

$$\begin{aligned} \det P_m (D_{\rm even} D_{\rm even}^*)^{1/2} P_m \;&=\; |\det P_m U_{\rm even} P_m| \cdot |\det P_m D_{\rm even} P_m| \\ &=\; |\det P_m U_{\rm even} P_m| \cdot \textstyle\prod_{k=1}^{2m} \cos\theta_k . \end{aligned}$$

Finally, to prove the last identity in (2.1.5), note that

$$\det P_m J^{1/2} P_m \;=\; \frac{\det[\,\langle J^{1/2} f_p, f_q\rangle\,]_{p,q=1}^m}{\det[\,\langle f_p, f_q\rangle\,]_{p,q=1}^m}$$

for all bases $f_1, \dots, f_m$ of the m-dimensional space ${\rm Ran} P_m$. Choosing the basis $1, \lambda, \dots, \lambda^{m-1}$ in the spectral representation of the operator J in the space $L^2(\nu_J(d\lambda))$ one obtains the identity

$$\det P_m J^{1/2} P_m \;=\; \frac{{\rm H}_m[\lambda^{1/2}\nu_J]}{{\rm H}_m[\nu_J]} \quad \text{and, similarly,} \quad \det P_m J P_m \;=\; \frac{{\rm H}_m[\lambda\nu_J]}{{\rm H}_m[\nu_J]}$$

As $\det P_m J P_m = [\det P_m D_{\rm even}^* P_m]^2 = [\prod_{k=1}^{2n} \cos\theta_k]^2$, this completes the proof. □

2.4.3 . Boundary magnetic field and the wetting phase transition

In this section we assume that $\theta_k = \theta < \frac{\pi}{4}$ for all $k \geq 2$, i.e., that we work with a fully homogeneous subcritical model but we allow the first interaction constant to have a different value. This can be trivially reformulated as inducing an additional magnetic field *at the first column* whose strength $h = 2J_1$ corresponds to θ_1 via (3.2.3). The main result is the following theorem which translates the abstract formula (2.1.5) into the concrete language of Toeplitz+Hankel determinants. Let

$$\begin{aligned} q := \tan\theta < 1\,, \qquad & r := 1 - \frac{\cos^2\theta_1}{\cos^2\theta} \in (-q^2; 1)\,, \\ w(z) := |1 - q^2 z|\,, \qquad & \xi(z) := \frac{(rz - q^2)(q^2 z - 1)}{(z - q^2)(q^2 z - r)}\,. \end{aligned} \tag{2.4.13}$$

Note that $\xi(z)\xi(z^{-1}) = 1$.

Theorem 2.4.2. In the setup described above, the following formula holds:

$$M_m \;=\; (1-r)^{-3/2} \det\,[\,\alpha_{k-n} - \beta_{k+n} + (1-r)^{3/2}\gamma_{k+n}\,]_{k,n=0}^{m-1}\,, \tag{2.4.14}$$

where

$$\alpha_s := \frac{1}{2\pi}\int_{-\pi}^{\pi} e^{-is\theta} w(e^{i\theta})d\theta\,, \qquad \beta_s := \frac{1}{2\pi}\int_{-\pi}^{\pi} e^{-is\theta}\xi(e^{i\theta})w(e^{i\theta})d\theta,$$

and $\gamma_s := c\cdot(q^2/r)^s$, $c = (r^2-q^4)r^{-3/2}(r-q^4)^{-1/2}$, if $r > q^2$ and $\gamma_s := 0$ otherwise.

Proof. Denote $a := \sin^2\theta\cos^2\theta = (q+q^{-1})^{-2}$. The entries of the Jacobi matrix J (see (2.1.4)) are given by

$$b_1 = (1-r)q^{-2}a\,, \quad a_1 = (1-r)^{1/2}a\,; \qquad b_k = 1-2a\,, \quad a_k = a\,, \quad k\geq 2.$$

Let $\varrho_k := (1-r\delta_{k,0})^{1/2}$, where $\delta_{k,0}$ is the Kronecker delta. The *continuous* spectrum of J has multiplicity 1 and equals to $[1-4a\,,1]$. The generalized eigenfunctions are

$$\psi_k(\zeta) := \varrho_k^{-1}\cdot[\zeta^k - \xi(\zeta)\zeta^{-k}], \quad \lambda(\zeta) := 1-a\cdot(2+\zeta+\zeta^{-1}), \quad \zeta = e^{i\theta},\ \theta\in[0,\pi].$$

The coefficient $\xi(\zeta)$ should satisfy the condition $(b_1-\lambda(\zeta))\psi_0(\zeta) = a_1\psi_1(\zeta)$ which leads to the formula (2.4.13). The matrix J also has the *eigenvalue*

$$\lambda(\zeta_0) \;=\; \frac{(1-r)(r-q^4)}{r(1+q^2)^2} \;\in\; (0,1-4a) \quad \text{if}\ \ \zeta_0 := q^2/r < 1$$

since $\xi(\zeta_0) = 0$. Note that

$$\begin{aligned}\frac{\varrho_k\varrho_n}{2\pi}\int_0^{\pi}\psi_n(e^{-i\theta})\psi_k(e^{i\theta})d\theta \;&=\; \frac{1}{2\pi i}\oint_{|\zeta|=1}[\,\zeta^{k-n} - \xi(\zeta^{-1})\zeta^{k+n}\,]\,\frac{d\zeta}{\zeta}\\ &=\; (1-r\delta_{k+n,0})\cdot\delta_{k,n} \;-\; c_0\zeta_0^{k+n-1},\end{aligned}$$

where $c_0 = 0$ if $r\leq q^2$ and

$$c_0 \;:=\; \operatorname*{res}_{z=\zeta_0}\xi(z^{-1}) \;=\; \frac{q^2(1-r)(r^2-q^4)}{r^2(r-q^4)} \quad \text{if}\ \ r > q^2.$$

Thus, the spectral decomposition of the basis vector $e_n = (\delta_{k,n})_{k\geq 0}$ reads as

$$\delta_{k,n} \;=\; \frac{1}{2\pi}\int_0^{\pi}\psi_n(e^{-i\theta})\psi_k(e^{i\theta})d\theta \;+\; \varrho_n^{-1}c_0\zeta_0^{n-1}\cdot\psi_k(\zeta_0).$$

Since $\lambda(e^{i\theta}) = (1+q^2)^{-2}(w(e^{it}))^2$, this gives the identity

$$\begin{aligned}\varrho_k\varrho_n\langle e_k, J^{1/2}e_n\rangle \;&=\; \frac{\varrho_k\varrho_n}{2\pi}\int_0^{\pi}\psi_n(e^{-i\theta})\psi_k(e^{i\theta})\frac{w(e^{i\theta})d\theta}{1+q^2} \;+\; c_0\zeta_0^{k+n-1}(\lambda(\zeta_0))^{1/2}\\ &=\; \varrho_k\varrho_n\cdot[(1+q^2)^{-1}(\alpha_{k-n}-\beta_{k+n}) + c_0(\lambda(\zeta_0))^{1/2}\zeta_0^{k+n-1}]\,.\end{aligned}$$

It remains to note that the normalizing factor $[\prod_{k=1}^{2n}\cos\theta_k\,]^{-1}$ in (2.1.5) equals to $(1-r)^{-1/2}\cdot(1+q^2)^k$ and hence (note also the two factors $\varrho_0 = (1-r)^{-1/2}$ in the first row and the first column of the matrix $J^{1/2}$)

$$M_m \;=\; (1-r)^{-3/2}\det\left[\alpha_{k-n}+\beta_{k+n}+(1-r)^{3/2}c\cdot\zeta_0^{k+n-1}\right]_{k,n=0}^{m-1},$$

where

$$c \;:=\; \frac{r(1+q^2)c_0(\lambda(\zeta_0))^{1/2}}{q^2(1-r)^{3/2}} \;=\; \frac{r^2-q^4}{r^{3/2}(r-q^4)^{1/2}}$$

as claimed. □

Remark 2.4.3 (*free boundary conditions*)**.** One can pass to the limit $r \to 1^-$ (which corresponds to $J_1 \to 0^+$) in the formula (2.4.14) since $\alpha_s = \alpha_{-s} = \beta_s + O(1-r)$ and $\alpha_0 = \beta_0 + O((1-r)^2)$ as $r \to 1^-$. (It is also not hard to adapt the proofs of Theorems 2.1.1 and 2.4.2 for this setup.) In particular, one can easily see that

$$\mathbb{E}^{+,0}_{\mathbb{H}^\diamond}[\sigma_{(-\frac{5}{2},0)}] \;=\; (1-q^4)^{1/2}, \qquad r=1,$$

where the sign '+' in the superscript indicates the boundary conditions at infinity and 0 stands for the value of the magnetic field h at the vertical boundary (free boundary conditions). Note that M_1 does *not* vanish at $h=0$ provided that $q<1$: the '+' boundary conditions at infinity break the spin-flip symmetry.

Remark 2.4.4 (*wetting phase transition*)**.** In fact, one can analytically continue the right-hand side of (2.4.14) to *negative* values of $(1-r)^{1/2}$. According to [73, 146], this corresponds to a wetting phase transition. Informally speaking, for small negative values $-h$ of the boundary magnetic field, the interface separating '+' boundary conditions at infinity from '−' ones on the imaginary line $i\mathbb{R}$ touches the boundary infinitely often and the '+' phase dominates in the bulk of the half-plane, while for big negative values $-h$ this interface 'breaks away' from $i\mathbb{R}$ and the '−' phase dominates in the bulk. For instance, one should have

$$\mathbb{E}^{+,-h}_{\mathbb{H}^\diamond}[\sigma_{(-\frac{5}{2},0)}] \;=\; -|1-r|^{3/2}(\alpha_0-\beta_0)+\gamma_0 \;=\; 2\gamma_0 - \mathbb{E}^{+,h}_{\mathbb{H}^\diamond}[\sigma_{(-\frac{5}{2},0)}]$$

provided that h is small enough. Due to Theorem 2.4.2, the mismatch $2\gamma_0$ disappears (which means that the boundary conditions at the vertical line dominate those at infinity) if $h \geq h_{\mathrm{crit}}(q)$, where the critical value $h_{\mathrm{crit}}(q)$ is specified by the condition $r=q^2$.

We refer the interested reader to [73, 146] and [123, Chapter XIII] for a discussion of this regime of the Ising model. (Note that the interpretation of the physics behind this effect given in the book [123] differs from the later work [73, 146].) In particular, [123, Fig. 13.7] suggests that

$$\lim_{m\to\infty} \mathbb{E}^{+,-h}_{\mathbb{H}^\diamond}[\sigma_{(-2m-\frac{1}{2},0)}] \;=\; (1-q^4)^{1/8} \quad \text{for all} \quad h < h_{\mathrm{crit}}(q)$$

while, for all $m \in \mathbb{N}_0$,

$$\mathbb{E}^{+,-h}_{\mathbb{H}^\diamond}[\sigma_{(-2m-\frac{1}{2},0)}] \;=\; -\mathbb{E}^{+,h}_{\mathbb{H}^\diamond}[\sigma_{(-2m-\frac{1}{2},0)}] \quad \text{if} \quad h \geq h_{\mathrm{crit}}(q)$$

since $\gamma_s = 0$ in the latter case. This means that the sign of the bulk magnetization should flip when the negative boundary magnetic field attains the value $-h_{\mathrm{crit}}(q)$. It would be interesting to derive this fact as well as to understand the profile of the function $M_m(h)$ in detail using Toeplitz+Hankel determinants (2.4.14).

2.5 . Geometric interpretation: isoradial graphs and s-embeddings

2.5.1 . Regular homogeneous grids and isoradial graphs

In this section we briefly discuss the geometric interpretation of the parameters

$$\exp[-2\beta J^{\mathrm{h}}] = x^{\mathrm{h}} = \tan\tfrac{1}{2}\theta^{\mathrm{h}}, \qquad \exp[-2\beta J^{\mathrm{v}}] = x^{\mathrm{v}} = \tan\tfrac{1}{2}\theta^{\mathrm{v}} \tag{2.5.1}$$

of the homogeneous Ising model on the square grid by putting it into a more general context of *Z-invariant* Ising models on isoradial graphs. We refer the reader interested in historical remarks on Z-invariance to the classical paper [13] due to Baxter and Enting, a standard source for the detailed treatment is [12, Sections 6 and 7]. We also refer the interested reader to the paper [6] and references therein, where the Z-invariance was first (to the best of our knowledge) discussed in a geometric context, as well as to the more recent work [129] due to Mercat. The latter paper popularized statistical mechanics models on *rhombic lattices* $G^\bullet \cup G^\circ$ in the probabilistic community ; the name *isoradial graphs* for the corresponding embeddings of the graph $G^\bullet$ itself was coined by Kenyon in [99] shortly afterwards. Below we adopt the notation from the recent paper [28] on this subject due to Boutillier, de Tilière, and Raschel and refer the interested reader to that paper for more references. The key idea of this geometric interpretation is that the combinatorial star-triangle transforms of the Ising model (which are known as the Yang–Baxter equation in the transfer matrices context) become local rearrangements of $G^\bullet \cup G^\circ$, e.g. see [28, Fig. 5].

In the notation of [28], one searches for a re-parametrization

$$x^{\mathrm{v}} = x(\theta \,|\, k) := \frac{\mathrm{cn}(\frac{2K}{\pi}\theta \,|\, k)}{1 + \mathrm{sn}(\frac{2K}{\pi}\theta \,|\, k)}, \qquad x^{\mathrm{h}} = x(\tfrac{\pi}{2} - \theta \,|\, k), \tag{2.5.2}$$

where cn and sn are the Jacobi elliptic functions, $\theta \in (0, \frac{\pi}{2})$, $k^2 \in (-\infty, 1)$, and $K = K(k)$ is the complete elliptic integral of the first kind, see [28, Section 2.2.2]. Once such a parametrization is found, it becomes useful to replace the square grid by a rectangular one, with horizontal mesh steps $2\cos\theta$ and vertical steps $2\sin\theta$, as the Ising model under consideration fits the framework of [28], with θ and $\frac{\pi}{2} - \theta$ being the half-angles of the rhombic lattice ; note that in [28] the Ising spins are assigned to *vertices* of an isoradial graph while in our paper they live on *faces*.

It is easy to see that the equations (2.5.1), (2.5.2) can be written as

$$\tan\theta^{\mathrm{h}} = \mathrm{sc}(\tfrac{2K}{\pi}\theta \,|\, k), \qquad \tan\theta^{\mathrm{v}} = \mathrm{sc}(K - \tfrac{2K}{\pi}\theta \,|\, k).$$

In particular, the parametrization (2.5.2) is always possible and

$$\tan\theta^{\mathrm{h}}\tan\theta^{\mathrm{v}} = (1-k^2)^{1/2}.$$

Furthermore, the criticality condition $\theta^{\mathrm{h}}+\theta^{\mathrm{v}} = \frac{1}{2}\pi$ is equivalent to $k^2 = 0$, and

$$\mathcal{M}(\theta^{\mathrm{h}},\theta^{\mathrm{v}}) \;=\; (1-(\tan\theta^{\mathrm{h}}\tan\theta^{\mathrm{v}})^2)^{1/8} \;=\; k^{1/4} \quad \text{if} \;\; k^2\in[0,1), \qquad (2.5.3)$$

a classical result of Baxter (see [12, Eq. (7.10.50)]). Moreover, the Z-invariance allows one to treat the homogeneous Ising model on the triangular/honeycomb lattices on the same foot with the model on the square grid, see [13, Fig. 2]: one has

$$\mathcal{M}_{\mathrm{tri}}(\theta_{\mathrm{tri}}) \;=\; \mathcal{M}_{\mathrm{hex}}(\theta_{\mathrm{hex}}) \;=\; k^{1/4} \quad \text{if} \;\; x_{\mathrm{tri}} = x(\tfrac{\pi}{6}\,|\,k), \;\; x_{\mathrm{hex}} = x(\tfrac{\pi}{3}\,|\,k), \;\; k\geq 0,$$

where we assume that the Ising model is considered on *faces* of the grid and use the same parametrization (3.2.3) of interaction constants as usual in our paper.

The importance of the particular way to draw the lattice becomes fully transparent at criticality, when $\theta = \theta^{\mathrm{h}} = \frac{\pi}{2}-\theta^{\mathrm{v}}$. (Due to Z-invariance, this condition reads as $\theta_{\mathrm{tri}} = \frac{\pi}{6}$ or $\theta_{\mathrm{hex}} = \frac{\pi}{3}$ for the homogeneous model on *faces* of the triangular or honeycomb lattices.) Indeed, under the isoradial embedding, the multiplicative factor in the asymptotics

$$D_m \;\sim\; \mathcal{C}_\sigma^2\cdot(2m\cos\theta)^{-1/4} \quad \text{as} \;\; m\to\infty$$

provided by Theorem 4.7.9 has a clear interpretation: $2m\cos\theta$ is nothing but the *geometric distance* between the two spins (located at m lattice steps from each other) under consideration.

Remark 2.5.1. Baxter's formula (2.5.3) suggests that the spontaneous magnetization under criticality equals to $k^{\frac{1}{4}}$ for the whole family of Ising models considered in [28] and not only on regular grids. Moreover, in the critical case $k=0$ the asymptotics $\mathbb{E}[\sigma_u\sigma_w] \;\sim \mathcal{C}_\sigma^2\cdot|u-w|^{-1/4}$ as $|u-w|\to\infty$ holds on all isoradial graphs, with the *universal* multiplicative constant $\mathcal{C}_\sigma^2$; see [42] for further details.

2.5.2 . S-embeddings of the layered zig-zag half-plane in the periodic case

We now move on from classical rhombic lattices to more general and flexible setup of s-embeddings suggested in [34] (see also [33] and [103, Section 7] for more details) as a tool to study critical Ising models on planar graphs. We start with discussing a geometric intuition behind the layered setup with *periodic* interaction constants $\theta_k = \theta_{k+2n}$ and conclude by formulating questions on the asymptotic behavior of the truncated determinants (2.1.5) as $m\to\infty$ in this setup.

The next lemma is a simple corollary of a general result given in [52] on the criticality condition for the Ising model on a bi-periodic planar graph.

Lemma 2.5.1. *Let $\theta_k = \theta_{k+2n}$ for all $k \geq 1$ and some $n \geq 1$. The layered Ising model in the zig-zag (half-)plane with the interaction constants $x_k = \tan\frac{1}{2}\theta_k$ between the $(k-1)$-th and k-th columns is critical (see [52] for a precise definition) if and only if the following condition holds:*

$$\prod_{k=1}^{2n} \tan\theta_k \;=\; 1. \tag{2.5.4}$$

Proof. According to [52, Theorem 1.1], the criticality condition reads as

$$\sum_{P\in\mathcal{E}_0(\mathcal{G})} x(P) \;=\; \sum_{P\in\mathcal{E}_1(\mathcal{G})} x(P)\,,$$

where $\mathcal{G}$ denotes the fundamental domain of the grid drawn on the *torus*, $\mathcal{E}_0(\mathcal{G})$ is the set of even subgraphs of $\mathcal{G}$ having the homology type $(0,0)$ modulo 2, and $\mathcal{E}_1(\mathcal{G})$ is the set of all other even subgraphs of $\mathcal{G}$ (i.e., those having the types $(0,1)$, $(1,0)$ or $(1,1)$ modulo 2). In our setup, the fundamental domain consists of $2n$ vertices and one easily sees that each even subgraph P of $\mathcal{G}$ either contains 0 or 2 edges linking the k-th and the $(k+1)$-th vertices, for all $k = 1,\dots,2n$, or contains exactly one of the two edges between these vertices, for all $k = 1,\dots,2n$. Therefore,

$$\sum_{P\in\mathcal{E}_0(\mathcal{G})} x(P) - \sum_{P\in\mathcal{E}_1(\mathcal{G})} x(P) \;=\; \prod_{k=1}^{2n}(1-x_k^2) - \prod_{k=1}^{2n}(2x_k).$$

Since $\tan\theta_k = 2x_k/(1-x_k^2)$, the claim easily follows. □

Recall that the same condition (2.5.4) describes the fact that the spectrum of the non-negative Jacobi matrix J begins at 0. In this case, it is easy to see that the unique (up to a multiplicative constant) periodic solution to the equation $J\psi^\circ = 0$ (in other words, a generalized eigenfunction corresponding to $\lambda = 0$) is given by

$$\psi^\circ_k \;=\; (\sin\theta_{2k-1})^{-1}\cdot\prod_{p=1}^{2k-2}\cot\theta_p\,, \quad k\geq 1\,. \tag{2.5.5}$$

Our next goal is to construct a *canonical s-embedding* $\mathcal{S}$ of the bi-periodic critical planar Ising model under consideration; see [33, Lemma 2.3] and [103, Lemma 13] for details. For $k\in\mathbb{N}_0$ and $s\in\mathbb{Z}$, let

$$\mathcal{S}((-k-\tfrac{1}{2},s)) = (-t^\bullet_k\,,s) \;\text{ if }\; k+s\notin 2\mathbb{Z}\,,$$
$$\mathcal{S}((-k-\tfrac{1}{2},s)) = (-t^\circ_k\,,s) \;\text{ if }\; k+s\in 2\mathbb{Z}\,,$$

where $t^\circ_0 < t^\bullet_1 < t^\circ_2 < t^\bullet_3 < \dots$ and $t^\bullet_0 < t^\circ_1 < t^\bullet_2 < t^\circ_3 < \dots$; see Fig. 2.5.1. Since the quadrilaterals with vertices $(-t^\bullet_k,s)$, $(-t^\circ_k,s+1)$, $(-t^\bullet_{k+1},s+1)$, $(-t^\circ_{k+1},s)$ should be tangential, we have

$$\begin{aligned} t^\bullet_{k+1} - t^\circ_k &= \tfrac{1}{2}[\tan\varphi_{k+1}+\tan\varphi_k],\\ t^\circ_{k+1} - t^\bullet_k &= \tfrac{1}{2}[\cot\varphi_{k+1}+\cot\varphi_k], \end{aligned} \qquad \text{where}\;\; \varphi_k := \tfrac{1}{2}\operatorname{arccot}(t^\circ_k - t^\bullet_k)\in(0,\tfrac{1}{2}\pi).$$

Moreover, the formula [34, Eq. (6.3)] for the value of the Ising interaction parameter gives the recurrence relation

$$\tan\varphi_{k+1} \;=\; \tan^2\theta_{k+1}\cdot\tan\varphi_k\,, \qquad k\in\mathbb{N}_0\,. \tag{2.5.6}$$

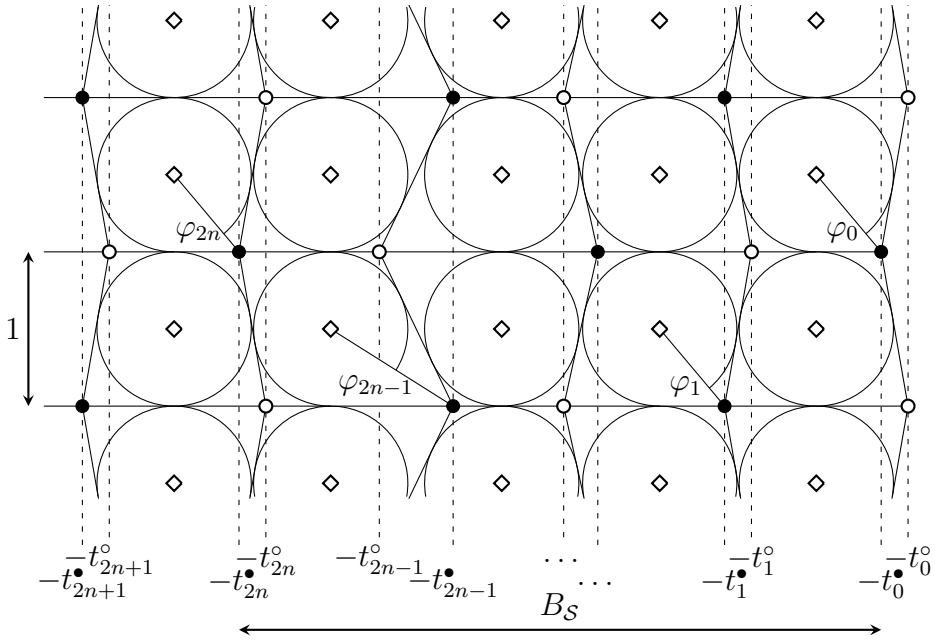

FIGURE 2.5.1 – Canonical s-embedding of a periodic critical layered Ising model, see [34, 33]. The slopes φ_k are uniquely determined by the recurrence (2.5.6) and by the condition (2.5.7) coming from the required periodicity of the function $\mathcal{Q}$ in the horizontal direction.

Finally, the condition that the 'origami map' function $\mathcal{Q}$ associated to $\mathcal{S}$ (or, equivalently, the function $L_{\mathcal{S}}$ in the notation of [34, Section 6]) is periodic in the horizontal direction reads as

$$\textstyle\sum_{k=0}^{2n-1} \tan\varphi_k \;=\; \sum_{k=0}^{2n-1} \cot\varphi_k\,. \tag{2.5.7}$$

It is easy to see that (2.5.6) and (2.5.7) define the angles φ_k uniquely and that the *width* of the horizontal period

$$B_{\mathcal{S}} \;:=\; t^\bullet_{k+2n} - t^\bullet_k \;=\; t^\circ_{k+2n} - t^\circ_k, \qquad k\in\mathbb{N}_0,$$

of thus constructed s-embedding $\mathcal{S}$ of the zig-zag half-plane $\mathbb{H}^\diamond$ equals to

$$\begin{aligned} B_{\mathcal{S}} \;&=\; \tfrac{1}{2}\big[\textstyle\sum_{k=0}^{2n-1}\tan\varphi_k + \sum_{k=0}^{2n-1}\cot\varphi_k\big] \;=\; \big[\textstyle\sum_{k=0}^{2n-1}\tan\varphi_k\cdot\sum_{k=0}^{2n-1}\cot\varphi_k\big]^{1/2} \\ &=\; \big[\textstyle\sum_{k=0}^{2n-1}\prod_{p=1}^{k}\tan^2\theta_p\cdot\sum_{k=0}^{2n-1}\prod_{p=1}^{k}\cot^2\theta_p\big]^{1/2}. \end{aligned}$$

A straightforward computation based upon (2.5.5) shows that this expression coincides with the formula (2.1.6) for the coefficient C_J in the asymptotics of the integrated density of states of the matrix J at 0. (For completeness of the presentation, we also discuss the proof of (2.1.6) in Section 2.5.3 below.) More precisely, one has

$$\begin{aligned} \textstyle\sum_{k=1}^{n}(\psi^\circ_k)^2 \;&=\; \textstyle\sum_{k=1}^{n}\big[(\sin\theta_{2k-1})^{-2}\prod_{p=1}^{2k-2}\cot^2\theta_p\big] \;=\; \sum_{k=1}^{2n}\prod_{p=1}^{k-1}\cot^2\theta_p\,, \\ \textstyle\sum_{k=1}^{n}(a_k\psi^\circ_k\psi^\circ_{k+1})^{-1} \;&=\; \textstyle\sum_{k=1}^{n}\big[(\cos\theta_{2k})^{-2}\prod_{p=1}^{2k-1}\tan^2\theta_p\big] \;=\; \sum_{k=1}^{2n}\prod_{p=1}^{k}\tan^2\theta_p\,, \end{aligned}$$

and therefore

$$n^{-1}B_{\mathcal{S}} \;=\; \Big[\, n^{-2}\textstyle\sum_{k=1}^{n}(\psi_k^\circ)^2 \cdot \sum_{k=1}^{n}(a_k\psi_k^\circ\psi_{k+1}^\circ)^{-1}\,\Big]^{1/2} \;=\; C_J\,. \qquad (2.5.8)$$

We conclude this section by coming back to the discussion of the link between the spectral properties of the matrix J and the asymptotic behavior of the magnetization M_m as $m \to \infty$. Contrary to the classical isoradial setup, in the periodic layered case we do *not* expect a regular behavior $M_m \sim \mathrm{const} \cdot m^{-1/8}$ uniformly over all m. Instead, one should expect an *oscillating* prefactor A_p depending on the 'type' of the column under consideration:

$$M_{nm+q} \;\sim\; A_p \cdot 2^{1/8}\mathcal{C}_\sigma(B_{\mathcal{S}}m)^{-1/8} \quad \text{for} \;\; 1 \le q \le n \;\; \text{and} \;\; m \to \infty,$$

where the main factor $2^{1/8}\mathcal{C}_\sigma(B_{\mathcal{S}}m)^{-1/8}$ is universal and accounts the geometry of the s-embedding, cf. $(2.5.8)$ and the asymptotics $(\mathrm{A}.9)$ in the homogeneous case. Note that such oscillating behavior of $(2.1.5)$ is fully consistent with the fact that $\mathrm{Supp}\,\nu_J$ has n bands in the periodic setup instead of a single segment in the homogeneous case. From our perspective, it would be interesting

— to justify the oscillatory behavior described above and, especially, to find spectral and geometric interpretations of the coefficients A_q ;

— to find a natural definition of the *average* magnetization over the period $\overline{M}_m = \overline{M}_m(M_{nm+1}, \ldots, M_{n(m+1)})$ such that

$$\overline{M}_m \;\sim\; 2^{1/8}\mathcal{C}_\sigma(B_{\mathcal{S}}m)^{-1/8} \quad \text{as} \;\; m \to \infty$$

(in other words, to find a natural average that makes 1 out of $A_1, \ldots, A_n$).

2.5.3 . Proof of the formula $(2.1.6)$

For convenience of the readers with a 'probabilistic' background we now sketch a computation of the integrated density of states of a periodic Jacobi matrix $(2.1.4)$ at the bottom edge of its spectrum, which is assumed to be $\lambda = 0$; see $(2.1.6)$ and $(2.5.8)$. Though this result seems to be quite standard, we were unable to find an explicit reference in the literature ; we thank Leonid Parnovski for indicating a convenient way of doing the required computation presented below.

Recall that we assume that $\theta_{k+2n} = \theta_k$ for all $k \ge 1$ and that $\prod_{k=1}^{2n}\tan\theta_k = 1$. Let $J^{[\mathbb{Z}]}$ denote the *doubly-infinite* periodic Jacobi matrix whose entries $-a_k$ and b_k, $k \in \mathbb{Z}$, are given by $(2.1.4)$. A straigtforward computation shows that the n-periodic vector

$$\psi^\circ = (\ldots\ \psi_{-1}^\circ\ \psi_0^\circ\ \psi_1^\circ\ \ldots)^\top, \qquad \psi_{pn+q}^\circ := \prod_{k=1}^{2q}\frac{\sin\theta_{k-1}}{\cos\theta_k}\cdot\psi_0^\circ,$$

solves the equation $J^{[\mathbb{Z}]}\psi^\circ = 0$; let us normalize ψ° so that $\sum_{q=1}^{n}(a_q\psi_q^\circ\psi_{q+1}^\circ)^{-1} = 1$.

Denote by $J^{[Nn]}$ the Jacobi matrix of size $Nn \times Nn$ with the same entries $-a_k, b_k$ and with *periodic* boundary conditions (i.e., we set $J^{[Nn]}_{1,Nn} = J^{[Nn]}_{Nn,1} := -a_1$); note that the choice of boundary conditions (being a rank two perturbation) is irrelevant when computing the number of eigenvalues of the truncation $P_{Nn}JP_{Nn}$ in a small window near $\lambda = 0$ as $N \to \infty$.

The matrix $J^{[Nn]}$ admits a factorization similar to that in the definition of the original matrix J (see $(2.1.4)$); in particular, $J^{[Nn]} \geq 0$. Clearly, $J^{[Nn]}\psi^\circ = 0$ and (small) eigenvalues of $J^{[Nn]}$ correspond to quasi-periodic eigenvectors $\psi_{s+n} = e^{it}\psi_s$, where $tN \in 2\pi\mathbb{Z}$. Let us now introduce an auxiliary function

$$g_s(t) := \exp\big[\, it \textstyle\sum_{q=1}^{s-1}(a_q\psi^\circ_q\psi^\circ_{q+1})^{-1}\big] \tag{2.5.9}$$

and denote

$$\begin{aligned} J^{[Nn]}(t) \;&:=\; (G^{[Nn]}(t))^{-1}J^{[Nn]}G^{[Nn]}(t)\,, \\ \text{where } G^{[Nn]}(t) \;&:=\; \operatorname{diag}\{g_s(t)\}_{s=1,\dots,Nn}. \end{aligned} \tag{2.5.10}$$

Due to the choice of the multiplicative normalization of the vector ψ° made above, we have $g_{s+n} = e^{it}g_s$. Therefore, studying eigenvalues of the matrix $J^{[Nn]}$ corresponding to quasi-periodic (i.e., $\psi_{s+n} = e^{it}\psi_s$) eigenvectors is equivalent to studying eigenvalues of the *family* of self-adjoint matrices $J^{[Nn]}(t)$ corresponding to *periodic* (i.e., $\psi_{s+n} = \psi_s$) eigenvectors, which are nothing but the eigenvalues of the $n \times n$ matrices $J^{[n]}(t)$ with $tN \in 2\pi\mathbb{Z}$.

The question is now reduced to the standard setup of the perturbation theory of (simple) lowest eigenvalues of matrices $J^{[n]}(t)$ as $t \to 0$. It is well known that both these eigenvalues $\lambda(t) \to 0$ and the corresponding, properly normalized, eigenvectors $\psi(t) \to \psi^\circ$ admit asymptotic expansions

$$\begin{aligned} \lambda(t) \;&=\; \lambda^{(1)}t + \lambda^{(2)}t^2 + \dots, \\ \psi(t) \;&=\; \psi^\circ + \psi^{(1)}t + \psi^{(2)}t^2 + \dots \end{aligned} \qquad \text{as } \; t \to 0,$$

where $\langle\psi^{(1)};\psi^\circ\rangle = 0$ and $\langle\psi^{(2)};\psi^\circ\rangle = -\frac{1}{2}\langle\psi^{(1)};\psi^{(1)}\rangle$. Moreover, it is easy to see from $(2.5.10)$ that $J^{[n]}(t) = J^{[n]} + J^{[n],(1)}t + J^{[n],(2)}t^2 + \dots$ as $t \to 0$, where $J^{[n],(1)}$ and $J^{[n],(2)}$ are two-diagonal matrices with entries

$$J^{[n],(1)}_{q+1,q} = -J^{[n],(1)}_{q,q+1} = i\cdot(\psi^\circ_q\psi^\circ_{q+1})^{-1}; \qquad J^{[n],(2)}_{q+1,q} = J^{[n],(2)}_{q,q+1} = \tfrac{1}{2}a_q^{-1}\cdot(\psi^\circ_q\psi^\circ_{q+1})^{-2}.$$

In particular, we have $J^{[n],(1)}\psi^\circ = 0$; note that this is exactly where a special choice of the function $(2.5.9)$ plays a very important role by simplifying the computations.

Considering the linear (in t) terms in the identity $J^{[n]}(t)\psi(t) = \lambda(t)\psi(t)$, we see that $J^{[n]}\psi^{(1)} = \lambda^{(1)}\psi^\circ$, which yields $\lambda^{(1)} = 0$ and $\psi^{(1)} = 0$ since $\langle\psi^{(1)};\psi^\circ\rangle = 0$ and ψ° is an eigenvector of $J^{[n]}$ corresponding to the simple eigenvalue $\lambda^\circ = 0$. Therefore, expanding the same identity up to the second order in t we obtain the equation

$$J^{[n]}\psi^{(2)} + J^{[n],(2)}\psi^\circ = \lambda^{(2)}\psi^\circ.$$

Since $\langle J^{[n]}\psi^{(2)},\psi^\circ\rangle = \langle \psi^{(2)}, J^{[n]}\psi^\circ\rangle = 0$, this allows us to compute the required coefficient

$$\lambda^{(2)} \;=\; \frac{\langle J^{[n],(2)}\psi^\circ,\psi^\circ\rangle}{\langle\psi^\circ,\psi^\circ\rangle} \;=\; \frac{\sum_{q=1}^n (a_q\psi_q^\circ\psi_{q+1}^\circ)^{-1}}{\sum_{q=1}^n(\psi_q^\circ)^2}$$
$$= \Bigl[\sum_{q=1}^n(\psi_q^\circ)^2\cdot\sum_{q=1}^n(a_q\psi_q^\circ\psi_{q+1}^\circ)^{-1}\Bigr]^{-1} \;=\; (nC_J)^{-2},$$

where in the third equality we used the prescribed multiplicative normalization of the vector ψ°; note that the final expression for C_J is invariant with respect to the choice of this normalization.

Therefore, we arrive at the asymptotics $\lambda(t) = (nC_J)^{-2}t^2 + \dots$ as $t\to 0$, which means that, for small enough λ_0 and $N\to\infty$, the $Nn\times Nn$ periodic Jacobi matrix $J^{[Nn]}$ has approximately $NnC_J\cdot\pi^{-1}\sqrt{\lambda_0}$ eigenvalues $\lambda(t)\le\lambda_0$ with $tN\in 2\pi\mathbb{Z}$. In other words, the integrated density of states of J behaves like $C_J\cdot\pi^{-1}\sqrt{\lambda}$ as $\lambda\to 0$, where the constant C_J is given by (2.1.6).

A . Appendix. Critical Ising model $\theta^{\mathrm{h}}=\theta^{\mathrm{v}}=\frac{\pi}{4}$: diagonal correlations and the half-plane magnetization via Legendre polynomials

In this appendix we work with the fully homogeneous critical (i.e., $\theta^{\mathrm{h}}=\theta^{\mathrm{v}}=\frac{\pi}{4}$) Ising model on the $\frac{\pi}{4}$-*rotated* square grid of mesh size $\sqrt{2}$. (Note that this setup is actually more similar to Section 2.4 rather than to Section 2.3.) We begin with a discussion of the famous result of Wu (see Theorem A.2 below) that provides an explicit expression of the diagonal spin-spin correlations in terms of factorials. Using the same approach as in the core part of our paper, we give a short proof of this theorem by reducing the computation to the norms of the classical *Legendre polynomials*. (As communicated to the authors by J.H.H. Perk, a similar link with Legendre functions and Wronskian identities was the starting point of their joint with H. Au-Yang treatment [143] of the two-point correlations at criticality via quadratic identities from [141]; see also Remark 2.3.5.) After this, we move to the magnetization M_m in the $(2m)$-th column of the zig-zag half-plane $\mathbb{H}^\diamond$ and note that it admits a similar explicit representation via factorials (see Theorem A.3) due to a simple *Schwarz reflection* argument, an identity which appears to be new.

Remark A.1. The interested reader is also referred to [32, Section 3] where the non-critical case $\theta=\theta^{\mathrm{h}}=\theta^{\mathrm{v}}<\frac{1}{4}\pi$ is handled in the same way, via the OPUC polynomials corresponding to the weight $w_q(t)=|1-q^2e^{it}|$ with $q:=\tan\theta<1$. It would be interesting to understand the precise link between asymptotics of these orthogonal polynomials obtained by Basor, Chen and Haq in [7] and asymptotics of the diagonal Ising correlations obtained by Perk and Au-Yang in [144].

Let $n \in \mathbb{N}_0$ and assume that the $\frac{\pi}{4}$-rotated square grid is shifted so that its vertices (resp., centers of faces) form the lattice $(-n-\frac{1}{2}+k, s)$ (resp., $(n+\frac{1}{2}+k, s)$) with $k, s \in \mathbb{Z}$ and $k+s \in 2\mathbb{Z}$. Let

$$D_n := \mathbb{E}[\sigma_{(-n+\frac{1}{2},0)}\sigma_{(n+\frac{1}{2},0)}]$$

be the (infinite-volume limit of the) diagonal spin-spin correlation at distance of n diagonal steps. Denote $\mathbf{v} := (-n-\frac{1}{2}, 0)$, $\mathbf{u} := (n+\frac{1}{2}, 0)$ and let

$$V(k,s) \;:=\; X_{[\mathbf{v},\mathbf{u}]}((k,s)), \qquad k, s \in \mathbb{Z},\; k+s+n \in 2\mathbb{Z},$$

recall that V is a spinor on the double covers branching over $\mathbf{v}$ and $\mathbf{u}$. It follows from Proposition 2.2.2 (or, equivalently, Proposition 2.2.3) that V satisfies the standard discrete harmonicity condition $[\Delta V](k,s) = 0$ for all k, s except at the points $(\pm n, 0)$ near the branchings, where

$$\begin{aligned}[\Delta V](k,s) \;:=\; & -V(k,s) \\ & +\; \tfrac{1}{4}[V(k-1,s-1)+V(k+1,s-1)+V(k-1,s+1)+V(k+1,s+1)].\end{aligned}$$

It directly follows from the definition of the observable $X_{[\mathbf{v},\mathbf{u}]}$ and the self-duality of the critical model that

$$V(-n,0) \;=\; V(n,0) \;=\; D_n\,. \tag{A.1}$$

Moreover, a straightforward computation similar to the proof of Proposition 2.2.2 implies that

$$\begin{array}{lll}[\Delta V](\pm n,0) \;=\; -\frac{1}{2}D_{n+1} & \text{if } n \geq 1\,, \\ [\Delta V](0,0) \;=\; -D_1 & \text{if } n = 0\,.\end{array} \tag{A.2}$$

Applying the optional stopping theorem as in the proof of Lemma 4.7.1, it is easy to see that the *uniformly bounded* discrete harmonic spinor V is uniquely defined by its values (A.1) near the branchings. Following exactly the same route as in Section 4.7.2 we now construct V explicitly; a similar idea was used in [76, Appendix A] to construct the harmonic measure of the tip in the slit plane, which can be viewed as an analogue of the function $V(k-n, s)$ for $n = \infty$.

Lemma A.1. *Let $P_n(x) := (2^n n!)^{-1}\frac{d}{dx}[(x^2-1)^n]$ be the n-th Legendre polynomial. Then, for all $k \in \mathbb{Z}$ and $s \in \mathbb{N}_0$ such that $n+k+s \in 2\mathbb{Z}$, one has*

$$V(k, \pm s) \;=\; \frac{C_n}{2\pi}\int_{-\pi}^{\pi} e^{-ikt}(y(t))^s P_n(\cos t)dt, \tag{A.3}$$

where $y(t) = (1-|\sin t|)/\cos t$ and C_n is chosen so that $V(\pm n, 0) = D_n$.

Proof. It is easy to see that

— the values $V(k,s)$ defined by (A.3) are uniformly bounded since $|y(t)| \leq 1$;

— $[\Delta V](k,s) = 0$ if $s \neq 0$ since $y(t) = \frac{1}{2}\cos t \cdot (1 + (y(t))^2)$;

— $V(k,0) = 0$ if $|k| > n$, thus one can view (A.3) as a function (spinor) defined on the *double cover* branching over $\mathbf{v}$ and $\mathbf{u}$ and vanishing over the real line outside the segment $[\mathbf{v},\mathbf{u}]$, this spinor satisfies the discrete harmonicity property at $(k,0)$ with $|k| > n$ due to symmetry reasons.

Moreover, the orthogonality in $L^2([-1,1])$ of $P_n(x)$ to all monomials $1, x, \dots, x^{n-1}$ gives

$$\begin{aligned} -[\Delta V](k,0) &= V(k,0) - \tfrac{1}{2}[V(k-1,1) + V(k+1,1)] \\ &= \frac{C_n}{2\pi}\int_{-\pi}^{\pi} e^{-ikt}(1 - y(t)\cos t)P_n(\cos t)dt \\ &= \frac{C_n}{2\pi}\int_{-\pi}^{\pi} \cos(kt)|\sin t|P_n(\cos t)dt \;=\; \frac{C_n}{\pi}\int_{-1}^{1} T_{|k|}(x)P_n(x)dx \;=\; 0 \end{aligned}$$

for all $|k| < n$, where $T_k(x) := \cos(k \arccos x)$ are the Chebyshev polynomials. Therefore, the Kadanoff–Ceva fermion $X_{[\mathbf{v},\mathbf{u}]}((k,s))$ must coincide with the right-hand side of (A.3) up to a multiplicative constant. □

The following theorem can be obtained as a simple corollary of Lemma A.1.

Theorem A.2 (Wu). The following explicit formula is fulfilled:

$$D_n \;=\; \left(\frac{2}{\pi}\right)^n \cdot \prod_{k=1}^{n-1}\left(1 - \frac{1}{4k^2}\right)^{k-n}, \quad n \geq 0. \tag{A.4}$$

Proof. Denote by $p_n := (2^n n!)^{-1} \cdot (2n)!/n!$ the leading coefficient of the Legendre polynomial P_n and let $t_n := 2^{n-1}$, $n \geq 1$ be the leading coefficient of the Chebyshev polynomial T_n, note that the value $t_0 = 1$ does not match the general case. It follows from (A.3) that $D_n = C_n \cdot 2^{-n} p_n$. On the other hand,

$$-[\Delta V](\pm n, 0) \;=\; \frac{C_n}{\pi}\int_{-1}^{1} T_n(x)P_n(x)dx \;=\; \frac{C_n t_n}{\pi p_n} \cdot \|P_n\|^2_{L^2([-1,1])} \;=\; \frac{2C_n t_n}{\pi(2n+1)p_n}\,.$$

Due to (A.2), we conclude that for *all* $n \geq 0$ the following recurrence relation holds:

$$\frac{D_{n+1}}{D_n} \;=\; \frac{2^{n+1}C_n}{\pi(2n+1)p_n} \;=\; \frac{2^{2n+1}}{\pi(2n+1)p_n^2} \;=\; \frac{2}{\pi} \cdot \frac{((2n)!!)^2}{(2n-1)!!(2n+1)!!}\,.$$

This easily gives (A.4) by induction. □

We now move on to an explicit expression for the magnetization in the $(2m)$-th column of the zig-zag half-plane $\mathbb{H}^\diamond$ with '+' boundary conditions:

$$M_m \;:=\; \mathbb{E}^+_{\mathbb{H}^\diamond}[\sigma_{(-2m-\frac{1}{2},0)}]\,.$$

Theorem A.3. The following identities are fulfilled for all $m \in \mathbb{N}_0$:

$$\frac{M_{m+1}}{M_m} \;=\; \frac{D_{2m+2}}{D_{2m+1}}\,, \qquad M_m \;=\; \left(\frac{2}{\pi}\right)^m \cdot \prod_{k=1}^{2m-1} \left(1-\frac{1}{4k^2}\right)^{\lfloor \frac{k}{2} \rfloor - m}. \tag{A.5}$$

Proof. Similarly to Section 2.4.1, let $\mathbf{v} = (-2m-\frac{3}{2}, 0)$ and

$$H(-k,s) \;:=\; X_{[\mathbf{v}]}((-k,s)), \qquad k \in \mathbb{N}_0,\; s \in \mathbb{Z},\; k+s \notin 2\mathbb{Z}$$

be the half-plane fermionic observable. This is a bounded discrete harmonic (except at $(-2m-1,0)$) spinor on the double cover of $\mathbb{H}^\diamond$ branching over $\mathbf{v}$ which satisfy the boundary conditions

$$H(0,s) \;=\; 2^{-1/2} \cdot [H(-1,s-1) + H(-1,s+1)], \quad s \notin 2\mathbb{Z}, \tag{A.6}$$

on the imaginary line (see (2.4.3) and (2.4.4)). Denote

$$\begin{matrix} V(\pm k,s) \;:=\; CH(k,s) & \text{if } k \in \mathbb{N}, \\ V(0,s) := 2^{-1/2} \cdot CH(0,s) & \text{if } k = 0, \end{matrix} \qquad s \in \mathbb{Z}, \quad k+s \notin 2\mathbb{Z}, \tag{A.7}$$

where $C := D_{2m+1}/M_m$; up to a change of the multiplicative normalization, this is nothing but the extension of H from the left half-plane to the full plane via the discrete Schwartz reflection. By construction, V is a spinor on the double cover of the full-plane branching over $\mathbf{v}$ and $\mathbf{u} := (2m+\frac{3}{2}, 0)$ which is discrete harmonic everywhere (including points on the imaginary line) except at points $(\pm(2m+1),0)$ near the branchings, where one has $V(\pm(2m+1),0) = D_{2m+1}$. Therefore, it coincides with the full-plane observable $X_{[\mathbf{v},\mathbf{u}]}((k,s))$ discussed above. In particular, (A.7) implies the identity

$$\tfrac{1}{2} D_{2m+2} \;=\; -[\Delta V](-2m-1,0) \;=\; -C \cdot [\Delta H](-2m-1,0) \;=\; C \cdot \tfrac{1}{2} M_{m+1}$$

which is equivalent to the first identity in (A.5). The explicit formula for M_m easily follows from the explicit formula (A.4) by induction. □

Remark A.4. Similarly, let $M_{m-\frac{1}{2}}$ denote the magnetization in the $(2m-1)$-th column of the critical homogeneous Ising model in the zig-zag plane. It is not hard to repeat the proof of Theorem A.3 in this situation and to obtain the identity

$$M_{m+\frac{1}{2}} \,/\, M_{m-\frac{1}{2}} \;=\; D_{2m+1} \,/\, D_{2m}, \quad m \in \mathbb{N}_0,$$

where we formally set $M_{-\frac{1}{2}} := \sqrt{2}$, this convention is the result of the additional factor relating the values of the half-plane and the full-plane observables on the imaginary line via (A.7). By induction, one easily gets the identity

$$M_{m+\frac{1}{2}} M_m \;=\; \sqrt{2} \cdot D_{2m+1}, \qquad m \in \tfrac{1}{2}\mathbb{N}_0, \tag{A.8}$$

and an explicit formula for $M_{m+\frac{1}{2}}$, which is similar to (A.5). Finally, a straightforward analysis gives the asymptotics

$$D_n \;\sim\; \mathcal{C}_\sigma^2 \cdot (2n)^{-1/4}, \quad M_m \;\sim\; 2^{1/8}\mathcal{C}_\sigma \cdot (2m)^{-1/8}, \quad n, m \to \infty, \tag{A.9}$$

where $\mathcal{C}_\sigma = 2^{\frac{1}{6}} e^{\frac{3}{2}\zeta'(-1)}$ is the same universal constant as in Theorem 4.7.9. Note that we prefer to encapsulate the factors $2n$ and $2m$ (rather than simply n and m), respectively, as they are equal to the geometric distance between the two spins under consideration and the distance from the spin $\sigma_{(-2m-\frac{1}{2},0)}$ to the boundary of the half-plane $\mathbb{H}^\diamond$, respectively.

3 - Universality of spin correlations in the Ising model on isoradial graphs

This chapter corresponds to the article [43], written with **Dmitry Chelkak** and **Konstantin Izyurov**, and is currently under revision for *The Annals of Probability*.

Abstract :

We prove universality of spin correlations in the scaling limit of the planar Ising model on isoradial graphs with uniformly bounded angles and Z-invariant weights. Specifically, we show that in the massive scaling limit, i. e., as the mesh size tends to zero at the same rate as the Baxter elliptic parameter tends to 1, the two-point spin correlations in the full plane converge to a universal rotationally invariant limit. These results, together with techniques developed to obtain them, are sufficient to extend to isoradial graphs the convergence results for multi-point spin correlations in bounded planar domains, which were previously known only on the square grid. We also give a simple proof of the fact that the infinite-volume magnetization in a subcritical Z-invariant Ising model is independent of the site and of the lattice. As compared to techniques already existing in the literature, we streamline the analysis of discrete (massive) holomorphic spinors near their ramification points, which also provides a solid ground for further generalizations.

Table des matières

3.1 . Introduction

3.1.1 . General context

Isoradial graphs, or, equivalently, rhombi tilings, were introduced by Duffin [59] as a natural family of embedded planar graphs admitting a nice discretization of complex analysis and potential theory. They latter attracted considerable attention both in the physics and the mathematics communities in connection with lattice models of two-dimensional statistical mechanics. Although the latter live on abstract planar graphs with some additional structure, e. g., weights on edges, it often turns out that embedding the graph isoradially sheds light on the behavior of the model at or near criticality. By now, there is an extensive literature on statistical mechanics on isoradial graphs ; e. g., see [26, 24, 25, 63, 66, 50, 51, 57, 80, 99, 111, 129] and references therein. Apart from being a natural framework for establishing universality, an additional motivation to study models on isoradial graph is that they form a flexible family to approximate arbitrary Riemann surfaces [129, 51, 50], for which regular lattices are too rigid.

A relevance of rhombi tilings for the two-dimensional statistical mechanics can be described as follows. As uncovered by Baxter [10, 8, 12], many models of statistical mechanics with local interactions have *Z-invariant weights*. The "invariance" here refers to the fact that the Y–Δ transform of the graph on which the model is defined leaves unchanged the partition function and many (if not all) observables of interest. As Baxter has shown, the flexibility this entails allows one to solve many such models exactly. Although these algebraic techniques does not directly rely upon embedding of graphs into the complex plane, it turns out that representing them as isoradial grids allows one to give a direct geometrical meaning to the parameters of the corresponding R-matrices. This is more than a numerical coincidence as the small mesh size limits of *critical* 2D lattice models are expected to have more symmetries than just the symmetries of the lattice : e. g., in this setup one expects the scaling, rotational and even *conformal* invariance. To exhibit such a symmetry, one needs to pick embeddings of graphs and the isoradial/rhombic lattices are known to be the correct choice provided that one can reformulate the lattice model under consideration using this geometric framework. For rhombic lattices, the Y–Δ moves are nothing but the so-called *cube flips*, which allow one to transform (big pieces of) different lattices into each other without affecting quantities of interest. Apart from being at the heart of physicists' predictions of the universality for Z-invariant lattice models, this idea also recently led to a rigorous proof of the rotational invariance of several Z-invariant lattice models ; we refer

the interested reader to [66] for further details.

In this paper we consider the critical and near-critical (aka massive) *Ising model* on isoradial graphs with Z-invariant weights. Before discussing our main results, let us first briefly mention the results available in the *square grid* setup. For the *critical* model (see also [32, 34] for more details), the convergence and conformal invariance was proven by Smirnov [160] for basic fermionic observables ; by Hongler and Smirnov [87, 84] for the energy density correlations ; and by the first two authors and Hongler [38] for spin correlations. Gheissari, Hongler, Park, Viklund and Kytölä studied more general local fields in [76, 85] and a unified framework to treat mixed correlations of all primary fields (i. e., fermions, energy densities, spins and disorders) was recently developed in [39]. Another aspect of conformal invariance is the convergence of interfaces and loop ensembles in the domain walls representation of the model to SLE_3 and CLE_3 ; see [49] and [18], respectively. Beyond the critical case, the *massive* limit of spin correlations in smooth domains and of fermionic observables in general (i .e., not necessarily smooth) ones was recently treated by S. C. Park in [137] and [138], respectively.

The *universality* – within the isoradial family – of basic fermionic observables was shown in [48] for the critical model and, very recently, in [138] for the massive one. These results admit a direct extension to the energy density correlations as the energy density field – in sharp contrast to spins themselves – can be directly expressed via fermions. However, the analysis of spin correlations is considerably more subtle. Of the aforementioned work, the proofs given in [38, 137] relied especially heavily on the properties of the square lattice, and hence they did not admit a simple generalization to the isoradial case. In this paper, we provide the missing ingredients and prove the universality for spin correlations on isoradial graphs, both in the critical and in the massive setup. This also paves a way to a proof of the universality of correlations of all primary fields [39] on isoradial graphs and possibly beyond, although we do not discuss it here.

3.1.2 . Main results

We work with the Z-invariant Ising model defined on (subsets of) an infinite planar isoradial grid $\Gamma^{\circ,\delta}$; note that the dual grid $\Gamma^{\bullet,\delta}$ is also isoradial with the same radii, and $\Lambda^\delta := \Gamma^{\circ,\delta} \cup \Gamma^{\bullet,\delta}$ forms a rhombi tiling of mesh size δ. Throughout the paper, we assume that all rhombi tilings satisfy the following bounded angle property for some (fixed) $\theta_0 > 0$:

$$\mathrm{BAP}(\theta_0): \text{ no rhombus has an angle smaller than } 2\theta_0.$$

The Z-invariant weights (per edge in the low-temperature – aka the *domain walls* – expansion of the model on $\Gamma^{\circ,\delta}$ or, equivalently, in the high-temperature expansion of the dual model on $\Gamma^{\bullet,\delta}$) are given by

$$x_e = \exp[-2\beta^\circ J_e^\circ] = \tanh[\beta^\bullet J_e^\bullet] \;=\; \tan\tfrac{1}{2}\widehat{\theta}_e, \qquad \sin\widehat{\theta}_e \;=\; \mathrm{sn}\left(\tfrac{2K}{\pi}\overline{\theta}_e \,|\, k\right), \tag{3.1.1}$$

where $\overline{\theta}_e$ is half of the angle of the rhombus containing e adjacent to a vertex of $\Gamma^{\bullet,\delta}$ (see Fig. 3.2.2), and $K = K(k)$ is the complete elliptic integral of the first kind; see [134, Eq. 19.2.8] (we routinely refer to the Digital Library of Mathematical Functions [134] in the above format). Thus, the edge weights are determined by the isoradial embedding of the graph plus a single temperature-like parameter, the *elliptic modulus* $k \in (0,1) \cup i\mathbb{R}_+$, or equivalently the *nome* $q \in \mathbb{R}$; see [134, Eq. 22.2.1]. We refer the reader to a recent work of Boutillier, de Tilière and Raschel [27, 28, 164] for an extensive discussion of thus defined Ising model and its links with dimers and uniform spanning trees. Note that $(3.1.1)$ agrees with the parametrization used in [28] for the interaction parameters $\beta^\bullet J_e^\bullet$ while we will typically work with the dual model defined on $\Gamma^{\circ,\delta}$ (i. e., we usually assign spins to *faces* of $\Gamma^\delta = \Gamma^{\bullet,\delta}$).

The critical point is $k = q = 0$, in which case $\widehat{\theta}_e = \overline{\theta}_e$. The case $q > 0$ and $k \in (0,1)$ gives rise to a sub-critical model on $\Gamma^{\bullet,\delta}$ and a super-critical model on $\Gamma^{\circ,\delta}$, while $q < 0$ and $k \in i\mathbb{R}_+$ correspond to the opposite situation. (Thus, the nome q has the same monotonicity as the temperature in the model on $\Gamma^{\circ,\delta}$.) Also, note that the parametrization $(3.1.1)$ is symmetric with respect to exchanging the roles of $\Gamma^{\bullet,\delta}$ and $\Gamma^{\circ,\delta}$ in the following sense : one also has

$$\tanh[\beta^\circ J_e^\circ] = \exp[-2\beta^\bullet J_e^\bullet] \;=\; \tan\tfrac{1}{2}\widehat{\theta}_e^*, \qquad \sin\widehat{\theta}_e^* \;=\; \operatorname{sn}\left(\tfrac{2K}{\pi}\overline{\theta}_e^* \,|\, k^*\right),$$

where $\widehat{\theta}_e + \widehat{\theta}_e^* = \frac{\pi}{2} = \overline{\theta}_e + \overline{\theta}_e^*$ and the dual elliptic parameter k^* is given by

$$k^* = \frac{ik}{\sqrt{1-k^2}} \quad \Leftrightarrow \quad q^* = -q\,. \tag{3.1.2}$$

This transform is nothing but a simple way of writing the *Kramers–Wannier duality* (e. g., see [60, Section 7.5] and [28, Section 4.5]) in the elliptic context. In particular, if one plugged the dual elliptic parameter k^* instead of k into the parametrization $(3.1.1)$, this would simply exchange the roles of $\Gamma^{\bullet,\delta}$ and $\Gamma^{\circ,\delta}$; e.g., see Proposition 3.1.3 below.

The main purpose of our paper is to study the *massive scaling limit*, as $\delta \to 0$ and simultaneously $q \to 0$, with the relation

$$q = \tfrac{1}{2}m\delta \tag{3.1.3}$$

between the two, where the parameter $m \in \mathbb{R}$ is called *mass*, alluding to a massive field theory conjecturally describing this limit. As a particular case, we study the scaling limit at criticality, $m = 0$. Our results are uniform with respect to lattices satisfying the uniformly bounded angles assumption $\mathrm{BAP}(\theta_0)$ for a fixed $\theta_0 > 0$, hence we do not assume that Λ^δ at each scale are related to each other in any way.

Throughout our paper, we use the notation $\mathbb{E}^{(m)}$ to denote the expectation in the Z-invariant Ising model defined on the isoradial grid of mesh size δ with

the elliptic parameter obtained from δ via (3.1.3). We write $\mathbb{E}^{(m),\mathrm{w}}$ and $\mathbb{E}^{(m),\mathrm{f}}$ for expectations considered in finite domains in order to specify the *wired* and *free* boundary conditions, respectively. (Recall that in our convention the spins are assigned to vertices of the dual lattice $\Gamma^{\circ,\delta}$, i.e., to the faces of $\Gamma^{\delta} = \Gamma^{\bullet,\delta}$. The wired boundary conditions mean that all spins at the boundary of a discrete domain have the same value.) Also, in Proposition 3.1.3 we use the notation $\mathbb{E}^{+}$ for the infinite volume limit of the sub-critical model with *plus* boundary conditions.

Theorem 3.1.1. For each $m \in \mathbb{R}$ there exists a function $\Xi(\cdot, m) : \mathbb{R}_+ \to \mathbb{R}_+$ such that the following holds in the massive scaling limit $q = \frac{1}{2} m\delta \to 0$:

$$\delta^{-\frac{1}{4}} \mathbb{E}^{(m)}_{\Gamma^{\circ},\delta}[\sigma_{u_1}\sigma_{u_2}] \;\to\; \mathcal{C}_\sigma^2 \cdot \Xi(|u_2 - u_1|, m) \;\text{ as }\; \delta \to 0\,, \tag{3.1.4}$$

where the constant $\mathcal{C}_\sigma = 2^{\frac{1}{6}} e^{\frac{3}{2}\zeta'(-1)}$ is independent of both the rhombic lattice Λ^δ and the mass m. One has $\Xi(r, 0) \equiv r^{-\frac{1}{4}}$ and $\Xi(r, m) \sim r^{-\frac{1}{4}}$ as $r \to 0$ for all m.

Proof. See Section 3.4.4 for the case $m = 0$ and Section 3.4.6 for $m \neq 0$. □

Remark 3.1.1. The explicit expression for $\Xi(r, m)$ in terms of Painlevé III transcendents is given by a celebrated formula of Wu, McCoy, Tracy and Barouch [166, 153, 94] for the massive model on the *square grid*; see also [137, Corollary 1.2 and Section 4.2]. The main content of Theorem 3.1.1 is that this result holds universally within the class of isoradial graphs; note in particular that the constant C_σ does not depend on the local geometry of Λ^δ near $u_{1,2}$. A similar result was hinted by Dubédat [57, Proposition 27] for magnetic correlators of the Gaussian free field; presumably, *at criticality* the convergence (3.1.4) can be alternatively derived therefrom via the combinatorial bosonization correspondence [58].

The left-hand side of (3.1.4) is a correlation in the infinite-volume thermodynamic limit, i. e., the limit of correlations in increasing finite domains $\Omega_1^\delta \subset \Omega_2^\delta \subset \ldots \subset \Gamma^\delta$ for a fixed temperature parameter q. The existence of such a limit can be shown by standard monotonicity arguments and RSW bounds at criticality; see Section 3.2.3 for details. Theorem 3.1.1 then concerns another limit as one lets both $q, \delta \to 0$ so that $q = \frac{1}{2} m\delta$. In fact, to prove Theorem 3.1.1 we rely upon the fact that the RSW bounds are uniform with respect to δ and q, which allows us to work in (sufficiently large) finite domains Ω^δ instead of Γ^δ. In particular, along the way we prove the convergence and universality for spin-spin correlations in smooth simply connected domains with appropriate boundary conditions : wired if $m \leq 0$ and free if $m \geq 0$. Our analysis also implies the following :

As in [38] and [137], one of the key ingredients of our proof in the case $m \leq 0$ is a (uniform) convergence result for the "discrete logarithmic derivatives"

$$\log \frac{\mathbb{E}^{(m),\mathrm{w}}_{\Omega^\delta}[\sigma_{u_1'}\sigma_{u_2}]}{\mathbb{E}^{(m),\mathrm{w}}_{\Omega^\delta}[\sigma_{u_1}\sigma_{u_2}]} \;=\; \mathrm{Re}\,[(u_1' - u_1)\mathcal{A}^{(m)}_{\Omega}(u_1, u_2)] + o(\delta) \tag{3.1.5}$$

where $u_1' \sim u_1$ are nearest neighbors on the lattice $\Gamma^{\circ,\delta}$ and the quantity $\mathcal{A}_\Omega^{(m)}(u_1,u_2)$ is expressed via the scaling limit of spinor fermionic observables; see Section 3.1.3 for a more detailed discussion. This result extends without any effort to multi-spin correlation, leading to convergence results for ratios of such correlations :

$$\frac{\mathbb{E}^{(m),\mathrm{w}}_{\Omega^\delta}[\sigma_{u_1'}\sigma_{u_2'}\dots\sigma_{u_n'}]}{\mathbb{E}^{(m),\mathrm{w}}_{\Omega^\delta}[\sigma_{u_1}\sigma_{u_2}\dots\sigma_{u_n}]} \;\to\; \frac{\langle\sigma_{u_1'}\sigma_{u_2'}\dots\sigma_{u_n'}\rangle^{(m),\mathrm{w}}_{\Omega}}{\langle\sigma_{u_1}\sigma_{u_2}\dots\sigma_{u_n}\rangle^{(m),\mathrm{w}}_{\Omega}} \;\text{ as }\; \delta\to 0\,, \tag{3.1.6}$$

where the "continuum correlation functions" in the right-hand side are defined as

$$\langle\sigma_{u_1}\sigma_{u_2}\dots\sigma_{u_n}\rangle^{(m),\mathrm{w}}_{\Omega} \;:=\; \exp\int \mathrm{Re}\,\big[\textstyle\sum_{s=1}^n \mathcal{A}_\Omega^{(m)}(u_s,u_1,\dots,u_{s-1},u_{s+1},\dots,u_n)du_s\big],$$

with an appropriate multiplicative normalization. Once the convergence (3.1.6) is established, the asymptotics (3.1.4) together with usual decorrelation arguments coming from RSW-type estimates for the random cluster (or Fortuin–Kasteleyn) representation of the model are enough to fix the explicit multiplicative normalization of the correlation functions. Thus, our analysis also implies the following :

Theorem 3.1.2. The results of [38, Theorem 1.2] for $m=0$ and [137, Theorem 1.1] for $m<0$ asserting convergence

$$\delta^{-\frac{n}{8}}\mathbb{E}^{(m),\mathrm{w}}_{\Omega^\delta}[\sigma_{u_1}\sigma_{u_2}\dots\sigma_{u_n}] \;\to\; \mathcal{C}_\sigma^n\cdot\langle\sigma_{u_1}\sigma_{u_2}\dots\sigma_{u_n}\rangle^{(m),\mathrm{w}}_{\Omega} \;\text{ as }\; \delta\to 0$$

of multi-point spin correlations in discrete approximations Ω^δ of bounded simply connected domains Ω (with smooth boundaries if $m<0$), hold true, without any change, for the massive Ising model on isoradial grids with Z-invariant weights.

We stress once again here that not only the continuous correlation functions are universal within this class of the lattices/weights, but also the constant $\mathcal{C}_\sigma$ in front.

Proof. The proof of (3.1.6) in the case $n=2$ is given in Corollary 3.4.10 for $m=0$ and in Corollary 3.4.16 for $m<0$. Since the analysis is local, it extends without any change to the case $n>2$. Given (3.1.6), the rest of the proofs in [38] and [137] amount to fixing the overall normalization by sending the points u_s pairwise to each other or to the boundary of Ω, and the only part of that argument that relied on the specific properties of the square lattice was the computation of the full-plane two-point correlation. This ingredient is now supplied by Theorem 3.1.1. □

Remark 3.1.2. In order to prove Theorem 3.1.1 for $m>0$ we rely upon an analogue of [38, Theorem 1.7] which gives the convergence of the ratio of the two-point correlations in dual Ising models. Thus, similarly to a work of S. C. Park [137], our methods do *not* directly imply an analogue of Theorem 3.1.2 for $m>0$. However, we believe that the techniques developed in

this paper for the analysis of spinor fermionic observables near their branching points allow to prove such a convergence, at least in smooth simply connected domains, following the framework of [39].

A sharp control of the discrete logarithmic derivative (3.1.5), in principle, suffices to recover the scaling function $\Xi(r,m)$ in the statement of Theorem 3.1.1, but not the fact that the constant C_σ is lattice-independent. In order to complete the proof, we use an additional *gluing argument* (see Section 3.2.4 for details), showing that a finite piece of an arbitrary isoradial grid can be glued, staying within the same family, to a piece of a regular (rectangular) lattice, so that the sizes of these pieces and the distance between them are comparable. Then, we can move the spins from the irregular part to the regular one, controlling how the correlation changes in the process, and establishing universality.

A similar argument can be applied to analyze the *magnetization in the infinite-volume limit* of the sub-critical model on a fixed isoradial grid Γ°, say, with $\delta = 1$. As a by-product of our analysis of the massive model, we also get the following result. We are not aware of its detailed proof in full generality in the literature, although it was probably known, at least for some particular lattices, in the folklore.

Proposition 3.1.3 (Baxter's formula)**.** For $q < 0$, the infinite-volume magnetization in the sub-critical Ising model on Γ° with Z-invariant weights is universal :

$$\mathbb{E}^+_{\Omega_n}[\sigma_u] \to (k^*)^{\frac{1}{4}} \text{ as } \Omega_n \uparrow \Gamma^\circ \quad \text{and} \quad \mathbb{E}_{\Gamma^\circ}[\sigma_{u_1}\sigma_{u_2}] \to (k^*)^{\frac{1}{2}} \text{ as } |u_1 - u_2| \to \infty.$$

For $q > 0$, similar results hold for the model on $\Gamma^\bullet$ with k^* replaced by k.

Proof. See Section 3.4.1. As in the case of Theorem 3.1.1 and the constant $\mathcal{C}_\sigma$, we do not compute these limits explicitly, but rather show that they are universal. To this end, we glue a large enough piece of a given isoradial grid to a piece of a rectangular lattice, on which we can apply the celebrated Onsager–Yang result [167, 123] in the form given by Baxter [12, Eq. 7.10.50] ; see also [40, Section 3] for a simplified derivation. (Note that the elliptic parameter k in [28] corresponds to k' of Baxter ; see footnote in [28, Section 2.2.2].) □

3.1.3 . Techniques and related projects

The general strategy of our proof of the key convergence result (3.1.5) follows that of [38, 137]. One introduces an observable, a properly normalized spin-fermion-disorder correlator, which, as a function of the position of the fermion, is a *massive s-holomorphic spinor* living on a double cover of the original discrete domain ramified at the positions of the spin and the disorder. (The notion of massive s-holomorphic functions on isoradial graphs and the regularity theory thereof were independently developed in a recent work of S.C.Park [138] ; see Section 3.3.1 for more details.) We then prove the convergence of this observable to a massive

holomorphic (i. e., satisfying the Dirac equation $\overline{\partial} f + im\overline{f} = 0$) limit as $\delta \to 0$; uniformly away from the boundary and from the branching points.

After this is done, one uses the fact that both spin-spin correlations in (3.1.5) can be recovered from the values of the observable by placing the fermion next to the disorder. We thus need a way to express a value of a massive s-holomorphic spinor next to its ramification point in terms of its values at a definite distance therefrom. This is where our main *technical innovation* comes into play : we introduce a very simple version of the Cauchy integral formula for spinors that allows one to do such a reconstruction using an explicit full-plane kernel, the discrete analogue of a spinor $e^{\mp i\frac{\pi}{4}} \cdot z^{-\frac{1}{2}} e^{\pm 2m|z|}$. Such kernels were essentially constructed by Dubédat in [57] for the critical case $m = 0$; we extend his construction to the massive setup using the theory of massive discrete exponentials, recently developed by Boutillier, de Tilière and Raschel in [27, 28]. The construction and the asymptotic analysis of the required branching kernels are presented in Section 3.5.

Recall that in [38, 137] a considerably more complicated reconstruction procedure was employed. In particular, it also required an explicit construction of discrete analogs of the kernels $e^{\mp i\frac{\pi}{4}} z^{\frac{1}{2}}$ (or their massive modifications) and an argument based on the symmetrization procedure and the discrete Beurling inequality; this technique is unavailable in the isoradial setup due to the lack of symmetries of the lattice. Thus, not only our new argument enables generalization of the results to the isoradial setup, it also leads to a much simpler proof in the square lattice case. In particular, the companion paper [39] devoted to a unified treatment of mixed correlations of primary fields, borrowed the arguments of the present paper in what concerns the analysis near the branching points. Moreover, this Cauchy formula can be written in a purely abstract form without any assumption on the embedding or weights of the model under consideration (see Lemma 3.3.14), which paves the way for further generalizations of the convergence results for spin correlations *beyond* the Z-invariant setup; cf. recent results on the convergence of fermionic observables on the so-called s-embeddings of planar weighted graphs [33].

Another – though not strictly necessary for our analysis – new idea implemented in this paper is a re-embedding of the massive Z-invariant Ising model on Λ^δ into the complex plane using the aforementioned *s-embeddings* $\mathcal{S}^\delta$; see Section 3.3.3 for more details. This allows us to benefit from a general regularity theory developed for s-holomorphic functions on s-embeddings in [33, Section 2] and [45, Section 6]. Under this procedure, the original massive s-holomorphic observables on Λ^δ and new s-holomorphic observables on $\mathcal{S}^\delta$ are linked by a simple explicit formula given in Proposition 3.3.19, which immediately allows us to deduce the a priori regularity of massive s-holomorphic functions on Λ^δ from the results of [33, 45]. Also, this provides a concrete illustration of a general phenomenology, which says that the mass in a planar Ising model manifests itself as the mean curvature of an s-embedding of the model into the Minkowski space $\mathbb{R}^{2+1}$; see [33, Section 2.7] for a discussion. Though, as already mentioned above, these re-embedding techniques

are not necessary for the analysis of the Z-invariant model (e. g., see [138], where the relevant a priori regularity estimates developed directly on Λ^δ), we believe that they are flexible enough to be applied to less rigid setups.

Recall that throughout this paper we assume that all isoradial grids satisfy the uniform bounded angles property $\mathrm{BAP}(\theta_0)$, which plays an essential role in several places of our analysis as we frequently use the fact that the graph distances on rhombic lattices are comparable with Euclidean ones : e. g., when passing from $(3.1.5)$ to $(3.1.6)$. However, there are certain indications that this assumption is not strictly relevant, at least at criticality. Notably, similar techniques can be applied to a 2D graphical expansion (e.,g., see [89, 109] and references therein) of the *quantum 1D Ising model*, leading to similar convergence results for correlation functions ; we refer the interested reader to a forthcoming paper [110] for more details. This expansion can be thought of as a 2D Ising model on a rectangular grid with an infinitesimally small aspect ratio, a limit that obviously cannot be achieved under $\mathrm{BAP}(\theta_0)$.

Finally, in terms of a framework developed in the companion paper [39] for the analysis of mixed correlations of primary fields in (possibly) multiply connected domains, this paper provides the following "building blocks" :

— an explicit construction and asymptotic analysis of required infinite-volume kernels $\mathcal{G}_{[u]}$, $\mathcal{G}_{[v]}$ and $\mathcal{G}_{(a)}$ (see Section 3.5 for more details) ;

— analysis of the two-point spin correlation in the full plane (Theorem 3.1.1).

Note that a work [138] of S. C. Park contains two more such "building blocks", namely

— a "quantitative convergence" of basic fermionic FK-Ising observables ;

— uniform RSW-type estimates for the massive FK-Ising model ; cf. [61].

Thus, the only remaining input required to extend the results of [39] to the massive Z-invariant model on isoradial grids is the analysis of solutions to certain Riemann-type boundary value problems for massive holomorphic functions *in continuum* (which is considerably more complicated for $m \neq 0$ than at criticality, cf. [138]).

Organization of the paper

We start Section 3.2 by fixing the notation and recalling the definition of the Z-invariant Ising model. We then recall the construction of fermionic observables via Kadanoff–Ceva order-disorder formalism, the propagation equation, and Smirnov's "integrating the square" procedure. We also recall a construction of the infinite volume limit of the model and describe the "star extension" procedure, which allows to glue a big piece of a given rhombic lattice to a regular one. In Section 3.3, we review the "massive discrete complex analysis" techniques, namely, the a priori regularity of "massive s-holomorphic functions" constructed from solutions to the spinor propagation equation, and the fact that subsequential limits of such functions satisfy the Dirac equation. We also state the properties of the

massive discrete holomorphic full-plane "kernels" used in our proofs, and introduce the aforementioned Cauchy integral formula. In Section 3.4, we prove the main results of the paper. For convenience of the reader we start with the critical case and then refer to it when discussing the massive setup. In Section 3.5, we construct the required full-plane kernels and perform the asymptotic analysis thereof, using the "massive discrete exponentials" of Boutillier, de Tilière, and Raschel [27].

Acknowledgements

We are grateful to S. C. Park for many fruitful discussions of the massive Ising model. We also would like to thank Cédric Boutillier, Béatrice de Tilière, Jhih-Huang Li, Ioan Manolescu, Paul Melotti and Yijun Wan for helpful comments and remarks. D. C. is a holder of the ENS–MHI chair funded by the MHI, whose support is gratefully acknowledged. The work of K. I. was supported by Academy of Finland via academy project "Critical phenomena in dimension two : analytic and probabilistic methods". The work of D. C. and R. M. was also partially supported by the ANR-18-CE40-0033 project DIMERS. Last but not least, we would like to thank the anonymous referee for carefully reading the first version of this paper and providing a useful feedback.

3.2 . Preliminaries and basic facts

3.2.1 . Notation : graphs, double covers, spin-disorder correlations

We rely upon the spin-disorder formalism of Kadanoff and Ceva [93] ; e. g. see [34, Section 2] or [39, Section 2] for more details and [37] for links of this approach with other combinatorial formalisms used to study the planar Ising model. For a planar graph $G = G^\bullet$, let

— G° be the graph dual to $G^\bullet$ (note that we typically work with the planar Ising model defined on G° and not on $G^\bullet$) ;

— $\Lambda(G)$ be a planar graph whose set of vertices is the union of $G^\bullet$ and G°, with edges connecting adjacent vertices $v \in G^\bullet$ and faces $u \in G^\circ$ of G ;

— $\diamondsuit(G)$ be the graph dual to $\Lambda(G)$, we often call its vertices $z \in \Lambda(G)$ *quads* referring to this duality (note that all faces of $\Lambda(G)$ have degree four) ;

— $\Upsilon(G)$ be the medial graph of $\Lambda(G)$ (i. e., vertices of $\Upsilon(G)$ are in a bijective correspondence with edges (uv) of $\Lambda(G)$), we often call its vertices $c \in \Upsilon(G)$ *corners* referring to the fact that they are in a bijective correspondence with corners of faces of G° (or of $G = G^\bullet$, note that faces of $\Upsilon(G)$ correspond either to $v \in G^\bullet$ or to $u \in G^\circ$ or to $z \in \diamondsuit(G)$) ;

— $\Upsilon^\times(G)$ be a double cover of $\Upsilon(G)$ that branches around *each* of its faces (e. g., see [129, Fig. 27] or [48, Fig. 6] or [33, Fig. 3]) ;

— more generally (e. g., see Fig. 3.2.1 for an example with $\varpi = [v, w]$), given a subset ϖ of vertices of $\Lambda(G) = G^\bullet \cup G^\circ$ let

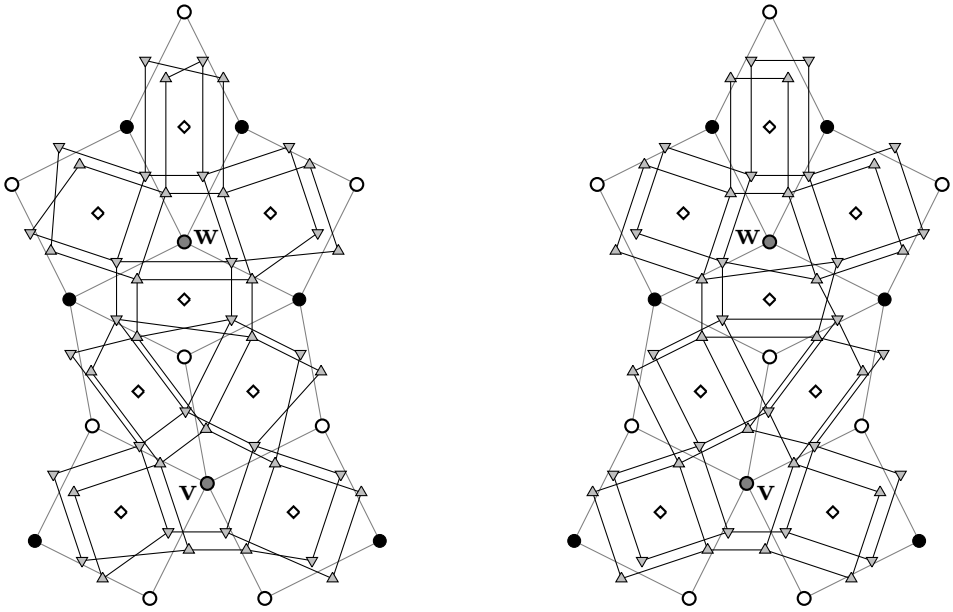

FIGURE 3.2.1 – Left : local structure of a double cover $\Upsilon^{\times}_{[v,w]}$ of the medial graph Υ ; vertices $v \in \Gamma^{\bullet}$ and $w \in \Gamma^{\circ}$ are marked in gray. Right : local structure of the corresponding double cover $\Upsilon_{[v,w]}$.

— $\Upsilon_{\varpi}(G)$ be a double cover of $\Upsilon(G)$ branching *only* around $w \in \varpi$,

— $\Upsilon^{\times}_{\varpi}(G)$ be a double cover ramified at all faces of $\Upsilon(G)$ *except* ϖ.

In our paper the graph G is usually a discrete domain on an isoradial grid $\Gamma^{\delta} = \Gamma^{\bullet,\delta}$ of mesh size $\delta \to 0$, which approximates a planar bounded simply connected domain $\Omega \subset \mathbb{C}$. We use the notation $\Omega^{\delta} \subset \Gamma^{\delta}$ for such approximations. We will often view vertices (dual vertices, etc.) as complex numbers giving their position in $\mathbb{C}$.

We often speak about *spinors* defined on double covers of graphs, which are functions on the double cover in question whose values at two lifts of the same vertex differ by the sign. Provided that an embedding of all these graphs into the complex plane is fixed, an important example of a spinor on $\Upsilon^{\times}(G)$ is given by

$$\eta_c \;:=\; \varsigma \cdot \exp\big[-\tfrac{i}{2}\arg(v(c)-u(c))\big], \qquad \varsigma := e^{i\frac{\pi}{4}}, \tag{3.2.1}$$

where $u(c) \in G^{\circ}$ and $v(c) \in G^{\bullet}$ are endpoints of the edge $(u(c)v(c))$ corresponding to the corner c. A particular choice of the prefactor ς is unimportant but influences the notation in what follows ; we choose the value $e^{i\frac{\pi}{4}}$ in order to keep the presentation consistent with [48] and [138] (note however that [38] and [137] use another convention $\varsigma = i$).

The (ferromagnetic) *nearest-neighbor* Lenz–Ising model on the *dual* graph G° is a random assignment of spins $\sigma_u \in \{\pm 1\}$ to the *faces* u of G such that the

probability of a spin configuration $\sigma = (\sigma_u)$ is proportional to

$$\mathbb{P}_G[\,\sigma\,] \propto \exp\,[\,\beta^\circ \textstyle\sum_{u\sim w} J^\circ_e \sigma_u \sigma_w\,]\,, \qquad e = (uw)^*, \tag{3.2.2}$$

where a positive parameter $\beta^\circ = 1/kT$ is called the *inverse temperature*, the sum is taken over all pairs of adjacent faces u, w of G (equivalently, edges e of G or quads $z \in \Lambda(G)$), and $J^\circ = (J^\circ_e)$ is a collection of positive interaction constants indexed by edges of G. Below we use the following *parametrization* of $\beta^\circ J^\circ_e$:

$$x_e \;=\; \tan \tfrac{1}{2}\widehat{\theta}_e \;:=\; \exp[\,-2\beta^\circ J^\circ_e\,]. \tag{3.2.3}$$

Note that the quantities $x_e \in (0,1)$ and $\widehat{\theta}_e := 2\arctan x_e \in (0, \frac{1}{2}\pi)$ have the same monotonicity as the temperature $(\beta^\circ)^{-1}$. We also often write $\widehat{\theta}_z$ instead of $\widehat{\theta}_e$ if a quad $z \in \Lambda(G)$ corresponds to an edge e of G. On isoradial graphs, we depart from arbitrary parameters $\widehat{\theta}_z$ and restrict to *Z-invariant weights* given in terms of a global elliptic parameter k and geometric angles $\overline{\theta}_e$ of the embedding by (3.1.1).

Note that $\tan\widehat{\theta}_z = (1+4q)\cdot\tan\overline{\theta}_z + O(q^2)$ as $q \to 0$, which implies that

$$\widehat{\theta}_z - \overline{\theta}_z \;=\; 4q\cdot\sin\overline{\theta}_z\cos\overline{\theta}_z + O(q^2) \;=\; 2\delta m \sin\overline{\theta}_z\cos\overline{\theta}_z + O(\delta^2) \tag{3.2.4}$$

in the massive limit $q = \frac{1}{2}m\delta \to 0$. In particular, $\widehat{\theta}_z = \overline{\theta}_z$ at criticality.

We denote by $\mathbb{E}^{(m),\mathrm{w}}_{\Omega^\delta}$ the expectation under the measure (3.2.2) with Z-invariant weights given by (3.1.1), with $q = \frac{1}{2}m\delta$. We will omit δ when we consider a fixed lattice of mesh $\delta = 1$. The superscript w stands for *wired* boundary conditions : since we use the convention that spins σ_u are assigned to faces of Ω^δ, instead of considering a single outer face u_{out} of Ω^δ one can think about all boundary points $u \in \Gamma^{\circ,\delta}$ as being wired to each other. Sometimes, we also fix the spin of u_{out} to be $+1$ (i. e., impose '+' boundary conditions) and write $\mathbb{E}^{+}_{\Omega^\delta}$ instead of $\mathbb{E}^{\mathrm{w}}_{\Omega^\delta}$.

The *Kramers–Wannier duality* (e. g., see [60, Section 7.5]) provides a link between the Ising model (on faces of Ω^δ) described above and another nearest-neighbor Ising model defined on vertices of Ω^δ with interaction parameters $\beta^\bullet J^\bullet_e$ such that $\tanh[\beta^\bullet J^\bullet_e] = \exp[-2\beta^\circ J^\circ_e]$ or, equivalently, $\sinh[2\beta^\circ J^\circ_e]\sinh[2\beta^\bullet J^\bullet_e] = 1$. In terms of the parametrization (3.2.3) this duality reads as

$$\exp[-2\beta^\circ J^\circ_e] = \tan\tfrac{1}{2}\widehat{\theta}_z, \qquad \exp[-2\beta^\bullet J^\bullet_e] = \tan\tfrac{1}{2}\widehat{\theta}^*_z, \qquad \widehat{\theta}_z + \widehat{\theta}^*_z = \tfrac{1}{2}\pi.$$

The angles $\widehat{\theta}^*_z$ also admit parametrization (3.1.1) with a dual elliptic parameter k^* ; the relation is simplest in terms of the nome $q^* = -q$; see (3.1.2). We denote the expectation in this dual model (defined on vertices of Ω^δ) as $\mathbb{E}^{(-m),\,\mathrm{f}}_{\Omega^*,\delta}$, where the superscript f stands for *free* boundary conditions and emphasizes that no restrictions on the boundary spins are imposed.

We use the Kadanoff–Ceva *disorder variables* : for a subset γ of edges of $G^\bullet$, put

$$\mu_\gamma \;:=\; \textstyle\prod_{u\sim w:(uw)\cap\gamma\neq\varnothing} e^{-2\beta^\circ J^\circ_{(uw)^*}\sigma_u\sigma_w}.$$

Up to the sign, the correlations of these variables with spins only depend on $\partial\gamma$ viewed as a chain modulo 2. Hence, we will simply write

$$\mu_\gamma = \mu_{v_1} \dots \mu_{v_m}, \quad \text{where} \quad \partial\gamma = \{v_1, \dots, v_m\}$$

inside such correlations. We have the following identity :

$$\mathbb{E}^{\mathrm{w}}_{\Omega^\delta}[\,\mu_{v_1} \dots \mu_{v_m} \sigma_{u_1} \dots \sigma_{u_n}\,] \;=\; \mathbb{E}^{\mathsf{free}}_{\Omega^{*,\delta}}[\,\mu_{u_1} \dots \mu_{u_n} \sigma_{v_1} \dots \sigma_{v_m}\,], \tag{3.2.5}$$

where $u_1, \dots, u_n \in \Omega^{\circ,\delta}$, $v_1, \dots, v_m \in \Omega^{\bullet,\delta}$, and both n, m are assumed to be even (otherwise, these correlators do not make sense) ; in fact, both sides of (3.2.5) lead to the same sums over subgraphs of $\Omega^\delta = \Omega^{\bullet,\delta}$ if one uses the low-temperature expansion for the left-hand side and the high-temperature expansion for the right-hand one. In particular, the disorder variables μ are dual objects to spins σ under the Kramers–Wannier duality. We refer the reader to [93, 37, 34, 39] for more details on the Kadanoff–Ceva formalism.

Remark 3.2.1. Recall also that under a natural rule for tracking the signs [39, Section 2.2], both sides of (3.2.5) change the sign when one of the vertices v_p makes a turn around one of u_q ; in other words one should view (3.2.5) as a spinor defined on an appropriate double cover of the set $(\Omega^{\bullet,\delta})^{\times m} \times (\Omega^{\circ,\delta})^{\times n}$ with the removed diagonal ($v_p = v_{p'}$ or $u_q = u_{q'}$ for some $p \neq p'$ or $q \neq q'$). In full generality, the extension of (3.2.5) onto the diagonal requires certain technicalities in fixing the signs. However, no problems of that kind arise in the simplest setup $m = 2$ that we only need below.

3.2.2 . Fermionic observables and functions H_X

The Kadanoff–Ceva fermionic variable χ_c is formally defined as $\chi_c := \mu_{v(c)}\sigma_{u(c)}$ and the corresponding fermionic observables read as

$$X_\varpi(c) \;:=\; \mathbb{E}^{\mathrm{w}}_G[\chi_c\, \mu_{v_1} \dots \mu_{v_{m-1}} \sigma_{u_1} \dots \sigma_{u_{n-1}}]\,, \quad c \in \Upsilon^\times_\varpi(G),$$

where $\varpi = \{v_1, \dots, v_{m-1}, u_1, \dots, u_{n-1}\}$ and we assume that both n, m are even.

Remark 3.2.2. Due to Remark 3.2.1, X_ϖ is a *spinor* on the double cover $\Upsilon^\times_\varpi(G)$. This implies that the product $\eta_c X_\varpi(c)$, where η_c is given by (3.2.1), is a spinor on the double cover $\Upsilon_\varpi(G)$, which branches *only* over points from ϖ ; see Fig. 3.2.1.

It is well known (e. g., see [129] or [37, Section 3.5] and references therein) that Kadanoff–Ceva fermionic observables satisfy the so-called *propagation equation*

$$X(c_{00}) \;=\; X(c_{01}) \cos\widehat{\theta}_z + X(c_{10}) \sin\widehat{\theta}_z\,, \tag{3.2.6}$$

which holds for each corner c_{00} and its neighbors c_{01}, c_{10} on the corresponding double cover $\Upsilon^\times_\varpi(G)$ such that all three are incident to the same quad z ; see

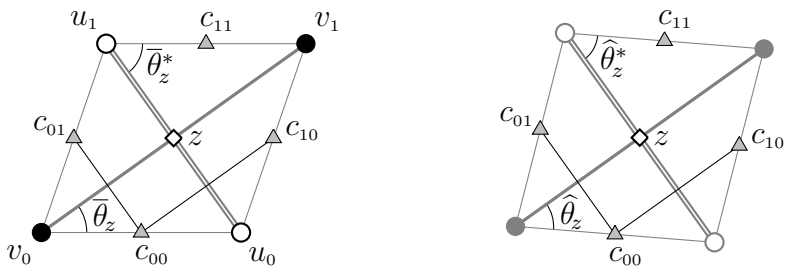

FIGURE 3.2.2 – Left : Local notation at a quad $z = (v_0u_0v_1u_1) \in \diamondsuit$. Identity (5.2.6) expresses the value $X(c_{00})$ of a Kadanoff–Ceva fermionic observable as a linear combination of $X(c_{01})$ and $X(c_{10})$ with coefficients $\cos\widehat{\theta}_z = \mathrm{cn}\left(\frac{2K}{\pi}\overline{\theta}_z \,|\, k\right)$ and $\sin\widehat{\theta}_z = \mathrm{sn}\left(\frac{2K}{\pi}\overline{\theta}_z \,|\, k\right)$, respectively. Right : Following [137, 138], to define the value $F(z) \in \mathbb{C}$ of the corresponding massive s-holomorphic function (aka Smirnov's fermionic observable) at $z \in \diamondsuit$, we imagine a tilted rhombus with edges $e^{\pm i(\widehat{\theta}_z - \overline{\theta}_z)}(v_p - u_q)$ centered at z and then apply the usual definition [48] of s-holomorphic functions to this 'virtual' rhombus.

Fig. 3.2.2 for the notation. A consequence of this identity is that, given a fermionic observable X, one can define (up to an additive constant) a function H_X on the graph $\Lambda(G)$ by prescribing its increments between neighboring vertices $u_q \in G^\circ$ and $v_p \in G^\bullet$ as

$$H_X(v_p) - H_X(u_q) \;:=\; (X(c_{pq}))^2. \tag{3.2.7}$$

(Note that for the critical Ising model on $\mathbb{Z}^2$, this is nothing but Smirnov's definition from [160, Lemma 3.6] ; see also Section 3.3.1 below.) More generally, if two observables X_1, X_2 are (locally) defined on the same double cover $\Upsilon^{\times}_{\varpi}(G)$, then one can extend the above definition and introduce a function $H[X_1, X_2]$, also defined up to an additive constant, by setting

$$H[X_1, X_2](v_p) - H[X_1, X_2](u_q) \;:=\; X_1(c_{pq})X_2(c_{pq}) \tag{3.2.8}$$

(this quantity does not depend on the lift of c_{pq} onto $\Upsilon^{\times}_{\varpi}(G)$; cf. Lemma 3.3.14.)

Remark 3.2.3. From the combinatorial perspective, considering a discrete simply connected domain $\Omega^\delta \subset \Gamma^\delta$ with wired boundary conditions boils down to identifying all 'white' vertices along the boundary with each other. In particular, all the values of H_X (or of $H[X_1, X_2]$) at 'white' boundary vertices $u \in \partial\Omega \cap G^\circ$ are the same, i. e., the function $H_X|_{G^\circ}$ always has *Dirichlet boundary conditions* in this case. However, note that this is not the case for boundary values of H_X on 'black' boundary vertices. Nevertheless, there exists a trick (originally suggested in [48, Section 3.6] in the critical setup) which allows to modify the grid Λ^δ near the boundary of Ω^δ staying in the isoradial

family and artificially define H_X on new obtained 'black' vertices so that it also has Dirichlet boundary values and all required 'discrete complex analysis estimates' hold true ; see Remark 3.3.10 below.

It is also convenient to extend the definition of H_X to the set $\diamondsuit(G)$ as follows :

$$\begin{array}{rcl} H_X(v_p) - H_X(z) & := & X(c_{p0})X(c_{p1})\cos\widehat{\theta}_z, \\ H_X(z) - H_X(u_q) & := & X(c_{0q})X(c_{1q})\sin\widehat{\theta}_z, \end{array} \tag{3.2.9}$$

where c_{p0} and c_{p1} are assumed to be chosen as neighbors on $\Upsilon^{\times}_{\varpi}(G)$ to avoid the ambiguity in the sign ; note that this definition is consistent with (5.2.16) due to the propagation equation (5.2.6). Let $\Lambda(G) \cup \diamondsuit(G)$ denotes a planar graph whose edges consist of all edges of $\Lambda(G)$ and edges linking each vertex $z \in \diamondsuit(G)$ to its four neighbors $z \sim w \in \Lambda(G)$.

The following lemma holds for all planar graphs and all interaction parameters.

Lemma 3.2.4. Let a function H_X be (locally) constructed via (3.2.9) and (5.2.16) from a fermionic observable X defined on a double cover $\Upsilon^{\times}_{\varpi}(G)$. Then, H_X satisfies

— the maximum principle on $\Lambda(G) \cup \diamondsuit(G)$ except at points of $\varpi \cap G^{\bullet}$;

— the minimum principle on $\Lambda(G) \cup \diamondsuit(G)$ except at points of $\varpi \cap G^{\circ}$.

Proof. See [33, Proposition 2.10], which proves both the maximum and the minimum principles for H_X in absence of (non)branching vertices, i. e., if $\varpi = \varnothing$. If $\varpi \neq \varnothing$, note that the value at a vertex $u \in \varpi \cap G^{\circ}$ is always smaller than the values at neighboring vertices from $G^{\bullet}$ due to (5.2.16), thus H_X cannot attain a maximum at u. Similarly, H_X cannot attain a minimum at a point $v \in \varpi \cap G^{\bullet}$. □

Remark 3.2.5. Let $w \in \varpi$ be an isolated point of ϖ and assume that $X(c) = 0$ at one of the nearby corners $w \sim c \in \Upsilon^{\times}_{\varpi}(G)$. Then, it is easy to see that the function H_X satisfies *both* the maximum and the minimum principle near w as its values at two neighboring vertices (one from G°, the other from $G^{\bullet}$) of c are the same.

3.2.3 . Infinite-volume of the Ising model with $q \neq 0$ and RSW estimates

Given an isoradial grid Λ^{δ} of mesh size δ and a point $u \in \mathbb{C}$ we denote by $\Lambda^{\delta}_R(u)$ a discretization of the square box

$$[\operatorname{Re} u - R\,, \operatorname{Re} u + R] \times [\operatorname{Im} u - R\,, \operatorname{Im} u + R]$$

on Λ^{δ} with appropriate boundary conditions which can vary depending on the context. We write Λ^{δ}_R instead of $\Lambda^{\delta}_R(0)$ if $u = 0$ and skip the superscript if $\delta = 1$.

It is well-known that spin-spin correlations $\mathbb{E}_G[\sigma_u\sigma_w]$ in the Ising model on a finite graph can be written as the probability that u and w are connected in the so-called Fortuin–Kasteleyn (or random cluster) representation of the model ; e. g., see [60, Section 7] for more details.

For the *critical* (i. e., $m = 0$) Ising model on isoradial grids it is well known that the following Russo–Seymour–Welsh-type estimate holds uniformly with respect to boundary conditions :

$$\mathbb{P}\big[\,\text{there exists a wired circuit in the annulus } \Lambda_{3R}(u) \setminus \Lambda_R(u)\,\big] \;\geq\; p_0 \;>\; 0.$$

(For a proof, one can, e. g., use [48, Theorem C] to show that crossings of rectangles with self-dual (i. e., wired/free/wired/free) boundary conditions have probability uniformly bounded away from zero, and then apply the proof of [61, Proposition 2.10] ; see also [33, Section 5.6].) In particular, the existence of such circuits implies the uniqueness of the infinite-volume Gibbs measure in the critical FK-Ising model and allows one to speak about infinite-volume correlations $\mathbb{E}_\Lambda[\sigma_u\sigma_w]$.

Assume now that $q = \frac{1}{2}m\delta \leq 0$. By monotonicity with respect to interaction parameters, the (uniform with respect to boundary conditions) existence of wired circuits in annuli $\Lambda_{3R}(u) \setminus \Lambda_R(u)$ also holds in this case. This allows one to define the *infinite-volume* limit of the sub-critical FK-Ising model on Λ and, moreover, implies the following uniform estimate :

> for each $\varepsilon > 0$ there exists $A = A(\varepsilon) \gg 1$ such that for all $m \leq 0$ and all $D \geq 1$ one has
>
> $$(1-\varepsilon)\cdot\mathbb{E}^{(m),\mathrm{w}}_{\Lambda_{AD}(u)}[\sigma_u\sigma_w] \;\leq\; \mathbb{E}^{(m)}_{\Lambda}[\sigma_u\sigma_w] \;\leq\; \mathbb{E}^{(m),\mathrm{w}}_{\Lambda_{AD}(u)}[\sigma_u\sigma_w] \quad (3.2.10)$$
>
> provided that $|w - u| \leq D$.

Indeed, the latter inequality in (3.2.10) is trivial due to the monotonicity with respect to boundary conditions. The former follows from the fact that

$$\mathbb{E}^{(m),\mathrm{f}}_{\Lambda_{AD}(u)}[\sigma_u\sigma_w] \;\geq\; \mathbb{P}^{(m),\mathrm{f}}_{\Lambda_{AD}(u)\setminus\Lambda_D(u)}\big[\,\text{there exists a wired circuit}\,\big]\times\mathbb{E}^{(m),\mathrm{w}}_{\Lambda_{AD}(u)}[\sigma_u\sigma_w],$$

which holds due to the FKG inequality and the monotonicity of the probability that u and w are connected with respect to a domain. (Note that the first factor can be made arbitrary close to 1 by choosing $A \geq 3^{\lfloor \log\varepsilon/\log(1-p_0)\rfloor+1}$.)

Remark 3.2.6. One can similarly use dual-wired circuits in order to define the infinite-volume limit of the off-critical FK-Ising model on Λ and the infinite-volume spin-spin correlations for $m \geq 0$. It is also worth noting that in the *massive* regime $q = \frac{1}{2}m\delta$, $\delta \to 0$, one also has uniform RSW-type estimates for *both* primary and dual crossings/circuits on scales $R \asymp 1$; see [61] and [138] for more details. Of course, this is a much deeper property of the massive Ising model as compared to the simple monotonicity with respect to m discussed above.

3.2.4 . 'Star extension' of a finite box on an isoradial grid

In order to prove the universality of spin-spin correlations with respect to a grid, i. e., the fact the correlations on two isoradial grids $\Gamma_1^{\circ,\delta}$ and $\Gamma_2^{\circ,\delta}$ behave in a similar way, we typically consider a 'mixed' rhombic lattice that contains large pieces of both Λ_1^δ and Λ_2^δ and analyse the Ising model on this lattice. This strategy relies upon a possibility to 'glue together' boxes of size R cut from different isoradial grids, with an additional requirement that these two pieces are located at $O(R)$ distance from each other.

Clearly, no problem arises if Λ_1^δ comes from a rectangular lattice while $\Lambda_2^\delta = \delta\mathbb{Z}^2$ (or, more generally, if both $\Lambda_{1,2}^\delta$ are obtained from rectangular lattices) ; see Fig. 3.2.3. Consider now an irregular rhombic lattice Λ satisfying the bounded angles property $\mathrm{BAP}(\theta_0)$. In this section we show that one can construct a new rhombic lattice $[\Lambda_R(u)]^\star$ satisfying the property $\mathrm{BAP}(\theta_0)$ such that

— Λ and $[\Lambda_R(u)]^\star$ have the same box $\Lambda_R(u)$ of size R centered at u ;

— the modified lattice $[\Lambda_R(u)]^\star$ contains infinite wedge-shaped subsets of rectangular grids located at distance at most $O(R)$ from the point u ; here and below the implicit constant in the estimate $O(R)$ depends on θ_0 only.

It is worth noting that these properties are scale invariant and thus the same procedure can be applied to rhombic lattices Λ^δ (with mesh size $\delta < R$) instead of Λ.

Recall that a *train-track* on Λ is a (infinite) sequence of adjacent rhombi such that they share a common direction of edges, called the transversal direction of the train-track (e. g., see [102] for a discussion of this notion). The construction of $[\Lambda_R(u)]^\star$ goes in two steps, see also Fig. 3.2.3 :

— **Step 1.** Let $\Theta_R(u) \supset \Lambda_R(u)$ be the *connected component* of the set of quads $z \in \diamondsuit$ such that *both* train-tracks passing through z intersect $\Lambda_R(u)$.

Lemma 3.2.7. The set $\Theta_R(u)$ has diameter $O(R)$ and is train-track-convex, i. e., if two rhombii lying on the same train-track belong to the set $\Theta_R(u)$, then the whole segment of the train-track between these rhombi belong to $\Theta_R(u)$.

Proof. Let $\mathcal{T}_R(u)$ denote the set of all train-tracks that intersect the box $\Lambda_R(u)$. It is easy to see that for each $t \in \mathcal{T}_R(u)$ the set of all rhombi $z \in t \cap \Theta_R(u)$ is a segment. Indeed, if $z, z' \in t$ are two consecutive rhombi on t such that $z \in \Theta_R(u)$ but $z' \notin \Theta_R(u)$, then the second train-track $t' \neq t$ passing through z' cannot intersect $\Lambda_R(u)$. Hence, $t' \cap \Theta_R(u) = \varnothing$, which implies that all further rhombi lying on t beyond z' cannot belong to the *connected* set $\Theta_R(u)$ as they are separated from $z \in \Theta_R(u)$ by t'. Thus, $\Theta_R(u)$ is train-track-convex.

To estimate the diameter of $\Theta_R(u)$, note that for each $t \in \mathcal{T}_R(u)$ the number of quads in $t \cap \Theta_R(u)$ cannot exceed the total number $|\mathcal{T}_R(u)|$ of train-tracks in $\mathcal{T}_R(u)$ (since each of the remaining train-tracks $t' \in \mathcal{T}_R(u)$ can intersect t at most once). Thus, the estimate $\operatorname{diam} \Theta_R(u) = O(R)$ follows from $|\mathcal{T}_R(u)| \leqslant 2|\partial\Lambda_R(u)| = O(R)$. □

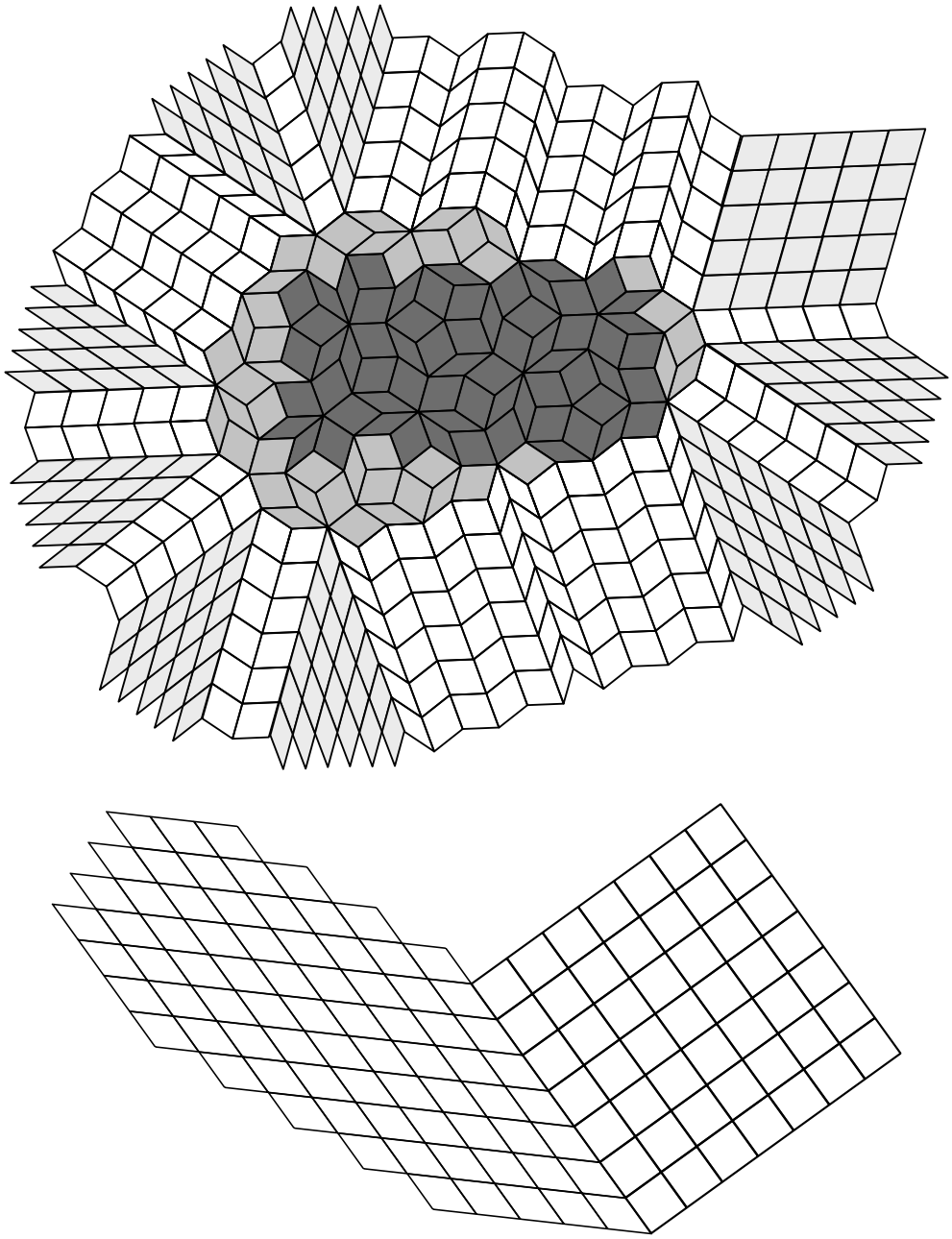

FIGURE 3.2.3 – TOP : the 'star extension' procedure for a rectangular box on a Penrose rhombic tiling. The box itself is colored dark gray and the rest of the corresponding set Θ is shown in gray. The boundary of Θ consists of nine train-tracks, extended infinitely outwards, the wedge-shaped parts of regular lattices are highlighted in light gray. The opening angles of the wedges are bounded from below by $2\theta_0$ of the $\mathrm{BAP}(\theta_0)$ property. For Penrose rhombic tilings, $2\theta_0 = \frac{\pi}{5}$; thus, in this case the boundary of Θ could not consist of more than ten train tracks. BOTTOM : a gluing of a regular rhombic lattice corresponding to a rectangular grid Λ^{rect} (on the left) with the square one (on the right).

The train-track convexity of $\Theta_R(u)$ implies that it is simply connected and its boundary $\partial\Theta_R(u)$ is a simple closed broken line such that no quad adjacent to it from outside can have two sides on $\partial\Theta_R(u)$. Let us divide these adjacent quads into (maximal) arcs τ_k, each of which is a part of a single-train track t_k. The above observation means that as we follow the boundary counterclockwise, the transversal directions of these train tracks also rotates counterclockwise, and the bounded angles property $\mathrm{BAP}(\theta_0)$ implies that it rotates at least $2\theta_0$ between two consecutive arcs ; in particular, there are at most π/θ_0 arcs. The construction of $[\Lambda_R(u)]^\star$ concludes as follows :

— **Step 2.** Duplicate (infinitely many times) each of the boundary arcs $\tau_k \subset t_k$ of $\Theta_R(u)$ in the transversal direction of t_k and fill the remaining wedge-shaped regions (of angle at least $2\theta_0$) by regular rhombic tilings ; see Fig. 3.2.3.

We call $[\Lambda_R(u)]^\star$ a *star extension* of $\Lambda_R(u)$. (In fact, we slightly abuse the notation since $[\Lambda_R(u)]^\star$ is not defined only by $\Lambda_R(u)$ and also depends on the structure of Λ near this box. However, this does not create any confusion in what follows.)

3.3 . Discrete complex analysis techniques

3.3.1 . Massive s-holomorphic functions on isoradial grids

In this section we discuss the notion of massive s-holomorphic functions on isoradial grids ; see also a recent paper [138] where this notion is discussed in more detail. Similarly to the critical case (see [48, Section 3.2]), given a real-valued Kadanoff–Ceva fermionic observable (i. e., a real-valued spinor on a subset of $\Upsilon^\times(\Lambda^\delta)$ satisfying the propagation equation $(5.2.6)$) one can construct a complex-valued Smirnov fermionic $F^{(m),\delta}$ observable (defined on a subset of $\diamondsuit^\delta$) in such a way that the propagation equation $(5.2.6)$ for $X^{(m),\delta}$ is replaced by the identities between projections of $F^{(m),\delta}$ onto certain directions ; see Definition 3.3.1 below.

The 'abstract' definition $(5.2.16)$ of functions $H_X^{(m),\delta}$ can be then – again, similarly to the critical case – thought of as considering the primitive of a discrete differential form $\frac{1}{2}\,\mathrm{Im}[(F^{(m),\delta}(z))^2 dz]$, which turns out to be closed on both $\Gamma^{\bullet,\delta}$ and $\Gamma^{\circ,\delta}$ up to certain local multiples that disappear in the limit $\delta \to 0$; see Lemma 3.3.3 and Remark 3.3.4 below. In Proposition 3.3.8 (see also 3.3.10) we prove (at least, for small enough δ) that the function $H^{(m),\delta}$ is subharmonic on $\Gamma^{\bullet,\delta}$ provided that $m \leq 0$ and superharmonic on $\Gamma^{\circ,\delta}$ provided that $m \geq 0$, thus generalizing to the massive setup a (rather mysterious) observation made by Smirnov in [160] for the critical Ising model on the square grid.

Further, we briefly discuss the a priori regularity properties of massive s-holomorphic functions ; see Proposition 3.3.11, this statement was obtained in [138]. We also suggest an alternative approach to this regularity theory, which relies upon a general framework developed in [33] and uses an *s-embedding* of the massive Ising model on Λ^δ into the complex plane ; see Section 3.3.3 for more details.

Finally, this reduction to the framework of [33] also directly implies that massive s-holomorphic functions on Λ^δ satisfy the discrete maximum principle (up to a multiplicative constant); see Lemma 3.3.12 below.

Recall that we use the notation $\eta_c = \varsigma \cdot \exp[-\frac{i}{2}\arg(v(c)-u(c))]$ for $c \in \Upsilon^\times(\Lambda^\delta)$, where $\varsigma = e^{i\frac{\pi}{4}}$; see (3.2.1). The following definition is adopted from [138].

Definition 3.3.1. Let $z \in \diamondsuit^\delta$ be a quad of a rhombic lattice Λ^δ with mesh size δ. Given a real-valued spinor $X^{(m),\delta}$ satisfying the three-terms identity (5.2.6) on corners adjacent to z we define a complex value $F^{(m),\delta}(z)$ by requiring that

$$\Pr[F^{(m),\delta}(z); \widehat{\eta}_{c,z}\mathbb{R}] = \delta^{-\frac{1}{2}} \cdot \widehat{\eta}_{c,z} X(c) \quad \text{for all} \quad c \sim z\,, \tag{3.3.1}$$

where

$$\widehat{\eta}_{c,z} \;:=\; \eta_c \cdot \exp\big[\mp \tfrac{i}{2}(\widehat{\theta}_z - \overline{\theta}_z)\big] \;=\; \varsigma \cdot \exp\big[-\tfrac{i}{2}(\arg(v(c)-z) \pm \widehat{\theta}_z)\big]$$

and the $\pm$ sign is chosen so that $\arg(v(c)-u(c)) = \arg(v(c)-z) \pm \overline{\theta}_z$; see Fig. 3.2.2.

Remark 3.3.2. Functions $F^{(m),\delta} : \diamondsuit^\delta \to \mathbb{C}$ satisfying the condition (3.3.1) were called *massive s-holomorphic* in [138] by analogy with more common s-holomorphic functions that appear in the case $m = 0$ (and hence $\widehat{\theta}_z = \overline{\theta}_z$); see [160, 48]. However, note that the values $\eta_c X^{(m),\delta}(c)$ differ from the values $F^{(m),\delta}(c)$ used in [160, 48, 138] and other related papers by the factor $\delta^{-\frac{1}{2}}$. We adopt this convention on *different* scalings of Kadanoff–Ceva (real-valued) and Smirnov (complex-valued) fermionic observables as it better fits the general framework developed in [33].

Lemma 3.3.3. Let $H_X^{(m),\delta}$ and $F^{(m),\delta}$ be constructed from the spinor $X^{(m),\delta}$ via identities (5.2.16) and (3.3.1), respectively. Then (see Fig. 3.2.2 for the notation),

$$\begin{aligned} H_X^{(m),\delta}(v_1) - H_X^{(m),\delta}(v_0) \;&=\; \frac{\cos\widehat{\theta}_z}{\cos\overline{\theta}_z} \cdot \tfrac{1}{2}\operatorname{Im}\left[(F(z))^2 \cdot (v_1 - v_0)\right], \\ H_X^{(m),\delta}(u_1) - H_X^{(m),\delta}(u_0) \;&=\; \frac{\sin\widehat{\theta}_z}{\sin\overline{\theta}_z} \cdot \tfrac{1}{2}\operatorname{Im}\left[(F(z))^2 \cdot (u_1 - u_0)\right]. \end{aligned}$$

Similar identities hold for functions $H[X_1^{(m),\delta}, X_2^{(m),\delta}] = \frac{1}{4}(H_{X_1+X_2}^{(m),\delta} - H_{X_1-X_2}^{(m),\delta})$.

Proof. Both formulas easily follow from a similar computation for $m = 0$ (e. g., see [48, Proposition 3.6]) performed for a 'virtual' rhombus with half-angle $\widehat{\theta}_z$ instead of $\overline{\theta}_z$; see Fig. 3.2.2 and [138, Lemma 2.5]. (The additional factor $\frac{1}{2}$ appears due to a tiny mismatch between the notation used in our paper and that in [160, 48, 138].) □

Remark 3.3.4. Below we often refer to the identities from Lemma 3.3.3 by writing

$$H_X^{(m),\delta} \;=\; \frac{1}{2}\int^{[(m),\delta]} \mathrm{Im}\,\big[\,(F^{(m),\delta}(z))^2 dz\,\big]$$

(or simply $\int^{[\delta]}$ if $m=0$). Though this identity is not true 'as is' even for discrete contour integrals due to the presence of additional factors $\cos\widehat{\theta}_z/\cos\overline{\theta}_z$ and $\sin\widehat{\theta}_z/\sin\overline{\theta}_z$ in one-step increments, these factors (uniformly under the assumption $\mathrm{BAP}(\theta_0)$) disappear as $\delta\to 0$. In other words, if functions $F^{(m),\delta}$ converge to a continuous function f, then the corresponding functions $H^{(m),\delta}$ converge to the function $h:=\frac{1}{2}\int \mathrm{Im}[(f(z))^2 dz]$.

The following lemma and its corollary are adopted from [138, Section A.1]. They imply that limits of massive s-holomorphic functions on refining isoradial grids Λ^δ, if they exist, are massive holomorphic, i. e., satisfy the equation (3.3.2).

Lemma 3.3.5. Let u^-vu^+ be a half-rhombus of an isoradial grid Λ^δ oriented counterclockwise (i. e., either $u^-=u_0$, $v=v_1$, $u^+=u_1$ or $u^-=u_1$, $v=v_0$, $u^+=u_0$ in the notation of Fig. 3.2.2) and $X^{(m),\delta}$ satisfies the identities (5.2.6). Then,

$$\frac{\sin\frac{1}{2}(\widehat{\theta}_z+\overline{\theta}_z)}{2\sin\overline{\theta}_z}\,F^{(m),\delta}(z)\,(u^--u^+) \;+\; F^{(m),\delta}(c^-)(v-u^-) \;+\; F^{(m),\delta}(c^+)(u^+-v)$$
$$=\; \frac{\sin\frac{1}{2}(\widehat{\theta}_z-\overline{\theta}_z)}{\delta\sin\overline{\theta}_z\cos\overline{\theta}_z}\,\overline{F^{(m),\delta}(z)}\cdot\mathrm{Area}(u^-vu^+)\,,$$

where the value $F^{(m),\delta}(z)$ is defined by (3.3.1) and $F^{(m),\delta}(c^\pm):=\eta_{c^\pm}\cdot\delta^{-\frac{1}{2}}X^{(m),\delta}(c^\pm)$. A similar identity (with the prefactor $\cos\frac{1}{2}(\widehat{\theta}_z+\overline{\theta}_z)/2\cos\overline{\theta}_z$ in the first term) holds for half-rhombi of the form v^-uv^+.

Proof. Let $v-u^\pm=\delta\cdot e^{i(\varphi_v\mp\overline{\theta}_z)}$, where $\varphi_v:=\arg(v-z)$. It follows from (3.3.1) that

$$\begin{aligned}F^{(m),\delta}(c^\pm) \;&=\varsigma e^{-\frac{i}{2}(\varphi_v\mp\overline{\theta}_z)}\cdot\tfrac{1}{2}\big[F^{(m),\delta}(z)\cdot\overline{\varsigma}e^{\frac{i}{2}(\varphi_v\mp\widehat{\theta}_z)}+\overline{F^{(m),\delta}(z)}\cdot\varsigma e^{-\frac{i}{2}(\varphi_v\mp\widehat{\theta}_z)}\big]\\ &=\tfrac{1}{2}\big[\,F^{(m),\delta}(z)\cdot e^{\pm\frac{i}{2}(\overline{\theta}_z-\widehat{\theta}_z)}+\overline{F^{(m),\delta}(z)}\cdot ie^{-i\varphi_v\pm\frac{i}{2}(\widehat{\theta}_z+\overline{\theta}_z)}\,\big],\end{aligned}$$

recall that $\varsigma=e^{i\frac{\pi}{4}}$. The desired identity follows by a straightforward computation as

$$u^+-u^-=2\delta\cdot ie^{i\varphi_v}\sin\overline{\theta}_z\quad\text{and}\quad\mathrm{Area}(u^-vu^+)=\delta^2\sin\overline{\theta}_z\cos\overline{\theta}_z.\qquad\square$$

Corollary 3.3.6. Let $F^{(m),\delta}$ be massive s-holomorphic functions on isoradial grids Λ^δ satisfying the uniform bounded angles condition $\mathrm{BAP}(\theta_0)$. Assume that $F^{(m),\delta}$ converge (on a certain open set $U\subset\mathbb{C}$) to a function $f^{(m)}:U\to\mathbb{C}$ as $\delta\to 0$. Then, $f^{(m)}$ is differentiable and satisfies the massive holomorphicity equation

$$\overline{\partial}f^{(m)}+im\overline{f^{(m)}}=0\,.\qquad(3.3.2)$$

Proof. It follows from the asymptotics (3.2.4) that

$$\frac{\sin\frac{1}{2}(\widehat{\theta}_z+\overline{\theta}_z)}{2\sin\overline{\theta}_z}\to\frac{1}{2}\,,\qquad \frac{\sin\frac{1}{2}(\widehat{\theta}_z-\overline{\theta}_z)}{\delta\sin\overline{\theta}_z\cos\overline{\theta}_z}\to m\ \text{ as }\ \delta\to 0\,,$$

uniformly with respect to z (provided that the condition $\mathrm{BAP}(\theta_0)$ holds). Therefore, summing the identity of Lemma 3.3.5 over any subset $V\subset U$ with smooth boundary, and passing to the limit, leads to the identity

$$\frac{1}{2}\oint_{\partial V} f^{(m)}(z)dz \;=\; m\iint_V \overline{f^{(m)}(z)}dA(z),$$

which is nothing but the weak form of the equation $i\overline{\partial}f^{(m)}=m\overline{f^{(m)}}$. A massive version of Morera's theorem (or Cauchy integral formula) then implies that any weak solution is differentiable. □

Remark 3.3.7. It is easy to see that, if $f^{(m)}$ satisfies the massive holomorphicity equation (3.3.2), then the primitive $h^{(m)}:=\frac{1}{2}\int \mathrm{Im}[(f^{(m)}(z))^2dz]$ is well defined and $\Delta h^{(m)}=-4m|f^{(m)}|^2$. In particular, the function $h^{(m)}$ is subharmonic if $m\le 0$.

In the next proposition we show that the subharmonicity property mentioned in Remark 3.3.7 also holds for *discrete* primitives of massive s-holomorphic functions on isoradial grids; a property that we need in the proof of Proposition 3.4.7. Note that the paper [138] also contains estimates of the discrete Laplacian

$$[\Delta^{\bullet,\delta}H^{(m),\delta}](v)\;:=\;(\mu^\delta(v))^{-1}\sum_{s=1}^{n}\tan\overline{\theta}_s\cdot(H^{(m),\delta}(v_s)-H^{(m),\delta}(v)),\quad(3.3.3)$$

where $v_1,\dots,v_n\in\Gamma^{\bullet,\delta}$ are the neighbors of $v\in\Gamma^{\bullet,\delta}$ and $\mu^\delta(v)=\frac{1}{2}\delta^2\sum_{s=1}^n\sin 2\theta_s$ is an appropriately chosen normalizing factor, which plays no role in the following inequality.

Proposition 3.3.8. Let $m\le 0$ and $\delta\le\delta_0(\theta_0)$ be small enough. Then, for each isoradial grid Λ^δ satisfying the condition $\mathrm{BAP}(\theta_0)$ and for each spinor $X^{(m),\delta}$ satisfying the propagation equation (5.2.6) near v, we have

$$[\Delta^{\bullet,\delta}H^{(m),\delta}](v)\;\ge\;0,\quad v\in\Gamma^{\bullet,\delta}\,,$$

where the function $H^{(m),\delta}$ is constructed from $X^{(m),\delta}$ via the identity (5.2.16). In other words, $H^{(m),\delta}$ is discrete subharmonic on $\Gamma^{\bullet,\delta}$ if $m\le 0$.

Remark 3.3.9. Similarly, the function $H^{(m),\delta}$ is superharmonic on $\Gamma^{\circ,\delta}$ if $m\ge 0$. If $m=0$, then *both* these properties hold (see [160, Lemma 3.8] and [48, Proposition 3.6]), which considerably simplifies the analysis at criticality.

Proof. We adopt the notation used in the proof of [48, Propostion 3.6]. Let $x_s \in \mathbb{R}$, $s = 1, \dots, n$, be the values of the spinor $X^{(m),\delta}$ at corners surrounding v. Then,

$$[\Delta^{\bullet,\delta} H^{(m),\delta}](v) \;=\; (\mu^\delta(v))^{-1} \sum_{s=1}^{n} \tan\overline{\theta}_s \cot^2 \widehat{\theta}_s \cdot [x_s^2 + x_{s+1}^2 \mp 2(\cos\widehat{\theta}_s)^{-1} x_s x_{s+1}],$$

where the sign $\mp$ stands for $-$ if $s = 1, \dots, n-1$ and for $+$ if $s = n$ (this convention corresponds to the fact that the double cover $\Upsilon^\times(\Lambda^\delta)$, on which the spinor $X^{(m),\delta}$ is defined, branches around v). We now expand this quadratic form in the parameter $q \to 0$. Since $\tan\widehat{\theta}_s = (1+4q)\tan\overline{\theta}_s + O(q^2)$ for all $s = 1, \dots, n$, this leads to the expression

$$(1-8q) Q^{(n)}_{\overline{\theta}_1,\dots,\overline{\theta}_n}(x_1, \dots, x_n) - 8q R^{(n)}_{\overline{\theta}_1,\dots,\overline{\theta}_n}(x_1, \dots, x_n) + O(q^2),$$

where the leading term

$$Q^{(n)}_{\overline{\theta}_1,\dots,\overline{\theta}_n}(x_1, \dots, x_n) \;=\; \sum_{s=1}^{n} \frac{\cos\overline{\theta}_s \cdot (x_s^2 + x_{s+1}^2) \mp 2 x_s x_{s+1}}{\sin\overline{\theta}_s} \;\geq\; 0$$

corresponds to the critical case $m = 0$ and

$$R^{(n)}_{\overline{\theta}_1,\dots,\overline{\theta}_n}(x_1, \dots, x_n) \;=\; \sum_{s=1}^{n-1} x_s x_{s+1} \sin\overline{\theta}_s - x_1 x_n \sin\overline{\theta}_n.$$

From the proof of [48, Proposition 3.6] it is easy to see that the (two-dimensional) kernel of the form $Q^{(n)}_{\overline{\theta}_1,\dots,\overline{\theta}_n}$ consists of vectors $x_s = \mathrm{cst} \cdot \cos\chi_s$, where $\chi_{s+1} = \chi_s - \overline{\theta}_s$ for all $s = 1, \dots, n-1$. A straightforward computation shows that

$$\begin{aligned} R^{(n)}_{\overline{\theta}_1,\dots,\overline{\theta}_n}(\cos\chi_1, \dots, \cos\chi_n) \;&=\; R^{(n-1)}_{\overline{\theta}_1,\dots,\overline{\theta}_{n-2},\overline{\theta}_{n-1}+\overline{\theta}_n}(\cos\chi_1, \dots, \cos\chi_{n-1}) \\ &+\; R^{(3)}_{\pi-\overline{\theta}_{n-1}-\overline{\theta}_n,\overline{\theta}_{n-1},\overline{\theta}_n}(\cos\chi_1, \cos\chi_{n-1}, \cos\chi_n) \end{aligned}$$

and that $R^{(3)}_{\overline{\theta}_1,\overline{\theta}_2,\overline{\theta}_3}(\cos\chi_1, \cos\chi_2, \cos\chi_3) = \sin\overline{\theta}_1 \sin\overline{\theta}_2 \sin\overline{\theta}_3$ if $\overline{\theta}_1 + \overline{\theta}_2 + \overline{\theta}_3 = \pi$.

Therefore, the form $R^{(n)}_{\overline{\theta}_1;\dots;\overline{\theta}_n}$ is strictly positive definite on the kernel of $Q^{(n)}_{\overline{\theta}_1;\dots;\overline{\theta}_n}$, which proves the required positivity property for small enough δ. □

Remark 3.3.10. It is worth noting that the so-called *'boundary modification trick'* (used in [48, Section 3.6] to control the boundary values of the function $H^{(m),\delta}_X$) admits a straightforward generalization to the massive setup. By definition, on the wired boundary of a discrete domain the function $H^{(m),\delta}_X$ satisfies Dirichlet boundary conditions $H^{(m),\delta}|_{\partial\Omega^{\circ,\delta}} = 0$ on 'white' boundary vertices. Following [48], in order to fit these boundary conditions and the

subharmonicity of $H_X^{(\delta),m}$ on 'black' inner vertices, one replaces each boundary half-rhombus by two rhombi with twice smaller angles and formally define $H_X^{(\delta),m}(v) := 0$ on newly constructed 'black' boundary vertices; see [48, Fig. 7]. For $m < 0$, such a modification *increases* the Laplacian (3.3.3) evaluated at near-to-boundary vertices since

$$\tan\overline{\theta}_z \cot^2\widehat{\theta}_z\cdot[2x^2-2(\cos\widehat{\theta}_z)^{-1}x^2] \;=\; -2x^2\tan\overline{\theta}_z\cot\widehat{\theta}_z\tan\tfrac{1}{2}\widehat{\theta}_z \;<\; -2x^2\tan\tfrac{1}{2}\overline{\theta}_z$$

due to $\widehat{\theta}_z < \overline{\theta}_z$ and the monotonicity of the function $\theta \mapsto \cot\theta\tan\frac{1}{2}\theta$ on $(0, \frac{1}{2}\pi)$.

In particular, after the 'boundary modification trick' from [48, Section 3.6] is performed, the function $H^{(m),\delta}$ *remains subharmonic* on 'black' vertices and has Dirichlet boundary conditions; similarly to the critical setup discussed in [48].

Proposition 3.3.11. Let refining isoradial grids Λ^δ satisfy the property $\mathrm{BAP}(\theta_0)$ and $F^{(m),\delta}$ be massive s-holomorphic functions on $\diamondsuit^\delta \cap U$. Assume that the functions $H^{(m),\delta} = \frac{1}{2}\int^{[(m),\delta]} \mathrm{Im}[(F^{(m),\delta}(z))^2 dz]$ remain uniformly bounded on compact subsets of U as $\delta \to 0$. Then $F^{(m),\delta}$ are also uniformly bounded and, moreover, (Hölder-)equicontinuous on compact subsets of U as $\delta \to 0$.

Proof. Without loss of generality assume that $m \le 0$, the other case follows by exchanging the roles of $\Gamma^{\bullet,\delta}$ and $\Gamma^{\circ,\delta}$. There are two different proofs of the required regularity estimates. For the first one – which actually gives the uniform *Lipschitzness* of functions $F^{(m),\delta}$ – we refer the reader to [138, Section 4.2] and notably to [138, Propositon 4.6 and Proposition A.7]. In this approach, one first estimates the L^2 norms of functions $F^{(m),\delta}$ on compacts via the maximum (or oscillations) of $H^{(\delta),m}$. Then, the pointwise estimate and the Lipschitzness of $F^{(m),\delta}$ can be obtained by applying an appropriate discrete massive Cauchy formula and using asymptotics of the massive s-holomorphic Cauchy kernel $\mathcal{G}_{(a)}$ discussed in Section 3.5 : see definition (3.5.15), Proposition 3.5.8 and asymptotics (3.5.30). Note also that one can give a similar proof by first estimating the L^4 norm of $F^{(m),\delta}$ (i. e., the L^2 norm of the gradient of $H^{(\delta),m}$) via a discrete version of the Caccioppoli inequality applied to bounded subharmonic (on $\Gamma^{\bullet,\delta}\cap U$) functions $H^{(m),\delta}$.

The second proof relies upon an s-embeddings framework developed in [33] and related to the context of this paper in Section 3.3.3 below. In this approach, one *re-embeds* the isoradial grid Λ^δ carrying the massive Ising model so as to obtain the Ising model on an appropriate s-embedding $\mathcal{S}^\delta$ While the (real-valued) Kadanoff–Ceva fermionic observables $X^{(m),\delta}$ and the functions $H^{(m),\delta}$ do not depend on a particular way in which the graph is embedded into $\mathbb{C}$, the complex values (Smirnov's observables) $F^{(\delta),m}(z)$ *change* to new values $F_{\mathcal{S}^\delta}(z)$ under this procedure; the relation between the two is given by

$$F^{(m),\delta}(z) \;=\; \mathcal{D}_+^\delta(z)\cdot F_{\mathcal{S}^\delta}(z) + \mathcal{D}_-^\delta(z)\cdot\overline{F_{\mathcal{S}^\delta}(z)}\,, \quad z\in\diamondsuit^\delta\,; \tag{3.3.4}$$

see Proposition 3.3.19 for the definition of coefficients $\mathcal{D}^\delta_\pm(z)$.

The Hölder regularity of massive s-holomorphic functions $F^{(m),\delta}$ on (subsets of) Λ^δ now follows from the regularity of s-holomorphic functions $F_{\mathcal{S}^\delta}$ on $\mathcal{S}^\delta$ (see [33, Section 2.6]) and from the fact that the mappings $z \mapsto \mathcal{S}^\delta(z)$ and $z \mapsto \mathcal{D}^\delta_\pm(z)$ are uniformly Lipschitz on compact subsets of Λ^δ due to Theorem 3.3.2. □

Lemma 3.3.12. Let Λ^δ satisfy the property BAP(θ_0), $F^{(m),\delta}$ be a massive s-holomorphic function defined inside a nearest-neighbor contour $C^\delta \subset \diamondsuit^\delta$. Then, provided that δ is small enough (depending on $\mathrm{diam}(C^\delta)$ and m only) we have

$$|F^{(m),\delta}(\cdot)| \;\le\; \mathrm{cst}(\theta_0, m, \mathrm{diam}(C^\delta)) \cdot \max_{z\in C^\delta} |F^{(m),\delta}(z)| \tag{3.3.5}$$

at all points lying inside C^δ, where the constant does not depend on δ and/or Λ^δ.

Proof. Without loss of generality, assume that 0 lies inside the contour C^δ and consider an s-embedding $\mathcal{S}^\delta$ of the massive Ising model on Λ^δ (see Section 3.3.3) below. Recall that the values $F^{(m),\delta}(z)$ and $F_{\mathcal{S}^\delta}(\mathcal{S}^\delta(z))$ are related to each other by the formula (3.3.4). The s-holomorphic (on $\mathcal{S}^\delta$) function $F_{\mathcal{S}^\delta}$ satisfies the maximum principle; see [33, Remark 2.9]. Therefore, a similar statement for $F^{(m),\delta}$ follows from the (uniform on bounded subsets) estimates

$$|\mathcal{D}^\delta_-(z)| \,/\, |\mathcal{D}^\delta_+(z)| \le \mathrm{cst} < 1 \quad \text{and} \quad |\mathcal{D}^\delta_+(z)| \le \mathrm{cst} < +\infty.$$

In their turn, these estimates follow from the identities $\mathcal{D}^\delta_\pm = \frac{1}{2}(\mathcal{F}^\delta_1 \mp i\mathcal{F}^\delta_i)$ and asymptotics of the functions $\mathcal{F}^\delta_1$, $\mathcal{F}^\delta_i$ given in Theorem 3.3.2. □

Remark 3.3.13. It is worth noting that the massive holomorphicity equation (3.3.2) implies that $\Delta f = 4m^2 f$ and thus a usual maximum principle for $|f|$. The same holds for massive s-holomorphic functions $F^{(m),\delta}$ defined on the square grid $\delta\mathbb{Z}^2$. Thus, it seems plausible that the constant prefactor in (3.3.5) is unnecessary at least as $\delta \to 0$. However, we do not know a proof of such a statement for irregular Λ^δ.

3.3.2 . Full-plane branching discrete kernels and their asymptotics

In our paper we very often use functions $H[X_1, X_2]$ constructed from two spinors X_1, X_2 satisfying the propagation equation (5.2.6), which are (locally) defined on slightly *different* double covers $\Upsilon^\times_{[v]}(G)$ and $\Upsilon^\times_{[u]}(G)$, where $v \in G^\bullet$ and $u \in G^\circ$ are neighboring vertices. Let the corner $c \in \Upsilon(G)$ be adjacent to both u and v. These two double covers (non-branching over u and non-branching over v) can be naturally identified with each other everywhere except the two lifts of c. Let $z^\pm \in \diamondsuit(G)$ be two quads adjacent to the edge (uv) of $\Lambda(G)$ so that u is the next vertex to v when going around z^+ counterclockwise; see Fig. 3.3.1. In what follows we assume that

> the lifts of $c = (uv)$ onto $\Upsilon^\times_{[v]}$ and $\Upsilon^\times_{[u]}$ are identified in such a way that the structure of these double covers around the quad z^+ is the same. (3.3.6)

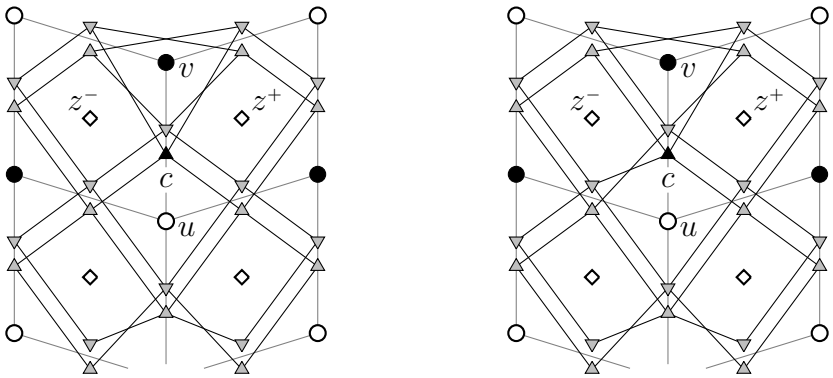

FIGURE 3.3.1 – Local structure of the double covers $\Upsilon^{\times}_{[u]}$, $u = u(c)$ (left) and $\Upsilon^{\times}_{[v]}$, $v = v(c)$ (right). These double covers can be identified with each other except at lifts of c. To choose such a lift (shown as a black triangular node) on both double covers *simultaneously* we use the convention (3.3.6) that their structure around the quad z^+ lying to the right of (uv) is the same.

Lemma 3.3.14. In the setup described above, let us define increments of the function $H[X_1, X_2] : \Lambda^\delta \to \mathbb{R}$ via the formula (3.2.8). Then, $H[X_1, X_2]$ has an additive monodromy $2X_1(c)X_2(c)$ when going around c counterclockwise. In particular, if $X_{1,2} = X^{(m),\delta}_{1,2}$ are defined on an isoradial grid Λ^δ and the massive s-holomorphic functions $F^{(m),\delta}_{1,2}$ are constructed from $X^{(m),\delta}_{1,2}$ according to Definition 3.3.1, then

$$2X_1^{(m),\delta}(c)X_2^{(m),\delta}(c) \;=\; \frac{1}{2}\oint^{[(m),\delta]} \mathrm{Im}\,[F_1^{(m),\delta}(z)F_2^{(m),\delta}(z)dz], \qquad (3.3.7)$$

where the discrete integral along a closed contour surrounding $c = (uv)$ in the right-hand side is understood in the sense of Lemma 3.3.3 and Remark 3.3.4.

Proof. Under the convention (3.3.6), the increments of the function $H[X_1, X_2]$ sum up to zero when going around all quads $z \in \diamondsuit(G)$ except $z = z^-$. The sum around z^- (when going counterclockwise) is $2X_1(c)X_2(c)$ since it would vanish if we used the opposite convention on the identification of $\Upsilon^{\times}_{[v]}(X_1)$ and $\Upsilon^{\times}_{[u]}(G)$ in (3.3.6). □

Remark 3.3.15. Note that a similar statement holds if, say, the spinor X_1 is (locally) defined on the double cover $\Upsilon^{\times}(G)$ while X_2 lives on $\Upsilon^{\times}_{[v(a),u(a)]}(G)$, where $a \in \Upsilon^{\times}(G)$. If $X_2 = \mathrm{G}_{(a)}$ is the massive Cauchy kernel on Λ^δ, this gives a Cauchy-type formula for massive s-holomorphic functions; see Fig. 3.5.1, definition (3.5.15) of $\mathrm{G}_{(a)}$, asymptotics (3.5.30), and [138, Section A.2] for more details.

In our paper we typically apply the formula (3.3.7) in a situation when $F_2^{(m),\delta}$ is a concrete massive s-holomorphic function, namely an analogue of the 'discrete $z^{-\frac{1}{2}}$ kernel on $\mathbb{Z}^{2}$' that was used in [38] (and of its massive analogue constructed in [137] for $m \leq 0$ and $w \in \Gamma^{\bullet,\delta}$). Similarly to the discrete Cauchy formula mentioned above, this formula provides a tool to reconstruct the value of X_1 (or F_1) right near the branching point v from its values on an arbitrary contour surrounding v.

We construct and analyze the aforementioned branching kernels in Section 3.5 ; the main result of this analysis is given by the following theorem. We assume that $m \leq 0$ but formulate the result for *both* $w = v \in \Gamma^{\bullet,\delta}$ and $w = u \in \Gamma^{\circ,\delta}$; a similar result for $m \geq 0$ follows by the duality.

Theorem 3.3.1. Let $m \leq 0$ and let an isoradial grid Λ^δ satisfy the bounded angles property $\mathrm{BAP}(\theta_0)$. For each $w \in \Lambda^\delta$ there exists a real-valued spinor $\mathrm{G}_{[w]}^{(m),\delta}$ defined on the double cover $\Upsilon_{[w]}^{\times}(\Lambda^\delta)$ and satisfying the propagation equation (5.2.6), such that

$$\mathrm{G}_{[w]}^{(m),\delta}(c) \;=\; 1 \quad \text{for all corners} \quad c \sim w \tag{3.3.8}$$

and that the massive s-holomorphic spinor $\mathcal{G}_{[w]}^{(m),\delta}$ constructed from $\mathrm{G}_{[w]}^{(m),\delta}$ according to Definition 3.3.1 has the following asymptotics as $\delta \to 0$:

$$\mathcal{G}_{[v]}^{(m),\delta}(z) \;=\; e^{-i\frac{\pi}{4}} \cdot \left(\frac{2}{\pi}\right)^{\frac{1}{2}} \frac{e^{2m|z-v|}}{\sqrt{z-v}} + \delta \cdot R_{\bullet}^{(m)}(z,v) + O(\delta^2) \quad \text{if} \quad w = v \in \Gamma^{\bullet,\delta},$$

$$\mathcal{G}_{[u]}^{(m),\delta}(z) \;=\; e^{i\frac{\pi}{4}} \cdot \left(\frac{2}{\pi}\right)^{\frac{1}{2}} \frac{e^{-2m|z-u|}}{\sqrt{z-u}} + \delta \cdot R_{\circ}^{(m)}(z,u) + O(\delta^2) \quad \text{if} \quad w = u \in \Gamma^{\circ,\delta},$$

where the sub-leading terms $R_{\bullet}^{(m)}$ and $R_{\circ}^{(m)}$ are uniformly bounded and uniformly Lipschitz in the second (i. e., v or u) argument provided that $|z-w|$ and $|z-w|^{-1}$ are uniformly bounded, and the error terms are uniform under the same assumptions.

Proof. See Section 3.5 : the spinors $\mathrm{G}_{[w]}$ are defined in (3.5.13–3.5.14), the identity (3.3.8) is checked in Proposition 3.5.8, and the asymptotics of $\mathrm{G}_{[w]}$ are given by (3.5.28–3.5.29). Note that these asymptotics do *not* contain corrections of order δ ; in other words, the terms $R_{\circ}^{(m)}$, $R_{\bullet}^{(m)}$ appear only along the reconstruction of $\mathcal{G}_{[w]}$ from $\mathrm{G}_{[w]}$ via Definition 3.3.1 and thus can be written explicitly. In particular, the fact that they are bounded and Lipschitz in the second variable trivially follows from (3.5.28–3.5.29). □

Remark 3.3.16. (i) Informally speaking, these kernels can be thought of as properly re-scaled infinite-volume correlators $\langle \chi_c \mu_v \sigma_\infty \rangle$ or $\langle \chi_c \mu_\infty \sigma_u \rangle$, respectively. This interpretation can be made rigorous if $w = v \in \Gamma^{\bullet,\delta}$ (and $m < 0$) by considering a limit of finite-volume correlators ; cf. the proof of Lemma 3.4.1

given below. Note that the exponential decay at infinity characterizes such a kernel uniquely up to a multiplicative normalization. (In fact, it is not hard to deduce from Lemma 3.2.4 and Remark 3.2.5 that already the estimate $O(R^{-1/2-\varepsilon})$ at infinity implies such a uniqueness property.) Moreover, the fact that (3.3.8) simultaneously holds for all $c \sim v$ is nothing but a re-statement of the universality of the magnetization in the sub-critical model. However, a similar interpretation for $w = u \in \Gamma^{\circ,\delta}$ (or $w = v \in \Gamma^{\bullet,\delta}$ and $m > 0$) is less transparent since in this case the kernel *grows* when $|z-u| \to \infty$ and thus does not admit a straightforward characterization.

(ii) In the critical case $m = 0$ the asymptotics simplify to

$$\mathcal{G}^{\delta}_{[w]}(z) \;=\; e^{\mp i\frac{\pi}{4}} \cdot \left(\tfrac{2}{\pi}\right)^{\frac{1}{2}} (z-w)^{-\frac{1}{2}} \;+\; O(\delta^2 \cdot |z-w|^{-\frac{5}{2}}), \tag{3.3.9}$$

where the constant prefactor is $e^{-i\frac{\pi}{4}}$ if $w = v \in \Gamma^{\bullet,\delta}$ and $e^{i\frac{\pi}{4}}$ if $w = u \in \Gamma^{\circ,\delta}$; see Section 3.5.3 for details.

(iii) In Section 3.4.1 we also rely upon the following statement. Let $\delta = 1$, $q = \frac{1}{2}m < 0$, and $w = v \in \Gamma^{\bullet}$. Then, the spinor $\mathrm{G}_{[v]} = \mathrm{G}^{(\delta),m}_{[v]}$ constructed in Theorem 3.3.1 satisfies the uniform bound

$$|\mathrm{G}_{[v]}(c)| \;=\; O(\exp(-\beta(q,\theta_0) \cdot |c-v|)) \;\text{ as }\; |c-v| \to \infty, \tag{3.3.10}$$

where a constant $\beta(q,\theta_0) > 0$ does not depend on Λ. We discuss this estimate (note that it does not directly follow from Theorem 3.3.1) in Section 3.5.4.

3.3.3 . S-embeddings of the massive isoradial Ising model

In this section we discuss the link of the massive Ising model on isoradial graphs considered in our paper with a general framework of *s-embeddings* recently developed in [33]. From a certain perspective, the material presented in this section can be viewed as an illustration of the general construction from [33]. However, note that we also rely upon this link – namely, upon Proposition 3.3.19 – when giving an (alternative to [138]) proof of the a priori regularity of massive s-holomorphic functions on isoradial grids and of the discrete maximum principle for such functions.

Recall that an s-embedding $\mathcal{S} = \mathcal{S}_{\mathcal{X}}$ of a given planar graph carrying a nearest-neighbor Ising model is constructed out of a complex-valued solution $\mathcal{X}$ of the propagation equation (5.2.6) or, equivalently, out of two (linear independent) real-valued solutions $\mathcal{X}_1$ and $\mathcal{X}_i$ of this equation such that $\mathcal{X} = \varsigma \cdot (\mathcal{X}_1 - i\mathcal{X}_i)$; recall that $\varsigma = e^{i\frac{\pi}{4}}$. This construction boils down to the definition (5.2.16) applied to $\mathcal{X}$. Namely, one has

$$\mathrm{Re}\,\mathcal{S}_{\mathcal{X}} = \; 2H[\mathcal{X}_1, \mathcal{X}_i]\,, \quad \mathrm{Im}\,\mathcal{S}_{\mathcal{X}} = \; H_{\mathcal{X}_1} - H_{\mathcal{X}_i}\,, \quad \mathcal{Q}_{\mathcal{X}} \;=\; H_{\mathcal{X}_1} + H_{\mathcal{X}_i}\,,$$

see [33] for more details on the definition of the auxiliary function $\mathcal{Q}_{\mathcal{X}} = H[\mathcal{X}, \overline{\mathcal{X}}]$.

In the context of the massive Ising model on an isoradial grid Λ^δ, the two spinors $\mathcal{X}_1^\delta$, $\mathcal{X}_i^\delta$ that one uses for a definition of an s-embedding $\mathcal{S}^\delta$ also give rise to massive s-holomorphic functions $\mathcal{F}_1^\delta$, $\mathcal{F}_i^\delta$ via Definition 3.3.1. Moreover, due to Lemma 3.3.3 (and using the notation of Remark 3.3.4) we have

$$\begin{aligned} \operatorname{Re}\mathcal{S}^\delta &= \tfrac{1}{2}\int^{[(m),\delta]} \operatorname{Im}\left[\, 2\mathcal{F}_1^\delta(z)\mathcal{F}_i^\delta(z)dz\,\right], \\ \operatorname{Im}\mathcal{S}^\delta &= \tfrac{1}{2}\int^{[(m),\delta]} \operatorname{Im}\left[((\mathcal{F}_1^\delta(z))^2 - (\mathcal{F}_i^\delta(z))^2)dz\right], \\ \mathcal{Q}^\delta &= \tfrac{1}{2}\int^{[(m),\delta]} \operatorname{Im}\left[((\mathcal{F}_1^\delta(z))^2 + (\mathcal{F}_i^\delta(z))^2)dz\right]. \end{aligned} \tag{3.3.11}$$

Remark 3.3.17. It is worth emphasizing that there is an enormous freedom in choosing $\mathcal{F}_1^\delta$ and $\mathcal{F}_i^\delta$ and not only those constructed in the forthcoming Theorem 3.3.2. If these functions converge (as $\delta \to 0$, on compact subsets of $\mathbb{C}$) to certain functions f_1, f_i, then so do $\mathcal{S}^\delta$ and $\mathcal{Q}^\delta$. Moreover, the limit of (3.3.11) is nothing but a conformal (or isothermal) parametrization of a constant curvature surface in the Minkowski space $\mathbb{R}^{2+1}$ by two massive holomorphic (i. e., satisfying the equation (3.3.2)) functions f_1, f_i; see [33, Section 2.7] for a discussion.

Theorem 3.3.2. Given $m \le 0$, on each isoradial grid Λ^δ satisfying the property $\mathrm{BAP}(\theta_0)$ there exist massive s-holomorphic functions $\mathcal{F}_1^\delta$, $\mathcal{F}_i^\delta$ such that the following asymptotics hold uniformly on compact sets as $\delta \to 0$:

$$\mathcal{F}_1^\delta(z) = \exp(-2m\operatorname{Im} z) + O(\delta), \qquad \mathcal{F}_i^\delta(z) = i\exp(2m\operatorname{Im} z) + O(\delta).$$

With a proper choice of additive constants in their definitions, the corresponding s-embeddings $\mathcal{S}^\delta$ and the function $\mathcal{Q}^\delta$ have the following asymptotics as $\delta \to 0$:

$$\begin{aligned} \mathcal{S}^\delta(z) &= \operatorname{Re} z + \tfrac{i}{4m}\sinh(4m\operatorname{Im} z) + O(\delta), \\ \mathcal{Q}^\delta(z) &= \tfrac{1}{4m}(1 - \cosh(4m\operatorname{Im} z)) + O(\delta), \end{aligned} \tag{3.3.12}$$

also uniformly on compact subsets of $\mathbb{C}$.

Proof. See Section 3.5.2 for the construction and Sections 3.5.4, 3.5.5 for the asymptotic analysis of $\mathcal{F}_1^\delta$ and $\mathcal{F}_i^\delta$. The asymptotics of $\mathcal{S}^\delta$ and $\mathcal{Q}^\delta$ easily follow from (3.3.11). □

In order to apply the results of [33, Section 2] we also need to check that $\mathcal{S}^\delta$ are *proper* s-embeddings, i. e., that no edge intersections arise when we re-embed the isoradial grids Λ^δ into the complex plane using $\mathcal{S}^\delta$. For the purposes of this paper it is enough to consider this re-embedding procedure on compact subsets only. Recall that we denote by Λ_R^δ the discretization of the box $[-R,R]\times[-R,R]$ on Λ^δ.

Proposition 3.3.18. For each $R > 0$ there exist $\delta_0 = \delta_0(R,\theta_0) > 0$ such that the following holds for all $\delta \le \delta_0$ and all isoradial grids satisfying the property $\mathrm{BAP}(\theta_0)$:

$\mathcal{S}^\delta$ is a proper embedding of the box Λ^δ_R satisfying the condition $\textsc{Unif}(\delta)$, i. e., all the lengths $|\mathcal{S}^\delta(v) - \mathcal{S}^\delta(u)|$, $u \sim v$, of edges in $\mathcal{S}^\delta(\Lambda^\delta_R)$ are uniformly comparable to δ and all the angles of quads in $\mathcal{S}^\delta(\Lambda^\delta_R)$ are uniformly bounded away from 0.

Proof. Let $u \sim v \in \Lambda^\delta_R$ and $c \in \Upsilon(\Lambda^\delta)$ be adjacent to both u and v. It follows from Definition 3.3.1 and a trivial estimate $\widehat{\eta}_{c,z} = \eta_c + O(\delta)$ that the edge length

$$\begin{aligned} |\mathcal{S}^\delta(v) - \mathcal{S}^\delta(u)| &= |\mathcal{X}^\delta(c)|^2 = (|\mathcal{X}^\delta_1(c)|^2 + |\mathcal{X}^\delta_i(c)|^2) \\ &= \delta \cdot \left[\left(\Pr[\mathcal{F}^\delta_1(z); \eta_c\mathbb{R}]\right)^2 + \left(\Pr[\mathcal{F}^\delta_i(z); \eta_c\mathbb{R}]\right)^2 + O(\delta) \right] \end{aligned}$$

is uniformly comparable to δ provided that $\delta \le \delta_0$ due to asymptotics of functions $\mathcal{F}^\delta_1$ and $\mathcal{F}^\delta_i$ given in Theorem 3.3.2. Similarly, if c and c' correspond to two adjacent edges of a quad z in $\mathcal{S}^\delta$, then it is easy to see that the quantity

$$\begin{aligned} \delta^{-1} \operatorname{Im}[\, \mathcal{X}^\delta(c)\overline{\mathcal{X}^\delta(c')}\,] &= \delta^{-1} \cdot [\mathcal{X}^\delta_1(c)\mathcal{X}^\delta_i(c') - \mathcal{X}^\delta_i(c)\mathcal{X}^\delta_1(c')] \\ &= |\mathcal{F}^\delta_1(z)||\mathcal{F}^\delta_i(z)| \cdot \operatorname{Im}[\, \eta_{c'}\overline{\eta}_c\,] + O(\delta) \end{aligned}$$

is uniformly bounded away from 0 and thus all the angles of quads in $\mathcal{S}^\delta(\Lambda^\delta_R)$ are uniformly bounded from below as required.

Thus, it remains to check that $\mathcal{S}^\delta$ is a proper embedding of Λ^δ_R. The computation given above also ensures that the increments $\mathcal{S}^\delta(v) - \mathcal{S}^\delta(u)$ around a given vertex of $\mathcal{S}^\delta$ (or around a given quad) are cyclically ordered in the same way as the increments $\eta_c^{-2} = -i \cdot (v - u)$ on the original isoradial grid Λ^δ. In other words, all quads in $\mathcal{S}^\delta$ are oriented in the same way as in Λ^δ and quads surrounding a given vertex do not overlap with each other. Now note that this local property implies the discrete argument principle : the number of times that $\mathcal{S}^\delta$ covers a point in $\mathbb{C}$ is equal the winding number of the image in $\mathcal{S}^\delta$ of a big contour surrounding this point in Λ^δ. This winding number is equal to 1 due to asymptotics (3.3.12) provided that δ is small enough, which completes the proof. □

Given an s-embedding $\mathcal{S}^\delta : \Lambda^\delta \to \mathbb{C}$ and a spinor X^δ (locally) defined on $\Upsilon^\times(\Lambda^\delta)$ one can construct an *s-holomorphic on* $\mathcal{S}^\delta$ function $F_{\mathcal{S}^\delta}$ by requiring that

$$X^\delta(c) = \operatorname{Re}\left[\, \overline{\varsigma}\mathcal{X}^\delta(c) \cdot F_{\mathcal{S}^\delta}(z)\,\right] \tag{3.3.13}$$

(see [33, Proposition 2.5]). The next proposition provides an explicit formula linking the function $F_{\mathcal{S}^\delta}$ and the massive s-holomorphic function $F^{(m),\delta}$ constructed from the same spinor X^δ via Definition 3.3.1.

Proposition 3.3.19. Let a spinor X^δ locally satisfy the propagation equation (5.2.6) on $\Upsilon^\times(\Lambda^\delta)$, the massive s-holomorphic (on Λ^δ) function $F^{(m),\delta}$ be

defined according to (3.3.2), and the function $F_{\mathcal{S}^\delta}$ be defined by (3.3.13). The following identity holds :

$$F^{(m),\delta}(z) \;= \mathcal{D}^\delta_+(z)\cdot F_{\mathcal{S}^\delta}(z) + \mathcal{D}^\delta_-(z)\cdot \overline{F_{\mathcal{S}^\delta}(z)}\,, \tag{3.3.14}$$

where the coefficients are given by $\mathcal{D}^\delta_\pm(z) = \frac{1}{2}(\mathcal{F}^\delta_1(z) \mp i\mathcal{F}^\delta_i(z))$.

Proof. For shortness, denote $\nu_c := \widehat{\eta}_{z,c}$. The formulas (3.3.2) and (3.3.13) imply that

$$\delta^{\frac{1}{2}}\cdot\big[\,\overline{\nu}_c F^{(m),\delta}(z) + \nu_c\overline{F^{(m),\delta}(z)}\,\big] \;=\; 2X(c) \;=\; \overline{\varsigma}\mathcal{X}^\delta(c)F_{\mathcal{S}^\delta}(z) + \varsigma\overline{\mathcal{X}^\delta(c)}\overline{F_{\mathcal{S}^\delta}(z)}.$$

for all $c\sim z$; note that these equations uniquely define the value $F^{(m),\delta}$. Therefore, the formula (3.3.14) is equivalent to the identity

$$\delta^{\frac{1}{2}}\cdot\big[\,\overline{\nu}_c\mathcal{D}^\delta_+(z) + \nu_c\overline{\mathcal{D}^\delta_-(z)}\,\big] = \overline{\varsigma}\mathcal{X}^\delta(c) = \mathcal{X}^\delta_1(c) - i\mathcal{X}^\delta_i(c), \quad c\sim z.$$

It remains to note that $\mathcal{X}^\delta_1(c) = \frac{1}{2}\delta^{\frac{1}{2}}\cdot[\,\overline{\nu}_c\mathcal{F}^\delta_1(z) + \nu_c\overline{\mathcal{F}^\delta_1(z)}\,]$ and similarly for $\mathcal{X}^\delta_i(c)$, again due to Definition 3.3.1. □

3.4 . Proofs of the main results

In this section we prove the main results of our paper. In particular, Theorem 3.1.1, i. e., the convergence of the re-scaled infinite-volume correlations $\delta^{-\frac{1}{4}}\mathbb{E}^{(m)}_{\Lambda^\delta}[\sigma_u\sigma_w]$ to a universal (i. e., independent of Λ^δ) rotationally invariant limit $\mathcal{C}^2_\sigma\cdot\Xi(|u-w|,m)$ is proven in Theorem 3.4.2 for $m=0$ and in Corollary 3.4.17 for $m\neq 0$. Along the way, we also prove convergence of spin-spin correlations in discrete approximations $\Omega^\delta\subset\Gamma^\delta$ of finite C^1-smooth domains $\Omega\subset\mathbb{C}$: see Corollary 3.4.12 and Theorem 3.4.4 for the critical and massive cases, respectively.

We start our exposition by giving a proof of Baxter's formula (Proposition 3.1.3) for the magnetization in the infinite-volume sub-critical model on isoradial graphs ; note that already this proof contains two important ideas that we also use later : gluing isoradial grids to each other via a procedure discussed in Section 3.2.4 and the reconstruction of values of spinor observables near their (non-)branching points via the explicit kernels from Section 3.3.2. In particular, Lemma 3.4.1 can be viewed as an off-critical single-spin version of the arguments used for the analysis of multi-point spin correlations on the square grid in [38] (at the critical point) and in [137] (in the massive regime). Let us repeat that our modification of these arguments, based upon Lemma 3.3.14, considerably simplifies the analysis as compared to [38, 137]. We analyze the spin correlations in the critical model on isoradial graphs in Sections 3.4.2–3.4.4. The massive model is discussed in Sections 3.4.5, 3.4.6 basing upon a similar strategy.

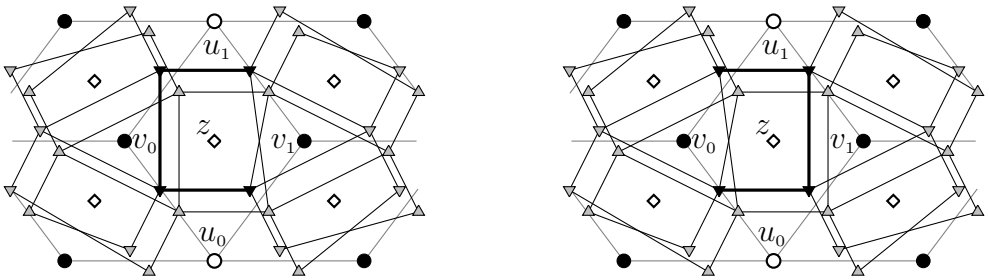

FIGURE 3.4.1 – If $v_0, v_1 \in \Gamma^\bullet$ be two vertices of a quad $z = (v_0u_0v_1u_1)$, the double covers $\Upsilon^\times_{[v_0]}$ (shown on the left) and $\Upsilon^\times_{[v_1]}$ (shown on the right) can be identified with each other except at lifts of corners $c_{pq} = (v_p u_q)$, $p = 0, 1$, $q = 0, 1$, surrounding z. In the proof of Lemma 3.4.1 we choose these lifts so that the incidence relations (3.4.1) hold ; these relations are shown by thick black lines in the figure.

3.4.1 . Baxter's formula for the magnetization in the sub-critical model

Throughout this section, $\delta = 1$ and $q = \frac{1}{2}m < 0$ are fixed.

Lemma 3.4.1. Let $m < 0$ and Λ be an infinite isoradial grid of mesh $\delta = 1$ satisfying the property BAP(θ_0). Then, the magnetization $\mathbb{E}^+_\Lambda[\sigma_u]$ does not depend on $u \in \Gamma^\circ$.

Proof. Let $z = (v_0u_0v_1u_1)$ be a rhombus on Γ ; see Fig. 3.2.2 for the notation. Consider the pointwise limit

$$X_{[v_0]}(c) \;:=\; \lim_{R\to\infty} \mathbb{E}^{\mathrm{w}}_{\Lambda_R}[\chi_c \mu_{v_0} \sigma_{u_{\mathrm{out}}}], \quad c \in \Upsilon^\times_{[v_0]},$$

which can also be thought of as the infinite-volume correlator $\mathbb{E}_\Lambda[\chi_c \mu_{v_0} \sigma_\infty]$. The existence of a limit follows from the fact that for each given c, one can fix a disorder line γ with $\partial\gamma = \{v(c), v_0\}$ and write

$$\mathbb{E}^{\mathrm{w}}_{\Lambda_R}[\chi_c \mu_{v_0} \sigma_{u_{\mathrm{out}}}] \;=\; \mathbb{E}^{\mathrm{w}}_{\Lambda_R}\Big[\sigma_{u(c)}\sigma_{u_{\mathrm{out}}} \textstyle\prod_{u\sim w:(uw)\cap\gamma\neq\varnothing} e^{-2\beta^\circ J^\circ_{(uw)^*}\sigma_u\sigma_w}\Big],$$

which is a finite linear combination of multipoint spin expectations since

$$e^{-2\beta^\circ J^\circ_{(uw)^*}\sigma_u\sigma_w} \;=\; \cosh(-2\beta^\circ J^\circ_{(uw)^*}) + \sigma_u\sigma_w \sinh(-2\beta^\circ J^\circ_{(uw)^*}).$$

Each of these expectations is decreasing as $R \to \infty$ due to the FKG inequality, which guarantees the convergence of $\mathbb{E}^{\mathrm{w}}_{\Lambda_R}[\chi_c \mu_{v_0} \sigma_{u_{\mathrm{out}}}]$.

Note that

$$X_{[v_0]}(c_{00}) \;=\; \lim_{R\to\infty} \mathbb{E}^{\mathrm{w}}_{\Lambda_R}[\sigma_{v_0}\sigma_{u_{\mathrm{out}}}] \;=\; \mathbb{E}^+_\Lambda[\sigma_{u_0}] \quad \text{and} \quad X_{[v_0]}(c_{01}) \;=\; \mathbb{E}^+_\Lambda[\sigma_{u_1}].$$

Let us now consider the function $H := H[X_{[v_0]}, \mathrm{G}_{[v_1]}]$, where $\mathrm{G}_{[v_1]}$ is the explicit infinite-volume kernel discussed in Theorem 3.3.1 and Remark 3.3.16(iii).

Since the two spinors $X_{[v_0]}$ and $\mathrm{G}_{[v_1]}$ are defined on slightly *different* double covers $\Upsilon^{\times}_{[v_0]}$ and $\Upsilon^{\times}_{[v_1]}$, the function H has an additive monodromy Z around the quad $(v_0u_0v_1u_1)$. Similarly to the proof of Lemma 3.3.14, it is easy to see that

$$\begin{aligned}\tfrac{1}{2}Z &= -X_{[v_0]}(c_{00})\mathrm{G}_{[v_1]}(c_{00}) + X_{[v_0]}(c_{10})\mathrm{G}_{[v_1]}(c_{10})\\ &= -X_{[v_0]}(c_{11})\mathrm{G}_{[v_1]}(c_{11}) + X_{[v_0]}(c_{01})\mathrm{G}_{[v_1]}(c_{01}),\end{aligned}$$

where we assume that the double covers $\Upsilon^{\times}_{[v_0]}$ and $\Upsilon^{\times}_{[v_1]}$ are identified with each other away from the quad $(v_0u_0v_1u_1)$ and that (see Fig. 3.4.1)

$$c_{11} \sim c_{01} \sim c_{00} \sim c_{01} \text{ on } \Upsilon^{\times}_{[v_0]} \quad \text{whilst} \quad c_{00} \sim c_{10} \sim c_{11} \sim c_{01} \text{ on } \Upsilon^{\times}_{[v_1]}. \tag{3.4.1}$$

On the other hand, the uniform boundedness of $X_{[v_0]}(c)$ and the exponential decay of $\mathrm{G}_{[v_1]}$ (as $|c - v_1| \to \infty$; see Remark 3.3.16(iii) and Section 3.5.4) imply that $Z = 0$ as we can move the integration contour in (3.3.7) far away from the branching. Thus,

$$X_{[v_0]}(c_{00})\mathrm{G}_{[v_1]}(c_{00}) = X_{[v_0]}(c_{10})\mathrm{G}_{[v_1]}(c_{10}).$$

Using the propagation equation (5.2.6) to write the value $\mathrm{G}_{[v_1]}(c_{00})$ as a linear combination of $\mathrm{G}_{[v_1]}(c_{10})$ and $\mathrm{G}_{[v_1]}(c_{11})$, and the value $X_{[v_0]}(c_{10})$ as a linear combination of $X_{[v_0]}(c_{00})$ and $X_{[v_0]}(c_{01})$, one can rewrite the last identity as

$$X_{[v_0]}(c_{00})\mathrm{G}_{[v_1]}(c_{11}) = X_{[v_0]}(c_{01})\mathrm{G}_{[v_1]}(c_{10}).$$

Recall that $\mathrm{G}_{[v_1]}(c_{11}) = \mathrm{G}_{[v_1]}(c_{10})$ due to the explicit construction of the kernel $\mathrm{G}_{[v_1]}$. This implies the desired identity $\mathbb{E}^+_\Lambda[\sigma_{u_0}] = X_{[v_0]}(c_{00}) = X_{[v_0]}(c_{01}) = \mathbb{E}^+_\Lambda[\sigma_{u_1}]$. □

Proposition 3.4.2. We have $\mathbb{E}_\Lambda[\sigma_u\sigma_w] \to (k^*)^{\frac{1}{2}}$ as $|u - w| \to \infty$ uniformly over isoradial lattices Λ and positions of points $u, w \in \Gamma^\circ$.

Proof. Denote by $D := |u-w|$ the (Euclidean) distance between u and w. The uniform RSW estimates (3.2.10) imply that for each $\varepsilon > 0$ one can find $A = A(\varepsilon) > 1$ such that

$$\mathbb{E}^{\mathrm{w}}_{\Lambda_{AD}(u)}[\sigma_u\sigma_w] - \varepsilon \le \mathbb{E}_\Lambda[\sigma_u\sigma_w] \le \mathbb{E}^{\mathrm{w}}_{\Lambda_{AD}(u)}[\sigma_u\sigma_w]$$

on each isoradial grid containing the box $\Lambda_{AD}(u)$ (and satisfying $\mathrm{BAP}(\theta_0)$).

Let us now replace Λ by the 'star extension' $[\Lambda_{AD}(u)]^\star$ of the box $\Lambda_{AD}(u)$ constructed in Section 3.2.4. For shortness, below we use the notation $\Lambda^\star := [\Lambda_{AD}(u)]^\star$; note that the the same reasoning applied to $\Lambda^\star$ instead of Λ implies that

$$\big|\, \mathbb{E}_\Lambda[\sigma_u\sigma_w] - \mathbb{E}_{\Lambda^\star}[\sigma_u\sigma_w] \,\big| \le \varepsilon. \tag{3.4.2}$$

According to the construction, on the modified lattice $\Lambda^\star$ we can find a 'white' vertex u' such that $|u'-u| \le CAD$ and that the box $\Lambda^\star_{AD}(u')$ is a piece of a rectangular grid; the constant C depends on θ_0 only. Denote by w' a 'white' vertex of $\Lambda^\star$ lying at distance D from u' and such that $w'-u'$ is one of the axial directions of this rectangular grid.

We claim that, for each grid $\Lambda^\star$ satisfying the bounded angles property $\mathrm{BAP}(\theta_0)$,

$$\big|\,\mathbb{E}_{\Lambda^\star}[\sigma_u\sigma_w] - \mathbb{E}_{\Lambda^\star}[\sigma_{u'}\sigma_{w'}]\,\big| \;=\; O(A(\varepsilon)D^2\exp(-\beta D)), \tag{3.4.3}$$

where a universal constant $\beta = \beta(q,\theta_0) > 0$ comes from the uniform exponential decay of the branching kernels $\mathrm{G}_{[v]}$; see (3.3.10) and Section 3.5.4. The proof of (3.4.3) goes along the same lines as the proof of Lemma 3.4.1. Namely, let $z = (v_0u_0v_1u_1)$ be a quad lying at distance D from the second 'white' vertex w under consideration. As in the proof of Lemma 3.4.1, let us consider a pointwise limit

$$X_{[v_0,w]}(c) \;:=\; \lim_{R\to\infty}\mathbb{E}^{\mathrm{w}}_{\Lambda^\star_R}[\chi_c\mu_{v_0}\sigma_w], \quad c\in\Upsilon^\times_{[v_0,w]},$$

and a function $H := H[X_{[v_0,w]},\mathrm{G}_{[v_1]}]$ defined in the vicinity of z of radius D. (Note that now the spinor $X_{[v_0,w]}$ has the second branching at w while $\mathrm{G}_{[v_1]}$ does not branch there, this is why H is not defined on the whole grid $\Lambda^\star$.) Let Z be the additive monodromy of the function H around z. The uniform boundedness of the fermionic observable $X_{[v_0,w]}$ and the uniform exponential decay of the kernel $\mathrm{G}_{[v_1]}$ imply that $Z = O(D\exp(-\beta D))$ since we can compute this monodromy along a contour running at distance D from z. Then, computing the monodromy Z similarly to the proof of Lemma 3.4.1 we obtain the estimate

$$\big|\,\mathbb{E}_{\Lambda^\star}[\sigma_{u_0}\sigma_w] - \mathbb{E}_{\Lambda^\star}[\sigma_{u_1}\sigma_w]\,\big| \;=\; O(D\exp(-\beta D)). \tag{3.4.4}$$

Moving a pair of points u,w step by step to u',w' so that they remain at distance (at least) D from each other we obtain the desired estimate (3.4.3).

Finally, let Λ^{rect} be a rectangular grid that extends the rectangular part $\Lambda^\star_{AD}(u')$ of $\Lambda^\star$. Similarly to (3.4.2), one has $\big|\,\mathbb{E}_{\Lambda^\star}[\sigma_{u'}\sigma_{w'}] - \mathbb{E}_{\Lambda^{\mathrm{rect}}}[\sigma_{u'}\sigma_{w'}]\,\big| \le \varepsilon$. Combining (3.4.2), (3.4.3) and this estimate, we see that

$$\big|\,\mathbb{E}_{\Lambda}[\sigma_u\sigma_w] - \mathbb{E}_{\Lambda^{\mathrm{rect}}}[\sigma_{u'}\sigma_{w'}]\,\big| \;\le\; 2\varepsilon + O(A(\varepsilon)D^2\exp(-\beta D)). \tag{3.4.5}$$

We can now rely upon explicit computations of the 'horizontal' spin-spin correlations $\mathbb{E}_{\Lambda^{\mathrm{rect}}}[\sigma_{u'}\sigma_{w'}]$ on rectangular grids; see [123, Section X.4] or [40, Theorem 3.6]. In particular, it is well known (see also Remark 3.4.3 below) that

$$\mathbb{E}_{\Lambda^{\mathrm{rect}}}[\sigma_{u'}\sigma_{w'}] \;\to\; (k^*)^{\frac12} \;\text{ as }\; |u'-w'|\to\infty. \tag{3.4.6}$$

Choosing first ε small enough and then D big enough in (3.4.5) allows us to conclude that $\mathbb{E}_{\Lambda}[\sigma_u\sigma_w] \to (k^*)^{\frac12}$ as $|u-w|\to\infty$, uniformly with respect to isoradial grids Λ satisfying the bounded angles condition $\mathrm{BAP}(\theta_0)$. $\square$

Remark 3.4.3. A careful reader could notice that above we used the – a priori nontrivial – fact that the limit in (3.4.6) does not depend on the (unknown) aspect ratio of the rectangular lattice Λ^{rect}. This can be avoided by making another comparison of correlations on Λ^{rect} and those on the *square lattice* $\mathbb{Z}^2$; recall that one can easily glue Λ^{rect} and $\mathbb{Z}^2$ staying inside the family of isoradial grids (see Fig. 3.2.3). The estimate (3.4.5) and a similar estimate for Λ^{rect} and $\mathbb{Z}^2$ imply that

$$\big|\, \mathbb{E}_{\Lambda}[\sigma_u\sigma_w] - \mathbb{E}_{\mathbb{Z}^2}[\sigma_{u'}\sigma_{w'}] \,\big| \;\le\; 4\varepsilon + O(A(\varepsilon)D^2\exp(-\beta D)).$$

In particular, this gives a self-contained proof of the existence of the universal (among isoradial grids) limit $\lim_{|u-w|\to\infty}\mathbb{E}_{\Lambda}[\sigma_u\sigma_w]$. Moreover, on the square lattice one can work with 'diagonal' spin-spin correlations instead of 'horizontal' ones, which considerably simplifies the computation of the limit ; e. g., see [32, Section 3].

Corollary 3.4.4. For all isoradial grids Λ satisfying the condition $\mathrm{BAP}(\theta_0)$ and for all $u\in\Gamma^\circ$ the magnetization $\mathbb{E}^+_{\Lambda}[\sigma_u]$ is equal to $(k^*)^{\frac14}$

Proof. It follows from Lemma 3.4.1 that, given Λ, the magnetization $\mathbb{E}^+_{\Lambda}[\sigma_u]$ does not depend on the position of $u\in\Gamma^\circ$; let us denote this common value by $M(\Lambda)$.

First, note that Proposition 3.4.2 and the FKG inequality imply that

$$(k^*)^{\frac12} \;=\; \lim_{R\to\infty}\mathbb{E}^{\mathrm{w}}_{\Lambda_R}[\sigma_u\sigma_{u'}] \;\ge\; \lim_{R\to\infty}\mathbb{E}^{+}_{\Lambda_R}[\sigma_u]\cdot\mathbb{E}^{+}_{\Lambda_R}[\sigma_{u'}] \;=\; (M(\Lambda))^2$$

and hence $M(\Lambda)\le(k^*)^{\frac14}$ for all Λ. To prove the inverse inequality note that, for large enough R, the FKG inequality also implies that

$$\mathbb{E}^{\mathrm{w}}_{\Lambda_R}[\sigma_u\sigma_{u'}] \;\le\; \mathbb{E}^{+}_{\Lambda_D(u)}[\sigma_u]\cdot\mathbb{E}^{+}_{\Lambda_{D'}(u')}[\sigma_{u'}] \quad\text{if}\quad \Lambda_D(u)\cap\Lambda_{D'}(u')=\varnothing.$$

Let us first consider the particular case when $\Lambda=\Lambda^{\mathrm{rect}}$ is a rectangular lattice. In this case, for each $\varepsilon>0$ one can choose $D=D'$ big enough so that

$$\mathbb{E}^{+}_{\Lambda_D(u)}[\sigma_u] \;=\; \mathbb{E}^{+}_{\Lambda_D(u')}[\sigma_{u'}] \;\le\; M(\Lambda^{\mathrm{rect}})+\varepsilon;$$

note that we used the translation invariance of Λ^{rect}. By first letting $R\to\infty$ in (3.4.1) and then $\varepsilon\to0$ one concludes that $M(\Lambda^{\mathrm{rect}})=(k^*)^{\frac14}$.

Let us now consider a general case. As above, given $\varepsilon>0$ and a vertex $u\in\Gamma^\circ$ near 0, one can choose $D=D(\varepsilon)$ large enough so that

$$\mathbb{E}^{+}_{\Lambda_D(u)}[\sigma_u] \;\le\; M(\Lambda)+\varepsilon.$$

Let $\Lambda^\star := [\Lambda_D(u)]^\star$ be the star extension of $\Lambda_D(u)$. By construction (see Fig. 3.2.3), $\Lambda^\star$ contains arbitrary large pieces of a certain rectangular grid Λ^{rect}

(whose aspect ratio can depend on $\Lambda^\star$, which in its turn depend on ε). One can now choose $D' = D'(\varepsilon)$ large enough so that

$$\mathbb{E}^+_{\Lambda^\star_{D'}(u')}[\sigma_{u'}] \;\leq\; M(\Lambda^{\mathrm{rect}}) + \varepsilon \;=\; (k^*)^{\frac{1}{4}} + \varepsilon$$

for a certain 'white' vertex u' of $\Lambda^\star$. Moreover, once D' is chosen, the vertex u' can be taken arbitrarily far from u. Passing to the limit $R \to \infty$, then $|u - u'| \to \infty$ and finally $\varepsilon \to 0$ in the inequality

$$\mathbb{E}^{\mathrm{w}}_{\Lambda_R}[\sigma_u \sigma_{u'}] \;\leq\; (M(\Lambda) + \varepsilon)((k^*)^{\frac{1}{4}} + \varepsilon)$$

we see that $M(\Lambda) \geq (k^*)^{\frac{1}{4}}$, which completes the proof. □

3.4.2 . Critical model : convergence of normalized observables $\mathbb{E}^{\mathbf{w}}_{\Omega^\delta}[\chi_c \mu_v \sigma_w]$

In this section we consider the critical Ising model in bounded discrete approximations $\Omega^\delta \subset \Gamma^\delta$ of a bounded simply connected domain $\Omega \subset \mathbb{C}$ with a C^1-smooth boundary. The convergence results discussed below can be viewed as generalizations of similar results obtained in [38] for the square grid $\Lambda^\delta = \delta\mathbb{Z}^2$; under an additional smoothness assumption on $\partial\Omega$. It is worth noting that we use this smoothness assumption only in order to give a simple proof of Proposition 3.4.7 following the paper [137], and that it can be removed by using techniques from [48] or from [39] instead ; see Remark 3.4.13 below. Let us emphasize that the proofs given in this section do *not* simply mimic those from [38] ; on the contrary, we considerably improve the strategy used in [38] even in the case $\Lambda^\delta = \delta\mathbb{Z}^2$ in what concerns the analysis of spinor observables near the branching points. In particular, we do *not* rely upon explicit '$z^{1/2}$-type' kernels (see [38, Lemma 2.17]).

Let $\Omega \subset \mathbb{C}$ be a bounded simply connected domain and Ω^δ be discrete approximation of Ω on isoradial grids Λ^δ with $\delta \to 0$. (As always in our paper we also assume that Λ^δ satisfy the bounded angles property $\mathrm{BAP}(\theta_0)$.) For simplicity, we also assume that the boundary $\partial\Omega$ of Ω is C^1-smooth and that Ω^δ approximate Ω in the Hausdorff sense so that $\mathrm{dist}(\partial\Omega^\delta; \partial\Omega) = O(\delta)$. However, it is worth noting that one can drop these regularity assumption by repeating the arguments developed in [48] in what concerns the near-to-the-boundary analysis of fermionic observables in rough domains Ω under the Carathéodory convergence $\Omega^\delta \to \Omega$; see also Remark 3.4.13 below.

Let v, w be distinct inner points of Ω ; for the sake of shortness we use the same notation for discrete approximations $v = v^\delta \in \Gamma^{\bullet,\delta}$ and $w = w^\delta \in \Gamma^{\circ,\delta}$ of these points. Also, let $u = u^\delta \in \Gamma^{\circ,\delta}$ be one of the neighboring 'white' vertices of v. Following [38], we consider the normalized real-valued fermionic observable

$$X^\delta_{[\Omega^\delta;v,w]}(c) \;:=\; \frac{\mathbb{E}^{\mathrm{w}}_{\Omega^\delta}[\chi_c \mu_v \sigma_w]}{\mathbb{E}^{\mathrm{w}}_{\Omega^\delta}[\sigma_u \sigma_w]}, \quad c \in \Upsilon^\times_{[v,w]}(\Omega^\delta), \tag{3.4.7}$$

and denote by $F^\delta_{[\Omega^\delta;v,w]}$ the complex-valued observables constructed from $X^\delta_{[\Omega^\delta;v,w]}$ according to (3.3.2) ; recall that $F^\delta_{[\Omega^\delta;v,w]}$ is an s-holomorphic spinor in Ω^δ branching

over v and w. Also,

$$X^{\delta}_{[\Omega^{\delta};v,w]}(c_{uv}) \;=\; 1, \tag{3.4.8}$$

where the corner c_{uv} is adjacent to both u and v.

In the forthcoming Theorem 3.4.1 (which can be viewed as a generalization to isoradial grids of a particular case $n = 2$ of [38, Theorem 2.16]; see also Remark 3.4.13) we prove the convergence of these discrete observables as $\delta \to 0$. The limit is a holomorphic spinor $f_{[\Omega;v,w]}$ on the double cover of Ω ramified over v and w that is uniquely defined by the following conditions :

— $f_{[\Omega;v,w]}$ is continuous in $\overline{\Omega} \setminus \{v, w\}$ and satisfies the Riemann-type boundary conditions $\mathrm{Im}[f_{[\Omega;v,w]}(\zeta)(\tau(\zeta))^{1/2}] = 0$ for all $\zeta \in \partial\Omega$, where $\tau(\zeta)$ denotes the tangent vector to $\partial\Omega$ at the point ζ oriented counterclockwise;

— the following asymptotics holds :

$$f_{[\Omega;v,w]}(z) \;=\; e^{-i\frac{\pi}{4}}(z-v)^{-\frac{1}{2}} + O(|z-v|^{\frac{1}{2}}) \;\text{ as }\; z \to v; \tag{3.4.9}$$

and there exists a (a priori unknown) constant $\mathcal{B}_{\Omega}(v, w) \in \mathbb{R}$ such that

$$f_{[\Omega;v,w]}(z) \;=\; e^{i\frac{\pi}{4}}\mathcal{B}_{\Omega}(v,w)\cdot(z-w)^{-\frac{1}{2}} + O(|z-w|^{\frac{1}{2}}) \;\text{ as }\; z \to w. \tag{3.4.10}$$

Remark 3.4.5. (i) Since $f_{[\Omega;v,w]}$ branches over the point w, the coefficient $\mathcal{B}_{\Omega}(v, w)$ is a priori defined only up to the sign. We fix this sign by requiring that $\mathcal{B}_{\Omega}(v, w) \geq 0$.

(ii) The uniqueness of the solution to this boundary value problem easily follows from considering the harmonic function $h := \int \mathrm{Im}[(f_1(z) - f_2(z))^2 dz]$: if f_1 and f_2 were two distinct solutions, then the function h would *not* have a singularity at the point $z = v$, would behave like $b \log|z-w| + O(1)$ with $b \geq 0$ as $z \to w$, and would have negative outer normal derivative along $\partial\Omega$, the sign which contradicts the Green formula; see also [38, Section 2.5].

(iii) If $\varphi : \Omega \to \Omega'$ is a conformal map, then it is easy to see that

$$f_{[\Omega;v,w]}(z) = f_{[\Omega';\varphi(v),\varphi(v)]}(\varphi(z)) \cdot (\varphi'(z))^{\frac{1}{2}}. \tag{3.4.11}$$

The solution in the upper-half plane $\Omega = \mathbb{H}$ can be written explicitly (see [38, Section 2.7]); in particular, this can be used to justify the existence of $f_{[\Omega;v,w]}$. Alternatively, one can get the existence of $f_{[\Omega;v,w]}$ directly from Theorem 3.4.1, not relying upon explicit formulas and/or the conformal covariance property (3.4.11).

Let us denote by H^{δ} the function constructed from the fermionic observable (3.4.7) via (5.2.16), where the additive constant in its definition is chosen so that H^{δ} satisfies the Dirichlet boundary conditions. Fix a small enough $r_0 > 0$ and denote

$$M^{\delta} \;:=\; \max_{\Omega(r_0)} |H^{\delta}|, \;\text{ where }\; \Omega(r_0) := \Omega \setminus (B(v, r_0) \cup B(w, r_0)). \tag{3.4.12}$$

The proof of the following estimate considerably simplifies the strategy used in [38].

Proposition 3.4.6. Assume that the estimate $M^\delta = O(1)$ holds as $\delta \to 0$. Then,

$$F^\delta_{[\Omega^\delta;v,w]} = O(1) \ \text{ as } \ \delta \to 0 \ \text{ uniformly on compact subsets of } \Omega \setminus \{v, w\}. \tag{3.4.13}$$

Proof. The a priori regularity estimates of s-holomorphic functions via the associated functions H_F (see Proposition 3.3.11), in particular, imply that

$$F^\delta_{[\Omega^\delta;v,w]} = O(1) \ \text{ as } \ \delta \to 0 \ \text{ uniformly on compact subsets of } \Omega(r_0).$$

Thus, to prove (3.4.13) we need to control the behavior of F^δ near v and w.

Consider now the explicit full-plane kernel $\mathrm{G}^\delta_{[v]}$ discussed in Section 3.3.2 and a spinor (defined, e. g., in a $3r_0$-vicinity of v)

$$X^{\delta,\dagger}(\cdot) \ := \ X^\delta_{[\Omega^\delta;v,w]}(\cdot) - \mathrm{G}^\delta_{[v]}(\cdot) \tag{3.4.14}$$

and let $F^{\delta,\dagger}$ and $H^{\delta,\dagger}$ be constructed from $X^{\delta,\dagger}$ via (3.3.2) and (5.2.16), respectively. Due to (3.4.8) and (3.3.8), we have $X^{\delta,\dagger}(c_{uv}) = 0$ and hence the function $H^{\delta,\dagger}$ satisfies *both* the maximum and the minimum principle near v (see Remark 3.2.5). Also, we know that $F^{\delta,\dagger} = O(1)$ and hence $H^{\delta,\dagger} = O(1)$ near the circle $\{z : |z - w| = 3r_0\}$, for an appropriate choice of the additive constants in the definition of $H^{\delta,\dagger}$. Therefore,

$$H^{\delta,\dagger} = O(1) \ \text{ as } \ \delta \to 0 \ \text{ uniformly in the } \textit{disc } B(v, 3r_0) := \{z : |z - v| < 2r_0\}.$$

It follows from Proposition 3.3.11 that

$$F^{\delta,\dagger}(z) = O(|z - v|^{-\frac{1}{2}}) \ \text{ and so } \ F^\delta_{[\Omega^\delta,v,w]}(z) = O(|z - v|^{-\frac{1}{2}}) \ \text{ for } z \in B(v, 2r_0)$$

due to the explicit asymptotics of $\mathcal{G}^\delta_{[v]}$ (see Theorem 3.3.1). In particular, F^δ remain uniformly bounded as $\delta \to 0$ on compact subsets of $\Omega \setminus (\{v\} \cup B(w, r_0))$.

A similar though slightly more involved argument can be applied near the second branching point $w \in \Gamma^{\circ,\delta}$; a complication is caused by the fact that now we do not have a prescribed value similar to (3.4.8) near w. However, it is not hard to see that these values remain uniformly bounded as $\delta \to 0$. Indeed, denote by c_w one of the corners adjacent to w and consider the function $H\big[X^\delta_{[\Omega^\delta;v,w]}, \mathrm{G}^\delta_{[v(c_w)]}\big]$. By Lemma 3.3.14, this function has the additive monodromy

$$\begin{aligned} 2X^\delta_{[\Omega^\delta;v,w]}(c_w)\mathrm{G}^\delta_{[v(c_w)]}(c_w) \ &= \ 2X^\delta_{[\Omega^\delta;v,w]}(c_w) \\ &= \ \frac{1}{2}\oint^{[\delta]}_{z:|z-w|=2r_0} \mathrm{Im}\,\big[F^\delta_{[\Omega^\delta;v,w]}(z)\mathcal{G}^\delta_{[v(c_w)]}dz\big]. \end{aligned}$$

Since the (complex-valued) kernels $\mathcal{G}^\delta_{[v(c_w)]}$ remain uniformly bounded at a definite distance from w as $\delta \to 0$ (see Theorem 3.3.1), we obtain the uniform estimate

$$X^\delta_{[\Omega^\delta;v,w]}(c_w) \ = \ O(1) \ \text{ as } \ \delta \to 0\,. \tag{3.4.15}$$

We can now repeat the arguments given above considering the spinor

$$X^{\delta}_{[\Omega^{\delta};v,w]}(\cdot) - X^{\delta}_{[\Omega^{\delta};v,w]}(c_w) \cdot \mathrm{G}^{\delta}_{[w]}(\cdot)$$

near the point w to prove that $F^{\delta}_{[\Omega^{\delta};v,w]}(z) = O(|z-w|^{-\frac{1}{2}})$ for $z \in B(w, 2r_0)$. □

Let us for a while take for granted the assumption $M^{\delta} = O(1)$ made in Proposition 3.4.6. It follows from the estimate (3.4.13) and from the a priori regularity of s-holomorphic functions (see Proposition 3.3.11) that the functions $F^{\delta}_{[\Omega^{\delta};v,w]}$ are also equicontinuous on compact subsets of $\Omega \setminus \{v, w\}$. Thus, one can apply the Arzelà–Ascoli theorem and find a subsequential limit

$$F^{\delta}_{[\Omega^{\delta};v,w]}(z) \;\to\; g_{[\Omega;v,w]}(z) \;\text{ as }\; \delta = \delta_k \to 0, \tag{3.4.16}$$

where the convergence is uniform on compact subsets of $\Omega \setminus \{v, w\}$. Trivially, each such a subsequential limit $g_{[\Omega;v,w]}$ is a spinor branching over v and w. Moreover, $g_{[\Omega;v,w]}$ is holomorphic due to Corollary 3.3.6. Let

$$h \;:=\; \tfrac{1}{2} \int \mathrm{Im}[(g_{[\Omega;v,w]}(z))^2 dz]; \tag{3.4.17}$$

note that h is a harmonic function in the punctured domain $\Omega \setminus \{v, w\}$ defined up to an additive constant.

As functions H^{δ} satisfy the Dirichlet boundary conditions (see Remarks 3.2.3 and Remark 3.3.10), it is natural to expect that the same holds for their subsequential limits (3.4.17). In the critical case $m = 0$, one can prove this fact without assuming that the boundary $\partial\Omega$ is smooth by using, e. g., the techniques developed in [48, Section 6]. However, we prefer to quote a more straightforward argument suggested by S. C. Park in [137, Proposition 22], which works in C^1-smooth domains only but instead has a great advantage of admitting a straightforward generalization to the $m < 0$ case. Let us emphasize that we will also rely upon Proposition 3.4.7 when discussing the massive setup in Section 3.4.6 ; namely, in the proof of Theorem 3.4.4.

Proposition 3.4.7. Let $m \le 0$ and assume that the boundary of Ω is C^1-smooth and that Ω^{δ} approximate Ω in the Hausdorff sense so that $\mathrm{dist}(\partial\Omega^{\delta}; \partial\Omega) = O(\delta)$ as $\delta \to 0$. Provided that the estimate $M^{\delta} = O(1)$ holds, the following are fulfilled :

(i) the uniform bound (3.4.13) holds up to the boundary of discrete domains $\partial\Omega^{\delta}$.

(ii) for each subsequential limit $g_{[\Omega;v,w]}$, the function h defined by (3.4.17) is continuous in $\overline{\Omega} \setminus \{v, w\}$ and satisfies Dirichlet boundary conditions at $\partial\Omega$;

(iii) moreover, $g_{[\Omega;v,w]}$ is continuous up to the boundary of Ω and satisfies Riemann-type boundary conditions $\mathrm{Im}[g_{[\Omega;v,w]}(\zeta)(\tau(\zeta))^{1/2}] = 0$ for all $\zeta \in \partial\Omega$, where $\tau(\zeta)$ denotes the tangent vector to $\partial\Omega$ at the point ζ oriented counterclockwise.

Proof. Recall that the functions H^δ are *sub*-harmonic on $\Gamma^{\bullet,\delta}$ due to Proposition 3.3.8 (or directly due to [48, Propostion 3.6] if $m = 0$) and that this property remains true if one performs the 'boundary modification trick' from [48, Section 3.6]; see also Remark 3.3.10 above. Therefore, a comparison with the discrete harmonic measure and the estimate $M^\delta = O(1)$ imply that $H^\delta(v) = O(\delta)$ at near-to-boundary vertices $v \in \Gamma^{\bullet,\delta}$ and hence $F^\delta_{[\Omega^\delta;v,w]}(z) = O(1)$ for all $z \in \partial\Omega^\delta$.

The discrete maximum principle for $|F^\delta|$ (which holds up to a universal multiplicative constant due to Lemma 3.3.12 or directly due to results of [33, Section 2.5] if $m = 0$) together with the uniform estimate (3.4.13) in the bulk of Ω^δ imply that

$$F^\delta_{[\Omega^\delta;v,w]} = O(1) \ \text{ as } \ \delta \to 0 \ \text{ uniformly in } \ \Omega^\delta \setminus (B(v,r_0) \cup B(w,r_0)),$$

including at the points close to the boundary $\partial\Omega^\delta$.

Now one easily sees that each subsequential limit (3.4.16) is uniformly bounded up to the boundary of Ω (i. e., on compact subsets of $\overline{\Omega} \setminus \{v,w\}$). In particular, the primitive $h = \frac{1}{2}\int \mathrm{Im}[(g_{[\Omega;v,w]}(z))^2 dz]$ is continuous in $\overline{\Omega}\setminus\{v,w\}$ and satisfies the Dirichlet boundary conditions at $\partial\Omega$.

Moreover, $\Delta h = 4m^2|g_{[\Omega;u,v]}|^2 = O(1)$ up to the boundary of a C^1-smooth domain Ω. Due to standard estimates, this implies that h is continuously differentiable and hence $g_{[\Omega;u,v]}$ is continuous *up to the boundary of* Ω, which allows one to speak about its boundary values. Finally, as pointed out in the proof of [137, Proposition 22], the discrete integration by parts argument used in [48, Remark 6.3] only relies upon the sub-harmonicity of function H^δ on $\Gamma^{\bullet,\delta}$ and thus can be applied verbatim to control the sign of the normal derivative of h provided that $m \le 0$. □

We are now in the position to prove the main result of this section. Note that we do *not* assume the bound $M^\delta = O(1)$ as $\delta \to 0$ anymore.

Theorem 3.4.1. The following holds uniformly on compact subsets of $\Omega \setminus \{v,w\}$:

$$F^\delta_{[\Omega^\delta;v,w]}(z) \ \to \ (\tfrac{2}{\pi})^{\frac{1}{2}} f_{[\Omega;v,w]}(z) \ \text{ as } \ \delta \to 0.$$

Moreover, this convergence is also uniform with respect to positions of v and w provided that v, w, z stay at definite distance from each other and from $\partial\Omega$.

Proof. We first prove the required result provided that $M^\delta = O(1)$ as $\delta \to 0$ and then rule out the impossible scenario $M^\delta \to \infty$ as $\delta = \delta_k \to \infty$.

If $M^\delta = O(1)$ as $\delta \to 0$ then we only need to prove that each subsequential limit $g_{[\Omega;v,w]}$ of s-holomorphic observables $F^\delta_{[\Omega^\delta;v,w]}$ solves the same boundary value problem as $f_{[\Omega;v,w]}$, up to the multiple $(2/\pi)^{1/2}$ in the asymptotics (3.4.9). (Recall that the existence of these subsequential limits $g_{[\Omega;v,w]}$ follows from Proposition 3.4.6 and the Arzelà–Ascoli theorem.) Proposition 3.4.7

guarantees that $g_{[\Omega;v,w]}$ satisfies the required Riemann-type boundary conditions at $\partial\Omega$. Therefore, it remains to analyze the asymptotics of $g_{[\Omega;v,w]}(z)$ as $z \to v$ and as $z \to w$.

It follows from the convergence results for s-holomorphic spinors $F^{\delta}_{[\Omega^\delta;v,w]}$ and $\mathcal{G}^{\delta}_{[v]}$ that the functions $H^{\delta,\dagger}$ (constructed from the fermionic observable (3.4.14) in a usual way) converge to a function

$$h^\dagger \ := \ \tfrac{1}{2}\int \mathrm{Im}[(g_{[\Omega;v,w]}(z) - (\tfrac{2}{\pi})^{\frac{1}{2}} e^{-i\frac{\pi}{4}}(z-v)^{-\frac{1}{2}})^2 dz]$$

on compact subsets of a *punctured* disc $B(v,2r_0)\setminus\{w\}$. However, the functions $H^{\delta,\dagger}$ remain uniformly bounded in the whole disc $B(v,2r_0)$ due to the discrete maximum principle. Therefore, the *harmonic* function $h^\dagger$ has a removable singularity at v and

$$g_{[\Omega;v,w]}(z) - (\tfrac{2}{\pi})^{\frac{1}{2}} e^{-i\frac{\pi}{4}}(z-v)^{-\frac{1}{2}} \ = \ O(|z-v|^{\frac{1}{2}}) \ \text{ as } \ z \to v$$

(the right-hand side automatically improves from $O(1)$ to $O(|z-v|^{\frac{1}{2}})$ since $g_{[\Omega;v,w]}$ has a square-root-type branching at v). A similar argument applies near the second branching point w. More precisely, using the estimate (3.4.15) and passing to a subsequence once more, we can assume that

$$X^{\delta}_{[\Omega^\delta;v,w]}(c_w) \ \to \ B \in \mathbb{R} \ \text{ as } \ \delta = \delta_k \to 0. \tag{3.4.18}$$

Then, the same argument as above implies that

$$g_{[\Omega;v,w]}(z) - B\cdot(\tfrac{2}{\pi})^{\frac{1}{2}} e^{i\frac{\pi}{4}}(z-w)^{-\frac{1}{2}} \ = \ O(|z-w|^{\frac{1}{2}}) \ \text{ as } \ z \to w.$$

Let us now rule out the scenario when $M^\delta \to \infty$ as $\delta = \delta_k \to 0$. In this hypothetical situation one can consider the re-scaled observables

$$\widetilde{F}^{\delta}_{[\Omega^\delta;v,w]} \ := \ (M^\delta)^{-\frac{1}{2}} \cdot F^{\delta}_{[\Omega^\delta;v,w]}$$

and repeat the arguments given above relying upon the identity $\max_{\Omega(r_0)}|\widetilde{H}^\delta| = 1$ for the corresponding functions $\widetilde{H}^\delta$. Each subsequential limit $\widetilde{g}_{[\Omega;v,w]}$ obtained in this way solves the same boundary value problem as $f_{[\Omega;v,w]}$ except that

$$\widetilde{g}_{[\Omega;v,w]}(z) \ = \ O(|z-v|^{\frac{1}{2}}) \ \text{ as } \ z \to v$$

since the re-scaled functions $(M^\delta)^{-\frac{1}{2}}\mathcal{G}^{\delta}_{[v]}$ vanish (on compact subsets of $\mathbb{C}\setminus\{v\}$) in the limit $\delta \to 0$. Similarly to Remark 3.4.5(ii), this boundary value problem does not admit a non-trivial solution, i. e., $\widetilde{g}_{[\Omega;v,w]}(z) = 0$ for all $z \in \Omega$. However, together with the uniform estimate $\widetilde{F}^{\delta}_{[\Omega^\delta;v,w]} = O(1)$ near the boundary of Ω^δ provided by Proposition 3.4.6, this implies that

$$\widetilde{H}^\delta \ \to \ 0 \ \text{ as } \ \delta \to 0 \ \text{ on compact subsets of } \ \overline{\Omega}\setminus\{v,w\},$$

which contradicts the normalization $\max_{\Omega(r_0)} |\widetilde{H}^\delta| = 1$.

Finally, note that we never used the fact that the positions of points $v^\delta = v$ and $w^\delta = w$ are fixed ; in all the arguments given above it is sufficient to assume that $u^\delta \to u$ and $w^\delta \to w$ as $\delta \to 0$. By compactness, this implies that all the convergence statements discussed above are uniform in u and w provided that these points stay at definite distance from each other and from $\partial\Omega$. □

3.4.3 . Critical model : convergence of ratios of spin-spin correlations

We now discuss several corollaries of Theorem 3.4.1 following the scheme designed in [38]. However, let us note that we give more straightforward proofs than those from [38]. The following result generalizes [38, Theorem 1.7] to isoradial grids.

Corollary 3.4.8. In the same setup as above, let $b \in \Omega^{\bullet,\delta}$ be adjacent to $w \in \Omega^{\circ,\delta}$ and recall that $v \sim u$. Then,

$$\frac{\mathbb{E}^{\mathrm{w}}_{\Omega^\delta}[\mu_v\mu_b]}{\mathbb{E}^{\mathrm{w}}_{\Omega^\delta}[\sigma_u\sigma_w]} \;=\; \frac{\mathbb{E}^{\mathrm{f}}_{\Omega^{*,\delta}}[\sigma_v\sigma_b]}{\mathbb{E}^{\mathrm{w}}_{\Omega^\delta}[\sigma_u\sigma_w]} \;\to\; \mathcal{B}_\Omega(v,w) \quad \text{as} \quad \delta \to 0\,. \tag{3.4.19}$$

Remark 3.4.9. Recall that, according to the Kramers–Wannier duality, the disorder-disorder correlator $\mathbb{E}^{\mathrm{w}}_{\Omega^\delta}[\mu_v\mu_b]$ is equal to the spin-spin correlation $\mathbb{E}^{\mathrm{f}}_{\Omega^{*,\delta}}[\sigma_v\sigma_b]$ in the *dual* Ising model on $\Omega^{*,\delta}$ with free boundary conditions.

Proof. Let $c_w \in \Upsilon^\times_{[v,w]}(\Omega^\delta)$ be adjacent to both w and b. By definition of the observable $X^\delta_{[\Omega^\delta;v,w]}$ (see (3.4.7)), we have $\mathbb{E}^{\mathrm{w}}_{\Omega^\delta}[\mu_v\mu_b]/\mathbb{E}^{\mathrm{w}}_{\Omega^\delta}[\sigma_u\sigma_w] = \pm X^\delta_{[\Omega^\delta;v,w]}(c_w)$. In fact, the convergence of the values $X^\delta_{[\Omega^\delta;v,w]}(c_w)$ has been already implicitly proven along the proof of Theorem 3.4.1. Indeed, each subsequential limit B in (3.4.18) has to be equal to $\mathcal{B}_\Omega(v,w)$ since the (a priori, unknown) coefficient in the asymptotics (3.4.10) is uniquely determined by the boundary problem itself.

Alternatively, one can consider the function $H\big[X^\delta_{[\Omega^\delta;v,w]}, \mathrm{G}^\delta_{[b]}\big]$ defined in a vicinity of w and note that its additive monodromy around c_w is equal to

$$\begin{aligned} 2X^\delta_{[\Omega^\delta;v,w]}(c_w) \;&=\; 2X^\delta_{[\Omega^\delta;v,w]}(c_w)\mathrm{G}^\delta_{[b]}(c_w) \\ &=\; \frac{1}{2}\oint^{[\delta]}_{z:|z-w|=2r_0} \mathrm{Im}\,\big[F^\delta_{[\Omega^\delta;v,w]}(z)\mathcal{G}^\delta_{[b]}(z)dz\big]; \end{aligned}$$

see Lemma 3.3.14. Using the convergence of $F^\delta_{[\Omega^\delta;v,w]}(z)$ and $\mathcal{G}^\delta_{[b]}(z)$ as $\delta \to 0$ near the circle $\{z : |z-w| = 2r_0\}$ we easily see that

$$X^\delta_{[\Omega^\delta;v,w]}(c_w) \;\to\; \frac{1}{2\pi}\oint^{[\delta]}_{z:|z-w|=2r_0} \mathrm{Im}\,\big[f_{[\Omega;v,w]}(z)(z-w)^{-\frac{1}{2}}dz\big] \;=\; \pm\mathcal{B}_\Omega(v,w),$$

where we used the asymptotics (3.4.10) in the last equation. (The potential ambiguity in the sign is caused by the fact that we work with spinors branching

over w rather than with single-valued holomorphic functions.) The $\pm$ sign can be easily fixed by noting that both $\mathbb{E}^{\mathrm{w}}_{\Omega^\delta}[\mu_v\mu_b]/\mathbb{E}^{\mathrm{w}}_{\Omega^\delta}[\sigma_u\sigma_w]$ and $\mathcal{B}_\Omega(v,w)$ are positive quantities. □

Following [38], let us introduce the quantity $\mathcal{A}_\Omega(v,w)\in\mathbb{C}$ as the sub-leading coefficient in the asymptotics of the spinor $f_{[\Omega;v,w]}$ at the point $z=v$:

$$f_{[\Omega;v,w]}(z) \;=\; e^{-\frac{\pi}{4}}(z-v)^{-\frac{1}{2}}\cdot\big(1+2\mathcal{A}_\Omega(v,w)(z-v)+O(|z-v|^2)\big). \quad (3.4.20)$$

Further, define the two-point spin correlation function $\langle\sigma_{u_1}\sigma_{u_2}\rangle^{\mathrm{w}}_\Omega$ as the exponential of the primitive of the following (closed) differential form :

$$\langle\sigma_{u_1}\sigma_{u_2}\rangle^{\mathrm{w}}_\Omega \;:=\; \exp\int^{(u_1,u_2)}\mathrm{Re}\,[\mathcal{A}_\Omega(v,w)dv+\mathcal{A}_\Omega(w,v)dw], \qquad (3.4.21)$$

normalized so that $\langle\sigma_{u_1}\sigma_{u_2}\rangle^{\mathrm{w}}_\Omega\sim|u_2-u_1|^{-\frac{1}{4}}$ as $u_2\to u_1$. For simply connected domains Ω, the function $\langle\sigma_{u_1}\sigma_{u_2}\rangle^{\mathrm{w}}_\Omega$ can be written explicitly (e. g., see [38, Eq. (1.2)]) ; it is also worth noting that the existence of such a primitive can be deduced from the convergence results discussed in Corollaries 3.4.10, 3.4.11 and Theorem 3.4.2 below. Also, let us define

$$\langle\sigma_{u_1}\sigma_{u_2}\rangle^{\mathrm{f}}_\Omega \;:=\; \mathcal{B}_\Omega(u_1,u_2)\cdot\langle\sigma_{u_1}\sigma_{u_2}\rangle^{\mathrm{w}}_\Omega\,. \qquad (3.4.22)$$

It is not hard to deduce from (3.4.11) that, for conformal maps $\varphi:\Omega\to\Omega'$,

$$\langle\sigma_{u_1}\sigma_{u_2}\rangle^{\mathfrak{b}}_\Omega \;=\; \langle\sigma_{\varphi(u_1)}\sigma_{\varphi(u_2)}\rangle^{\mathfrak{b}}_{\Omega'}\cdot|\varphi'(u_1)|^{\frac{1}{8}}|\varphi'(u_2)|^{\frac{1}{8}}. \qquad (3.4.23)$$

for both wired ($\mathfrak{b}=\mathrm{w}$) and free ($\mathfrak{b}=\mathrm{f}$) boundary conditions.

The following result generalizes [38, Theorem 1.5] to the isoradial setup ; it is worth noting that the proof given below considerably simplifies the arguments used in [38] even in the square grid case $\Lambda^\delta=\delta\mathbb{Z}^2$.

Corollary 3.4.10. In the same setup as above, let $u_0,u_1\in\Gamma^{\circ,\delta}$ be two neighboring 'white' vertices adjacent to $v\in\Gamma^{\bullet,\delta}$. Then, the following asymptotics hold :

$$\frac{\mathbb{E}^{\mathrm{w}}_{\Omega^\delta}[\sigma_{u_1}\sigma_w]}{\mathbb{E}^{\mathrm{w}}_{\Omega^\delta}[\sigma_{u_0}\sigma_w]} \;=\; 1+\mathrm{Re}\,[(u_1-u_0)\cdot\mathcal{A}_\Omega(v,w)]+o(\delta),$$

where the error term is uniform with respect to $v,w\in\Omega$ provided that they remain at a definite distance from each other and from $\partial\Omega$.

Proof. Let $v(c_{0,1})=v$, $u(c_{0,1})=u_{0,1}$, and assume that $c_{0,1}\in\Upsilon^\times_{[v;w]}(\Omega^\delta)$ are chosen to be adjacent on the double cover. Consider the observable (3.4.7) with $u=u_0$ and note that

$$\frac{\mathbb{E}^{\mathrm{w}}_{\Omega^\delta}[\sigma_{u_1}\sigma_w]}{\mathbb{E}^{\mathrm{w}}_{\Omega^\delta}[\sigma_{u_0}\sigma_w]}-1 \;=\; X^\delta_{[\Omega^\delta;v,w]}(c_1)-X^\delta_{[\Omega^\delta;v,w]}(c_0).$$

Using Lemma 3.3.14 as in the proof of Corollary 3.4.8 we see that

$$X^{\delta}_{[\Omega^\delta;v,w]}(c_1) - X^{\delta}_{[\Omega^\delta;v,w]}(c_0) \\ = \frac{1}{4}\oint^{[\delta]}_{z:|z-v|=2r_0} \mathrm{Im}\,[F^{\delta}_{[\Omega^\delta;v,w]}(z)\cdot(\mathcal{G}^{\delta}_{[u_1]}(z)-\mathcal{G}^{\delta}_{[u_0]}(z))dz].$$

Note that the asymptotics (3.3.9) contain no $O(\delta)$ term. Therefore,

$$\mathcal{G}^{\delta}_{[u_1]}(z)-\mathcal{G}^{\delta}_{[u_0]}(z) \;=\; \tfrac{1}{2}(u_1-u_0)\cdot e^{i\frac{\pi}{4}}(\tfrac{2}{\pi})^{\frac{1}{2}}(z-v)^{-\frac{3}{2}}+O(\delta^2) \;\text{ as }\; \delta\to 0.$$

Since we also know that $F^{\delta}_{[\Omega^\delta;v,w]}(z)\to(\frac{2}{\pi})^{\frac{1}{2}}f_{[\Omega;v,w]}(z)$ as $\delta\to 0$ (uniformly near the circle $\{z:|z-v|=2r_0\}$, see Theorem 3.4.1), this gives

$$\frac{\mathbb{E}^{\mathrm{w}}_{\Omega^\delta}[\sigma_{u_1}\sigma_w]}{\mathbb{E}^{\mathrm{w}}_{\Omega^\delta}[\sigma_{u_0}\sigma_w]}-1 \;=\; \frac{1}{4\pi}\oint_{z:|z-v|=2r_0}\mathrm{Im}\Big[(u_1-u_0)\cdot\frac{e^{i\frac{\pi}{4}}f_{[\Omega;v,w]}(z)dz}{(z-v)^{\frac{3}{2}}}\Big]+o(\delta) \\ =\; \mathrm{Re}\,[(u_1-u_0)\cdot\mathcal{A}_\Omega(v,w)]+o(\delta),$$

where we used definition (3.4.20) of the coefficient $\mathcal{A}_\Omega(v,w)$ in the last equation. □

Corollary 3.4.11. In the same setup as above, the following holds :

$$\frac{\mathbb{E}^{\mathrm{w}}_{\Omega^\delta}[\sigma_{u'}\sigma_{w'}]}{\mathbb{E}^{\mathrm{w}}_{\Omega^\delta}[\sigma_u\sigma_w]} \;\to\; \frac{\langle\sigma_{u'}\sigma_{w'}\rangle^{\mathrm{w}}_{\Omega}}{\langle\sigma_u\sigma_w\rangle^{\mathrm{w}}_{\Omega}} \;\text{ as }\; \delta\to 0,$$

uniformly with respect to $u,u',w,w'\in\Omega$ provided that all these four points stay at a definite distance $\rho>0$ from $\partial\Omega$ and that $|u-w|\geq\rho$ and $|u'-w'|\geq\rho$.

Proof. The asymptotics provided by Corollary 3.4.10 can be equivalently written as

$$\log\frac{\mathbb{E}^{\mathrm{w}}_{\Omega^\delta}[\sigma_{u_1}\sigma_w]}{\mathbb{E}^{\mathrm{w}}_{\Omega^\delta}[\sigma_{u_0}\sigma_w]} \;=\; \mathrm{Re}\,[(u_1-u_0)\cdot\mathcal{A}_\Omega(v,w)]+o(\delta).$$

Summing these expression along appropriate paths connecting u to u' and w to w' inside Ω^δ and using definition (3.4.21) of the continuous correlation functions $\langle\sigma_u\sigma_w\rangle^{\mathrm{w}}_{\Omega}$ one easily gets the result. □

3.4.4 . Critical model : universality of the full-plane spin-spin correlations

In this section we consider the critical Ising model on infinite isoradial grids Λ with $\delta=1$ and prove that the two-point correlations $\mathbb{E}_\Lambda[\sigma_u\sigma_w]$ have *universal* (i. e., independent of Λ) rotationally invariant asymptotics as $|u-w|\to\infty$.

Theorem 3.4.2. Let $\mathcal{C}_\sigma=2^{\frac{1}{6}}e^{\frac{3}{2}\zeta'(-1)}$. The following asymptotics hold :

$$\mathbb{E}_\Lambda[\sigma_u\sigma_w] \;\sim\; \mathcal{C}_\sigma^2\cdot|u-w|^{-\frac{1}{4}} \quad\text{as}\quad |u-w|\to\infty, \tag{3.4.24}$$

uniformly with respect to Λ provided that it satisfies the property $\mathrm{BAP}(\theta_0)$.

Proof. The proof is similar to the proof of Proposition 3.4.2 for the subcritical model, see also Remark 3.4.3. More precisely, it goes in the following three steps :

i. prove that the asymptotics (3.4.24) holds if $\Lambda = \mathbb{Z}^2$ is the square grid ;

ii. prove that (3.4.24) holds uniformly over the class of rectangular grids Λ^{rect} ;

iii. prove that the same asymptotics is fulfilled for all isoradial grids.

The proofs of steps (ii) and (iii) are similar to each other and are based upon gluing large pieces of Λ^{rect} and $\mathbb{Z}^2$ in step (ii), and the 'star extension' construction discussed in Section 3.2.4, which allows to glue a large piece of Λ with a piece of a rectangular grid in step (iii). Thus, we only discuss steps (i) and (iii) below.

Step (i) follows from (ia) the explicit computation of 'diagonal' correlations on the square grid due to Wu [123, Section XI.4], see also [40, Appendix] for a short proof of this result ; and (ib) the fact that these asymptotics are rotationally invariant ; see [38, Remark 2.6] (and [148] where this result was proven by other techniques).

To prove (ib), let us fix $\varepsilon > 0$ and let $A = A(\varepsilon) \gg 1$ be chosen so that the RSW estimates (3.2.10) hold. Denote $\rho = \rho(\varepsilon) := 1/A(\varepsilon)$ and $\delta := 2\rho \cdot |u - w|^{-1}$. Let the scaled grid $\delta\mathbb{Z}^2$ be also shifted so that u and w become the (approximations of) points $\pm\alpha\rho$ on $\delta\mathbb{Z}^2$, where $|\alpha| = 1$. Denote by $\mathbb{D}^\delta$ the discretization of the unit disc $\mathbb{D} := \{z : |z| < 1\}$ on $\delta\mathbb{Z}^2$. It follows from (3.2.10) that

$$\frac{\mathbb{E}^{\mathrm{w}}_{\mathbb{D}^\delta}[\sigma_{\alpha\rho}\sigma_{-\alpha\rho}]}{\mathbb{E}_{\delta\mathbb{Z}^2}[\sigma_{\alpha\rho}\sigma_{-\alpha\rho}]} = 1 + O(\varepsilon), \quad \text{uniformly in } \delta.$$

At the same time, Corollary (3.4.11) and the rotational invariance of continuous correlation functions $\langle\sigma_{\alpha\rho}\sigma_{-\alpha\rho}\rangle^{\mathrm{w}}_{\mathbb{D}} = \langle\sigma_{\rho}\sigma_{-\rho}\rangle^{\mathrm{w}}_{\mathbb{D}}$ imply that

$$\frac{\mathbb{E}^{\mathrm{w}}_{\mathbb{D}^\delta}[\sigma_{\alpha\rho}\sigma_{-\alpha\rho}]}{\mathbb{E}^{\mathrm{w}}_{\mathbb{D}^\delta}[\sigma_{\rho}\sigma_{-\rho}]} = 1 + o_{\delta\to 0}(1) \quad \text{for each fixed } \rho(\varepsilon).$$

Using (3.2.10) once again to compare $\mathbb{E}^{\mathrm{w}}_{\mathbb{D}^\delta}[\sigma_{\rho}\sigma_{-\rho}]$ and $\mathbb{E}_{\delta\mathbb{Z}^2}[\sigma_{\rho}\sigma_{-\rho}]$ we see that

$$\frac{\mathbb{E}_{\delta\mathbb{Z}^2}[\sigma_{\alpha\rho}\sigma_{-\alpha\rho}]}{\mathbb{E}_{\delta\mathbb{Z}^2}[\sigma_{\rho}\sigma_{-\rho}]} \;=\; 1 + O(\varepsilon) + o_{\delta\to 0}(1)$$

Choosing first ε small enough and then $|u - w| = 2\rho(\varepsilon) \cdot \delta^{-1}$ big enough one obtains the required rotational invariance property (ib).

We now discuss step (iii), recall that step (ii) can be done following exactly the same lines by replacing the pair Λ, Λ^{rect} of isoradial grids by Λ^{rect} and $\delta\mathbb{Z}^2$ in the argument given below ; cf. Remark 3.4.3. Let $A = A(\varepsilon) \gg 1$, $\rho = \rho(\varepsilon) := 1/A(\varepsilon)$ and $\delta := 2\rho \cdot |u - w|^{-1}$ be chosen as above. Also, let Λ^δ be the grid Λ scaled by the factor δ, rotated and shifted so that u and w become the points $\pm\rho$ on Λ^δ.

Further, let $\Lambda_1^\delta = \Lambda_1^\delta(0)$ be the discretization of the box $[-1,1]\times[-1,1]$ on Λ^δ and denote by $\Lambda^{\star,\delta} := [\Lambda_1^\delta]^\star$ the 'star extension' of this box (see Section 3.2.4). Recall that $\Lambda^{\star,\delta}$ contains pieces of rectangular lattices located at $O(1)$ distance (uniformly in δ) from the origin. Therefore, there we can find a point $z\in\mathbb{C}$ such that $|z|\le C = C(\theta_0)$ and that the box $\Lambda_1^{\star,\delta}(z)$ of size 2×2 centered at z is a subset of a rectangular grid $\Lambda^{\mathrm{rect},\delta}$.

Finally, denote by $\Omega\subset\mathbb{C}$ the disc of radius $C+1$ centered at $\frac{1}{2}z$. Corollary 3.4.11 implies the convergence

$$\frac{\mathbb{E}^{\mathrm{w}}_{\Omega^\delta}[\sigma_\rho\sigma_{-\rho}]}{\mathbb{E}^{\mathrm{w}}_{\Omega^\delta}[\sigma_{z+\rho}\sigma_{z-\rho}]} \;\to\; \frac{\langle\sigma_\rho\sigma_{-\rho}\rangle^{\mathrm{w}}_{\Omega}}{\langle\sigma_{z+\rho}\sigma_{z-\rho}\rangle^{\mathrm{w}}_{\Omega}} \;=\; 1 \quad\text{as}\quad \delta\to 0,$$

where Ω^δ stands for the discretization of the disc Ω on the modified grid $\Lambda^{\star,\delta}$.

At the same time, the RSW estimates (3.2.10) give

$$\begin{aligned}
\mathbb{E}^{\mathrm{w}}_{\Omega^\delta}[\sigma_\rho\sigma_{-\rho}] \;&\le\; \mathbb{E}^{\mathrm{w}}_{\Lambda_1^\delta(0)}[\sigma_\rho\sigma_{-\rho}] \;\le\; (1-\varepsilon)^{-1}\cdot\mathbb{E}_{\Lambda^\delta}[\sigma_\rho\sigma_{-\rho}],\\
\mathbb{E}^{\mathrm{w}}_{\Omega^\delta}[\sigma_\rho\sigma_{-\rho}] \;&\ge\; (1-\varepsilon)\cdot\mathbb{E}^{\mathrm{w}}_{\Lambda_1^\delta(0)}[\sigma_\rho\sigma_{-\rho}] \;\ge\; (1-\varepsilon)\cdot\mathbb{E}_{\Lambda^\delta}[\sigma_\rho\sigma_{-\rho}]
\end{aligned}$$

and similarly for $\mathbb{E}^{\mathrm{w}}_{\Omega^\delta}[\sigma_{z-\rho}\sigma_{z+\rho}]$ and $\mathbb{E}_{\Lambda^{\mathrm{rect},\delta}}[\sigma_{z+\rho}\sigma_{z-\rho}]$. Therefore,

$$\frac{\mathbb{E}_{\Lambda^\delta}[\sigma_\rho\sigma_{-\rho}]}{\mathbb{E}_{\Lambda^{\mathrm{rect},\delta}}[\sigma_{z+\rho}\sigma_{z-\rho}]} \;=\; 1+O(\varepsilon)+o_{\delta\to 0}(1),$$

where the error term $O(\varepsilon)$ is uniform in δ. Moreover, it follows from step (ii) applied to the re-scaled grid $\delta^{-1}\Lambda^{\mathrm{rect},\delta}$ with mesh size 1 that

$$\mathbb{E}_{\Lambda^{\mathrm{rect},\delta}}[\sigma_{z+\rho}\sigma_{z-\rho}] \;=\; \mathcal{C}_\sigma^2\cdot(2\rho\delta^{-1})^{-\frac{1}{4}}\cdot(1+o_{\delta\to 0}(1)).$$

Since $\delta = 2\rho\cdot|u-w|^{-1}$, we arrive at the asymptotics

$$\mathbb{E}_\Lambda[\sigma_u\sigma_w] \;=\; \mathbb{E}_{\Lambda^\delta}[\sigma_\rho\sigma_{-\rho}] \;=\; \mathcal{C}_\sigma^2\cdot|u-w|^{-\frac{1}{4}}\cdot(1+O(\varepsilon)+o_{|u-w|\to\infty}(1)),$$

with the uniform (in u,w) error term $O(\varepsilon)$. By first choosing ε small enough and then $|u-w|$ large enough one obtains the required asymptotics (3.4.24). □

It is easy to see that Theorem 3.4.2 allows to pass from the convergence of *ratios* of two-point spin correlations in finite domains discussed in Corollary 3.4.11 to the convergence of these correlations themselves; see also Remark 3.4.13 below.

Corollary 3.4.12. Let $\Omega\subset\mathbb{C}$ be a bounded simply connected domain with C^1-smooth boundary and assume that $u,w\in\Omega$, $u\ne w$. Let isoradial grids Λ^δ satisfy the property $\mathrm{BAP}(\theta_0)$ and discrete domains $\Omega^\delta\subset\Gamma^\delta$ approximate Ω in the Hausdorff sense so that $\mathrm{dist}(\partial\Omega^\delta;\partial\Omega) = O(\delta)$. Then,

$$\begin{aligned}
\delta^{-\frac{1}{4}}\mathbb{E}^{\mathrm{w}}_{\Omega^\delta}[\sigma_u\sigma_w] \;&\to\; \mathcal{C}_\sigma^2\cdot\langle\sigma_u\sigma_w\rangle^{\mathrm{w}}_{\Omega}\,,\\
\delta^{-\frac{1}{4}}\mathbb{E}^{\mathrm{f}}_{\Omega^\delta}[\sigma_u\sigma_w] \;&\to\; \mathcal{C}_\sigma^2\cdot\langle\sigma_u\sigma_w\rangle^{\mathrm{f}}_{\Omega}
\end{aligned}\qquad\text{as}\quad \delta\to 0.$$

Proof. Let $\rho > 0$ be small enough. It follows from Corollary 3.4.11 that

$$\frac{\mathbb{E}^{\mathrm{w}}_{\Omega^\delta}[\sigma_u\sigma_w]}{\mathbb{E}^{\mathrm{w}}_{\Omega^\delta}[\sigma_u\sigma_{u+\rho}]} \cdot \frac{\langle\sigma_u\sigma_{u+\rho}\rangle^{\mathrm{w}}_{\Omega}}{\langle\sigma_u\sigma_w\rangle^{\mathrm{w}}_{\Omega}} \;=\; 1 + o_{\delta\to 0}(1) \quad \text{for each fixed } \rho > 0.$$

Recall that the multiplicative normalization of the continuous correlation functions (3.4.21) is fixed so that

$$\langle\sigma_u\sigma_{u+\rho}\rangle^{\mathrm{w}}_{\Omega} \;=\; \rho^{-\frac{1}{4}} \cdot (1 + o_{\rho\to 0}(1)).$$

At the same time, the RSW estimates (3.2.10) imply that

$$\frac{\mathbb{E}^{\mathrm{w}}_{\Omega^\delta}[\sigma_u\sigma_{u+\rho}]}{\mathbb{E}_{\Lambda^\delta}[\sigma_u\sigma_{u+\rho}]} \;=\; 1 + o_{\rho\to 0}(1) \quad \text{uniformly in } \delta \le \delta_0(\rho).$$

Finally, due to Theorem 3.4.2 we have the asymptotics

$$\mathbb{E}_{\Lambda^\delta}[\sigma_u\sigma_{u+\rho}] \;=\; \mathcal{C}_\sigma^2 \cdot (\delta^{-1}\rho)^{-\frac{1}{4}} \cdot (1 + o_{\delta\to 0}(1)) \quad \text{for each fixed } \rho > 0.$$

Combining these asymptotics together, first choosing ρ small enough, and then δ small enough we obtain the required convergence result for $\delta^{-\frac{1}{4}}\mathbb{E}^{\mathrm{w}}_{\Omega^\delta}[\sigma_u\sigma_w]$.

Recall that the continuous correlation functions $\langle\sigma_u\sigma_w\rangle^{\mathrm{f}}_{\Omega}$ are defined by (3.4.22). The convergence of spin-spin correlations with free boundary conditions follows from the Kramers–Wannier duality, Corollary 3.4.8, and the convergence of spin-spin correlations in the dual isoradial model with wired boundary conditions. □

Remark 3.4.13. (i) Recall that we used the smoothness assumption on $\partial\Omega$ only in Proposition 3.4.7, which claims the correct boundary conditions of subsequential limits (3.4.16) of discrete fermionic observables. In the critical setup, this smoothness assumption can be dropped, e. g., by using techniques from [48, Section 6] instead.

(ii) The simplification/generalization of the proofs from [38] discussed above is not restricted to the two-point correlations and applies to all results of that paper. In particular, for all $n \ge 1$ the convergence

$$\delta^{-\frac{n}{8}}\mathbb{E}^{\mathrm{w}}_{\Omega^\delta}[\sigma_{u_1}\dots\sigma_{u_n}] \;\to\; \mathcal{C}_\sigma^n \cdot \langle\sigma_{u_1}\dots\sigma_{u_n}\rangle^{\mathrm{w}}_{\Omega} \quad \text{as} \quad \delta \to 0$$

holds uniformly over the class of isoradial discretizations $\Omega^\delta \subset \Gamma^\delta$, at least provided that Λ^δ satisfy the uniformly bounded angles property $\mathrm{BAP}(\theta_0)$.

(iii) We refer the interested reader to a recent paper [39] for a discussion of further generalizations, e. g., (a) convergence results for more involved correlations and (b) techniques that can be used to control the boundary values of fermionic observables.

3.4.5 . Massive model : definitions of correlation functions in continuum

We now move to the analysis of the massive model. In this section we define relevant two-point spin correlation functions *in continuum*, assuming that $m < 0$ and that Ω is a C^1-smooth domain. Note that, contrary to the conformally invariant case $m = 0$ discussed above, this smoothness assumption plays a much more important role in what follows. In particular, it greatly simplifies the discussion of the *uniqueness* of solutions of the corresponding boundary value problems (which can be avoided if $m = 0$ due to the conformal covariance identity (3.4.11)). We refer the interested reader to a recent paper [138] by S. C. Park, where certain techniques allowing to treat Riemann-type boundary value problems for massive fermionic observables in rough domains Ω were developed.

The definitions given below generally follow those from [137]. However, note that we avoid the explicit use of Bessel functions in order to keep the discussion as light as possible ; we refer the interested reader to [137] for more information on massive holomorphic functions and their singularities. It is worth noting that below we use a slightly different notation $\mathcal{A}^{(m)}_{\Omega}(v,w)$ instead of $\mathcal{A}_{\Omega}(v,w\,|\,m)$ etc used in [137].

Given $m < 0$, let us denote by $f^{(m)}_{[\Omega;v,w]}$ a spinor on the double cover $[\Omega; v, w]$ of a smooth domain Ω ramified over v and w such that

— $f^{(m)}_{[\Omega;v,w]}$ satisfies the massive holomorphicity equation (3.3.2) in $\Omega \setminus \{v, w\}$;

— $f^{(m)}_{[\Omega;v,w]}$ is continuous in $\overline{\Omega} \setminus \{v, w\}$ and satisfies the Riemann-type boundary conditions $\mathrm{Im}[f^{(m)}_{[\Omega;v,w]}(\zeta)(\tau(\zeta))^{1/2}] = 0$ for all $\zeta \in \partial\Omega$, where $\tau(\zeta)$ denotes the tangent vector to $\partial\Omega$ at the point ζ oriented counterclockwise ;

— the following asymptotics near the branching points v, w hold :

$$f^{(m)}_{[\Omega;v,w]}(z) \;=\; e^{-i\frac{\pi}{4}}\frac{e^{2m|z-v|}}{\sqrt{z-v}} + O(|z-v|^{\frac{1}{2}}), \qquad z \to v, \tag{3.4.25}$$

$$f^{(m)}_{[\Omega;v,w]}(z) \;=\; e^{i\frac{\pi}{4}}\mathcal{B}^{(m)}_{\Omega}(v,w)\cdot\frac{e^{-2m|z-w|}}{\sqrt{z-w}} + O(|z-w|^{\frac{1}{2}}), \quad z \to w, \tag{3.4.26}$$

where $\mathcal{B}^{(m)}_{\Omega}(v,w) \in \mathbb{R}$ is an (a priori unknown) coefficient defined up to the sign, which we fix by requiring that $\mathcal{B}^{(m)}_{\Omega}(v,w) \geq 0$.

Recall that the massive holomorphicity condition $\overline{\partial} f + im\overline{f} = 0$ implies that the primitive $h := \int \mathrm{Im}[(f(z))^2 dz]$ is well-defined and that $\Delta h := -8m|f|^2$. In particular, h is sub-harmonic provided that $m < 0$. Thus, the argument given in Remark 3.4.5(ii) applies and gives the *uniqueness* of a solution $f^{(m)}_{[\Omega;v,w]}$ to this boundary value problem ; see [137, Proposition 17]. However, contrary to the critical case, for $m < 0$ one cannot claim the *existence* of this solution via the conformal

covariance and an explicit formula in a reference domain. Instead, $f^{(m)}_{[\Omega;v,w]}$ can be obtained as a subsequential limit of discrete observables; see Theorem 3.4.3 below.

Lemma 3.4.14. Let Ω be a smooth simply connected domain, $m \leq 0$. Then, one has

$$\mathcal{B}^{(m)}_{\Omega}(v,w) \to 1 \quad \text{as} \quad w \to v, \quad \text{for each} \quad v \in \Omega. \tag{3.4.27}$$

Proof. Let us emphasize that this fact is *not* trivial if $m \neq 0$ because of the lack of conformal invariance and explicit formulas. However, one can analyze the behavior of the coefficient $\mathcal{B}^{(m)}_{\Omega}(v,w)$ by comparing it with $\mathcal{B}_{\Omega}(v,w) = \mathcal{B}^{(0)}_{\Omega}(v,w)$, which is explicit. We refer the reader to [137, Lemmas 28 and 29] for the proof of (3.4.27). □

We are now in the position to define the coefficients $\mathcal{A}^{(m)}_{\Omega}(v,w) \in \mathbb{C}$. Similarly to (3.4.20), they are introduced by requiring that

$$f^{(m)}_{[\Omega;v,w]}(z) \;=\; e^{-i\frac{\pi}{4}} \frac{e^{2m|z-v|}}{(z-v)^{\frac{1}{2}}} \cdot \big(1 + 2\mathcal{A}^{(m)}_{\Omega}(v,w)\cdot(z-v) + O(|z-v|^2)\big) \tag{3.4.28}$$

as $z \to v$. Let us emphasize that the *existence* of such an asymptotic expansion for $m < 0$ is much less trivial than (3.4.20) for $m = 0$. As discussed, e. g., in [137] (see Eq. (2.16) and (2.17) of that paper), spinor solutions to the massive holomorphicity equation (3.3.2) considered near their branching points admit expansions via half-integer modified Bessel functions $e^{\pm i\nu \arg z} I_{\nu}(2|mz|)$. In their turn, the function $I_{\nu}(r)$ are power series in r; see [134, Eq. 10.25.2]. It remains to check that the last factor in the expansion (3.4.28) cannot contain other linear terms than $\mathrm{cst}\cdot(z-v)$, which we leave to the reader as a simple exercise.

The next step is to define for $m < 0$, similarly to (3.4.21) and (3.4.22),

$$\langle \sigma_{u_1}\sigma_{u_2}\rangle^{(m),\mathrm{w}}_{\Omega} \;:=\; \exp \int^{(u_1,u_2)} \mathrm{Re}\,[\mathcal{A}^{(m)}_{\Omega}(v,w)dv + \mathcal{A}^{(m)}_{\Omega}(w,v)dw], \tag{3.4.29}$$

$$\langle \sigma_{u_1}\sigma_{u_2}\rangle^{(-m),\mathrm{f}}_{\Omega} \;:=\; \mathcal{B}^{(m)}_{\Omega}(u_1,u_2)\cdot \langle \sigma_{u_1}\sigma_{u_2}\rangle^{(m),\mathrm{w}}_{\Omega}. \tag{3.4.30}$$

Again, a priori it is not obvious that the differential form in (3.4.29) is exact. However, this can be immediately derived from an analogue of Corollary 3.4.10 in the massive case; see Corollary 3.4.16 below. Still, there remains a question of fixing the multiplicative normalization in (3.4.29), which we do by requiring that

$$\langle \sigma_{u_1}\sigma_{u_2}\rangle^{(m),\mathrm{w}}_{\Omega} \;\sim\; |u_2-u_1|^{-\frac{1}{4}} \;\sim\; \langle \sigma_{u_1}\sigma_{u_2}\rangle^{(-m),\mathrm{f}}_{\Omega} \quad \text{as} \quad u_2 \to u_1. \tag{3.4.31}$$

The existence of such a normalization (for $m < 0$) follows from the monotonicity of spin-spin correlations in discrete

$$\mathbb{E}^{(m),\mathrm{w}}_{\Omega^{\delta}}[\sigma_{u_1}\sigma_{u_2}] \;\geq\; \mathbb{E}^{\mathrm{w}}_{\Omega^{\delta}}[\sigma_{u_1}\sigma_{u_2}]\,, \qquad \mathbb{E}^{(-m),\mathrm{f}}_{\Omega^{*,\delta}}[\sigma_{v_1}\sigma_{v_2}] \;\leq\; \mathbb{E}^{\mathrm{f}}_{\Omega^{*,\delta}}[\sigma_{v_1}\sigma_{v_2}]\,,$$

convergence results (3.4.34), (3.4.19), and from Lemma 3.4.14 (applied for both $m < 0$ and $m = 0$); see the proof of Theorem 3.4.4.

We define the full-plane correlation functions as

$$\langle\sigma_{u_1}\sigma_{u_2}\rangle_{\mathbb{C}}^{(m)} := \lim_{\Omega\uparrow\mathbb{C}}\langle\sigma_{u_1}\sigma_{u_2}\rangle_{\Omega}^{(m),\mathrm{w}}, \quad \langle\sigma_{u_1}\sigma_{u_2}\rangle_{\mathbb{C}}^{(-m)} := \lim_{\Omega\uparrow\mathbb{C}}\langle\sigma_{u_1}\sigma_{u_2}\rangle_{\Omega}^{(-m),\mathrm{f}},$$

where the limits are taken along arbitrary sequences of smooth domains exhausting the complex plane. These limits exist and are non-trivial since for $\Omega\subset\Omega'$ one has

$$\begin{aligned}\langle\sigma_{u_1}\sigma_{u_2}\rangle_{\Omega}^{(m),\mathrm{w}} &\geq \langle\sigma_{u_1}\sigma_{u_2}\rangle_{\Omega'}^{(m),\mathrm{w}} \geq \langle\sigma_{u_1}\sigma_{u_2}\rangle_{\mathbb{C}} = |u_2-u_1|^{-\frac{1}{4}},\\ \langle\sigma_{u_1}\sigma_{u_2}\rangle_{\Omega}^{(-m),\mathrm{f}} &\leq \langle\sigma_{u_1}\sigma_{u_2}\rangle_{\Omega'}^{(-m),\mathrm{f}} \leq \langle\sigma_{u_1}\sigma_{u_2}\rangle_{\mathbb{C}} = |u_2-u_1|^{-\frac{1}{4}}\end{aligned}$$

due to Theorem 3.4.4 and similar inequalities in discrete. The rotational invariance of the full-plane correlation functions

$$\langle\sigma_{u_1}\sigma_{u_2}\rangle_{\mathbb{C}}^{(m)} = \Xi(|u_2-u_1|,m), \quad m\in\mathbb{R},$$

follows from the rotational invariance of finite-volume correlation functions $(3.4.29)$, $(3.4.30)$ and of the corresponding boundary value problems in large discs. Finally, we have $\Xi(r,m)\sim r^{-\frac{1}{4}}$ as $r\to 0$ due to $(3.4.31)$ and the aforementioned monotonicity with respect to Ω, which allows to pass to the limit $\Omega\uparrow\mathbb{C}$ in these asymptotics.

3.4.6 . Massive model : convergence results

We now discuss generalizations of the results from Section 3.4.3 to the massive setup. Throughout this section we assume that $\Omega\subset\mathbb{C}$ is a C^1-smooth bounded simply connected domain and $m<0$.

As in Section 3.4.3, let v,w be distinct inner points of Ω; recall that we use the same notation for their discrete approximations. Also, let $u=u^\delta\in\Omega^{\circ,\delta}$ be such that $u\sim v=v^\delta\in\Omega^{\bullet,\delta}$ and $b=b^\delta\in\Omega^{\bullet,\delta}$ be such that $b\sim w=w^\delta\in\Omega^{\circ,\delta}$. Consider the normalized real-valued fermionic observable

$$X^{(m),\delta}_{[\Omega^\delta;v,w]}(c) := \frac{\mathbb{E}^{(m),\mathrm{w}}_{\Omega^\delta}[\chi_c\mu_v\sigma_w]}{\mathbb{E}^{(m),\mathrm{w}}_{\Omega^\delta}[\sigma_u\sigma_w]}, \quad c\in\Upsilon^\times_{[v,w]}(\Omega^\delta), \tag{3.4.32}$$

and let $F^{(m),\delta}_{[\Omega^\delta;v,w]}$ be the corresponding massive s-holomorphic spinor in Ω^δ branching over v and w; see Definition 3.3.1.

Theorem 3.4.3. Let $m<0$ and Ω be a C^1-smooth bounded simply connected domain. For each $v,w\in\Omega$, $v\neq w$, the following holds uniformly on compact subsets of $\Omega\setminus\{v,w\}$:

$$F^{(m),\delta}_{[\Omega^\delta;v,w]}(z) \to (\tfrac{2}{\pi})^{\frac{1}{2}} f^{(m)}_{[\Omega;v,w]}(z) \text{ as } \delta\to 0, \tag{3.4.33}$$

where a massive holomorphic spinor $f^{(m)}_{[\Omega;v,w]}$ solves the boundary value problem described in Section 3.4.5. The convergence is also uniform with respect to v,w

provided that v, w, z stay at definite distance from each other and from $\partial\Omega$. Moreover,

$$\frac{\mathbb{E}^{(m),\mathrm{w}}_{\Omega^\delta}[\,\mu_v\mu_b\,]}{\mathbb{E}^{(m),\mathrm{w}}_{\Omega^\delta}[\sigma_u\sigma_w]} \;=\; \frac{\mathbb{E}^{(-m),\,\mathrm{f}}_{\Omega^{*,\delta}}[\sigma_v\sigma_b]}{\mathbb{E}^{(m),\mathrm{w}}_{\Omega^\delta}[\sigma_u\sigma_w]} \;\to\; \mathcal{B}^{(m)}_\Omega(v,w) \quad \text{as} \quad \delta\to 0. \tag{3.4.34}$$

Proof. The proof of (3.4.33) repeats the proof of Theorem 3.4.1, including that of Proposition 3.4.7, which goes through for C^1-smooth domains and $m<0$ as pointed out by Park in [137, Proposition 22] in the square grid context $\Lambda^\delta=\delta\mathbb{Z}^2$. Working with irregular isoradial grids Λ^δ instead, it is worth noting that

- the a priori regularity estimates of massive s-holomorphic functions $F^{(m),\delta}$ via the corresponding functions H^δ are given by Proposition 3.3.11 ;
- sub-sequential limits of massive s-holomorphic functions satisfy the massive holomorphicity equation (3.3.2) due to Corollary 3.3.6 ;
- the proof of Proposition 3.4.7 relies upon
  - the sub-harmonicity of the function $H^{\bullet,\delta}$ discussed in Proposition 3.3.8 (see also Remark 3.3.10) ;
  - the maximum principle for the function $|F^{(m),\delta}|$, which holds true (up to a multiplicative constant) due to Lemma 3.3.12.

The only small difference with the critical case $m=0$ is the analysis near the branching point w and the proof of (3.4.34). Recall that the asymptotics of explicit full-plane kernels $\mathcal{G}^{(m),\delta}_{[w]}$ are given in Theorem 3.3.1. Let c_w be adjacent to both w and b. Then, we can still use Lemma 3.3.14 to see that

$$2X^{(m),\delta}_{[\Omega^\delta;v,w]}(c_w) \;=\; \frac{1}{2}\oint_{z:|z-w|=2r_0}^{[(m),\delta]} \mathrm{Im}\,[F^{(m),\delta}_{[\Omega^\delta;v,w]}(z)\mathcal{G}^{(m),\delta}_{[b]}(z)dz], \tag{3.4.35}$$

where the discrete contour integral in the right-hand side is understood in the sense of Remark 3.3.4. (In particular, note that one can easily estimate the value $X^{(m),\delta}(c_w)$ via the values of $F^{(m),\delta}$ near the contour $\{z:|z-w|=2r_0\}$; in other words, the proof of convergence (3.4.33) literally mimics that of Theorem 3.4.1.)

In order to prove the convergence (3.4.34) note that, for each fixed $r_0>0$, the discrete contour integral in the identity (3.4.35) converges as $\delta\to 0$:

$$X^{(m),\delta}_{[\Omega^\delta;v,w]}(c_w) \underset{\delta\to 0}{\to} \frac{1}{2\pi}\oint_{z:|z-w|=2r_0} \mathrm{Im}\left[f^{(m)}_{[\Omega;v,w]}(z)\cdot e^{-i\frac{\pi}{4}}\frac{e^{2m|z-w|}}{\sqrt{z-w}}dz\right]$$

and that the limit does not depend on r_0. Using the asymptotic expansion (3.4.26) we can write

$$\begin{aligned}&\frac{1}{2\pi}\oint_{z:|z-w|=2r_0} \mathrm{Im}\left[f^{(m)}_{[\Omega;v,w]}(z)\cdot e^{-i\frac{\pi}{4}}\frac{e^{2m|z-w|}}{\sqrt{z-w}}dz\right]\\ =\;&\frac{1}{2\pi}\oint_{z:|z-w|=2r_0} \mathrm{Im}\left[\left(\pm\frac{\mathcal{B}^{(m)}_\Omega(v,w)}{z-w}+O(1)\right)dz\right] \;=\; \pm\mathcal{B}^{(m)}_\Omega(v,w)+O(r_0),\end{aligned}$$

which implies that this quantity equals $\pm\mathcal{B}_\Omega^{(m)}(v,w)$ as it cannot depend on r_0. Therefore, we have the convergence

$$X^{(m),\delta}_{[\Omega^\delta;v,w]}(c_w) \;=\; \frac{\mathbb{E}^{(m),\mathrm{w}}_{\Omega^\delta}[\,\mu_v\mu_b\,]}{\mathbb{E}^{(m),\mathrm{w}}_{\Omega^\delta}[\sigma_u\sigma_w]} \;\to\; \mathcal{B}_\Omega^{(m)}(v,w) \quad \text{as} \quad \delta\to 0,$$

(the $\pm$ sign is fixed by the fact that both sides of (3.4.34) are positive quantities). □

Remark 3.4.15. A careful reader could have noticed that the proof of Theorem 3.4.3 also relies upon the following fact : if $f^{(m)}$ is a massive holomorphic spinor in a punctured vicinity of a branching point w (or, similarly, v), then the boundedness of the function $h := \int \mathrm{Im}[(f^{(m)}(z))^2 dz]$ near w implies that $f^{(m)}(z) = O(|z-w|^{\frac{1}{2}})$. To prove this fact, one can, e. g., first argue that $f^{(m)}(z) = O(|z-w|^{-\frac{1}{2}})$ as $z\to w$ due to standard a priori estimates of $f^{(m)}$ via $h = O(1)$, and then improve this estimate to $O(|z-w|^{\frac{1}{2}})$ by using Bers' similarity principle (e. g., see [137, Lemma 14]).

Similarly to the critical case, it is not hard to deduce from Theorem 3.4.3 the following analogues of Corollary 3.4.10 and Corollary 3.4.11.

Corollary 3.4.16. (i) In the same setup as above, let $u_{0,1}\in\Gamma^\delta$ be two neighboring 'white' vertices adjacent to $v\in\Gamma^{\bullet,\delta}$. Then, the following asymptotics hold :

$$\frac{\mathbb{E}^{(m),\mathrm{w}}_{\Omega^\delta}[\sigma_{u_1}\sigma_w]}{\mathbb{E}^{(m),\mathrm{w}}_{\Omega^\delta}[\sigma_{u_0}\sigma_w]} \;=\; 1+\mathrm{Re}\,\big[(u_1-u_0)\cdot\mathcal{A}_\Omega^{(m)}(v,w)\big]+o(\delta) \quad \text{as} \quad \delta\to 0, \quad (3.4.36)$$

where the error term is uniform with respect to $v,w\in\Omega$ provided that they remain at a definite distance from each other and from $\partial\Omega$.

(ii) Let $\rho>0$ and $u_1,u_2,u_1',u_2'\in\Omega$ be such that $|u_2-u_1|\geq\rho$, $|u_2'-u_1'|\geq\rho$ and assume also that all these four points are at least ρ-away from $\partial\Omega$. Then,

$$\log\frac{\mathbb{E}^{(m),\mathrm{w}}_{\Omega^\delta}[\sigma_{u_1'}\sigma_{u_2'}]}{\mathbb{E}^{(m),\mathrm{w}}_{\Omega^\delta}[\sigma_{u_1}\sigma_{u_2}]} \;\to\; \int_{(u_1,u_2)}^{(u_1',u_2')}\mathrm{Re}\,\big[\,\mathcal{A}_\Omega^{(m)}(v,w)dv+\mathcal{A}_\Omega^{(m)}(w,v)dw\,\big] \quad \text{as} \quad \delta\to 0,$$

where the integral can be computed along any smooth path $(v_t,w_t)\in\Omega\times\Omega$ such that, for all t, the points v_t,w_t stay at distance at least ρ from each other and from $\partial\Omega$.

Proof. (i) Similarly to the proof of Corollary 3.4.10 and the proof of Theorem 3.4.3(ii), for each $r_0>0$ we can write the identity

$$\begin{aligned}\frac{\mathbb{E}^{(m),\mathrm{w}}_{\Omega^\delta}[\sigma_{u_1}\sigma_w]}{\mathbb{E}^{(m),\mathrm{w}}_{\Omega^\delta}[\sigma_{u_0}\sigma_w]}-1 \;&=\; X^{(m),\delta}_{[\Omega^\delta;v,w]}(c_1)-X^{(m),\delta}_{[\Omega^\delta;v,w]}(c_0)\\ &=\; \frac{1}{4}\oint_{z:|z-v|=2r_0}^{[(m),\delta]}\mathrm{Im}\,[F^{(m),\delta}_{[\Omega^\delta;v,w]}(z)\cdot(\mathcal{G}^{(m),\delta}_{[u_1]}(z)-\mathcal{G}^{(m),\delta}_{[u_0]}(z))dz]\,,\end{aligned}$$

where $c_{0,1}$ is adjacent to both $v \in \Omega^{\bullet,\delta}$ and $u_{0,1} \in \Omega^{\circ,\delta}$, and the discrete contour integral in the right-hand side is understood in the sense of Remark 3.3.4. Since $R(z,u)$ in the asymptotics given in Theorem 3.3.1 is a Lipshitz function of the second argument, for each fixed $r_0 > 0$ we have a (uniform in z) asymptotics

$$\begin{aligned}\mathcal{G}^{(m),\delta}_{[u_1]}(z) \;-\; \mathcal{G}^{(m),\delta}_{[u_0]}(z) \;&=\; e^{i\frac{\pi}{4}}\left(\frac{2}{\pi}\right)^{\frac{1}{2}}\left[\frac{e^{-2m|z-u_1|}}{\sqrt{z-u_1}} - \frac{e^{-2m|z-u_0|}}{\sqrt{z-u_0}}\right] + O(\delta^2)\\ &=\; e^{i\frac{\pi}{4}}\left(\frac{2}{\pi}\right)^{\frac{1}{2}}\frac{e^{-2m|z-v|}}{\sqrt{z-v}}\cdot\left[\frac{u_1-u_0}{2(z-v)} + \frac{2m\,\mathrm{Re}[(z-v)(\overline{u}_1-\overline{u}_0)]}{|z-v|}\right] + O(\delta^2)\,.\end{aligned}$$

At the same time, Theorem 3.4.3(i) and the definition (3.4.28) imply that

$$F^{\delta}_{[\Omega^\delta;v,w]}(z) \;=\; e^{-i\frac{\pi}{4}}\left(\frac{2}{\pi}\right)^{\frac{1}{2}}\frac{e^{2m|z-v|}}{\sqrt{z-v}}\cdot\left[1+2\mathcal{A}^{(m)}_{\Omega}(v,w)(z-v)+O(r_0^2)\right]+o_{\delta\to 0}(1),$$

uniformly in z, where the error term $O(r_0^2)$ does not depend on δ.

It is easy to see that the contour integrals $\oint \ldots dz$ of functions $(z-v)^{-2}$, $|z-v|^{-1}$ and $|z-v|(z-v)^{-2}$ along a circle centered at v vanish. Therefore,

$$\begin{aligned}&\delta^{-1}\cdot\left[\frac{\mathbb{E}^{\mathrm{w}}_{\Omega^\delta}[\sigma_{u_1}\sigma_w]}{\mathbb{E}^{\mathrm{w}}_{\Omega^\delta}[\sigma_{u_0}\sigma_w]} - 1\right]\\ &\qquad=\; \frac{1}{2\pi}\oint_{z:|z-v|=2r_0}\mathrm{Im}\left[\left(\frac{\delta^{-1}(u_1-u_0)\mathcal{A}^{(m)}_{\Omega}(v,w)}{z-v} + O(1)\right)dz\right] + o_{\delta\to 0}(1)\\ &\qquad=\; \mathrm{Re}\left[\delta^{-1}(u_1-u_0)\mathcal{A}^{(m)}_{\Omega}(v,w)\right] + o_{\delta\to 0}(1)\end{aligned}$$

since the $O(1)$ term in the integrand gives a contribution $O(r_0)$, which does not depend on δ and can be made as small as needed before choosing δ small enough.

(ii) The proof repeats the proof of Corollary 3.4.11 and boils down to multiplying the asymptotics (3.4.36) along discrete paths going from (u_1,u_2) to (u_1',u_2'). □

The next theorem, in particular, provides an analogue of Corollary 3.4.12 in the massive case. Note that we change the order of statements as compared to Section 3.4.3 and prove this result *before* the analogue of Theorem 3.4.2. This shortcut is possible due to the fact that we can now use the critical model in order to control the multiplicative normalization of spin-spin correlations in Ω^δ and do not need to consider the full-plane limit first (as it was in the proof of Corollary 3.4.12).

Theorem 3.4.4. (i) Let $m < 0$ and Ω be a C^1-smooth bounded simply connected domain. Then, one can define a function $\langle\sigma_{u_1}\sigma_{u_2}\rangle^{(m),\mathrm{w}}_{\Omega}$ according

to (3.4.28) such that the asymptotics $\langle\sigma_{u_1}\sigma_{u_2}\rangle_\Omega^{(m),\mathrm{w}} \sim |u_2-u_1|^{-\frac{1}{4}}$ as $u_2 \to u_1$ holds for each $u_1 \in \Omega$.

(ii) Let discrete domains $\Omega^\delta \subset \Gamma^\delta$ approximate $\Omega \subset \mathbb{C}$ in the Hausdorff sense so that $\mathrm{dist}(\partial\Omega^\delta;\partial\Omega) = O(\delta)$. Then, for each $u, w \in \Omega$, $u_1 \neq u_2$, one has the convergence

$$\begin{array}{rcll} \delta^{-\frac{1}{4}}\mathbb{E}^{(m),\mathrm{w}}_{\Omega^\delta}[\sigma_u\sigma_w] & \to & \mathcal{C}_\sigma^2\cdot\langle\sigma_u\sigma_w\rangle_\Omega^{(m),\mathrm{w}}, & \\ \delta^{-\frac{1}{4}}\mathbb{E}^{(-m),\mathrm{f}}_{\Omega^\delta}[\sigma_u\sigma_w] & \to & \mathcal{C}_\sigma^2\cdot\langle\sigma_u\sigma_w\rangle_\Omega^{(-m),\mathrm{f}} & \text{as } \delta\to 0, \end{array}$$

where the limits (continuous correlation functions) are defined by (3.4.29)–(3.4.31), and the universal constant $\mathcal{C}_\sigma = 2^{\frac{1}{6}}e^{\frac{3}{2}\zeta'(-1)}$ does not depend neither on m nor on Λ^δ.

Proof. (i) It immediately follows from Corollary 3.4.16 that the differential form

$$\mathcal{L}_\Omega^{(m)}(v,w) \;:=\; \mathrm{Re}\,[\mathcal{A}_\Omega^{(m)}(v,w)dv + \mathcal{A}_\Omega^{(m)}(w,v)dw],$$

defined on the set $\{(v,w)\in\Omega\times\Omega : v\neq w\}$, is exact. Now note that

$$1 \le \frac{\mathbb{E}^{(m),\mathrm{w}}_{\Omega^\delta}[\sigma_{u_1}\sigma_{u_2}]}{\mathbb{E}^{\mathrm{w}}_{\Omega^\delta}[\sigma_{u_1}\sigma_{u_2}]} \le \frac{\mathbb{E}^{(m),\mathrm{w}}_{\Omega^\delta}[\sigma_{u_1}\sigma_{u_2}]}{\mathbb{E}^{(-m),\mathrm{f}}_{\Omega^{*,\delta}}[\sigma_{v_1}\sigma_{v_2}]}\cdot\frac{\mathbb{E}^{\mathrm{f}}_{\Omega^{*,\delta}}[\sigma_{v_1}\sigma_{v_2}]}{\mathbb{E}^{\mathrm{w}}_{\Omega^\delta}[\sigma_{u_1}\sigma_{u_2}]} \underset{\delta\to 0}{\to} \frac{\mathcal{B}_\Omega(u_1,u_2)}{\mathcal{B}_\Omega^{(m)}(u_1,u_2)} \tag{3.4.37}$$

due to the monotonicity of spin-spin correlations with respect to the interaction parameters, Theorem 3.4.3(ii) and Corollary 3.4.8. Together with Lemma 3.4.14 this gives the estimate

$$\limsup_{\delta\to 0}\left|\log\frac{\mathbb{E}^{(m),\mathrm{w}}_{\Omega^\delta}[\sigma_{u_1'}\sigma_{u_2'}]}{\mathbb{E}^{(m),\mathrm{w}}_{\Omega^\delta}[\sigma_{u_1}\sigma_{u_2}]} - \log\frac{\mathbb{E}^{\mathrm{w}}_{\Omega^\delta}[\sigma_{u_1'}\sigma_{u_2'}]}{\mathbb{E}^{\mathrm{w}}_{\Omega^\delta}[\sigma_{u_1}\sigma_{u_2}]}\right| \;=\; o_{u_2\to u_1}(1) + o_{u_2'\to u_1'}(1)$$

and hence, by passing to the limit $\delta\to 0$ and applying Corollary 3.4.16(ii) and Corollary 3.4.10, we have

$$\int_{(u_1,u_2)}^{(u_1',u_2')} (\mathcal{L}_\Omega^{(m)}(v,w) - \mathcal{L}_\Omega(v,w)) \;=\; o_{u_2\to u_1}(1) + o_{u_2'\to u_1'}(1),$$

where $\mathcal{L}_\Omega(v,w) := \mathcal{L}_\Omega^{(0)}(v,w) = d\langle\sigma_v\sigma_w\rangle^{\mathrm{w}}_\Omega$. Therefore, one can choose a primitive

$$\mathcal{R}_\Omega^{(m)} \;:=\; \exp\textstyle\int(\mathcal{L}_\Omega^{(m)} - \mathcal{L}_\Omega)$$

so that it is continuous up to the diagonal $u_1 = u_2$ and, moreover, $\mathcal{R}_\Omega^{(m)}(u,u) = 1$ for all $u\in\Omega$. We can now define $\langle\sigma_{u_1}\sigma_{u_2}\rangle_\Omega^{(m),\mathrm{w}} := \mathcal{R}_\Omega^{(m)}(u_1,u_2)\cdot\langle\sigma_{u_1}\sigma_{u_2}\rangle^{\mathrm{w}}_\Omega$.

(ii) Given $u, w\in\Omega$, let us also consider another pair points $u', w'\in\Omega$ such that the distance $|w'-u'|$ is small. Combining Corollary 3.4.16 and the esti-

mate (3.4.37) applied to u' and w' we see that

$$\begin{aligned}\frac{\langle\sigma_u\sigma_w\rangle_\Omega^{(m),\mathrm{w}}}{\langle\sigma_{u'}\sigma_{w'}\rangle_\Omega^{(m),\mathrm{w}}} &\le \liminf_{\delta\to0}\frac{\mathbb{E}_{\Omega^\delta}^{(m),\mathrm{w}}[\sigma_u\sigma_w]}{\mathbb{E}_{\Omega^\delta}^{\mathrm{w}}[\sigma_{u'}\sigma_{w'}]}\\ &\le \limsup_{\delta\to0}\frac{\mathbb{E}_{\Omega^\delta}^{(m),\mathrm{w}}[\sigma_u\sigma_w]}{\mathbb{E}_{\Omega^\delta}^{\mathrm{w}}[\sigma_{u'}\sigma_{w'}]} \le \frac{\langle\sigma_u\sigma_w\rangle_\Omega^{(m),\mathrm{w}}}{\langle\sigma_{u'}\sigma_{w'}\rangle_\Omega^{(m),\mathrm{w}}}\cdot(1+o_{w'\to u'}(1))\end{aligned}$$

Using the convergence $\delta^{-\frac14}\mathbb{E}_{\Omega^\delta}^{\mathrm{w}}[\sigma_{u'}\sigma_{w'}]\to\mathcal{C}_\sigma^2\cdot\langle\sigma_{u'}\sigma_{w'}\rangle_\Omega^{\mathrm{w}}$ (see Corollary 3.4.12) and the fact that $\langle\sigma_{u'}\sigma_{w'}\rangle_\Omega^{(m),\mathrm{w}}\sim\langle\sigma_{u'}\sigma_{w'}\rangle_\Omega^{\mathrm{w}}$ as $w'\to u'$, the previous estimate can be written as

$$\begin{aligned}\mathcal{C}_\sigma^2\cdot\langle\sigma_u\sigma_w\rangle_\Omega^{(m),\mathrm{w}}\cdot(1-o_{w'\to u'}(1)) &\le \liminf_{\delta\to0}\delta^{-\frac14}\mathbb{E}_{\Omega^\delta}^{(m),\mathrm{w}}[\sigma_u\sigma_w]\\ \le \limsup_{\delta\to0}\delta^{-\frac14}\mathbb{E}_{\Omega^\delta}^{(m),\mathrm{w}}[\sigma_u\sigma_w] &\le \mathcal{C}_\sigma^2\cdot\langle\sigma_u\sigma_w\rangle_\Omega^{(m),\mathrm{w}}\cdot(1+o_{w'\to u'}(1)).\end{aligned}$$

By choosing first w' close enough to u' and then δ small enough this implies the convergence $\delta^{-\frac14}\mathbb{E}_{\Omega^\delta}^{(m),\mathrm{w}}[\sigma_u\sigma_w]\to\mathcal{C}_\sigma^2\cdot\langle\sigma_u\sigma_w\rangle_\Omega^{(m),\mathrm{w}}$.

Finally, a similar result for $\delta^{-\frac14}\mathbb{E}_{\Omega^\delta}^{(-m),\mathrm{f}}[\sigma_u\sigma_w]$ follows from the Kramers–Wannier duality, convergence (3.4.34), and the convergence of spin-spin correlations in the dual isoradial model with wired boundary conditions. □

We conclude this section by deducing the convergence of the spin-spin correlations in the full plane from Theorem 3.4.4.

Corollary 3.4.17. Let $u,w\in\mathbb{C}$ and $m\in\mathbb{R}\setminus\{0\}$. Then, uniformly with respect to isoradial grids Λ^δ satisfying the uniformly bounded angles property $\mathrm{BAP}(\theta_0)$, we have the convergence

$$\delta^{-\frac14}\mathbb{E}_{\Lambda^\delta}^{(m)}[\sigma_u\sigma_w]\ \to\ \mathcal{C}_\sigma^2\cdot\Xi(|u-w|,m)\ \text{ as }\ \delta\to0,$$

where

$$\Xi(|u-w|,m)\ =\ \langle\sigma_u\sigma_w\rangle_{\mathbb{C}}^{(m)}\ =\ \begin{cases}\lim_{\Omega\uparrow\mathbb{C}}\langle\sigma_u\sigma_w\rangle_\Omega^{(m),\mathrm{w}} & \text{if } m<0,\\ \lim_{\Omega\uparrow\mathbb{C}}\langle\sigma_u\sigma_w\rangle_\Omega^{(m),\mathrm{f}} & \text{if } m>0.\end{cases}$$

Proof. Let $B_R^\delta\subset\Lambda^\delta$ denote the discretization of the disc $B_R:=B(\frac12(u+w),R)\subset\mathbb{C}$. For $m<0$, it follows from the RSW estimates (3.2.10) that

$$\mathbb{E}_{\Lambda^\delta}^{(m)}[\sigma_u\sigma_w]\ =\ \mathbb{E}_{B_R^\delta}^{(m),\mathrm{w}}[\sigma_u\sigma_w]\cdot(1+o_{R\to\infty}(1))\ \text{ as }\ R\to\infty,$$

uniformly in δ. By definition of the infinite-volume correlations in continuum,

$$\langle\sigma_u\sigma_w\rangle_{\mathbb{C}}^{(m)}\ =\ \langle\sigma_u\sigma_w\rangle_{B_R}^{(m)}\cdot(1+o_{R\to\infty}(1)).$$

Finally, for each fixed R, Theorem 3.4.4(ii) provides the asymptotics

$$\delta^{-\frac{1}{4}}\mathbb{E}^{(m),\mathrm{w}}_{B_R^\delta}[\sigma_u\sigma_w] \;=\; \mathcal{C}_\sigma^2\cdot\langle\sigma_u\sigma_w\rangle^{(m)}_{B_R}\cdot(1+o_{\delta\to0}(1)).$$

Choosing first R big enough and then δ small enough we obtain the required convergence of the infinite-volume correlations in the case $m<0$.

The proof for $m>0$ is similar and relies upon the convergence of the finite-volume correlations $\delta^{-\frac{1}{4}}\mathbb{E}^{(m),\mathrm{f}}_{B_R^\delta}[\sigma_u\sigma_w]$, which is also given by Theorem 3.4.4(ii). □

3.5 . Construction and asymptotic analysis of full-plane kernels

In this section, we construct and analyze massive s-holomorphic functions

— $\mathcal{F}_1,\mathcal{F}_i$ (discrete analogues of $e^{-2m\,\mathrm{Im}\,z}$ and $ie^{2m\,\mathrm{Im}\,z}$; see Theorem 3.3.2), which were used to construct an s-embedding in Section 3.3.3 ;

— $\mathcal{G}_{[v]}$, $\mathcal{G}_{[u]}$ (discrete analogues of $e^{\mp i\pi/4}\cdot z^{-1/2}e^{\pm2m|z|}$; see Theorem 3.3.1), which are the main tool used in our paper ;

— massive Cauchy kernels $\mathcal{G}_{(a)}$, where $a\in\Upsilon^\times$ is a (lift onto $\Upsilon^\times$ of a) given edge of Λ ; see Section 3.5.2 and, in particular, Remark 3.5.7 for more details.

Although not strictly necessary for the present paper, the latter kernel $\mathcal{G}_{(a)}$ can be used to establish the regularity of massive s-holomorphic functions (see [138] and the proof of Proposition 3.3.11) and also to prove the convergence of energy correlations ; we thus include its construction and analysis for reference purposes.

For shortness, *from now onwards we omit the superscripts* $(m),\delta$ *in the notation.* Also, in this section we prefer to work with $q=\frac{1}{2}m\delta>0$ in order to keep the moduli $k,K(k),K'(k)$ real ; for $q<0$ it suffices to apply the Kramers–Wannier duality.

Remark 3.5.1. Recall that this duality amounts to exchanging the lattices $\Gamma^{\bullet,\delta}\leftrightarrow\Gamma^{\circ,\delta}$ and, simultaneously, changing the sign of q and m. In order to keep the definition of η_c and of massive s-holomorphic functions invariant under this procedure, one also needs to simultaneously replace the global prefactor ς in (3.2.1) by $\pm i\varsigma$; note that this also leaves the equation $\overline{\partial}f+\varsigma^2m\overline{f}=0$ unchanged. In order to keep this dependence on ς transparent, we do *not* rely upon the explicit convention $\varsigma=e^{i\frac{\pi}{4}}$ in what follows and formulate all results in a slightly more invariant way.

The results given below are formulated in terms of real-valued spinors $\mathcal{X}_1$, $\mathcal{X}_i$, $\mathrm{G}_{[v]}$, $\mathrm{G}_{[u]}$, $\mathrm{G}_{(a)}$ satisfying the three-terms identity (5.2.6) rather than in terms of massive s-holomorphic functions $\mathcal{F}_1$, $\mathcal{F}_i$, $\mathcal{G}_{[v]}$, $\mathcal{G}_{[u]}$, $\mathcal{G}_{(a)}$ themselves ; recall that the correspondence between the two is provided by Definition 3.3.1.

3.5.1 . Discrete exponentials

We heavily rely upon the existence of particular solutions to the three-terms equation (5.2.6) on isoradial graphs, the *discrete exponentials*. At criticality, they were first introduced by Mercat [129] and Kenyon [99], and for $q \neq 0$ by Boutillier, de Tilière and Raschel [27]. In this section, we review their construction, with slight modifications made in order to fit our setup.

Given $c \in \Upsilon^\times$ (i. e., a lift onto the double cover of the mid-point of an edge $(u(c)v(c))$ of the rhombic lattice Λ with $u(c) \in \Gamma^\circ$ and $v(c) \in \Gamma = \Gamma^\bullet$), let

$$\alpha_c \;:=\; \arg(v(c) - u(c)).$$

Note that these angles are typically denoted by $\overline{\alpha}_c$ in [27, 28, 164], similarly to the notation $\overline{\theta}_e$ for the half-angles of rhombi that we used above. However, we prefer to simply write α_c and $\theta_e := \overline{\theta}_e$ throughout this section in order not to create a confusion with the complex conjugation. At the same time, we will use the notation

$$\check{\alpha}_c := \tfrac{2K}{\pi}\alpha_c \qquad \text{and} \qquad \check{\theta}_e := \tfrac{2K}{\pi}\theta_e \tag{3.5.1}$$

for the "elliptic" quantities that are denoted by α_c and θ_e in [27, 28, 164].

We start by recalling the construction of discrete exponentials in the *critical* Ising model, i. e., if $m = 0$ and $\widehat{\theta}_e = \theta_e = \check{\theta}_e$. Given $\lambda \in \mathbb{C} \smallsetminus \{0\}$, we set

$$\begin{aligned}
\mathbf{e}(\lambda\,; v(c), c) \;&:=\; \bar{\varsigma}\eta_c \cdot (2\lambda)^{-1/2} \cdot (1 + \lambda \cdot (v(c) - c)) \\
&=\; (2e^{i\alpha_c}\lambda)^{-1/2} \cdot (1 + \tfrac{\lambda}{2}(v(c) - u(c))), \qquad (3.5.2)\\
\mathbf{e}(\lambda\,; u(c), c) \;&:=\; \bar{\varsigma}\eta_c \cdot (2\lambda)^{-1/2} \cdot (1 + \lambda \cdot (u(c) - c)) \\
&=\; (2e^{i\alpha_c}\lambda)^{-1/2} \cdot (1 - \tfrac{\lambda}{2}(v(c) - u(c))), \qquad (3.5.3)
\end{aligned}$$

and $\mathbf{e}(\lambda\,; c, v(c)) := \mathbf{e}(\lambda\,; v(c), c)^{-1}$, $\mathbf{e}(\lambda\,; c, u(c)) := \mathbf{e}(\lambda\,; u(c), c)^{-1}$, where the additional factors $\bar{\varsigma}\eta_c$ and $(2\lambda)^{-1/2}$ are introduced to fit the forthcoming definition outside of criticality ; see (3.5.4–3.5.5) and Remark 3.5.4. We then define

$$\mathbf{e}(\lambda\,; x, x_0) := \prod_{k=1}^{N} \mathbf{e}(\lambda\,; x_k, x_{k-1}), \quad x, x_0 \in \Lambda \cup \Upsilon^\times,$$

the product is taken over an arbitrary path $x_0 \sim x_1 \sim \cdots \sim x_N = x$, where x_k and x_{k-1} are adjacent points of $\Upsilon^\times$ and Λ (or vice versa). Note that, using the path of just two steps, we get

$$\mathbf{e}(\lambda\,; v(c), u(c)) \;=\; \frac{1 + \frac{\lambda}{2}(v(c) - u(c))}{1 - \frac{\lambda}{2}(v(c) - u(c))},$$

recovering the usual definition of discrete exponentials on Λ as in [99]. This also shows that $\mathbf{e}(\lambda\,; x, x_0)$ does not depend on the path chosen. In particular,

— for fixed λ and x_0, the discrete exponential $\mathbf{e}(\lambda\,; \cdot, x_0)$ is a well-defined function on Λ and a well-defined spinor on $\Upsilon^\times$;

— for fixed x, x_0, the discrete exponential $\mathbf{e}(\cdot\,; x, x_0)$ is a well-defined function of $\lambda \in \mathbb{C} \smallsetminus \{0\}$ if both $x, x_0 \in \Lambda$ or both $x, x_0 \in \Upsilon^\times$, and is a spinor branching over $\lambda = 0$ if one of x, x_0 belongs to Λ and the other to $\Upsilon^\times$.

Lemma 3.5.2. For each $x_0 \in \Lambda \cup \Upsilon^\times$ and $\lambda \in \mathbb{C} \smallsetminus \{0\}$, the complex-valued spinor $\mathbf{e}(\lambda\,; \cdot, x_0) : \Upsilon^\times \to \mathbb{C}$ satisfies the three-terms identity (5.2.6) with $\widehat{\theta}_e = \theta_e = \check{\theta}_e$.

Proof. Denoting $X_{pq} := \mathbf{e}(\lambda\,; c_{pq}, x_0)$ and $\alpha_{pq} := \alpha_{c_{pq}}$ (see Fig. 3.2.2), we have

$$X_{01} = X_{00} \cdot \frac{e^{-\frac{i\alpha_{00}}{2}} \cdot (1 + \frac{\lambda\delta}{2} e^{i\alpha_{00}})}{e^{-\frac{i\alpha_{01}}{2}} \cdot (1 + \frac{\lambda\delta}{2} e^{i\alpha_{01}})}; \quad X_{10} = X_{00} \cdot \frac{e^{-\frac{i\alpha_{00}}{2}} \cdot (1 - \frac{\lambda\delta}{2} e^{i\alpha_{00}})}{e^{-\frac{i\alpha_{10}}{2}} \cdot (1 - \frac{\lambda\delta}{2} e^{i\alpha_{10}})}.$$

Taking into account that $\alpha_{01} = \alpha_{00} + 2\theta_e$ and $\alpha_{10} = \alpha_{00} - \pi + 2\theta_e$, the required identity (5.2.6) boils down to an elementary identity

$$1 + \tfrac{\lambda\delta}{2} e^{i(\alpha_{00} + 2\theta_e)} \;=\; e^{i\theta_e} \cdot (1 + \tfrac{\lambda\delta}{2} e^{i\alpha_{00}}) \cdot \cos\theta_e \;-\; i e^{i\theta_e} \cdot (1 - \tfrac{\lambda\delta}{2} e^{i\alpha_{00}}) \cdot \sin\theta_e,$$

which is straightforward to check. □

We now proceed to defining the discrete exponentials outside criticality, following [27, 28, 164]; recall that in this section we assume that $q > 0$ and hence $k, k' \in (0, 1)$ and the complete elliptic integrals of the first kind $K(k), K'(k)$ are real; the opposite case follows from the Kramers–Wannier duality.

Throughout this section to each "elliptic" variable (e. g., $\check{\nu} \in \mathbb{T}(k)$) that can be an argument of an elliptic function corresponds a "Euclidean" variable ν that can be plugged into a trigonometric function and vice versa; the relation is (cf. (3.5.1))

$$\check{\nu} \;=\; \tfrac{2K}{\pi}\nu.$$

Given a value $\frac{1}{2}\check{\mu} \in \mathbb{T}(k) := \mathbb{C}/(4K\mathbb{Z} + 4iK'\mathbb{Z})$ and $c \in \Upsilon^\times$, define

$$\mathbf{e}(\check{\mu} \,|\, k\,; v(c), c) \;:=\; (k')^{\frac{1}{4}} \cdot \mathrm{sd}\left(\tfrac{1}{2}(\check{\mu} - \check{\alpha}_c) \,|\, k\right), \tag{3.5.4}$$

$$\mathbf{e}(\check{\mu} \,|\, k\,; u(c), c) \;:=\; -i(k')^{-\frac{1}{4}} \cdot \mathrm{cd}\left(\tfrac{1}{2}(\check{\mu} - \check{\alpha}_c) \,|\, k\right). \tag{3.5.5}$$

Recall that $\mathrm{sd}\,(\check{w} + 2K \,|\, k) \;=\; -\mathrm{sd}\,(\check{w} \,|\, k)$ and $\mathrm{cd}\,(\check{w} + 2K \,|\, k) \;=\; -\mathrm{cd}\,(\check{w} \,|\, k)$, hence the quantities (3.5.4–3.5.5) change the sign under the transform $\alpha_c \mapsto \alpha_c + 2\pi$. This is why they are defined for $c \in \Upsilon^\times$ (and not for $c \in \Upsilon$), similarly to (3.5.2–3.5.3). Let us also emphasize the fact that the functions (3.5.4–3.5.5) of $\frac{1}{2}\mu \in \mathbb{T}(k)$ are *not* well-defined on the torus $\mu \in \mathbb{T}(k)$ itself, rather being *spinors* on $\mathbb{T}(k)$; see (3.5.7–3.5.9).

As in the critical case, we extend the definition of $\mathbf{e}(\check{\mu} \,|\, k\,; x, x_0)$ to arbitrary $x, x_0 \in \Lambda \cup \Upsilon^\times$ by multiplying along paths. In particular, this gives

$$\mathbf{e}(\check{\mu} \,|\, k\,; v(c), u(c)) \;=\; i\sqrt{k'} \cdot \mathrm{sc}\left(\tfrac{1}{2}(\check{\mu} - \check{\alpha}_c) \,|\, k\right). \tag{3.5.6}$$

as in [27, Eq.15]. Since $\mathrm{sc}\,(w+2K\,|\,k)=\mathrm{sc}\,(w\,|\,k)$, the latter expression is actually independent on the choice of the lift of c onto $\Upsilon^\times$. Moreover, the identity

$$\mathrm{sc}\,(\check{w}+K\,|\,k)\,\mathrm{sc}\,(\check{w}\,|\,k)\;=\;-(k')^{-1}$$

(see [134, Eq. 22.4.3]) guarantees that multiplying (3.5.6) around a quad yields 1. This proves that $\mathbf{e}(\check{\mu}\,|\,k\,;x,x_0)$ is independent of the choice of the path.

For a fixed x_0 and a fixed $c\in\Upsilon^\times$, the periodicity properties of the discrete exponential $\mathbf{e}(\cdot):=\mathbf{e}(\cdot\,|\,k\,;c,x_0)$, easily read off [134, Eq. 22.4.1], are as follows :

$$\mathbf{e}(\check{\mu}+4K)=\mathbf{e}(\check{\mu})=\mathbf{e}(\check{\mu}+4iK') \qquad \text{if } x_0=c_0\in\Upsilon^\times; \tag{3.5.7}$$

$$-\mathbf{e}(\check{\mu}+4K)=\mathbf{e}(\check{\mu})=\mathbf{e}(\check{\mu}+4iK') \qquad \text{if } x_0=u\in\Gamma^\circ; \tag{3.5.8}$$

$$-\mathbf{e}(\check{\mu}+4K)=\mathbf{e}(\check{\mu})=-\mathbf{e}(\check{\mu}+4iK') \qquad \text{if } x_0=v\in\Gamma^\bullet. \tag{3.5.9}$$

Lemma 3.5.3 ([28, Proposition 36])**.** The discrete exponentials $c\mapsto\mathbf{e}(\check{\mu}\,|\,k\,;c,x_0)$ satisfy the propagation equation (5.2.6) on $\Upsilon^\times$ provided that $\sin\widehat{\theta}_e=\mathrm{sc}\left(\check{\theta}_e\,|\,k\right)$.

Proof. Similarly to the proof of Lemma 3.5.2, this boils down to checking the identity

$$1\;=\;\frac{\mathrm{sd}\left(\frac{1}{2}(\check{\mu}-\check{\alpha}-2\check{\theta})\,|\,k\right)}{\mathrm{sd}\left(\frac{1}{2}(\check{\mu}-\check{\alpha})\,|\,k\right)}\mathrm{cn}\left(\check{\theta}\,|\,k\right)+\;\frac{\mathrm{cd}\left(\frac{1}{2}(\check{\mu}-\check{\alpha}-2\check{\theta})\,|\,k\right)}{\mathrm{cd}\left(\frac{1}{2}(\check{\mu}-\check{\alpha}-2\check{K})\,|\,k\right)}\mathrm{sn}\left(\check{\theta}\,|\,k\right).$$

Denote $\check{w}:=\frac{1}{2}(\check{\mu}-\check{\alpha})$. Since $\mathrm{cd}\,(\check{w}-K\,|\,k)=\mathrm{sn}\,(\check{w}\,|\,k)$, this is equivalent to

$$\mathrm{sn}\,(\check{w}\,|\,k)\;=\;\mathrm{sd}\left(\check{w}-\check{\theta}\,|\,k\right)\mathrm{cn}\left(\check{\theta}\,|\,k\right)\mathrm{dn}\,(\check{w}\,|\,k)+\mathrm{cd}\left(\check{w}-\check{\theta}\,|\,k\right)\mathrm{sn}\left(\check{\theta}\,|\,k\right).$$

The latter identity follows from the fact that the two sides are co-periodic (see [134, Eq. 22.4.1]), and have the same poles and residues. Namely, by [134, Eq. 22.5.1], the LHS has a pole at iK' with residue $\frac{1}{k}$, while the RHS has a pole at iK' with residue $-i\mathrm{cn}\,(\theta\,|\,k)\,\mathrm{sd}\,(iK'-\theta\,|\,k)$, and at $K+iK'+\theta$ with residue

$$-i(kk')^{-1}\mathrm{cn}\,(\theta\,|\,k)\,\mathrm{dn}\,(K+iK'+\theta\,|\,k)-k^{-1}\mathrm{sn}\,(\theta\,|\,k)\,;$$

the former expression equals to $\frac{1}{k}$ and the latter to 0 by [134, Table 22.4.3]. □

Remark 3.5.4. Note that our modified definition (3.5.2–3.5.3) of discrete exponentials at criticality is nothing but a particular case of the more general elliptic construction (3.5.4–3.5.5) corresponding to $k=0$, $k'=1$, $K=\frac{\pi}{2}$, $K'=+\infty$. More precisely, the limiting form of (3.5.4–3.5.5) as $\delta=1$ and $k\to 0$ is

$$\mathbf{e}(\mu\,|\,0\,;v(c),c)\;=\;\sin\tfrac{1}{2}(\mu-\alpha_c)\;=\;\tfrac{1}{2i}e^{-\frac{i}{2}\alpha_c}e^{i\frac{\mu}{2}}\cdot(1-e^{-i\mu}e^{i\alpha_c}),$$

$$\mathbf{e}(\mu\,|\,0\,;u(c),c)\;=\;-i\cdot\cos\tfrac{1}{2}(\mu-\alpha_c)\;=\;\tfrac{1}{2i}e^{-\frac{i}{2}\alpha_c}e^{i\frac{\mu}{2}}\cdot(1+e^{-i\mu}e^{i\alpha_c}),$$

which coincides with (3.5.2–3.5.3) if $e^{-i\mu}=-\frac{1}{2}\lambda$. Thus, we have the identity

$$\mathbf{e}(\mu\,|\,0\,;x,x_0)\;=\;\mathbf{e}(-2e^{-i\mu}\,;x,x_0)\;\;\text{provided that}\;\;\delta=1. \tag{3.5.10}$$

3.5.2 . Definition and basic properties of the full-plane kernels

In this section we introduce real-valued spinors

— $\mathcal{X}_1$, $\mathcal{X}_i$ defined on $\Upsilon^\times$;

— $\mathrm{G}_{[u]}$, $\mathrm{G}_{[v]}$ (where $u \in \Gamma^\circ$ and $v \in \Gamma^\bullet$) defined on $\Upsilon^\times_{[u]}$ and $\Upsilon^\times_{[v]}$, respectively ;

— and the massive Cauchy kernel $\mathrm{G}_{(a)}$, where $a \in \Upsilon^\times$, defined on the double cover $\Upsilon^\times_{(a)} := \Upsilon^\times_{[v(a),u(a)]}$, which can be naturally identified with $\Upsilon^\times$ except the two lifts of the corner a itself ; see Fig. 3.5.1 and Remark 3.5.7 below.

These spinors satisfy (see Proposition 3.5.8 below) the propagation equation $(5.2.6)$, which allows one to construct massive s-holomorphic functions $\mathcal{F}_1$, $\mathcal{F}_i$, $\mathcal{G}_{[u]}$, $\mathcal{G}_{[v]}$, and $\mathcal{G}_{(a)}$ out of them via Definition 3.3.1.

For $w_1, w_2 \in \mathbb{C}$ such that $w_1 \neq w_2$, denote

$$\varphi_{w_1 w_2} := \arg(w_1 - w_2), \qquad \check{\varphi}_{w_1 w_2} := \tfrac{2K}{\pi} \cdot \varphi_{w_1 w_2}.$$

Also, let $o \in \Gamma^{\circ,\delta}$ be the closest to the origin vertex of $\Gamma^{\circ,\delta}$. We define

$$\delta^{-\frac{1}{2}} \mathcal{X}_1(c) := -ik^{-1} \cdot \mathbf{e}(\tfrac{4K}{\pi} \arg \varsigma + 2iK' \,|\, k \,; c, o)\,, \tag{3.5.11}$$

$$\delta^{-\frac{1}{2}} \mathcal{X}_i(c) := -ik^{-1} \cdot \mathbf{e}(\tfrac{4K}{\pi} \arg \varsigma - 2K + 2iK' \,|\, k \,; c, o)\,; \tag{3.5.12}$$

$$\mathrm{G}_{[u]}(c) := -\frac{(k')^{\frac{1}{4}}}{2\pi} \int_{\check{\varphi}_{cu}-2iK'}^{\check{\varphi}_{cu}+2iK'} \mathbf{e}(\check{\mu} \,|\, k \,; c, u)\, d\check{\mu}\,, \tag{3.5.13}$$

$$\mathrm{G}_{[v]}(c) := -\frac{i(k')^{\frac{1}{4}}}{2\pi} \int_{\check{\varphi}_{cv}-2K-2iK'}^{\check{\varphi}_{cv}+2K+2iK'} \mathbf{e}(\check{\mu} \,|\, k \,; c, v)\, d\check{\mu}\,; \tag{3.5.14}$$

$$\mathrm{G}_{(a)}(c) := \frac{i}{2\pi} \int_{\check{\varphi}_{ca}-2iK'}^{\check{\varphi}_{ca}+2iK'} \frac{\mathbf{e}(\check{\mu} \,|\, k \,; c, a)}{\mathrm{cd}\left(\frac{1}{2}(\check{\mu} - \check{\alpha}_a) \,|\, k\right) \mathrm{sn}\left(\frac{1}{2}(\check{\mu} - \check{\alpha}_a) \,|\, k\right)}\, d\check{\mu}\,; \tag{3.5.15}$$

where the integrals in (3.5.13–3.5.15) are computed along *straight* segments : vertical in $(3.5.13)$, $(3.5.15)$ and 'diagonal' in $(3.5.14)$. Note that the integrands are meromorphic functions of $\check{\mu}$, so one only has to specify the homotopy classes of the paths of integration with respect to the poles of discrete exponentials $\mathbf{e}(\cdot \,|\, k \,; c, x_0)$, which belong to the set $\mathrm{Im}\, \check{\mu} \in 4K'\mathbb{Z}$ due to (3.5.4–3.5.6).

It is not hard to see that symmetries of the elliptic functions involved imply that all the quantities (3.5.11–3.5.15) are real. However, note that one can avoid checking this fact by taking the real part in the above definitions ; this operation is obviously compatible with the propagation equation $(5.2.6)$ and with asymptotics (3.5.26–3.5.30) discussed below.

We begin by listing several important comments on the definitions (3.5.13–3.5.13).

Remark 3.5.5. Because of (3.5.7–3.5.9) and [134, Table 22.4.3], each of the three integrals in (3.5.13–3.5.15) is half the integral over the twice longer

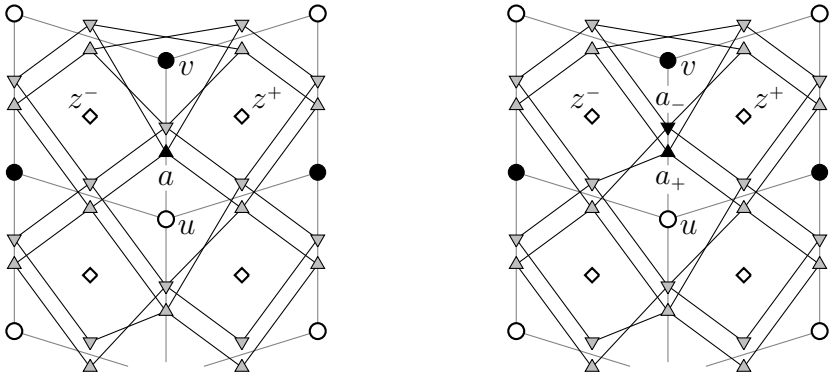

FIGURE 3.5.1 – Given $a \in \Upsilon^\times$ (shown as a black triangular node in the left picture), the double cover $\Upsilon^\times_{(a)} = \Upsilon^\times_{[v(a),u(a)]}$ (shown on the right) can be identified with $\Upsilon^\times$ except at the lifts of a. We choose $a_+ \in \Upsilon^\times_{(a)}$ so that the branching structure of the two double covers around the quad z^+ is the same, and similarly for a_- and z^-.

(vertical or 'diagonal') segment, which can be thought of as a period of the twice bigger torus $\check{\mu} \in \mathbb{C}/(8K\mathbb{Z} + 8iK'\mathbb{Z})$ on which the integrand is naturally defined.

Remark 3.5.6. The fact that the spinors $\mathrm{G}_{[u]}(c)$, $\mathrm{G}_{[v]}(c)$ are defined on $\Upsilon^\times_{[u]}$, $\Upsilon^\times_{[v]}$, respectively (and not simply on $\Upsilon^\times$) follows from the anti-periodicity (3.5.8-3.5.9) of discrete exponentials in the horizontal direction and the fact that $\check{\varphi}_{cu}$ increases by $\frac{2K}{\pi} \cdot 2\pi = 4K$ when c makes a turn around u; see also Proposition 3.5.8 below.

Remark 3.5.7. Definition (3.5.15) of the kernel $\mathrm{G}_{(a)}(c)$ does not make sense for $c = a$; this corresponds to the fact that the double covers $\Upsilon^\times$ and $\Upsilon^\times_{(a)}$ have different branching structures near a. Let $a_+ \in \Upsilon^\times_{(a)}$ (resp., a_-) be such that, if one identifies it with $a \in \Upsilon^\times$, then the two double covers have the same structure around the quad $z^\pm$ lying to the right (resp., to the left) of $(u(a)v(a))$ as in (3.3.6); see Fig. 3.5.1. To define $\mathrm{G}_{(a)}(c)$ for $c = a^\pm$ we choose some $\varphi_{a_\pm a}$ so that

$$\varphi_{a_+ a} - \varphi_{v(a)u(a)} \ \in \ (-\pi, 0), \qquad \varphi_{a_- a} - \varphi_{v(a)u(a)} \ \in \ (0, \pi)$$

and use the same definition (3.5.15) with $\mathbf{e}(\check{\mu} \,|\, k\,; a_\pm, a) := 1$; it is easy to see that the result actually does not depend on the choices of $\check{\varphi}_{a_+ a} \in (\check{\alpha}_a - 2K, \check{\alpha}_a)$ and $\check{\varphi}_{a_- a} \in (\check{\alpha}_a, \check{\alpha}_a + 2K)$. Note that $\mathrm{G}_{(a)}(a_+) = -\mathrm{G}_{(a)}(a_-)$ due to [134, Table 22.4.3].

Proposition 3.5.8. (i) The spinors (3.5.13–3.5.15) satisfy the propagation equation (5.2.6) on $\Upsilon^{\times}_{[u]}$, $\Upsilon^{\times}_{[v]}$ and $\Upsilon^{\times}_{(a)}$, respectively; in the latter case one should use the value at a_+ (resp., at a_-) to recover the equation to the right (resp., to the left) of $(u(a)v(a))$.

(ii) Let $c \in \Upsilon^{\times}$ and assume that the angle $\varphi_{cu} = \arg(c-u)$, $u = u(c)$, is chosen so that $\frac{1}{2}\varphi_{cu} = \frac{1}{2}\alpha_c$. (Recall that this condition corresponds to specifying one of the two sheets of the double cover $\Upsilon^{\times}_{[u]}$ around u; cf. Remark 3.5.6.) Then, $\mathrm{G}_{[u(c)]}(c) = 1$ for all $k \in (0,1)$.

(iii) A similar identity $\mathrm{G}_{[v(c)]}(c) = 1$ holds under the convention $\frac{1}{2}\varphi_{cv} = \frac{1}{2}(\alpha_c - \pi)$.

(iv) We also have the identity $\mathrm{G}_{(c)}(c_\pm) = \pm 1$ for all $c \in \Upsilon^{\times}$ and $k \in (0,1)$.

Proof. Due to Lemma 3.5.3, the discrete exponentials $c \mapsto \mathbf{e}(\check{\mu} \,|\, k\,; c, x)_0$ satisfy the equation (5.2.6). Therefore so do each of the functions (3.5.13–3.5.15) provided that one can shift the contours of integration used to define its values around a given quad to the same position, not crossing the poles of the integrands. This follows from the same considerations as in [99, Theorem 4.2] and [27, Theorem 12].

For $u = u(c)$, applying [134, Eq. 22.14.7] we obtain the identity

$$\begin{aligned} \mathrm{G}_{[u(c)]}(c) \;&=\; -\frac{i}{2\pi}\int_{\check{\varphi}_{cu}-2iK'}^{\check{\varphi}_{cu}+2iK'} \mathrm{dc}\left(\tfrac{1}{2}(\check{\mu}-\check{\alpha}_c)\,|\,k\right) d\check{\mu} \\ &=\; -\frac{i}{2\pi}\int_{-2iK'}^{2iK'} \mathrm{dc}\left(\tfrac{1}{2}\check{\mu}\,|\,k\right) d\check{\mu} = -\frac{i}{\pi}\log\left(\mathrm{nc}\left(\tfrac{1}{2}\check{\mu}\,|\,k\right)+\mathrm{sc}\left(\tfrac{1}{2}\check{\mu}\,|\,k\right)\right)\Big|_{-2iK'}^{2iK'}. \end{aligned}$$

Note that $\mathrm{nc}\,(\pm iK'\,|\,k) = 0$ and $\mathrm{sc}\,(\pm iK'\,|\,k) = \pm i$; see [134, Eq. 22.5.1, 22.4.3]. Thus, the value $\mathrm{G}_{[u(c)]}(c)$ belongs to the set $1+2\mathbb{Z}$. Since it could only depend continuously on k, in fact it does *not* depend on k at all. The concrete value 1 of the answer can be justified, e. g., by considering the limit

$$\int_{-2iK'}^{2iK'} \mathrm{dc}\left(\tfrac{1}{2}\check{\mu}\,|\,k\right) d\check{\mu} \;\to\; \int_{-i\infty}^{i\infty} \frac{dt}{\cos(t/2)} \;=\; 2\pi i \quad \text{as} \quad k \to 0\,.$$

The computation for $\mathrm{G}_{[v(c)]}(c)$ is similar. For $\mathrm{G}_{(c)}(c_+)$, we get by [134, Eq. 22.13(i)]

$$\frac{i}{2\pi}\int_{-0-2iK'}^{-0+2iK'} \mathrm{dc}\left(\tfrac{1}{2}\check{\mu}\,|\,k\right)\mathrm{ns}\left(\tfrac{1}{2}\check{\mu}\,|\,k\right) d\mu \;=\; \frac{i}{\pi}\log \mathrm{sc}\left(\tfrac{1}{2}\check{\mu}\,|\,k\right)\Big|_{-0-2iK'}^{-0+2iK'} \;\in\; 1+2\mathbb{Z}$$

and, once again, the choice of the value 1 can be justified by considering $k \to 0$. □

3.5.3 . Asymptotics at criticality

Before analyzing the asymptotics of the full-plane kernels (3.5.28–3.5.30) in the massive regime, let us first briefly discuss the degenerate case $q = 0$ and $\delta = 1$.

Changing the variable $\lambda := -2e^{-i\mu}$ according to (3.5.10) (see also [27, Remark 13]), one sees that in this case (3.5.13) reads as

$$\mathrm{G}_{[u]}(c) \;=\; -\frac{i}{2\pi}\int_{(\overline{u}-\overline{c})\mathbb{R}_+}\frac{\mathbf{e}(\lambda\,;c,u)}{\lambda}\,d\lambda \;=\; -\frac{i}{2\pi}\int_{(\overline{u}-\overline{c})\mathbb{R}_+}\frac{\mathbf{e}(2\lambda\,;c,u)}{\lambda}\,d\lambda\,.$$

The behaviour of these integrals for $|c-u|\gg\delta=1$ is governed by the behavior of the integrands near 0 and ∞ (e. g., see [99] or [47, Appendix]). Note that we have

$$\begin{aligned}\lambda^{-1}\mathbf{e}(2\lambda\,;c,u) \;&=\; \lambda^{-1}\mathbf{e}(2\lambda\,;c,u(c))\cdot\mathbf{e}(2\lambda\,;u(c),u)\\ &=\; 2\varsigma\overline{\eta}_c\cdot\lambda^{-\frac{1}{2}}\cdot\exp\left[2(c-u)\lambda+O(\lambda^2)+O(|c-u|\lambda^3)\right]\;\text{ as }\;\lambda\to 0.\end{aligned}$$

since $\mathbf{e}(2\lambda\,;v,u)=\exp\left[2\lambda(v-u)+O(\lambda^3)\right]$ for $u\sim v$ and thus only the first factor contributes to the $O(\lambda^2)$ term. A similar computation shows that

$$\lambda^{-1}\mathbf{e}(2\lambda\,;c,u) \;=\; -2\overline{\varsigma}\eta_c\cdot\lambda^{-\frac{3}{2}}\cdot\exp\left[2(\overline{c}-\overline{u})\lambda^{-1}+O(\lambda^{-2})+O(|c-u|\lambda^{-3})\right]$$

as $\lambda\to\infty$. Using the Laplace method as in [99, 47, 57] one obtains asymptotics

$$\begin{aligned}\mathrm{G}_{[u]}(c) \;&=\; -\tfrac{i}{\pi}\cdot\left[\varsigma\overline{\eta}_c\cdot(2(u-c))^{-\frac{1}{2}}-\overline{\varsigma}\eta_c\cdot\overline{(2(u-c))^{-\frac{1}{2}}}\right]\cdot\Gamma(\tfrac{1}{2})+O(|c-u|^{-\frac{5}{2}})\\ &=\; (\tfrac{2}{\pi})^{\frac{1}{2}}\,\mathrm{Re}\left[\overline{\eta}_c\cdot\varsigma(c-u)^{-\frac{1}{2}}\right]+O(|c-u|^{-\frac{5}{2}})\end{aligned}$$

as $|c-u|\to\infty$. After an appropriate scaling as $\delta\to 0$, this reads as

$$\mathcal{G}_{[u]}(z) \;=\; \left(\frac{2}{\pi}\right)^{\frac{1}{2}}\cdot\frac{\varsigma}{\sqrt{z-u}}+O(\delta^2|z-u|^{-\frac{5}{2}}),\quad z\in\diamondsuit,$$

in terms of the corresponding s-holomorphic functions $\mathcal{G}_{[u]}$ associated with $\mathrm{G}_{[u]}$ via Definition 3.3.1; this is nothing but asymptotics (3.3.9) for $w=u\in\Gamma^\circ$. A similar result for $\mathrm{G}_{[v]}$, with the multiple $-i\varsigma$ instead of ς, follows by the duality; see Remark 3.5.1.

Remark 3.5.9. A similar analysis at criticality applies to discrete Cauchy kernels

$$\mathrm{G}_{(a)}(c) \;=\; \frac{2ie^{i\alpha_a}}{\pi}\int_{(\overline{a}-\overline{c})\mathbb{R}_+}\frac{\mathbf{e}(2\lambda\,;c,a)}{1-\lambda^2e^{2i\alpha_a}}\,d\lambda\,,$$

a degenerate case of (3.5.15) for $q=0$ and $\delta=1$; see also (3.5.10). Using the Laplace method as above one gets the asymptotics

$$\begin{aligned}\mathrm{G}_{(a)}(c) \;&=\; \tfrac{2i}{\pi}\cdot\left[e^{i\alpha_a}\eta_a\overline{\eta}_c\cdot(2(a-c))^{-1}-e^{-i\alpha_a}\overline{\eta}_a\eta_c\cdot\overline{(2(a-c))^{-1}}\right]+O(|c-a|^{-3})\\ &=\; \tfrac{2}{\pi}\cdot\mathrm{Re}\left[\overline{\eta}_c\cdot\overline{\eta}_a(-i\varsigma^2)(c-a)^{-1}\right]+O(|c-a|^{-3})\end{aligned}$$

as $|c-a|\to\infty$ and $\delta=1$. Again, this results extends to $\delta\to 0$ by scaling arguments and reads as

$$\delta^{-\frac{1}{2}}\mathcal{G}_{(a)}(z) \;=\; \frac{2}{\pi}\cdot\frac{(-i\varsigma^2)\cdot\overline{\eta}_a}{z-a}+O(\delta^2|z-a|^{-3}),\quad z\in\diamondsuit,\qquad(3.5.16)$$

in terms of the corresponding s-holomorphic functions; see Definition 3.3.1.

3.5.4 . Asymptotics and estimates of discrete exponentials

We start with giving a proof of the estimate (3.3.10) for the sub-critical model (i.e., $k > 0$ and $\delta = 1$ are fixed). We need to show that the full plane kernel $\mathrm{G}_{[u]}(c)$, $u \in \Gamma^\circ$, decays exponentially fast as $|c-u| \to \infty$; the required estimate (3.3.10) follows by the duality. Here and below we rely upon the following fact (e. g., see [24, Lemma 17]) :

— Under condition $\mathrm{BAP}(\theta_0)$, given u and c one can find a (so-called *minimal*) nearest-neighbor path $u = w_0 \sim w_1 \sim \ldots \sim w_n$ on Λ with $w_n \sim c$ such that all angles $\varphi_{w_{j+1}w_j} = \arg(w_{j+1} - w_j)$, as well as φ_{cw_n}, belong to a segment of length $\pi - 2\theta_0$ (which also contains the direction φ_{cu}). We denote by φ^Λ_{cu} the midpoint of this segment.

Proof of the estimate (3.3.10). By construction, the function $\mathbf{e}(\cdot \,|\, k\,; c, u)$ does not have poles in the strip $|\operatorname{Re}(\check\mu - \check\varphi^\Lambda_{cu})| \le K - \check\theta_0$, which means that one can replace $\check\varphi_{cu}$ by $\check\varphi^\Lambda_{cu}$ in the definition (3.5.13) of $\mathrm{G}_{[u]}(c)$. Note that the function $\operatorname{sc}(\cdot \,|\, k)$ is analytic in the strip $|\operatorname{Re}\check z| \leqslant \frac12 K$ and periodic in the vertical direction, and that

$$k' \cdot \bigl|\operatorname{sc}(\check z \,|\, k)\bigr|^2 \;=\; k' \cdot \bigl|\operatorname{sc}(\check z \,|\, k)\operatorname{sc}(\check z \mp K \,|\, k)\bigr| \;=\; 1 \quad \text{if} \quad \operatorname{Re} z = \pm\tfrac12 K$$

due to [134, Eq. 22.4.3] and since $\check z \mp K = -\overline{\check z}$ if $\operatorname{Re} z = \pm\frac12 K$. Therefore, the maximum principle gives a simple estimate

$$\xi \;:=\; \sup_{\check z:\,|\operatorname{Re}\check z| \le \frac12 (K - \check\theta_0)} \bigl|i\sqrt{k'} \cdot \operatorname{sc}(\check z \,|\, k)\bigr| < 1. \tag{3.5.17}$$

Due to (3.5.6), we see that $\bigl|\mathbf{e}(\check\mu \,|\, k\,; w_n, u)\bigr| \le \xi^n$ if $\operatorname{Re}\check\mu = \check\varphi^\Lambda_{cu}$. Since $|\varphi_{cw_n} - \varphi^\Lambda_{cu}| \le \frac{\pi}{2}$, the last factor $\mathbf{e}(\check\mu \,|\, k\,; c, w_n)$ is uniformly bounded, which implies that the integrand in (3.5.13) is uniformly exponentially small as $|c-u| \to \infty$. □

We now move on to the massive setup $q = \frac12 m\delta \to 0$, $m > 0$. The asymptotic expansions of elliptic parameters via the nome $q = \exp(-\pi K'/K)$ are, as per [134, Eq. 22.2.1–2 and 20.2.1–4] :

$$\begin{aligned} &k = 4q^{\frac12}(1 - 4q + O(q^2)), \quad && K = \tfrac{\pi}{2}(1 + 4q + 4q^2 + O(q^3)), \\ &k' = 1 - 8q + O(q^2), && K' = -\tfrac12 \log q + O(|q \log q|). \end{aligned} \tag{3.5.18}$$

Similarly to the critical case discussed in the previous section, the main contribution to the integrals (3.5.13–3.5.15) comes from neighborhoods of endpoints of the corresponding segments. It is thus convenient to introduce a shifted variable

$$\check\nu \;:=\; \check\mu - 2iK';$$

recall also that the periodicity (3.5.7–3.5.8) imply that one can compute these integrals over segments lying in the strip $|\operatorname{Im}\check\nu| \le 2K'$ instead of $\operatorname{Im}\check\nu \in [-4K', 0]$.

In terms of the variable $\check\nu$, the definitions (3.5.4–3.5.6) read as (see [134, Eq. 22.4.3])

$$\mathbf{e}(\check\mu\,|\,k\,;v(c),c) \;=\; (k')^{\frac14}\cdot \mathrm{sd}\left(\tfrac12(\check\mu-\check\alpha_c)\,|\,k\right) \;=\; ik^{-1}(k')^{\frac14}\cdot \mathrm{nc}\left(\tfrac12(\check\nu-\check\alpha_c)\,|\,k\right),$$
$$\mathbf{e}(\check\mu\,|\,k\,;u(c),c) \;=\; -i(k')^{-\frac14}\mathrm{cd}\left(\tfrac12(\check\mu-\check\alpha_c)\,|\,k\right) \;=\; -ik^{-1}(k')^{-\frac14}\cdot \mathrm{dc}\left(\tfrac12(\check\nu-\check\alpha_c)\,|\,k\right),$$

which gives

$$\mathbf{e}(\check\mu\,|\,k\,;w_{j+1},w_j) \;=\; -\sqrt{k'}\cdot \mathrm{nd}\left(\tfrac12(\check\nu-\check\varphi_{w_{j+1}w_j})\,|\,k\right) \tag{3.5.19}$$

for all pairs of neighboring vertices $w_j\sim w_{j+1}$ on Λ.

In what follows, we will always have $z=\frac12(\nu-\varphi_{**})$ for some $\varphi_{**}\in\mathbb{R}$. We also introduce a real variable $y\in\mathbb{R}$ by requiring that

$$\mathrm{Im}\,\check z \;=\; \tfrac12\,\mathrm{Im}\,\check\nu \;=\; K'y \quad\Leftrightarrow\quad \mathrm{Im}\,z \;=\; \tfrac12\,\mathrm{Im}\,\nu \;=\; (-\tfrac12\log q)\cdot y\,.$$

Using [134, Eq. 22.2.6 and Eq. 20.2.3–4] and the estimate $|\cos(2nz)|\le q^{-n|y|}$ to bound the higher (i.e., $n\ge 2$) terms in the expansions of the Jacobi theta functions, it is easy to see that the following uniform asymptotics hold :

$$\sqrt{k'}\cdot \mathrm{nd}\,(\check z\,|\,k) \;=\; \frac{\theta_4(z,q)}{\theta_3(z,q)} \;=\; \frac{1-2q\cos(2z)+O(q^{4-2|y|})}{1+2q\cos(2z)+O(q^{4-2|y|})} \quad\text{if}\quad |\,\mathrm{Im}\,\check z|\le K'; \tag{3.5.20}$$

the latter condition is equivalent to say that $|y|\le 1$.

It is worth noting that we only have the estimate $|q\cos(2z)|=O(q^{1-|y|})=O(1)$ if working in the full strip $|\,\mathrm{Im}\,z'|\le K'$, which is obviously not sufficient to develop asymptotic expansions in (3.5.20). (Recall also that the function $\mathrm{nd}\,(\check z\,|\,k)$ has poles on the lines $|\,\mathrm{Im}\,\check z|=K'$.) However, the main contributions to the expressions (3.5.13)–(3.5.15) come from a vicinity of the real line, where such an asymptotic analysis is possible ; see below. In order to neglect the remaining parts of the integrals, we also need an appropriate estimate of (3.5.20) for $|y|\in[\frac12,1]$.

Denote

$$\Pi_{q,\theta_0} \;:=\; \{z=\tfrac{\pi}{2K}\check z\in\mathbb{C}:\,|\,\mathrm{Re}\,\check z|\le \tfrac12 K-\check\theta_0\,,\;\tfrac12K'\le|\,\mathrm{Im}\,\check z|\le K'\}$$

and note that the map $z\mapsto 2q\cos 2z=q\cdot(e^{2iz}+e^{-2iz})$ sends the region Π_{q,θ_0} into the region $\{\zeta\in\mathbb{C}:|\arg\zeta|\leqslant\frac{\pi}{2}-\theta_0\,,\;q^{\frac12}-q^{\frac32}\leqslant|\zeta|\leqslant 1-q^2\}$. Therefore,

$$\log\left|\sqrt{k'}\,\mathrm{nd}\,(\check z\,|\,k)\right| \;\le\; -2(q^{\frac12}-q^{\frac32})\cdot\sin\theta_0+O(q^2) \quad\text{if}\quad z\in\Pi_{q,\theta_0}. \tag{3.5.21}$$

As in the proof of the estimate (3.3.10) discussed above, let us now consider a minimal path $u=w_0\sim w_1\sim\ldots\sim w_n\sim c$, where $n\asymp\delta^{-1}|c-u|$, and apply the estimate (3.5.21) to each of the factors (3.5.19). We see that there exists a constant $\mathrm{cst}(\theta_0)>0$ such that

$$\log|\mathbf{e}(\check\mu\,|\,k\,;c,u)| \;\le -\mathrm{cst}(\theta_0)\cdot q^{-\frac12}\cdot m|c-u| \tag{3.5.22}$$

as $q = \frac{1}{2}m\delta \to 0$, for all $\check{\mu} = \check{\nu} + 2iK'$ such that

$$\operatorname{Re}\check{\nu} = \check{\varphi}^{\Lambda}_{cu} \quad \text{and} \quad K' \le |\operatorname{Im}\check{\nu}| \le 2K'.$$

(Note also that the last factor $\mathbf{e}(\check{\nu} + 2iK' \,|\, k\,; c, w_n)$ is uniformly bounded for such $\check{\nu}$.)

We now move to the analysis of discrete exponentials in the strip $|\operatorname{Im}\check{z}| \le \frac{1}{2}K'$, which corresponds to $|y| \le \frac{1}{2}$. Since $|q\cos(2z)| \le q^{1-|y|}$, in this region the asymptotics (3.5.20) give

$$\mathbf{e}(\check{\mu} \,|\, k\,; w_{j+1}, w_j) \;=\; -\exp\left[-4q\cos(\nu - \varphi_{w_{k+1}w_j}) + O(q^{3-3|y|})\right], \quad (3.5.23)$$

for all edges $w_j \sim w_{j+1}$ of Λ, uniformly in the strip $|\operatorname{Im}\check{z}| \le \frac{1}{2}K'$.

Let $u = w_0 \sim w_1 \sim \ldots \sim w_{2n} = u(c) \sim c$, where $w_j \in \Lambda$ and $n = O(\delta^{-1}|c-u|)$ be a nearest-neighbor path going from u to c. Using [134, Eq. 22.2.3–9 and 20.2.1–4] again, one also sees that

$$\operatorname{cd}(\check{z} \,|\, k) \;=\; \cos(z)\cdot\exp\left[2q - 2q\cos(2z) + O(q^{2-|y|})\right], \qquad |\operatorname{Im}\check{z}| \le \tfrac{1}{2}K',$$

since $|q^{(1+\frac{1}{2})^2}\cos(3z)/\cos z| = O(q^{\frac{9}{4}-|y|})$ and thus the second (and further) terms in the expansion of the Jacobi theta function θ_2 are absorbed into the error term.

It follows from geometric considerations that

$$\textstyle\sum_{j=0}^{2n-1}\cos(\nu - \varphi_{w_{j+1}w_j}) + \frac{1}{2}\cos(\nu - \alpha_c) \;=\; \delta^{-1}|c-u|\cdot\cos(\nu - \varphi_{cu})$$

for all $\nu \in \mathbb{R}$, which is therefore identically true for all $\nu \in \mathbb{C}$. Multiplying asymptotics (3.5.23) along the path $u = w_0 \sim w_1 \sim \ldots \sim w_{2n} = u(c)$ and taking into account the last term

$$\begin{aligned}\mathbf{e}(\check{\mu} \,|\, k\,; c, u(c)) \;&=\; ik\cdot(k')^{\frac{1}{4}}\operatorname{cd}\left(\tfrac{1}{2}(\check{\nu} - \check{\alpha}_c) \,|\, k\right)\\ &=\; ik\cdot\cos(\tfrac{1}{2}(\nu-\alpha_c))\cdot\exp[-2q\cos(\nu-\alpha_c) + O(q^{2-|y|})]\end{aligned}$$

we conclude that

$$\begin{aligned}&\mathbf{e}(\check{\mu} \,|\, k\,; c, u) \qquad\qquad (3.5.24)\\ &\quad=\; ik\cdot\cos(\tfrac{1}{2}(\nu-\alpha_c))\cdot\exp\left[-2m|c-u|\cos(\nu-\varphi_{cu}) + O(q^{2-3|y|})\right]\\ &\quad=\; ik\cdot\exp\left[-2m|c-u|\cos(\nu-\varphi_{uc})\right]\cdot\left(\cos(\tfrac{1}{2}(\nu-\alpha_c)) + O(q^2 e^{\frac{7}{2}|\operatorname{Im}\nu|})\right)\end{aligned}$$

as $q = \frac{1}{2}m\delta \to 0$, uniformly over $|c-u| = O(1)$ and provided that $\check{\mu} = \check{\nu} + 2iK'$ is such that $\operatorname{Im}\check{\nu} = 2K'y$ or, equivalently, $\operatorname{Im}\nu = (-\log q)\cdot y$ with $|y| \le \frac{1}{2}$.

Remark 3.5.10. It is easy to see that the estimate (3.5.22) and the asymptotics (3.5.24) remain true if one replaces $u \in \Gamma^\circ$ by $v \in \Gamma^\bullet$. However, a slightly more accurate consideration is required for the contribution of the

first step $a \sim u(a) = w_0$ to the integrand in the definition (3.5.15) of $\mathcal{G}_{(a)}$, $a \in \Upsilon^\times$. In this case we have

$$\begin{aligned}\frac{\mathbf{e}(\check\mu \,|\, k\,; u(a), a)}{\operatorname{cd}\left(\frac12(\check\mu - \check\alpha_a)\,|\,k\right)\operatorname{sn}\left(\frac12(\check\mu - \check\alpha_a)\,|\,k\right)} &= -i(k')^{-\frac14}\cdot \operatorname{ns}\left(\tfrac12(\check\mu - \check\alpha_a)\,|\,k\right)\\ &= -ik(k')^{-\frac12}\cdot (k')^{\frac14}\operatorname{cd}\left(\tfrac12(\check\nu - \check\varphi_{w_0 a})\,|\,k\right)\end{aligned}$$

due to [134, Eq. 22.4.3] and since $\alpha_a = \varphi_{v(a)a} = \varphi_{u(a)a} - \pi$. This means that $\mathbf{e}(\check\mu \,|\, k\,; c, a)$ admits a similar asymptotics to (3.5.24) with the prefactor $k^2(k')^{-\frac12}$ instead of ik, an additional multiple $\cos(\frac12(\nu - \varphi_{u(a)a})) = \sin(\frac12(\nu - \alpha_a))$ and with the error term $O(q^2 e^{4|\operatorname{Im}\nu|})$ instead of $O(q^2 e^{\frac72|\operatorname{Im}\nu|})$.

3.5.5 . Asymptotics of the massive full-plane kernels (3.5.11–3.5.15)

We are now ready to compute the required asymptotics of the spinors $\mathcal{X}_1$, $\mathcal{X}_i$, G_u, $\mathrm{G}_{[v]}$ and $\mathrm{G}_{(a)}$. In order to formulate the result for the latter one, denote

$$f(z) := (-i\varsigma^2)\cdot 4|m| e^{-i\arg z} K_1(2|mz|), \qquad f^\star(z) := 4im K_0(2|mz|),$$

where K_1 and K_0 are modified Bessel functions of the second kind (see [134, Section 10.25]). Also, let

$$f^{[\eta]}(z) := \tfrac12[\,\overline\eta f(z) + \eta f^\star(z)\,] \quad \text{for} \quad \eta \in \mathbb{C}, \tag{3.5.25}$$

this is a special solution of the massive holomorphicity equation $\overline\partial f + \varsigma^2 m \overline f = 0$ that behaves like a Cauchy kernel $(-i\varsigma^2)\overline\eta\cdot z^{-1}$ at the origin; cf. (3.5.16). Let $m > 0$ be fixed and recall that $K = K(k) = \frac\pi2(1 + 2m\delta + O(\delta^2))$ as $\delta \to 0$; see (3.5.18). We claim that the following asymptotics hold as $q = \frac12 m\delta \to 0$:

$$\delta^{-\frac12}\mathcal{X}_1(c) = \operatorname{Re}\Big[\,\overline\eta_c \cdot e^{-2m\operatorname{Re}[\overline\varsigma^2(c-o)]}\,\Big] + O(\delta^2)\,, \tag{3.5.26}$$

$$\delta^{-\frac12}\mathcal{X}_i(c) = \operatorname{Re}\Big[\,\overline\eta_c \cdot ie^{2m\operatorname{Re}[\overline\varsigma^2(c-o)]}\,\Big] + O(\delta^2)\,; \tag{3.5.27}$$

$$\delta^{-\frac12}\mathrm{G}_{[u]}(c) = K^{-\frac12}\cdot\operatorname{Re}\left[\,\overline\eta_c\cdot\varsigma\frac{e^{-2m|c-u|}}{\sqrt{c-u}}\,\right] + O(\delta^2)\,, \tag{3.5.28}$$

$$\delta^{-\frac12}\mathrm{G}_{[v]}(c) = K^{-\frac12}\cdot\operatorname{Re}\left[\,\overline\eta_c\cdot(-i\varsigma)\frac{e^{2m|c-v|}}{\sqrt{c-v}}\,\right] + O(\delta^2)\,; \tag{3.5.29}$$

$$\delta^{-1}\mathrm{G}_{(a)}(c) = \frac{2}{\pi}\cdot\operatorname{Re}\Big[\,\overline\eta_c f^{[\eta_a]}(c-a)\,\Big] + O(\delta^2)\,, \tag{3.5.30}$$

where (3.5.26–3.5.27) are uniform on compact subsets and (3.5.28–3.5.30) are uniform provided that $|c-w| = O(1)$ and $|c-w|^{-1} = O(1)$, where $w = u, v, a$, respectively. More generally, the same asymptotics hold if $\delta \to 0$ and $q \to 0$ simultaneously so that $m := 2q\delta^{-1}$ stays uniformly bounded away from 0 and ∞.

Remark 3.5.11. Similar asymptotics for $m < 0$ follow by the duality, which amounts to exchanging the lattices $\Gamma^\circ \leftrightarrow \Gamma^\bullet$, changing the sign of q and m, and

replacing ς by $\pm i\varsigma$; see Remark 3.5.1. In particular, note that (3.5.26–3.5.27) provide, via Definition 3.3.1, a proof of Theorem 3.3.2. Similarly, (3.5.28–3.5.29) and Definition 3.3.1 yield Theorem 3.3.1 since $K = \frac{\pi}{2} + O(q)$ as $q \to 0$.

Proof of the asymptotics (3.5.26–3.5.27). This immediately follows from definitions (3.5.11–3.5.12) of the spinors $\mathcal{X}_1$, $\mathcal{X}_i$ and asymptotics (3.5.24) of discrete exponentials. Indeed, for $\nu \in \mathbb{R}$, note that

$$\cos(\tfrac{1}{2}(\nu-\alpha_c)) \;=\; \mathrm{Re}[\,\overline{\eta}_c \cdot \varsigma e^{-i\frac{\nu}{2}}\,] \quad \text{and} \quad |c-o|\cos(\nu-\varphi_{co}) \;=\; \mathrm{Re}[\,e^{-i\nu}(c-o)\,]\,.$$

Therefore, (3.5.24) directly yields (3.5.26–3.5.27). □

Proof of the asymptotics (3.5.28). Recall that, due to periodicity reasons, the integral in (3.5.13) is equal to the integral over a shifted segment $\check{\mu} \in [\check{\varphi}_{cu}; \check{\varphi}_{cu}+4iK']$, i. e., $\nu \in [\check{\varphi}_{cu}-2iK'; \check{\varphi}_{cu}+2iK']$. This contour can be deformed, without crossing the poles of the integrand, to the broken line passing through the points

$$\check{\varphi}^{\Lambda}_{cu} - 2iK'; \quad \check{\varphi}^{\Lambda}_{cu} - iK'; \quad \check{\varphi}_{cu} - iK'; \quad \check{\varphi}_{cu} + iK'; \quad \check{\varphi}^{\Lambda}_{cu} + iK'; \quad \check{\varphi}^{\Lambda}_{cu} + 2iK'.$$

The contribution of the first and the last (vertical) segments to the integral (3.5.13) is stretch-exponentially small as $q \to 0$ due to the estimate (3.5.22). The contribution of horizontal segments at height $\pm iK'$ is also stretch-exponentially small due to the asymptotics (3.5.24) and since $|\varphi^{\Lambda}_{cu} - \varphi_{cu}| \le \frac{\pi}{2} - \theta_0$.

Let $\rho_{cu} := 2m|c-u|$. On the middle segment

$$\mathrm{Re}\,\check{\nu} \;=\; \check{\varphi}_{cu}, \qquad |\,\mathrm{Im}\,\check{\nu}| \;\le\; K'$$

the asymptotics (3.5.24) reads as

$$\mathbf{e}(\check{\mu}\,|\,k\,;c,u) \;=\; ik \cdot \exp\,[-\rho_{cu}\cosh(\mathrm{Im}\,\nu)\,] \cdot \big(\cos(\tfrac{1}{2}(\nu-\alpha_c)) + O(q^2 e^{\frac{7}{2}|\,\mathrm{Im}\,\nu|})\big);$$

Provided that $\rho_{cu} \ge \mathrm{cst} > 0$, this yields the asymptotics

$$\mathrm{G}_{[u]}(c) \;=\; -\frac{(k')^{\frac{1}{4}}}{2\pi} \cdot ik \cdot \frac{2iK}{\pi} \cdot \Big[\int_{-\infty}^{+\infty} e^{-\rho_{cu}\cosh t}\cos(\tfrac{1}{2}(it+\varphi_{cu}-\alpha_c))\,dt + O(q^2)\Big],$$

where $t = \mathrm{Im}\,\nu$ and we used the fact the integrand is stretch-exponentially small in $q \to 0$ outside the segment $|t| \le K' \sim -\frac{1}{2}\log q$.

The leading term can be evaluated explicitly by writing

$$\cos(\tfrac{1}{2}(it+\varphi_{cu}-\alpha_c)) \;=\; \cosh(\tfrac{1}{2}t)\cos(\tfrac{1}{2}(\varphi_{cu}-\alpha_c)) - i\sinh(\tfrac{1}{2}t)\sin(\tfrac{1}{2}(\varphi_{cu}-\alpha_c))$$

and using [134, Eq. 10.32.9 and Eq. 10.39.2], which gives

$$\int_{-\infty}^{+\infty} e^{-\rho_{cu}\cosh t}\cosh(\tfrac{1}{2}t)\,dt \;=\; (2\pi/\rho_{cu})^{\frac{1}{2}} \cdot e^{-\rho_{cu}}. \tag{3.5.31}$$

To complete the proof, it remains to note that (see (3.5.18))

$$\frac{k\,(k')^{\frac14}K}{\pi^2}\cdot\Big(\frac{\pi}{m}\Big)^{\frac12} \;=\; \delta^{\frac12}K^{-\frac12}\cdot(1+O(q^2)) \quad\text{as}\quad q=\tfrac12 m\delta\to 0$$

and that $\cos(\frac12(\varphi_{cu}-\alpha_c))\cdot|c-u|^{-\frac12} = \mathrm{Re}\,[e^{\frac{i}{2}\alpha_c}(c-u)^{-\frac12}] = \mathrm{Re}[\,\overline{\eta}_c\cdot\varsigma\,(c-u)^{-\frac12}]$. □

Proof of the asymptotics (3.5.29). The treatment of $\mathrm{G}_{[v]}(c)$ only differs in the computation of the leading term, which we now perform; recall that the asymptotics (3.5.24) and the estimate (3.5.22) remain true if one replaces $u\in\Gamma^\circ$ by $v\in\Gamma^\bullet$. Instead of the integral

$$\int_{\varphi_{cu}-i\infty}^{\varphi_{cu}+i\infty} e^{-\rho_{cu}\cos(\nu-\varphi_{cu})}\cos(\tfrac12(\nu-\alpha_c))d\nu$$

that gave rise to the leading term in the asymptotics (3.5.28) we now need to consider a similar integral computed, e. g., along the broken line

$$\nu\;\in\;[\varphi_{cv}-i\infty\,;\varphi_{cv}]\,\cup\,[\varphi_{cv}\,;\varphi_{cv}+2\pi]\,\cup\,[\varphi_{cv}+2\pi\,;\varphi_{cv}+2\pi+i\infty]\,.$$

We write this integral as the sum of (a) the integral computed over the vertical line $[\varphi_{cv}-i\infty\,;\varphi_{cv}+i\infty]$ that was already evaluated in (3.5.31), and (b) a similar integral computed over the contour

$$\nu=\varphi_{cv}+it,\quad\text{where}\quad t\;\in\;\Gamma\;:=\;[+\infty\,;0]\,\cup\,[0\,;-2\pi i]\,\cup\,[-2\pi i\,;-2\pi i+\infty]\,;$$

note that we have

$$\cos(\tfrac12(\nu-\alpha_c)) \;=\; \tfrac12(e^{-\frac{t}{2}}e^{\frac{i}{2}(\varphi_{cv}-\alpha_c)}+e^{\frac{t}{2}}e^{-\frac{i}{2}(\varphi_{cv}-\alpha_c)})\,.$$

It follows from [134, Eq. 10.32.12 and Eq. 10.39.1] that

$$\begin{aligned}\int_\Gamma e^{-\rho_{cv}\cosh t}e^{\mp\frac{t}{2}}dt \;&=\; \pm i\int_{+\infty+i\pi}^{+\infty-i\pi} e^{\,\rho_{cv}\cosh t}e^{\mp\frac{t}{2}}dt\\ &=\; \pm 2\pi\cdot I_{\pm\frac12}(\rho_{cv}) \;=\; \pm(2\pi/\rho_{cv})^{\frac12}\cdot(e^{\rho_{cv}}\mp e^{-\rho_{cv}})\,,\end{aligned}$$

which gives

$$\begin{aligned}&\int_\Gamma e^{-\rho_{cv}\cosh t}\cos(\tfrac12(\varphi_{cv}+it-\alpha_c))dt\\ &\qquad=\;(2\pi/\rho_{cv})^{\frac12}\cdot(ie^{\rho_{cv}}\sin(\tfrac12(\varphi_{cv}-\alpha_c))-e^{-\rho_{cv}}\cos(\tfrac12(\varphi_{cv}-\alpha_c)))\,.\end{aligned}$$

The second term cancels out with the contribution (a) of the line $\mathrm{Re}\,\nu=\varphi_{cv}$. Taking into account the additional factor i in (3.5.14) as compared to (3.5.13), we obtain the following expression for the leading term in the asymptotics (3.5.29) :

$$K^{-\frac12}\cdot\sin(\tfrac12(\alpha_c-\varphi_{cv}))|c-v|^{-\frac12}\cdot e^{2m|c-v|}+O(\delta^2)\,.$$

It remains to note that

$$\sin(\tfrac12(\alpha_c-\varphi_{cv}))|c-v|^{-\frac12} \;=\; \mathrm{Im}\,[\varsigma\,\overline{\eta}_c\cdot(v-c)^{-\frac12}] \;=\; \mathrm{Re}\,[\overline{\eta}_c\cdot(-i\varsigma)(v-c)^{-\frac12}].\;\square$$

Proof of the asymptotics (3.5.30). Due to Remark 3.5.10, the integrand in the definition (3.5.15) behaves similarly to the integrand in (3.5.13). Following the same lines as in the proof of (3.5.28) we obtain the asymptotics

$$\mathrm{G}_{(a)}(c) \;=\; \frac{i}{2\pi}\cdot k^2(k')^{-\frac{1}{2}}\cdot\frac{2iK}{\pi}\cdot\Big[\int_{-\infty}^{+\infty} e^{-\rho_{ca}\cosh t}\,V(t)dt + O(q^2)\Big],$$

where $\rho_{ca} = 2m|c-a|$ and

$$\begin{aligned} V(t) \;&=\; \sin(\tfrac{1}{2}(\varphi_{ca}+it-\alpha_a))\cdot\cos(\tfrac{1}{2}(\varphi_{ca}+it-\alpha_c)) \\ &=\; \tfrac{1}{2}\cosh t\cdot\sin(\varphi_{ca}-\tfrac{1}{2}(\alpha_a+\alpha_c)) + \tfrac{i}{2}\sinh t\cdot\cos(\varphi_{ca}-\tfrac{1}{2}(\alpha_a+\alpha_c)) \\ &+\; \tfrac{1}{2}\sin(\tfrac{1}{2}(\alpha_c-\alpha_a)). \end{aligned}$$

Using [134, Eq. 10.32.9] we get

$$\begin{aligned} \int_{-\infty}^{\infty} e^{-\rho\cdot\cosh t}\,V(t)dt \;&=\; K_1(\rho_{ca})\sin(\varphi_{ca}-\tfrac{1}{2}(\alpha_a+\alpha_c)) + K_0(\rho_{ca})\sin(\tfrac{1}{2}(\alpha_c-\alpha_a)) \\ &=\; -K_1(\rho_{ca})\cdot\mathrm{Im}[\,e^{-i\varphi_{ca}}\cdot\varsigma^2\overline{\eta}_c\overline{\eta}_a\,] + K_0(\rho_{ca})\cdot\mathrm{Im}[\,\overline{\eta}_c\eta_a\,] \\ &=\; -\mathrm{Re}\,[\,\overline{\eta}_c\cdot(\overline{\eta}_a\cdot(-i\varsigma^2)e^{-i\varphi_{ca}}K_1(\rho_{ca}) + \eta_a\cdot iK_0(\rho_{ca}))] \\ &=\; -\mathrm{Re}\,[\,\overline{\eta}_c\cdot(2m)^{-1}f^{[\eta_a]}(2m|c-a|)\,], \end{aligned}$$

see definition (3.5.25) of the massive Cauchy kernel $f^{[\eta]}$. Finally, it easily follows from (3.5.18) that

$$\frac{k^2(k')^{-\frac{1}{2}}K}{\pi^2} \;=\; \frac{8q}{\pi}\cdot(1+O(q^2)) \;=\; \frac{4m\delta}{\pi}\cdot(1+O(\delta^2)),$$

which completes the computation. □

4 - Conformal invariance in the Quantum Ising model

This chapter corresponds to the article [110], written with **Jhih-Huang** Li and currently submitted to the arXiv.

Abstract :

We introduce Kadanoff–Ceva order-disorder operators in the quantum Ising model. This approach was first used for the classical planar Ising model [93] and recently put back to the stage [37, 34]. This representation turns out to be equivalent to the loop expansion of Sminorv's fermionic observables and is particularly interesting due to its simple and compact formulation. Using this approach, we are able to extend different results known in the classical planar Ising model, such as the conformal invariance / covariance of correlations and the energy-density, to the spin-representation of the (1+1)-dimensional quantum Ising model.

4.1 . Introduction

The one-dimensional quantum Ising model is a quantum spin chain defined on $\mathbb{Z}$. Given two positive parameters $\tau, \theta > 0$, the interaction of the system is described by the following Hamiltonian,

$$\mathbf{H} = -\theta \sum_{x \sim y} \sigma_x^{(3)} \sigma_y^{(3)} - \tau \sum_{x \in V} \sigma_x^{(1)},$$

acting on the Hilbert space $\bigotimes_{\mathbb{Z}} \mathbb{C}^2$. In the above definition, θ is the intensity of the interaction between neighboring particles and τ is the intensity of the interaction with the transverse field. We recall that the $\frac{1}{2}$-spin Pauli matrices $\sigma^{(1)}$ and $\sigma^{(3)}$ are given by

$$\sigma^{(1)} = \begin{pmatrix} 0 & 1 \\ 1 & 0 \end{pmatrix}, \quad \sigma^{(3)} = \begin{pmatrix} 1 & 0 \\ 0 & -1 \end{pmatrix},$$

which act on the state space of a spin $\mathbb{C}^2 \cong \mathrm{Span}(|+\rangle, |-\rangle)$, where we identify $|+\rangle$ with $(1,0)$ and $|-\rangle$ with $(0,1)$, for instance. The operators $\sigma_x^{(1)}$ is defined by the tensor product which takes the Pauli matrix $\sigma^{(1)}$ at coordinate x and identity operator elsewhere ; the same applies to $\sigma_x^{(3)}$. As consequence, the operator $\mathbf{H}$ makes sense and acts effectively on $\bigotimes_{\mathbb{Z}} \mathbb{C}^2$.

The one-dimensional quantum Ising model is an exactly solvable one-dimensional quantum model [145]. The quantization $e^{-\beta H}$ of the Gibbs measure of the classical Ising model will be the operator of our interest and the ground state, or the limit of the operator when $\beta \to \infty$, is the quantum state, or the probability measure we are interested in.

This ground state has several graphical representations, such as the usual spin-representation, the FK-representation or the random-current representation. Readers may have a look at [89] for a nice and complete exposition on this topic. These representations are useful in interpreting results from the classical Ising model [81, 20, 22, 109], and in particular, it has been shown that the ground state of the one-dimensional quantum Ising model goes through a continuous phase transition at $\rho = \rho_c := 2$ [20, 63].

In this paper, we will tackle a finer study of the behavior of the model at the critical point $\rho_c = 2$ on one side, and the magnetization in the spin subcritical regime on the other side. The main tool is based on an approach of fermionic observables using Kadanoff–Ceva correlators, which, to our knowledge, has not been done yet for the quantum Ising model. This approach allows us to derive, in a more systematic way, local relations of the observables, leading to results for the space-time representation of the quantum model. Similar local relations were obtained previously FK-loop representation [21, 109].

This formalism allows us to derive the horizontal full-plane spin-spin correlations at any temperature, and in any directions at criticality. We also prove the convergence of the energy density (Theorem 4.3.1 and Theorem 4.3.2) and n-spin correlations (Theorem 4.3.7) in simply-connected domains. The last mentioned results have a particularly nice physical interpretation when considering the space-time representation of the one-dimensional quantum Ising model.

Moreover, this approach also provides us a way to compute the magnetization in the spin sub-critical regime, see Theorem 4.7.6.

The paper is organized as follows. In Section 4.2 we recall the definition of the model and its multiple equivalent representations. In Section 4.4, we introduce the Kadanoff–Ceva formalism in the semi-discrete lattice and use it to define mixed-correlators. In Sections 4.5 and 4.6, we recall the main tools to study boundary value problems (BVP) that arise naturally from semi-discrete fermionic observables, and prove the convergence to their continuous counterparts.

Those tools were originally used to prove conformal invariance of the interface on the square lattice [162, 160, 65], which were generalized later to isoradial graphs [48]. Recently, the first author used them in a similar way in the quantum model [109, Sec. 4]. The convergence of BVP allows then to derive the existence and the conformal invariance of the scaling limit. Finally, in Section 4.7, we follow the formalism of [40] to rederive directly in the semi-discrete lattice full-plane asymptotics of correlations.

Acknowledgments J.-H. L. acknowledges support from EPRSC through grant EP/R024456/1. R.M. acknowledges the support from the ANR-18CE40-0033 project DIMERS. This research was initiated during the stay of the second author at the University of Warwick. J.-H. L. is grateful to Nikolaos Zygouras for his support at University of Warwick and to Hugo Duminil-Copin and Stanislav Smirnov for

introducing him to the quantum Ising model. R.M. is grateful to the University of Warwick for its hospitality, Dmitry Chelkak, Sung-Chul Park and Konstantin Izyurov for fruitful discussions.

4.2 . The quantum Ising model

4.2.1 . Semi-discrete graph notations

Here we recall some definitions from [109, Sec. 3.1], given a simply connected domain $\Omega \subseteq \mathbb{C}$ and $\delta > 0$. We write $\Omega_\delta^\bullet$ for the semi-discretized *primal domain* of Ω and Ω_δ° for the dual of $\Omega_\delta^\bullet$, which is called the *dual domain*. Mathematically, one can take for instance $\Omega_\delta^\bullet = \Omega \cap 2\delta(\mathbb{Z} \times \mathbb{R})$ and $\Omega_\delta^\circ = \Omega \cap \delta(2\mathbb{Z}+1) \times \mathbb{R})$. We call the joint domain $\Lambda(\Omega_\delta) = \diamondsuit(\Omega_\delta) := \Omega_\delta^\bullet \cup \Omega_\delta^\circ$ the *medial domain*. The graphs $\Lambda(\Omega_\delta)$ and $\diamondsuit(\Omega_\delta)$ have the same vertex set but are denoted differently to be closer to the current litterature and avoid confusions on local relations of s-holomorphic functions and the primitive of their square. We discuss their graph properties in the following paragraph. In this article, unless otherwise specified, u (resp. v) mostly denotes a point on the primal (resp. dual) lattice.

We say that v and u are neighbours in $\Lambda(\Omega_\delta)$ if they share the same vertical cordinate while their horizontal cordinate only differs by $\pm\delta$. This makes $\Lambda(\Omega_\delta)$ a bipartite graph, whose edges (linking primal to dual vertices) are in bijection with the *corner graph* $\Upsilon(\Omega_\delta)$ (also called *midedge domain* in [109]). Given $p \in \Lambda(\Omega_\delta)$, write p^- (resp. p^+) its closest left (resp. right) vertex in $\Lambda(\Omega_\delta)$ (hence $p^\pm$ belong to the graph which is dual to the one containing p).

A corner c (or a *mid-edge*) is the middle of the segment formed by two neighbours in $\Lambda(\Omega_\delta)$. We write u_c (resp. v_c) its neighboring primal (resp. dual) vertex make the identification $c = (v_c u_c)$. We also write c^- (resp. c^+) the closest left (resp. right) corner with the same vertical cordinate as c. The set of edges linking nearby corners is in bijection with the diamond graph $\diamondsuit(\Omega_\delta)$ i.e. for any neighbouring corners $c_{1,2}$, we set $z := z(c_1, c_2)$ the middle of segment $[c_1 c_2]$, which belongs to $\diamondsuit(\Omega_\delta)$. See Figure 4.2.1.

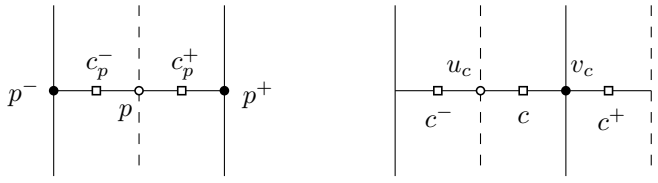

FIGURE 4.2.1 – Notations

4.2.2 . The model

Let Ω be a domain in $\mathbb{C}$. Denote $\Omega_\delta^\bullet$ (resp. Ω_δ°) the semi-discretized primal (resp. dual) domain of Ω. We will study the quantum Ising model defined on $\Omega_\delta^\bullet$ with + boundary condition, or its dual model, the quantum Ising model defined on

Ω_δ° with free boundary condition. Both models are defined as a Radon-Nikodym derivative with respect to some Poisson point processes.

Note that the following probability measures in different representations are only well-defined on bounded domains. For unbounded domains, we follow a classical approach. We construct compatible measures on a sequence of increasing bounded domains whose limit is the unbounded one, and the weak limit of the sequence of measures will be the measure on the unbounded domain.

Given two positive parameters τ and θ. We write $\eta_\tau^\bullet$ to be the Poisson point process of intensity τ on primal lines of $\Omega_\delta^\bullet$. Similary, η_θ° denotes the Poisson point process of intensity θ on dual lines of Ω_δ°. The two Poisson point processes $\eta_\tau^\bullet$ and η_θ° are assumed to be independent. We write $\eta_{\tau,\theta}$ to be the tensor product $\eta_\tau^\bullet \otimes \eta_\theta^\circ$. We also write $\mathrm{Leb}^\bullet$ (resp. Leb°) for the one-dimensional Lebesgue measure on primal lines of $\Omega_\delta^\bullet$ (resp. dual lines of Ω_δ°). We drop the superscript and write Leb if the context is clear.

The FK representation

The FK representation is defined through the Poisson point process $\eta_{\tau,\theta}$. To define the notion of connected components for the FK representation, we shall see the points on primal lines to be death points (denoted D) and the points on dual lines to be bridges (denoted B) connected neighboring lines. As such, the FK measure is given by the Random-Nikodym derivative,

$$\frac{\mathrm{d}\mathbb{E}_{\tau,\theta}^{\mathsf{FK}}(\omega)}{\mathrm{d}\eta_{\tau,\theta}(D,B)} \propto 2^{k(\omega)},$$

where $k(\omega)$ counts the number of connected components in ω with some prescribed boundary condition that is omitted in the above notation.

The space-time spin representation

The space-time spin representation is defined through the Poisson point process $\eta_\tau^\bullet$ on the primal lines. Write D for a (countable) set of points given by this point process, which are called *death points*. A function $\sigma : \Omega_\delta^\bullet \to \{+1, -1\}$ is said to be a *spin configuration* (compatible with D) if it is constant on each connected component of $\Omega_\delta^\bullet \backslash D$. Write $\Sigma(D)$ for the set of spin configurations compatible with D. Note that if $\sigma \in \Sigma(D)$ for some countable set D, then $\sigma \in \Sigma(D')$ for any $D' \supseteq D$. This shows that $\Sigma(D)$ is increasing for inclusion and that $\Sigma(D)$'s are not pairwise disjoint.

The spin measure is characterized as follows. Given a measurable function $F : \bigcup \Sigma(D) \to \mathbb{R}$, its expectation is given by

$$\mathbb{E}_{\tau,\theta}^{\mathsf{spin}}[F(\sigma)] := \frac{\eta_\tau^\bullet \left[\sum_{\sigma \in \Sigma(D)} F(\sigma) \exp\left(-\frac{\theta}{2}\mathcal{H}(\sigma)\right)\right]}{\eta_\tau^\bullet \left[\sum_{\sigma \in \Sigma(D)} \exp\left(-\frac{\theta}{2}\mathcal{H}(\sigma)\right)\right]}, \tag{4.2.1}$$

where $\theta > 0$ and $\mathcal{H}$ denotes the Hamiltonian,

$$\mathcal{H}(\sigma) := -\mathsf{Leb}^\circ(\varepsilon_v), \qquad \text{where} \quad \varepsilon_v = \sigma_{v^+}\sigma_{v^-} \text{ for } v \in \Omega_\delta^\circ.$$

The denominator in the above Equation $(4.2.1)$ is called the *partition function*,

$$Z(\tau,\theta) := \eta_\tau^\bullet\left[\sum_{\sigma\in\Sigma(D)} \exp\left(-\tfrac{\theta}{2}\mathcal{H}(\sigma)\right)\right] = \eta_\tau^\bullet\left[\sum_{\sigma\in\Sigma(D)} \exp\left(\tfrac{\theta}{2}\cdot \mathsf{Leb}^\circ(\varepsilon_v)\right)\right]. \tag{4.2.2}$$

Note that we could have defined $\Sigma'(D)$ to be the subset of $\Sigma(D)$ such that $\sigma \in \Sigma'(D)$ changes value at *every* point of D. As such, $\Sigma'(D)$'s are disjoint and the following Radon-Nikodym derivative makes sense. For $\sigma \in \Sigma'(D)$, one defines

$$\frac{\mathrm{d}\mathbb{E}^{\mathsf{spin}}_{\tau,\theta}(\sigma)}{\mathrm{d}\eta_\tau^\bullet(D)} \propto \exp\left(-\tfrac{\theta}{2}\mathcal{H}(\sigma)\right).$$

In this case, $(4.2.1)$ and $(4.2.2)$ stay the same except that $\Sigma(D)$ is replaced by $\Sigma'(D)$ in the summations.

Additionally, we can define the energy density $\psi_\sigma : \Omega_\delta^\circ \to \{+1,-1\}$ by $\psi_\sigma(v) = \varepsilon_v$ for $v \in \Omega_\delta^\circ$. Let $E_+(\sigma) = \psi_\sigma^{-1}(+1)$, $E_-(\sigma) = \psi_\sigma^{-1}(-1)$ and $S_\pm(\sigma) = \mathsf{Leb}^\circ(E_\pm(\sigma))$. Using the fact that $S_+(\sigma) + S_-(\sigma) = \mathsf{Leb}^\circ(\Omega_\delta^\circ)$ is a constant not depending on σ (but on Ω_δ°) and that $\mathcal{H}(\sigma) = S_+(\sigma) - S_-(\sigma)$, we can rewrite,

$$\frac{\mathrm{d}\mathbb{E}^{\mathsf{spin}}_{\tau,\theta}(\sigma)}{\mathrm{d}\eta_\tau^\bullet(D)} \propto \exp(-\theta S_-(\sigma)) \propto \exp(\theta S_+(\sigma)). \tag{4.2.3}$$

Let A be a subset of points in $\Omega_\delta^\bullet$ and write $\sigma_A = \prod_{x\in A}\sigma_x$ for a spin configuration $\sigma \in \coprod \Sigma'(D) = \bigcup \Sigma'(D)$. We have,

$$\mathbb{E}^{\mathsf{spin}}_{\tau,\theta}(\sigma_A) = \frac{\eta_\tau^\bullet\left[\sum_{\sigma\in\Sigma'(D)} \sigma_A \exp\left(-\theta S_-(\sigma)\right)\right]}{\eta_\tau^\bullet\left[\sum_{\sigma\in\Sigma'(D)} \exp\left(-\theta S_-(\sigma)\right)\right]}, \tag{4.2.4}$$

Random-parity representation

The random-parity representation is particularly useful to write the n-spin correlation in an alternative way. It is defined with respect to the Poisson point process $\eta^\circ_{\theta/2}$ defined on Ω_δ°, which, in the aforementioned FK-representation, can be interpreted as bridges. Write B for a (countable) set of points given by $\eta^\circ_{\theta/2}$. Denote $B^\pm \subseteq \Omega_\delta^\bullet$ the set of extremities of bridges in B, i.e. $B^\pm = \bigcup_{e\in B}\{e^+, e^-\}$.

Consider additionally a finite subset $A \subseteq \Omega_\delta^\bullet$ called *source*. A function $\psi : \Omega_\delta^\bullet \to \{0,1\}$ is said to be a *random-parity function*, with source A and compatible with B, if (a) it is continuous on $\Omega_\delta^\bullet \backslash (A \cup B^\pm)$ and (b) the subgraph $(A \cup B^\pm, \psi^{-1}(1))$ has an even degree at vertices in $B^\pm$ and an odd degree at vertices in A. Define $I(\psi) = \mathsf{Leb}^\bullet(\psi^{-1}(1))$ to be the one-dimension Lebesgue measure of $\psi^{-1}(1)$. Write $\Psi_A(B)$ for the set of such random-parity functions.

The random-parity function being defined for any finite source A, the n-spin correlation reads,

$$\mathbb{E}^{\mathsf{spin}}_{\tau,\theta}(\sigma_A) = \frac{\eta^{\circ}_{\theta/2}\left[\sum_{\psi\in\Psi_A(B)}\exp\left(-2\tau I(\psi)\right)\right]}{\eta^{\circ}_{\theta/2}\left[\sum_{\psi\in\Psi_\varnothing(B)}\exp\left(-2\tau I(\psi)\right)\right]} \tag{4.2.5}$$

Same as we said just after $(4.2.2)$, we could have also defined $\Psi'_A(B)$ (resp. $\Psi'_\varnothing(B)$) with a mandatory discontinuity at *every* point of $A\cup B^{\pm}$ (resp. $B^{\pm}$) and replaced $\Psi_A(B)$ and $\Psi_\varnothing(B)$ with $\Psi'_A(B)$ and $\Psi'_\varnothing(B)$ in $(4.2.5)$.

4.2.3 . FK-spin coupling

Given a spin configuration σ and a FK configuration ω, we say that they are *compatible* if x and y are in the same component in ω, then the spins σ_x and σ_y coincide. Below is the construction of the Edward-Sokal coupling for the quantum Ising model.

Given a FK configuration ω sampled according to $\mathbb{E}^{\mathsf{FK}}_{\tau,\theta}$, define a (random) spin configuration σ in the following way. To each connected component of ω, we choose a spin ($+$ or $-$) uniformly at random. We write $\mathbb{P}_1$ for this measure.

Conversely, given a spin configuration σ sampled according to $\mathbb{E}^{\mathsf{spin}}_{\tau,\theta}$, define a (random) FK configuration ω by adding Poisson points of parameter θ on the dual lines where the neighboring spins coincide, which are bridges connected different components having the same spin. We write $\mathbb{P}_2$ for this measure. Using elementary properties of the Poisson point processes, one can show that the two measures $\mathbb{P}_1$ and $\mathbb{P}_2$ have the same distribution.

4.2.4 . Kramers-Wannier duality

The space-time spin representation and the random-parity representation are dual representations to each other. To be more precise, the space-time spin representation corresponds to the so-called *low-temperature* expansion. A spin configuration defined on $\Omega^{\bullet}_{\delta}$ is in bijection with collection of contours on Ω°_{δ} which appear as interfaces between + and - spins, see Equation $(4.2.3)$ and Figure 4.2.2. As such, the spin measure is exactly the measure defined on the set of contours.

In a similar manner, the random-parity representation corresponds to the so-called *high-temperature* expansion. It does not consist in rewriting the probability measure configuration-wise. Instead, it gives an alternative way to rewrite the n-point correlation, after summing/integrating over spin configurations, using contours and paths as in Equation $(4.2.5)$. An example is given in Figure 4.2.2.

Note that the Kramers-Wannier duality reads as,

$$(\tau^\star,\theta^\star) = (\tfrac{\theta}{2}, 2\tau). \tag{4.2.6}$$

It is an involution, i.e. $((\tau^\star)^\star,(\theta^\star)^\star) = (\tau,\theta)$. The self-dual point is given by $\frac{\tau}{\theta} = 2$ which is also the critical point of the quantum Ising model, see [20, 63].

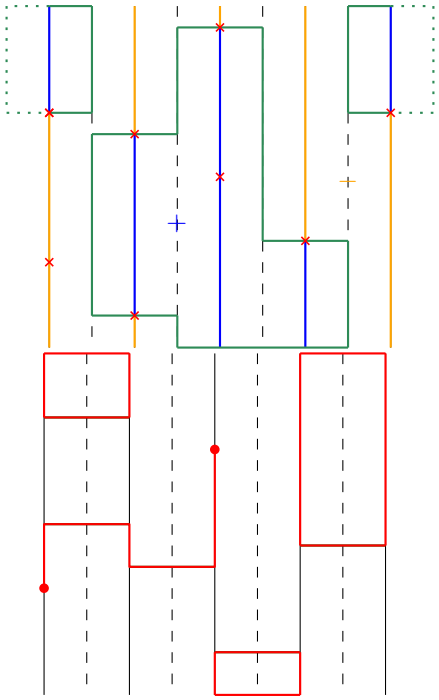

FIGURE 4.2.2 – We work with a primal domain with free boundary condition. **Left :** An example of the space-time spin representation with + spin in blue and - spin in orange. The contours separating different spins are given in green. **Right :** An example of the random-parity representation with source given by two points.

We remind the reader that the "usual" way of talking about sub- or super-criticality differs in the spin- and the FK-representation. Due to the coupling mentioned in Section 4.2.3, the existence of an infinite cluster in the FK-representation is equivalent to a positive spontaneous magnetization. However, in the FK setting, we usually refer this case as *super-critical*, whereas in the spin setting, we usually refer this as *sub-critical*.

4.2.5 . From discrete to semi-discrete

The different representations described above can be seen as their corresponding representations in the classical two-dimension Ising model on a flattened lattice. As shown in Figure 4.2.3, there are two types of edges, long "horizontal" edges of length $\frac{\delta}{2}\cos\frac{\varepsilon}{2}$ and short "vertical" edges of length $\frac{\delta}{2}\sin\frac{\varepsilon}{2}$ in the flattend lattice $\mathcal{G}^\varepsilon$ and we note that when $\varepsilon \to 0$, it "converges" to the semi-discrete lattice.

At discrete level, let us fix the parameters as follows. To each edge e one associates the coupling constant $J_e > 0$ which only depends on the type, horizontal or vertical : each horizontal edge e has the same coupling constant J_h and each vertical edge has the same coupling constant J_v. And we recall that the Hamiltonian

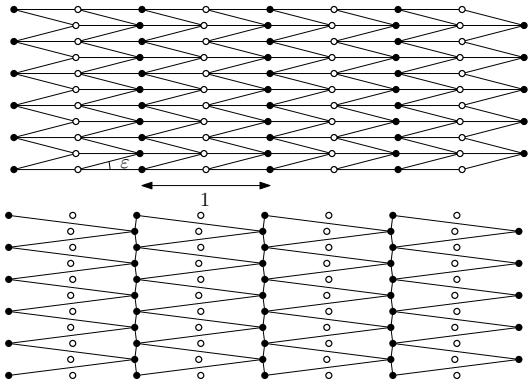

FIGURE 4.2.3 – The flattened lattice $\mathcal{G}^\varepsilon$ which "converges" to the semi-discrete lattice in the limit. **Left :** The isoradial representation (diamond graph) when $\delta = \frac{1}{2}$. **Right :** The primal lattice with dual vertices.

in the discrete model is given by

$$\mathcal{H}(\sigma) = -\sum_{e \in E} J_e \sigma_x \sigma_y, \qquad \text{where } e = (x, y) \text{ for } e \in E.$$

Note that in the above expression, one drops the additional parameter β which is the inverse temperature. One can include it in J_e and the regime of the model (subcritical, critical, supercritical) is thus determined by how the parameters J_e are chosen.

In the low-temperature expansion, a spin configuration is in bijection with a collection of contours in the dual lattice. For each edge e in the primal lattice, the weight of its dual edge is given by $t_e^\star = e^{-2J_e}$. The coupling constatans J_h and J_v are chosen such that $1 - t_h^\star \sim \theta\varepsilon$ and $t_v^\star \sim \tau\varepsilon$. Recall that the dual of a horizontal edge is vertical and vice versa. As such, when the limit $\varepsilon \to 0$ is taken, one obtains contours defined by Poisson Point Processes as weak limit of families of i.i.d. Bernoulli random variables whose parameters are scaled as described above.

In the corresponding high-temperature expansion, we make use of $\tanh(J_e) = \frac{1-t_e^\star}{1+t_e^\star}$. This gives $\tanh(J_h) \sim \frac{\theta}{2}\varepsilon$ and $1 - \tanh(J_v) \sim 2\tau\varepsilon$. Using the same argument to obtain Poisson Point Processes, this also confirms that the dual model is given by parameters as shown in $(4.2.6)$.

Above we describe the procedure from discrete to semi-discrete in the spin-representation. When it comes to the FK-representation, we refer interested readers to [63, Sec. 5.1].

This similarity between the discrete model and the semi-discrete representation of the quantum model suggests that the same results in the classical Ising model are expected to hold in the quantum setting. However, when dealing with universality of results in the discrete setting, one important assumption is the so-called *bounded-angle property*, i.e. angles of the graph need to be uniformly bounded away from

0 and π. This property does not survive in the procedure from discrete to semi-discrete for obvious reasons.

In [63], authors obtained finer estimations in this particular procedure from discrete to semi-discrete, thus extending phase transition results from discrete graphs described in Figure 4.2.3 to the semi-discrete lattice $2\mathbb{Z} \times \mathbb{R}$. This approach might be tempting knowing universality of spin-correlation on isoradial graphs proven in [43], provided they keep the bounded angle-property. Still, in this case, additional difficulties rise due to local normalizing factor appearing before smashing the grid in the vertical direction. Thus, we prefer to present a more straightforward and elegant method by working directly in the semi-discrete setting, following the spirit of [109].

4.3 . Results

In this section, we give a summary of the main results proved in this paper. They are expressed in terms of the space-time spin representation of the quantum Ising model. They also extend a series of results proved on isoradial graphs [87, 83, 38, 43] to the semi-discrete lattice, showing the existence and the conformal covariance of a scaling limit in simply connected domains. Such an extension has previously been made for interfaces in the FK-loop representation [109], but more work is required in this paper for general correlations, one of the reasons being that normalizing factors depending on the mesh size δ of the lattice are now required.

For concision, we mostly state those results for with $+$ boundary conditions, although one can extend them to any boundary condition composed of a finite sequence of boundary arc in $\{+, -, \mathrm{f}\}$ using the theory developped in [39]. For more general boundary conditions, the scaling limit is simply muliplied by a conformally invariant factor. It is also enough to prove the convergence results in smooth domains, since the monotonicity with respect to boundary conditions and approximations by smooth domains allow to prove convergence in general domains once it is done in smooth domains.

Since the (1+1)-dimensional quantum Ising model has several equivalent representations, the results will be stated in the three following settings. Unless otherwise specified, the model is considered at its criticality, i.e., $\theta = \theta^\star$.

1. In Ω_δ, which is the semi-discretization by $2\delta(\mathbb{Z}\times\mathbb{R})$ of a given simply connected domain $\Omega \subset \mathbb{C}$. The quantum Ising measure at the criticality will be denoted by $\mathbb{E}_{\Omega_\delta^\bullet}$ in this case.
2. In $\mathbb{H}_\delta := 2\delta(\mathbb{Z} \times \mathbb{R})$, which can be regarded as the graphical time-evolution of the quantum Ising model on $2\delta\mathbb{Z}$, or as the special case $\Omega = \mathbb{H}$ in the first point. The quantum Ising measure at the criticality will be denoted by $\mathbb{E}_{\mathsf{QI}_\delta}$ in this case.
3. In $\mathcal{R}_\delta(k)$, where $\mathcal{R}_\delta(k)$ stands for the semi-discretization by $2\delta(\mathbb{Z} \times \mathbb{R})$ of $\mathcal{R}(k)$, which is the rectangle defined in Appendix 4.9. We have that

$\mathcal{R}(k) = (-K(k), K(k)) \times (0, K'(k))$, where, for $k \in (0,1)$,

$$K(k) := \int_0^1 \frac{\mathrm{d}s}{\sqrt{(1-s^2)(1-k^2s^2)}}$$

is the complete elliptic integral of the first kind, and $K'(k) = K(\sqrt{1-k^2})$. Since $k \mapsto K(k)/K'(k)$ is a diffeomorphism between $(0,1)$ and $(0,+\infty)$, the set $\{\mathcal{R}(k), k \in (0,1)\}$ describes all the possible aspect ratios of a rectangle. More details are given in Appendix 4.9. This can be understood as the thermodynamic limit of a finite-size quantum Ising model where we scale both the number of vertices and the time together by δ^{-1}. The corresponding quantum Ising measure at the criticality will be denoted by $\mathbb{E}_{\mathsf{QI}_\delta(k)}$.

In the second (resp. the third) setting, due to the natural space-time representation, we introduce some additional notations. For a space-time point (x^δ, t) in $\mathbb{H}_\delta$ (resp. $\mathcal{R}_\delta(k)$

Our first result states the conformal covariance of the horizontal energy density in simply connected domains.

Theorem 4.3.1. *Let $a \in \Omega$ an interior point of a simply connected domain approximated by $a^\delta \in \Omega_\delta^\bullet$. Set $\varepsilon_{a^\delta} := \sigma_{a^\delta}\sigma_{a^\delta+2\delta} - \mathbb{E}^+_{\mathbb{C}_\delta}[\sigma_{a^\delta}\sigma_{a^\delta+2\delta}] = \sigma_{a^\delta}\sigma_{a^\delta+2\delta} - \frac{2}{\pi}$ the* energy density *random variable. For the critical space-time representation of the quantum Ising model, one has*

$$\tfrac{1}{\delta}\,\mathbb{E}^+_{\Omega_\delta^\bullet}[\varepsilon_{a^\delta}] \underset{\delta\to 0}{\longrightarrow} \tfrac{1}{\pi}\ell_\Omega(a), \tag{4.3.1}$$

where $\ell_\Omega(a)$ is the hyperbolic metric of Ω at the point a, i.e. $\ell_\Omega(a)$ is twice *the modulus of the derivative at a of any conformal from $\mathbb{D}$ to Ω vanishing at a. The above convergence is uniform over points remaining at a definite distance from $\partial\Omega$.*

The substraction of the full-plane energy density $\mathbb{E}^+_{\mathbb{C}_\delta}[\sigma_{a^\delta}\sigma_{a^\delta+2\delta}] = \frac{2}{\pi}$ (see Remark 4.7.8) is necessary to underline the influence of the domain Ω. Indeed, using standard Russo-Seymour-Welch type estimates [63] and comparaison between boundary conditions, one can easily see that $\mathbb{E}^+_{\Omega_\delta}[\varepsilon_{a^\delta}] \to 0$ as $\delta \to 0$. The effect of the boundary of Ω reads in the sub-leading term of the expansion of $\mathbb{E}^+_{\Omega_\delta}[\sigma_{a^\delta}\sigma_{a^\delta+2\delta}]$.

One can also state a more general result involving several energy density variables, whose proof is based upon the special case $r = 1$ and the Pfaffian structure of the Ising Model.

Theorem 4.3.2. *Let $a_1, \dots, a_n \in \Omega$ be distinct interior points of Ω, approximated respectively by $a_1^\delta, \dots, a_n^\delta$ in $\Omega_\delta^\bullet$. In the setup of the previous theorem, one has*

$$\tfrac{1}{\delta^n}\,\mathbb{E}^+_{\Omega_\delta^\bullet}[\varepsilon_{a_1^\delta}\dots\varepsilon_{a_n^\delta}] \underset{\delta\to 0}{\longrightarrow} \langle \varepsilon_{a_1}\dots\varepsilon_{a_n}\rangle^+_\Omega, \tag{4.3.2}$$

where the multiple energy correlator is a conformally covariant quantity defined via (4.5.16)*. Moreover, the convergence is uniform over points* $a_1, \dots, a_n$ *remaining at a definite distance from each other and from the boundary.*

Let $\mathbb{K}(a_1, \dots, a_r)$ be the $r \times r$ matrix defined by $\mathbb{K}_{i,j} := \mathbf{1}_{i \neq j}(a_i - a_j)^{-1}$ and denote Pf the usual Pfaffian operator on matrices.

Theorem 4.3.3. *Consider the critical Ising quantum spin chain on* $2\delta\mathbb{Z}$*, fix* $(x_k)_{1 \leqslant k \leqslant r}$ *distinct points of* $\mathbb{R}$ *approximated by* $(x_k^\delta)_{1 \leqslant k \leqslant r}$ *on* $2\delta\mathbb{Z}$*. Fix also a sequence of positive instants* $(t_k)_{1 \leqslant k \leqslant r}$*. For a space-time configuration* (x^δ, t) *in* $2\delta\mathbb{Z} \times \mathbb{R}_+^\star$*, denote* $\varepsilon_{x^\delta}^{(t)} := \sigma_{x^\delta}^{(t)} \sigma_{x^\delta + 2\delta}^{(t)} - \frac{2}{\pi}$ *the horizontal energy density at site* x^δ *at time* t*. On has*

$$\tfrac{1}{\delta}\,\mathbb{E}^+_{\mathrm{QI}_\delta}\big[\varepsilon_{x^\delta}^{(t)}\big] \underset{\delta \to 0}{\longrightarrow} \tfrac{1}{\pi t}, \quad \tfrac{1}{\delta}\,\mathbb{E}^{\mathrm{f}}_{\mathrm{QI}_\delta}\big[\varepsilon_{x^\delta}^{(t)}\big] \underset{\delta \to 0}{\longrightarrow} -\tfrac{1}{\pi t}, \tag{4.3.3}$$

$$\tfrac{1}{\delta^n}\,\mathbb{E}^+_{\mathrm{QI}_\delta}\big[\varepsilon_{x_1^\delta}^{(t_1)} \dots \varepsilon_{x_n^\delta}^{(t_n)}\big] \underset{\delta \to 0}{\longrightarrow} \big(\tfrac{2}{i\pi}\big)^n \mathrm{Pf}\big[\mathbb{K}(x_1 + \mathrm{i}\,t_1, \dots, x_n + \mathrm{i}\,t_n, x_1 - \mathrm{i}\,t_1, \dots, x_n - \mathrm{i}\,t_n)\big],$$

$$\tfrac{1}{\delta}\,\mathbb{E}^+_{\mathrm{QI}_\delta(k)}\big[\varepsilon_{x^\delta}^{(t)}\big] \underset{\delta \to 0}{\longrightarrow} \tfrac{1}{\pi}\tfrac{\mathrm{cn}((\,|\,x) + \mathrm{i}\,t, k)\mathrm{dn}(x + \mathrm{i}\,t, k)}{\mathrm{Im}\,\mathrm{sn}(x + \mathrm{i}\,t, k)}, \tfrac{1}{\delta}\mathbb{E}^{\mathrm{f}}_{\mathrm{QI}_\delta(k)}\big[\varepsilon_{x^\delta}^{(t)}\big] \underset{\delta \to 0}{\longrightarrow} -\tfrac{1}{\pi}\tfrac{\mathrm{cn}(x + \mathrm{i}\,t, k)\mathrm{dn}(x + \mathrm{i}\,t, k)}{\mathrm{Im}\,\mathrm{sn}(x + \mathrm{i}\,t, k)},$$

where cn, dn, sn denote usual Jacobi theta elliptic function, QI^δ *denotes critical the quantum spin chain on* $2\delta\mathbb{Z}$ *while* $QI^\delta(k)$ *denotes the quantum spin chain on* $(-K(k), K(k)) \cap 2\delta\mathbb{Z}$ *until time* $K'(k)$*.*

Remark 4.3.4. The convergence un the upper-half plane is invariant by translation, which comes directly from translation invarariance of the model. One also notices that the energy density blows up near time $t = 0$. For example, in the case of + boundary conditions, both nearby spins involved in the energy density are more likely to be correlated as they feel the + imposed at the boundary when they approach it. With the f boundary conditon, it is the other way around and the nearby spins are less likely to be correlated as approaching the boundary.

We now state the results concerning the general spin-correlations, i.e. the correlations between spins at macroscopic distances from each other.

Theorem 4.3.5. *Let* Ω *be a simply connected domain and* $a_1, \dots, a_n \in \Omega$ *distinct interior points approximated respectively by* $a_1^\delta, \dots, a_n^\delta$ *in* $\Omega_\delta^\bullet$*. Let also* $b_1, \dots, b_n \in \Omega$ *be distinct interior points approximated respectively by* $b_1^\delta, \dots, b_n^\delta$ *in* $\Omega_\delta^\bullet$*. For the critical space-time representation of the quantum Ising model one has*

$$\frac{\mathbb{E}^+_{\Omega_\delta^\bullet}[\sigma_{a_1^\delta} \dots \sigma_{a_n^\delta}]}{\mathbb{E}^+_{\Omega_\delta^\bullet}[\sigma_{b_1^\delta} \dots \sigma_{b_n^\delta}]} \underset{\delta \to 0}{\longrightarrow} \frac{\langle \sigma_{a_1} \dots \sigma_{a_n} \rangle^+_\Omega}{\langle \sigma_{b_1} \dots \sigma_{b_n} \rangle^+_\Omega}, \tag{4.3.4}$$

where the function $\langle \sigma_{(\cdot)} \dots \sigma_{(\cdot)} \rangle^+_\Omega$ *is defined in* (4.5.19)*. The convergence is again uniform over points remaining at a definite distance from each other and from the boundary.*

Using Krammer-Wannier duality and the formalism of disorders (which can be understood as dual-spins), one can also prove the convergence of correlation ratios between primal and dual model.

Theorem 4.3.6. *Let $u_1^\delta \in \Omega_\delta^\bullet$ and $v_1^\delta \in \Omega_\delta^\circ$ approximating $a_1 \in \Omega$ (respectively $u_2^\delta \in \Omega_\delta^\bullet$ and $v_2^\delta \in \Omega_\delta^\circ$ approximating $a_2 \in \Omega$). One has*

$$\frac{\mathbb{E}^{\mathrm{f}}_{\Omega_\delta^\circ}[\sigma_{v_1^\delta}\sigma_{v_2^\delta}]}{\mathbb{E}^{+}_{\Omega_\delta^\bullet}[\sigma_{u_1^\delta}\sigma_{u_2^\delta}]} \underset{\delta\to 0}{\longrightarrow} \mathcal{B}_\Omega(a_1,a_2), \tag{4.3.5}$$

where the coefficient $\mathcal{B}_\Omega(a_1,a_2)$ is defined in (4.5.20) via the expansion of the boundary value problem (4.5.12) near one of its branchings.

Using the last two theorems and an induction, one can recover the convergence of rescaled correlation, with a fully explicit lattice dependant normalization. The next theorem states this complete result.

Theorem 4.3.7. *Set $\mathcal{C} := 2^{\frac{1}{6}} e^{\frac{3}{2}\zeta'(-1)}$. Under the previous hypothesis, given $a_1,\dots,a_n$ interior points of Ω approximated by $a_1^\delta,\dots,a_n^\delta$ in $\Omega_\delta^\bullet$, one has*

$$\delta^{-\frac{n}{8}}\ \mathbb{E}^{+}_{\Omega_\delta^\bullet}[\sigma_{a_1^\delta}\dots\sigma_{a_n^\delta}] \underset{\delta\to 0}{\longrightarrow} \mathcal{C}^n \langle \sigma_{a_1}\dots\sigma_{a_n}\rangle^+_\Omega. \tag{4.3.6}$$

The convergence is uniform over points remaining at a definite distance from each other and from the boundary.

Once the previous theorem is proven, one can compute explicit formulas in specific domains to recover analytic expressions of correlation. Those expressions can be used to compute space-time correlations of the one dimensional quantum Ising model. The next theorem provides those formulas for the two most natural setups.

Theorem 4.3.8. *Consider the critical one dimensional Ising quantum spin chain on $2\delta\mathbb{Z}$. Set $x_1,\dots,x_n$ horizontal cordinates approximatated by $x_1^\delta,\dots,x_n^\delta$ and $t_1,\dots,t_n$ positives times. Let $\sigma^{(t)}_{x^\delta}$ be the spin variable x^δ at time t. One has the space-time spin-spin correlations,*

$$\delta^{-\frac{n}{8}}\ \mathbb{E}^{+}_{\mathrm{QI}_\delta}[\sigma^{(t_1)}_{x_1^\delta}\dots\sigma^{(t_n)}_{x_n^\delta}] \underset{\delta\to 0}{\longrightarrow} \mathcal{C}^n \prod_{r=1}^n (\tfrac{2}{t_r})^{\frac{1}{8}} \Big(2^{-\frac{n}{2}} \sum_{\mu\in\{\pm1\}^n} \prod_{1\leqslant r<m\leqslant n} \Big|\tfrac{(x_r-x_m)^2+(t_r-t_m)^2}{(x_r-x_m)^2+(t_r+t_m)^2}\Big|^{\frac{\mu_r\mu_m}{4}}\Big)^{\frac{1}{2}},$$

$$\frac{\mathbb{E}^{+}_{\mathrm{QI}_\delta(k)}[\sigma^{(t_1)}_{x_1^\delta}\dots\sigma^{(t_n)}_{x_n^\delta}]}{\mathbb{E}^{+}_{\mathrm{QI}_\delta}[\sigma^{(t_1)}_{x_1^\delta}\dots\sigma^{(t_n)}_{x_n^\delta}]} \underset{\delta\to 0}{\longrightarrow} \prod_{j=1}^n |\mathrm{cn}(x_j+it_j,k)\mathrm{dn}(x_j+it_j,k)|.$$

In particular, the one-point function and the two-point function write,

$$\delta^{-\frac{1}{8}}\ \mathbb{E}^{+}_{\mathrm{QI}_\delta}[\sigma^{(t)}_{x}] \underset{\delta\to 0}{\longrightarrow} \mathcal{C}(\tfrac{2}{t})^{\frac{1}{8}},$$

$$\delta^{-\frac{1}{4}}\ \mathbb{E}^{+}_{\mathrm{QI}_\delta}[\sigma^{(t_1)}_{x_1}\sigma^{(t_2)}_{x_2}] \underset{\delta\to 0}{\longrightarrow} \mathcal{C}^2(\tfrac{1}{t_1t_2})^{\frac{1}{8}} \big[\big|\tfrac{(x_1-x_2)^2+(t_1+t_2)^2}{(x_1-x_2)^2+(t_1-t_2)^2}\big|^{\frac{1}{4}} + \big|\tfrac{(x_1-x_2)^2+(t_1-t_2)^2}{(x_1-x_2)^2+(t_1+t_2)^2}\big|^{\frac{1}{4}}\big]^{\frac{1}{2}},$$

$$\delta^{-\frac{1}{4}}\ \mathbb{E}^{\mathrm{f}}_{\mathrm{QI}_\delta}[\sigma^{(t_1)}_{x_1}\sigma^{(t_2)}_{x_2}] \underset{\delta\to 0}{\longrightarrow} \mathcal{C}^2(\tfrac{1}{t_1t_2})^{\frac{1}{8}} \big[\big|\tfrac{(x_1-x_2)^2+(t_1+t_2)^2}{(x_1-x_2)^2+(t_1-t_2)^2}\big|^{\frac{1}{4}} - \big|\tfrac{(x_1-x_2)^2+(t_1-t_2)^2}{(x_1-x_2)^2+(t_1+t_2)^2}\big|^{\frac{1}{4}}\big]^{\frac{1}{2}}.$$

The lattice dependant scaling factor $\delta^{\frac{n}{8}}\mathcal{C}^n$ is obtained by replacing the expectation in bounded regions by the expectation in the full-plane. Theorems 4.3.3 and 4.3.8 can be seen as a byproduct of the space-time interpretation for the critical 1D Ising model, as well as explicit formulas for correlation functions in the upper-half plane and in rectangles.

In the above-mentioned theorems, explicit lattice scaling factors appear and are related to the full-plane asymptotics of the two points functions, which we compute explicitely, already on the semi-discrete lattice. We developp a formalism, close to the one introduced in [40], that allows to derive the desired asymptotics in the vertical direction. Combined with the convergence of correlation ratios mentioned above, it implies in particular the rotational invariance of the critical model, together with its explicit two point function.

Theorem 4.3.9. *For the critical space-time representation of the quantum Ising model in full-plane $\mathbb{C}_1$, one has the asymptotic*

$$\mathbb{E}^+_{\mathbb{C}_1}[\sigma_0\sigma_z] \underset{z\to\infty}{\sim} \mathcal{C}^2|2z|^{-\frac{1}{4}}. \tag{4.3.7}$$

In particular, the critical model is rotationally invariant. The uniqueness of the Gibbs measure at criticality allows to drop $+$ boundary condition at infinity from the definition. We now pass to the results outside of criticality, obtained by the same formalism of Topelitz+Hankle determinants.

Theorem 4.3.10. *For the sub-critical $(\theta < \theta^\star)$ space-time representation of quantum Ising model in $\mathbb{C}_1$ with parameters $(\theta, \theta^\star)$ and $+$ boundary conditions at infinity, the spontaneous magnetization satisfies*

$$\mathcal{M}(\theta,\theta^\star) \ := \lim_{n\to\infty} \mathbb{E}^+_{\mathbb{C}_1}[\sigma_0\sigma_n]^{1/2} \ = \ (\theta^2+\theta^{\star 2})^{-\frac{1}{2}}(1-(\tfrac{\theta}{\theta^\star})^2)^{\frac{1}{8}}. \tag{4.3.8}$$

This result generalizes the full-plane magnetization result below criticality proven for rectangular grids in [40] and in general Z-invariant isoradial graphs with bounded angles in [43]. It is known by [63] that above criticality, the spin-spin correlation decays exponentially fast. In particular, using quasi-multiplicativity arguments, one can see that the so-called *correlation length* [63, Thm. 1.5] in the horizontal direction ξ is well defined. The next result gives its exact value, extending to the horizontal direction the result proved in [14].

Theorem 4.3.11. *For the super-critical $(\theta > \theta^\star)$ quantum Ising model in full-plane $\mathbb{C}_1$ with parameters $(\theta, \theta^\star)$ and $+$ boundary conditions at infinity, one has*

$$\xi = \lim_{n\to\infty} -\tfrac{1}{n}\log \mathbb{E}^+_{\mathbb{C}_1}[\sigma_0\sigma_n] = \tfrac{1}{2}\log(\tfrac{\theta}{\theta^\star}). \tag{4.3.9}$$

An interesting question would be interesting to find a way to exploit this first result to prove at least the exponential decay in all directions. As for the general correlation length expression (which is not isotropic), it looks to be a more challenging task and is not adressed here.

4.4 . Disorder insertion

We are interested in the space-time spin representation of the quantum Ising model on the primal domain $\Omega_\delta^\bullet$ with $+$ boundary condition. The underlying Poisson point process is of parameter τ on primal lines (death points) and the coupling constant is denoted by θ. The latter parameter is also the underlying Poisson point process for bridges in the FK representation, but not needed here for the spin representation.

Its dual model is the quantum Ising model defined on the dual domain Ω_δ° with free boundary condition whose underlying Poisson point process is of parameter $\tau^\star$ on dual lines and whose coupling constant is given by $\theta^\star$. The relation between these parameters $(\tau^\star, \theta^\star) = (\frac{\theta}{2}, 2\tau)$ is given in $(4.2.6)$. Recall that the critical point is also the self-dual point, and the choice of parameters we make will be $\tau^\star = \tau = \frac{1}{4\delta}$ and $\theta^\star = \theta = \frac{1}{2\delta}$. Only the ratio $\frac{\theta}{\tau}$ determines for the regime of the model, but this particular choice allows us to have some nice isotropic property as explained in [109] and will be discussed later in Section 4.4.2 and 4.4.4.

4.4.1 . Definition

Below we give the formal definition of the disorder operator which is valid for any parameters. In particular we do *not* assume the self-dual condition $(4.2.6)$, which will not be used when working with the model outside of criticality.

As in the discrete setup, the disorder insertion has two possible equivalent definitions. It can be seen as the ratio of partition functions between a modified model and the original one, or as an expectation of a random variables defined along disorder lines in the primal graph. More precisely,

Definition 4.4.1. For pairwise disjoint vertices $(v_i)_{1\leqslant i\leqslant 2n}$ in the dual domain Ω_δ°, we define the disorder operator by

$$\mathbb{E}^+_{\Omega_\delta^\bullet,\tau,\theta}[\mu_{v_1}\dots\mu_{v_{2n}}] := \frac{Z(\tau,\tilde\theta)}{Z(\tau,\theta)} = \mathbb{E}^+_{\Omega_\delta^\bullet,\tau,\theta}\left[\exp\left(-\theta\cdot \mathrm{Leb}^\circ(\mathbb{1}_{v\in L_1\cup\dots\cup L_n}\varepsilon_v)\right)\right], \tag{4.4.1}$$

where $(L_i)_{1\leqslant i\leqslant n}$ is a path collection pairing vertices in $(v_i)_{1\leqslant i\leqslant 2n}$.

The parameter $\tilde\theta$ here is defined to be $-\theta$ along all (L_i) and θ elsewhere. By reversing along the lines (L_i) the coupling constants, we make the model anti-ferromagnetic there. The partition functions $Z(\tau,\theta)$ and $Z(\tau,\tilde\theta)$ are defined in $(4.2.2)$. We need to check that the above definition does not depend either on (a) how the vertices v_i are paired or (b) the path taken between two vertices.

Indeed, it is enough to check the second condition since by deforming paths, the first one is a special case of the second. More precisely, we deform a path so that it goes through another disorder vertex, cut the path and glue in a different manner from that vertex. See Figure 4.4.1 for an illustration. The definition $(4.4.1)$ can also be generalized to an odd number or disorders, but since there is no such

a pairing of disorders, the quantitiy is zero. If two disorders are located at the same vertex, we formally pair them together and say they cancel each other (i.e. $\mu_v \mu_v = 1$ almost surely).

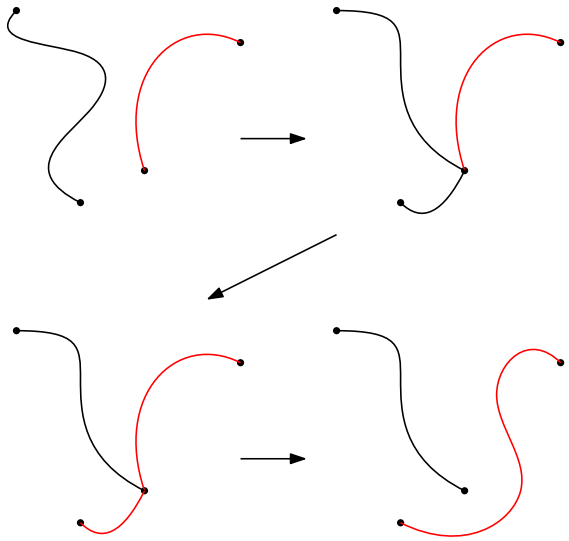

FIGURE 4.4.1 – Path deformation showing that the way the disorder lines pair vertices up does not matter.

Now, we show that the definition $(4.4.1)$ is path-independent. It is enough to show this for a disorder line connecting v_1 to v_2. Let L_1 and $\tilde{L}_1$ be two such paths. Write θ_1 and $\tilde{\theta}_1$ as in the definition of the partition function $(4.4.1)$. Write Λ for the (closed) region delimited by L_1 and $\tilde{L}_1$, L_Λ for the collection of dual lines in Λ (boundary included). For a spin configuration σ, write σ_{Λ^c} for σ restricted on Λ^c and $\tilde{\sigma}$ for the configuration which coincides with σ on Λ^c but with reversed sign on Λ. Then,

$$\begin{aligned}
\frac{Z(\tilde{\theta}_1)}{Z(\theta)} &\overset{(1)}{=} Z(\theta)^{-1} \cdot \eta_\tau^\bullet \left[\sum_{\sigma \in \Sigma(D)} C(\sigma_{\Lambda^c}) \exp\left(\tfrac{\tilde{\theta}_1}{2} \cdot \mathsf{Leb}^\circ(\mathbb{1}_{v \in L_\Lambda} \varepsilon_v)\right) \right] \\
&\overset{(2)}{=} Z(\theta)^{-1} \cdot \eta_\tau^\bullet \left[\sum_{\sigma \in \Sigma(D)} C(\tilde{\sigma}_{\Lambda^c}) \exp\left(\tfrac{\theta_1}{2} \cdot \mathsf{Leb}^\circ(\mathbb{1}_{v \in L_\Lambda} \varepsilon_v)\right) \right] \\
&\overset{(3)}{=} Z(\theta)^{-1} \cdot \eta_\tau^\bullet \left[\sum_{\sigma \in \Sigma(D)} C(\sigma_{\Lambda^c}) \exp\left(\tfrac{\theta_1}{2} \cdot \mathsf{Leb}^\circ(\mathbb{1}_{v \in L_\Lambda} \varepsilon_v)\right) \right],
\end{aligned}$$

where D is sampled according to $\eta_\tau^\bullet$. In the above computation, the first (1) line is the definition and $C(\sigma_{\Lambda^c})$ is some constant depending only on the spin outside of Λ. In the second line (2), we flip all the spins inside Λ which is equivalent to switching the coupling constant from $\tilde{\theta}_1$ to θ_1. It is possible to do so due to the

following equality in distribution for any finite set $X \subseteq \Omega_\delta^\bullet$,

$$\mathcal{L}(D \mid X \subseteq D) = \mathcal{L}(D) \cup X.$$

Finally, in the last line (3), we use the bijection $\sigma \mapsto \tilde{\sigma}$.

Using the duality between the space-time spin representation and the random-parity representation, one can see the disorders as a dual spin configuration, for the dual model with dual parameters, e.g.

$$\mathbb{E}^+_{\Omega_\delta^\bullet,\tau,\theta}[\mu_{v_1} \dots \mu_{v_n}] = \mathbb{E}^{\mathrm{f}}_{\Omega_\delta^\circ,\tau^\star,\theta^\star}[\sigma_{v_1} \dots \sigma_{v_n}], \tag{4.4.2}$$

where $(\tau^\star, \theta^\star) = (\frac{\theta}{2}, 2\tau)$ is given in $(4.2.6)$. Note again that above we defined the disorder operator when n is even. When the number of disorders is odd, the LHS of $(4.4.2)$ is zero because the disorders do not pair up ; the RHS is also zero because under the free boundary condition, the measure is invariant under the globlal spin-flip.

We can give another interpretation of $Z(\tau, \tilde{\theta})$ in $(4.4.1)$ using the quantum Ising model defined on some double cover. This viewpoint will turn out to be very useful later for the definition of mixed correlators $(4.4.7)$.

Let $\mathcal{D}_\delta = \Omega_\delta^\bullet$, Ω_δ° or $\Upsilon(\Omega_\delta)$. A double cover of $\mathcal{D}_\delta$ is formally defined as the disjoint union of two identical copies (also called sheets) $\mathcal{D}_\delta \sqcup \mathcal{D}_\delta$ with the following additional data telling about its branching structure :

— $\mathbf{v} = (v_1, \dots, v_n)$ where $v_1, \dots, v_n \in \Omega_\delta^\circ$ if $\mathcal{D}_\delta = \Omega_\delta^\bullet$ or $\Upsilon(\Omega_\delta)$;

— $\mathbf{u} = (u_1, \dots, u_m)$ where $u_1, \dots, u_m \in \Omega_\delta^\bullet$ if $\mathcal{D}_\delta = \Omega_\delta^\circ$ or $\Upsilon(\Omega_\delta)$.

We denote this double cover by $[\Omega_\delta^\bullet, \mathbf{v}]$, $[\Omega_\delta^\circ, \mathbf{u}]$ and $[\Upsilon(\Omega_\delta), \mathbf{v}, \mathbf{u}]$ respectively. Its branching structure is described as follows :

— If $\mathcal{D}_\delta = \Omega_\delta^\bullet$, the cuts are described by *any* pairing of v_i's ;

— if $\mathcal{D}_\delta = \Omega_\delta^\circ$, the cuts are described by *any* pairing of u_j's ;

— if $\mathcal{D}_\delta = \Upsilon(\Omega_\delta)$, the cuts are described by *any* pairing of v_i's and u_j's.

See Figure 4.4.2 for an illustration in the case of $[\Omega_\delta^\bullet, v_1, v_2]$.

Given $v_1, \dots, v_n \in \Omega_\delta^\circ$.

— Let $[\Omega_\delta^\bullet, \mathbf{v}]$ be the double cover of $\Omega_\delta^\bullet$ that branches over $v_1, \dots, v_n \in \Omega_\delta^\circ$. We consider the quantum Ising model on $[\Omega_\delta^\bullet, \mathbf{v}]$.

— The Poisson point process $\eta_\tau^\bullet$ is sampled on one copy and is taken to be the same on the other copy.

— A spin configuration σ on the double cover $[\Omega_\delta^\bullet, \mathbf{v}]$ should satisfy the *sign-flip symmetry* : $\sigma_u \sigma_{u^\#} = -1$ for any $u \in [\Omega_\delta^\bullet, \mathbf{v}]$ (we recall that $u^\#$ is the other fiber in $[\Omega_\delta^\bullet, \mathbf{v}]$ of the natural projection of u in $\Omega_\delta^\bullet$).

— Given a finite set of death points D, denote by $\Sigma(D)$ the set of spin configurations on the double cover $[\Omega_\delta^\bullet, \mathbf{v}]$ satisfying the sign-flip symmetry. Note that this does not depend on $v_1, \dots, v_n$ but only on D.

As such, the quantity $Z(\tau, \tilde{\theta})$ can be rewritten as the partition function of the Ising model defined on the double cover $[\Omega_\delta^\bullet, \mathbf{v}]$ with a modified Hamiltonian [1]. Denoting this quantity by $Z^{\mathbf{v}}(\tau, \theta)$, we can write,

$$Z^{\mathbf{v}}(\tau, \theta) = \eta_\tau^\bullet \left[\sum_{\sigma \in \Sigma(D)} \exp\left(-\tfrac{\theta}{2} \cdot \mathcal{H}^{\mathbf{v}}(\sigma) \right) \right] \tag{4.4.3}$$

$$= \eta_\tau^\bullet \left[\sum_{\sigma \in \Sigma(D)} \exp\left(\tfrac{\theta}{2} \cdot \tfrac{1}{2} \mathsf{Leb}^\circ(\varepsilon_p) \right) \right], \tag{4.4.4}$$

where the Hamiltonian $\mathcal{H}^{\mathbf{v}}(\sigma)$ is defined to be $-\frac{1}{2}\mathsf{Leb}^\circ(\varepsilon_v)$,

$$\mathcal{H}^{\mathbf{v}}(\sigma) = -\frac{1}{2}\mathsf{Leb}^\circ(\varepsilon_v) = -\frac{1}{2}\int_{[\Omega_\delta^\bullet, \mathbf{v}]} \varepsilon_v |\mathrm{d}v|. \tag{4.4.5}$$

Note that the factor $\frac{1}{2}$ comes from the fact that when working on the double cover, the contribution coming from each *planar* pair of neighboring spins is counted twice. In particular, the energy density $\varepsilon_v = \sigma_{v^-}\sigma_{v^+}$ now takes into account the structure of the double cover. More precisely, if v lies on one of the disorder lines, then v^- and v^+ belong to two different sheets, and that is where the sign-flip symmetry makes the difference.

The quantum Ising measure on this double cover is characterized by

$$\mathbb{E}^+_{[\Omega_\delta^\bullet, \mathbf{v}], \tau, \theta}\left[F(\sigma)\right] = Z^{\mathbf{v}}(\tau, \theta)^{-1} \cdot \eta_\tau^\bullet \left[\sum_{\sigma \in \Sigma(D)} F(\sigma) \exp\left(-\tfrac{\theta}{2} \cdot \mathcal{H}^{\mathbf{v}}(\sigma) \right) \right], \tag{4.4.6}$$

for any measurable function $F : \cup\Sigma(D) \to \mathbb{R}$.

Using this interpretation, for given $v_1, \dots, v_n \in \Omega_\delta^\circ$ and $u_1, \dots, u_m \in \Omega_\delta^\bullet$, we can introduce the *mixed correlator*,

$$\mathbb{E}^+_{\Omega_\delta^\bullet, \tau, \theta}[\mu_{v_1} \dots \mu_{v_n} \sigma_{u_1} \dots \sigma_{u_m}] := \mathbb{E}^+_{\Omega_\delta^\bullet, \tau, \theta}[\mu_{v_1} \dots \mu_{v_n}] \mathbb{E}^+_{[\Omega_\delta^\bullet, \mathbf{v}]}\left[\sigma_{u_1} \dots \sigma_{u_m}\right]. \tag{4.4.7}$$

In other words, denote $\mathcal{DB}(\Omega_\delta, m, n)$ the double cover of $(\Omega_\delta^\circ)^n \times (\Omega_\delta^\bullet)^m$ with the following branching structure. For $\mathbf{v} = (v_1, \dots, v_n) \in (\Omega_\delta^\circ)^n$ and $\mathbf{u} = (u_1, \dots, u_m) \in (\Omega_\delta^\bullet)^m$, we fix a path collection connecting v_i's to the boundary and another path collection connecting u_j's to the boundary. When u_j's wind around v_i's, the cuts are given by the path collection of v_i's; similarly, when v_i's wind around u_j's, the cuts are given by the path collection of u_j's.

Using the duality between representations, one has, for any integers n and m,

$$\mathbb{E}^+_{\Omega_\delta^\bullet, \tau, \theta}[\mu_{v_1} \dots \mu_{v_n} \sigma_{u_1} \dots \sigma_{u_m}] = \mathbb{E}^{\mathrm{f}}_{\Omega_\delta^\circ, \tau^\star, \theta^\star}[\sigma_{v_1} \dots \sigma_{v_n} \mu_{u_1} \dots \mu_{u_m}]. \tag{4.4.8}$$

1. The partition function sums "twice" the contribution of each pair of spins (on two sheets)

In what follows, we write this last quantity as $\langle \mu_{v_1} \dots \mu_{v_n} \sigma_{u_1} \dots \sigma_{u_m} \rangle$ or, equivalently, $\langle \sigma_{v_1} \dots \sigma_{v_n} \mu_{u_1} \dots \mu_{u_m} \rangle$, since the object at stake is now canonical and does not "favor" spins or disorders (i.e. primal or dual spins). Note that these quantities are defined on the double cover $\mathcal{DB}(\Omega_\delta, m, n)$ with the branching structure described above. Such a function is called *spinor* because the sign flips when replacing u (resp. v) by $u^\#$ (resp. $v^\#$).

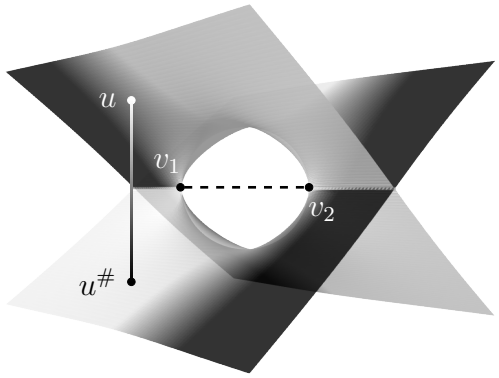

FIGURE 4.4.2 – A graphical representation of $\Omega_\delta^{\bullet[v_1,v_2]}$ locally around the branching given by $v_1, v_2 \in \Omega_\delta^\circ$. The vertices $u, u^\# \in \Omega_\delta^\bullet$ are two different vertices belonging to the same fiber.

4.4.2 . Local propagation Equation

The local propagation equation for Kadanoff–Ceva fermions (also called Dostenko propagation equation in [129]) in the classical Ising model [93] has an equivalent in the graphical representation of the quantum Ising model. Instead of having a three-term relation, we have a two-term relation which involves a vertical derivative of the order-disorder operator. This is due to the degeneration when we squeeze the rectangular lattice to obtain the semi-discrete lattice.

Proposition 4.4.2. *Let $\mathcal{O}$ be a mixed correlator. For a dual vertex v on the double cover,*

$$\partial_y \langle \mu_v \mathcal{O} \rangle = \partial_y \langle \mu_{v+\mathrm{i}\,y} \mathcal{O} \rangle_{|y=0} := \lim_{y \to 0} \frac{1}{y} \big[\langle \mu_{v+\mathrm{i}\,y} \mathcal{O} \rangle - \langle \mu_v \mathcal{O} \rangle \big], \tag{4.4.9}$$

where for all small enough y, $v + \mathrm{i}\,y$ needs to be chosen such that it belongs to the same sheet of the double cover as v. Moreover, this derivative satisfies the following two-term relation,

$$\partial_y \langle \mu_v \mathcal{O} \rangle = \mathrm{sgn}(\mathcal{O}, v) \cdot \theta \langle \mu_v \sigma_{v^-} \sigma_{v^+} \mathcal{O} \rangle, \tag{4.4.10}$$

where v^- and v^+ are chosen to belong to the same sheet of the double cover and $\mathrm{sgn}(\mathcal{O}, v)$ takes value in $\{0, \pm 1\}$ depending on the path L that pairs v with

another dual vertex in $\mathcal{O}$*,*

$$\mathrm{sgn}(\mathcal{O}, v) = \begin{cases} 0 & \textit{if such a path } L \textit{ does not exist,} \\ +1 & \textit{if } L \textit{ leaves } v \textit{ from above,} \\ -1 & \textit{if } L \textit{ leaves } v \textit{ from below.} \end{cases} \tag{4.4.11}$$

Note that it is indeed important to take the quantity $\mathrm{sgn}(\mathcal{O}, v)$ into account since the mixed correlators $\langle \mu_{v+\mathrm{i}\,y}\mathcal{O}\rangle$ and $\langle \mu_v \sigma_{v^-}\sigma_{v^+}\mathcal{O}\rangle$ are defined on a double cover where cuts depend on how the path L changes.

Proof. If the path L defined as in the statement does not exist, then $\mathcal{O}$ has an even number of disorders and $\langle \mu_{v+\mathrm{i}\,y}\mathcal{O}\rangle$ is identically 0 for small enough y. The right side of (4.4.10) is also identically zero for the same reason.

Assume that L exists. Using (4.4.1) and (4.4.7), we get,

$$\begin{aligned} Z(\tau,\theta)\cdot\partial_y\langle \mu_{v+\mathrm{i}\,y}\mathcal{O}\rangle_{|y=0} &= \partial_y \eta_\tau^\bullet\left[\sum_{\sigma\in\Sigma(D)}\mathcal{O}_\sigma \exp\left(-\tfrac{\theta}{2}\cdot\mathcal{H}^{[v+\mathrm{i}\,y,\mathbf{v}]}(\sigma)\right)\right]_{|y=0}, \\ &= \theta\cdot\mathrm{sgn}(\mathcal{O},v)\cdot\eta_\tau^\bullet\left[\sum_{\sigma\in\Sigma(D)}\mathcal{O}_\sigma \exp\left(-\tfrac{\theta}{2}\cdot\mathcal{H}^{[v,\mathbf{v}]}(\sigma)\right)\sigma_{v^-}\sigma_{v^+}\right], \end{aligned}$$

where we use the dominated convergence to switch the expectation $\eta_\tau^\bullet$ and the partial derivative ∂_y along with (4.4.15). This gives the final result (4.4.10). □

Proposition 4.4.3. *Let* $\mathcal{O}$ *be a mixed correlator. For a primal vertex* u *on the double cover,*

$$\partial_u\langle\sigma_u\mathcal{O}\rangle = \partial_u\langle\sigma_{u+\mathrm{i}\,y}\mathcal{O}\rangle_{|y=0} := \lim_{y\to 0}\frac{1}{y}\big[\langle\sigma_{u+\mathrm{i}\,y}\mathcal{O}\rangle - \langle\mu_u\mathcal{O}\rangle\big], \tag{4.4.12}$$

where for all small enough y*,* $u+\mathrm{i}\,y$ *needs to be chosen such that it belongs to the same sheet of the double cover as* u*. Moreover, this derivative satisfies the following two-term relation,*

$$\partial_y\langle\sigma_u\mathcal{O}\rangle = \mathrm{sgn}(\mathcal{O},u)\cdot\theta^\star\langle\sigma_u\mu_{u^-}\mu_{u^+}\mathcal{O}\rangle, \tag{4.4.13}$$

where $\mathrm{sgn}(\mathcal{O},u)$ *takes value in* $\{\pm 1\}$ *depending on the path* L *that connects* u *with the boundary (thus actually no dependency on* $\mathcal{O}$*),*

$$\mathrm{sgn}(\mathcal{O},u) = \begin{cases} +1 & \textit{if } L \textit{ leaves } u \textit{ from above,} \\ -1 & \textit{if } L \textit{ leaves } u \textit{ from below.} \end{cases} \tag{4.4.14}$$

Proof. One simply uses proposition 4.4.2 together with the duality relation (4.4.8). □

Lemma 4.4.4. *We use the notations from Proposition 4.4.2 and write* $\mathbf{v}$ *for the set of all the disorders in* $\mathrm{Supp}(\mathcal{O})$*. Then, we have,*

$$\partial_y \mathcal{H}^{[v+\mathrm{i}\,y,\mathbf{v}]}(\sigma)_{|y=0} := \lim_{y\to 0} \frac{\mathcal{H}^{[v+\mathrm{i}\,y,\mathbf{v}]}(\sigma) - \mathcal{H}^{[v,\mathbf{v}]}(\sigma)}{y} = -\operatorname{sgn}(\mathcal{O},v)\cdot 2\sigma_{v^-}\sigma_{v^+}, \tag{4.4.15}$$

where v^- *and* v^+ *are chosen to be on the same sheet of the double cover.*

Proof. We show the result in the case that $\operatorname{sgn}(\mathcal{O},v) = 1$ and $y > 0$, the computation in the other cases is similar.

Write $v_1 = v$ and $v_2 = v + \mathrm{i}\,y$ with $y > 0$. Compute the difference of the two following Hamiltonians using (4.4.5),

$$\begin{aligned}
&\mathcal{H}^{[v_1,\mathbf{v}]}(\sigma) - \mathcal{H}^{[v_2,\mathbf{v}]}(\sigma)\\
&\overset{(1)}{=} -\frac{1}{2}\int_{\Omega^{[v_1,\mathbf{v}]}} \mathbb{1}_{v\in[v_1,v_2]\cup[v_1^\#,v_2^\#]}\sigma_{v^-}\sigma_{v^+}|\mathrm{d}v| + \frac{1}{2}\int_{\Omega^{[v_2,\mathbf{v}]}} \mathbb{1}_{v\in[v_1,v_2]\cup[v_1^\#,v_2^\#]}\sigma_{v^-}\sigma_{v^+}|\mathrm{d}v|\\
&\overset{(2)}{=} -\int_{\Omega^{[v_1,\mathbf{v}]}} \mathbb{1}_{v\in[v_1,v_2]}\sigma_{v^-}\sigma_{v^+}|\mathrm{d}v| + \int_{\Omega^{[v_2,\mathbf{v}]}} \mathbb{1}_{v\in[v_1,v_2]}\sigma_{v^-}\sigma_{v^+}|\mathrm{d}v|\\
&\overset{(3)}{=} \int_{\Omega^{[v_1,\mathbf{v}]}} \mathbb{1}_{v\in[v_1,v_2]}\sigma_{(v^-)^\#}\sigma_{v^+}|\mathrm{d}v| + \int_{\Omega^{[v_2,\mathbf{v}]}} \mathbb{1}_{v\in[v_1,v_2]}\sigma_{v^-}\sigma_{v^+}|\mathrm{d}v|\\
&\overset{(4)}{=} 2\int_{\Omega^{[v_2,\mathbf{v}]}} \mathbb{1}_{v\in[v_1,v_2]}\sigma_{v^-}\sigma_{v^+}|\mathrm{d}v|.
\end{aligned} \tag{4.4.16}$$

In the second equality (2), we use the fact that both sheets of the double cover contributes equally to the integrals. In the third equality, (3), we use the sign-flip symmetry for the double cover $\Omega^{[v_1,\mathbf{v}]}$. In the first term of the last equality (4), on Ω and for $v \in [v_1, v_2]$, the primal vertices $(v^-)^\#$ and v^+ belong to the same sheet, thus can be rewritten with the cut point v_1 shifted to v_2.

To conclude the proof, we divide (4.4.16) by y and take the limit to obtain the desired formula (4.4.15). □

4.4.3 . Construction of observables via correlators

In the following subsections, we will define two special correlators used in the convergence proofs of the critical model, which are constructed out of mixed correlators of the type $\mathcal{O}$. We also prove they satisfy the so-called s-holomorphicity property, which makes discrete correlators regular already in discrete. As for mixed corelator of the form $\mathcal{O}$, the construction is appropriate on some double cover. We precise here those definitions.

Definition 4.4.5. Let $\tilde{F} : \Omega_\delta^\circ \times \Omega_\delta^\bullet \to \mathbb{C}$ be a function defined on $\mathcal{DB}(\Omega_\delta, 1, 1)$. We say that

— $\tilde{F}$ has the sign-flip property around $v \in \Omega_\delta^\circ$ if $\tilde{F}(v, u^\#) = -\tilde{F}(v, u)$ for all $u \in \mathcal{DB}(\Omega_\delta, 0, 1)$,

— $\tilde{F}$ has the sign-flip property around $u \in \Omega_\delta^\bullet$ if $\tilde{F}(v^\#, u) = -\tilde{F}(v, u)$ for all $v \in \mathcal{DB}(\Omega_\delta, 1, 0)$,

— $\tilde{F}$ has the sign-flip property (everywhere) if the above two items are true for all $v \in \Omega_\delta^\circ$ and $u \in \Omega_\delta^\bullet$.

In the above statement, $p^\#$ denotes the *other fiber* of p on the appropriate double cover.

As it is the case in the discrete case, we specify the notion of *sign-flip symmetry*, which will appear naturally later.

Definition 4.4.6. Let $F : \Upsilon(\Omega_\delta) \to \mathbb{C}$ be a function defined on the corner semi-discrete lattice such that for each $c \in \Upsilon(\Omega_\delta)$, $F(c)$ depends only on $v_c \in \Omega_\delta^\circ$ and $u_c \in \Omega_\delta^\bullet$. We may write $F(c) = \tilde{F}(v_c, u_c)$. We say that F has the *sign-flip* property at $c \in \Upsilon(\Omega_\delta)$ if

— $v \mapsto \tilde{F}(u_c, v)$ has the sign-flip property around u_c,

— $u \mapsto \tilde{F}(u, v_c)$ has the sign-flip property around v_c.

Definition 4.4.7. Let $\eta_c := [\mathrm{i}(v_c - u_c)]^{-1/2}$ be the semi-discrete *Dirac spinor*.

Note that η_c is defined up to the sign, which explains the need of the double cover structure described above. The sign of η_c depends on the choice of v_c and u_c. In other words, η_c has the sign-flip property around *all* vertices of $\Upsilon(\Omega_\delta)$.

Definition 4.4.8. Let $\varpi = (u_1, \dots, u_{n-1}, v_1, \dots, v_{m-1}) \in (\Omega_\delta^\bullet)^{n-1} \times (\Omega_\delta^\circ)^{m-1}$ and $\mathcal{O} = \mu_{v_1} \dots \mu_{v_{m-1}} \sigma_{u_1} \dots \sigma_{u_{n-1}}$. For a corner $c \in [\Upsilon(\Omega_\delta), \varpi]$ set formally $\chi_c := \mu_{v_c} \sigma_{u_c}$, where v_c (resp. u_c) is the neighboring dual (resp. primal) vertex. This allows to define the complexified correlator Ψ_ϖ on $[\Upsilon(\Omega_\delta), \varpi]$ by

$$\Psi_\varpi := c \mapsto \eta_c \langle \chi_c \mathcal{O} \rangle = \eta_c \langle \chi_c \mu_{u_1} \dots \mu_{u_{n-1}} \sigma_{v_1} \dots \sigma_{v_m - 1} \rangle. \tag{4.4.17}$$

The next proposition shows that the complexified correlator is properly defined and satifies the spinor property.

Proposition 4.4.9. *In the context of the definition* (4.4.8)*, the complexified correlator Ψ_ϖ is well defined on $[\Upsilon(\Omega_\delta), \varpi]$. Moreover Ψ_ϖ has the sign-flip property i.e. for $c, c^\#$ corners of $[\Upsilon(\Omega_\delta), \varpi]$, one has $\Psi_\varpi(c) = -\Psi_\varpi(c^\#)$, which means that Ψ_ϖ changes its sign when c makes a turn around one of the v_p or u_q.*

Proof. As explained above and in [39, Rmk. 2.5, Lem. 2.6, Def. 2.7], the correlator $\langle \chi_c \mathcal{O} \rangle$ can be viewed a *single* multivalued function on *one* double cover. The presence of nearby branchings at c and the multiplication by η_c (which branches around all points of $\Upsilon(\Omega_\delta)$) kills the branching structure around each point except those of ϖ. Finally, the spinor property comes from the spinor property of η_c since replacing χ_c by $\chi_{c^\#}$ doesen't change the sign of $\langle \chi_c \mathcal{O} \rangle$ but the one of η_c.

□

4.4.4 . s-holomorphicity and fermionic correlators

We recall now the definition of a semi-discrete s-holomorphic function [109, Sec. 3.7], which is a natural generalisation of the isoradial case. In particular, we show that mixed correlators introduced above give rise to s-holomorphic functions. Contrarily to the FK-loop representation [109], the approach of disorder insertion described in previous sections provides the s-holomorphicity property almost directly (i.e. there is no need to look at combinatorial bijections between local loop configurations). Below we define the notion of s-holomorphicity, which can be viewed in both the corner and diamond lattices, and provide a simple way to switch point of view depending on the context.

Definition 4.4.10. Let $F : \Upsilon(\Omega_\delta) \to \mathbb{C}$ be a function defined on the *corner* semi-discrete lattice. It is said to be *corner s-holomorphic* if it satisfies the two following properties.

1. *Parallelism* : for $c \in \Upsilon(\Omega_\delta)$, we have $F(c) /\!\!/ \eta_c\mathbb{R}$ where η_c is defined in (4.4.7) In other words,
   - $F(c) \in \nu\mathbb{R}$ if u_c is on the left and v_c is on the right (western corners),
   - $F(c) \in \mathrm{i}\,\nu\mathbb{R}$ if u_c is on the right and v_c is on the left (eastern corners),

   where $\nu = e^{-\mathrm{i}\frac{\pi}{4}}$.
2. *Holomorphicity* : for any corner $c \in \Upsilon(\Omega_\delta)$, we have $\overline{D}^{(\delta)}F(c) = 0$.

Note that in the above definition, the semi-discrete derivative is given by

$$\overline{D}^{(\delta)}F(c) := \frac{1}{2}\left[D_x^{(\delta)}F(c) - \frac{\partial_y F(c)}{\mathrm{i}}\right] = \frac{1}{2}\left[\frac{F(c^+) - F(c^-)}{2\delta} - \frac{\partial_y F(c)}{\mathrm{i}}\right]. \tag{4.4.18}$$

Definition 4.4.11. Let $F^\diamond : \diamondsuit(\Omega_\delta) \to \mathbb{C}$ be a function defined on the *diamond* semi-discrete domain. It is said to be *diamond s-holomorphic* if it satisfies the two following properties.

1. *Projection* : for every $c = c(z_c^-, z_c^+) \in \Upsilon(\Omega_\delta)$, we have
$$\mathrm{Proj}[F^\diamond(z_c^-), \eta_c\mathbb{R}] = \mathrm{Proj}[F^\diamond(z_c^+), \eta_c\mathbb{R}] \tag{4.4.19}$$
   where $\mathrm{Proj}(X, \eta\mathbb{R})$ denotes the usual projection of X on the line $\eta\mathbb{R}$, i.e.
$$\mathrm{Proj}[X, \eta\mathbb{R}] = \tfrac{1}{2}[X + \eta^2\overline{X}].$$
2. *Holomorphicity* : for all vertex z on the medial domain $\diamondsuit(\Omega_\delta)$, we have $\overline{D}^{(\delta)}F^\diamond(z) = 0$.

In the convergence proofs, we mainly work with *diamond* holomorphic function, since they behave as continous holomorphic function as the lattice mesh-size goes to 0. In fact, this passage to complexed valued diamond holomorphic function appears crucial to study the scaling limits, since corner holomorphic functions have a prescribed complex argument, thus cannot behave like holomorphic ones. In fact, there is a natural bijection between *corner* and *diamond* s-holomorphic functions on $\Upsilon(\Omega_\delta)$ and those on $\diamondsuit(\Omega_\delta)$. The next proposition explicits this very simple link.

Proposition 4.4.12. *Given a* corner *s-holomorphic function $F : \Upsilon(\Omega_\delta) \mapsto \mathbb{C}$, one can define $F^\diamond : z \in \diamondsuit(\Omega_\delta) \mapsto \mathbb{C}$ by :*

$$F^\diamond(z) := F(c_z^-) + F(c_z^+).$$

Then, the function $F^\diamond$ is diamond *s-holomorphic.*
Conversely, given an diamond *s-holomorphic function $F^\diamond : \diamondsuit(\Omega_\delta) \mapsto \mathbb{C}$, one can define $F : c \in \Upsilon(\Omega_\delta) \mapsto \mathbb{C}$ by*

$$F(c) := \mathrm{Proj}[F^\diamond(z_c^-), \eta_c\mathbb{R}] = \mathrm{Proj}[F^\diamond(z_c^+), \eta_c\mathbb{R}].$$

Then, the function F is corner *s-holomorphic.*

When the context is clear, we will drop the denomination corner or diamond s-holomorphic functions and just call them s-holomorphic functions, passing from one to the other using Proposition 4.4.12. As a consequence of the projection properties mentioned earlier, one can see as in [33, Eq. (2.20) and Rmk. 2.9] that $F^\diamond$ satisfies the maximum principle, i.e. for any connected set S of $\diamondsuit(G)$ (where neighbours are either at a distance 2δ from each other or belong to same vertical axis), the maximum of $|F^\diamond|$ is attained at the boundary of S.

We now prove that the correlator Ψ_ϖ introduced in Definition 4.4.8 is s-holomorphic at the critical isotropic point. We first need to compute the vertical derivative of mixed correlator.

Lemma 4.4.13. *Let $c \in \Upsilon(\Omega_\delta)$ be a corner and $\mathcal{O}$ a mix correlator. Let the partial derivative ∂_y be taken with respect to the vertical variation of c, i.e.,*

$$\partial_y\langle\chi_c\mathcal{O}\rangle := \partial_y\langle\chi_{c+\mathrm{i}\,y}\mathcal{O}\rangle_{|y=0}.$$

Then, this derivative is given according to the positions of $v := v(c)$ and $u := u(c)$ where $c = (v(c), u(c))$.

— *If v is on the left and u is on the right, then,*

$$\partial_y\langle\chi_c\mathcal{O}\rangle = \mathrm{sgn}(\mathcal{O}, v)\cdot\theta\langle\chi_{c^-}\mathcal{O}\rangle + \mathrm{sgn}(\mathcal{O}, u)\cdot\theta^\star\langle\chi_{c^+}\mathcal{O}\rangle. \qquad (4.4.20)$$

— *If v is on the right and u is on the left, then,*

$$\partial_y\langle\chi_c\mathcal{O}\rangle = \mathrm{sgn}(\mathcal{O}, v)\cdot\theta\langle\chi_{c^+}\mathcal{O}\rangle + \mathrm{sgn}(\mathcal{O}, u)\cdot\theta^\star\langle\chi_{c^-}\mathcal{O}\rangle. \qquad (4.4.21)$$

Proof. First note that for any primal vertex u and dual vertex v, we have,

$$\begin{aligned}\partial_y\langle\mu_{v+\mathrm{i}\,y}\sigma_{u+\mathrm{i}\,y}\mathcal{O}\rangle_{|y=0} &= \partial_y\langle\mu_{v+\mathrm{i}\,y}\sigma_u\mathcal{O}\rangle_{|y=0} + \partial_y\langle\mu_v\sigma_{u+\mathrm{i}\,y}\mathcal{O}\rangle_{|y=0}\\ &= \mathrm{sgn}(\mathcal{O},v)\cdot\theta\langle\mu_v\sigma_{v^-}\sigma_{v^+}\sigma_u\mathcal{O}\rangle + \mathrm{sgn}(\mathcal{O},u)\cdot\theta^\star\langle\sigma_u\mu_{u^-}\mu_{u^+}\mu_v\mathcal{O}\rangle.\end{aligned}$$

The above result follows from (4.4.10) and (4.4.13) by respectively choosing v^-, v^+ on the same sheet and u^-, u^+ on the same sheet. Now the lemma follows from a direct application of the above formula. Let us write it for the first item,

$$\begin{aligned}\partial_y\langle\chi_c\mathcal{O}\rangle &= \partial_y\langle\mu_v\sigma_u\mathcal{O}\rangle\\ &= \mathrm{sgn}(\mathcal{O},v)\cdot\theta\langle\mu_v\sigma_{v^-}\sigma_{v^+}\sigma_u\mathcal{O}\rangle + \mathrm{sgn}(\mathcal{O},u)\cdot\theta^\star\langle\sigma_u\mu_{u^-}\mu_{u^+}\mu_v\mathcal{O}\rangle\\ &= \mathrm{sgn}(\mathcal{O},v)\cdot\theta\langle\mu_v\sigma_{v^-}\mathcal{O}\rangle + \mathrm{sgn}(\mathcal{O},u)\cdot\theta^\star\langle\sigma_u\mu_{u^+}\mathcal{O}\rangle\\ &= \mathrm{sgn}(\mathcal{O},v)\cdot\theta\langle\chi_{c^-}\mathcal{O}\rangle + \mathrm{sgn}(\mathcal{O},u)\cdot\theta^\star\langle\chi_{c^+}\mathcal{O}\rangle.\end{aligned}$$

□

Proposition 4.4.14. *Let Ψ_ϖ be the correlator as defined in* (4.4.17)*. As long as $c^\pm\notin\varpi$, one has,*

— *If v is on the left and u is on the right, then,*

$$\partial_y\Psi_\varpi(c) = \mathrm{i}[\theta^\star\Psi_\varpi(c^+) - \theta\Psi_\varpi(c^-)]. \tag{4.4.22}$$

— *If v is on the right and u is on the left, then,*

$$\partial_y\Psi_\varpi(c) = \mathrm{i}[\theta\Psi_\varpi(c^+) - \theta^\star\Psi_\varpi(c^-)]. \tag{4.4.23}$$

In particular, at critical and isotropical point $\theta=\theta^\star=\frac{1}{2\delta}$, it is corner s-holomorphic on $[\Upsilon(\Omega_\delta),\varpi]$ (when $c^\pm\notin\varpi$).

Proof. Let $\Psi_\varpi(c)=\eta_c\langle\chi_c\mathcal{O}\rangle$ where c is a corner of $[\Upsilon(\Omega_\delta),\varpi]$ and $\mathcal{O}$ is a mixed order-disorder operator. Since η_c stays constant when c varies vertically, we only need to compute the first derivative of $\langle\chi_c\mathcal{O}\rangle$ which is done in the above Lemma 4.4.13. Moreover, if η is chosen such that its cuts coincide with those of $\langle\chi_c\mathcal{O}\rangle$, we have the following relation,

$$\frac{\eta_{vv^+}}{\eta_{vv^-}} = \frac{[\mathrm{i}(v-v^+)]^{-1/2}}{[\mathrm{i}(v-v^-)]^{-1/2}} = \left(\frac{v-v^+}{v-v^-}\right)^{-1/2} = -\,\mathrm{sgn}(\mathcal{O},v)\cdot\mathrm{i}, \tag{4.4.24}$$

since $v-v^+ = e^{\mathrm{sgn}(\mathcal{O},v)\,\mathrm{i}\,\pi}(v-v^-)$. Similarly, we also have,

$$\frac{\eta_{uu^+}}{\eta_{uu^-}} = \frac{[\mathrm{i}(u^+-u)]^{-1/2}}{[\mathrm{i}(u^--u)]^{-1/2}} = \left(\frac{u^+-u}{u^--u}\right)^{-1/2} = -\,\mathrm{sgn}(\mathcal{O},u)\cdot\mathrm{i} \tag{4.4.25}$$

since $u^+-u = e^{\mathrm{sgn}(\mathcal{O},u)\,\mathrm{i}\,\pi}(u^--u)$.

Let us complete the computation for the first item. Assume that v is on the left and u is on the right of the corner c. From (4.4.25), we have $\eta_{c^+} = -\operatorname{sgn}(\mathcal{O}, u) \cdot \mathrm{i}\,\eta_c$; from (4.4.24), we have $\eta_{c^-} = \operatorname{sgn}(\mathcal{O}, v) \cdot \mathrm{i}\,\eta_c$. Combine these two relations with (4.4.20), we find (4.4.22). A similar computation results in (4.4.23). □

Proposition 4.4.15. *Let $\Psi = \Psi_\varpi$ be the correlator as defined in* (4.4.17)*. If c is not nearby one of the branchings ϖ, it satisfies the following local relations,*

$$\partial_{yy}\Psi(c) = (\theta^2 + \theta^{\star 2})\Psi(c) - \theta\theta^\star\big[\Psi(c^{++}) + \Psi(c^{--})\big]. \tag{4.4.26}$$

Proof. Assume that $c = (v, u)$ is a corner such that v is on the left and u is on the right. Then, the corners c^+ and c^- are of the opposite type. We can take the vertical derivative to (4.4.22)

$$\begin{aligned}\partial_{yy}\Psi(c) &= \mathrm{i}[\theta^\star\partial_y\Psi(c^+) - \theta\partial_y\Psi(c^-)]\\ &= \mathrm{i}\left[\theta^\star \cdot \mathrm{i}[\theta\Psi(c^{++}) - \theta^\star\Psi(c)] - \theta \cdot \mathrm{i}[\theta\Psi(c) - \theta^\star\Psi(c^{--})]\right]\\ &= (\theta^2 + \theta^{\star 2})\Psi(c) - \theta\theta^\star\big[\Psi(c^{++}) + \Psi(c^{--})\big]\end{aligned}$$

The computation is the same if c is of the other type. □

The above proposition suggests the following definition for the massive Laplacian operator $\Delta^{(m)} = \Delta^{(m)}_{(\theta,\theta^\star)}$,

$$\Delta^{(m)}_{(\theta,\theta^\star)}\Psi(c) = \Delta^{(m)}\Psi(c) := -\Psi(c) + \frac{1}{\theta^2 + \theta^{\star 2}}\big[\partial_{yy}\Psi(c) + \theta\theta^\star\big[\Psi(c^{++}) + \Psi(c^{--})\big]. \tag{4.4.27}$$

The equation (4.4.26) is equivalent to $\Delta^{(m)}\Psi(c) = 0$. The massive Laplacian $\Delta^{(m)}$ can be interpreted as the infinitesimal generator of the semi-discrete Brownian Motion with horizontal killing rate $1 - \frac{2\theta\theta^\star}{\theta^2+\theta^{\star 2}}$. At the critical and isotropical point of the quantum Ising model $\theta = \theta^\star = \frac{1}{2\delta}$, the massive Laplacian operator (4.4.27) gets simplified and one recovers the (normalized) semi-discrete Laplacian operator,

$$\Delta^{(\delta)}\Psi(c) := \frac{1}{2}\partial_{yy}\Psi(c) + \frac{1}{2\delta^2}\big[\Psi(c^{++}) + \Psi(c^{--}) - 2\Psi(c)\big]. \tag{4.4.28}$$

This shows that the correlator Ψ is harmonic at the critical and isotropical point and massive harmonic otherwise. This massive harmonicity will be used to derive asymptotics of correlations in the infinite volume limit.

4.4.5 . The energy and spin correlators

We introduced above a general formalism for fermionic correlators. We focus now on two specific choices of $\mathcal{O}$ which that are useful to prove the existence of a scaling limit at criticality for energy density and spin-correlations. In several papers following Smirnov's seminal work [160] on the planar critical Ising model, those observables were introduced in terms of their loops expansion, but we prefer using

here the Kadanoff–Ceva formalism developped above. The global strategy is to use the fermionic correlator 4.4.7 as a functional of corners. We recall that given $\varpi := (v_1, \dots, v_{n-1}, u_1, \dots, u_{m-1}) \in (\Omega_\delta^\bullet)^{n-1} \times (\Omega_\delta^\circ)^{m-1}$ and $c \in [\Upsilon(\Omega_\delta), \varpi]$, we defined $\Psi_\varpi(c) = \eta_c \langle \chi_c \mu_{v_1} \dots \mu_{v_{m-1}} \sigma_{u_1} \dots \sigma_{u_{n-1}} \rangle$ on $[\Upsilon(\Omega_\delta), \varpi]$.

The energy correlator We fix a corner $a = (v_a u_a) \in \Upsilon(\Omega_\delta)$ and set $\varpi = \{u_a, v_a\}$. We define the graph $\Omega_{\delta,a} := (\Omega_\delta \backslash \{a\}) \cup \{a^\pm\}$ where the two corner $a^\pm$ are *different* but located at a, i.e. a is replaced by two corner $a^\pm$, and combinatorially, a^+ is a neighbour to the right part of the graph near a while a^- is a neighbour of the left part of the graph near a. We are now able to define the energy correlator using $\mathcal{O} = \mu_{v_a} \sigma_{u_a}$. The next definition precises this setup.

Definition 4.4.16. Fix a corner $a = (v_a u_a) \in \Upsilon(\Omega_\delta)$. We define the energy correlator double-valued at a by setting for $c \neq a^\pm \in \Omega_{\delta,a}$

$$\Psi^{\mathcal{E}}_{\Omega_\delta,a}(c) := \eta_c \langle \sigma_{u_a} \mu_{v_a} \sigma_{u(c)} \mu_{v(c)} \rangle_{\Omega_\delta} = \eta_c \langle \chi_c \chi_a \rangle_{\Omega_\delta} \tag{4.4.29}$$

with $\Psi^{\mathcal{E}}_{\Omega_\delta,a}(a^\pm) = \pm \eta_a$.

The next proposition precises its main characteristics of $\Psi^{\mathcal{E}}_{\Omega_\delta,a}$.

Proposition 4.4.17. *The energy correlator defined in* (4.4.29) *is well defined and is s-holomorphic everywhere.*

The catchpoint of the above definition is that one should not look at $\Psi^{\mathcal{E}}_{\Omega_\delta,a}$ as a spinor on a double cover, but rather see $\Psi^{\mathcal{E}}_{\Omega_\delta,a}$ as a *planar* observable, i.e., not defined on the double cover, with a discrete singularity at a.

Proof. This is a consequence of [39, Lem. 2.9 and Rmk. 2.13], or [43, Fig. 6]. The introduction of $\Omega_{\delta,a}$ amounts to introducing a cut $\gamma_a = [u_a v_a]$ in the double cover $[\Upsilon(\Omega_\delta), u_a, v_a]$ which branches around u_a and v_a. A priori, the above correlator $\eta_c \langle \sigma_{u_a} \mu_{v_a} \sigma_{u(c)} \mu_{v(c)} \rangle_{\Omega_\delta}$ is well defined on $[\Upsilon(\Omega_\delta), u_a, v_a]$ that branches around nearby points u_a and v_a. The two sets $[\Upsilon(\Omega_\delta), u_a, v_a]$ and $\Upsilon(\Omega_\delta)$ *can be identified* except at the corner a. In terms of observables, this "planarity" statement can be easily seen since whenever c winds around *both* branchings at the same time in $[\Upsilon(\Omega_\delta), u_a, v_a]$, it simply returns to the same sheet, i.e. the branching effets around v_a and u_a simply kill each other. One can thus restrict $\langle \sigma_{u_a} \mu_{v_a} \sigma_{u(c)} \mu_{v(c)} \rangle_{\Omega_\delta}$ to one of its sheets to get the identification with $\Omega_{\delta,a}$. Still, in this sheet restriction, one has to prescribe the representant of a. The split of a in $a^\pm$ and the choice of valuation $\pm\eta_a$ preserves the local holomorphicity relation (which holds $\Omega_{\delta,a}$), provided we assume that $a^\pm$ interact (in a combinatorial way) respectively with right and the left and the part of the edge $[v_a u_a]$. □

In particular, the associated *diamond* observable $\Psi^{\mathcal{E},\diamond}_{\Omega_\delta,a}$ is not s-holomorphic at a (since the associated projections only match up to the sign). Still, as mentioned in the previous paragraph, using the corners $a^\pm$ instead of a, one can preserve the projection property and thus construct $\Psi^{\mathcal{E},\diamond}_{\Omega_\delta,a}$. We also define the full-plane observable (see appendix 4.8) $G_{(a)}$ in a combinatorial way, which turns out to have exactly the *same* singularity as $\Psi^{\mathcal{E},\diamond}_{\Omega_\delta,a}$. In particular, since $\Psi^{\mathcal{E},\diamond}_{\Omega_\delta,a}$ and $G_{(a)}$ have the same singularity at a, their difference $\Psi^{\mathcal{E},\diamond}_{\Omega_\delta,a} - G_{(a)}$ is now s-holomorphic *everywhere* in $\diamondsuit(\Omega_\delta)$ (i.e. there is no need to use the graph Ω_a where a is replaced by $a^\pm$).

Assuming for example that a is a western corner, the definition of the fermionic correlator, the identity $\mu_{v_a}\mu_{v_a} = 1$ and the computation $G_{(a)}(a+\delta) = \eta_{a+\delta}\frac{2}{\pi} = \eta_{a+\delta}\langle\sigma_{u_a}\sigma_{u_{a+2\delta}}\rangle^+_{\mathbb{C}_\delta}$ directly yields that

$$[\Psi^{\mathcal{E},\diamond}_{\Omega_\delta,a} - G_{(a)}][v_a] = \eta_{a+\delta}[\langle\sigma_{u_a}\sigma_{u_{a+2\delta}}\rangle^+_{\Omega^\bullet_\delta} - \langle\sigma_{u_a}\sigma_{u_{a+2\delta}}\rangle^+_{\mathbb{C}_\delta}], \tag{4.4.30}$$

is the normalized energy density at u_a up to an explicit modular factor. One can deduce the same way that

$$[\Psi^{\mathcal{E},\diamond}_{\Omega_\delta,a} - G_{(a)}][u_a] = \eta_{a-\delta}[\langle\mu_{v_a}\mu_{v_{a-2\delta}}\rangle^+_{\Omega^\bullet_\delta} - \langle\mu_{v_a}\mu_{v_{a-2\delta}}\rangle^+_{\mathbb{C}_\delta}], \tag{4.4.31}$$

Remark 4.4.18. One could see alternatively $G_{(a)}$ as the limit of functions $\Psi^{\mathcal{E},\diamond}_{\Omega_\delta,a}$ when $\Omega_\delta \uparrow \mathbb{C}_\delta$.

The spin correlator Let $u_1, u_2, \ldots, u_n \in \Omega^\bullet_\delta$ be distinct vertices and $v \in \Omega^\circ_\delta$ be a dual vertex neighbouring u_1. Denote $\varpi = \{v, u_2, \ldots, u_n\}$. We now define the spin correlator depending on the mixed correlator $\mathcal{O} = \mu_v\sigma_{u_2}\ldots u_n$ using only one dual vertex.

Definition 4.4.19. Given $u_1, u_2, \ldots, u_n, v$ as above, one defines the spin correlator $\Psi^{\mathcal{S}}_{[\Upsilon(\Omega_\delta),\varpi]}$ for $c \in [\Upsilon(\Omega_\delta), \varpi]$ by

$$\Psi^{\mathcal{S}}_{[\Upsilon(\Omega_\delta),\varpi]}(c) := \eta_c\langle\sigma_{u_c}\mu_{v_c}\mu_v\sigma_{u_2}\ldots\sigma_{u_n}\rangle_{\Omega_\delta}. \tag{4.4.32}$$

The next proposition discusses the properties of $\Psi^{\mathcal{S}}_{[\Upsilon(\Omega_\delta),\varpi]}$.

Proposition 4.4.20. *The correlator defined in* (4.4.32) *is a spinor, s-holomorphic everywhere on* $[\Upsilon(\Omega_\delta), \varpi]$ *and only branches over the points of* ϖ*. Moreover, one has the identity* $\Psi^{\mathcal{S}}_{\Omega_\delta,\varpi}(c(u_1v)) = \pm\mathbb{E}^+_{\Omega_\delta}[\sigma_{u_1}\ldots\sigma_{u_n}]$*, depending on the fiber* $c(u_1v)$ *taken for evaluation.*

Proof. This is a simple consequence of the consturctions of $\mathcal{O}$ and η. For the last claim, one sees that $\langle\sigma_{u_1}\mu_v\mu_v\sigma_{u_2}\ldots\sigma_{u_n}\rangle_{\Omega_\delta} = \langle\sigma_{u_1}\sigma_{u_2}\ldots\sigma_{u_n}\rangle_{\Omega_\delta} = \mathbb{E}^+_{\Omega_\delta}[\sigma_{u_1}\ldots\sigma_{u_n}]$. □

4.5 . Riemann-type boundary value problems

As already mentioned, Smirnov introduced in [160] (via their loop representation) complexified fermionic observables in the isoradial context, which happen to be a very powerfull tool to study the scaling limits of the Ising model defined grids with thinner and thinner mesh size. The most remarkable feature of those scaling limits is their conformal invariance/covariance i.e. sclaling limits compose nicely under conformal maps. In the next paragraph, we recall the semi-discrete integration procedure for the imaginary part of the square a fermionic observable, which is the key tool to pass from semi-discrete to continuum and prove conformal invariance.

4.5.1 . Discrete Integration procedure

Let $F_\delta^{(1)}, F_\delta^{(2)} : \Upsilon(\Omega_\delta) \to \mathbb{C}$ be corner s-holomorphic functions. The next definition precises how to construct a bilinear form that can be interpreted as the imaginary part of the primitive of their product.

Definition 4.5.1. Let $H_\delta = H[F_\delta^{(1)}, F_\delta^{(2)}] := \langle F_\delta^{(1)}, F_\delta^{(2)} \rangle : \Lambda(\Omega_\delta) \to \mathbb{R}$ be defined by the following rules. The integration with respect to $\mathrm{d}z$ is the path integral.

1. If v_1 and v_2 are both in Ω_δ° and such that $\operatorname{Re} v_1 = \operatorname{Re} v_2$, define

$$H_\delta(v_2) - H_\delta(v_1) := \int_{v_1}^{v_2} [F_\delta^{(1)}(c_z^-)\overline{F_\delta^{(2)}}(c_z^+) - \overline{F_\delta^{(2)}}(c_z^-)F_\delta^{(1)}(c_z^+)]\mathrm{d}z. \tag{4.5.1}$$

2. If u_1 and u_2 are both in $\Omega_\delta^\bullet$ and such that $\operatorname{Re} u_1 = \operatorname{Re} u_2$, define

$$H_\delta(u_2) - H_\delta(u_1) := -\int_{u_1}^{u_2} [F_\delta^{(1)}(c_z^-)\overline{F_\delta^{(2)}}(c_z^+) - \overline{F_\delta^{(2)}}(c_z^-)F_\delta^{(1)}(c_z^+)]\mathrm{d}z. \tag{4.5.2}$$

3. If v and u are horizontal neighbours in $\Lambda(\Omega_\delta)$ with $v \in \Omega_\delta^\circ$ and $u \in \Omega_\delta^\bullet$, define

$$H_\delta(v) - H_\delta(u) := -\delta F_\delta^{(1)}(c_{vu})\overline{F_\delta^{(2)}(c_{vu})}. \tag{4.5.3}$$

Note that (4.5.1) and (4.5.2) are *path integrations*. It can be easily checked that H_δ is locally (and hence globally) well defined up to *one* additive constant on $\Lambda(\Omega_\delta)$, by showing that the sum of differences (4.5.1), (4.5.2) and (4.5.3) along any closed contour is zero. This check is easy on elementary rectangles and extends to any contour. Below we show the computation on elementary rectangles.

Consider two corners c_1 and c_2 such that $\operatorname{Re} c_1 = \operatorname{Re} c_2$. For $i = 1, 2$, write

$c_i = (v_i, u_i)$ and assume that v_i is on the left and u_i is on the right. Then,

$$\begin{aligned}
&[H_\delta(v_2) - H_\delta(v_1)] - [H_\delta(u_2) - H_\delta(u_1)] \\
&\quad = \int_{c_1}^{c_2} [F_\delta^{(1)}(c^-)\overline{F_\delta^{(2)}}(c) - \overline{F_\delta^{(2)}}(c^-)F_\delta^{(1)}(c)]\mathrm{d}c \\
&\qquad + \int_{c_1}^{c_2} [F_\delta^{(1)}(c)\overline{F_\delta^{(2)}}(c^+) - \overline{F_\delta^{(2)}}(c)F_\delta^{(1)}(c^+)]\mathrm{d}c \\
&\quad = \int_{c_1}^{c_2} F_\delta^{(1)}(c)[\overline{F_\delta^{(2)}}(c^+) - \overline{F_\delta^{(2)}}(c^-)] - \overline{F_\delta^{(2)}}(c)[F_\delta^{(1)}(c^+) - F_\delta^{(1)}(c^-)]\mathrm{d}c \\
&\quad = \mathrm{i}\,\delta \int_{c_1}^{c_2} F_\delta^{(1)}(c) \cdot \partial_y \overline{F_\delta^{(2)}}(c) + \overline{F_\delta^{(2)}}(c) \cdot \partial_y F_\delta^{(1)}(c)\mathrm{d}c \\
&\quad = \mathrm{i}\,\delta \int_{c_1}^{c_2} \partial_y [F_\delta^{(1)}(c)\overline{F_\delta^{(2)}}(c)]\mathrm{d}c = -\mathrm{i} \int_{c_1}^{c_2} \partial_y [H_\delta(v_c) - H_\delta(u_c)]\mathrm{d}c.
\end{aligned}$$

One can also easily check that H_δ is a bilinear form on the Hermitian space of corner s-holomorphic functions. Given a complex-valued function $F_\delta : \Upsilon(\Omega_\delta) \to \mathbb{C}$ defined at corners (requiring F_δ to be a spinor when defined on the double cover) one can define a *primitive* of its square by simply posing $H_\delta = H_\delta[F_\delta] := \langle F_\delta, F_\delta \rangle$. This recovers the definition of the primitive H_δ in [109, Sec. 4.3] where the integrals are one-dimensional integrals instead of path integrals. Recall that for $z \in \Lambda(\Omega_\delta)$, we defined

$$F_\delta^\diamond(z) := F_\delta(c_z^+) + F_\delta(c_z^-). \tag{4.5.4}$$

Proposition 4.4.12 ensures that $F_\delta^\diamond$ is s-holomorphic on $\diamondsuit(\Omega_\delta)$. The following proposition states that the primitive H_δ has a nice interpretation in terms of $F_\delta^\diamond$. We omit the proof here since they can be found in [109, Sec. 4.3].

Proposition 4.5.2. *The bilinear form $H_\delta = H_\delta[F_\delta]$ has the following properties :*

1. *H_δ is well defined simultaneously on $\Omega_\delta^\bullet$ and Ω_δ° up to* one *additive constant.*
2. *One can interpret H_δ as the primitive of the imaginary part of $(F_\delta^\diamond)^2$ i.e.*
   (a) *Let $z, z' \in \diamondsuit(\Omega_\delta)$ such that $\operatorname{Re} z = \operatorname{Re} z'$ and $[zz'] \subset \diamondsuit(\Omega_\delta)$. Then we have*
   $$H_\delta(z') - H_\delta(z) = \operatorname{Im} \int_z^{z'} \mathrm{i} \cdot (F_\delta^\diamond(\nu))^2 \mathrm{d}\nu. \tag{4.5.5}$$
   (b) *Let $z \in \diamondsuit(\Omega_\delta)$ such that $z^-, z^+ \in \diamondsuit(\Omega_\delta)$. Then,*
   $$H_\delta(z^+) - H_\delta(z^-) = \operatorname{Im}[F_\delta^\diamond(z)^2(z^+ - z^-)]. \tag{4.5.6}$$
3. *H^δ is subharmonic on primal lines and superharmonic on dual lines, i.e.,*
   $$\Delta^{(\delta)} H_\delta(u) \geqslant 0 \quad \text{and} \quad \Delta^{(\delta)} H_\delta(v) \leqslant 0$$
   for all $u \in \Omega_\delta^\bullet$ and $v \in \Omega_\delta^\circ$, provided $F_\delta^\diamond$ doesen't branch over u or v.

One can see as in [38, Rmk. 3.8] that the above sub/super harmonicity property *is preserved near one of the branchings* when the corner holomorphic observable *vanished* at a corner nearby the branching, while it fails if the observable does not vanish near the branching. One can also see that (which is a consequence of [109, Prop. 3.15] and the sub/super harmonicity property) the semi-discrete primitive of the square H satisfies the maximum and minimum principle i.e. in a connected set S of $\Lambda(\Omega_\delta)$ where the observable has no branchings (or vanishes near its branchings as described above), the maximum and the minimum of H is attained at the boundary of S. When integrating observables definded on a double cover with a finite number of branchings, this integration procedure kills the branching structure and provides a well-defined function *on the planar domain*. We now present a trick already mentioned in [43, Lem. 3.14] that takes advantages of the previous integration procedure to extract values of observables near their branchings.

Proposition 4.5.3. *Let $F_v^\diamond$ and $G_u^\diamond$ two diamond s-holomorphic spinors that branch respectively over $v \in \Omega_\delta^\circ$ and $u \in \Omega_\delta^\bullet$, separated by a corner $c = c(v,u)$. Let $\mathcal{C}$ be a* planar *closed contour formed by lines of $\Lambda(\Omega_\delta)$ and medial edges, surrounding v and u but no other branching of $F_v^\diamond$ and $G_u^\diamond$. We have then*

$$\mathrm{Im}\,\big[\oint_{\mathcal{C}} F_v^\diamond(z) G_u^\diamond(z)\mathrm{d}z\big] = \pm 2\delta F_v(c)\overline{G_u(c)}, \tag{4.5.7}$$

where $\pm$ only depends on the orientation of $\mathcal{C}$ and the sheet of the lift of c.

Proof. The s-holomorphic functions $F_v^\diamond$ and $G_u^\diamond$ are locally defined on two *slightly different* double-covers, branching respectively around v and u. One can naturally identify those two double-covers except at the two lifts of c. Consider the planar contour $\mathcal{C}$ defined by $p_1 \sim p_2 \sim \cdots \sim p_r \sim p_{r+1} = p_1$ as in Figure 4.5.1. In our notations, either $p_i \sim p_{i+1}$ are two neighbours $\Lambda(\Omega_\delta)$ or $\mathrm{Re}[p_i] = \mathrm{Re}[p_{i+1}]$.

The integration procedure introduced in Definition 4.5.1 for the product of $F_v^\diamond$ and $G_u^\diamond$ is local and hence well defined away from the branchings. In particular, local increments of $H[F_v^\diamond, G_u^\diamond]$ are well defined. Modifying step by step the contour (as done with pink arrows), it is possible to replace $\mathcal{C}$ by any interior elementary rectangle surrounding c and passing by v and u. Splitting this last rectangle into two elementary rectangles containing the segment $[vu]$, the only remaing contribution comes from the two horizontal segments (drawn in red and blue), where the non-identification of double-covers at c implies the increments *do not* cancel each other. Fix a lift c_0 of c to the double cover branching around v. Up to a global sign (depending on the orientation of the contour and the choice of the lift c_0), the total increment of the two horizontal rectangles is

$$\delta F_v(c_0)\overline{G_u(c_0)} - \delta F_v(c_0)\overline{G_u(c_0^\#)}. \tag{4.5.8}$$

The mismatch obtained is $\pm 2\delta F_v(c_0)\overline{G_u(c_0)}$ using the spinor property. □

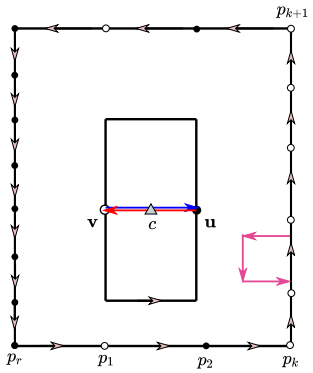

FIGURE 4.5.1 – Illustration of the proof of Proposition 4.5.3 : One first modifies a contour surrouding $c, \mathbf{v}, \mathbf{u}$ without changing the integral around $\mathcal{C}$ (local moves represented by pink arrows) to get a standard rectangle passing by $\mathbf{v}, \mathbf{u}$ and surrounding c. We then split the rectangle in two different elementary rectangle, containing the segment $[uv]$. Due to the non-identification of double-covers at c, the increments in red and blue are *the same* and sum up to $\pm 2\delta F_v(c)\overline{G_u(c)}$.

4.5.2 . Characterisation of observables via semi-discrete boundary values problems

For a semi-discrete simply connected region $\mathcal{R}_\delta$ and $z_{ext} \in \partial\mathcal{R}_\delta$, one defines $v_{out}(z_{ext})$ to be the unit normal vector at z oriented towards the exterior of $\mathcal{R}_\delta$. It is a classical fact [109, 48] that the s-holomorphicity condition (4.4.10) applied at a boundary vertex z_{ext} implies that $\mathrm{Im}[F^\diamond(z_{ext})v_{out}^{1/2}(z_{ext})] = 0$. The latter fact reads as $H_\delta = H[F_\delta]$ being constant along the boundary of $\mathcal{R}_\delta$. Since the primitivation procedure in Definition 4.5.1 is defined up to an additive constant, one can always assume that H_δ vanishes along the boundary. We write now the energy and spin observables (4.4.29) (4.4.32) as solutions to semi-discrete Riemann-type boundary value problems. We keep the notations introduced earlier, with $a \in \Upsilon(\Omega_\delta)$, $\varpi = \{v, u_2, \dots, u_n\}$, and c_0 one of the lifts of $c(vu_1)$ in $[\Upsilon(\Omega_\delta), \varpi]$. We consider the following boundary value problems $\mathcal{P}^{\mathcal{E}}_{\Omega_\delta,a}$ and $\mathcal{P}^{\mathcal{S}}_{\Omega_\delta,\varpi^\delta}$, whose respective solutions are denoted $F_{\mathcal{E}} = F^{\mathcal{E}}_{\Omega_\delta,a}$ and $F_{\mathcal{S}} = F^{\mathcal{S}}_{\Omega_\delta,\varpi^\delta}$

$$\mathcal{P}^{\mathcal{E}}_{\Omega_\delta,a} : \begin{cases} F_{\mathcal{E}} \text{ is double-valued } \pm 1 \text{ at } a^\pm \text{ as in (4.4.29).} \\ F_{\mathcal{E}} \text{ is } s\text{-holomorphic everywhere in } \Omega_{a,\delta}. \\ H_\delta[F_{\mathcal{E}}] \text{ vanishes on } \partial\Omega_\delta. \end{cases} \tag{4.5.9}$$

$$\mathcal{P}^{\mathcal{S}}_{\Omega_\delta,\varpi^\delta} : \begin{cases} F_{\mathcal{S}} \text{ is a spinor on } [\Upsilon(\Omega_\delta), \varpi] \text{ branching around } v, u_2, \dots, u_n. \\ F_{\mathcal{S}}(c_0) = 1. \\ F_{\mathcal{S}} \text{ is } s\text{-holomorphic everwhere in } [\Upsilon(\Omega_\delta), \varpi] \text{ (e.g. even near the branchings).} \\ H_\delta[F_{\mathcal{S}}] \text{ vanishes on } \partial\Omega_\delta. \end{cases} \tag{4.5.10}$$

Lemma 4.5.4. *The observables $F^{\mathcal{E}}_{\Omega_\delta,a}$ and $\mathbb{E}^+_{\Omega_\delta}[\sigma_{u_1}\dots\sigma_{u_n}]^{-1}F^{\mathcal{S}}_{\Omega_\delta,\varpi^\delta}$ are respectively the unique solutions to $\mathcal{P}^{\mathcal{E}}_{\Omega_\delta,a}$ and $\mathcal{P}^{\mathcal{S}}_{\Omega_\delta,\varpi^\delta}$.*

Proof. The results of the previous sections imply that $F^{\mathcal{E}}_{\Omega_\delta,a}$ and $\frac{F^{\mathcal{S}}_{\Omega_\delta,\varpi^\delta}}{\mathbb{E}^+_{\Omega_\delta}[\sigma_{u_1}\dots\sigma_{u_n}]}$ are indeed solutions to the corresponding boundary value problems. To prove their uniqueness, consider $\hat{F}_{\mathcal{E},\mathcal{S}}$ as the differences of two distinct solutions to the corresponding boundary value problems. For the energy-energy boundary value problem $\mathcal{P}^{\mathcal{E}}_{\Omega_\delta,a}$, the double valuations at a cancel each-other, hence the observable $\hat{F}_{\mathcal{E}}$ is s-holomorphic everywhere thus $H_\delta[\hat{F}_{\mathcal{E}}]$ is well defined on Ω_δ and satisfies the maximum and the minimum principle. Since H_δ vanishes at the boundary, it implies that both H_δ and $\hat{F}_{\mathcal{E}}$ identically vanish. For the spin boundary value problem $\mathcal{P}^{\mathcal{S}}_{\Omega_\delta,\varpi^\delta}$, one sees that $\hat{F}_{\mathcal{S}}$ vanishes near the branching v, preserving the subharmonicity of H_δ at v. Thus H_δ is subharmonic everywhere and vanishes on the boundary, as a conesequence, it vanishes everywhere. Assume that $\hat{F}_{\mathcal{S}}$ is not trivial. In particular H is not constant, and its maximum has to be attained at the boundary. This implies as in [39, Prop. 2.16 and (4.7)] that the sign $\overline{\eta_c}\hat{F}_{\mathcal{S}}$ has to be preserved when traveling along the boundary. This is incompatible with the fact that $\overline{\eta_c}\hat{F}_{\mathcal{S}}$ branches around any of the other branchings. One can then conclude that $\hat{F}_{\mathcal{S}}$ is trivial. □

4.5.3 . Continuous boundary values problem

The previous paragraph characterizes semi-discrete observables by semi-discrete Riemann-type boundary value problems. The overall strategy to prove the convergence of different Ising-related quantities starts by proving the convergence of semi-discrete observables to their natural continuous counterparts, which arise naturally from associated continuous boundary problems. For completeness, we recall simple facts on solutions to those continuous boundary value problems, which are summurized in a very complete way in [39, Sec. 3 and 5].

Given a simply connected domain Ω, a and $\varpi = \{u_1, u_2, \dots, u_n\}$, consider $\mathcal{P}^{\mathcal{E}}_{\Omega,a}$ and $\mathcal{P}^{\mathcal{S}}_{\Omega,\varpi}$ the following Riemann-Hilbert boundary value problems, whoses respective solutions are denoted by $f_{\mathcal{E}} = f^{\mathcal{E}}_{\Omega,a}$ and $f_{\mathcal{S}} = f^{\mathcal{S}}_{\Omega,\varpi}$.

$$\mathcal{P}^{\mathcal{E}}_{\Omega,a}: \begin{cases} f_{\mathcal{E}} \text{ is holomorphic everywhere in } \Omega\backslash\{a\}. \\ f_{\mathcal{E}} - \frac{1}{\pi(z-a)} \text{ is bounded near } a. \\ H_{\mathcal{E}} := \operatorname{Im}\int^z f^2_{\mathcal{E}}(\nu)\mathrm{d}\nu \text{ vanishes on } \partial\Omega. \end{cases} \tag{4.5.11}$$

$$\mathcal{P}^{\mathcal{S}}_{\Omega,\varpi}: \begin{cases} f_{\mathcal{S}} \text{ is an holomorphic spinor in } [\Upsilon(\Omega_\delta), \varpi]. \\ H_{\mathcal{S}} := \operatorname{Im}\int^z f^2_{\mathcal{S}}(\nu)\mathrm{d}\nu \text{ is bounded from above near } u_2, \dots, u_n. \\ H^\dagger_{\mathcal{S}} := \operatorname{Im}\int^z [f_{\mathcal{S}}(\nu) - \frac{e^{\mathrm{i}\frac{\pi}{4}}}{\sqrt{\nu-u_1}}]^2\mathrm{d}\nu \text{ is bounded near } u_1. \\ H_{\mathcal{S}} \text{ vanishes on } \partial\Omega. \end{cases} \tag{4.5.12}$$

Each of the above boundary value problems has a unique solution, see [39]. We explain briefly the ideas behind. The uniqueness proof goes as in the semi-discrete treated above, while the existence comes from explicit constructions, first in a concrete domain then mapped to general domains using conformal rules. Given a conformal map $\varphi : \Omega \to \varphi(\Omega)$ between two simply connected domains, one has

$$f^{\mathcal{E}}_{\Omega,a}(z) = |\varphi'(a)| \cdot f^{\mathcal{E}}_{\varphi(\Omega),\varphi(a)}[\varphi(z)], \tag{4.5.13}$$

$$f^{\mathcal{S}}_{\Omega,\varpi}(z) = \prod_{k=1}^{n} |\varphi'(u_k)|^{\frac{1}{8}} \cdot f^{\mathcal{S}}_{\Omega,\varphi(\varpi)}[\varphi(z)]. \tag{4.5.14}$$

The link between Ising-related quantities and their scaling limits read near the singularities of $f^{\mathcal{E}}_{\Omega,a}$ and $f^{\mathcal{S}}_{\Omega,\varpi}$. For the solution to $\mathcal{P}^{\mathcal{E}}_{\Omega,a}$, one has the expansion

$$f^{\mathcal{E}}_{\Omega,a}(z) - \frac{1}{\pi(z-a)} \overset{z\to a}{\longrightarrow} \frac{1}{2\pi}\ell_\Omega(a), \tag{4.5.15}$$

where $l_\Omega(a)$ is the conformal modulus of Ω seen from a **[hongler-smirnov]**.

For the multiple energy correlation function, first recall that we write $\mathbb{K}(a_1, \dots, a_r)$ for the $r \times r$ matrix with coefficients $\mathbb{K}_{i,j} = \mathbf{1}_{i\neq j}(a_i - a_j)^{-1}$. Given distinct points $a_1, \dots, a_r$ of $\mathbb{H}$, set

$$\langle \varepsilon_{a_1}\varepsilon_{a_2}\dots\varepsilon_{a_r}\rangle^+_{\mathbb{H}} := (\tfrac{2}{i\pi})^n \mathrm{Pf}(a_1, \dots, a_r, \overline{a_1}, \dots, \overline{a_r}), \tag{4.5.16}$$

where Pf denotes the usual Pfaffian operator. Given $\varphi : \mathbb{H} \to \Omega$ a conformal map, one can define the continuous energy correlation in Ω via

$$\langle \varepsilon_{a_1}\varepsilon_{a_2}\dots\varepsilon_{a_r}\rangle^+_{\mathbb{H}} := \prod_{k=1}^{r} |\varphi'(a_k)| \cdot \langle \varepsilon_{\varphi(a_1)}\varepsilon_{\varphi(a_2)}\dots\varepsilon_{\varphi(a_r)}\rangle^+_{\Omega}. \tag{4.5.17}$$

One can also see that the solution to $\mathcal{P}^{\mathcal{S}}_{[\Upsilon(\Omega_\delta),\varpi]}$ admits an expansion near u_1 of the form

$$f^{\mathcal{S}}_{\Omega,\varpi}(z) = e^{\mathrm{i}\frac{\pi}{4}}\big[\frac{1}{\sqrt{z-u_1}} + 2\mathcal{A}_{[\Omega,u_1,\dots,u_n]}\sqrt{z-u_1} + O((z-u_1)^{\frac{3}{2}})\big]. \tag{4.5.18}$$

This expansion allows us to define the coefficient $\mathcal{A}_{(u_1,\dots,u_n)} := \mathcal{A}_{[\Omega,u_1,\dots,u_n]}$. Now, one can *define* the *continuous correlation fuction*

$$\langle \sigma_{u_1}\dots\sigma_{u_n}\rangle^+_{\Omega} := \exp\big(\mathrm{Re}\big[\int^{(u_1,\dots,u_n)} \sum_{k=1}^{n} \mathcal{A}_{(x_1,\dots,x_n)}\mathrm{d}x_k\big]\big), \tag{4.5.19}$$

with a normalization chosen so that $\langle \sigma_{u_1}\dots\sigma_{u_n}\rangle^+_{\Omega} \sim \frac{1}{|u_2-u_1|^{\frac{1}{4}}}\langle \sigma_{u_3}\dots\sigma_{u_n}\rangle^+_{\Omega}$ as $u_1 \to u_2$. The above integration should be understood as an integration on the space of n-tuples living on Ω^n.

In the special case $n = 2$, one can also define the coefficient $\mathcal{B}_\Omega(u_1, u_2) \in \mathbb{R}$ via the expansion of $f^{\mathcal{S}}_{\Omega,\varpi}$ near u_2, such that

$$f^{\mathcal{S}}_{\Omega,\varpi} = \frac{e^{-i\frac{\pi}{4}}}{(z-u_2)^{\frac{1}{2}}}\mathcal{B}_\Omega(u_1, u_2) + O(z-u_2)^{\frac{1}{2}}. \tag{4.5.20}$$

Due to the branching structure, the coefficient $\mathcal{B}_\Omega(u_1, u_2)$ is defined up to the sign, thus one can simply chose it to be non-negative. This allows us to define the correlation function with free boundary conditions, which is at stake in the convergence of the model with f boundary conditions.

$$\langle \sigma_{u_1}\sigma_{u_2}\rangle^{\mathrm{f}} := \mathcal{B}_\Omega(u_1, u_2) \cdot \langle \sigma_{u_1}\sigma_{u_2}\rangle^{+}. \tag{4.5.21}$$

For a conformal mapping φ and $\mathfrak{b} \in \{+, \mathrm{f}\}$, one has the conformal rule

$$\langle \sigma_{u_1}\sigma_{u_2}\rangle^{\mathfrak{b}}_{\Omega} = \langle \sigma_{\varphi(u_1)}\sigma_{\varphi(u_2)}\rangle^{\mathfrak{b}}_{\varphi(\Omega)} \cdot |\varphi'(u_1)|^{\frac{1}{8}}|\varphi'(u_2)|^{\frac{1}{8}}. \tag{4.5.22}$$

4.6 . Derivation of main theorems

The proofs of convergence of semi-discrete Ising quantities start by proving that semi-discrete fermionic observables constructed out of mixed correlators converge to their continuous counterparts. The general strategy is to prove the existence of subseqential limits (for the topology of the uniform convergence on compacts) and that any of those sub-sequential limits (now viewed in continuum) is solution to a continuous boundary value problem. As in the isoradial case, the precompactness is achieved by using the semi-discrete primitive of the imaginary part of the square. Next lemma recalls a sufficient condition for the family $(F^{\diamond}_\delta)_{\delta>0}$ to be precompact via some control on $(H_\delta)_{\delta>0}$.

Lemma 4.6.1 (Precompactness of s-holomorphic functions)**.** *Let $Q \subset \Omega$ be a rectangular domain such that $9Q \subset \Omega$. Let $(F^{\diamond}_\delta)_{\delta>0}$ be a family of diamond s-holomorphic functions on $\Lambda(\Omega_\delta)$ and $H_\delta = \operatorname{Im}\int F^{\diamond 2}_\delta$. If $(H_\delta)_{\delta>0}$ is uniformly bounded on $9Q_\delta$, then $(F^{\diamond}_\delta)$ is precompact on Q_δ.*

Proof. This result is proven in [109, Thm. 5.3]. □

4.6.1 . Convergence of semi-discrete observable to continous ones

In this subsection we prove the convergence of properly normalized semi-discrete fermionic observables in the semi-discrete lattice to their continuous counterpart. Those proofs follow the path of the isoradial case. Recall that the observables $\Psi^{\mathcal{E}}_{\Omega_\delta,a}$ and $\Psi^{\mathcal{S}}_{\Omega_\delta,\varpi}$ are respectively the unique solution to $\mathcal{P}^{\mathcal{E}}_{\Omega_\delta,a}$ and $\mathcal{P}^{\mathcal{S}}_{\Omega_\delta,\varpi}$. As mentioned in Section 4.3, it is enough to prove the convergence results when Ω is smooth, since the analoguous theorems for general domains can be deduced using results in smooth domain, monotonicity with respect to boundary conditions and FKG inequality.

Proposition 4.6.2. *Let a be an interior point of Ω. Then the sequence of observables $(\delta^{-1}F^{\mathcal{E}}_{\Omega_\delta,a})_{\delta>0}$ converges to $\overline{\eta_a}f^{\mathcal{E}}_{\Omega,a}$, uniformly on compact subsets of $\Omega\backslash\{a\}$.*

Proof. Denote $F^\dagger_\delta := \delta^{-1}(F^{\mathcal{E}}_{\Omega_\delta,a} - G_{(a)})$ where $G_{(a)}$ is constructed in Appendix 4.8, $H_\delta := \mathrm{Im}[\int(\delta^{-1}F^{\mathcal{E}}_{\Omega_\delta,a})^2(\nu)\mathrm{d}\nu]$ and $H^\dagger_\delta := \mathrm{Im}[\int(F^\dagger_\delta)^2(\nu)\mathrm{d}\nu]$, both chosen with proper additive constants so that H_δ vanishes on $\partial\Lambda(\Omega_\delta)$ and $H^\dagger_\delta$ vanishes at some fixed interior point different from a (this second choice is irrelevant). We also set $(M^\delta_r)^2 := \max_{\Omega_\delta\backslash B(a,r)} |H^\delta|$. Since the singularities of $F^{\mathcal{E}}_{\Omega_\delta,a}$ and $G_{(a)}$ cancel each other, the observable $F^\dagger_\delta$ is s-holomorphic everywhere. There are now two potential scenarii (the second one is in fact impossible) :

Scenario 1 : For any $r > 0$, the family $(M^\delta_r)_{\delta>0}$ is uniformly bounded by a constant $C(r)$. Using the precompactness lemma 4.6.1, one can extrat a subsequential limit from the family $(\delta^{-1}F^{\mathcal{E}}_{\Omega_\delta,a})_{\delta>0}$ such that $\delta^{-1}F^{\mathcal{E}}_{\Omega_\delta,a} \to f$, $H_\delta \to h = \mathrm{Im}[\int^z f^2(\nu)\mathrm{d}\nu]$ and $H^\dagger_\delta \to h^\dagger = \mathrm{Im}[\int^z(f - \frac{\overline{\eta_a}}{\pi(\nu-a)})^2\mathrm{d}\nu]$ uniformly on compact subsets of $\Omega\backslash\{a\}$, with f holomorphic away from a, h harmonic except at a and *vanishing* along the boundary of Ω. To obtain this last claim, one has to prove that the semi-discrete boundary conditions of H_δ survive when passing to the limit in continuum (i.e. the function h has Dirichlet boundary conditions). One can first use the boundary modification trick from [109, Lem. 5.1] and modify the weights of the Laplacian operator (4.4.27) at the boundary to preserve the sub-harmonicity of H_δ on $\Omega^\bullet_\delta$ even at the boundary. Using the subharmnocitity of H_δ on $\Omega^\bullet_\delta$, the superharmonicity of H_δ on Ω°_δ, the maximum principle for H_δ and the fact that H_δ vanishes along the boundary one gets

$$-C(r_0)(1 - \mathrm{hm}^{\Omega_\delta\backslash B(a,r)}_{\partial\Omega_\delta}(z)) \leqslant H_\delta(z) \leqslant C(r_0)(1 - \mathrm{hm}^{\Omega_\delta\backslash B(a,r)}_{\partial\Omega_\delta}(z)),$$

where $\mathrm{hm}^{\Omega_\delta\backslash B(a,r)}_{\partial\Omega_\delta}(z)$ stands for the harmonic measure of $\partial\Omega_\delta$ in $\Omega_\delta\backslash B(a,r)$, with respect to the random walk started at z. Due to uniform crossing estimates for the random walk generated by the Laplacian operator (4.4.27), $\mathrm{hm}^{\Omega_\delta\backslash B(a,r)}_{\partial\Omega_\delta}(z)$ goes to 1 (uniformly in δ) as z approaches $\partial\Omega_\delta$.

On the other hand, the convergence of $\delta^{-1}G_{(a)}$ to $\frac{\overline{\eta_a}}{\pi(z-a)}$ and the maximum principle applied to $H^\dagger_\delta$ ensures that $H^\dagger_\delta$ is uniformly bounded near a *already in semi-discrete* (since at a fixed definite distance from a, $F^\dagger_\delta$ converges to $f - \frac{\overline{\eta_a}}{\pi(z-a)}$). In particular, $F^\dagger_\delta$ is uniformly bounded near a. Passing to the limit $f - \frac{\overline{\eta_a}}{\pi(z-a)}$ is then uniformly bounded near a (due to the maximum principle applied to the s-holomorphic functions $F^\dagger_\delta$). We can thus identify f as $\overline{\eta_a}f^{\mathcal{E}}_{\Omega,a}$.

Scenario 2 : Conversly, assume that $M^\delta_{r_0} \to \infty$ along some subsequence for some $r_0 > 0$ and consider $\tilde{F}^{\mathcal{E}}_{\Omega_\delta,a} := \frac{F^{\mathcal{E}}_{\Omega_\delta,a}}{M^\delta_{r_0}}$, $\tilde{F}^\dagger_\delta := \frac{F^\dagger_\delta}{M^\delta_{r_0}}$, $\tilde{H}_\delta := \frac{H_\delta}{(M^\delta_{r_0})^2}$ and $\tilde{H}^\dagger_\delta := \frac{H^\dagger_\delta}{(M^\delta_{r_0})^2}$. We first apply the Harnack inequality to the functions $\tilde{H}_\delta$ [109, Prop. 3.25] to deduce that $\tilde{H}_\delta$ is uniformly bounded on *any compact subset* away from a. This way, one can repeat the previous reasoning to extract a subsequential limit from $(\delta^{-1}\tilde{F}^{\mathcal{E}}_{\Omega_\delta,a})_{\delta>0}$ and $(\tilde{H}_\delta)_{\delta>0}$ that converge respectively (uniformly on compact subets of $\Omega\backslash\{a\}$) to $\tilde{f}$ and $\tilde{h} = \mathrm{Im}[\int \tilde{f}^2(\nu)\mathrm{d}\nu]$, with $\tilde{h} = 0$ on $\partial\Omega$. Up to another extraction, we can also assume that the sequence of points $(z_\delta)_{\delta>0}$ in $\Omega\backslash B(a, \frac{r_0}{2})$ such that $\tilde{H}_\delta(z_\delta) = 1$ converges to z_∞. Since $(\delta M^\delta_{r_0})^{-1} G_{(a)}$ now converges to 0, we have (still uniformly on compact subsets of $\Omega\backslash\{a\}$) $\tilde{H}^\dagger_\delta \to \tilde{h}^\dagger = \tilde{h} + \mathrm{cst} = \mathrm{Im}[\int \tilde{f}^2\mathrm{d}\nu]$. In particular, since $\tilde{h}^\dagger$ is bounded away from a and satisfies the maximum principle near a (since $\tilde{F}^\dagger_\delta$ has no singularity), hence so does $\tilde{h}$. In particular, f has no singularity at a, and thus is trivial. This is not compatible with the Dirichlet boundary conditions of $\tilde{h}$ and the fact that $\tilde{h}(z_\infty) = 1$. □

Let $\varpi^\delta = \{v^\delta, u^\delta_2, \dots, u^\delta_n\}$ be points of Ω_δ, at a definite distance from each other, approximating respectively interior points $\varpi = \{u_1, \dots, u_n\}$ of Ω, with the usual convention that $v^\delta \in \Omega^\circ_\delta$ and $u^\delta_2, \dots, u^\delta_n \in \Omega^\bullet_\delta$, and $v^\delta \sim u^\delta_1$.

Proposition 4.6.3. *In the above mentioned context, the family of semi-discrete observables* $(\mathbb{E}^+_{\Omega_\delta}[\sigma_{u_1} \dots \sigma_{u_n}]^{-1}\delta^{-\frac{1}{2}} F^{\mathcal{S}}_{\Omega_\delta,\varpi^\delta})_{\delta>0}$ *converges to* $(\frac{1}{\pi})^{\frac{1}{2}} f^{\mathcal{S}}_{\Omega,\varpi}$ *uniformly on compact subsets of* $[\Upsilon(\Omega_\delta), \varpi]\backslash\varpi$.

Proof. We keep the notations of the previous proof. Denote for the rest of the proof $F_\delta := \delta^{-\frac{1}{2}}\mathbb{E}^+_{\Omega_\delta}[\sigma_{u_1} \dots \sigma_{u_n}]^{-1} F^{\mathcal{S}}_{\Omega_\delta,\varpi}$, $F^\dagger_\delta := F_\delta - \delta^{-\frac{1}{2}} G_{[v]}$, $H_\delta := \mathrm{Im}[\int (F_\delta)^2(\nu)\mathrm{d}\nu]$ and $H^\dagger_\delta := \mathrm{Im}[\int (F^\dagger_\delta)^2(\nu)\mathrm{d}\nu]$, with H_δ vanishing along $\partial\Omega_\delta$ and $H^\dagger_\delta$ vanishing at a point different from the punctures. One can see that $F^\dagger_\delta$ vanishes near the branching v^δ. We also set $(M^\delta_r)^2 := \max_{\Omega\backslash\cup_{i=1\dots n} B(u_i,r)} |H^\delta|$. There are two potential scenarii (the second one is again impossible).

Scenario 1 : If for any $r > 0$, $(M^\delta_r)_{\delta>0}$ is bounded by a constant $C(r)$. Using the precompactness Lemma 4.6.1, one can extract a subsequential limit from the family $(F_\delta)_{\delta>0}$ as $\delta \to 0$. Any subsequential limit f of F_δ is an holomorphic spinor on $[\Upsilon(\Omega_\delta), \varpi]$ and h is harmonic function away from the branchings. The sub/super harmonicity of H_δ, the boundary modification trick and the control of semi-discrete harmonic measures in smooth domains allow to preserve again boundary conditions from semi-discrete to continuum, i.e. $H_\delta \to h = \mathrm{Im}[\int f^2\mathrm{d}\nu]$ uniformly on compact subsets of $\Omega\backslash\varpi$, with $h = 0$ on $\partial\Omega$. Since $F^\dagger_\delta$ vanishes near v^δ, one can use the maximum and the minimum principle in semi-discrete for $H^\dagger_\delta$ near v^δ and the convergence (away from u_1)

of $F_\delta^\dagger$ to $f-(\frac{1}{\pi})^{\frac{1}{2}}\frac{e^{\frac{i\pi}{4}}}{\sqrt{\nu-u_1}}$ to deduce that $H_\delta^\dagger \to h^\dagger = \mathrm{Im}[\int (f-(\frac{1}{\pi})^{\frac{1}{2}}\frac{e^{\frac{i\pi}{4}}}{\sqrt{\nu-u_1}})^2 \mathrm{d}\nu]$, the latter convergence being uniform near u_1. This ensures that $h^\dagger$ is bounded from above and from below near u_1. By subharmonicity property of H_δ, we see that H_δ is bounded from above near $u_2^\delta, \dots, u_n^\delta$ *already in semi-discrete*, which implies the same one sided bound for h near $u_2, \dots, u_n$. This allows to identify f as a multiple of $f^{\mathcal{S}}_{\Omega,\varpi}$ and the normalizing constant is fixed by the asymptotic near u_1.

Scenario 2 : If $M_r^\delta \to \infty$ along some subsequence, one normalizes again by M_r^δ as in the previous proposition and extracts a new subsequential limit $\tilde{f}$, which remains an holomorphic spinor on $[\Upsilon(\Omega_\delta), \varpi]$ and such that the function $\tilde{h} = \mathrm{Im}[\int \tilde{f}^2 \mathrm{d}\nu]$ is harmonic in $\Omega \backslash \varpi$, satisfies Dirichlet Boudary condition, is bounded from below near $u_2, \dots, u_n$ and has a positive outer normal derivative. We know that $\tilde{H}_\delta^\dagger$ satisfies the maximum principle in semi-discrete at a small definite distance from v^δ. Moreover $\tilde{h} = \tilde{h}^\dagger + \mathrm{cst}$ thanks to the normalization by M_r^δ. Thus $\tilde{h}$ is bounded from below near all points $u_1, \dots, u_n$. This implies that $\tilde{h}$ vanishes identically. It remains to adapt the proof of [38, Lem. 3.10] which states that no subsequential limits of $(M_r^\delta)^{-2} H^\delta$ is trivial. This (somewhat technical) proof only relies upon the same sub/super harmonicity arguments, and readily adapts. □

Having explicit asymptotics of the kernels $G_{[u]}$, $G_{[v]}$ and $G_{(a)}$, one can prove the same statement only using one side of the sub/super harmonicity property of functions H^δ, at least in smooth domains (e.g. [43]). It could be even possible in principle to bypass the use of all sub/super harmonicity properties using ideas of [33].

4.6.2 . Derivation of the main theorems

We are now going to use the kernels constructed explicitely and the convergence theorems for s-holomorphic functions arising from boundary value problems to derive Theorems 4.3.7 and 4.3.2. It is important to notice that, comparing to the isoradial case, one has to be careful due to the denegeracy of the lattice in the vertical direction. In particular, the use of the Dotsenko propagation equation becomes crucial to derive the results in the vertcical direction. We start with the proof of Theorem 4.3.5 which is the convergence proof for correlation ratios of general spin-spin correlations.

Proof. As before, we work with Ω_δ, an approximation of a bounded smooth simply connected domain Ω. We assume that $\varpi^\delta = \{v^\delta, u_2^\delta, \dots, u_n^\delta\}$ approximate respectively the interior points $u_1, \dots, u_n$ of Ω, remaining at a definite distance from each other and from the boundary. For simplicity of proof reading, we denote $F^\diamond_{v^\delta} := \delta^{-\frac{1}{2}} F^{\mathcal{S}}_{\Omega_\delta, \varpi^\delta}$. We start the proof of Theorem 4.3.5 with the derivation of correlation ratio in the horizontal direction.

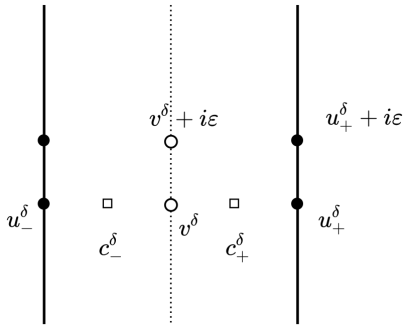

FIGURE 4.6.1 – Configuration of points used to derive convergence of correlation ratios, in the horizontal and the vertical direction. We chose v^δ and $v^\delta + i\varepsilon$ (respectively u_+^δ and $u_+^\delta + i\varepsilon$) to be on the same sheet of the double cover. For the proof in the vertical direction, deforming the contour leads to computing the two increments passing by c_+^δ, which compensate each other due the opposite values of $\mathrm{sgn}(\mathcal{O}_{c_+^\delta}, v^\delta)$ depending on the position of corners compared to v^δ.

Correlation ratio in the horizontal direction Consider the vertices $v^\delta, u_-^\delta, u_+^\delta$ and $c_\pm^\delta = (v^\delta u_{c_\pm^\delta})$ as in Figure 4.6.1. Fix a (small) positive number $r > 0$ and let $\mathcal{C}_r^\delta$ be a semi-discrete square of width $2r$ centered at v^δ, oriented counter-clockwise. We apply the integration trick of Proposition 4.5.3 twice with the contour $\mathcal{C}_r^\delta$ to the functions $F_{v^\delta}^\diamond$ and $\delta^{-\frac{1}{2}} G_{[u_-^\delta]}^\diamond$ on one hand, and to the functions $F_{v^\delta}^\diamond$ and $\delta^{-\frac{1}{2}} G_{[u_+^\delta]}^\diamond$ on the other hand. One gets,

$$\begin{aligned}
\frac{2\delta \cdot \delta^{-\frac{1}{2}} F_{v^\delta}(c_+^\delta) \cdot \delta^{-\frac{1}{2}} \overline{G_{[u_+^\delta]}(c_+^\delta)}}{2\delta \cdot \delta^{-\frac{1}{2}} F_{v^\delta}(c_-^\delta) \cdot \delta^{-\frac{1}{2}} \overline{G_{[u_-^\delta]}(c_-^\delta)}} &= \frac{\int_{\mathcal{C}_r^\delta} \mathrm{Im}[F_{v^\delta}^\diamond(z)\delta^{-\frac{1}{2}} G_{[u_+^\delta]}^\diamond(z)\mathrm{d}z]}{\int_{\mathcal{C}_r^\delta} \mathrm{Im}[F_{v^\delta}^\diamond(z)\delta^{-\frac{1}{2}} G_{[u_-^\delta]}^\diamond(z)\mathrm{d}z]} \\
&= \frac{1 + \dfrac{\int_{\mathcal{C}_r^\delta} \mathrm{Im}\left[F_{v^\delta}^\diamond(z)\delta^{-\frac{1}{2}}(G_{[u_+^\delta]}^\diamond(z) - G_{[u_-^\delta]}^\diamond(z))\mathrm{d}z\right]}{\int_{\mathcal{C}_r^\delta} \mathrm{Im}\left[F_{v^\delta}^\diamond(z)\delta^{-\frac{1}{2}}(G_{[u_+^\delta]}^\diamond(z) + G_{[u_-^\delta]}^\diamond(z))\mathrm{d}z\right]}}{1 - \dfrac{\int_{\mathcal{C}_r^\delta} \mathrm{Im}\left[F_{v^\delta}^\diamond(z)\delta^{-\frac{1}{2}}(G_{[u_+^\delta]}^\diamond(z) - G_{[u_-^\delta]}^\diamond(z))\mathrm{d}z\right]}{\int_{\mathcal{C}_r^\delta} \mathrm{Im}\left[F_{v^\delta}^\diamond(z)\delta^{-\frac{1}{2}}(G_{[u_+^\delta]}^\diamond(z) + G_{[u_-^\delta]}^\diamond(z))\mathrm{d}z\right]}}.
\end{aligned}$$

The convergence of the spin fermionic observable given in Proposition 4.6.3 ensures that,

$$\frac{F_{v^\delta}^\diamond(z)}{\mathbb{E}_{\Omega_\delta^\bullet}^+[\sigma_{u_+^\delta} \dots \sigma_{u_n^\delta}]} = \frac{e^{\mathrm{i}\frac{\pi}{4}}}{\sqrt{\pi}}\Big(\frac{1}{\sqrt{z-u_1}} + 2\mathcal{A}_{(u_1,\dots,u_n)}\sqrt{z-v} + O((z-v)^{\frac{3}{2}})\Big),$$

uniformly in $z \in \Omega_{\varpi_\delta}^\diamond$ remaining at a fixed distance from the punctures and

the boundary, where the coefficient $\mathcal{A} = \mathcal{A}_{(\Omega,u_1,\dots,u_n)}$ is defined in (4.5.18). Additionally, the asymptotic of the kernels $G^{\diamond}_{[u^\delta_\pm]}$ away from their branchings gives,

$$\delta^{-\frac{1}{2}}(G^{\diamond}_{[u^\delta_+]}(z) - G^{\diamond}_{[u^\delta_-]}(z)) = \frac{e^{-i\frac{\pi}{4}}}{\sqrt{\pi}}\frac{(u^\delta_+ - u^\delta_-)}{2(z-v)^{\frac{3}{2}}} + O\Big(\frac{\delta^2}{(z-v)^{\frac{5}{2}}}\Big).$$

One first multiplies the two previous asymptotics, then uses classical bounds on interpolation of countour integrals via their discretization, together with the fact that integrals of the continuous limits do *not* depend on the contour of integration. Since r can be chosen arbitrarily small, the residue theorem ensures that when $\delta \to 0$,

$$\begin{aligned}
&\mathrm{Im}\,[\int_{\mathcal{C}^\delta_r} \frac{F^{\diamond}_{v^\delta}(z)}{\mathbb{E}^+_{\Omega^\bullet_\delta}[\sigma_{u^\delta_+}\dots\sigma_{u^\delta_n}]}\delta^{-\frac{1}{2}}(G^{\diamond}_{[u^\delta_+]}(z) - G^{\diamond}_{[u^\delta_-]}(z))\mathrm{d}z] \\
&= 2\,\mathrm{Re}[\mathcal{A}\cdot(u^\delta_+ - u^\delta_-)] + O(r\delta) + o(\delta) \\
&= 4\delta\mathrm{Re}[\mathcal{A}_{(u_1,\dots,u_n)}] + o(\delta).
\end{aligned}$$

Similarly, for $\delta \to 0$, one has,

$$\mathrm{Im}\,[\int_{\mathcal{C}^\delta_r} \frac{F^{\diamond}_{v^\delta}(z)}{\mathbb{E}^+_{\Omega^\bullet_\delta}[\sigma_{u^\delta_+}\dots\sigma_{u^\delta_n}]}\delta^{-\frac{1}{2}}(G^{\diamond}_{[u^\delta_+]}(z) + G^{\diamond}_{[u^\delta_-]}(z))\mathrm{d}z] = 4 + o(1),$$

where o is uniform provided that $u_1,\dots,u_n$ remain at a definite distance from each other and from the boundary. Finally, it is enough to notice that $|G_{[u^\delta_+]}(c^\delta_+)| = |G_{[u^\delta_-]}(c^\delta_-)| = 1$ to conclude that,

$$\frac{\mathbb{E}^+_{\Omega^\bullet_\delta}[\sigma_{u^\delta_+}\dots\sigma_{u^\delta_n}]}{\mathbb{E}^+_{\Omega^\bullet_\delta}[\sigma_{u^\delta_-}\dots\sigma_{u^\delta_n}]} = 1 + 2\delta\mathrm{Re}[\mathcal{A}_{(u_1,\dots,u_n)}] + o(\delta). \tag{4.6.1}$$

Correlation ratio in the vertical direction The proof in the vertical direction is more tedious and requires the use of the propagation equation (4.4.10) and the asymptotics of correlation ratio in the horizontal direction derived in (4.6.1). We first fix $v^\delta, v^\delta + i\varepsilon, u^\delta_+, u^\delta_+ + i\varepsilon, u^\delta_-$ as in Figure 4.6.1, assuming $v^\delta, v^\delta + i\varepsilon$ and $u^\delta_+, u^\delta_+ + i\varepsilon, u^\delta_-$ are taken respectively on the same sheet. Applying the previous reasoning on a macroscopic contour $\mathcal{C}^\delta_r$ of small radius r one gets,

$$\frac{\mathbb{E}^+_{\Omega^\bullet_\delta}[\sigma_{u^\delta_+ + i\varepsilon}\dots\sigma_{u^\delta_n}]}{\mathbb{E}^+_{\Omega^\bullet_\delta}[\sigma_{u^\delta_+}\dots\sigma_{u^\delta_n}]} = \frac{1 + \dfrac{\mathrm{Im}\,[\int_{\mathcal{C}^\delta_r} F^{\diamond}_{v^\delta+i\varepsilon}(z)\delta^{-\frac{1}{2}}G_{[u^\delta_+ + i\varepsilon]}(z) - F^{\diamond}_{v^\delta}(z)\delta^{-\frac{1}{2}}G^{\diamond}_{[u^\delta_+]}(z)\mathrm{d}z]}{\mathrm{Im}\,[\int_{\mathcal{C}^\delta_r} F^{\diamond}_{v^\delta+i\varepsilon}(z)\delta^{-\frac{1}{2}}G^{\diamond}_{[u^\delta_+ + i\varepsilon]}(z) + F^{\diamond}_{v^\delta}(z)\delta^{-\frac{1}{2}}G^{\diamond}_{[u^\delta_+]}(z)\mathrm{d}z]}}{1 - \dfrac{\mathrm{Im}\,[\int_{\mathcal{C}^\delta_r} F^{\diamond}_{v^\delta+i\varepsilon}(z)\delta^{-\frac{1}{2}}G_{[u^\delta_+ + i\varepsilon]}(z) - F^{\diamond}_{v^\delta}(z)\delta^{-\frac{1}{2}}G^{\diamond}_{[u^\delta_+]}(z)\mathrm{d}z]}{\mathrm{Im}\,[\int_{\mathcal{C}^\delta_r} F^{\diamond}_{v^\delta+i\varepsilon}(z)\delta^{-\frac{1}{2}}G^{\diamond}_{[u^\delta_+ + i\varepsilon]}(z) + F^{\diamond}_{v^\delta}(z)\delta^{-\frac{1}{2}}G^{\diamond}_{[u^\delta_+]}(z)\mathrm{d}z]}}. \tag{4.6.2}$$

We use the factorization

$$F^{\diamond}_{v^\delta+i\varepsilon}(z)G^{\diamond}_{[u^\delta_+ +i\varepsilon]}(z) - F^{\diamond}_{v^\delta}(z)G^{\diamond}_{[u^\delta_+]}(z)$$
$$= F^{\diamond}_{v^\delta}(z)\big(G^{\diamond}_{[u^\delta_+ +i\varepsilon]}(z) - G^{\diamond}_{[u^\delta_+]}(z)\big) + \big(F^{\diamond}_{v^\delta+i\varepsilon}(z) - F^{\diamond}_{v^\delta}(z)\big)G^{\diamond}_{[u^\delta_+ +i\varepsilon]}(z),$$

and treat separately the two terms on the RHS of the previous equality.

First term Using the differentiability of the correlator with respect to its branching position (see (4.8.7)), one can write the expansion,

$$G^{\diamond}_{[u^\delta_+ +i\varepsilon]}(z) - G^{\diamond}_{[u^\delta_+]}(z) = i\varepsilon\partial_y G^{\diamond}_{[u^\delta_+]}(z) + o(\varepsilon), \tag{4.6.3}$$

where o is uniform provided ε is small enough. Thus, integrating on $\mathcal{C}^\delta_r$, one finds

$$\operatorname{Im}\big[\int_{\mathcal{C}^\delta_r} F^{\diamond}_{v^\delta}(z)\delta^{-\frac{1}{2}}\big(G^{\diamond}_{[u^\delta_+ +i\varepsilon]}(z) - G^{\diamond}_{[u^\delta_+]}(z)\big)\mathrm{d}z\big]$$
$$= \varepsilon \operatorname{Im}\big[\int_{\mathcal{C}^\delta_r} \mathrm{i}\,\delta^{-\frac{1}{2}}\partial_y G^{\diamond}_{[u^\delta_+]}(z)F^{\diamond}_{v^\delta}(z)\mathrm{d}z\big] + o(\varepsilon).$$

Second term We take advantage of the propagation equation stated previously. To simplify the proof reading of the following lines, we introduce the Kadanoff–Ceva correlator $Y_{[v^\delta,u^\delta_-,u^\delta_+]}(c) := \delta^{-\frac{1}{2}}\eta_c\langle\mu_{v_c}\sigma_{u_c}\mu_{v^\delta}\sigma_{u^\delta_+}\sigma_{u^\delta_-}\sigma_{u_2}\dots\sigma_{u_n}\rangle_{\Omega_\delta}$, where $u^\delta_\pm$ are taken on the same sheet as in Proposition 4.4.2. We also denote by $Y^{\diamond}_{[v^\delta,u^\delta_-,u^\delta_+]}$ its associated diamond s-holomorphic extension, see Proposition 4.4.12. One sees that $Y^{\diamond}_{[v^\delta,u^\delta_-,u^\delta_+]}$ branches only around the three vertices $v^\delta, u^\delta_-, u^\delta_+$. In that case, Proposition 4.4.2 reads,

$$\delta^{-\frac{1}{2}}\big(\langle\mu_{v_c}\sigma_{u_c}\mu_{v^\delta+i\varepsilon}\sigma_{u^\delta_2}\dots\sigma_{u^\delta_n}\rangle_{\Omega_\delta} - \langle\mu_{v_c}\sigma_{u_c}\mu_{v^\delta}\sigma_{u^\delta_2}\dots\sigma_{u^\delta_n}\rangle_{\Omega_\delta}\big)$$
$$= (2\delta)^{-1}\operatorname{sgn}(\mathcal{O}(c),v^\delta)Y_{[v^\delta,u^\delta_-,u^\delta_+]}(c) + O(\varepsilon^2),$$

where O is uniform over corners c remaining at a fixed distance away from $u^\delta_+, u^\delta_2\dots u^\delta_n$. Moreover, one notices that, provided r is small enough, the function $\operatorname{sgn}(\mathcal{O}(c),v^\delta)Y_{[v^\delta,u^\delta_-,u^\delta_+]}$ has the branching structure of $\langle\mu_{v_c}\sigma_{u_c}\mu_{v^\delta}\sigma_{u^\delta_2}\dots\sigma_{u^\delta_n}\rangle_{\Omega_\delta}$ (this can be seen as a feature of Proposition 4.4.2). Using again the expansion (4.6.3) and integrating on $\mathcal{C}^\delta_r$, one has,

$$\operatorname{Im}\big[\int_{\mathcal{C}^\delta_r}\big(F^{\diamond}_{v^\delta+i\varepsilon}(z) - F^{\diamond}_{v^\delta}(z)\big)\delta^{-\frac{1}{2}}G^{\diamond}_{[u^\delta_+ +i\varepsilon]}(z)\mathrm{d}z\big]$$
$$= \varepsilon\cdot(2\delta)^{-1}\operatorname{Im}\big[\int_{\mathcal{C}^\delta_r}\operatorname{sgn}(\mathcal{O}(z),v^\delta)Y^{\diamond}_{[v^\delta,u^\delta_-,u^\delta_+]}(z)\delta^{-\frac{1}{2}}G^{\diamond}_{[u^\delta_+]}(z)\mathrm{d}z\big] + o(\varepsilon).$$

A similar treatment shows that

$$\operatorname{Im}\big[\int_{\mathcal{C}^\delta_r} F^{\diamond}_{v^\delta+i\varepsilon}(z)\delta^{-\frac{1}{2}}G^{\diamond}_{[u^\delta_+ +i\varepsilon]}(z) + F^{\diamond}_{v^\delta}(z)\delta^{-\frac{1}{2}}G^{\diamond}_{[u^\delta_+]}(z)\mathrm{d}z\big]$$
$$= 2\operatorname{Im}\big[\int_{\mathcal{C}^\delta_r} F^{\diamond}_{v^\delta}(z)\delta^{-\frac{1}{2}}G^{\diamond}_{[u^\delta_+]}(z)\mathrm{d}z\big] + o_{\varepsilon\to 0}(1).$$

Putting the previous asymptotics all together in (4.6.2) and taking the logarithm, one deduces that $\partial_y \log \mathbb{E}^+_{\Omega^\bullet_\delta}[\sigma_{u_1^\delta}\dots\sigma_{u_n^\delta}]$ exists and is given by,

$$\frac{\mathrm{Im}\,[\int_{\mathcal{C}_r^\delta} \mathrm{i}\,\delta^{-\frac{1}{2}}\partial_y G^\diamond_{[u_+^\delta]}(z)F^\diamond_{v^\delta}(z)\mathrm{d}z] + \mathrm{Im}\,[\int_{\mathcal{C}_r^\delta} \frac{\mathrm{sgn}(\mathcal{O}(z),v^\delta)Y^\diamond_{[v^\delta,u_-^\delta,u_+^\delta]}(z)}{2\delta}\delta^{-\frac{1}{2}}G^\diamond_{[u_+^\delta]}(z)\mathrm{d}z]}{\mathrm{Im}\,[\int_{\mathcal{C}_r^\delta} F^\diamond_{v^\delta}(z)\delta^{-\frac{1}{2}}G^\diamond_{[u_+^\delta]}(z)\mathrm{d}z]}. \tag{4.6.4}$$

We are now going to evaluate the contribution of the above terms as $\delta \to 0$. Repeating computations similar to the proof in the horizontal direction, one sees that,

$$\mathrm{Im}\,[\int_{\mathcal{C}_r^\delta} F^\diamond_{v^\delta}(z)\delta^{-\frac{1}{2}}G^\diamond_{[u_+^\delta]}(z)\mathrm{d}z] = 2\mathbb{E}^+_{\Omega^\bullet_\delta}[\sigma_{u_+^\delta}\dots\sigma_{u_n^\delta}] + o_{\delta\to 0}(\mathbb{E}^+_{\Omega^\bullet_\delta}[\sigma_{u_+^\delta}\dots\sigma_{u_n^\delta}]),$$

$$\begin{aligned}\mathrm{Im}\,[\int_{\mathcal{C}_r^\delta} \mathrm{i}\,\delta^{-\frac{1}{2}}\partial_y G^\diamond_{[u_+^\delta]}(z)F^\diamond_{v^\delta}(z)\mathrm{d}z] &= 2\mathbb{E}^+_{\Omega^\bullet_\delta}[\sigma_{u_+^\delta}\dots\sigma_{u_n^\delta}]\,\mathrm{Re}\,[i\mathcal{A}_{(u_1,\dots,u_n)}]\\ &\quad + o_{\delta\to 0}(\mathbb{E}^+_{\Omega^\bullet_\delta}[\sigma_{u_+^\delta}\dots\sigma_{u_n^\delta}]),\end{aligned}$$

since the asymptotics of the derivative of the full-plane correlator away from its branching is given by (see (4.8.7))

$$\delta^{-\frac{1}{2}}\partial_y G_{[u_+^\delta]}(z) = -\frac{\mathrm{i}}{2\sqrt{\pi}(z-u)^{\frac{3}{2}}} + O(\frac{\delta}{(z-u)^{\frac{5}{2}}}).$$

Now, we treat now the remaining term and prove it *vanishes identically*. One first notes that the double covers $\Omega_{[v^\delta]}$ and $\Omega_{[u_+^\delta,v^\delta,u_-^\delta]}$ can be canonically identified. This only amounts to change the sheets of *both* corners $c_\pm^\delta$ neighbouring v^δ. Thus, one can use the integration procedure of Proposition 4.5.3 applied to the correlators $\mathrm{sgn}(O(z),v^\delta)Y^\diamond_{[v^\delta,u_-^\delta,u_+^\delta]}$ and $\delta^{-\frac{1}{2}}G^\diamond_{[u_+^\delta]}$ to modify the contour and make it an elementary one passing by c_+^δ. This is indeed a fair operation since $\mathrm{sgn}(O(z),v^\delta)$ is locally constant away from the branchings. Thus, by contour deformation, the only terms that do not *trivially* cancel out are the increments of $H[Y^\diamond_{[v^\delta,u_-^\delta,u_+^\delta]},\delta^{-\frac{1}{2}}G^\diamond_{[u_+^\delta]}(z)]$ along the segment $[v^\delta u_+^\delta]$ (since the two double covers $\Omega_{[v^\delta]}$ and $\Omega_{[u_+^\delta]}$ are *not* identified at lifts of c_+^δ. We claim that those two increments in fact *do* compensate each other. Indeed, fix a lift of c_+^δ in $\Omega_{[v^\delta]}$. Since the contour is oriented counter-clockwise, the "upper" increment passing by c_+^δ is oriented from left to right. Up to a global sign choice, the sum of those two increments (as in the proof of Proposition 4.5.3) equals,

$$\delta\cdot(+1)F_{v^\delta}(c_+^\delta)\delta^{-\frac{1}{2}}G_{[u_+^\delta]}(c_+^\delta) - \delta\cdot(-1)F_{v^\delta}(c_+^\delta)\delta^{-\frac{1}{2}}G_{[u_+^\delta]}((c_+^\delta)^\#), \tag{4.6.5}$$

where in the above equation $(+1)$ in the first term comes from the sign of the 'upper' increment $\mathrm{sgn}(\mathcal{O}_{c_+^\delta},v^\delta) = +1$ (i.e. coming from a deformation of

the contour in the part of the graph *above* v^δ) while (-1) in the second term comes from the sign of the 'lower' increment $\mathrm{sgn}(\mathcal{O}_{c_+^\delta}, v^\delta) = +1$ (coming from a deformation of the contour in the part of the graph *below* v^δ). Thus (4.6.5) vanishes.

In conclusion, one can conclude that

$$\partial_y \log \mathbb{E}^+_{\Omega^\bullet_\delta}[\sigma_{u_1^\delta} \dots \sigma_{u_n^\delta}] = \mathrm{Re}[\mathrm{i}\, \mathcal{A}_{(u_1,\dots,u_n)}] + o_{\delta\to 0}(1), \tag{4.6.6}$$

where $o_{\delta\to 0}(1)$ is uniform in bounded compact subsets of Ω. Whenever one has the two asymptotics (4.6.1) and (4.6.6), it is enough to integrate them along a sequence of paths linking b_1^δ to a_1^δ, b_2^δ to a_2^δ ... b_n^δ to a_n^δ to recover that

$$\frac{\mathbb{E}^+_{\Omega^\bullet_\delta}[\sigma_{a_1^\delta} \dots \sigma_{a_n^\delta}]}{\mathbb{E}^+_{\Omega^\bullet_\delta}[\sigma_{b_1^\delta} \dots \sigma_{b_n^\delta}]} \underset{\delta\to 0}{\longrightarrow} \exp\big(\mathrm{Re}\big[\int_{(b_1,\dots,b_n)}^{(a_1,\dots,a_n)} \sum_{k=1}^n \mathcal{A}_{(x_1,\dots,x_n)} \mathrm{d}x_k\big]\big). \tag{4.6.7}$$

This concludes the proof.

□

One can now use a similar scheme to prove Theorem 4.3.6.

Proof. Let $v_2^\delta \in \Omega_\delta^\circ$ be a neighbour of u_2^δ. Repeating the previous integration formula 4.5.3 to extract values near the branchings with the observables $F_\delta^\diamond := \delta^{-\frac{1}{2}} \mathbb{E}^+_{\Omega_\delta}[\sigma_{u_1^\delta}\sigma_{u_2^\delta}]^{-1} F^{\mathcal{S}}_{\Omega_\delta,\{v_1^\delta,u_2^\delta\}}$ and $\delta^{-\frac{1}{2}} G_{[v_2^\delta]}$ via a macroscopic countour $\mathcal{C}_r^\delta$ at a small distance $r > 0$ from u_2^δ, one gets

$$2\, \frac{\mathbb{E}^+_{\Omega^\bullet_\delta}[\mu_{v_1^\delta}\mu_{v_2^\delta}]}{\mathbb{E}^+_{\Omega^\bullet_\delta}[\sigma_{u_1^\delta}\sigma_{u_2^\delta}]} = \mathrm{Im}\big[\int_{\mathcal{C}_r^\delta} \delta^{-\frac{1}{2}} G^\diamond_{[v_2^\delta]}(z) F^\diamond_\delta(z) \mathrm{d}z\big]. \tag{4.6.8}$$

Using the asymptotics

$$f^{\mathcal{S}}_{\Omega,\varpi} = \frac{1}{\sqrt{\pi}} \frac{e^{-\mathrm{i}\frac{\pi}{4}}}{(z-u_2)^{\frac{1}{2}}} \mathcal{B}_\Omega(u_1,u_2) + O((z-u_2)^{\frac{1}{2}}),$$
$$\delta^{-\frac{1}{2}} G^\diamond_{[v_2^\delta]}(z) = \frac{1}{\sqrt{\pi}} \frac{e^{\mathrm{i}\frac{\pi}{4}}}{(z-u_2)^{\frac{1}{2}}} + O(\frac{\delta^2}{(z-v)^{\frac{5}{2}}}),$$

one gets the result exactly as in the previous proof (taking again r arbitrarily small). To conclude, one uses Krammers–Wannier duality to note that $\mathbb{E}^+_{\Omega^\bullet_\delta}[\mu_{v_1^\delta}\mu_{v_2^\delta}] = \mathbb{E}^{\mathrm{f}}_{\Omega^\circ_\delta}[\sigma_{v_1^\delta}\sigma_{v_2^\delta}]$.

□

Now that once Theorem 4.3.5 is proven, one has to find the proper normalizing factors in front of the correlation ratio to prove completely Theorem 4.3.7. This goes by a comparaison with the full-plane lattice. This proof is done here by induction over n and recalls elements introduced in [38].

Proof. We start with the case $n = 2$. Define $\langle \sigma_a \sigma_b \rangle^+_{\mathbb{C}} := |b-a|^{\frac{1}{4}}$. In this case, Theorem 4.3.5 implies that,

$$\frac{\delta^{-\frac{1}{4}} \mathcal{C}^2 \mathbb{E}^+_{\Omega_\delta}[\sigma_a \sigma_b]}{\langle \sigma_a \sigma_b \rangle^+_\Omega} = \Big(\frac{\langle \sigma_a \sigma_{b'} \rangle^+_\Omega}{\langle \sigma_a \sigma_b \rangle^+_\Omega} \cdot \frac{\mathbb{E}^+_{\Omega_\delta}[\sigma_a \sigma_b]}{\mathbb{E}^+_{\Omega_\delta}[\sigma_a \sigma_{b'}]} \Big) \cdot \frac{\mathbb{E}^+_{\Omega_\delta}[\sigma_a \sigma_{b'}]}{\mathbb{E}^+_{\mathbb{C}_\delta}[\sigma_a \sigma_{b'}]} \cdot \frac{\mathbb{E}^+_{\mathbb{C}_\delta}[\sigma_a \sigma_{b'}]}{\delta^{-\frac{1}{4}} \mathcal{C}^2 \langle \sigma_a \sigma_{b'} \rangle_{\mathbb{C}}} \cdot \frac{\langle \sigma_a \sigma_{b'} \rangle^+_{\mathbb{C}}}{\langle \sigma_a \sigma_b \rangle^+_\Omega}.$$

Sending δ to 0 first makes the first term on the RHS on both lines converge to 1. Sending then b' to a and using the fact that $\lim_{b' \to a} \lim_{\delta \to 0} \frac{\mathbb{E}^+_{\Omega_\delta}[\sigma_a \sigma_b]}{\mathbb{E}^+_{\mathbb{C}_\delta}[\sigma_a \sigma_{b'}]} = 1$ (which is true by FKG inequality and the fact that $\mathcal{B}(a, b')$ goes to 1 as b' approches a), it simply remains to notice that $\langle \sigma_a \sigma_{b'} \rangle^+_{\mathbb{C}} (\langle \sigma_a \sigma_{b'} \rangle^+_\Omega)^{-1}$ goes to 1 as b' goes to a. The latter is true when $\Omega = \mathbb{H}$ and holds by conformal invariance for general domains.
For $n = 1$, one notices that,

$$\frac{\mathbb{E}^+_{\Omega_\delta}[\sigma_a]^2}{\delta^{\frac{1}{4}} \mathcal{C}^2 (\langle \sigma_a \rangle^+_\Omega)^2} = \Big(\frac{1}{(\langle \sigma_a \rangle^+_\Omega)^2} \frac{\mathbb{E}^+_{\Omega_\delta}[\sigma_a]}{\mathbb{E}^+_{\Omega_\delta}[\sigma_b]} \Big) \cdot \frac{\mathbb{E}^+_{\Omega_\delta}[\sigma_a] \mathbb{E}^+_{\Omega_\delta}[\sigma_b]}{\mathbb{E}^+_{\Omega_\delta}[\sigma_a \sigma_b]} \cdot \frac{\mathbb{E}^+_{\Omega_\delta}[\sigma_a \sigma_b]}{\delta^{\frac{1}{4}} \mathcal{C}^2}. \tag{4.6.9}$$

By sending δ to 0, the first term converges to $(\langle \sigma_a \rangle^+_\Omega \langle \sigma_b \rangle^+_\Omega)^{-1}$ and the last term converges to $\langle \sigma_a \sigma_b \rangle^+_\Omega$. As b approaches the boundary, the second term can be made arbitrarily close to 1 (uniformly in δ, this is a consequence of GHS inequality and the fact that $\mathcal{B}_\Omega(a, b)$ goes to 0 in that regime). Still when b approaches the boundary, the product $\langle \sigma_a \sigma_b \rangle^+_\Omega (\langle \sigma_a \rangle^+_\Omega \langle \sigma_b \rangle^+_\Omega)^{-1}$ is arbitrarily close to 1. For $n \geqslant 3$, assume that the result is already proven for all $n' < n$. One decomposes

$$\begin{aligned} \frac{\mathbb{E}^+_{\Omega_\delta}[\sigma_{a_1} \dots \sigma_{a_n}]}{\mathcal{C}^n \delta^{\frac{n}{8}} \langle \sigma_{a_1} \dots \sigma_{a_n} \rangle^+_\Omega} &= \frac{\mathbb{E}^+_{\Omega_\delta}[\sigma_{a_1} \dots \sigma_{a_n}]}{\mathbb{E}^+_{\Omega_\delta}[\sigma_b \sigma_{a_2} \dots \sigma_{a_n}]} \cdot \frac{\langle \sigma_b \sigma_{a_2} \dots \sigma_{a_n} \rangle^+_\Omega}{\langle \sigma_{a_1} \dots \sigma_{a_n} \rangle^+_\Omega} \\ &\quad \times \frac{\mathbb{E}^+_{\Omega_\delta}[\sigma_b \sigma_{a_2} \dots \sigma_{a_n}]}{\mathbb{E}^+_{\Omega_\delta}[\sigma_b] \mathbb{E}^+_{\Omega_\delta}[\sigma_{a_2} \dots \sigma_{a_n}]} \\ &\quad \times \frac{\mathbb{E}^+_{\Omega_\delta}[\sigma_b]}{\mathcal{C} \delta^{\frac{1}{8}}} \cdot \frac{\mathbb{E}^+_{\Omega_\delta}[\sigma_{a_2} \dots \sigma_{a_n}]}{\mathcal{C}^{n-1} \delta^{\frac{n-1}{8}}} \cdot \frac{1}{\langle \sigma_b \sigma_{a_2} \dots \sigma_{a_n} \rangle^+_\Omega}. \end{aligned}$$

Sending first δ to 0, the RHS of the first line converges to 1 (due to Theorem 4.3.5). As b approaches the boundary, the second line can be made arbitrarily close to 1 (one side is FKG inequality while the other one is Russo–Seymour–Welsh type estimates), uniformly in δ small enough. Finally, the last line converges to $\langle \sigma_b \rangle^+_\Omega \langle \sigma_{a_2} \dots \sigma_{a_n} \rangle^+_\Omega (\langle \sigma_b \dots \sigma_{a_n} \rangle^+_\Omega)^{-1}$ due to the induction hypothesis. It is then enough to note that the last mentionned quantity can be be made arbitrarily close to 1 provided b is close enough to the boundary (this is due to the structure of continuous correlation function, see [39, Sec. 5]). □

We now pass to the proof of convergence of Theorems 4.3.1 and 4.3.2. For simplicity, we only sketch the proof of multiple-energy correlations since it can be

derived clasically by induction using the Pfaffian structure of the model, up to the amount of introducing the formalism of multi-point spin-dirsorder correlator (i.e. introducing a correlator as a function depending on several corners).

Proof. We start with the case $n = 1$. One first notices within the derivation of Proposition 4.6.2 that the function $F_\delta^\dagger := \delta^{-1}(F^{\mathcal{E}}_{\Omega_\delta,a} - G_{(a)})$ converges to $\overline{\eta_a}[f^{\mathcal{E}}_{\Omega,a} - \frac{1}{\pi}\frac{1}{z-a}]$ *uniformly* on compact subsets of Ω (since $F_\delta^\dagger$ has no singularity). In particular the convergence holds at v_a and u_a. On the other hand, one has the expansion $f^{\mathcal{E}}_{\Omega,a}(z) = \overline{\eta_a}[\frac{1}{\pi(z-a)} + \frac{1}{2\pi} l_\Omega(a) + O(z-a)]$ near a, which allows to identify the limit of $F_\delta^\dagger[v_a] = \overline{\eta_a}\delta^{-1}\mathbb{E}^+_{\Omega_\delta^\bullet}[\varepsilon_{a^\delta}]$, $F_\delta^\dagger[u_a] = -\overline{\eta_a}\delta^{-1}(\mathbb{E}^+_{\Omega_\delta^\bullet}[\mu_a\mu_{a-2\delta}] - \mathbb{E}^+_{\mathbb{C}_\delta^\bullet}[\mu_a\mu_{a-2\delta}])$.

For the n-point energy case, one can reccursively construct as in the semi-discrete case a multi-point fermionic correlator [39, Sec. 2.4] as a function of $2r$ corners

$$G(c_1, c_2, \dots, c_{2r}) \mapsto \eta_{c_1}\eta_{c_2}\dots\eta_{c_{2r}}\langle\chi_{c_1}\chi_{c_2}\dots\chi_{c_{2r}}\rangle_{\Omega_\delta}, \tag{4.6.10}$$

with proper double valuations at the corners c_i and consistent choices of η_c. One gets that away from its diagonal (when the c_i's are distinct), one has

$$G(c_1, c_2, \dots, c_{2r}) = \mathrm{Pf}\big[\eta_{c_k}\eta_{c_l}\langle\chi_{c_k}\chi_{c_l}\rangle_{\Omega_\delta}\big]_{1\leqslant k,l\leqslant 2r}. \tag{4.6.11}$$

Multiple energy correlation can be recovered as values of G near their diagonal (i.e. taking the corners $c_k \sim c_{k+r}$ to be adjacent) and the convergence of the single energy density proved in the previous lines together with the Pfaffian formula (4.6.11) directly yields the result. □

The proof of Theorems 4.3.8 and 4.3.3 is a simple application of Theorems 4.3.7 and 4.3.2 with explicit formulas for solution to boundary value problmes, which can be found in [39, Sec. 7] for the upper-half plane, and in the appendix for rectangles.

We are now able to prove Theorem 4.3.9 that states rotational invariance of the model at criticality.

Proof. Fix $\varepsilon > 0$ and $\vec{s}$ a unitary vector. Let $\mathbb{D}_R^\delta$ be the approximation of $\mathbb{D}(0,R)$ by $\mathbb{C}_\delta$. There exist $R(\varepsilon) > 0$ large enough such that, uniformy in δ and s,

$$1 - \varepsilon \leqslant \frac{\mathbb{E}^+_{\mathbb{D}_R^\delta}[\sigma_{-s}\sigma_s]}{\mathbb{E}^+_{\mathbb{C}_\delta}[\sigma_{-s}\sigma_s]} \leqslant 1 + \varepsilon$$

Moreover, now one can use the convergence theorem in $\mathbb{D}_R^\delta$, which states that $\mathbb{E}^+_{\mathbb{D}_R^\delta}[\sigma_{-s}\sigma_s]\mathbb{E}^+_{\mathbb{D}_R^\delta}[\sigma_{-1}\sigma_1]^{-1}$ converges [2] to $\langle\sigma_{-s}\sigma_s\rangle^+_{\mathbb{D}_R}(\langle\sigma_{-s}\sigma_s\rangle^+_{\mathbb{D}_R})^{-1} = 1$. Hence, the quantity $\langle\sigma_{-s}\sigma_s\rangle^+_{\mathbb{D}_R^\delta}(\langle\sigma_{-s}\sigma_s\rangle^+_{\mathbb{D}_R^\delta})^{-1}$ goes to 1 as $\delta \to 0$. Sending δ to 0 then

2. This comes from the rotational invariance of $\langle\sigma_{-s}\sigma_s\rangle^+_{\mathbb{D}_R}$, which comes itself from the rotational invariance of the associated boundary value problem.

ε to 0, one can deduce that $\mathbb{E}^+_{\mathbb{C}_\delta}[\sigma_{-s}\sigma_s]\mathbb{E}^+_{\mathbb{C}_\delta}[\sigma_{-1}\sigma_1]^{-1}$ is arbitrarily close to 1 as δ goes to 0. We conclude by using the asymptotics in the vertical direction derived in Theorem 4.7.9.

□

4.7 . Orthogonal polynomials and full-plane expectation

In this section, we discuss full-plane spin-spin correlations in the horizontal direction (taken in the infinite volume limit) for the quantum Ising model, at and below the criticality. In the homogeneous square-grid case, those results are known since the 70's with the work of McCoy and Wu [124], and were originally derived relying upon the formalism of Toeplitz determinants. Here, we follow the strategy of [40], where a simplification using modern techniques only using the theory of *real-valued* orthogonal polynomials was developed. This last mentioned method admits a generalization to the case of the quantum Ising model. Instead of using known results for rectangular grids and then smashing the lattice (which can raise problems when exchanging limits), we prefer remaining with the formalism of disorder insertion in the semi-discrete lattice to derive results for the quantum model.

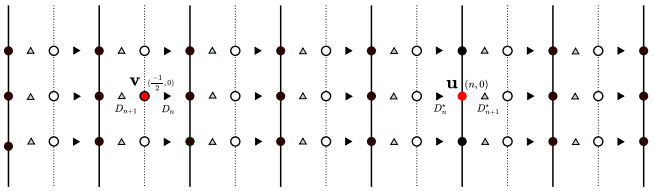

FIGURE 4.7.1 – Local picture for the full-plane observable with two branchings (denoted in red).

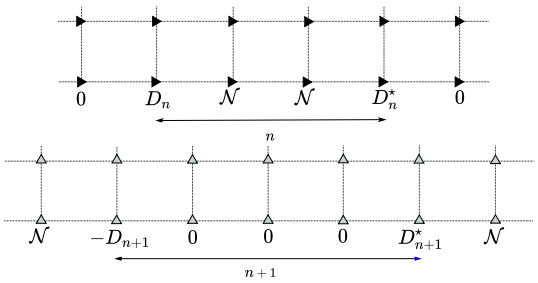

FIGURE 4.7.2 – Symmetrized (left) and antisymmetrized (right) semi-discrete boundary value problems in the upper-half plane.

4.7.1 . Full-plane observable with two branchings

Assume that the semi-discrete lattice on which the Ising model is so that its primal vertices coincide with $\mathbb{Z}\times\mathbb{R}$ and its dual vertices are $(\mathbb{Z}+\frac{1}{2})\times\mathbb{R}$, see Fig. 4.7.1. It is knwon [63] that at and below criticality, the quantum Ising model only admits two extremal Gibbs measures (coming from '+' and '−' boundary conditions at infinity). Those extremal measure are in particular translationally invariant in the infinite volume limit. Given $n\geq 0$, we define the horizontal and next-to-horizontal correlations

$$\begin{aligned} D_n &:= \mathbb{E}_{\mathbb{Z}\times\mathbb{R}}\big[\sigma^{\bullet}_{(0,0)}\sigma^{\bullet}_{(n,0)}\big], \qquad & D^{\star}_n &:= \mathbb{E}^{\star}_{(\mathbb{Z}\times\mathbb{R})^{\star}}\big[\sigma^{\circ}_{(-\frac{1}{2},0)}\sigma^{\circ}_{(n-\frac{1}{2},0)}\big],\\ D_{n+1} &:= \mathbb{E}_{\mathbb{Z}\times\mathbb{R}}\big[\sigma^{\bullet}_{(-1,0)}\sigma^{\bullet}_{(n,0)}\big], \qquad & D^{\star}_{n+1} &:= \mathbb{E}^{\star}_{(\mathbb{Z}\times\mathbb{R})^{\star}}\big[\sigma^{\circ}_{(-\frac{1}{2},0)}\sigma^{\circ}_{(n+\frac{1}{2},0)}\big],\\ \widetilde{D}_{n+1} &:= \partial_y\big[\mathbb{E}_{\mathbb{Z}\times\mathbb{R}}\big[\sigma^{\bullet}_{(-1,y)}\sigma^{\bullet}_{(n,0)}\big]\big]_{y=0}, \qquad & \widetilde{D}^{\star}_{n+1} &:= \partial_y\big[\mathbb{E}^{\star}_{(\mathbb{Z}\times\mathbb{R})^{\star}}\big[\sigma^{\circ}_{(-\frac{1}{2},y)}\sigma^{\circ}_{(n+\frac{1}{2},y)}\big]\big]_{y=0}, \end{aligned}$$

where the expectations in the second column are taken for the *dual* quantum Ising model with dual parameters (see Section 4.2.4). In particular, one can view those dual expectactions as disorder-disorder correlations for the quantum Ising model defined on $\Omega^{\bullet}$.

Let $\mathbf{v}=(-\frac{1}{2},0)$ and $\mathbf{u}=(n,0)$. Below we rely upon the *full-plane* observable $F_{[\mathbf{v},\mathbf{u}]}$ which can be thought of as a subsequential limit of observables defined on an increasing sequence $(G_n)_{n\geqslant 0}$ of finite graphs exhausting the semi-discrete lattice. The existence of this pointwise (subsequential) limit is justified by the bound

$$\big|\langle\mu_{v(c)}\mu_{\mathbf{v}}\sigma_{u(c)}\sigma_{\mathbf{u}}\rangle_{G_n}\big| \;\leq\; \langle\mu_{v(c)}\mu_{\mathbf{v}}\rangle_{G_n} \;=\; \mathbb{E}^{\star}_{G_n^{\bullet}}[\sigma^{\circ}_{v(c)}\sigma^{\circ}_{\mathbf{v}}] \;\leq\; 1, \tag{4.7.1}$$

together by the equicontinuity of correlators (so it is enough to apply the diagonal process on $(\mathbb{Z}\pm\frac{1}{4})\times\mathbb{Q}$). The uniqueness of the limit (and hence its non dependance on the exhaustion used above) follows from Lemma 4.7.1. Let $[\mathbb{Z}\times\mathbb{R};\mathbf{v},\mathbf{u}]$ denote the double cover of the lattice $\mathbb{Z}\times\mathbb{R}$ branching over $\mathbf{v}$ and $\mathbf{u}$. We now introduce the following *symmetrized* and *anti-symmetrized* versions of the observable $F_{[\mathbf{v},\mathbf{u}]}(\cdot)$ on eastern and western corners, respectively (see Fig. 4.7.1) :

$$X^{\mathrm{sym}}_{[\mathbf{v},\mathbf{u}]}(c) := \tfrac{e^{\mathrm{i}\frac{\pi}{4}}}{2}[F_{[\mathbf{v},\mathbf{u}]}(c)+F_{[\mathbf{v},\mathbf{u}]}(\bar{c})], \quad c\in[(\mathbb{Z}-\tfrac{1}{4})\times\mathbb{R};\mathbf{v},\mathbf{u}], \tag{4.7.2}$$

$$X^{\mathrm{anti}}_{[\mathbf{v},\mathbf{u}]}(c) := \tfrac{e^{-i\frac{\pi}{4}}}{2}[F_{[\mathbf{v},\mathbf{u}]}(c)-F_{[\mathbf{v},\mathbf{u}]}(\bar{c})], \quad c\in[(\mathbb{Z}+\tfrac{1}{4})\times\mathbb{R};\mathbf{v},\mathbf{u}], \tag{4.7.3}$$

where the continuous conjugation $z\mapsto\bar{z}$ on $[(\mathbb{Z}\pm\frac{1}{4})\times\mathbb{R};\mathbf{v},\mathbf{u}]$ is defined so it maps the segment $[\pm\frac{1}{4},n\pm\frac{1}{4}]\times\{0\}$ between $\mathbf{v}$ and $\mathbf{u}$ to itself (i.e., the conjugate of each point located over this segment is on the *same* sheet of the double cover). Once $z\mapsto\bar{z}$ is specified in between of the branching points, it can be 'continuously' extended to the entire double cover $[(\mathbb{Z}\pm\frac{1}{4})\times\mathbb{R};\mathbf{v},\mathbf{u}]$. In particular, the points c located over the real line but outside of the segment $[\pm\frac{1}{4},n\pm\frac{1}{4}]$ are mapped by $z\mapsto\bar{z}$ to their counterparts $c^{\#}$ on the *other* sheet of the double cover.

We now list some basic properties of the observables $X^{\mathrm{sym}}_{[\mathbf{v},\mathbf{u}]}$ and $X^{\mathrm{anti}}_{[\mathbf{v},\mathbf{u}]}$ and show they are sufficient to characterize them uniquely. Due to $(4.7.1)$ we have

$$\big|X^{\mathrm{sym}}_{[\mathbf{v},\mathbf{u}]}(k-\tfrac{1}{4},s)\big|\leq 1 \quad\text{and}\quad \big|X^{\mathrm{anti}}_{[\mathbf{v},\mathbf{u}]}(k+\tfrac{1}{4},s)\big|\leq 1 \quad\text{for all}\quad (k,s)\in\mathbb{Z}\times\mathbb{R}.$$

Equation (4.4.27) ensures that the observables $X^{\mathrm{sym}}_{[\mathbf{v},\mathbf{u}]}$ and $X^{\mathrm{anti}}_{[\mathbf{v},\mathbf{u}]}$ are massive harmonic away from the branching points $\mathbf{v}, \mathbf{u}$. In particular, one has

$$[\Delta^{(m)} X^{\mathrm{sym}}_{[\mathbf{v},\mathbf{u}]}]((k-\tfrac{1}{4}, s)) = 0 \quad \text{and} \quad [\Delta^{(m)} X^{\mathrm{anti}}_{[\mathbf{v},\mathbf{u}]}]((k+\tfrac{1}{4}, s)) = 0 \quad \text{if} \ \ s \neq 0. \tag{4.7.4}$$

Moreover, the spinor property of the observable $F_{[\mathbf{v},\mathbf{u}]}$ coupled with the above described choice of the conjugation ensures

$$X^{\mathrm{sym}}_{[\mathbf{v},\mathbf{u}]}((k-\tfrac{1}{4},0))=0, \ k \notin [0,n], \quad [\Delta^{(m)} X^{\mathrm{sym}}_{[\mathbf{v},\mathbf{u}]}]((k-\tfrac{1}{4},0))=0, \ k \in [1,n-1]; \tag{4.7.5}$$

$$X^{\mathrm{anti}}_{[\mathbf{v},\mathbf{u}]}((k+\tfrac{1}{4},0))=0, \ k \in [1,n], \quad [\Delta^{(m)} X^{\mathrm{anti}}_{[\mathbf{v},\mathbf{u}]}]((k+\tfrac{1}{4},0))=0, \ k \notin [0,n+1]. \tag{4.7.6}$$

Finally, the definition of $F_{[\mathbf{v},\mathbf{u}]}$ as a correlator imply (recall $\sigma_u \sigma_u = 1$, $\mu_v \mu_v = 1$)

$$X^{\mathrm{sym}}_{[\mathbf{v},\mathbf{u}]}((-\tfrac{1}{4},0)) = D_n, \qquad X^{\mathrm{sym}}_{[\mathbf{v},\mathbf{u}]}((n-\tfrac{1}{4},0)) = D^\star_n; \tag{4.7.7}$$

$$X^{\mathrm{anti}}_{[\mathbf{v},\mathbf{u}]}((-\tfrac{3}{4},0)) = -D_{n+1}, \qquad X^{\mathrm{anti}}_{[\mathbf{v},\mathbf{u}]}((n+\tfrac{1}{4},0)) = D^\star_{n+1}, \tag{4.7.8}$$

where we assume that these pairs of corners are located on the *same sheet* of the double cover $[(\mathbb{Z} \pm \frac{1}{4}) \times \mathbb{R}; \mathbf{v}, \mathbf{u}]$ *as viewed from the upper half-plane* ; this explains why the value D_{n+1} at $(-\frac{3}{4}, 0)$ comes with an opposite sign.

Lemma 4.7.1. *(i) The uniformly bounded observable $X^{\mathrm{sym}}_{[\mathbf{v},\mathbf{u}]}$ given by* (4.7.2) *is uniquely characterized by the properties* (4.7.4), (4.7.5) *and its values* (4.7.7) *near* $\mathbf{v}$ *and* $\mathbf{u}$.

(ii) Similarly, the uniformly bounded observable $X^{\mathrm{anti}}_{[\mathbf{v},\mathbf{u}]}$ given by (4.7.3) *is uniquely characterized by the properties* (4.7.4), (4.7.6) *and its values* (4.7.8) *near* $\mathbf{v}$ *and* $\mathbf{u}$.

Proof. (i) Let X_1 and X_2 be two bounded spinors satisfying (4.7.4), (4.7.5) and (4.7.7). Let $(Z_k)_{k \geqslant 0}$ be the semi-discrete Brownian Motion with killing started at $c \in [(\mathbb{Z} - \frac{1}{4}) \times \mathbb{R}; \mathbf{u}, \mathbf{v}]$ that corresponds to the massive Laplacian $\Delta^{(m)}$. This semi-discrete Brownian Motion almost surely hits the points located over the set $\{(k-\frac{1}{4}, 0), k \notin [1, n-1]\}\}$ or dies. Since the process $(X_1 - X_2)(Z_k)$ is a bounded martingale with respect to the canonical filtration, the optional stopping theorem yields $X_1(c) - X_2(c) = 0$. The proof of (ii) is similar. □

The next lemma allows one to construct explicitely $X_{[\mathbf{v},\mathbf{u}]}$ in Section 4.7.2 to get a recurrence relation between consecutive spin-spin full-plane correlations. For $n \geq 1$, denote

$$L_n := -\frac{\theta}{\theta^2 + \theta^{\star 2}} \cdot \widetilde{D}_n, \qquad L^\star_n := -\frac{\theta^\star}{\theta^2 + \theta^{\star 2}} \cdot \widetilde{D}^\star_n. \tag{4.7.9}$$

Lemma 4.7.2. *For each $n \geq 1$, the following identities are fulfilled :*

$$-[\Delta^{(m)} X^{\mathrm{sym}}_{[\mathbf{v},\mathbf{u}]}]((-\tfrac{1}{4},0)) = L_{n+1}, \qquad -[\Delta^{(m)} X^{\mathrm{sym}}_{[\mathbf{v},\mathbf{u}]}]((n-\tfrac{1}{4},0)) = L^{\star}_{n+1}; \tag{4.7.10}$$

$$-[\Delta^{(m)} X^{\mathrm{anti}}_{[\mathbf{v},\mathbf{u}]}]((-\tfrac{3}{4},0)) = -L_{n}, \qquad -[\Delta^{(m)} X^{\mathrm{anti}}_{[\mathbf{v},\mathbf{u}]}]((n+\tfrac{1}{4},0)) = L^{\star}_{n}, \tag{4.7.11}$$

with the same choice of points on the double covers $[(\mathbb{Z}\pm\frac{1}{4})\times\mathbb{Z};\mathbf{v},\mathbf{u}]$ as above. If $n=0$, the identities (4.7.10) *should be replaced by $-[\Delta^{(m)} X^{\mathrm{sym}}_{[\mathbf{v},\mathbf{u}]}]((-\frac{1}{4},0)) = L_1 + L^{\star}_1$ while* (4.7.11) *hold with $L_0 := \frac{\theta^{\star}}{\theta^2+\theta^{\star 2}}$ and $L^{\star}_0 := \frac{\theta}{\theta^2+\theta^{\star 2}}$.*

Proof. We proof the first item. Due to the symetrization procedure (which amounts to take a cut of the double cover in the horizontal axis, outside of the branchings) the value of $X^{\mathrm{sym}}_{[\mathbf{v},\mathbf{u}]}$ at $(-\frac{5}{4},0)$ vanishes. Thus one can reapply the strategy of the proof of (4.4.26) but this time, and $[\Delta^{(m)} X^{\mathrm{sym}}_{[\mathbf{v},\mathbf{u}]}]$ equals $e^{\mathrm{i}\frac{\pi}{4}}\frac{\theta\theta^{\star}}{\theta^2+\theta^{\star 2}} F_{[\mathbf{v},\mathbf{u}]}(-\frac{5}{4},0)$. Applying the equation (4.4.13) at $c=(-\frac{5}{4},0)$ gives

Applying the equation (4.4.21) at $c=(-\frac{3}{4},0)$

$$\tilde{D}_{n+1} = \mathrm{sgn}(\mathcal{O},u)\cdot\theta^{\star}\langle\chi_{(-\frac{5}{4},0)}\mathcal{O}\rangle.$$

The check of the sign $\mathrm{sgn}(\mathcal{O},u) = -1$ is left to the reader. The other items are proved in a similar maner. □

4.7.2 . Construction via the Fourier transform and orthogonal polynomials

In this subsection, we construct explicitely in Lemma 4.7.4 and Lemma 4.7.5 two bounded functions satisfying the properties (4.7.4)–(4.7.8) using Fourier transform and orthogonal polynomials techniques. Due to the uniqueness statement proved in Lemma 4.7.1, these solutions must coincide with $X^{\mathrm{sym}}_{[\mathbf{v},\mathbf{u}]}$ and $X^{\mathrm{anti}}_{[\mathbf{v},\mathbf{u}]}$. Instead of the double covers $[(\mathbb{Z}\pm\frac{1}{4})\times\mathbb{R};\mathbf{u},\mathbf{v}]$, we work only in the upper half-plane $\mathbb{Z}\times\mathbb{R}_+$ only (the link between the two setups is fully explained in Lemma 4.7.3).

Given a function $V : \mathbb{Z}\times\mathbb{R}\to\mathbb{R}$, we keep the definition (4.4.27) for the massive Laplacian $[\Delta^{(m)}V](k,s)$ when $s>0$ and introduce the values

$$[\mathcal{N}V](k,0) := -\frac{1}{2}\left[\partial_y^{+}V(k,0) + \partial_y^{-}V(k,0)\right], \tag{4.7.12}$$

where ∂_y^{+} and ∂_y^{-} stand respectively for the vertical partial derivative in the upper and the lower half planes. The operator $\mathcal{N}$ should be understood as a version of the normal second derivative of V at $(k,0)$, thus leaving the functions at stake in their respective half-planes. We now define two intermediate explicit problems $[\mathbf{P}^{\mathbf{sym}}_{\mathbf{n}}]$ and $[\mathbf{P}^{\mathbf{anti}}_{\mathbf{n}}]$ whose solutions are useful to derive a reccurence relation on spin-spin expectation in the full-plane. As a consequence of the uniqueness Lemma 4.7.1, solving those problems is equivalent to construct the functions $X^{\mathrm{sym}}_{[\mathbf{v},\mathbf{u}]}$ and $X^{\mathrm{anti}}_{[\mathbf{v},\mathbf{u}]}$, respectively ; see also Fig. 4.7.2.

— $[\mathbf{P_n^{sym}}]$: given $n \geq 1$, construct a bounded function $V : \mathbb{Z} \times \mathbb{R} \to \mathbb{R}$ such that the following conditions are fulfilled :

$$[\Delta^{(m)}V](k,s) = 0 \text{ if } s > 0; \qquad [\mathcal{N}V](k,0) = 0 \text{ for } k \in [\![1, n-1]\!];$$
$$V(k,0) = 0 \text{ for } k \notin [\![0,n]\!]; \qquad V(0,0) = D_n \text{ and } V(n,0) = D_n^\star\,.$$

— $[\mathbf{P_{n+1}^{anti}}]$: given $n \geq 0$, construct a bounded function $V : \mathbb{Z} \times \mathbb{R} \to \mathbb{R}$ such that the following conditions are fulfilled :

$$[\Delta^{(m)}V](k,s) = 0 \text{ if } s > 0; \qquad [\mathcal{N}V](k,0) = 0 \text{ for } k \notin [\![0,n+1]\!];$$
$$V(k,0) = 0 \text{ for } k \in [\![1,n]\!]; \qquad V(0,0) = -D_{n+1}; \quad V(n+1,0) = D_{n+1}^\star\,.$$

Lemma 4.7.3. *Assume that V_n^{sym} (resp., V_{n+1}^{anti}) is a solution to $[\mathrm{P}_{\mathrm{n}}^{\mathrm{sym}}]$ (resp., $[\mathrm{P}_{\mathrm{n+1}}^{\mathrm{anti}}]$). Then, the following holds :*

$$[\mathcal{N}V_n^{\mathrm{sym}}](0,0) = L_{n+1}, \qquad [\mathcal{N}V_n^{\mathrm{sym}}](n,0) = L_{n+1}^\star; \tag{4.7.13}$$
$$[\mathcal{N}V_{n+1}^{\mathrm{anti}}](0,0) = -L_n, \qquad [\mathcal{N}V_{n+1}^{\mathrm{anti}}](n+1,0) = L_n^\star. \tag{4.7.14}$$

Proof. Take a section of the double cover $[(\mathbb{Z} \pm \frac{1}{4}) \times \mathbb{R}; \mathbf{v}, \mathbf{u}]$ with an horizontal cut along the segment $[-\frac{1}{2}, n] \times \{0\}$ for the problem $[\mathrm{P}_{\mathrm{n}}^{\mathrm{sym}}]$ and outside the segment $[-\frac{1}{2}, n] \times \{0\}$ (in the horizontal axis) for the problem $[\mathrm{P}_{\mathrm{n+1}}^{\mathrm{anti}}]$. Define two functions respectively on the right and left corners of the lattice by

$$V_{[\mathbf{v},\mathbf{u}]}^{\mathrm{sym}}((\pm k - \tfrac{1}{4}, s)) := V_n^{\mathrm{sym}}(k,s) \qquad V_{[\mathbf{v},\mathbf{u}]}^{\mathrm{anti}}((\pm k + \tfrac{1}{4}, s)) := \pm V_{n+1}^{\mathrm{anti}}(k,s).$$

Since both functions vanish on their respective cuts, they can be viewed as bounded spinors on the double covers $[(\mathbb{Z} \pm \frac{1}{4}) \times \mathbb{R}; \mathbf{v}, \mathbf{u}]$, which satisfy the entire set of conditions described in (4.7.4)–(4.7.8). Using the uniqueness Lemma 4.7.1, this allows to identify $X_{[\mathbf{v},\mathbf{u}]}^{\mathrm{sym}} = V_{[\mathbf{v},\mathbf{u}]}^{\mathrm{sym}}$ and $V_{[\mathbf{v},\mathbf{u}]}^{\mathrm{anti}} = V_{[\mathbf{v},\mathbf{u}]}^{\mathrm{anti}}$. The identities (4.7.13), (4.7.14) are now easily deduced from (4.7.10), (4.7.11) and the definition (4.7.12). □

Let V be a solution to the problem $[\mathrm{P}_{\mathrm{n}}^{\mathrm{sym}}]$. We are going to construct V explicitly, starting first with a heuristic and more intuitive argument. Assume for a moment that all the Fourier series

$$\widehat{V}_s(e^{\mathrm{i}\,t}) := \textstyle\sum_{k\in\mathbb{Z}} V(k,s) e^{\mathrm{i}\,kt}, \quad s \geq 0, \quad t \in [0, 2\pi],$$

are well-defined. Using the massive harmonicity condition $[\Delta^{(m)}V](k,s) = 0$ for $s \neq 0$, this implies (provided the serie/derivation exchange is proper) that

$$[1 - \frac{2\theta\theta^\star}{\theta^2 + \theta^{\star 2}} \cos t] \cdot \widehat{V}_s(e^{\mathrm{i}\,t}) \;=\; \frac{1}{\theta^2 + \theta^{\star 2}} \widehat{V}_s''(e^{\mathrm{i}\,t}), \tag{4.7.15}$$

where the derivative in the above equation is taken with respect to the variable s. A general solution to the differential equation (4.7.15) is a linear combination of the functions $e^{\pm s w(t)}$ where $w(t) := w(t; \theta, \theta^\star)$ solves the quadratic equation,

$$1 - \frac{2\theta\theta^\star}{\theta^2 + \theta^{\star 2}} \cos t = \frac{w(t)^2}{\theta^2 + \theta^{\star 2}}.$$

Let $w(t;\theta,\theta^\star)$ to be the non-negative root of the above equation, i.e.,

$$w(t;\theta,\theta^\star) = \sqrt{(\theta^2+\theta^{\star 2}) - 2\theta\theta^\star\cos t} = |\theta - \theta^\star e^{\mathrm{i}\,t}|.$$

At level $s=0$, the function $\widehat{V}_0(e^{\mathrm{i}\,t}) = Q_n(e^{\mathrm{i}\,t})$ is an unknown trigonometric polynomial of degree n. Since we want Fourier series $\widehat{V}_s$ with *bounded* coefficients, we are tempted to state that $\widehat{V}_s(e^{\mathrm{i}\,t}) = Q_n(e^{\mathrm{i}\,t})\cdot e^{-sw(t;\theta,\theta^\star)}$ for $s \geqslant 0$. A direct computation at level $s=0$ proves that

$$\textstyle\sum_{k\in\mathbb{Z}}[\mathcal{N}V](k,0)e^{\mathrm{i}\,kt} \;=\; w(t;\theta,\theta^\star)Q_n(e^{\mathrm{i}\,t}). \tag{4.7.16}$$

The crucial point here is that the LHS of the previous equation *should not contai-nany monomials of the family* $\{e^{\mathrm{i}\,t},\dots,e^{\mathrm{i}(n-1)t}\}$, which simply reads as an orthogonality condition for $Q_n(e^{\mathrm{i}\,t})$. Let us make now rigourous the previous analysis to construct and identify the unique solution to the problem $[\mathrm{P}^{\mathrm{sym}}_{\mathrm{n}}]$.

Lemma 4.7.4. *Let $n\geq 1$. If a trigonometric polynomial $Q_n(e^{\mathrm{i}\,t}) = D_n + \cdots + D_n^\star e^{\mathrm{i}\,nt}$ of degree n has prescribed free (D_n) and leading ($D_n^\star$) coefficients and is orthogonal to the family $\{e^{\mathrm{i}\,t},\dots,e^{\mathrm{i}(n-1)t}\}$ with respect to the measure $w(t;\theta,\theta^\star)\frac{dt}{2\pi}$ on the unit circle, then the semi-discrete function defined by*

$$V(k,s) := \tfrac{1}{2\pi}\textstyle\int_{-\pi}^{\pi} e^{-ikt}Q_n(e^{\mathrm{i}\,t})e^{-sw(t;\theta,\theta^\star)}\mathrm{d}t$$

is uniformly bounded and solves $[\mathrm{P}^{\mathrm{sym}}_{\mathrm{n}}]$ in the upper half-plane. Moreover,

$$\langle Q_n, 1\rangle_{\frac{w}{2\pi}dt} = L_{n+1} \quad \textit{and} \quad \langle Q_n, e^{\mathrm{i}\,nt}\rangle_{\frac{w}{2\pi}dt} = L^\star_{n+1}, \tag{4.7.17}$$

where the scalar product is taken with respect to the same measure on the unit circle.

Proof. The values of $V(k,s)$ defined above are uniformly bounded since $|e^{-sw(t;\theta,\theta^\star)}| \leq 1$. The massive harmonicity property $[\Delta^{(m)}V](k,s)=0$ for $s>0$ is straightforward and the properties required for $V(k,0)$ and $[\mathcal{N}F](k,0)$ follow directly from the assumptions made on Q_n. The identities in (4.7.13) give (4.7.17). □

On can perform a similar construction to solve $[\mathrm{P}^{\mathrm{anti}}_{\mathrm{n+1}}]$, see Fig. 4.7.2. The only difference is that at level $s=0$, it is now required that $\widehat{V}_0(e^{\mathrm{i}\,t})$ does not contain monomials $e^{\mathrm{i}\,t},\dots,e^{\mathrm{i}(n+1)t}$ while

$$\textstyle\sum_{k\in\mathbb{Z}}[\mathcal{N}V](k,0)e^{\mathrm{i}\,kt} \;=\; w(t;\theta,\theta^\star)\widehat{V}_0(e^{\mathrm{i}\,t}) \;=\; -L_n + \cdots + L_n^\star e^{\mathrm{i}(n+1)t} \tag{4.7.18}$$

is a trigonometric polynomial of degree $n+1$. In other words, the polynomial in the RHS has to be ortgonal to $\{e^{\mathrm{i}\,t},\dots,e^{\mathrm{i}\,nt}\}$ with respect to the weight

$$w^{\#}(t;\theta,\theta^\star) \;:=\; (w(t;\theta,\theta^\star))^{-1}, \qquad t\in[0,2\pi]. \tag{4.7.19}$$

provided that $w^{\#}$ is integrable on the unit circle. One can easily see from its definition that this integrability condition holds if and only if $\theta\neq\theta^\star$. The special case $\theta=\theta^\star$ corresponds the model at criticality and will require modification as explained in Section 4.7.4.

Lemma 4.7.5. *Let $n \geq 0$ and assume that $\theta \neq \theta^\star$. If a trigonometric polynomial $Q^{\#}_{n+1}(e^{\mathrm{i}\,t}) = -L_n + \cdots + L^\star_n e^{\mathrm{i}(n+1)t}$ of degree $n+1$ has prescribed free $(-L_n)$ and leading $(L^\star_n)$ coefficients is orthogonal to the family $\{e^{\mathrm{i}\,t}, \ldots, e^{\mathrm{i}\,nt}\}$ with respect to the measure $w^{\#}(t;\theta,\theta^\star)\frac{dt}{2\pi}$, then the function defined by*

$$V(k,s) := \tfrac{1}{2\pi}\int_{-\pi}^{\pi} e^{-ikt} Q^{\#}_{n+1}(e^{\mathrm{i}\,t}) e^{-sw(t;\theta,\theta^\star)} w^{\#}(t;\theta,\theta^\star)dt \tag{4.7.20}$$

is uniformly bounded and solves $[\mathrm{P}^{\mathrm{anti}}_{\mathrm{n+1}}]$. *Moreover,*

$$\langle Q^{\#}_{n+1}, 1\rangle_{\frac{w^{\#}}{2\pi}dt} = -D_{n+1} \quad \textit{and} \quad \langle Q^{\#}_{n+1}, e^{\mathrm{i}(n+1)t}\rangle_{\frac{w^{\#}}{2\pi}dt} = D^\star_{n+1}, \tag{4.7.21}$$

where the scalar product is taken with respect to the same measure on the unit circle.

Proof. The proof is identical to the one of Lemma 4.7.4. □

4.7.3 . Horizontal spin-spin correlations below criticality

In this section, we derive the asymtotics of the horizontal spin-spin correlations D_n (as $n \to \infty$) by combining Lemmas 4.7.4 and 4.7.5. We assume that $\theta < \theta^\star$ and recall that $D^\star_n \to 0$ as $n \to \infty$. The latter claim is classical, and can be derived from the monotonicity of D_n with respect to the temperature together with the fact that $D_n = D^\star_n \to 0$ as $n \to \infty$ at cricicality, result which is discussed in the very next section. Even without the next section, one can simply mention RSW estimates at criticality to conclude.

Theorem 4.7.6. *Let $\theta < \theta^\star$. The spontaneous magnetization $\mathcal{M}(\theta,\theta^\star)$ of the quantum Ising model defined below satisfies*

$$\mathcal{M}(\theta,\theta^\star) \;:=\; \lim_{n\to\infty} D_n^{1/2} \;=\; (\theta^2+\theta^{\star 2})^{-\frac{1}{2}}(1-(\tfrac{\theta}{\theta^\star})^2)^{\frac{1}{8}}. \tag{4.7.22}$$

Since we developped a formalism fitted to [40], this proofs goes as in Theorem 3.6. The next lemma has exactly the same proof as in [40].

Lemma 4.7.7. *Set $\Phi_n(z) := z^n + \cdots - \alpha_{n-1}$ be the n-th unitary orthogonal polynomial with respect to the measure $w(t;\theta,\theta^\star)\frac{dt}{2\pi}$ on the unit circle. We also set $\Phi^\star_n(z) := z^n\Phi_n(z^{-1}) = -\alpha_{n-1}z^n + \cdots + 1$ the polynomial reciprocal to Φ_n. Moreover, write $\beta_n := \|\Phi_n\|^2 = \langle \Phi_n, e^{\mathrm{i}\,nt}\rangle = \langle \Phi^\star_n, 1\rangle$ and $\beta^{\#}_n := \|\Phi^{\#}_n\|^2$, where $\Phi^{\#}_n$ is the n-th unitary orthogonal polynomial with respect to the measure defined in* (4.7.19). *Then,*

$$\begin{aligned} L^2_{n+1} - (L^\star_{n+1})^2 &= \beta_n\beta_{n-1}\cdot(D^2_n - (D^\star_n)^2) \quad \textit{for} \;\; n \geq 1,\\ D^2_{n+1} - (D^\star_{n+1})^2 &= \beta^{\#}_{n+1}\beta^{\#}_n \cdot (L^2_n - (L^\star_n)^2) \quad \textit{for} \;\; n \geq 0. \end{aligned}$$

As a consequence, by applying the above two formulas recursively, we also have,

$$D^2_{2m+1} - (D^\star_{2m+1})^2 = \prod_{k=0}^{2m+1}\beta^{\#}_k \cdot \prod_{k=0}^{2m-1}\beta_k \cdot (L^2_0 - (L^\star_0)^2), \tag{4.7.23}$$

where $L^2_0 - (L^\star_0)^2 = \frac{\theta^2-\theta^{\star 2}}{(\theta^2+\theta^{\star 2})^2}$.

Now we can complete the proof of Theorem 4.7.6.

Proof. Recall that $D^{\star}_{2m+1} \to 0$ as $m \to \infty$. It remains to apply the Szego theory (e.g., see [79, Sec. 5.5] or [159, Thm. 8.1 and 8.5]) to the weights $w(t;\theta,\theta^{\star})$ and $w^{\#}(t;\theta,\theta^{\star})$. Let $q = \theta/\theta^{\star}$. We can write

$$w(t;\theta,\theta^{\star}) \ = \theta^{*} w_q(t), \qquad \text{where } w_q(t) = |1 - qe^{\mathrm{i}\,t}|,$$

Since $w^{\#}(t;\theta,\theta^{\star}) = (w(t;\theta,\theta^{\star}))^{-1}$, we have

$$\lim_{m\to\infty} \prod_{k=0}^{2m+1} \beta_k^{\#} \cdot \prod_{k=0}^{2m-1} \beta_k \ = \ \theta^{*-2} \cdot G^2, \tag{4.7.24}$$

where

$$\log G = \frac{1}{4\pi} \iint_{\mathbb{D}} \frac{\mathrm{d}}{\mathrm{d}z} \Big| \log(1-qz) \Big|^2 \mathrm{d}A(z) = \sum_{k\geqslant 1} \frac{q^{2k}}{4k} = -\frac{1}{4} \log(1-q^2).$$

Moreover,

$$L_0^2 - (L_0^{\star})^2 = \frac{\theta^2 - \theta^{\star 2}}{(\theta^2 + \theta^{\star 2})^2} = \frac{1}{\theta^{\star 2}} \frac{1-q^2}{(1+q^2)^2}.$$

Putting all the factors together, one gets (4.7.22).

□

Remark 4.7.8. In the proof of lemma 4.7.7, one uses the identities (3.24) and (3.26) from [40], which are

$$\begin{bmatrix} L^{\star}_{n+1} \\ L_{n+1} \end{bmatrix} = \beta_{n-1} \begin{bmatrix} 1 & \alpha_{n-1} \\ \alpha_{n-1} & 1 \end{bmatrix} \begin{bmatrix} D^{\star}_{n} \\ D_{n} \end{bmatrix}, \tag{4.7.25}$$

$$\begin{bmatrix} D^{\star}_{n+1} \\ -D_{n+1} \end{bmatrix} = \beta_{n}^{\#} \begin{bmatrix} 1 & \alpha_{n}^{\#} \\ \alpha_{n}^{\#} & 1 \end{bmatrix} \begin{bmatrix} L^{\star}_{n} \\ -L_{n} \end{bmatrix}. \tag{4.7.26}$$

We notice that, (4.7.26) applied to $n = 0$ provides the formula,

$$D_1 = \frac{\beta_0^{\#}}{\theta^2 + (\theta^{\star})^2} \cdot [\theta^{\star} - \alpha_0^{\#}\theta],$$

which is the *energy density* of the quantum Ising model.

Note that Equation (4.7.23) becomes useless at criticality since $\theta = \theta^{\star}$ and thus $L_0 = L_0^{\star}$. The asymptotic analysis needs to be treated in differently as explained in the following section.

4.7.4 . Asymptotics of horizontal correlations D_n as $n \to \infty$ at criticality

We now work at the critical and isotropical point of the model, i.e., $\theta = \theta^\star$. We generalize to the quantum Ising model the classical result by Mc-Coy and Wu that states that spin-spin correlations D_m decay like $m^{-1/4}$ when $m \to \infty$. The power-law type decay can be deduced by usual RSW arguments, but finding the correct asymptotic requires some additional work, which we perform now. We keep following the formalism of [40]. The proof of the next theorem goes as the one of Theorem 3.9 and we only give its outlines.

Theorem 4.7.9. *Let $\mathcal{C}_\sigma := 2^{\frac{1}{6}} e^{\frac{3}{2}\zeta'(-1)}$. For the critical quantum Ising model, one has the asymptotic as $m \to \infty$*

$$D_m \ \sim \ \mathcal{C}_\sigma^2 \cdot (2m)^{-1/4}. \tag{4.7.27}$$

Proof. A straightforward computation shows that

$$w_c(t) = 2(\sin \tfrac{1}{2}t)^2 \, .$$

thus the weight $w_c^\# := w_c^{-1}$ is not integrable anymore and the arguments of the proof of Theorem 4.7.6 have to be modified. We still can remark that $D_n = D_n^\star$, $L_n = L_n^\star$ by Kramers–Wannier duality. Still one can keep using (4.7.25). This allows to switch to the framework of orthogonal polynomials on the *the segment* $[-1, 1]$ instead of the working with weights defined on the unit circle. Let

$$\overline{w}_c(x) \ := \ [\, 1 - x^2 \,]^{1/2} \, , \quad x \in [-1; 1], \tag{4.7.28}$$

and $P_n(x) = x^n + \dots$ be the unitary orthogonal polynomial of degree n on the segment $[-1, 1]$ for the weight $\overline{w}_c(x)$. The trigonometric polynomial

$$Q_n(e^{\mathrm{i}\, t}) \ := \ D_n \cdot e^{\frac{1}{2}\, \mathrm{i}\, nt} \cdot 2^n P_n(\cos \tfrac{1}{2}t)$$

fits the construction given in Lemma 4.7.4 to solve $[\mathrm{P}_{\mathrm{n}}^{\mathrm{sym}}]$ (it has the proper orthogonality relations with prescribed proper free and leading coefficients D_n (recall that P_n is unitary). The formula (4.7.17) gives for $n \geqslant 1$

$$L_{n+1} = \frac{1}{2\pi} \int_{-\pi}^{\pi} Q_n(e^{\mathrm{i}\, t}) w_c(t) dt = \pi^{-1} 2^{2n} \cdot \|P_n\|^2_{\overline{w}_c dx} \cdot D_n. \tag{4.7.29}$$

An analoguous computation for $n = 0$ gives (using $D_0 = 1$ and due to the modification required in Lemma 4.7.2 for the case $n = 0$),

$$2L_1 \ = \ 2\pi^{-1} \textstyle\int_{-1}^{1} P_0(x) \overline{w_c}(x) dx = 2\pi^{-1} \cdot \|P_0\|^2_{\overline{w_c} dx} \tag{4.7.30}$$

We construct similarly a solution to $[\mathrm{P}_{\mathrm{n+1}}^{\mathrm{anti}}]$ treated in Lemma 4.7.5 in the supercritical regime. Denote $P_n^\#(x)$ be the unitary orthogonal polynomial of degree n on the segment $[-1, 1]$ for the weight,

$$\overline{w}_c^\#(x) \ := \ [\, 1 - x^2 \,]^{-1/2} \, , \quad x \in [-1, 1], \tag{4.7.31}$$

and,

$$Q_{n+1}^{\#}(e^{\mathrm{i}\,t}) \;:=\; L_n \cdot (e^{\mathrm{i}\,t}-1)e^{\frac{1}{2}\,\mathrm{i}\,nt} \cdot 2^n P_n^{\#}(\cos\tfrac{1}{2}t).$$

The formula (4.7.20) indeed provides a solution to the problem $[\mathrm{P}_{\mathrm{n+1}}^{\mathrm{anti}}]$, and now the product $(e^{\mathrm{i}\,t}-1)w_c^{\#}(t)$ *becomes integrable* in unit circle as the additional factor $(e^{\mathrm{i}\,t}-1)$ removes the singularity of $w_c^{\#}$ at $t=0$. Finally, the computation (4.7.21) is still valid and implies for $n \geqslant 0$,

$$D_{n+1} = -\frac{1}{2\pi}\int_{-\pi}^{\pi} Q_{n+1}^{\#}(e^{\mathrm{i}\,t})w_c(t)^{-1}dt = \pi^{-1}2^{2n} \cdot \|P_n^{\#}\|^2_{\overline{w}_c^{\#}dx} \cdot L_n. \qquad (4.7.32)$$

Since $L_0 = 1$ (see Lemma 4.7.2). Using the reccurence relations (4.7.30), (4.7.29) for $n = 1, \ldots, m-1$, and (4.7.32) for $n = 0, \ldots, m$, one gets

$$D_{m+1}D_m \;=\; \pi^{-2m-1}2^{2m^2}\prod_{k=0}^{m-1}\|P_k\|^2_{\overline{w_c}dx} \cdot \prod_{k=0}^{m}\|P_k^{\#}\|^2_{\overline{w_c}^{\#}dx}\,, \qquad (4.7.33)$$

where the weights $w_c(x)$ and $w_c^{\#}(x)$ on $[-1,1]$ are given by (4.7.28) and (4.7.31). This is a classical problem of orthogonal theory, and going back to the unit circle with a $|t|$-type singularity of the weights appears when $e^{\mathrm{i}\,t}=1$. General results (accounted, e.g., in [55]) ensure that,

$$D_{m+1}D_m \;\sim\; 2^{2/3}e^{6\zeta'(-1)}(2m)^{-1/2}, \quad m \to \infty,$$

To conclude, it is enough to prove that $D_{m+1} \sim D_m$ as $m \to \infty$. This can be seen in the convergence of horizontal correlation ratios in a finite box 4.3.5 and Russo-Seymour-Welsh estimates to pass to the full-plane. □

4.7.5 . Asymptotics of correlations above criticality

Proposition 4.7.10. *The horizontal correlation lenght equals* $\xi = \frac{1}{2}\log(\frac{\theta}{\theta^\star})$.

Proof. One first notices that using (4.7.25) and (4.7.26), one has, for all n,

$$D_{n+2} = q_n D_n + r_n, \qquad (4.7.34)$$

with $q_n = \beta_{n+1}^{\#}\beta_{n-1}(1-\alpha_{n+1}^{\#}\alpha_{n-1})$ and $r_n = \beta_{n+1}^{\#}\beta_{n-1}(\alpha_{n-1}-\alpha_{n+1}^{\#})D_n^\star$. The above formula gives, by induction, the following formula,

$$D_{2n} = \left(D_0 + \sum_{j=0}^{n-1}\frac{r_j}{\prod_{k=0}^{j}q_k}\right)\prod_{m=0}^{n-1}q_m. \qquad (4.7.35)$$

Note that $\alpha_{n+1}^{\#}$ and α_{n-1} converge to 0 exponentially fast [159, Thm. 9.1] with the same exponential rate $\lim_{n\to\infty}|\alpha_n|^{1/n} = \lim_{n\to\infty}|\alpha_n^{\#}|^{1/n} = R^{-1}$, with $R = \theta^\star/\theta > 1$ given by the radius of the disk on which w has an analytic continuation. We also know that D_n converges to 0 as n tends to ∞. Moreover, using (4.7.24), when n tends to infinity, we have that the product

$\prod_{m=0}^{n-1} q_m$ converges to a positive constant and that $\beta_{n+1}^{\#}\beta_{n-1}$ tends to 1. The aforementioned convergences all together imply that the factor

$$D_0 + \sum_{j=0}^{n-1} \frac{r_j}{\prod_{k=0}^{j} q_k}$$

goes to 0 as $n \to \infty$, and can be consequently rewritten as the remainder of a converging infinite series,

$$-\sum_{j=n}^{\infty} \frac{r_j}{\prod_{k=0}^{j} q_k}.$$

The ratio of the two consecutive terms in the above remainder is given by,

$$\frac{r_{j+1}/q_{j+1}}{r_j} = \frac{\alpha_j - \alpha_{j+2}^{\#}}{\alpha_{j-1} - \alpha_{j+1}^{\#}} \frac{1}{\beta_{j+1}^{\#}\beta_{j-1}} \frac{1}{1 - \alpha_{j+2}^{\#}\alpha_j}, \tag{4.7.36}$$

which tends to R^{-1} as explained below. Thus, the whold remainder (4.7.36) converges exponentially fast at rate R^{-1}.

We prove now the annouced fact that the given ratio converges to R^{-1}. The last two terms in (4.7.36) converge to 1 exponentially fast. Let $D(z) = \theta^{\frac{1}{2}}(1 - \frac{1}{R}z)^{\frac{1}{2}}$ and $D^{\#}(z) = \theta^{-\frac{1}{2}}(1 - \frac{1}{R}z)^{-\frac{1}{2}}$ the Szego functions naturally associated to the weights w and $w^{\#}$. Let $D^{-1}(z) = \sum_{j=0}^{\infty} d_{j,-1} z^j$ and $(D^{\#})^{-1}(z) = \sum_{j=0}^{\infty} d_{j,-1}^{\#} z^j$ their decomposition as power series.

Asymptotically, we have $d_{j,-1} = \theta^{-\frac{1}{2}}\binom{-\frac{1}{2}}{j} R^{-j} \sim \theta^{-\frac{1}{2}}(-1)^j \Gamma(\frac{1}{2})^{-1} j^{-\frac{1}{2}}$ and $d_{j,-1}^{\#} = \theta^{\frac{1}{2}}\binom{\frac{1}{2}}{j} R^{-j} \sim \theta^{\frac{1}{2}}(-1)^j \Gamma(-\frac{1}{2})^{-1} j^{-\frac{3}{2}}$. We now use the corollary (2) of Theorem 7.2.1 [159, Thm. 7.2.1] that states that the asymptotics on $d_{j,-1} d_{j,-1}^{\#}$ imply directly that $\alpha_j \sim (C_1) R^{-j} j^{-\frac{1}{2}}$ and $\alpha_j \sim C_1^{\#} R^{-j} j^{\frac{1}{2}}$. This concludes the proof.

□

4.8 . Construction of infinite volume correlators

In this section, we construct infinite-volume correlators in the semi-discrete lattice, which we rely on to identify the scaling limit fermionic observables in general simply connected domains. Those constructions are similar to the isoradial case, and are made out of a proper integration of the so-called discrete exponentials, introduced in the semi-discrete lattice in [109], following the path of [100, 12, 48]. One of the key features here is to extend discrete exponentials to the entire semi-discrete lattice, including the corner graph.

Definition 4.8.1. Let $\delta > 0$. Take $p \in \Lambda(\Omega_\delta) \cup \Upsilon(\Omega_\delta)$ be a vertex on either the medial graph or the corner graph. Fix $\lambda \in \mathbb{C}$. We define the *semi-discrete exponential* $\exp_\delta(\lambda, \cdot, p)$ *normalized at* p using the following reccursion rules.

— $\exp_\delta(\lambda, p, p) := 1$.

— $\exp_\delta(\lambda, q, p) := \exp_\delta\left[\frac{\lambda(q-p)}{(1+\frac{\lambda\delta}{2})(1-\frac{\lambda\delta}{2})}\right]$ for any q such that $\mathrm{Re}(q) = \mathrm{Re}(p)$.

— $\exp_\delta(\lambda, c, p) := \exp_\delta(\lambda, q, p)(1 + \lambda(c - q))^{-1}$ for each pair of adjacent vertices $q \in \Lambda(\Omega_\delta)$ and $c \in \Upsilon(\Omega_\delta)$.

Moreover, the reccursion rules ensure that if $u \sim v$ are neighbours in $\Lambda(\Omega_\delta)$, we have,

$$\exp_\delta(\lambda, v, p) = \exp_\delta(\lambda, u, p)\frac{1 + \frac{\lambda\delta}{2}(v - u)}{1 - \frac{\lambda\delta}{2}(v - u)}.$$

One can easily check that the semi-discrete exponential is well-defined and also this definition coincides with the one from [109] if we restrict it to the semi-discrete medial lattice.

Lemma 4.8.2. *Given $p_0 \in \Lambda(\Omega_\delta)$ and $\lambda \in \mathbb{C}$, the function $c \mapsto \exp(\lambda, c, p_0)$ is discrete holomorphic everywhere.*

Proof. This is a straightforward computation that we precise here. Assume that $\delta = 1$, fix $\lambda \in \mathbb{C}$ and set $F = \exp_1(\lambda, \cdot, p_0)$. Assuming that $c^- \sim c \sim c^+$ are naturally ordered neighbors, one has,

$$F(c^+) = \frac{1 + \frac{\lambda}{2}}{1 - \frac{\lambda}{2}} F(c), \quad F(c^-) = \frac{1 - \frac{\lambda}{2}}{1 + \frac{\lambda}{2}} F(c), \quad \partial_y F(c) = \frac{\mathrm{i}\,\lambda}{(1 + \frac{\lambda}{2})(1 - \frac{\lambda}{2})} F(c).$$

Thus checking discrete holomorphicity (4.4.11) amounts to verify that

$$F(c)\big[\frac{1}{2}\big(\frac{1 + \frac{\lambda}{2}}{1 - \frac{\lambda}{2}} - \frac{1 - \frac{\lambda}{2}}{1 + \frac{\lambda}{2}}\big) - \frac{1}{i}\frac{i\lambda}{(1 + \frac{\lambda}{2})(1 - \frac{\lambda}{2})}\big] = 0$$

which holds.

□

We are now in position to construct the infinite-volume correlators out of semi-discrete exponentials.

Definition 4.8.3 (Infinite-volume energy correlator)**.** Given $a \in \Upsilon(\Omega_\delta)$, we define the full-plane energy correlator normalized at a by setting for $c \neq a \in \Upsilon(\Omega_\delta)$

$$\eta_c\langle\chi_c\chi_a\rangle_{\mathbb{C}_\delta} := \frac{1}{2\pi}\int_{-\mathbb{R}_+\overline{c-a}} \frac{\overline{\eta_a}\exp_\delta(\lambda, c, a)}{1 - i\overline{\eta_a}^2\frac{\lambda^2}{4}}\mathrm{d}\lambda. \tag{4.8.1}$$

The previous definition should be understood at $a^\pm$ by

$$\eta_a\langle\chi_{a^\pm}\chi_a\rangle_{\mathbb{C}_\delta} := \pm\frac{1}{2\pi}\int_{\mathbb{R}_+} \frac{\overline{\eta_a}}{1 - i\overline{\eta_a}^2\frac{\lambda^2}{4}}\mathrm{d}\lambda. \tag{4.8.2}$$

We also denote $G_{(a)} := \eta_a\langle\chi_c\chi_a\rangle^\diamond_{\mathbb{C}_\delta}$ its diamond s-holomorphic counterpart.

Definition 4.8.4 (Infinite-volume spin correlators)**.** Given $u \in \Omega_\delta^\bullet$ and $v \in \Omega_\delta^\circ$, we also define the infinite volume correlators $\eta_c \langle \chi_c \sigma_u \rangle_{[\mathbb{C}_\delta, u]}$ and $\eta_c \langle \chi_c \mu_v \rangle_{[\mathbb{C}_\delta, v]}$ by setting

$$\eta_c \langle \chi_c \sigma_u \rangle_{[\mathbb{C}_\delta, u]} := \frac{e^{-\frac{i\pi}{4}}}{2\pi} \int_{-\mathbb{R}_+ \overline{c-u}} \frac{1}{\lambda^{1/2}} \exp_\delta(\lambda, c, u) \mathrm{d}\lambda, \tag{4.8.3}$$

$$\eta_c \langle \chi_c \mu_v \rangle_{[\mathbb{C}_\delta, v]} := \frac{e^{\frac{i\pi}{4}}}{2\pi} \int_{-\mathbb{R}_+ \overline{c-v}} \frac{1}{\lambda^{1/2}} \exp_\delta(\lambda, c, v) \mathrm{d}\lambda. \tag{4.8.4}$$

The correlators $\langle \chi_c \sigma_u \rangle_{[\mathbb{C}_\delta, u]}$ and $\langle \chi_c \mu_v \rangle_{[\mathbb{C}_\delta, v]}$ are respectively defined in $[\mathbb{C}_\delta, u]$ and $[\mathbb{C}_\delta, v]$, the double covers of the semi-discrete lattice $\mathbb{C}_\delta$ respectively branching around u and v. We also denote $G^\diamond_{[u]} := \langle \chi_c \sigma_u \rangle^\diamond_{[\mathbb{C}_\delta, u]}$ and $G^\diamond_{[v]} := \langle \chi_c \mu_v \rangle^\diamond_{[\mathbb{C}_\delta, v]}$ the naturally associated diamond s-holomorphic extensions.

Proposition 4.8.5. *The energy correlator $\langle \chi_c \chi_a \rangle^\diamond_{\mathbb{C}_\delta}$, double valued at $a^\pm$ as in* (4.4.29)*, is corner s-holomorphic* everywhere *(even at $a^\pm$ with the proper graph modifications). Moreover, uniformly on compact subsets of $\mathbb{C} \backslash \{a\}$, one has the asymptotic $\delta^{-1} G_{(a)}(z) = \frac{\overline{\eta_a}}{\pi(z-a)}(1 + O(\delta))$ as $\delta \to 0$. Finally, one has $G_{(a)}(a + \delta) = \eta_{a+\delta} \frac{2}{\pi}$.*

Proof. The corner discrete holomorphicity comes from the fact that one can (using simple deformation of contours) replace the line $-\mathbb{R}_+ \overline{c-a}$ by a contour surrounding all the poles of the integrand at nearby corners. One can then use the same contour for nearby corners and the corner discrete holomorphicity comes directly from the one of discrete exponentials. In order to compute asymptotics, a simple rescaling of the grid allows to work with $\delta = 1$ and $|c - a| \to \infty$. One can cut the integral in 3 parts : $|\lambda| \leqslant |c-a|^{-\frac{1}{3}}$, $\lambda \in [|c-a|^{-\frac{1}{3}}; |c-a|^{+\frac{2}{3}}]$ and $|\lambda| \geqslant |c-a|^{\frac{2}{3}}$. Using the fact that $\eta_c^2 = \frac{i}{v_c - u_c}$, the integrand $\exp(\lambda, c, a)(1 - i\overline{\eta_a}^2 \frac{\lambda^2}{4})^{-1}$ has the following asymptotics

- $\overline{\eta_a} \exp\left(\lambda(c-a) + O(\lambda^2) + O(|c-a|\lambda^3)\right)$ as $\lambda \to 0$.
- $4\eta_a \eta_c^2 \lambda^{-2} \exp\left(4\lambda^{-1}\overline{(c-a)} + O(\lambda^{-2}) + O(|c-a|\lambda^{-3})\right)$ as $\lambda \to \infty$.
- $\exp(\lambda, c, a)(1 - \mathrm{i}\,\overline{\eta_a}^2 \frac{\lambda^2}{4})^{-1} = O\big(\exp(-|c-a|^{\frac{1}{2}})\big)$ for $\lambda \in [|c-a|^{-\frac{1}{3}}; |c-a|^{+\frac{2}{3}}]$ as in the proof of [109, Prop. 3.20].

Applying the Laplace method one directly gets the asymptotic expansion

$$\eta_c \langle \chi_c \chi_a \rangle_{\mathbb{C}_1} = \frac{1}{2\pi}\Big(\frac{\overline{\eta}_a}{c-a} + \frac{\eta_a \eta_c^2}{\overline{c-a}}\Big) + O(|c-a|^{-2}) \quad \text{as} \quad |c-a| \to \infty$$

The values at $a^\pm$ and at $a + \delta$ are obtained by a straightfoward computation. The check of complex sign of the projection $\eta_c \langle \chi_c \chi_a \rangle_{\mathbb{C}_\delta}$ is left as an exercice to the reader (e.g. see Remark in [43, Sec. 5.2]).

□

Proposition 4.8.6. *The correlator $\eta_c\langle\chi_c\sigma_u\rangle_{[\mathbb{C}_\delta,u]}$ is a well-defined corner s-holormophic function everywhere on $[\mathbb{C}_\delta, u]$. Moreover, one has the asymptotic expansion*

$$\delta^{-\frac{1}{2}}G^{\diamond}_{[u]}(z) = \frac{1}{\sqrt{\pi}}\frac{e^{-\frac{i\pi}{4}}}{\sqrt{z-u}} + O(\frac{\delta^2}{(z-u)^{\frac{5}{2}}}),$$

which is uniform on compact subsets away from u. Similarly, the correlators $\eta_c\langle\chi_c\mu_v\rangle_{[\mathbb{C}_\delta,v]}$ is a well-defined corner s-holormophic function everywhere on the double cover $[\mathbb{C}_\delta, v]$. One also has the asymptotic expansion

$$\delta^{-\frac{1}{2}}G^{\diamond}_{[v]}(z) = \frac{1}{\sqrt{\pi}}\frac{e^{\frac{i\pi}{4}}}{\sqrt{z-v}} + O(\frac{\delta^2}{(z-u)^{\frac{5}{2}}}),$$

which is uniform on compact subsets away from v. At corner neighbouring their branchings, both corner s-holomorphic correlators have an absolute value 1, with appropriate complex sign.

Proof. The spirit of the proof is very similar to that of the energy correlator. Deforming again the half-line into contour (this time avoiding the poles of discrete exponentials and u) and using the a asymptotics of discrete exponentials allows to transfer the discrete holomorphicity of discrete exponentials to the discrete holomorphicity of the correlators. Rescaling again the lattice, we work with $\delta = 1$ when $|c-u| \to \infty$. This time the integrand has the asymptotics,

- $e^{-\frac{i\pi}{4}}\lambda^{-\frac{1}{2}}\exp\left(\lambda(c-u) + O(|c-u|^2\lambda^2)\right)$ as $\lambda \to 0$.
- $2e^{\frac{i\pi}{4}}\eta_c^2\lambda^{-\frac{3}{2}}\exp\left(4\lambda^{-1}\overline{(c-u)} + \mathcal{O}(|c-u|^{-2}\lambda^{-2})\right)$ as $\lambda \to \infty$.
- $\lambda^{-\frac{1}{2}}\exp(\lambda, c, u) = O\big(\exp(-|c-u|^{\frac{1}{2}})\big)$ for $\lambda \in [|c-u|^{-\frac{1}{3}}; |c-u|^{+\frac{2}{3}}]$ as in the proof of [109, Prop. 3.20].

This proves again that the integral is well defined and the Laplace method provides the announced asymptotics. The spinor property comes from the spinor property of the function $\lambda^{-\frac{1}{2}}$ and the values near the branchings are computed using the residue theorem. The check of complex sign of the projection $\eta_c\langle\chi_c\sigma_u\rangle_{[\mathbb{C}_\delta,u]}$ (i.e. not only the complex sign of its asymptotic which is given by the above computation) is left as an exercice to the reader (e.g. see Remark in [43, Sec. 5.2]).

□

Proposition 4.8.7. *The correlator $G_{[u^\delta]}$ is differentiable with respect to the position of its branching u, i.e. uniformly over z's at a fixed distance from u^δ, one has the asymptotic expansion*

$$\delta^{-\frac{1}{2}}\partial_y G_{[u^\delta]}(z) := \lim_{\varepsilon\to 0}\frac{G_{[u^\delta+i\varepsilon]}(z) - G_{[u^\delta]}(z)}{\varepsilon} = -\frac{1}{\sqrt{\pi}}\frac{i}{2(z-u)^{\frac{3}{2}}} + O(\frac{\delta}{(z-u)^{\frac{5}{2}}}), \tag{4.8.5}$$

where the asymptotic is given when $\delta \to 0$.

Proof. Let c^δ be a fixed corner, away from the u^δ and $u^\delta + i\varepsilon$. By translation invariance of the lattice, one clearly has $G_{[u^\delta+i\varepsilon]}(c^\delta + \mathrm{i}\,\varepsilon) = G_{[u^\delta]}(c^\delta)$, thus we immediately deduce that $G_{[u^\delta+i\varepsilon]}(c^\delta) = G_{[u^\delta]}(c^\delta - i\varepsilon)$. This implies that,

$$\begin{aligned}\frac{G_{[u^\delta+i\varepsilon]}(c^\delta) - G_{[u^\delta]}(c^\delta)}{\varepsilon} &= \frac{G_{[u^\delta]}(c^\delta - i\varepsilon) - G_{[u^\delta]}(c^\delta)}{\varepsilon} \\ &\xrightarrow[\varepsilon\to 0]{} \partial_y G_{[u^\delta]}(c^\delta) = -i\frac{G_{[u^\delta]}(c^\delta+\delta) - G_{[u^\delta]}(c^\delta-\delta)}{2\delta},\end{aligned}$$

where the last equality is justified by the fact that $G_{[u^\delta]}(\cdot)$ is discrete holomorphic away from u. The announced asympotic is now easily recovered by the two terms asymptotics of $G_{[u^\delta]}$ away from its branching. □

4.9 . Hyperbolic metric on a rectangular domain

Let $0 < k < 1$ and define $\mathcal{R}(k)$ to be the rectangle given by $(-K(k), K(k)) \times (0, K'(k))$, where K denotes the complete elliptic integral of the first kind,

$$K(k) = \int_0^1 \frac{\mathrm{d}t}{\sqrt{(1-t^2)(1-k^2t^2)}},$$

and K' denotes its complementary, i.e. $K'(k) = K(\sqrt{1-k^2})$. Note that $k \mapsto K(k)/K'(k)$ is strictly increasing with limits 0 and $+\infty$ when k tends to 0 and 1. Hence, the whole family $\{\mathcal{R}(k), 0 < k < 1\}$ describes all the rectangles of all the possible aspect ratios.

Proposition 4.9.1. *Let $0 < k < 1$. The following Schwarz–Christoffel mapping f_k transforms the upper half-plane $\mathbb{H}$ into the rectangle $\mathcal{R}(k)$,*

$$f_k(z) = \int_0^z \frac{\mathrm{d}t}{\sqrt{(1-t^2)(1-k^2t^2)}}.$$

Proof. We can easily see that f_k is indeed a Schwarz–Christoffel mapping where $-k^{-1}$, -1, 1 and k^{-1} are mapped to vertices of the resulting polygon with angles all equal to $\frac{\pi}{2}$, thus a rectangle. Moreover, the images of -1 and 1 via f_k can be computed as follow, $f_k(1) = K(k)$, $f_k(-1) = -K(k)$. Finally, we compute $f_k(k^{-1}) - f_k(1) = \mathrm{i}\,K'(k)$ by a change of variables, similarly for $f_k(-k^{-1}) - f_k(-1)$. □

The hyperbolic metric of a simply connected domain $\mathcal{D}$ is defined by

$$\ell_{\mathcal{D}}(a) = \frac{2|h'(a)|}{1-|h(a)|^2}, \qquad a \in \mathcal{D}, \tag{4.9.1}$$

where h is *any* conformal map sending $\mathcal{D}$ to the unit disk $\mathbb{D}$. It is important to note that such a conformal map is well-defined only up to a Möbius transformation, which does not change the metric defined via (4.9.1).

Proposition 4.9.2. *Given $k > 1$. The hyperbolic metric on $\mathcal{R}(k)$ is given by*

$$\ell_{\mathcal{R}(k)}(a) = \frac{\mathrm{cn}(a,k)\mathrm{dn}(a,k)}{\mathrm{Im}\,\mathrm{sn}(a,k)}, \qquad a \in \mathcal{R}(k).$$

Proof. Let $g : \mathbb{H} \to \mathbb{D}$ be a conformal map between the upper half-plane and the unit disk given by $g(z) = \frac{z-\mathrm{i}}{z+\mathrm{i}}$ for $z \in \mathbb{H}$. Then the map $h := g \circ f_k^{-1}$ is a conformal map between $\mathcal{R}(k)$ and $\mathbb{D}$. Moreover, f_k^{-1} is the inverse of an elliptic integral and is given by the Jacobi elliptic function $a \mapsto sn(a,k)$. Then the result follows by applying (4.9.1) and the properties of the Jacobi elliptic functions. □

5 - Crossing estimates on general s-embeddings

This chapter corresponds to the article [117], written alone and currently available at the webpage of the author.

Abstract :

We prove Russo-Seymour-Welsh type crossing estimates for the FK-Ising model on general s-embeddings satisfying the assumption $\textsc{Lip}(\kappa,\delta)$ with an additional geometrical constrain $\textsc{Lenght-Exp-Fat}(\delta)$. This results extends the work Chelkak on 'flat' s-embeddings providing a class of Ising models without any bounded angle type property where crossing estiamtes at large scale are bounded away from 0 and 1, extending previously known results on the critical and near critical isoradial grids.

5.1 . Introduction, main results and perspectives

5.1.1 . General context

The Ising model, introduced a century ago by Lenz, is one of the most studied models in the statistical mechanics. Its planar version (i.e., the model in $2D$ with nearest-neighbor interactions) have received extensive attention and shows a profuse structure of correlations (see e.g. the monographs [72, 123, 136]). We focus in this paper on the model with no exterior magnetic field, and contrarily to usual conventions, we prefer working with the ferromagnetic model defined on *faces* (denoted by G°) of a planar graph G (whose vertices are denoted by $G^\bullet$). If G is a finite connected graph and $\beta = 1/kT$ a positive number called inverse temperature, one attaches to each edge $e \in E(G)$ separating the two faces $v^\circ_\pm(e) \in G^\circ$ a coupling constant $J_e > 0$. The partition function of the model is given by

$$\mathcal{Z}(G) \;:=\; \sum_{\sigma:G^\circ\to\{\pm1\}} \exp\big[\,\beta \sum_{e\in E(G)} J_e \sigma_{v^\circ_-(e)}\sigma_{v^\circ_+(e)}\,\big]. \tag{5.1.1}$$

The domain walls representation (see e.g. [37, Sec 1.2]) allows to rewrite $\mathcal{Z}(G)$ as

$$\mathcal{Z}(G) \;=\; 2\textstyle\prod_{e\in E(G)}(x(e))^{-1/2} \times \sum_{C\in\mathcal{E}(G)} \prod_{e\in C} x(e), \text{ where } x(e) := \exp[-2\beta J_e]$$

and $\mathcal{E}(G)$ denotes the set of even sub-graphs of G. Naturally identifying an edge e of G to the associated face $z(e)$ of the bipartite graph $\Lambda(G) := G^\bullet \cup G^\circ$ allows to set an *abstract parametrization* (i.e. without any geometric interpretation) of the coupling constant J_e given by

$$\theta_{z(e)} \;:=\; 2\arctan x(e) \;\in\; (0, \tfrac{1}{2}\pi). \tag{5.1.2}$$

This abstract definition does *not* require to fix an embedding of G into $\mathbb{C}$ and was used by Chelkak to introduce the notion of *s-embeddings* in [34, 33], aiming to

study large scale properties of weighted planar graphs (G, x) carrying critical or near-critical (in some way that is not precised here) Ising weights $x(e)$. This study is already rather complete and precise in tn the isoradial context. In particular, this embedding procedure introduced by Chelkak already allowed him to analyze (in some cases) the scaling limit of discrete fermionic observables, in the spirit of the pioneering work of Smirnov [162, 160] on the square grid and further generalization on critical and near critical isoradial grids [48, 38, 138, 39, 137, 87]. The notion of s-embeddings is in fact encapsulated in the more general framework of *t-embeddings* or *Coloumb gauges*, which is centered in the study of the bipartite dimer model [103, 45, 44]. This later fact allows to benefit from the regularity theory of discrete harmonic and holomorphic functions developed there, under rather mild geometrical assumptions (see [45, Sec. 6]).

The long term motivation of [33] is to provide an embedding procedure adapted to the study large scale properties of weighted graphs which are potentially locally irregular, including some graphs sorted at random (where no kind of bounded angle type property should be expected). This could in principle target the study of the Ising model in random environments, and in the best case scenario, help understanding critical random maps equipped with the Ising model -which presumably converges to the *Liouville Quantum Gravity* (e.g. see [67]) but also deterministic graphs sorted with random coupling constants (e.g. $\mathbb{Z}^2$ with i.i.d. coupling constants). We clearly emphasize that the current paper doesn't treat at all any such difficult questions, which rather provides a really flexible framework to attack the question of crossing estimates in a broad class of lattices.

In the current paper, we prove usual Russo-Seymour-Welsh crossing estimates for the associated FK-Ising model (see [60, Sec. 5] for the usual statement on the square grid) under the assumption $\textsc{Lip}(\kappa,\delta)$, together with a mild geometrical assumption $\textsc{Lenght-Exp-Fat}(\delta)$. In particular, *we do not rely upon any bounded angle or comparable length assumptions*, but rather assume that the embeddings start to be non-smashed above some scale δ (defined via the assumption $\textsc{Lip}(\kappa,\delta)$) and that, at macroscopic distances compared to δ, the share of exponentially small faces (in δ^{-1}) is negligeble in the overall picture (see below the precise definition of the assumption $\textsc{Lenght-Exp-Fat}(\delta)$). This hints that the s-embeddings framework might be part of an interesting path for the analysis of the critical or near critical Ising model on general weighted graphs, possibly chosen at random (whether randomness is chosen on the local geometry or on the weights). The roadmap would consist in first re-imbedding an abstract weighted graph via the s-embeddings framework and then try to apply the strategy developed in the present article. Let us emphasize that in order to apply the aforementionned strategy, one should first ensure the possibility to construct a *proper* s-embedding associated to the abstract weighted graph G, where faces that do not overlap each other. This existence of a proper s-embedding associated to G remains a difficult question in full generality and *is not a priori automatic for general infinite grids*.

The idea of Chelkak to construct embeddings suited to the study of the critical Ising model already allowed to prove in [33, Theorem 1.2] the conformal invariance of properly embedded critical double-periodic graphs (setup where the criticality condition was derived by Cimasoni and Duminil-Copin in [52, Theorem 1.1]) and more generally for regular graphs with 'flat' origami functions $\mathcal{Q}^\delta = O(\delta)$. In the critical double-periodic case, even finding the correct cannonical embedding [33, Lemma 2.3] and proving the convergence of FK-Ising interfaces to SLE(16/3) remained open before the work of Chelkak. The convergence of the FK-observable in arbitrary rough domains was also made quantitative in δ , which was not known even in the critical square grid case. In the present paper, we answer one of Chelkak's questions [33, Section 1.4 (I)] and treat the case $\mathcal{Q}^\delta \not\to 0$, also removing bounded angles type assumptions on the local geometry. Among the consequence of our current work on already studied models, there is

— An alternative derivation of the RSW property for the FK-Ising model on critical Z-invariant isoradial lattices as in [48]. Our result extends beyond the scope of the paper of Chelkak and Smirnov, as it allows to replace the bounded angle property by the assumption $\textsc{Lenght-Exp-Fat}(\delta)$ introduced below. The removal of bounded angle property allows in particular to rederive the RSW property for the FK representation of the quantum Ising model [62, Section 5].

— An alternative derivation of the RSW property for the *massive* Z-invariant model on isoradial grids as in [138], using the re-embedding procedure of [43, Section 3.3].

— An alternative derivation of the RSW property for double-periodic graphs given in [33].

— The derivation of the RSW property for the FK-Ising model on circle patterns introduced in [113] with bounded angles. The result was not known there and in that case complements the dichotomy between the three phases of the model, proving that correlation decay polyniomially fast with the distance. One also notes that our proof goes beyond the bounded angle property assumption made there.

We emphasize once again that our theorem goes beyond the aforementioned list and is constructed to be applied in a way more general class of weighted graphs.

5.1.2 . Main results

In order to keep the presentation compact, we postpone to section 5.2 the precise definition of the construction of an s-embeddings $\mathcal{S}$. Discussing large scale properties of a grid $\mathcal{S}$, one should first define the notion of *scale* associated to $\mathcal{S}$. In the case of grids with comparable edges-lengths and non-smashed angles, a quite natural definition (recalled below) was introduced in [33, Section 1.3].

Definition 5.1.1 ($\textsc{Unif}(\delta)$)**.** We say that the s-embedding $\mathcal{S}^\delta$ satisfies the assumption $\textsc{Unif}(\delta)$ if there exists constants $r_0, \theta_0 > 0$ such that all edge

lengths of $\mathcal{S}^\delta$ are uniformly comparable to δ i.e. for any two neighboring vertices $v^\bullet \in G^\bullet$ and $v^\circ \in G^\circ$

$$r_0\delta \ \leq \ |\mathcal{S}^\delta(v^\bullet) - \mathcal{S}^\delta(v^\circ)| \ \leq \ (r_0)^{-1}\delta$$

and all angles of quads in $\mathcal{S}^\delta$ are uniformly bounded from below by θ_0. In particular, from the Ising model combinatorics perspective, under this assumption, all interaction parameters defined via (5.1.2) are uniformly bounded away from 0 and from 1, as a direct consequence of the formula (5.2.11).

We provide now a more general definition of the *scale* of the s-embedding $\mathcal{S}^\delta$, using the origami map $\mathcal{Q}$ defined in Definition 5.2.2. In words, the origami map $\mathcal{Q}$ can be viewed as a real valued function defined by its increments beween neighbouring vertices $v^\bullet, v^\circ$ of the bipartite graph $G^\bullet \cup G^\circ$ with the local incremental rule given by $\mathcal{Q}(\mathcal{S}^\delta(v^\bullet)) - \mathcal{Q}(\mathcal{S}^\delta(v^\circ)) := |\mathcal{S}^\delta(v^\bullet) - \mathcal{S}^\delta(v^\circ)|$ i.e $\mathcal{Q}$ adds distances when going from vertices of G° to vertices of $G^\bullet$ and substracts distances in the other direction (see Definition 5.2.2 and below for a precise statement and the extension of $\mathcal{Q}$ to the entire plane). A definition of the scale of the embedding can be proposed using the following assumption $\textsc{Lip}(\kappa,\delta)$ repeating the idea of [45].

Hypothèse 5.1.1 ($\textsc{Lip}(\kappa,\delta)$)**.** There exists a positive constant $\kappa < 1$ such that

$$|\mathcal{Q}^\delta(v') - \mathcal{Q}^\delta(v)| \leq \kappa \cdot |\mathcal{S}^\delta(v') - \mathcal{S}^\delta(v)| \quad \text{if} \quad |\mathcal{S}^\delta(v') - \mathcal{S}^\delta(v)| \geq \delta. \qquad (5.1.3)$$

One can then construct a *definition* of the notion of scale δ of the s-embedding $\mathcal{S}^\delta$ using the assumption $\textsc{Lip}(\kappa,\delta)$ following the framework of [45]. Fix some positive $\kappa < 1$. The scale δ of the embedding is the *minimal* length δ starting at which the assumption $\textsc{Lip}(\kappa,\delta)$ holds.

When speaking about the scaling limit of a sequence of s-embeddings $(\mathcal{S}^\delta)_{\delta>0}$, this limit is taken along a subsequence of s-embeddings $(\mathcal{S}^{\delta_n})_{\delta_n}$ with $\delta_n \to 0$ as $n \to \infty$ and *all* s-embeddings $\mathcal{S}^{\delta_n}$ satisfy $\mathrm{Lip}(\kappa, \delta_n)$ for the *same* $\kappa < 1$. For grids satisfying $\textsc{Unif}(\delta)$, the definition of the scale using $\textsc{Lip}(\kappa,\delta)$ coincides with the parameter δ up to bounded (only depending on r_0, θ_0)) factor. When working with irregular local geometries, we introduce another mild assumption $\textsc{Lenght-Exp-Fat}(\delta)$ that quantifies the degree of degeneracy allowed to still be able to perform some meaningful analysis. This restriction on the local geometry is a reinforcement of the assumption $\textsc{Exp-Fat}(\delta)$ recall below, which ensures precompactness of s-holomorphic functions (see Theorem 5.2.18).

Hypothèse 5.1.2. We say that a family of proper s-embeddings $(\mathcal{S}^\delta)_{\delta>0}$ satisfies the assumption $\textsc{Lenght-Exp-Fat}(\delta)$ on a macroscopic ball $B \subset \mathbb{C}$ if for each $\gamma > 0$:

$$\lim_{\delta\to 0} \sum_{z\in\diamondsuit\cap B, r_z\leqslant \exp(-\gamma\delta^{-1})} \mathrm{diam}(z) = 0,$$

where r_z is the radius of the tangential circle associated to the face z of $G^\circ \cup G^\bullet$ defined in section 5.2.

The second assumption is stronger that the Assumption denoted EXP-FAT(δ) which was first introduced in [45, Assumption 1.2] to quantify the local degeneracies allowed for the embeddings. We recall now that original assumption.

Hypothèse 5.1.3. We say that a family of proper s-embeddings $\mathcal{S}^\delta$ satisfies the assumption EXP-FAT(δ) on an open subset $U \subset \mathbb{C}$ if for each $\gamma > 0$:

after removing all quads $(\mathcal{S}^\delta)^\diamond(z)$ with $r_z \geq \exp(-\gamma\delta^{-1})$ from U, the maximal diameter of all vertex-connected components goes to 0 when $\delta \to 0$.

Explained in words, the assumption EXP-FAT(δ) means that the connected components of faces with an exponentially small radius (in δ^{-1}) do *not* form macroscopic regions, while the assumption LENGHT-EXP-FAT(δ) reads as the fact that the total $\mathcal{H}^1$ measure of exponentially small faces (still in δ^{-1}) is small as $\delta \to 0$.

Under the assumptions LIP(κ,δ) and LENGHT-EXP-FAT(δ) , boxes of macroscopic size satisfy the usual Russo-Seymour-Welsh box crossing property for the associated FK-Ising model (see e.g. [60, Chapter 4] for precise defintions and basic property of that model). This result is already known for critical and near critical Ising model on isoradial grids (see [48, Theorem 6.1] and [138, Theorem 1.2]) as well as for 'flat' s-embeddings (see [33, Theorem 1.3]). The proof of such theorem starts with a proof of a lower bound for the magnetization of the spin-Ising model with 4 alterating boundary conditions.

Theorem 5.1.1. Let $x_1 < x_2$, $y_1 < y_2$, $\mathcal{R} := (x_1, x_2) \times (y_1, y_2) \subset \mathbb{C}$, and $(\mathcal{S}^\delta)_{\delta>0}$ be s-embeddings satisfying the assumptions LIP(κ,δ) and LENGHT-EXP-FAT(δ) .
Let $\mathcal{R}^\delta = [\mathcal{R}(x_1, x_2; y_1, y_2)]^{\circ\bullet\circ\bullet}_{\mathcal{S}^\delta}$ be a discretization of $\mathcal{R}$ whose boundary stays $o_{\delta\to 0}(1)$ from the boundaries of $\mathcal{R}$. We consider the Ising model in $\mathcal{R}^\delta$ with wired boundary conditions on the approximations $(b^\delta c^\delta)^\circ$ and $(d^\delta a^\delta)^\circ$ of horizontal segments and free boundary conditions the approximations $(a^\delta b^\delta)^\bullet$ and $(c^\delta d^\delta)^\bullet$ of the vertical segments. Then one has

$$\liminf_{\delta\to 0} \mathbb{E}^{\circ\bullet\circ\bullet}_{\mathcal{R}^\delta}[\sigma_{(b^\delta c^\delta)^\circ}\sigma_{(d^\delta a^\delta)^\circ}] \;\geq\; \text{cst} \;>\; 0,$$

where the constant cst > 0 only depends on κ and the ratio $|x_2-x_1|\cdot|y_2-y_1|^{-1}$.

Proof. The theorem is a consequence of monotonicity with respect to boundary conditions (e.g. [60, Section 4]) and the proof of analoguous crossing in extended shapes constructed in section 5.3. □

The next theorem follows from Theorem 5.1.1. Given $u \in \mathbb{C}$ and $d > 0$, denote the annulus

$$\square(u,d) \;:=\; ([\operatorname{Re} u - 3d, \operatorname{Re} u + 3d] \times [\operatorname{Im} u - 3d, \operatorname{Im} u + 3d]) \\ \smallsetminus ((\operatorname{Re} u - d, \operatorname{Re} u + d) \times (\operatorname{Im} u - d, \operatorname{Im} u + d))$$

and let $\mathbb{P}^{\text{free}}_{\square^\delta(u,d)}$ be the probability measure in the random cluster (or Fortuin-Kasteleyn) representation of the Ising model with free boundary conditions on *both* the outer and the inner boundaries of $\square^\delta(u,d)$. Then we have the following theorem :

Theorem 5.1.2. There exists a constant $p_0 > 0$ only depending on κ such that for all $u \in \mathbb{C}$, $d > 0$, and all s-embeddings $\mathcal{S}^\delta$ satisfying $\textsc{Lip}(\kappa,\delta)$ and $\textsc{Lenght-Exp-Fat}(\delta)$ and covering the disc $B(u,5d)$, one has

$$\liminf_{\delta\to 0} \mathbb{P}^{\text{free}}_{\square^\delta(u,d)}\big[\,\text{there exists a wired circuit in } \square^\delta(u,d)\,\big] \;\geq\; p_0.$$

A similar uniform estimate holds for the dual model.

Proof. Once Theorem 5.1.1 is derived, one can apply the strategy of [61, Proposition 2.10] recalled in detail in [33, Sec 5.6].) □

In the case of s-embeddings satisfying $\textsc{Unif}(\delta)$, both theorems hold not only at macroscopic distances but also starting at distances $d \geqslant L_0\delta$, for some L_0 only depending on constants in $\textsc{Unif}(\delta)$. One can also note that the same proof works at mesoscopic scales compared to δ (e.g. δ^α for $0 < \alpha < 1$), modifying accurately the hypotheses on the degeneracy of the grid. With the current given proofs, it is possible to weaken the assumption $\textsc{Lenght-Exp-Fat}(\delta)$, working on grids that satisfy $\textsc{Exp-Fat}(\delta)$ and requiring that $\textsc{Lenght-Exp-Fat}(\delta)$ only holds in some macroscopic (but arbitrarly small) regions of compacts of the embedding.

To prove Theorem 5.1.1, we use the *geometrical flexibility* of the s-embeddings setup in order to extend the discretization of a rectangle in $\mathcal{S}^\delta$ by periodic layers of kites, and paste those kites to pieces of the square lattice (see Fig 5.3.3 in section 5.3.1). Once this extension is done, the proof goes by contradiction. One first assumes that Theorem 5.1.1 doesn't hold and repeat the scheme introduced in [48, Section 6]. Namely, if the magnetization $\mathbb{E}^{\circ\bullet\circ\bullet}_{\mathcal{R}^\delta}[\sigma_{(b^\delta c^\delta)^\circ}\sigma_{(d^\delta a^\delta)^\circ}]$ vanishes when δ goes to 0, one can find a sequence of 4-points observables $(F^\delta)_{\delta>0}$, together with the associated function $(H^\delta)_{\delta>0}$ (see definition 5.2.5), converging respectively to f and h. In the boundary arcs attached to the square lattice pieces, one can prove (using directly the arguments of [48, Section 6]) that the continous function h inherits the Dirichlet boundary conditions from its discrete counterparts. In this square lattice region, simple estimates on the complex phase of the discrete functions F^δ near the boundary arc impose that their continuous limit f vanishes identically at the boundary (and thus in entire region tilled by square lattices). This

scenario is finally ruled out by using an additional analytic tool, namely the Stoïlov factorization of the primitive $I_{\mathbb{C}}$ of f, which imposes that f should be identically 0 everywhere.

Directions of generalization A first direction of generalization would concern extending the previous results only assuming $\text{EXP-FAT}(\delta)$. One way to procede could be based on a procedure that increases the lenghts of s-embeddings pictures would allow to use the same strategy as the one presented here. Another interesting line of research would be to extend the strategy of [64] to prove the so called 'Strong-RSW' property by boostraping Theorem 5.1.2 for $\text{UNIF}(\delta)$ grids. We are not able to handle such problem as for now, since a similar strategy requires a comparison between primal and dual one arm exponents in the half-plane, that we are not able to derive as for now and leave for further researches.

Acknowledgements. The author is grateful to Dmitry Chelkak for introducing him to this field, constant support as well as careful reading of earlier versions of this manuscript. The author is also greatly indebted to Sung-Chul Park and Mikhail Basok for crucial help in the continuous analysis as well as to Niklas Affoter Konstantin Izyurov, Francois Jacopin, Seginus Mowlavi, Mendes Oulamara and Yijun Wan for useful discussions and helpful remarks.

5.2 . Definitions and crash introduction to s-embeddings

We recall in the section the construction of s-embeddings given in [33, Section 3], as well as the construction of Kadanoff-Ceva correlators and the regularity theory of s-holomorphic functions. The notations we use in this paper follow *exactly* those of [33] and agree with those of [37, Section 3] and [34].

5.2.1 . Notation and Kadanoff–Ceva formalism

We fix G a planar graph (allowing multi-edges and vertices of degree two but forbidding loops and vertices of degree one) with the combinatorics of the plane or of the sphere, considered up to homeomorphisms preserving cyclic ordering of edges around each vertex. In the sphere case, we prescribe one of the faces of G and call it the *outer* face of G. We denote $G = G^\bullet$ the original graph whose vertices are denoted by $v^\bullet \in G^\bullet$ and G° its dual, whose vertices are denoted by $v^\circ \in G^\circ$. The faces of the bipartite graph $\Lambda(G) := G^\circ \cup G^\bullet$ (with natural incidence relation) are in bijection with edges of G. We also denote $\diamondsuit(G)$ the graph dual to $\Lambda(G)$, whose vertices are often denoted by $z \in \diamondsuit(G)$ and called quads. Finally, we denote by $\Upsilon(G)$ the medial graph of $\Lambda(G)$. The vertices of $\Upsilon(G)$ are in bijection with edges $(v^\bullet v^\circ)$ of $\Lambda(G)$. The vertices $c \in \Upsilon(G)$ are called corners of G. To make the formalism consistent, one needs to consider several *double covers* of $\Upsilon(G)$, see e.g. [129, Fig. 27] or [33, Fig 3.A] for relevant pictures. Denote by $\Upsilon^\times(G)$ the double cover that branches over *all* faces of $\Upsilon(G)$ (each $v^\bullet \in G^\bullet, v^\circ \in G^\circ, z \in \diamondsuit(G)$). When G is finite, this statement remains meaningful as $\#(G^\bullet)+\#(G^\circ)+\#(\diamondsuit(G))$

is even due to the Euler Theorem. Given $\varpi = \{v_1^\bullet, \dots, v_m^\bullet, v_1^\circ, \dots, v_n^\circ\} \subset \Lambda(G)$ where n, m are even, denote by $\Upsilon_{\varpi}^{\times}(G)$ the double cover of $\Upsilon(G)$ branching over all its faces *except* those ϖ, and by $\Upsilon_{\varpi}(G)$ the double cover of $\Upsilon(G)$ branching *only* over those ϖ. We call a *spinor* a function defined on one of the aforementioned double covers whose value at two different lifts of the same corner differ by a multiplicative factor -1.

In this paper, we consider the Ising model on *faces* of G, including the outer face in the disc case, i.e. the model assigns ± 1 random variables to vertices of G° with a partition function given by $(5.1.1)$. The domain walls representation [37, Section 1.2] (also called low-temperature expansion) assigns a spin configuration $\sigma : G^\circ \to \{\pm 1\}$ to a subset C of edges of G that separates spins of opposite signs ; this expansion is a 2-to-1 mapping from spin configurations onto the set $\mathcal{E}(G)$ of even subgraphs of G, depending on the value of the spin of the outer face.

Given $v_1^\circ, \dots, v_n^\circ \in G^\circ$ where n is even, fix a subgraph $\gamma^\circ = \gamma_{[v_1^\circ, \dots, v_n^\circ]} \subset G^\circ$ with odd degree at vertices of $v_1^\circ, \dots, v_n^\circ$ and even degree at all other vertices of G°. On can represent such configuration as a collection of paths on G° linking pairwise vertices of $v_1^\circ, \dots, v_n^\circ$. Denote

$$x_{[v_1^\circ, \dots, v_n^\circ]}(e) \ := \ (-1)^{e \cdot \gamma_{[v_1^\circ, \dots, v_n^\circ]}} x(e), \quad e \in E(G),$$

where $e \cdot \gamma = 0$ if e doesn't cross γ and $e \cdot \gamma = 1$ otherwise. One can see that

$$\mathbb{E}\big[\sigma_{v_1^\circ} \dots \sigma_{v_n^\circ}\big] \ = \ x_{[v_1^\circ, \dots, v_n^\circ]}(\mathcal{E}(G))/x(\mathcal{E}(G)), \tag{5.2.1}$$

where $x(\mathcal{E}(G)) := \sum_{c \in \mathcal{E}(G)} x(C)$, $x(C) := \prod_{e \in C} x(e)$, and similarly for $x_{[v_1^\circ, \dots, v_n^\circ]}$.

For m even and $v_1^\bullet, \dots, v_m^\bullet \in G^\bullet$, fix again subgraph $\gamma^\bullet = \gamma^{[v_1^\bullet, \dots, v_m^\bullet]} \subset G^\bullet$ with even degree at all vertices of $G^\bullet$ except those of $v_1^\bullet, \dots, v_m^\bullet$. Following the formalism of Kadanoff and Ceva[93], one changes the signs of the interaction constants $J_e \mapsto -J_e$ on edges $e \in \gamma^\bullet$. This inversion (which is equivalent to replace $x(e)$ by $x(e)^{-1}$ makes the model *anti-ferromagnetic* along those edges favoring locally configurations with disaligned spins, and is shorten by the notation $\mu_{v_1^\bullet} \dots \mu_{v_m^\bullet}$. More precisely, we introduce the random variable

$$\mu_{v_1^\bullet} \dots \mu_{v_m^\bullet} \ := \ \exp\big[-2\beta \textstyle\sum_{e \in \gamma^{[v_1^\bullet, \dots, v_m^\bullet]}} J_e \sigma_{v_-^\circ(e)} \sigma_{v_+^\circ(e)} \big],$$

the domain walls representation of σ shows that (e.g. [37, Propositon 1.3])

$$\mathbb{E}\big[\mu_{v_1^\bullet} \dots \mu_{v_m^\bullet}\big] \ = \ x(\mathcal{E}^{[v_1^\bullet, \dots, v_m^\bullet]}(G))/x(\mathcal{E}(G)), \tag{5.2.2}$$

where $\mathcal{E}^{[v_1^\bullet, \dots, v_m^\bullet]}$ denotes the set of subgraphs of G with even degrees at all vertices except at those of $v_1^\bullet, \dots, v_m^\bullet$ and odd degrees at the last mentioned. This again doesn't depend on the choice of $\gamma^\bullet$. A generalization of $(5.2.1)$ and $(5.2.2)$ reads as (e.g. [37, Propositon 3.3])

$$\mathbb{E}\big[\mu_{v_1^\bullet} \dots \mu_{v_m^\bullet} \sigma_{v_1^\circ} \dots \sigma_{v_n^\circ}\big] \ = \ x_{[v_1^\circ, \dots, v_n^\circ]}(\mathcal{E}^{[v_1^\bullet, \dots, v_m^\bullet]}(G))/x(\mathcal{E}(G)), \tag{5.2.3}$$

where $\mu_{v_1^\bullet} \dots \mu_{v_m^\bullet}$ are understood as above. The sign of this last expression in fact depends on the parity number of intersections between γ° and $\gamma^\bullet$. There is *no* canonical way to chose of that sign in $(5.2.3)$ staying on the Cartesian product $(G^\bullet)^{\times m} \times (G^\circ)^{\times n}$. However, one can first fix $\mathcal{S} : \Lambda(G) \to \mathbb{C}$ is an *arbitrarily* chosen embedding of G, and consider a natural double cover of this Cartesian product, whose branching structure is the one of the spinor $[\prod_{p=1}^m \prod_{q=1}^n (\mathcal{S}(v_p^\bullet) - \mathcal{S}(v_q^\circ))]^{1/2}$. As discussed in great details in [39, Section 2.2], the expectations of the form $(5.2.3)$ can be seen as *spinors* on the above described double cover of $(G^\bullet)^{\times m} \times (G^\circ)^{\times n}$. When treating mixed correlation of the type $(5.2.3)$, an extension of the usual Kramers-Wannier duality (again [37, Propositon 3.3]) implies that the roles played by the graphs $G^\bullet$ and G° are now equivalent.

One can also consider correlators with neighbouring disorders $v^\bullet(c) \in G^\bullet$ and spins $v^\circ(c) \in G^\circ$, separated by a corner c, denote

$$\chi_c := \mu_{v^\bullet(c)} \sigma_{v^\circ(c)}, \tag{5.2.4}$$

Using equation $(5.2.3)$, one can then define the Kadanoff–Ceva *fermionic observables* by

$$X_\varpi(c) := \mathbb{E}[\chi_c \mu_{v_1^\bullet} \dots \mu_{v_{m-1}^\bullet} \sigma_{v_1^\circ} \dots \sigma_{v_{n-1}^\circ}]. \tag{5.2.5}$$

The above remarks state that $X_\varpi(c)$ is a priori defined up to the sign but becomes well defined when passing to $\Upsilon_\varpi^\times(G)$. Around a quad $z = (v_0^\bullet, v_0^\circ, v_1^\bullet, v_1^\circ)$ whose vertices are listed in the counterclockwise order (see [33, Figure 3.A] for the notation), that Kadanoff–Ceva fermionic observables satisfy a local linear propagation equation, whose coefficients are determined by the Ising interaction parameters. This propagation equation appeared in the works of [56], [142] and [129, Section 4.3]) and reads as follows :

$$X(c_{pq}) = X(c_{p,1-q}) \cos\theta_z + X(c_{1-p,q}) \sin\theta_z, \tag{5.2.6}$$

where the corner $c_{pq} = (v_p^\bullet v_q^\circ)$ and the lifts of c_{pq}, $c_{p,1-q}$ and of $c_{1-p,q}$ to $\Upsilon_\varpi^\times(G)$ are neighbors. One can see that the solutions to $(5.2.6)$ are *spinors* on $\Upsilon_\varpi^\times(G)$.

We conclude this reminder on Kadanoff-Ceva correlators by recalling the definition of the spinor η_c that is a special solution to the propagation equation $(5.2.6)$ on isoradial grids. Given an embedding $\mathcal{S} : \Lambda(G) \to \mathbb{C}$ of $\Lambda(G)$ into the complex plane, denote

$$\eta_c := \varsigma \cdot \exp\big[-\tfrac{i}{2} \arg(\mathcal{S}(v^\bullet(c)) - \mathcal{S}(v^\circ(c)))\big], \qquad \varsigma := e^{i\frac{\pi}{4}}, \tag{5.2.7}$$

where the prefactor $\varsigma = e^{i\frac{\pi}{4}}$ is chosen to be consistent with [48, 33]. As explained previously, one can avoid the sign ambiguity in the definition $(5.2.7)$ by passing to the double cover $\Upsilon^\times(G)$, understanding the products $\eta_c X_\varpi(c) : \Upsilon_\varpi(G) \to \mathbb{C}$ as defined on the double cover $\Upsilon_\varpi(G)$ than only branches over ϖ. Below, we use the notation $(5.2.7)$ even when $\mathcal{S}$ is not isoradial.

5.2.2 . Definition of s-embeddings

We present now in a consise way the explicit embedding procedure first proposed by Chelkak [34, Section 6] and was developped in great details in [33]. We start by recalling the concrete definition of an s-embedding given in [33, Definition 2.1], based upon the Kadanoff-Ceva formalism recalled in section 5.2.1.

Definition 5.2.1. Let (G, x) be a weighted planar graph with the combinatorics of the plane and $\mathcal{X} : \Upsilon^\times(G) \to \mathbb{C}$ a solution to the propagation equation (5.2.6). We say that $\mathcal{S} = \mathcal{S}_\mathcal{X} : \Lambda(G) \to \mathbb{C}$ is an s-embedding of (G, x) associated to $\mathcal{X}$ if for each $c \in \Upsilon^\times(G)$, we have

$$\mathcal{S}(v^\bullet(c)) - \mathcal{S}(v^\circ(c)) = (\mathcal{X}(c))^2. \tag{5.2.8}$$

For $z \in \diamondsuit(G)$, denote by $\mathcal{S}^\diamond(z) \subset \mathbb{C}$ the quadrilateral whose vertices are $\mathcal{S}(v_0^\bullet(z))$, $\mathcal{S}(v_0^\circ(z))$, $\mathcal{S}(v_1^\bullet(z))$, $\mathcal{S}(v_1^\circ(z))$. The s-embedding $\mathcal{S}$ is said to be *proper* if the quadrilaterals $\mathcal{S}^\diamond(z) = (\mathcal{S}(v_0^\bullet(z))\mathcal{S}(v_0^\circ(z))\mathcal{S}(v_1^\bullet(z))\mathcal{S}(v_1^\circ(z)))$ do not overlap with each other, and non-degenerate if no quads $\mathcal{S}^\diamond(z)$ degenerates to a segment. In particular, the convexity of $\mathcal{S}^\diamond(z)$ is not required.

This definition extends to the set $\diamondsuit(G)$ by setting [33, eq (2.5)]

$$\begin{aligned} \mathcal{S}(v_p^\bullet(z)) - \mathcal{S}(z) &:= \mathcal{X}(c_{p0})\mathcal{X}(c_{p1})\cos\theta_z, \\ \mathcal{S}(v_q^\circ(z)) - \mathcal{S}(z) &:= -\mathcal{X}(c_{0q})\mathcal{X}(c_{1q})\sin\theta_z, \end{aligned} \tag{5.2.9}$$

where c_{p0} and c_{p1} (respectively, c_{0q} and c_{1q}) are neighbors on $\Upsilon^\times(G)$. The propagation equation (5.2.6) implies directly the consistency of both definitions (5.2.8) and (5.2.9). The second object of crucial relevance in the s-embeddings framework is the so called origami map, whose definition [33, Definition 2.2] is recalled below (see also [103, 45]).

Definition 5.2.2. Given $\mathcal{S} = \mathcal{S}_\mathcal{X}$, one can construct the *origami* function $\mathcal{Q} = \mathcal{Q}_\mathcal{X} : \Lambda(G) \to \mathbb{R}$, up to a global additive constant by declaring its increments to be

$$\mathcal{Q}(v^\bullet(c)) - \mathcal{Q}(v^\circ(c)) \;:=\; |\mathcal{X}(c)|^2 \;=\; |\mathcal{S}(v^\bullet(c)) - \mathcal{S}(v^\circ(c))|\,. \tag{5.2.10}$$

Once again, the propagation equation (5.2.6) implies directly the consistency of the definition (5.2.2). In words, this implies that *alternate sum of edge-lenghts around a quad vanishes*, which means for the geometrical picture that $\mathcal{S}^\diamond(z)$ is *a tangential quadrilateral to a circle* centered at $\mathcal{S}(z)$. We denote by r_z the radius of the circle, which can be recovered from χ, using e.g. [33, eq (2.7)]. If one denotes φ_{vz} the half-angle of the quad $\mathcal{S}^\diamond(z)$ at $\mathcal{S}(v)$, the Ising weight θ_z (in the parametretrization (5.1.2)) can be recovered from $\mathcal{S}$ using the formula [33, eq (2.8)]

$$\tan\theta_z \;=\; \left(\frac{\sin\varphi_{v_0^\bullet z}\sin\varphi_{v_1^\bullet z}}{\sin\varphi_{v_0^\circ z}\sin\varphi_{v_1^\circ z}}\right)^{1/2}. \tag{5.2.11}$$

As explained in [33, Section 2.3] (see also [103, Section 7]), one can see that if $\mathcal{S}$ is proper and non-degenerate, the map $\mathcal{S} : \Lambda(G) \cup \diamondsuit(G) \to \mathbb{C}$ as a *t-embedding* $\mathcal{T}$ and $\eta_{c^\bullet} = \eta_{c^\circ} := \overline{\varsigma}\eta_c$ as an origami square root (see [45, Definition 2.4]) of $\mathcal{T}$. This identification allows (e.g. [45, Appendix]) to extend $\mathcal{Q}$ in a piece-wise (and complex valued inside faces) linear way to the entire plane, and not only on edges of $\Lambda(G)$.

5.2.3 . s-holomorphic functions and associated functions H_F and $I_{\mathbb{C}}$

We recall here the notion of *s-holomorphic functions*, introduced first for the critical square grid by Smirnov [160, Defition 3.1] and generalized in the isoradial context by Chelkak and Smirnov in [48, Definition 3.1], where its name was coined. Under the briefly recalled link between s/t-embeddings, the s-holomorphic functions are special cases of *t-holomorphic* functions introduced in the dimers context in [45, Definition 3.2]. We recall now the definition general definition on s-embeddings, given in [33, Definition 2.4].

Definition 5.2.3. A function F defined on a subset of $\diamondsuit(G)$ is called s-holomorphic if

$$\Pr[F(z)\,;\eta_c\mathbb{R}] \;=\; \Pr[F(z')\,;\eta_c\mathbb{R}] \tag{5.2.12}$$

for each pair of quads $z, z' \in \diamondsuit(G)$ adjacent to the same edge $(v^\circ(c)v^\bullet(c))$ in $\mathcal{S}$.

The next proposition generalizes beyond the isoradial setup (e.g. [48, Lemma 3.4]) the link between real valued solutions to the propagation equation (5.2.6) and s-holomorphic functions. This link was already presented in [33, Proposition 2.5] and in [45, Appendix].

Proposition 5.2.4. Let $\mathcal{S} = \mathcal{S}_{\mathcal{X}}$ be a proper s-embedding and F an s-holomorphic on a subset of $\diamondsuit(G)$. Then, the spinor X defined at corners $c \in \Upsilon^\times(G)$ belonging to the face $z \in \diamondsuit(G)$ by

$$\begin{aligned} X(c) \;&:=\; |\mathcal{S}(v^\bullet(c)) - \mathcal{S}(v^\circ(c))|^{\frac{1}{2}} \cdot \mathrm{Re}[\overline{\eta}_c F(z)] \\ &=\; \mathrm{Re}[\overline{\varsigma}\mathcal{X}(c)\cdot F(z)] \;=\; \overline{\varsigma}\mathcal{X}(c)\cdot \Pr[F(z)\,;\eta_c\mathbb{R}] \end{aligned} \tag{5.2.13}$$

satisfies the propagation equation (5.2.6) around z.

Conversely for $X : \Upsilon^\times(G) \to \mathbb{R}$ a unique real valued solution to (5.2.6), there exists a s-holomorphic function F such that (5.2.13) is fulfilled.

When F and X are linked by (5.2.13), it is possible to reconstruct the value of F at $z \in \diamondsuit$ from the values of X at any pair of corners $c_{pq}(z) \in \Upsilon^\times(G)$, e.g. [33, Corollary 2.6]

$$F(z) \;=\; -i\varsigma \cdot \frac{\overline{\mathcal{X}(c_{01}(z))}\, X(c_{10}(z)) - \overline{\mathcal{X}(c_{10}(z))}\, X(c_{01}(z))}{\mathrm{Im}[\,\overline{\mathcal{X}(c_{01}(z))}\,\mathcal{X}(c_{10}(z))}, \tag{5.2.14}$$

.

To study the regularity of s-holomorphic functions as well as the behavior of their scaling limit, one uses their 'primitive' and a generalization of the 'primitive' of the imaginary part of their square. The former is heavily studied in [45, Proposition 6.15] and will is useful to derive local regularity theory for discrete functions as well as the local equation satisfied by subsequential limits in continuum, while the latter was introduced by Smirnov in [160] on the critical square grid and has since been interpreted in several different contexts to identify the scaling limit of fermionic observables. We start with the primitive $I_{\mathbb{C}}$ of an s-holomorphic function. In [33, Section 2.5 of], s-holomorphic functions are described as gradients of harmonic functions on the associated S-graphs, specializing in the Ising context the technology developed in [45, Section 4.2] for t-holomorphic functions. Given an s-holomorphic function F on $\diamondsuit(G)$, one can define *in the entire plane* (up to a global additive constant) [33, Section 2.3]

$$I_{\mathbb{C}}[F] := \int (\overline{\varsigma} F d\mathcal{S} + \varsigma \overline{F} d\mathcal{Q}) \tag{5.2.15}$$

As for the primitive of the square H, we start by recalling first its *combinatorial* definition (i.e. which doesn't require any particular embedding into the plane) for spinors on $\Upsilon^{\times}(G)$ satisfying (5.2.6). Afterwards, we precise its analytic interpretation in the context of s-embeddings. This definition which is a generalisation of the original work of Smirnov can be found in the following form in [33, Definition 2.8].

Definition 5.2.5. Given X a spinor on $\Upsilon^{\times}(G)$ satisfying (5.2.6), one defines the function H_X up to a global additive constant on $\Lambda(G) \cup \diamondsuit(G)$ by setting

$$\begin{array}{rcll} H_X(v_p^{\bullet}(z)) - H_X(z) & := & X(c_{p0}(z))X(c_{p1}(z))\cos\theta_z, & p = 0,1, \\ H_X(v_q^{\circ}(z)) - H_X(z) & := & -X(c_{0q}(z))X(c_{1q}(z))\sin\theta_z, & q = 0,1, \\ H_X(v_p^{\bullet}(z)) - H_X(v_q^{\circ}(z)) & := & (X(c_{pq}(z)))^2, & \end{array} \tag{5.2.16}$$

similarly to (5.2.8) and (5.2.9).

The consistency of the above definition follows from once again from the propagation equation (5.2.6). Passing to an s-embedding $\mathcal{S}$ of (G, x), one can use the correspondence between X and F recalled in Proposition 5.2.4 to interpret H_X via an s-holomorphic function F. More precisely, it is possible to define [33, eq (2.17)]

$$H_F := \int \tfrac{1}{2}\operatorname{Re}(\overline{\varsigma}^2 F^2 d\mathcal{S} + |F|^2 d\mathcal{Q}) = \int \tfrac{1}{2}(\operatorname{Im}(F^2 d\mathcal{S}) + \operatorname{Re}(|F|^2 d\mathcal{Q})), \tag{5.2.17}$$

on $\Lambda(G) \cup \diamondsuit(G)$. The function H_F extends linearly to a piece-wise affine function on each faces of the t-embedding $\mathcal{T} = \mathcal{S}$ (but not on each face of $\diamondsuit(G)$ as each

face of $\mathcal{T}$ has its own origami square root $d\mathcal{Q}$), at least if one doesen't handle of G (see [45, Proposition 3.10]). The next lemma links to each other definitions (5.2.16) and (5.2.17) as shown in [33, Lemma 2.9].

Lemma 5.2.6. Let F defined $\diamondsuit(G)$ and X defined on $\Upsilon^\times(G)$ be related by the identity (5.2.13). Then, the functions H_F and H_X coincide up to a global additive constant.

If $\mathcal{S}$ is an isoradial grid, the origami map $\mathcal{Q}$ is constant on both $G^\bullet$ and G°, thus H_F is the primitive of $\frac{1}{2}\,\mathrm{Im}[F^2 d\mathcal{S}]$, recovering the original definition given in [48, Section 3.3]. We now recall the comparison principle for functions $H_F = H_X$ associated with s-holomorphic functions. This statement is due to Park and can be found in [33, Proposition 2.11]. In particular, when one of the observables in the following proposition is identically 0, this proposition becomes a *maximum principle*.

Proposition 5.2.7. Let spinors $X, Y : \Upsilon^\times(G) \to \mathbb{R}$ both satisfy the propagation equation (5.2.6) and the associated functions $H_X, H_Y : \Lambda(G) \cup \diamondsuit(G) \to \mathbb{R}$ be defined via (5.2.16). Then, the difference $H_X - H_Y$ cannot have an extremum at an interior vertex of its domain of definition.

In particular if H_X is bounded at the boundary of a domain (which is trivially the case for the observables defined in section 5.3.2), then $H_X = H_F$ is bounded everywhere in the domain.

5.2.4 . Regularity theory for s-holomorphic functions

One of the goals of this subsection is to recall in a concise way the regularity theory of s-holomorphic functions, which is developed in [33, Sect 2.6], adapting to the Ising context results from [45, Section 6]. We start by recalling that this regularity theory requires adding some (mild) geometrical constrains on potential local degeneracies of the embedding. The highest level of degeneracies authorized up to now in the s/t-embeddings setups so that one can still extract sub-sequential limits is made via the assumption Exp-Fat(δ) introduced [45, Assumption 1.2]. In this article, we always assume that Lip(κ,δ) and Exp-Fat(δ) hold (recall that they hold with a huge margin under Unif(δ)). In that case, an s-holomorphic function F satisfies a standard Harnack-type estimate that controls $|F|^2$ via the oscillations of H_F (see [33, Corrolary 2.20] for the original proof).

Corollary 5.2.8. Let $\kappa < 1$ and a sequence of s-embeddings $\mathcal{S}^\delta$ satisfying Lip(κ,δ) and Exp-Fat(δ) in a disc $U = B(u, r)$. Assume that F^δ is an s-holomorphic function on $\mathcal{S}^\delta$ and that $\max_{v:\mathcal{S}(v)\in U} |H_{F^\delta}(v)| \leq M$ for all δ. Then, the following uniform (as $\delta \to 0$) estimate holds :

$$|F^\delta(z)|^2 = O(r^{-1}M) \quad \text{if} \quad \mathcal{S}^\delta(z) \in B(u, \tfrac{1}{2}r). \tag{5.2.18}$$

In particular, the functions H_{F^δ} are uniformly Lipschitz on compact subsets of U.

Under the assumptions of Corollary 5.2.8, [33, Remark 2.11] also ensures that the functions F^δ, form a precompact family in the topology of the uniform convergence on compacts of $B(u,r)$ as $\delta \to 0$. Indeed, those functions are uniformly bounded and β-Hölder (see [33, Theorem 2.17]) on scales above $\mathrm{cst}(\kappa)\cdot\delta$.

5.2.5 . Subsequential limits of s-holomorphic functions

We discuss now the behavior of subsequential limits of s-holomorphic functions, under the general hypothesis $\mathrm{LIP}(\kappa,\delta)$, repeating a discussion already made by Chelkak in [33, Section 2.7]. In what follows, we work with proper s-embeddings $\mathcal{S}^\delta$ all satisfying the assumption $\mathrm{LIP}(\kappa,\delta)$ as $\delta \to 0$, such that their respective images cover a given ball $U = B(u,r) \subset \mathbb{C}$. As the functions $\mathcal{Q}^\delta$ all are κ-lipchitz above scale $\asymp \delta$ and defined up to an additive constant, there exist a sub-sequence $\delta_k \to 0$ and a κ-Lipchitz function $\vartheta : U \to \mathbb{R}$ such that uniformly on compacts of U,

$$\mathcal{Q}^{\delta_k} \circ (\mathcal{S}^{\delta_k})^{-1} \to \vartheta. \tag{5.2.19}$$

Assuming now we are in the setup of Corollary 5.2.8 and that $(5.2.19)$, consider let $f : U \to \mathbb{C}$ be a subsequential limit of s-holomorphic functions F^δ on $\mathcal{S}^\delta$. Then following [33, Proposition 2.21] and setting $\varsigma = e^{i\frac{\pi}{4}}$ as in $(5.2.7)$, the differential form $\frac{1}{2}(\overline{\varsigma} f dz + \varsigma \overline{f} d\vartheta)$ is *closed*. This comes as a natural counterpart of the definition of the primitive $I_{\mathbb{C}}$ in $(5.2.15)$. With a consistent choice of additive constants, the associated functions H_{F^δ} converge uniformly on compact subsets of U to $h := \frac{1}{2}\int(\mathrm{Im}(f^2 dz) + |f|^2 d\vartheta)$.

The previous condition on closed form is *not* easily tractable and hard to interpret in termps of local relations satisfied by f. In [33, Sec 2.7], Chelkak provided a *nicer* description when passing to the conformal parametrization of the an appropriate surface in the Minkowski space $\mathbb{R}^{2,1}$. The author is deeply indebted to Dmitry Chelkak and Mikhail Basok for explanations that lead to the following paragraph, most of it being already present in [33, Sec 2.7].

On first recalls that the function ϑ is κ-Lipschitz, thus differentiable almost everywhere. Chelkak then considers [33, eq (2.26)] an orientation-preserving *conformal parametrization* of the space-like surface $(z,\vartheta(z))_{z\in U}$ equipped with a positive metric coming from the ambient Minkowski space

$$\mathbb{D} \ni \zeta \;\mapsto\; (z,\vartheta) \in U \times \mathbb{R} \;\subset \mathbb{C}\times\mathbb{R} \;\cong \mathbb{R}^{2+1} \tag{5.2.20}$$

As noted in [33, below (2.26)] when ϑ is a smooth function, the angles (measured in $\mathbb{R}^{2,1}$) of infinitesimal increments are preserved by mapping $(5.2.20)$ if and only *everywhere* in $\mathbb{D}$ one has [33, eq (2.27)]

$$z_\zeta \overline{z}_\zeta \;=\; (\vartheta_\zeta)^2 \quad \text{and} \quad |z_\zeta| > |\vartheta_\zeta| \geq |\overline{z}_\zeta|\,, \tag{5.2.21}$$

where $z_\zeta := \partial z/\partial\zeta$ (similarly, $\overline{z}_\zeta$ and ϑ_ζ) stands for the Wirtinger derivative.

If one wants to generalize this discussion without any smoothness assumption on ϑ, one can note that conformal parametrization of $(5.2.21)$ can be equivalently

rewritten as a Beltrami equation for the *quasi-conformal* map $z \mapsto \zeta(z)$:

$$\zeta_{\bar{z}} = \mu(z)\zeta_z, \tag{5.2.22}$$

(or in an equivalent way to $z_\zeta = -\overline{\mu(\zeta)}z_\zeta$), with the Beltrami coefficient μ fixed by the equation

$$\frac{\bar{\mu}}{1+|\mu|^2} = -\frac{\vartheta_z^2}{1-2|\vartheta_z|^2}, \tag{5.2.23}$$

This equivalence can be seen by plugging the identity $\vartheta_\zeta = \vartheta_z z_\zeta + \vartheta_{\bar{z}}\bar{z}_\zeta$ (which uses the fact that ϑ is real valued) into $(5.2.21)$, which rewrites as $-\overline{\mu} = (\vartheta_z - \overline{\mu}\vartheta_{\bar{z}})^2$. Since $\vartheta_{\bar{z}} = \overline{\vartheta_z}$, this gives $(5.2.23)$. Moreover the function $z \mapsto \vartheta(z)$ is κ-Lipchitz for some $\kappa < 1$, which proves that $|\vartheta_z| \leqslant \frac{\kappa}{2}$ and ensures that $|\mu| \leqslant \mathsf{cst}(\kappa) < 1$. For a general κ-Lipchitz function, one can now proceed as follows

— Compute the Beltrami coefficient $\mu \in L^\infty$ from the equation $(5.2.23)$ *almost everywhere* as ϑ is differentiable almost everywhere for the Lebesgue measure.

— Use the Ahlors-Bers's measurable Riemann mapping theorem [3, Chapter 5] to solve the Beltrami equation $(5.2.22)$, constructing a quasi-conformal uniformization $\zeta : U \mapsto \mathbb{D}$ such that $(5.2.21)$ holds almost everywhere in $\mathbb{D}$.

In the $\zeta \in \mathbb{D}$ parametrization, one can make a convenient change of variables as in [33, eq. (2.28)], by defining the functions

$$\varphi(\zeta) := \ \bar{\varsigma} f(z(\zeta)) \cdot (z_\zeta)^{1/2} + \varsigma \overline{f(z(\zeta))} \cdot (\bar{z}_\zeta)^{1/2} \tag{5.2.24}$$

Under this change of variables, $I_{\mathbb{C}}[f] := \int \bar{\varsigma} f(z(\zeta)) f(z) dz + \varsigma \overline{f(z)} d\vartheta$ reads as

$$g(\zeta) = \int \bar{\varsigma}\varphi(\zeta) \cdot z_\zeta^{\frac{1}{2}} d\zeta + \varsigma \overline{\varphi(\zeta)} \cdot (z_{\bar{\zeta}})^{\frac{1}{2}} d\bar{\zeta}. \tag{5.2.25}$$

Computing their Wirtinger derivatives and using the almost everywhere relation $(5.2.21)$, one sees directly that g satisfies a *conjugate* Beltrami equation

$$g_{\overline{\zeta}} = \overline{\nu} \cdot \overline{g_\zeta} \qquad \text{with} \qquad \nu := -\frac{(\bar{z}_\zeta)^{\frac{1}{2}}}{(z_\zeta)^{\frac{1}{2}}} = -\frac{\vartheta_\zeta}{z_\zeta} \tag{5.2.26}$$

where the Beltrami coefficent ν is bounded away from 1 as one can see from $\vartheta_\zeta = \vartheta_z z_\zeta + \vartheta_{\bar{z}}\bar{z}_\zeta$ that $|\nu| < 2|\vartheta_z| \leqslant \kappa < 1$. Moreover g is defined as a primitive of a continuous differential form and thus inherits some a priori regularity from it. One can, as long as f is locally bounded that

— The function g has bounded distortion (see e.g. [3, eq.(2.27)]), smaller than $\frac{1+\kappa}{1-\kappa}$.

— The function g also belongs to $L^{1,2}_{loc}$. Indeed one has the formula $g_\zeta = \overline{\varsigma} f(z(\zeta)) z_\zeta + \varsigma \bar{f}(z(\zeta)) \vartheta_\zeta$ and $f(z(\zeta))$ is locally bounded. Moreover the Jacobian at z satisfies $\mathrm{Jac}(z) := |z_\zeta|^2 - |z_{\bar{\zeta}}|^2 \geqslant (1-\kappa^2)|z_\zeta|^2$, while $(5.2.21)$ ensures that $|z_{\bar{\zeta}}| \leqslant \kappa |z_\zeta|$ in the ζ parametrization. Computing area integrals of $\int |z_\zeta|^2 d^2\zeta \leqslant (1-\kappa^2)^{-1} \int \mathrm{Jac}(z) d^2 z = (1-\kappa^2)^{-1} \mathrm{Area}(\Omega) < \infty$ alows to conclude.

Combining the two previous observations, one can apply the Stoïlov factorization stated in Corollary $5.3.3$ of [3] which allows to write the factorization $g = \underline{g} \circ p$ with $p : \Omega \to \Omega$ a $\beta(\kappa)$-Hölder homeomorphism and $\underline{g}$ an holomorphic function. In particular, g cannot be constant in an open set except if it is constant everywhere.

5.3 . A proof of crossing estimates under the hypothesis Unif(δ)

In this section, we give a complete proof of Theorem 5.1.1 under the hypothesis $\textsc{Unif}(\delta)$. This proof contains already all conceptual ingredients required, and a generalisation to wilder local geometries (that will be carried out in the following sections) only requires being more carefull and efficient in the extension of a piece of an s-embedding. We start this section by describing an explicit procedure to weld a piece of a given s-embedding $\mathcal{S}^\delta$ to a piece of the square lattice.

5.3.1 . Extension of a topological rectangle with a piece of the square lattice

One starts with $(\mathcal{S}^\delta)_{\delta>0}$, a sequence of s-embeddings, each satisfying the hypothesis $\textsc{Unif}(\delta)$ for the *same* parameters θ_0, r_0. It is clear that up to increasing the value of δ by a factor that only depends on θ_0, r_0, there exist $\kappa < 1$ such that each grids satisfies $\textsc{Lip}(\kappa,\delta)$. We aim to extend the approximation of a rectangle of a fixed aspect ratio in $\mathcal{S}^\delta$ such that :

— All the tangential quadrilaterals of the extended picture have a radius $r_z \geqslant \delta^{200}$.

— The extended picture contains two macroscopic pieces of the square grid lattice whose faces all have a radius $r_z \geqslant \delta^{200}$.

We limit ourselves to the extension of a rectangle $\mathcal{R}_\delta$ that approximates up to $o_{\delta\to 0}(1)$ the rectangle $[-\frac{1}{2}, \frac{1}{2}] \times [-3, 3]$ (the rectangles with other aspect ratios can be treated similarly), chosen with boundary quads in the left and right side all having a radius $r_z \geqslant \delta^2$. . Making such a choice of vertical boundaries is trivial under the hypothesis $\textsc{Unif}(\delta)$ since all faces $z \in \diamondsuit(G)$ of the original picture in $\mathcal{S}^\delta$ have a radius $r_z \geqslant \mathrm{cst} \cdot \delta$, for some constant cst only depending on constants in $\textsc{Unif}(\delta)$. We also denote $\mathcal{R}'_\delta$ the approximation of $[-\frac{1}{2}, \frac{1}{2}] \times [-5, 5]$, assuming its discrete vertical boundary in $\mathcal{S}^\delta$ contains the respective approximations of the vertical boundaries of $\mathcal{R}_\delta$. The main output of this section is the next proposition.

Proposition 5.3.1. *Given $\mathcal{R}_\delta$ in $\mathcal{S}^\delta$, and provided δ is small enough, one construct (see Figure 5.3.3) a finite piece of a proper s-embedding $\mathcal{R}_\delta^{\mathbf{ext}}$, approximating up $o_{\delta\to 0}(1)$ the domain $([\frac{-1}{2};\frac{1}{2}]\times[-5;5])\cup([\frac{1}{2};\frac{3}{4}]\times[-4;-5])\cup([-\frac{3}{4};\frac{1}{2}]\times[4;5])$, such that :*

- *All quads of $\mathcal{R}_\delta^{\mathbf{ext}}$ have a radius r_z larger than δ^{200}.*
- *One has $\mathcal{R}_\delta\subseteq\mathcal{R}_\delta^{\mathbf{ext}}$ and the left and right 'vertical' boundaries of $\mathcal{R}_\delta$ belong the boundary of $\mathcal{R}_\delta^{\mathbf{ext}}$.*
- *There exists a horizontal line $y_0^\delta=-\frac{7}{2}+o_{\delta\to 0}(1)$ such that below this line, the tangential quadrilateral of $\mathcal{R}_\delta^{\mathbf{ext}}$ are kites with horizontal symmetry axis, all having a radius r_z larger than δ^{200}.*
- *There exists a horizontal line $y_1^\delta=\frac{7}{2}+o_{\delta\to 0}(1)$ such that above this line, the tangential quadrilateral of $\mathcal{R}_\delta^{\mathbf{ext}}$ are kites with horizontal symmetry axis, all having a radius r_z larger than δ^{200}.*
- *$\mathcal{R}_\delta^{\mathbf{ext}}$ contains two pieces of a square lattice with an associated r_z larger than δ^{200} in the regions $[\frac{1}{2};\frac{3}{4}]\times[-5;-\frac{9}{2}]$ and $[-\frac{3}{4};\frac{1}{2}]\times[\frac{9}{2};5]$.*
- *$\mathcal{R}_\delta^{\mathbf{ext}}$ satisfies $\textsc{Lip}(\kappa,5\delta)$.*

The proof is done by an explicit construction combining several steps and simple geometrical features on tangential quadrilaterals. From a geometrical standpoint, extending a finite piece of an s-embedding, while remaining in the s-embedding setup (i.e. requiering that all faces $\Lambda(G)$ are tangential quadrilaterals) is *not* a trivial question. Still, one can remark that if all boundary vertices are aligned along a straight line, there exist a rather simple extension procedure using periodic layers of kites. Before starting the precise descrpiton of the construction, we recall simple geometrical features on tangential quadrilaterals in the following sequence of claims, that should be read with the associated pictures of Figure 5.3.1.

Let $z=(v_0^\circ v_0^\bullet v_1^\circ v_1^\bullet)$ be a tangential quadrilateral centered at $\hat{z}$ with an inner circle of radius r_z. Then one has :

(A) The area of the tangential quadrilateral is a product of the radius of the inner circle r_z by the half-perimeter of z. In the rest of this article, we bound from below on multiple occasions the radius of a newly constructed tangential quadrilateral. This is done by bounding from *below* the area of z and from *above* its perimeter.

(B) Let $\varphi_{v,z}$ be one of the half-angles of z at v (i.e. the angle formed by an edge containing v and the bisector that links v to $\hat{z}$). Then there exists a universal constant C such that $\varphi_{v,z}\geqslant C\tan\varphi_{v,z}\geqslant C\frac{r_z}{\delta}$. The first inequality is true when $\varphi_{v,z}$ goes to 0 and is not used for larger values of $\varphi_{v,z}$. The second inequality is a direct computation using the straight triangle formed by $v,\hat{z}$ and the orthogonal projection of $\hat{z}$ on one of the edges containing v.

(C) Fix an edge $e=[v^\circ v^\bullet]\in z$ of a tangential quadrilateral attached to vertices v° and $v^\bullet$ whose respective angles are $\varphi_{v^\circ,z}$ and $\varphi_{v^\bullet,z}$. The length of the edge e equals $r_z(\cot(\varphi_{v^\circ,z})+\cot(\varphi_{v^\bullet,z}))\geqslant r_z\sin(\varphi_{v^\circ,z}+\varphi_{v^\bullet,z})$.

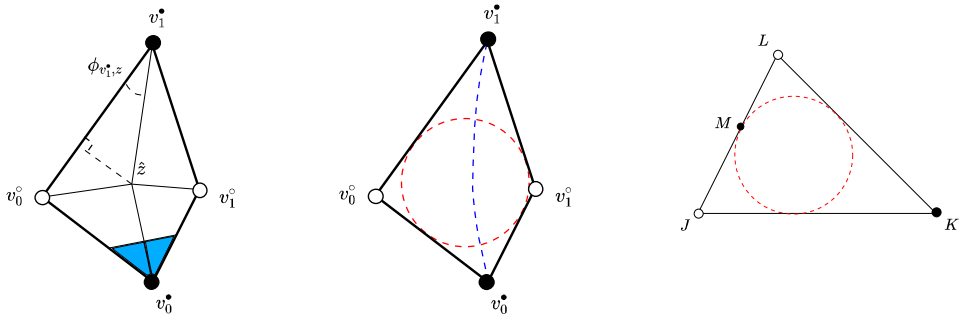

FIGURE 5.3.1 – (Left) Notations for the tangential quadrilateral with center $\hat{z}$. The four bisectors intersect at the center $\hat{z}$ of the tangential quadrilateral. (Middle) Hyperbola $\mathcal{C}$ drawn in blue denoting in claim (D) the set of points such that $(v_0^\circ v_0^\bullet v_1^\circ v^\bullet)$ is a tangential quadrilateral. (Right) Transformation described in (E) of a triangle into a tangential quadrilateral by adding as a vertex to tangent point of $\mathfrak{C}$ and one of its sides.

(D) Fix three vertices $v_{0,1}^\circ$ and $v_0^\bullet$. The set $\mathcal{C}$ of points $v^\bullet$ such that $(v_0^\circ v_0^\bullet v_1^\circ v^\bullet)$ is a tangential quadrilateral is an *hyperbola* (potentially degenerated to a line) passing through $v_0^\bullet$ and $v_1^\bullet$. Indeed, denoting (x, y) the coordinates of $v^\bullet$ and writing the equality $|v^\bullet - v_0^\circ| - |v^\bullet - v_1^\circ| = |v_0^\bullet - v_0^\circ| - |v_0^\bullet - v_1^\circ|$, one recovers the algebraic equation of a conical. This conical is clearly unbounded and admits the bisector of the angle $(v_0^\circ v_0^\bullet v_1^\circ)$ as an asymptote when $v^\bullet$ goes to infinity.

(E) Let $T = (JKL)$ be a triangle (whose vertices are labeled in the counter-clockwise order) and consider $\mathfrak{C}$ the circle of radius r tangential to its three sides. Consider e.g. M the point at the intersection of $\mathfrak{C}$ and the segment $[JL]$. Then one can view the quadrilateral $(JKLM)$(still labeling vertices in the counter-clockwise order) as a tangential quadrilateral, whose tangential circle is $\mathfrak{C}$.

We explain now how to *slice* horizontally a piece of an s-embedding to extend it afterwards by periodic layers of kites. We start by giving a very concrete method to replace the interesection of a tangential quadrilateral and a closed half-plane by several tangential quadrilaterals whose bottom boundary vertices are *all aligned along the border of that half-plane*.

Definition 5.3.1. Let $z \in \diamondsuit(G)$ a tangential quadrilateral and y a horizontal level intersecting z. We say that $Z \subseteq \overline{z}$ is a horizontal alignment of z at level y if

— Z is the union of at most 3 tangential quadrilaterals.

— $Z = \overline{z} \cap (y + \overline{\mathbb{H}})$ i.e. Z is the intersection of z and the close half plane above level y.

The next lemma ensures that it is possible to perfom a horizontal alignment of a given tangential quadrilateral.

Lemma 5.3.2. *Let z a tangential quadrilateral and y a vertical level (represented by the line passing by) that intersects z at a level that doesen't contain its highest vertex. Then there exist an horizontal alignement of z at level y.*

Proof. The proof is made by an explicit construction using geometrical claims recalled above about tangential quadrilaterals. We make a dichotomy depending on the number of vertices of z below level y.

(1) There is only one vertex of z below level y

Up to swapping colors, one can assume that the vertex below level y is $v_0^\bullet$. Let $\mathcal{C}$ the be hyperbola (see claim (D)) of points $v^\bullet$ such that $(v_0^\circ v_1^\bullet v_1^\circ v^\bullet)$ is a tangential quadrilateral. This hyperbola is a continuous curve *inside* z containing the points $v_0^\bullet$ and $v_1^\bullet$. A continuity argument ensures the existence of a point $\tilde{v}^\bullet$ with $\mathrm{Im}[\tilde{v}^\bullet] = y$ such that $(v_0^\circ v_1^\bullet v_1^\circ \tilde{v}^\bullet)$ is a tangential quadrilateral. As a consequence (e.g. checking the alternate sum of edge-lenghts), the quadrilateral $(v_0^\circ v_0^\bullet v_1^\circ \tilde{v}^\bullet)$ is also tangential. Set now the points $\tilde{v}_0^\bullet$ and $\tilde{v}_1^\bullet$ to be respectively the intersections of the segments $[v_0^\circ v_0^\bullet]$ and $[v_0^\circ v_1^\bullet]$ with the level y. Using the claim (E), one can transform the triangles $(\tilde{v}^\bullet v_0^\circ \tilde{v}_0^\bullet)$ and $(\tilde{v}^\bullet v_1^\circ \tilde{v}_1^\bullet)$ as tangential quadrilaterals by adding repectively the vertices $\tilde{v}_{0,y}^\circ$ and $\tilde{v}_{1,y}^\circ$ to the segments $[\tilde{v}_0^\bullet \tilde{v}^\bullet]$ and $[\tilde{v}_1^\bullet \tilde{v}^\bullet]$.

(2) There are two vertices of z below level y

We make a dichotomy of two subcases that appear here.

(a) The two vertices of different colors $v_0^\bullet$ and v_0° that are below level y. Consider first $\mathcal{C}_1$ the hyperbola of points $v^\bullet$ such that $(v_0^\circ v_0^\bullet v_1^\circ v^\bullet)$ is a tangential quadrilateral linking continuously $v_0^\bullet$ to $v_1^\bullet$ *inside* z. There exist again of a point $\tilde{v}^\bullet$, with $\mathrm{Im}[\tilde{v}^\bullet] = y$, such that $(v_0^\circ v_0^\bullet v_1^\circ \tilde{v}^\bullet)$ is a tangential quadrilateral. As previously, the quadrilateral $(v_0^\circ v_1^\bullet v_1^\circ \tilde{v}^\bullet)$ is tangential. One then reapply the same strategy, this time to the tangential quadrilateral $(v_0^\circ v_1^\bullet v_1^\circ \tilde{v}^\bullet)$ to construct *inside* $(v_0^\circ v_0^\bullet v_1^\circ \tilde{v}^\bullet)$ a tangential quadrilateral $(v_1^\circ v_1^\bullet \tilde{v}^\circ \tilde{v}^\bullet)$ with $\mathrm{Im}[\tilde{v}^\circ] = y$. Set this time $\tilde{v}_0^\bullet$ and $\tilde{v}_0^\circ$ the respective intersections of the segments $[v_1^\circ v_0^\bullet]$ and $[v_1^\bullet v_0^\circ]$ with the line y. Using claim (E), one can construct two tangential quadrilaterals out of the triangles $(\tilde{v}_0^\bullet v_1^\circ v_0^\bullet)$ and $(\tilde{v}_{0,y}^\circ v_1^\bullet v_0^\circ)$ by adding respectively one white vertex to the segment $[\tilde{v}_0^\bullet v^\bullet]$ and one black vertex to the segment $[\tilde{v}_0^\circ \tilde{v}^\circ]$, both located on the axis y.

(b) The two vertices $v_0^\bullet$ and $v_1^\bullet$ below level y are of the same color (that we assume to be black here up to swapping colors). In that case, $(v_0^\circ v_0^\bullet v_1^\circ v^\bullet)$ is non convex and $\overline{z} \cap (y + \overline{\mathbb{H}})$ is formed by two triangles containing respectively v_0° and v_1°. Denote by $\tilde{v}_{00}^\bullet, \tilde{v}_{01}^\bullet, \tilde{v}_{10}^\bullet, \tilde{v}_{11}^\bullet$ the intersections of respectively $[v_0^\bullet v_0^\circ], [v_0^\bullet v_1^\circ], [v_1^\bullet v_0^\circ], [v_1^\bullet v_1^\circ]$ and this axis y. Then the triangles $(\tilde{v}_{10}^\bullet \tilde{v}_{10}^\bullet v_0^\circ)$ and

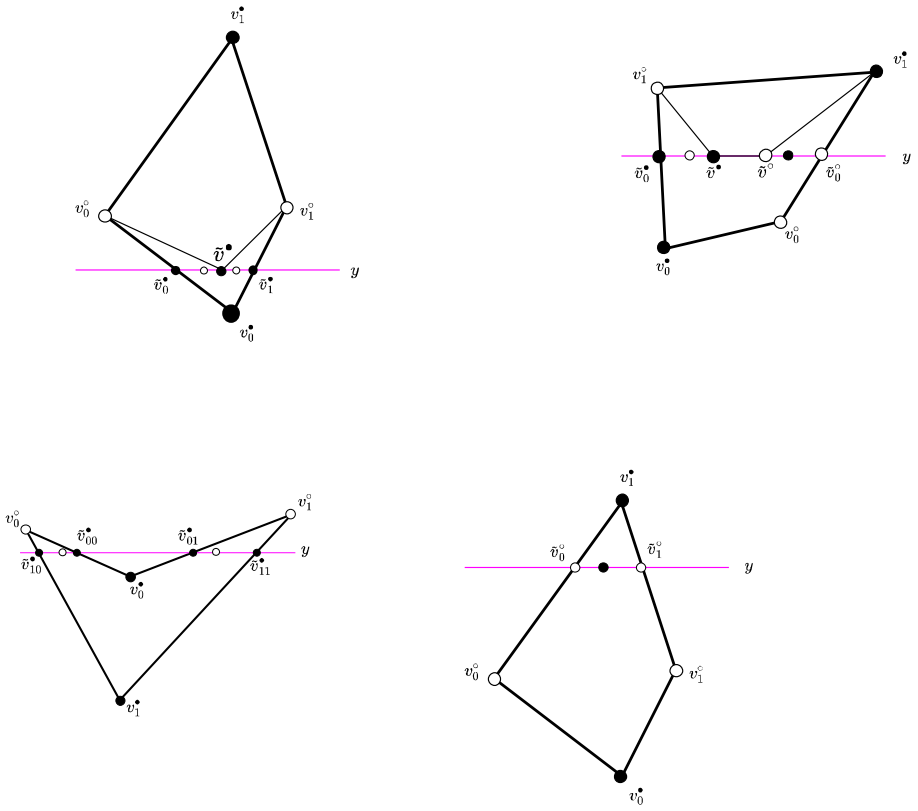

FIGURE 5.3.2 – Top : (Left) Case 1 (Right) Case 2a. Bottom : (Left) Case 2b (Right) Case 3

$(\tilde{v}_{01}^\bullet \tilde{v}_{11}^\bullet v_1^\circ)$ can be viewed as tangential quadrilaterals by adding two white vertices to the segments $[\tilde{v}_{10}^\bullet \tilde{v}_{00}^\bullet]$ and $[\tilde{v}_{01}^\bullet \tilde{v}_{11}^\bullet]$.

(3) There are three vertices of z below level y

Assume e.g. that $v_1^\bullet$ lies above level y. The consider $\tilde{v}_0^\circ$ and $\tilde{v}_1^\circ$ the intersections of y and the segments $[v_1^\bullet v_0^\circ]$ and $[v_1^\bullet v_1^\circ]$. Then one can view the triangle $(v_1^\bullet \tilde{v}_0^\circ \tilde{v}_1^\circ)$ as a tangential quadrilateral by adding a black vertex to the segment $[\tilde{v}_0^\circ \tilde{v}_1^\circ]$.

□

In order to apply regularity theory for s-holomorphic function, one needs to check the hypothesis EXP-FAT(δ) , which could fail if some of the quads produced by this slicing procedure have a too small radius r_z. We explain in what follows that under the assumptionn UNIF(δ) , there is only a negligeable share of vertical levels that produce too small tangential quadrilaterals, thus one can find a vertical level y that produces fat-enough quadrilaterals.

Definition 5.3.2. Let y be a horizontal a level that intersects the tangential quad z. We say that y is a *β-bad level* for z if one of the tangential quadrilaterals constructed during the horizontal allingnement of Lemma 5.3.2 has a radius r_z smaller than β. The complement of *β-bad levels* are called *β-good levels.*

The next proposition upper bounds the share of bad levels in a tangential quadrilateral z of a grid satisying $\textsc{Unif}(\delta)$. In words, it shows that $\beta-$bad levels (for a small β) are only those close to the horizontal lines containing vertices of z.

Proposition 5.3.3. *Let z be a tangential quadrilateral of a grid satisfying $\textsc{Unif}(\delta)$. Then provided δ is small enough, the (vertical) one dimensional Lebesgue measure of δ^{30}-bad levels intersecting z is at most $4\delta^4$.*

Proof. Recall that all the angles $\varphi_{v,z}$ of the tangential quadrilateral are bounded from below under the assumption $\textsc{Unif}(\delta)$. Fix a horizontal level y, at a vertical distance at least δ^4 from the 4 horizontal lines containing the vertices of z and perform an horizontal alignment at level y following Lemma 5.3.2. We keep exactly the notations of that lemma and separate the four sub-cases to treat, depending on the number of vertices below level y. We still denote $\hat{z}$ the center of the tangential quadrilateral.

(1) There is only one vertex of z below the axis y

One claims that, provided δ is small enough, the area of the tangential quadrilaterals $(v_0^\circ v_1^\bullet v_1^\circ \tilde{v}^\bullet)$ and $(v_0^\circ v_0^\bullet v_1^\circ \tilde{v}^\bullet)$ is larger than $\text{cst} \times \delta^8$ for some constant cst only depending on constants in $\textsc{Unif}(\delta)$. Indeed, consider e.g. the triangle (which is filled in blue in the left Figure 5.3.1) $T_{(v_0^\circ v_0^\bullet v_1^\circ \tilde{v}^\bullet)}(v_0^\bullet, \delta^4) = T(v_0^\bullet, \delta^4) \subseteq (v_0^\circ v_0^\bullet v_1^\circ \tilde{v}^\bullet)$, isoscele at $v_0^\bullet$ such that

— The symmetry axis of $T(v_0^\bullet, \delta^4)$ is the bisector of the angle $(v_0^\circ v_0^\bullet v_1^\circ)$

— Two sides of $T(v_0^\bullet, \delta^4)$ belong respectively to the segments $[v_0^\circ v_0^\bullet]$ and $[v_1^\circ v_0^\bullet]$.

— The height of $T(v_0^\bullet, \delta^4)$ (along the bisector of the angle $(v_0^\circ v_0^\bullet v_1^\circ)$) is δ^4.

Since the angle $\widehat{\varphi_{v_0^\bullet, z}}$ is bounded from below, the area $A_{(v_0^\circ v_0^\bullet v_1^\circ \tilde{v}^\bullet)}$ of $T(v_0^\bullet, \delta^4)$ and thus the area of $(v_0^\circ v_0^\bullet v_1^\circ \tilde{v}^\bullet)$ is larger than $\text{cst} \times \delta^8$. Moreover, the perimeter $\text{Per}_{(v_0^\circ v_0^\bullet v_1^\circ \tilde{v}^\bullet)}$ of $(v_0^\circ v_0^\bullet v_1^\circ \tilde{v}^\bullet)$ is at most 4δ (it is a general fact that if a convex polygon lies *inside* another one, the perimeter of the outer-one is larger than the interior one). We then deduce that

1. $r_{(v_0^\circ v_0^\bullet v_1^\circ \tilde{v}^\bullet)} = 2A_{(v_0^\circ v_0^\bullet v_1^\circ \tilde{v}^\bullet)} \text{Per}^{-1}_{(v_0^\circ v_0^\bullet v_1^\circ \tilde{v}^\bullet)} \geqslant \text{cst} \times \delta^8 \cdot \delta^{-1} \geqslant \delta^8$ using claim (A) provided δ is small enough.
2. The angles $\widehat{v_0^\bullet v_0^\circ \tilde{v}^\bullet}$ and $\widehat{v_0^\bullet v_1^\circ \tilde{v}^\bullet}$ are both bounded from below by the quantity $Cr_{(v_0^\circ v_0^\bullet v_1^\circ \tilde{v}^\bullet)}\delta^{-1} \geqslant C\delta^8 \cdot \delta^{-1} \geqslant \delta^8$, where the absolute constant C comes from claim (B) and δ is chosen small enough.
3. One can compute directly the area of the triangle $[v_0^\bullet v_0^\circ \tilde{v}^\bullet]$, which is exactly equal to $\frac{1}{2} \sin \widehat{v_0^\bullet v_0^\circ \tilde{v}^\bullet} \, |\tilde{v}_0^\bullet - v_0^\circ||\tilde{v}^\bullet - v_0^\circ| \geqslant \frac{1}{4}\delta^8 \cdot \delta^4 \cdot \delta^4 \geqslant \delta^{17}$. As the

perimeter of $[v_0^\bullet v_0^\circ \tilde{v}^\bullet]$ is again smaller than 10δ, one gets $r_{v_0^\bullet v_0^\circ \tilde{v}^\bullet \tilde{v}_{0,y}^\circ} \geqslant \delta^{17}$ repeating exactly the area/perimeter argument given in step 1.

The same result holds for the triangle $(v_0^\bullet v_1^\circ \tilde{v}^\bullet)$ viewed as a tangential quadrilateral.

(2) There are two vertices of opposite color of z below the axis y

Recall that the horizontal alignement is constructed by modifying along the appropriate hyperbola $(v_0^\bullet v_1^\circ v_1^\bullet v_0^\circ)$ into $(\tilde{v}^\bullet v_1^\circ v_1^\bullet v_0^\circ)$ and then modifying along the appropriate hyperbola $(\tilde{v}^\bullet v_1^\circ v_1^\bullet v_0^\circ)$ into $(\tilde{v}^\bullet v_1^\circ v_1^\bullet \tilde{v}^\circ)$.

Repeating the arguments of the case with one vertex below the axis y, one gets

— The angles $\widehat{v_0^\bullet v_1^\circ \tilde{v}^\bullet}$ and $\widehat{\tilde{v}^\circ v_1^\bullet v_0^\circ}$ are larger than δ^8, as in (2). The radii of the tangential quadrilaterals associated to the triangles $(\tilde{v}_0^\bullet v_1^\circ \tilde{v}^\bullet)$ and $(\tilde{v}_0^\circ v_1^\bullet \tilde{v}^\circ)$ are then larger than δ^{17} as (3).

— The tangential quadrilateral $(v_0^\circ \tilde{v}^\bullet v_1^\circ v_1^\bullet)$ has an area at least δ^8 as in (1). Following this time (2) and (3), the angle $\widehat{\tilde{v}^\bullet v_1^\circ v_1^\bullet}$ and the radius $r_{v_0^\circ \tilde{v}^\bullet v_1^\circ v_1^\bullet}$ are both larger than δ^8.

— One can now consider the triangle $T_{(v_0^\circ \tilde{v}^\bullet v_1^\circ v_1^\bullet)}(v_1^\circ, \delta^9) = T(v_1^\circ, \delta^9)$, isoscele at v_1° whose height along the bisector of $(v_0^\circ \tilde{v}^\bullet v_1^\circ v_1^\bullet)$ is δ^9. This triangle is contained in $(v_0^\circ \tilde{v}^\bullet v_1^\circ v_1^\bullet)$ and has an area $\frac{1}{2} \sin \widehat{\tilde{v}^\bullet v_1^\circ v_1^\bullet} \cdot \delta^9 \cdot \delta^9 \geqslant \delta^{27}$. One can then conclude that $r_{v_1^\circ \tilde{v}^\bullet \tilde{v}_1^\circ v_1^\bullet} \geqslant \delta^{27}$ as in (1).

(3) Remaining cases To handle the remaining cases (corresponding to 2b and 3 in Lemma 5.3.2) it is sufficient to note that in e.g. the case where three vertices of z are below the axis y, the triangle $T_{(v_0^\bullet v_0^\circ v_1^\bullet v_1^\circ)}(v_1^\bullet, \delta^4) = T(v_1^\bullet, \delta^4)$ is *inside* the triangle $(\tilde{v}_0^\circ v_1^\bullet \tilde{v}_0^\circ)$ has an area at least $\text{cst}\delta^8$. The tangential quadrilateral associated to $(\tilde{v}_0^\circ v_1^\bullet \tilde{v}_0^\circ)$ has then a radius $r_z \geqslant \delta^8$ as in (3).

All together, this proves that the one dimensional Lebesgue measure of δ^{30}-bad levels intersecting z is at most $4\delta^4$.

□

Remark 5.3.3. One can note that in the previous proof, one uses a rather general scheme to obtain a bound from below of the radius of the newly constructed tangential quadrilaterals after perfoming an horizontal alignement. An a priori lower bound on the area and an upper bound on the edge-lenghts gives a bound on the angles and radii. In particular if one replaces the bounded angle property by a lower bound on angles (which can be itself derived via a lower bound on radii following claim (B)), one can apply the same strategy with appropriate changes in the result.

We are now in position to prove Proposition 5.3.1

Proof. The proof is done by an explicit construction and should be followed with Figure 5.3.3. We only treat the bottom boundary, the upper one can be

treated similarly. Provided δ is small enough, Proposition 5.3.3 ensure that the vertical Lebesgue measure of δ^{30}-bad levels for one concrete quadrilateral is at most $O(\delta^4)$. Under the assumption $\textsc{Unif}(\delta)$ there are at most $O(\delta^{-2})$ tangential quadrilaterals in a region of bounded area, thus it exists a good level $y_0^\delta = -\frac{7}{2} + o_{\delta\to 0}(1)$. We detail now the step by step construction of the desired extension $\mathcal{R}_\delta^{\mathbf{ext}}$.

Step 1 : Slicing $\mathcal{S}^\delta$ to align all vertices of $\Lambda(G)$ into a horizontal line. One performs a horizontal alignement at level y_0^δ of *all* tangential quadrilaterals intersecting level y_0^δ. In that case, Proposition 5.3.3 implies that the lower boundary of the sliced picture is now formed by a sequence of tangential quadrilaterals with radius $r_z \geqslant \delta^{30}$. Moreover, in the proof of Proposition 5.3.3, one sees that the angles of the tangential quadrilaterals attached to the axis y_0^δ are *all* larger than δ^{10}, which implies that the sum of two consecutive angles in each of those quadrilaterals is in $[2\delta^{10}; 2\pi - 2\delta^{10}]$. One can now conclude, using claim (C) on geometrical features of tangential quadrilaterals, that the distance between two consecutive vertices (which are of opposite color) on the axis y_0^δ is larger than $\delta^{30}\sin(2\delta^{10}) \geqslant \delta^{40}$ provided δ is chosen small enough.

Step 2 : Create a second layer of horizontally aligned vertices
Once we have a discrete boundary aligned in the horizontal axis y_0^δ, one can extend this boundary from below, using again tangential (at white vertices of y_0^δ) quadrilaterals of triangular shape. More formally, let $G^\circ_{y_0^\delta}$ be the set of white vertices belonging to the axis y_0^δ. We extend the discrete boundary at level y_0^δ by creating a layer of quadrilaterals, tangential at vertices of $G^\circ_{y_0^\delta}$, such that their second white vertex lies *exactly* the level $y_0^\delta - 2\delta^{80}$ (drawn with blue dashes in Fig 5.3.3). Given three consectuive vertices $v_1^\bullet \sim v^\circ \sim v_2^\bullet$, consider the circle of radius r, centered at the point $(\mathrm{Re}[v^\circ], \mathrm{Im}[v^\circ] - r)$ and $T(r)$ the triangle tangential to the segment $[v_1^\bullet v_2^\bullet]$ at v° (see Fig 5.3.3) and denote v_r° its third vertex. As r goes to 0, $T(r)$ is smashed to the segment $[v_1^\bullet v_2^\bullet]$ and v_r° goes to v°. On the other hand $\mathrm{Im}[v_r^\circ]$ is strictly decreasing towards $-\infty$ up the value $r_0 > 0$ such that the tangents to the circle $\mathfrak{C}(r_0)$ passing respectively by $v_{1,2}^\bullet$ become parallel. As both $|v_{1,2}^\bullet - v^\circ|$ are larger than δ^{40}, one can easily see that $r_0 \geqslant \delta^{80}$ (as the two tangents to $\mathfrak{C}(r_0)$ passing by $v_{1,2}^\bullet$ clearly still intersect for $r \leqslant \delta^{80}$).

Consider now the hyperbola $\mathcal{C}$, which represents the set of vertices v_r° such that $(v_1^\bullet v^\circ v_2^\bullet v_r^\circ)$ is a tangential quadrilateral (see the geometrical claim (D)). By symmetry reasons, the tangent to $\mathcal{C}$ at the point $v^\circ \in \mathcal{C}$ is the vertical axis passing by v°. Let us now write the equality $|v_r^\circ - v_1^\bullet| - |v_r^\circ - v_2^\bullet| = |v^\circ - v_1^\bullet| - |v^\circ - v_2^\bullet|$ and use Taylor expansions as $|v_r^\circ - v^\circ|$ goes to 0. In the leading term, it reads as :

$$\langle \frac{v_1^\bullet - v^\circ}{|v_1^\bullet - v^\circ|} | v_r^\circ - v^\circ \rangle + O(\frac{|v_r^\circ - v^\circ|}{|v_1^\bullet - v^\circ|}) = \langle \frac{v_2^\bullet - v^\circ}{|v_2^\bullet - v^\circ|} | v_r^\circ - v^\circ \rangle + O(\frac{|v_r^\circ - v^\circ|}{|v_2^\bullet - v^\circ|}),$$

which imposes that $v_r^\circ - v^\circ$ is (at first order) vertical near v°. Going to the second term of the previous expansion, one can see that this expansion is a good one as long as $|v_r^\circ - v^\circ| \leqslant \delta^{60}$. More precisely, the difference between $i\,\mathrm{Im}[v_r^\circ - v^\circ]$ and $(v_r^\circ - v^\circ)$ is bounded by $\frac{1}{10}|v_r^\circ - v^\circ|$. In particular chosing then the unique r so that $\mathrm{Im}[v_r^\circ] = y_0^\delta - 2\delta^{80}$ proves the existence of a quadrilateral $(v_1^\bullet v^\circ v_1^\bullet v_r^\circ)$, tangential at v°, such that $\mathrm{Im}[v_r^\circ] = y_0^\delta - 2\delta^{80}$. The radius of the tangential circle associated to any of those newly constructed quads is at least δ^{120} as the area of $T(r)$ is $\frac{1}{2}|v_2^\bullet - v_1^\bullet| \times 2\delta^{40} \geqslant \delta^{120}$. Moreover the distance between two consecutive vertices v_r° lying on the axis $y_0^\delta - 2\delta^{80}$ is at most δ^{45} (as they are respectively $\frac{1}{2}\delta^{80}$ hotizontally away from their white counterparts in y_0^δ).

Step 3 : Symmetrize the picture to get a layer of kites

One can now symmetrize the boundary with respect to the (blue dashed) axis $y_0^\delta - 2\delta^{80}$ to construct *kites* whose bottom white vertices are all aligned along the axis $y_0^\delta - 4\delta^{80}$. Those symetrized edges are drawn in green. Repeating the previous area argument, all the associated radii of the newly formed quads are larger than δ^{85}. We finally replicate this symetrization vertically until the axis $y = -5 + o_{\delta\to 0}(1)$. Those edges are drawn in green in Fig 5.3.3.

Step 4 : Add the squares at the bottom right

Let $x_{\min}^\delta$ and $x_{\max}^\delta$ denote respectively the minimal and the maximal x horizontal coordinate of the lower boundary at the level y_0^δ used to slice (those coordinates are respectively $o_{\delta\to 0}(1)$ from $\mp\frac{1}{2}$). One can close vertically the left and right vertical boundaries of the extension using again 'triangular' shapes by adding vertical vertices with coordinates $(x_{\max}, y_0^\delta - (2k+1)\delta^{80})$ and $(x_{\min}, y_0^\delta - (2k+1)\delta^{80})$ for $k \geqslant 0$ some large enough integer, until the new boundary touches the level $y = -5 + o_{\delta\to 0}(1))$. This forms a sequence of alternating vertices of $G^\circ \cup G^\bullet$ separated vertically by a distance $2\delta^{80}$. These segments are colored in orange. Below the axis $y = -\frac{9}{2}$, one creates tangential quadrilaterals of triangular shapes, attached to the orange edges, whose vertices are located at position of the form $(x_{\max}, y_0^\delta - (2k+1)\delta^{80})$,$(x_{\max}, y_0^\delta - (2k+2)\delta^{80})$, $(x_{\max}, y_0^\delta - (2k+3)\delta^{80})$ and $(x_{\max} + 2\delta^{80}, y_0^\delta - (2k+2)\delta^{80})$ and then continues the picture to the right with squares in $\Lambda(G)$ whose diagonal between white vertices is *horizontal* and of length $4\delta^{80}$. This concludes the construction.

To check the fact that the constructed grid satisfies $\mathrm{Lip}(\kappa, 5\delta)$, it is enough to notice that in the original part of the grid it already holded, in the kite region is holds as $|\mathcal{Q}(x + iy) - \mathcal{Q}(x + iy_0^\delta)| \leqslant 2\delta$ (as we copy periodically). As the transition region between the original grid and the kite region is of vertical depht smaller than δ, one can simply bound the derivative of the origami map by 1 there to recover that the assumption $\mathrm{Lip}(\kappa, 5\delta)$ holds for the entire extended picture.

□

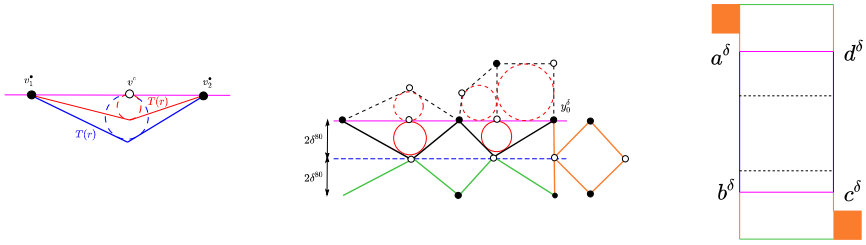

FIGURE 5.3.3 – (Left) Scheme used in step (3) to extend the grid below the level y_0^δ. We draw several triangles $T(r)$ with different radii r. (Center) Local picture near the boundary after the entire extension procedure. The slicing level y_0^δ is drawn in purple, the piece that belonged to the original picture before slicing is dashed, the lateral boundary used to construct a square grid piece is drawn in in orange. (Right) : Final shape containing the square grid pieces colored in orange. While considering the Ising model on the next section, we discretize the blue arcs with *free* boundary condition and the remaining of the boundary of $\Omega_\delta = (a^\delta b^\delta c^\delta d^\delta)$ as *wired* arcs.

We denote $a^\delta, b^\delta, c^\delta, d^\delta$ the vertices at the junction between the original piece of $\mathcal{S}^\delta$ and its extension $\mathcal{R}_\delta^{\mathbf{ext}}$ ordered counter-clockwise with a^δ lying in the top left. More precisely, a^δ lies at $(-\frac{1}{2}; \frac{7}{2}) + o_{\delta\to 0}(1)$, b^δ lies at $(-\frac{1}{2}; -\frac{7}{2}) + o_{\delta\to 0}(1)$,$c^\delta$ lies at $(\frac{1}{2}; -\frac{7}{2}) + o_{\delta\to 0}(1)$ and d^δ lies at $(\frac{1}{2}; \frac{7}{2}) + o_{\delta\to 0}(1)$. The two square grid regions are called the square grid districts and are colored in orange and we require that the vertices of G° approximating the horizontal arc of the bottom right district *all belong to the same horizontal axis*.

5.3.2 . Proof of Theorems 5.1.1 and 5.1.2 under Unif(δ)

We now prove Theorem 5.1.1 that allows to deduce Theorem 5.1.2 as recalled in Section 5.1. The proof of positive magnetization between opposite boundaries in the alternating wired/free/wired/free spin-Ising setup is done first in the domain $\mathcal{R}_{\mathbf{ext}}^\delta$ constructed in section 5.3.1 and then deduced in $\mathcal{R}^\delta$ using standard monotonicity arguments with respect to boundary conditions (e.g. [60, Theorem 7.6]). Since the graphs highly lack symmetries, the main tool to prove the positive magnetization is to work by *contradiction* in a discrete 4-points setup (alternating wired and free boundary conditions on the four arcs). Namely, one can construct in the extended domain a sequence s-holomorphic functions F^δ out of 4-points Kadanoff-Ceva correlators and prove their convergence to a continuous function f together with the convergence of the associated H^δ to a continuous function h, which inherits Dirichlet boudary from discrete, at least in the square lattice districts. If the magnetization vanishes under some sub-sequence $\delta \to 0$, the only way to reconcile discrete estimates for F^δ and continuous estimates for f is to have the

latter vanishing identically in the sqaure districts, which is in its turn impossible.

The idea to prove the positive magnetization using observables dates back to Smirnov and was first implemented in [48, Section 6] on isoradial grids. It was then applied by Chelkak in [33, Section 5], *without using the comparison* between functions H^δ and discrete harmonic functions, as this approach is not possible outside of the isoradial context. Here, the introduction of pieces of a square lattice near the wired arcs allows re-use the original technology introduced for isoradial grids in [48, Section 5], modulo some uniqueness principle for solutions to Beltrami equations. In this section we keep using the Kadanoff-Ceva formalism instead of the loop representation for the FK-model used in [48, Section 6]. As a simplification, one notes that in order to prove the non-vanishing magnetization in the limit, there is *no need* of the rewiring procedure for the wired/free/wired/free setup introduced in [48, eq (6.3) and (6.4)] and we present here a more transparent derivation. Still, let us note that the rewiring procedure remains useful if one wants to prove *convergence* of magnetization in the same 4 points setup.

Let $(\Omega_\delta; a^\delta, b^\delta, c^\delta, d^\delta)$ be a discrete simply connected domain of an s-embedding $\mathcal{S}^\delta$, with two *wired* boundary arcs $(b^\delta c^\delta)^\circ$, $(d^\delta a^\delta)^\circ$ and a two *dual-wired* boundary arcs $(c^\delta d^\delta)^\bullet$ and $(a^\delta b^\delta)^\bullet$. One can now define the Kadanoff–Ceva four points observable by setting $X^\delta(\cdot) := \mathbb{E}_{\Omega_\delta}[\chi_{(\cdot)}\mu_{(c^\delta d^\delta)^\bullet}\sigma_{(d^\delta a^\delta)^\circ}]$ via $(5.2.5)$ and gets

$$\begin{aligned} X^\delta(a^\delta) &= \pm\mathbb{E}_{\Omega_\delta}[\mu_{(a^\delta b^\delta)^\bullet}\mu_{(c^\delta d^\delta)^\bullet}], & X^\delta(d^\delta) &= \pm 1,\\ X^\delta(b^\delta) &= \pm\mathbb{E}_{\Omega_\delta}[\mu_{(a^\delta b^\delta)^\bullet}\mu_{(c^\delta d^\delta)^\bullet}\sigma_{(b^\delta c^\delta)^\circ}\sigma_{(d^\delta a^\delta)^\circ}], & X^\delta(c^\delta) &= \pm\mathbb{E}_{\Omega_\delta}[\sigma_{(b^\delta c^\delta)^\circ}\sigma_{(d^\delta a^\delta)^\circ}]. \end{aligned}$$

Choosing properly the global additive constant in the definition of H_{X^δ} associated to X^δ via $(5.2.16)$, one has

$$\begin{aligned} H_{X^\delta}((c^\delta d^\delta)^\bullet) &= 1, & H_{X^\delta}((d^\delta a^\delta)^\circ) &= 0,\\ H_{X^\delta}((a^\delta b^\delta)^\bullet) &= 1-\mathbb{E}[\mu_{(a^\delta b^\delta)^\bullet}\mu_{(c^\delta d^\delta)^\bullet}]^2, & H_{X^\delta}((b^\delta c^\delta)^\circ) &= 1-\mathbb{E}[\sigma_{(b^\delta c^\delta)^\circ}\sigma_{(d^\delta a^\delta)^\circ}]^2. \end{aligned}$$

We focus on the situation where $\Omega_\delta = (b^\delta, c^\delta, d^\delta, a^\delta)$ is the topological rectangle $\mathcal{R}_\delta^{\mathbf{ext}}$ constructed in Section 5.3.1, approximating the domain $\Omega = ([\frac{-1}{2}; \frac{1}{2}]\times[-5;5]) \cup ([\frac{1}{2}; \frac{3}{4}]\times[-4;-5]) \cup ([-\frac{3}{4}; \frac{1}{2}]\times[4;5])$. One denotes by F^δ and $H^\delta = H_{F^\delta} = H_{X^\delta}$ the functions naturally associated to X^δ via $(5.2.14)$ and $(5.2.16)$. Using the maximum principle for H^δ coming from Proposition 5.2.7, one directly deduces from the boundary conditions $(5.3.2)$ that the functions H_{F^δ} are uniformly bounded on Ω_δ. Recall that all the faces of $\mathcal{R}_\delta^{\mathbf{ext}}$ have *by construction* a radius $r_z \geqslant \delta^{100}$ (as one can see in the proof of Proposition 5.3.1), thus the assumption $\textsc{Exp-Fat}(\delta)$ is fullfiled, as well as the assumption $\textsc{Lip}(\kappa, 5\delta)$ (which is again an output of Proposition 5.3.1). In particular, one can apply the regularity theory for s-holomorphic functions recalled in Section 5.2.4 and conclude that there exist a subsequential limit of the family $(F^\delta)_{\delta>0}$ such that, uniformly on compacts of Ω,

$$F^\delta \to f, \quad H_{F^\delta} \to h = \tfrac{1}{2}\int \mathrm{Im}[(f(z))^2 dz] + |f(z)|^2 d\vartheta.$$

In general $d\vartheta \neq 0$, and f is *not* holomorphic. Still, the function f *is* holormorphic inside in the regions $[\frac{1}{2}, \frac{3}{4}] \times [-5, -4]$ and $[-\frac{3}{4}; \frac{1}{2},] \times [4; 5]$, as ϑ is constant there. This also implies that $h = \frac{1}{2} \int \mathrm{Im}[(f(z))^2 dz]$ is a harmonic function in those regions. Assuming $\mathbb{E}_{\Omega_\delta}[\sigma_{(b^\delta c^\delta)^\circ} \sigma_{(d^\delta a^\delta)^\circ}] \to 0$ as $\delta \to 0$, we have $H_{X^\delta}((b^\delta c^\delta)^\circ) = 1 - \mathbb{E}_{\Omega_\delta}[\sigma_{(b^\delta c^\delta)^\circ} \sigma_{(d^\delta a^\delta)^\circ}]^2$ that goes to 1 as δ goes to 0. The contradiction is obtained in three steps :

— We show that h has Dirichlet boundary 0 in a piece of the arc of the top left region and has Dirichlet boundary 1 in a piece of the bottom right region.

— In this scenario, the only way to reconcile discrete and continous estimates in the bottom right district is the one when f vanishes identically in the bottom right district.

— The Sloïlov factorization of the primitive $I_{\mathbb{C}}$ implies that the function f should actually vanish everywhere in Ω, contradicting the change of boundary values of h in different districts.

The author is grateful to Mikhail Basok for pointing out the Sloïlov factorization allowing to obtain the final contradiction.

Proof. **Step 1 : Boundary behavior of the continuous functions f and h**

Recall that $H_{X^\delta}((b^\delta c^\delta)^\circ) = 1 - \mathbb{E}_{\Omega_\delta}[\sigma_{(b^\delta c^\delta)^\circ} \sigma_{(d^\delta a^\delta)^\circ}]^2 \to 1$ at the wired arc $(b^\delta c^\delta)$. This statement remains in particular true at the horizontal arcs of the bottom right square grid district. *In the square grid districts and a priori only there*, one can apply [48, Proposition 3.6] and deduce directly that

— The function H_{F^δ} is *sub-harmonic* on G° for the natural Laplacian on G° defined in [48, eq (3.1)].

— The function H_{F^δ} is *super-harmonic* on $G^\bullet$ for the natural Laplacian on $G^\bullet$ defined in [48, eq (3.1)].

One can then apply the *boundary modification trick* of [48, Lemma 3.14, Remark 3.15] to compare H^δ with discrete harmonic functions and prove exactly as in [48, Theorem 4.3]) that discrete Dirichelet boundary conditions survive when passing to continuum i.e. h extends continuously to 1 at the horizontal arc of the bottom right square grid district. In continuum, the 1 Dirichlet boundary conditions of h at the horizontal segment $[\frac{1}{2}; \frac{3}{4}] \times \{-5\}$ and the fact that $h \leqslant 1$ imply that f extends continuously up to the bottom boundary. This implies that $f^2 \in \mathbb{R}^-$ near that arc, i.e. $f \in i\mathbb{R}$, as shown in [33, Proof of Theorem 1.3].

Step 2 : Boundary behavior of discrete F^δ

For discrete observables, at a boundary quad z of the arc approximating the horizontal segment $[\frac{1}{2}; \frac{3}{4}] \times \{-5\}$, the increment of H_{F^δ} between two consecutive (from left to right) white vertices vanishes identically on the one hand (this is a direct consequence of (5.3.2)) and is on the other hand proportional to $\mathrm{Im}[F^\delta(z)^2]$. This allows to conclude that $F^\delta(z)^2 \in \mathbb{R}$ and one can even go

beyond that observation, as the value of the boundary argument of $F^\delta(z)$ is given directly by the formula [33, Lemma 5.3], which implies that $F^\delta(z) \in \mathbb{R}$. In particular $F^\delta(z)$ is purely real at the boundary, which means that $\mathrm{Im}[F^\delta]$ vanishes identically there.

In the square grid region, $z' \mapsto \mathrm{Im}[F^\delta(z')]$ is a martingale for the standard random walk on quads (i.e. the probability to leave from one $z \in \diamondsuit(G)$ to one of its four neighbours is $\frac{1}{4}$). This is a simple implication of the discrete Cauchy-Riemann equation satisfied by F^δ (see e.g. [38, eq (3.1)]). Set $z_0 = (\frac{5}{8}; -5+s)$ and denote by $\mathcal{R}^\delta_{s^{\frac{1}{4}}}$ the square of width $2s^{\frac{1}{4}}$ centered at $(\frac{5}{8}; -5+s^{\frac{1}{4}})$. Using the standard gamblers ruin estimates for random walks on $\mathbb{Z}^2$, the probability that the random walk associated to $\mathrm{Im}[F^\delta(z')]$ leaves $\mathcal{R}^\delta_{s^{\frac{1}{4}}}$ from its top side is $O(s^{\frac{3}{4}})$ and the probability that it leaves $\mathcal{R}^\delta_{s^{\frac{1}{4}}}$ from one of its vertical sides at a height ρ (from its bottom boundary) is bounded by $\rho^{\frac{1}{2}+\varepsilon}$ for some $\varepsilon > 0$ independant of s and $\tilde{\delta}$. We apply now the optional stopping theorem to the stopping time the walk started at z_0 leaves $\mathcal{R}^\delta_{s^{\frac{1}{4}}}$. One then has

— The contribution of the bottom side of $\mathcal{R}^\delta_{s^{\frac{1}{4}}}$ vanishes identically as $\mathrm{Im}[F^\delta]$ vanishes there (which is a consequence of the construction of the cut).

— The contribution of the top side is bounded by $O(s^{\frac{3}{4}} \cdot s^{-\frac{1}{8}})$ as F^δ is bounded there by $s^{-\frac{1}{8}}$ in the top segments of $\mathcal{R}^\delta_{s^{\frac{1}{4}}}$.

— The contribution of the vertical sides is polynomial in s, as the probability to leave from one of the vertical sides at a height ρ from the bottom side is bounded by $\rho^{\frac{1}{2}+\varepsilon}$ and we have the upper bound $|F^\delta(z)| = O(\mathrm{dist}(z, \partial\Omega)^{-\frac{1}{2}})$.

In conclusion $|\mathrm{Im}[F^\delta(z_0)]| = O(s^{\beta''})$ for some positive exponent β''. Sending first δ to 0 and then s to 0 implies that f vanishes at $(\frac{5}{8}; -5)$. The same reasoning ensures f vanishes in the entire arc $[\frac{1}{2}; \frac{3}{4}] \times \{-5\}$. Since f is holomorphic in the region $[\frac{1}{2}, \frac{3}{4}] \times [-5, -4]$ and vanishes in a boundary arc, it vanishes everywhere in $[\frac{1}{2}, \frac{3}{4}] \times [-5, -4]$. This implies in particular that its primitive $I_{\mathbb{C}}$ is constant there. On can also note that a similar reasoning on survival of Dirichlet boundary conditions applied at the top left square grid district proves that $h = 0$ near the arc $[-\frac{3}{4}; \frac{1}{2}] \times \{5\}$.

Step 3 : Final contradiction using the Stoïlov factorization

We are now in position to conclude the final contradiction. Consider the function $g(\zeta) = I_{\mathbb{C}}(\zeta)$ defined by (5.2.25) in the ζ conformal parametrization of $(z, \vartheta(z))$. As explained in section 5.2.5, g satisfies a conjugate Beltrami equation (5.2.26) with a Beltrami coefficient which is bounded away from 1, only depending on κ. Since f vanishes in the bottom square grid region, g is constant there, thus constant everywhere in Ω. In return, this proves that f

vanishes everywhere in Ω. This contradicts the change of boundary values from 0 to 1 for the function h between the two opposite square grid districts. $\square$

5.4 . Extension of the proof under the assumption Lenght-Exp-Fat(δ)

We explain now how to adapt the preceeding methods to prove crossing estimates under the assumption LENGHT-EXP-FAT(δ) . Those modifications are rather mild and the only additional constrains compared to the proof under the assumption UNIF(δ) is to ensure that tangential quadrilaterals constructed when slicing horizontally and extending the original picture do not have a too small radius r_z. This allows to apply then the regularity theory for s-holomorphic functions developped in the section 5.2.4 and extract sub-sequential limits. Once this is done, all the arguments presented in the section 5.3.2 apply in the exact same way. We explain here how to adapt the proofs and statements given section 5.3 to recover the same the final contradiction if Theorem 5.1.1 doesen't hold. The main additional ingredient of this section is Proposition 5.3.1 which is a clear generalisation of Propositon 5.4.1.

Fix $\gamma > 0$ and denote once again the rectangle $\mathcal{R}_\delta^\gamma$ approximating up to $o_{\delta\to 0}(1)$ the rectangle $[-\frac{1}{2},\frac{1}{2}]\times[-3,3]$, chosen with boundary quads in the left and right side all having a radius $r_z \geqslant \exp(-\gamma\delta^{-1})$. Provided δ is small enough, such a choice is always possible under the assumption LENGHT-EXP-FAT(δ) (and even under the assumption EXP-FAT(δ)). We also denote $\mathcal{R}_\delta^{'\gamma}$ the approximation of $[-\frac{1}{2},\frac{1}{2}]\times[-5,5]$, assuming its discrete vertical boundary in $\mathcal{S}^\delta$ contains the respective approximations of the vertical boundaries of $\mathcal{R}_\delta^\gamma$, and is also formed by quadrilaterals all having a radius $r_z \geqslant \exp(-\gamma\delta^{-1})$. The main output of this section is the next proposition.

Proposition 5.4.1. *Given $\gamma > 0$, chose $\mathcal{R}_\delta^\gamma$ as above in $\mathcal{S}^\delta$, assuming the sequence of embeddings satisfy the assumption* LENGHT-EXP-FAT(δ) *. Provided δ is small enough, one can construct a finite piece of a proper s-embedding $\mathcal{R}_\delta^{\gamma,\mathbf{ext}}$, approximating up $o_{\delta\to 0}(1)$ the domain $([\frac{-1}{2};\frac{1}{2}]\times[-5;5])\cup([\frac{1}{2};\frac{3}{4}]\times[-4;-5])\cup([-\frac{3}{4};\frac{1}{2}]\times[4;5])$, such that :*

- $\lim_{\delta\to 0}\sum_{r_z\leqslant\exp(-250\gamma\delta^{-1})} diam(z) = 0$, *where the sum is taken on quads of $\mathcal{R}_\delta^{\gamma,\mathbf{ext}}$.*
- *One has $\mathcal{R}_\delta^\gamma \subseteq \mathcal{R}_\delta^{\gamma,\mathbf{ext}}$ and the left and right 'vertical' boundaries of $\mathcal{R}_\delta^\gamma$ belong the boundary of $\mathcal{R}_\delta^{\gamma,\mathbf{ext}}$.*
- *There exists a horizontal line $y_0^\delta = -\frac{7}{2} + o_{\delta\to 0}(1)$ such that below the line y_0^δ, the tangential quadrilateral of $\mathcal{R}_\delta^{\gamma,\mathbf{ext}}$ are kites with horizontal symmetry axis, all having a radius r_z larger than $\exp(-250\gamma\delta^{-1})$.*
- *There exists a horizontal line $y_1^\delta = \frac{7}{2} + o_{\delta\to 0}(1)$ such that above the line y_1^δ, the tangential quadrilateral of $\mathcal{R}_\delta^{\gamma,\mathbf{ext}}$ are kites with horizontal symmetry axis, all having a radius r_z larger than $\exp(-250\gamma\delta^{-1})$.*

— $\mathcal{R}_\delta^{\gamma,\mathbf{ext}}$ *contains two pieces of a square lattice with an associated* r_z *larger than* $\exp(-250\gamma\delta^{-1})$ *in the regions* $[\frac{1}{2};\frac{3}{4}]\times[-5;-4]$ *and* $[-\frac{3}{4};\frac{1}{2}]\times[4;5]$.
— $\mathcal{R}_\delta^{\gamma,\mathbf{ext}}$ *satisfies* $\textsc{Lip}(\kappa, 5\delta)$.

In order to prove Proposition 5.4.1, one starts once again by proving the existence of a *good* horizontal slicing level, which is done by quantifying the share of bad levels defined in Proposition 5.3.3.

Proposition 5.4.2. *Let* z *be a tangential quadrilateral with a radius* $r_z \geqslant \exp(-\gamma\delta^{-1})$ *and whose edge-lenghts are smaller than* δ. *Then provided* δ *is small enough, the (vertical) one dimensional Lebesgue measure of* $\exp(-40\gamma\delta^{-1})$*-bad levels intersecting* z *is at most* $4\exp(-4\gamma\delta^{-1})$.

Proof. We keep exactly the notations and methods used in the proof of Proposition 5.3.3. Using claim (B) on the geometrical features of tangential quadrilateral, the angles $\varphi_{v,z}$ are now bounded from below (provided δ is small enough) by $\delta^{-1}\exp(-\gamma\delta^{-1}) \geqslant \exp(-\gamma\delta^{-1})$, as $r_z \geqslant \exp(-\gamma\delta^{-1})$ and the edge-lengths are smaller than δ. Fix an horizontal level y, at a vertical distance at least $\exp(-4\gamma\delta^{-1})$ from the 4 axes containing the vertices of z and perform an horizontal alignment at level y. Again, we treat separately the four sub-cases depending on the number of vertices below level y and still denote by $\hat{z}$ the center of the tangential quadrilateral z.

(1) There is only one vertex of z below the axis y

The area of the tangential quadrilaterals $(v_0^\circ v_1^\bullet v_1^\circ \tilde{v}^\bullet)$ and $(v_0^\circ v_0^\bullet v_1^\circ \tilde{v}^\bullet)$ are larger than $\frac{1}{2}\exp(-\gamma\delta^{-1})\exp(-4\gamma\delta^{-1})\exp(-4\gamma\delta^{-1}) \geqslant \exp(-10\gamma\delta^{-1})$. This can be seen once again computing e.g. for $(v_0^\circ v_0^\bullet v_1^\circ \tilde{v}^\bullet)$ the area of the isocele triangle at $v_0^\bullet$ denoted by $T_{(v_0^\circ v_0^\bullet v_1^\circ \tilde{v}^\bullet)}(v_0^\bullet, \exp(-4\gamma\delta^{-1}))$, whose angle at $v_0^\bullet$ is now larger than $\exp(-\gamma\delta^{-1})$. This implies the following bounds, provided δ is small enough :

1. $r_{(v_0^\circ v_0^\bullet v_1^\circ \tilde{v}^\bullet)} = 2A_{(v_0^\circ v_0^\bullet v_1^\circ \tilde{v}^\bullet)}\mathrm{Per}^{-1}_{(v_0^\circ v_0^\bullet v_1^\circ \tilde{v}^\bullet)} \geqslant \exp(-10\gamma\delta^{1})\cdot\delta^{-1} \geqslant \exp(-10\gamma\delta^{-1})$.
2. The angles $\widehat{v_0^\bullet v_0^\circ \tilde{v}^\bullet}$ and $\widehat{v_0^\bullet v_1^\circ \tilde{v}^\bullet}$ are both bounded from below by the quantity $Cr_{(v_0^\circ v_0^\bullet v_1^\circ \tilde{v}^\bullet)}\delta^{-1} \geqslant C\exp(-10\gamma\delta^{-1})\cdot\delta^{-1} \geqslant \exp(-10\gamma\delta^{-1})$.
3. The area of the triangle $[v_0^\bullet v_0^\circ \tilde{v}^\bullet]$ can be computed explicitely and is now larger than $\frac{1}{4}\exp(-10\gamma\delta^{-1})\cdot\exp(-4\gamma\delta^{-1})\cdot\exp(-4\gamma\delta^{-1}) \geqslant \exp(-20\gamma\delta^{-1})$. As the perimeter of $[v_0^\bullet v_0^\circ \tilde{v}^\bullet]$ is still smaller than 10δ, one gets the lower bound $r_{v_0^\bullet v_0^\circ \tilde{v}^\bullet \tilde{v}^\circ_{0,y}} \geqslant \exp(-20\gamma\delta^{-1})$.

The same result holds for the triangle $(v_0^\bullet v_1^\circ \tilde{v}^\bullet)$.

(2) There are two vertices of opposite color of z below the axis y

Repeating exactly the arguments of the similar case in the proof of Proposition 5.3.3 one has

— The angles $\widehat{v_0^\bullet v_1^\circ \tilde{v}^\bullet}$ and $\widehat{\tilde{v}^\circ v_1^\bullet v_0^\circ}$ are larger than $\exp(-10\gamma\delta^{-1})$ while the radii of the tangential quadrilaterals associated to the triangles $(\tilde{v}_0^\bullet v_1^\circ \tilde{v}^\bullet)$ and $(\tilde{v}_0^\circ v_1^\bullet \tilde{v}^\circ)$ are then larger than $\exp(-20\gamma\delta^{-1})$.

— The tangential quadrilateral $(v_0^\circ \tilde{v}^\bullet v_1^\circ v_1^\bullet)$ has an area at least $\exp(-10\gamma\delta^{-1})$ which implies that both the angle $\widehat{\tilde{v}^\bullet v_1^\circ v_1^\bullet}$ and the radius $r_{v_0^\circ \tilde{v}^\bullet v_1^\circ v_1^\bullet}$ are larger than $\exp(-10\gamma\delta^{-1})$.

— Considering the triangle $T_{(v_0^\circ \tilde{v}^\bullet v_1^\circ v_1^\bullet)}(v_1^\circ, \exp(-12\gamma\delta^{-1}))$ contained in $(v_0^\circ \tilde{v}^\bullet v_1^\circ v_1^\bullet)$ whose area is $\frac{1}{2}\sin\widehat{\tilde{v}^\bullet v_1^\circ v_1^\bullet}\cdot\exp(-12\gamma\delta^{-1})\cdot\exp(-12\gamma\delta^{-1}) \geqslant \exp(-40\gamma\delta^{-1})$ one can conclude that $r_{v_1^\circ \tilde{v}^\bullet \tilde{v}_1^\circ v_1^\bullet} \geqslant \exp(-40\gamma\delta^{-1})$.

(3) Remaining cases The remaining cases are solved noting once again e.g. for the sub-case where three vertices of z are below the axis y that the triangle $T_{(v_0^\bullet v_0^\circ v_1^\bullet v_1^\circ)}(v_1^\bullet, \exp(-4\gamma\delta^{-1}))$ is *inside* the triangle $(\tilde{v}_0^\circ v_1^\bullet \tilde{v}_0^\circ)$ and has an area at least $\exp(-10\gamma\delta^{-1})$ as the angle of z at $v_0^\bullet$ is bounded from below by $\exp(-\gamma\delta^{-1})$. In particular the tangential quadrilateral associated to the triangle $(\tilde{v}_0^\circ v_1^\bullet \tilde{v}_0^\circ)$ has a radius $r_z \geqslant \exp(-10\gamma\delta^{-1})$.

All together, this proves that the one dimensional Lebesgue measure of $\exp(-40\gamma\delta^{-1})$-bad levels intersecting z is at most $4\exp(-4\gamma\delta^{-1})$.

□

We are now in position to prove Proposition 5.4.1.

Proof. The proof mimicks the proof of Proposition 5.3.1 and only the differences are highlighted here. We use the hypothesis Lenght-Exp-Fat(δ) for $\gamma > 0$ fixed. Provided δ is small enough, the Lebesgue measure of vertical levels y in $[-4;4]$ intersecting quads with a radius $r_z \leqslant \exp(-\gamma\delta^{-1})$ is $o_{\delta\to 0}(1)$. Consider A_γ the set of $y \in [-4;4]$ such that the vertical level y *do not* intersect any quad with $r_z < \exp(-\gamma\delta^{-1})$ i.e. any level of A_γ only intersects quads such that $r_z \geqslant \exp(-\gamma\delta^{-1})$. There are at most $O(\exp(2\gamma\delta^{-1}))$ different quads intersecting A_γ, since the overall area of a macroscopic rectangle is bounded from above. Using Proposition 5.3.3, the one dimensional Lebesgue measure of $\exp(-40\gamma\delta^{-1})$-bad levels intersecting a given quad of A_γ is at most $\exp(-4\gamma\delta^{-1})$. Thus the Lebesgue measure of $\exp(-40\gamma\delta^{-1})$-good levels is $8 - o_{\delta\to 0}(1)$ and has a point near $y_0^\delta = -\frac{7}{2}$. Fix such a level y_0^δ in A_γ near $-\frac{7}{2}$ assuming moreover that all vertices of $\Lambda(G)$ intersecting A_γ are at a vertical distance $\exp(-4\gamma\delta^{-1})$ from y_0. This is alwas possible since there are at most $O(\exp(2\gamma\delta^{-1}))$ different quads that intersect A_γ. We detail once again step by step the construction of the extension.

Step 1 : Slicing $\mathcal{S}^\delta$ to align all vertices of $\Lambda(G)$ into a horizontal line.

One performs a horizontal alignement to *all* tangential quadrilaterals intersecting level y_0^δ. One deduces from Proposition 5.4.2 that the lower boundary of the sliced picture is formed by bipartite sequence of vertices separated by a distance at least $\exp(-60\gamma\delta^{-1})$ from each other.

Step 2 : Create a second layer of horizontally aligned vertices

One repeats the Step 2 of the proof of Proposition 5.3.1 and creates a second layer of vertically aligned vertices of G° at the horizontal axis $y_0^\delta -$

$2\exp(-120\gamma\delta^{-1})$ using triangular shapes $T(r)$. The radius of any of those newly constructed quads is at least $\exp(-200\gamma\delta^{-1})$ as the area of the associated triangle is $\frac{1}{2}|v_2^\bullet - v_1^\bullet| \times 2\exp(-120\gamma\delta^{-1}) \geqslant \exp(-200\gamma\delta^{-1})$.

Step 3 : Symmetrize the picture to get a layer of kites

Symmetrize the boundary with respect to the axis $y_0^\delta - 2\exp(-120\gamma\delta^{-1})$ to construct *kites* whose bottom white vertices are all aligned along the axis $y_0^\delta - 4\exp(-120\gamma\delta^{-1})$. All the associated radii of the newly formed quads are larger than $\exp(-200\gamma\delta^{-1})$. One can now replicate this symetrization vertically until the axis $y = -5 + o_{\delta\to 0}(1)$.

Step 4 : Add the squares at the bottom right

Repeat *motus mutandis* Step 4 of the proof of Proposition 5.3.1 replacing the distance δ^{80} by $\exp(-120\gamma\delta^{-1})$.

The fact that $\mathrm{Lip}(\kappa, 5\delta)$ still holds is proven exactly as in Proposition 5.3.1. □

We are now in position to prove the theorem under LENGHT-EXP-FAT(δ)

Proof of Theorem 5.1.1 under the assumption LENGHT-EXP-FAT(δ) . For any fixed $\gamma > 0$, provided δ is small enough, one can construct a topological rectangle $\mathcal{R}_\delta^{\mathbf{ext},\gamma}$ with all the properties of Proposition 5.4.1. In particular, under the assumption LENGHT-EXP-FAT(δ) , one can consider a sequence of s-embeddings $\mathcal{R}_\delta^{\gamma_\delta,\mathbf{ext}}$, with γ_δ going to 0 as δ goes to 0 that satisfy the assumption EXP-FAT(δ) . It is then possible to work again by contradiction and extract a sub-sequential limit (using EXP-FAT(δ) and LIP($\kappa, 5\delta$)) of 4-points observables defined in the domains $\mathcal{R}_\delta^{\gamma_\delta,\mathbf{ext}}$ to conclude exactly as in Section 5.3.2.

□

6 - Convergence of fermionic observables on s-embeddings with smooth limiting surface

This chapter corresponds to an article in preparation [116], written alone.

6.1 . Convergence of fermionic observables on s-embeddings with smooth limiting surface

In this chapter, we prove the convergence of the FK-Dobrushin observables defined in approximations of smooth domains of the plane, in the case where the limiting origami map ϑ is a smooth function. This result proves the existence of a scaling limit for the model, which is *not* locally a holomorphic function, but admits a nicer description (after a change of variables) as a solution to a massive Dirac equation on conformal parametrization of the surface $(z, \vartheta(z)) \in \mathbb{R}^{2,1}$ (see [33, Below (2.28)]). The nature of this scaling limit in continuum was understood by Chelkak in [33, Section 2.7] and we provide here the technical tools to derive the convergence of the FK observables, when both ϑ and the domain Ω are smooth. A more general convergence is expected to hold without imposing any assumption on the smoothness of ϑ. In that last case, the description of the scaling limit should be done via solutions to conjugate Beltrami equations, but is *not* included here. The main obstacle to a generalization in the case of a rough limiting origami map turns out to be proving uniqueness of solutions to some Riemann-Hilbert type boundary value problem. In this chapter, we make the following assumptions :

— We work with a sequence $(\mathcal{S}^\delta)_{\delta>0}$ of s-embeddings, each satisfying the assumption $\textsc{Unif}(\delta)$ for the *same* positive constants r_0, θ_0.

— We assume that the functions $\mathcal{Q}^\delta$ converge to a $\mathcal{C}^2$ smooth function ϑ uniformly on compacts of the plane. Note that the pre-compactness of the family $(\mathcal{Q}^\delta)_{\delta>0}$ is always true, as those functions are 1-lipchitz and defined up to an additive constant.

— The discrete domains Ω^δ on which the FK observables are defined approximate in the Carathéodory sense (see [47, Sect 3.2]) a simply connected domain Ω with a $\mathcal{C}^1$ smooth boundary.

Given the methods we use in our proof, the first assumption could be in principle weakened to an assumption similar to $\textsc{Lenght-Exp-Fat}(\delta)$ without changing any conceptual ingredient. We do not include such a generalization here to simplify proof-reading. The assumption on the smoothness of ϑ is mainly done to prove the *uniqueness* of solutions to the naturally associated Riemann-Hilbert type

boundary value problem in continuum. Let us still mention that a generalization of the comparison principle stated in [138, Lemma 3.6] to functions ϑ whose second derivatives are in some L^p space is plausible and would lead to a similar convergence statement with the proof presented here. Finally, the purpose of the domain smoothness assumption is to enable the use of the discrete *comparison principle* in special topological rectangles to provide a short derivation of survival of Dirichlet boundary conditions when passing to the continuous limit of the functions H^δ. The study of convergence in rough domains, as performed in [138, 46], is seriously more evolved, from both the discrete and continuous analysis perspective, even in the case of smooth functions ϑ and is left for further researches. Let us still mention the case of 'flat' s-embeddings (assuming $\mathcal{Q}^\delta = O(\delta)$), where the convergence of the FK-observables in arbitrary rough domains was proved by Chelkak (see [33, Theorem 1.2]), extending already known results for the critical model on isoradial grids that satisfy the bounded angle property [48, Theorem A and B] and proving conformal invariance of the model.

In what follows, we fix a bounded simply connected domain Ω whose boundary is $\mathcal{C}^1$ smooth. One distinguishes two boundary points $a, b \in \partial\Omega$, considered as prime ends. Let Ω^δ be a discrete domain with two marked corners $a^\delta, b^\delta \in \partial\Omega^\delta$ such that $(\Omega^\delta, a^\delta, b^\delta)$ approximates (Ω, a, b) up to $o_{\delta\to 0}(1)$ in the Carathéodory sense. One can define the FK-Dobrushin correlator X^δ on $(\Omega^\delta, a^\delta, b^\delta)$ with *wired* boundary conditions on the arc $(b^\delta a^\delta)^\circ$ and *free* boundary conditions on the arc $(a^\delta b^\delta)^\bullet$ by setting

$$X^\delta(c) := \mathbb{E}^{\mathsf{w},\mathsf{f}}_{(\Omega^\delta, a^\delta, b^\delta)}[\chi_c \sigma_{(b^\delta a^\delta)^\circ} \mu_{(a^\delta b^\delta)^\bullet}]. \tag{6.1.1}$$

The correlator X^δ induces an s-holomorphic function F^δ defined via (5.2.14), together with a function $H^\delta = H^\delta_X = H_{F^\delta}$ defined via (5.2.17) and (5.2.16). A straightforward computation shows that $|X^\delta(a^\delta)| = |X^\delta(b^\delta)| = 1$, thus one can choose the additive constant in the definition of H^δ such that $H^\delta \equiv 0$ on the arc $(b^\delta a^\delta)^\circ$ and $H^\delta \equiv 1$ on the arc $(a^\delta b^\delta)^\bullet$. It is then possible to use the maximum principle recalled in Proposition 5.2.7 to see that $0 \leqslant H^\delta \leqslant 1$ in the entire domain Ω^δ.

Controlling the values of H^δ *at a small macroscopic distance from the boundary* is a rather delicate question in the general s-embeddings setup, to which we provide here a completely novel approach, by proving first a similar statement for observables defined in a local *comparison* domain, which has nicer boundary arcs. To conclude for H^δ near the boundary of Ω, it is then enough to use the *comparison principle* recalled in Proposition 5.2.7. We describe now the main result of this chapter.

Theorem 6.1.1. Let $(\Omega^\delta, a^\delta, b^\delta)_{\delta>0}$ be discrete domains with wired boundary conditions on the arc $(b^\delta a^\delta)^\circ$ and free boundary conditions on the arc $(a^\delta b^\delta)^\bullet$, approximating in the Carathéodory sense a simply connected domain

(Ω, a, b), with two different marked points a, b in its $\mathcal{C}^1$ smooth boundary. If the functions $(\mathcal{Q}^\delta)_{\delta>0}$ converge to a $\mathcal{C}^2$ smooth function ϑ as $\delta \to 0$, then the s-holomorphic functions $(F^\delta)_{\delta>0}$ converge to the unique continuous fonction f such that

— the differential form $(f dz + i\overline{f} d\vartheta)$ is closed in Ω,

— $h := \frac{1}{2}\int \mathrm{Im}[f^2 dz] + |f|^2 d\vartheta$ extends continuously to 0 in the arc (ba) and to 1 in the arc (ab).

In order to prove this theorem, we first focus on treating observables defined in a local domain near a given boundary point, chosen with *nice* discrete boundary cuts. In that case, the general interpretation of projections of s-holomorphic functions as *harmonic functions* (in some particular sense) becomes extremely useful. We give now a reminder on the interpretation of the harmonicity of projections of s-holomorphic functions defined on an s-embedding $\mathcal{S}^\delta$ via random walks on the associated S-graphs. The next section repeats a discussion made in [33, Section 2.5].

6.1.1 . Short reminder on the link between s-holomorphic functions and S-graphs

We first recall the notion of *S-graphs* associated to s-embeddings, which are the key object to derive the regularity theory for discrete s-holomorphic functions (see [33, Section 2.3]). We follow exactly the notations of [33, Section 2.6] and recall the arguments given there. We start with following definition, introduced first in the dimers context (see e.g. [45] and references therein) and adapted to the s-embeddings setup in [33, Definition 2.7]

Definition 6.1.1. Given a proper and non-degenerate s-embedding $\mathcal{S} : \Lambda(G) \to \mathbb{C}$ whose associated origami map is $\mathcal{Q} : \Lambda(G) \to \mathbb{R}$ and an unimodular number α, we call the map $\mathcal{S} + \alpha^2\mathcal{Q} : \Lambda(G) \to \mathbb{C}$ an S-graph associated to $\mathcal{S}$. The S-graph is called *non-degenerate* if for all $v \neq v'$, one has $(\mathcal{S} + \alpha^2\mathcal{Q})(v) \neq (\mathcal{S} + \alpha^2\mathcal{Q})(v')$.

When $\mathcal{S}$ is a proper and non-degenerate s-embedding, degeneracies in the S-graph $\mathcal{S}+\alpha^2\mathcal{Q}$ happen exactly at edges $(v^\circ v^\bullet)$ such that $\mathcal{S}(v^\bullet)-\mathcal{S}(v^\circ) \in -\alpha^2\mathbb{R}_+$. One can see using (5.2.10) that for a quad $z = (\mathcal{S}(v_0^\bullet)\mathcal{S}(v_0^\circ)\mathcal{S}(v_1^\bullet)\mathcal{S}(v_1^\circ)) \in \diamondsuit(G)$ and $p, q \in \{0, 1\}$, the following geometrical observation, first stated in [33, eq (2.13)], holds

$$\mathrm{Re}[\,\overline{\alpha}^2(\mathcal{S} + \alpha^2\mathcal{Q})(v_p^\bullet(z))\,] \;\geq\; \mathrm{Re}[\,\overline{\alpha}^2(\mathcal{S} + \alpha^2\mathcal{Q})(v_q^\circ)(z)\,], \tag{6.1.2}$$

with an equality possible if and only if $\mathcal{S} + \alpha^2\mathcal{Q}$ is degenerate. In that case, one of the edges $(\mathcal{S}(v_p^\bullet(z))\mathcal{S}(v_q^\circ(z)))$ is collapsed into a point in the $\mathcal{S} + \alpha^2\mathcal{Q}$ plane. Geometrically, the image $(\mathcal{S} + \alpha^2\mathcal{Q})^\diamond(z)$ of a tangential quadrilateral $\mathcal{S}^\diamond(z)$ in a non-degenerate S-graph is a *non-convex* quadrilateral (see e.g. [33, Fig. 3 (C)]).

We recall now how the introduction of S-graphs is useful, as they provide an interpretation to projections of s-holomorphic functions as harmonic functions. The catch-point of this discussion is Proposition 6.1.3, that states that $\Pr[F\,;\alpha\mathbb{R}]$ is a harmonic function with respect to some directed random walk denoted $\widetilde{X}_t$ on vertices of the S-graph $\mathcal{S}-i\overline{\alpha}^2\mathcal{Q}$. This means that $\operatorname{Re}F$ can be seen as harmonic for some random walk on $\mathcal{S}-i\mathcal{Q}$ while $\operatorname{Im}F$ can be seen as a harmonic function for *another* random walk on $\mathcal{S}+i\mathcal{Q}$. We only work here on *non-degenerated* S-graphs. Indeed, the theory extends directly to the degenerate case as the law of the associated random walks is continuous with respect to the variable $\alpha\in\mathbb{T}$. The appropriate modifications in the degenerate case are explicited in [45, Remark 4.7 and Remark 4.18].

There is a priori an inconsistency of notation in the previous paragraph, as the function $\Pr[F(z)\,;\alpha\mathbb{R}]$ is defined on quads of $\diamondsuit(G)$ while the announced harmonic functions on S-graphs are defined on the image of $\Lambda(G)$ by $\mathcal{S}+\alpha^2\mathcal{Q}$. We clarify now this ambiguity following [33, Definition 2.13]. Given $\mathcal{S}$ a proper non-degenerate s-embedding and $\alpha\in\mathbb{T}$, let $z\mapsto v^{(\alpha)}(z)$ be the map that sends z to the pre-image of the *non-convex* vertex of the quad $(\mathcal{S}+\alpha^2\mathcal{Q})^\diamond(z)$. In the bulk, this mapping $z\mapsto v^{(\alpha)}(z)$ is actually a bijection between $\diamondsuit(G)$ and $\Lambda(G)$, that depends on the value of α. This bijection changes at values of α where $\mathcal{S}+\alpha^2\mathcal{Q}$ becomes degenerate. We recall now the definition of a continuous time random walk X_t in $\mathcal{S}+\alpha^2\mathcal{Q}$, introduced in [33, Definition 2.14], whose transition rates admit a natural geometrical interpretation.

Definition 6.1.2. Given $\mathcal{S}+\alpha^2\mathcal{Q}$ a non-degenerate S-graph, set $X_t=X_t^{(\alpha)}$ the continuous time random walk on $\Lambda(G)$ defined such that :

(i) the only non-vanishing outgoing jump rates from $v(z)=v^{(\alpha)}(z)$ are those towards the three other vertices of the quad $(\mathcal{S}+\alpha^2\mathcal{Q})^\diamond(z)$;

(ii) these three non-vanishing jump rates are chosen so that both processes $(\mathcal{S}+\alpha^2\mathcal{Q})(X_t)$ and $\operatorname{Tr}\operatorname{Var}[(\mathcal{S}+\alpha^2\mathcal{Q})(X_t)]-t$ are martingales.

As noted in [33, (2.19)], the *invariant measure* μ for the continuous time random walk X_t is independant from α and is given explicitly by $\mu(v(z)):=\frac{1}{2}\text{Area}(\mathcal{S}^\diamond(z))$ i.e. the invariant measure has a fully geometrical meaning in $\mathcal{S}$. One can then define $\widetilde{X}_t=\widetilde{X}_t^{(\alpha)}$ as the *time reversal* random walk of $X_t=X_t^{(\alpha)}$ with respect to the invariant measure μ. The relevance of backward walks was first noticed in [45, Proposition 4.17] in the dimers context and was then translated to the Ising context in [33, Prop 2.16]. We emphasize once again that the next proposition is the key takeaway point of this reminder, and was first stated in [33, Proposition 2.16].

Proposition 6.1.3. Let F be an s-holomorphic function defined on $\mathcal{S}$ and $\alpha\in\mathbb{T}$. Then the function $\Pr[F\,;\alpha\mathbb{R}]$ is a martingale with respect to the backward walk $\widetilde{X}_t=\widetilde{X}_t^{(i\varsigma\overline{\alpha})}$ on $\mathcal{S}-\varsigma^2\overline{\alpha}^2\mathcal{Q}=\mathcal{S}-i\overline{\alpha}^2\mathcal{Q}$.

6.1.2 . Construction of discrete half plane

In this subsection, we recall the definition and the construction of discrete half-planes coming from S-graphs. Those special cuts, when mapped back to $\mathcal{S}$, induce fermionic observables with a *nicer close to boundary behavior*. As for now, we fix a sequence of s-embeddings $(\mathcal{S}^\delta)_{\delta>0}$ satisfying $\mathrm{LIP}(\kappa,\delta)$ and work for a fixed grid $\mathcal{S}^\delta$, where δ is chosen small enough. The construction of the discrete half-planes of $\mathcal{S}^\delta$ was first performed in [33, Section 5.1], and we focus here on discrete half-planes in $\mathcal{S}^\delta$ coming from the S-graph $\mathcal{S}^\delta - i\mathcal{Q}^\delta$. The modifications for other values of α are rather straightforward and detailed in [33, Section 5.1]. In order to simplify proof-reading, we identify the vertices in $\mathcal{S}^\delta$ with their images in $\mathcal{S}^\delta - i\mathcal{Q}^\delta$, via the bijection $z \mapsto v^{(i)}(z)$, and only work with non-degenerated S-graphs (which is always possible on compacts of the plane by a small rotation). We use the hat $\hat{}$ notation for elements of S-graphs.

Fix an horizontal line in the $\mathcal{S}^\delta - i\mathcal{Q}^\delta$ plane that doesn't contain any vertex of $(\mathcal{S}^\delta - i\mathcal{Q}^\delta)(\Lambda(G))$ and assume (which is always possible up to a vertical shift of $\mathcal{S}^\delta$) that this line is the horizontal axis $y = 0$. In that case, the geometrical inequality (6.1.2) ensures that in any concave quadrilateral $(\mathcal{S}^\delta - i\mathcal{Q}^\delta)^\diamond(z)$, the two 'black' vertices lie *below* the two 'white' vertices. Let $\hat{G}^\bullet_{(-)} \subseteq \mathcal{S}^\delta - i\mathcal{Q}^\delta$ (respectively $\hat{G}^\bullet_{(+)} \subseteq \mathcal{S}^\delta - i\mathcal{Q}^\delta$) be the set of vertices of the $\mathcal{S}^\delta - i\mathcal{Q}^\delta$ plane with *negative* (respectively *positive*) vertical coordinate. The set $\hat{G}^\bullet_{(-)}$ is connected. Indeed for $\hat{v}^\bullet_1 \in \hat{G}^\bullet_{(-)}$, let $\hat{v}^\bullet_2$ be the other 'black' vertex of the quadrilateral $(\mathcal{S}^\delta - i\mathcal{Q}^\delta)^\diamond(z)$ convave at $\hat{v}^\bullet_1$. Then the concavity at $\hat{v}^\bullet_1$ and the fact that $\hat{v}^\circ_{1,2}$ are strictly above $\hat{v}^\bullet_1$ impose that $\hat{v}^\bullet_2$ lies strictly *below* $\hat{v}^\bullet_1$. As the graph is locally finite, one can iterate such a consideration to prove connecteness of $\hat{G}^\bullet_{(-)}$. We recall now the definition of the discrete upper half-plane introduced in [33, Definition 5.1]

Definition 6.1.4. Let $\partial\hat{\mathbb{H}}^\circ_{\mathcal{S}^\delta}$ be the simple path of the $\mathcal{S}^\delta - i\mathcal{Q}^\delta$ plane that separates $\hat{G}^\bullet_{(-)}$ from $\hat{G}^\bullet_{(+)}$. One denotes $\partial\mathbb{H}^\circ_{\mathcal{S}^\delta} \subseteq G^\circ \cup \diamondsuit(G)$ its premiage in the $\mathcal{S}^\delta$ plane. The discrete upper-half plane is the connected component of the $\mathcal{S}^\delta$ plane that lies above $\partial\mathbb{H}^\circ_{\mathcal{S}^\delta}$.

An example of a piece of $\partial\mathbb{H}^\circ_{\mathcal{S}^\delta}$ is given in [33, Figure 6]. As emphasized below [33, Definition 2.2], $\partial\hat{\mathbb{H}}^\circ_{\mathcal{S}^\delta}$ is a *simple path*. When pulling back to $\mathcal{S}^\delta$, on views the set $\partial\mathbb{H}^\circ_{\mathcal{S}}$ as a sequence of neighboring vertices of G°, each pair of neighbors being separated by a quad $z \in \partial\mathbb{H}^\circ_{\mathcal{S}}$. As a consequence of the construction, for any two adjacent vertices $\hat{v}^\circ_1, \hat{v}^\circ_2$ of $\partial\mathbb{H}^\circ_{\mathcal{S}^\delta}$, the quad $(\hat{v}^\circ_1\hat{v}^\bullet_1\hat{v}^\circ_2\hat{v}^\bullet_2)$ in $\mathcal{S}^\delta - i\mathcal{Q}^\delta$ contains exactly one black vertex $\hat{v}^\bullet_1 \in \hat{G}^\bullet_{(+)}$ while the other black vertex $\hat{v}^\bullet_2$ belongs to $\hat{G}^\bullet_{(-)}$. It is also easy to note that all points of $\partial\hat{\mathbb{H}}^\circ_{\mathcal{S}^\delta}$ lie at most at a distance 4δ from the axis $y = 0$ in the $\mathcal{S}^\delta - i\mathcal{Q}^\delta$ plane (as all edges of $\mathcal{S}^\delta$ are of length smaller than δ and $\mathcal{Q}^\delta$ is a 1-lipchitz function).

Lemma 6.1.1. *Let $\alpha \in \mathbb{T}$ and fix $\hat{\mathcal{L}}$ a (straight) segment of lenght $l \geqslant 100\delta$ in $\mathcal{S}^\delta - i\alpha^2\mathcal{Q}^\delta$ plane, parallel to the direction $\alpha^2\mathbb{R}$ and parametrized in the positive*

direction of $\alpha^2\mathbb{R}_+$. *Then there exist a polygonal line* $\hat{\mathcal{D}}$ *of the* $\mathcal{S}^\delta - i\alpha^2\mathcal{Q}^\delta$ *plane formed by adjacent edges of* $\mathcal{S}^\delta - i\alpha^2\mathcal{Q}^\delta$ *such that*

— $\hat{\mathcal{D}}$ *is a simple path that remains at a distance at most* 4δ *from* $\hat{\mathcal{L}}$.

— $\hat{\mathcal{D}}$ *belongs to a discrete half-plane in* $\mathcal{S}^\delta - i\alpha^2\mathcal{Q}^\delta$.

We denote $\mathcal{D} \subset \Lambda(G)$ *the pre-image such a polygonal line* $\hat{\mathcal{D}}$ *in* $\mathcal{S}^\delta$.

The polygonal line $\hat{\mathcal{D}}$ is called an *adapted straight cut* to $\mathcal{S}^\delta - i\alpha^2\mathcal{Q}^\delta$. In the case of $\alpha = 1$, the above lemma simply means that provided δ is small enough, any horizontal segment $\hat{\mathcal{L}}$ in the $\mathcal{S}^\delta - i\mathcal{Q}^\delta$ plane of length at least 100δ can be approximated by simple path formed by edges of $\mathcal{S}^\delta - i\mathcal{Q}^\delta$ at a distance at most 4δ.

Proof. This is a simple consequence of the construction of discrete half-planes recalled above, from which we only keep a finite piece to construct $\hat{\mathcal{D}}$. □

To construct discrete half-planes in $\mathcal{S}^\delta - i\alpha^2\mathcal{Q}^\delta$, one repeats the same procedure using a line parallel to $\alpha^2\mathbb{R}$ and the geometrical inequality (6.1.2). Let us also mention that similar constructions of discrete half-planes of the form $\partial\mathbb{H}^\bullet_{\mathcal{S}^\delta}$ are possible and are precised at the end of [33, Section 5.2].

The focus on construction of discrete half-planes is based on the following observation

— When the backward walk in an S-graph jumps across a discrete half-plane, it is possible to *redistribute* its values to nearby boundary quads of $\partial\mathbb{H}^\circ_{\mathcal{S}^\delta}$ while maintaining the martingale property, which allows to keep applying the optional stopping theorem [33, Definition 5.5 and Lemma 5.6].

In the following discussion, we keep exactly the notation of [33, Section 5.3]. As mentionned in the previous lines, one needs to be careful about the interpretation of the projection $\mathrm{Re}[\beta F]$ as a harmonic function *near the boundary of* $\partial\mathbb{H}^\circ_{\mathcal{S}^\delta}$. Indeed, consider a boundary vertex $v^\circ \in \partial\mathbb{H}^\circ_{\mathcal{S}^\delta}$ corresponding to a quad $z \in \diamondsuit(G)$ via the bijection $z \mapsto v^{(-i\beta^2)}(z)$. Then, it can happen that the values $\mathrm{Re}[\beta F(z)]$ are distributed *outside of* $\mathbb{H}^\circ_{\mathcal{S}^\delta}$, which doesn't allow to apply the optional stopping theorem for martingales stopped at the boundary of $\partial\mathbb{H}^\circ_{\mathcal{S}^\delta}$ (as $\mathrm{Re}[\beta F]$ is not defined outside of the domain). Following the notation of [33, Definition 5.5 Lemma 5.6 and 5.7], fix $z_\pm \in \partial\mathbb{H}^\circ_{\mathcal{S}^\delta}$ attached to a boundary vertex $v^\circ \in \partial\mathbb{H}^\circ_{\mathcal{S}^\delta}$. If $\mathrm{Re}[\beta F(z)]$ is sent outside of $\mathbb{H}^\circ_{\mathcal{S}^\delta}$ by the backward walk, one can *redistribute* the value $\mathrm{Re}[\beta F(z)]$ sent to quads outside of $\mathbb{H}^\circ_{\mathcal{S}^\delta}$ to $\mathrm{Re}[\beta F(z_\pm)]$ while maintaining the martingale property, at least if the boundary is chosen coming from a discrete half-plane. To see that, list (as in [33, Lemma 5.6]) in the counterclockwise order $z_+ = z_0, \dots, z_n = z_- \in \mathbb{H}^\circ_{\mathcal{S}^\delta}$ the neighbors of v° in $\mathbb{H}^\circ_{\mathcal{S}^\delta}$. Working e.g. near a wired arc, one has the identity (which is a direct analogue of [33, eq (5.9)])

$$\sum_{k=1}^{n}\Big(\frac{\mathrm{Re}[\overline{\beta}\eta_{k+1}]}{\mathrm{Im}[\overline{\beta}\eta_{k+1}]}-\frac{\mathrm{Re}[\overline{\beta}\eta_{k}]}{\mathrm{Im}[\overline{\beta}\eta_{k}]}\Big)\,\mathrm{Re}[\beta F(z_k)]+\Big(\frac{\mathrm{Re}[\overline{\beta}\eta_{1}]}{\mathrm{Im}[\overline{\beta}\eta_{1}]}-\frac{\mathrm{Re}[\overline{\beta}\eta_{out}]}{\mathrm{Im}[\overline{\beta}\eta_{out}]}\Big)k_+^{(\beta)}\,\mathrm{Re}[\beta F(z_+)]$$
$$+\Big(\frac{\mathrm{Re}[\overline{\beta}\eta_{out}]}{\mathrm{Im}[\overline{\beta}\eta_{out}]}-\frac{\mathrm{Re}[\overline{\beta}\eta_{n}]}{\mathrm{Im}[\overline{\beta}\eta_{n}]}\Big)k_-^{(\beta)}\,\mathrm{Re}[\beta F(z_-)],$$

where the coefficients $k_\pm^{(\beta)}$ are given by

$$k_+^{(\beta)}:=\frac{\mathrm{Im}[\mathcal{X}(c_{++})\overline{\mathcal{X}(c_{+-})}]}{\mathrm{Im}[\mathcal{X}(c_{+-})\overline{\mathcal{X}(c_{out})}]}\cdot\frac{\mathrm{Im}[\varsigma\overline{\beta\mathcal{X}(c_{out})}]}{\mathrm{Re}[-i\overline{\varsigma}\beta(\mathcal{X}(c_{++})-\mathcal{X}(c_{+-}))]},\tag{6.1.3}$$

$$k_-^{(\beta)}:=-\frac{\mathrm{Im}[\mathcal{X}(c_{--})\overline{\mathcal{X}(c_{-+})}]}{\mathrm{Im}[\mathcal{X}(c_{-+})\overline{\mathcal{X}(c_{out})}]}\cdot\frac{\mathrm{Im}[\varsigma\overline{\beta\mathcal{X}(c_{out})}]}{\mathrm{Re}[-i\overline{\varsigma}\beta(\mathcal{X}(c_{-+})-\mathcal{X}(c_{--}))]}.\tag{6.1.4}$$

This observation is similar to the one of [33, Lemma 5.6], replacing formally in the proof F by βF, η by $\overline{\beta}\eta$ and $\mathcal{X}$ by $\beta\mathcal{X}$. If one wants to apply the redistribution procedure to $z_\pm$, one needs to check that the redistribution coefficients $k_\pm^{(\beta)}$ for the backward walk on $\mathcal{S}^\delta-i\beta^2\mathcal{Q}^\delta$ are positive. With the boundary cuts chosen in the kite region in Section 6.1.3 *for the FK observable in the comparison domain*, it will be the case. Considering e.g. the coefficient $k_+^{(\beta)}$, one has (from the discussion below $(6.1.5)$ in Section 6.1.4) up to a global choice of sign in the definition of the Dirac spinor $\mathcal{X}_\varepsilon$ of the comparison domain (in the setup used in Section 6.1.5) :

— The observable F_ε^δ has a boundary argument in $[-\frac{\pi}{4};\frac{\pi}{4}]$ and is positively colinear to $\exp\left(i\varsigma(\overline{\mathcal{X}_\varepsilon(c_{++})}-\overline{\mathcal{X}_\varepsilon(c_{+-})})\right)$.

— One works with $\beta\in\mathbb{T}$ such that $|\arg(\beta)|\leqslant\frac{\pi}{4}-\mathsf{cst}(\kappa)$. In that case one directly deduces that $\mathrm{Re}[-i\overline{\varsigma}\beta(\mathcal{X}_\varepsilon(c_{++})-\mathcal{X}_\varepsilon(c_{+-}))]$ is positive.

This is sufficient to conclude on the positivity of $k_+^{(\beta)}$ when $|\arg(\beta)|\leqslant\frac{\pi}{4}-\mathsf{cst}(\kappa)$ since (fixing the sign of $\mathcal{X}_\varepsilon(c_{out})$ in a 'continuous counterclockwise turn' starting from $\mathcal{X}_\varepsilon(c_{-+})$ in the notation of [33, Figure 7]), one sees that

— the first factor in $k_+^{(\beta)}$ is positive, exactly as in the proof of [33, Lemma 5.7] (this first factor is in fact independant from β)

— If v° corresponds to z_k for $1\leqslant k\leqslant n-1$ via the bijection $v^{(-i\beta^2)}$, this then means that the ray $i\overline{\beta}^2\mathbb{R}_+$ lies in between $(\mathcal{S}(v_k^\bullet)-\mathcal{S}(v^\circ))\mathbb{R}_+$ and $(\mathcal{S}(v_{k+1}^\bullet)-\mathcal{S}(v^\circ))\mathbb{R}_+$. This implies in particular (with the notation of [33, Figure 7]) that the ray $i\overline{\beta}^2\mathbb{R}_+$ lies in between $(\mathcal{S}(v_+^\bullet)-\mathcal{S}(v^\circ))\mathbb{R}_+$ and $(\mathcal{S}(v_-^\bullet)-\mathcal{S}(v^\circ))\mathbb{R}_+$ and implies that $\mathrm{Im}[\varsigma\overline{\beta\mathcal{X}_\varepsilon(c_{out})}]$ is positive (still as in the proof of [33, Lemma 5.7]).

Let us emphasize that the possibility to redistribute the walk while maintaining the martingale property (which amounts to check that $k_\pm^{(\cdot)}$ is positive) is not only true for the value $(\cdot)=\beta$ that will be fixed in the third step of Section 6.1.3 but also for values $\beta e^{i\pm\varphi_0(\kappa)}$ for some small enough positive constant $\varphi_0(\kappa)$ that only depends on κ.

6.1.3 . Surgery and extension of the original domain

One of the key ideas we introduce in the chapter to control the values of the functions H^δ *macroscopically* close to the boundary of Ω_δ (that is still assumed to approximate a bounded $\mathcal{C}^1$ smooth domain Ω) is to control first the boundary values of the function H^ε_δ associated to a correlator defined in a local topological rectangle around a given boundary point. This topological rectangle will be chosen such that a part of its boundary contains the pre-image of properly chosen straight cuts. Recall here that we assumed that the functions $\mathcal{Q}^\delta$ converge uniformly to a $\mathcal{C}^2$ smooth function ϑ as $\delta \to 0$. All the different surgeries described below are *local* near one of the boundary points and the structure of Ω away from that boundary point is irrelevant to our construction.

Step 1 : Surgery in Ω

One first orients the boundary of Ω in the counterclockwise direction and parametrize it by a smooth arc $\gamma : [0;1] \mapsto \mathbb{C}$. Fiz a point $\gamma(t_0) = z \in \partial\Omega$. One can define $\vec{u} = \vec{u}(z)$ the *unitary tangent vector* at z, oriented in the same direction as $\partial\Omega$, a well as $\vec{\tau} = \vec{\tau}(z)$, the outer normal at $z \in \partial\Omega$. Fix $\varepsilon > 0$ a small number. For l_0 small enough, consider the *square* $\Omega_z^{l_0} := z + ([-5l_0; 5l_0]\cdot\vec{u}) \times ([-5l_0; 5l_0]\cdot\vec{\tau})$ of width $10l_0$ and centered at z. One can make the following observations :

- $\gamma^{-1}(\Omega_z^{l_0})$ is a finite union of disjoint intervals $[t_j^-; t_j^+]$ such that $t_0 \in [t_{j_0}^-; t_{j_0}^+]$.
- The arc (drawn in red in Figure 6.1.1) $\mathcal{C}_{z,\varepsilon,l_0} := \gamma([t_{j_0}^-; t_{j_0}^+])$ is smooth and connects the two opposite sides of the square $\Omega_z^{l_0}$ inside the rectangle $z + ([-5l_0; 5l_0] \cdot \vec{u}) \times ([-\varepsilon l_0; \varepsilon l_0] \cdot \vec{\tau})$
- Considering the two connected components of $\Omega_z^{l_0}$ separated by $\mathcal{C}_{z,\varepsilon,l_0}$, the one on the *left* of $\vec{u}$ is entirely included in Ω (if l_0 is chosen small enough).

It is possible that the boundary of Ω is self-touching at z, but with an arc (oriented in natural parametrization of γ) coming from the connected component of $\Omega_z^{l_0}$ that is *on the right* of $\vec{u}(z)$. This is a consequence of the fact that the interior of Ω is always on the *left* of the tangent vector $\vec{u}(z)$.

Step 2 : Extension of $\mathcal{S}^\delta$ by periodic layers of kites

We describe now the second step of the surgery procedure, which focuses on modifying the graphs at the discrete level. We keep working near the boundary point $z = 0$, still assuming that $\vec{u} = 1$, $\vec{\tau} = -i$. This construction is a simple consequence of the extension procedure described in the proof of [117, Proposition 3.1]. Fix $l_0 = l_0(z = 0)$ (that is a local quantity that depends on $z = 0$) small enough to be able to apply Step 1. Using the work of [117, Section 3] and under the hypothesis $\textsc{Unif}(\delta)$, one can find a level $y_0^\delta = -2\varepsilon l_0 + o_{\delta\to}(1)$ and perform a extension from *below* of rectangle $[-4l_0; 4l_0] \times ([-2\varepsilon l_0; \varepsilon l_0] + o_{\delta\to}(1))$ while remaining in the s-embedding setup such that

- below the level y_0^δ, the extension of $[-4l_0; 4l_0] \times ([-2\varepsilon l_0; \varepsilon l_0] + o_{\delta\to 0}(1))$ fills the rectangle $[-4l_0; 4l_0] \times ([-4\varepsilon l_0, \varepsilon l_0])$ by periodic (in the vertical direction)

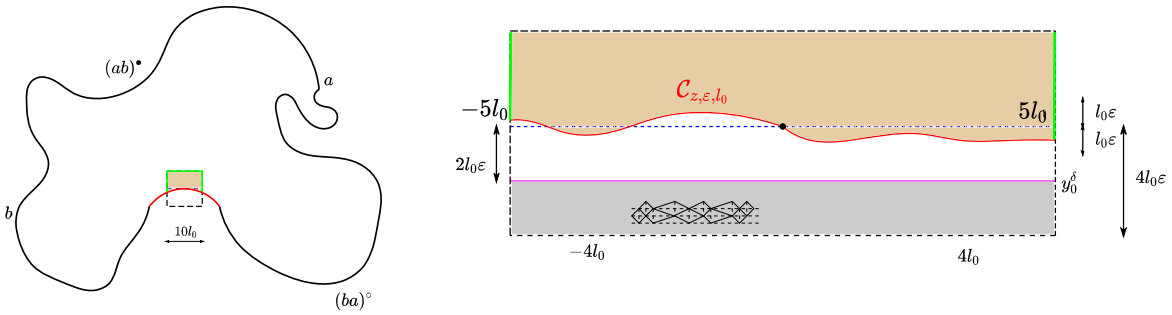

FIGURE 6.1.1 – (Left) Global picture of the domain Ω with wired arc $(ba)^\circ$ and free arc $(ab)^\bullet$. The boundary arc $\mathcal{C}_{z,\varepsilon,l_0}$ near $z=0$ is drawn in red. The green arc corresponds to the free arc of the discrete comparison domain $\Omega^\delta_{z,\varepsilon,l_0}$. The interior of Ω is filled in orange pale. (Right) Zoom near the boundary point $z=0$. The zone in grey is filled with kites (below the axis $y=-2\varepsilon l_0$ drawn in purple) by the surgery procedure described in Step 2.

layers of *kites*, whose symmetry axes are horizontal.

— All the faces of the extended picture have a radius $r_z \geqslant \delta^{200}$.

— The entire extended picture satisfies $\mathrm{Lip}(\kappa, 5\delta)$.

The kites region is filled in grey in Figure 6.1.1. As a consequence of the periodical copy procedure in the vertical direction, below the level y_0^δ, one has $d\mathcal{Q}^\delta_{ext} = 0$ between two vertically aligned vertices of the same kite (for both colors). In particular, as $\delta \to 0$, one can see in the region $[-4l_0; 4l_0] \times [-4\varepsilon l_0, -2\varepsilon l_0]$ that $d\vartheta_{ext} = 0$ *in the vertical direction*, while $d\vartheta_{ext}(x+iy) = d\vartheta_{ext}(x - 2il_0\varepsilon)$ for any $x \in [-4l_0; 4l_0]$ and $y \leqslant -2l_0\varepsilon$.

Step 3 : Choice of the boundary of the extended domain

Fix a small number $\varepsilon > 0$ and assume we are still in the setup where $z=0$, $\vec{u}=1$, $\vec{\tau}=-i$. Also assume that $\mathcal{Q}^\delta(0)=0$, which is always possible up to a proper choice of additive constant. Recall that ϑ (which still denotes as for now the limiting origami map *before the surgery procedure* of Step 2) is differentiable at $z=0$. It is possible to choose l_0 small enough such that

— The construction of the domain $\Omega^{l_0}_z$ given in Step 1 is possible.

— The kites surgery given in Step 2 is possible.

— There exist $a, b \in \mathbb{R}$, such that $\vartheta(x,y) = ax + by + (|x| + |y|)p(x,y)$ for any (x,y) in the square of width $10l_0$ centered at $z=0$, with an error term $p(x,y)$ satisfying $|p(x,y)| \leqslant \varepsilon^2$.

Using the κ-lipchitzness of ϑ for a small enough multiple of the unitary vector $(a^2+b^2)^{-\frac{1}{2}}(a,b)$, one can see that $a^2+b^2 \leqslant \kappa^2$.

As recalled at the end of Step 2, the discrete surgery procedure amounts to copy the boundary of the original graph (after slicing it in the horizontal direction) in the vertical direction. It produces then a vanishing vertical increment of $d\mathcal{Q}^\delta_{ext}$ for any two vertically aligned adjacent vertices of the same color. This implies that *after the surgery procedure*, (whose embedding after adding the kites is still denoted by $\mathcal{S}^\delta$), one has the following estimates for $\mathcal{Q}^\delta_{ext}$:

— $\mathcal{Q}^\delta_{ext}(x,y) = ax + by + p(x,y)(|x|+|y|) + o_{\delta\to 0}(1)$ if $y \geqslant -2\varepsilon l_0$,

— $\mathcal{Q}^\delta_{ext}(x,y) = ax - 2b\varepsilon l_0 + p(x,y)(|x|+|y|) + o_{\delta\to 0}(1)$ if $y \leqslant -2\varepsilon l_0$.

for some function $|p(x,y)| \leqslant \varepsilon^2$ in the entire rectangle $[-4l_0; 4l_0] \times [-4l_0\varepsilon; 4l_0]$. In what follows, we write $\mathcal{Q}^\delta = \mathcal{Q}^\delta_{ext}$ and assume the above surgery consisting in adding the kites near $z = 0$ has already been done at discrete level.

We are now going to define the boundary of the discrete extended domain in the $\mathcal{S}^\delta$ plane, by pulling-back straight cuts of properly chosen S-graphs. The choice of the S-graph used to construct the discrete boundary near a given point is made to send segments parallel to the tangent at $z \in \partial\Omega$ to *almost* straights cuts in the corresponding S-graph (i.e. small segments parallel to the tangent at z in the $\mathcal{S}^\delta$ plane are sent close to segments parallel to $\beta^2\mathbb{R}$ in the $\mathcal{S}^\delta - i\beta^2\mathcal{Q}^\delta$ plane). The following description still concerns the case $z = 0$, $\vec{u} = 1$, $\vec{\tau} = -i$ and can be easily adapted for any boundary point.

Let $\beta \in \mathbb{U}$ be chosen such that $\beta^2 = \cos(2\beta_0) + i\sin(2\beta_0)$, with $\sin(2\beta_0) + a = 0$ and $\cos(2\beta_0) > 0$. Since $|a| \leqslant \kappa$, one can choose $|\beta_0| \leqslant \frac{\pi}{4} - \mathrm{cst}(\kappa)$ for some positive constant $\mathrm{cst}(\kappa)$ only depending on κ. We keep identifying the vertices in the $\mathcal{S}^\delta$ plane with their counterparts in S-graphs, writing the latter with hats. We define now the boundary of the extended domain as follows. For $t \in [-4\varepsilon l_0; \varepsilon^{\frac{1}{2}} l_0]$, set

— $\hat{v}^\delta_t := [\mathcal{S}^\delta - i\beta^2\mathcal{Q}^\delta](it)$ as the image of the point it in the $\mathcal{S}^\delta - i\beta^2\mathcal{Q}^\delta$ plane.

— $\hat{L}^\delta_t := 3\beta^2\cos(2\beta_0)[-l_0; l_0] + \hat{v}^\delta_t$ as a *straight segment* in the $\mathcal{S}^\delta - i\beta^2\mathcal{Q}^\delta$ plane passing by $\hat{v}^\delta_t$ and parallel to the direction $\beta^2\mathbb{R}$. We emphasize that $\hat{L}^\delta_t$ is *not* an approximation by some edges of the discrete set $[\mathcal{S}^\delta - i\beta^2\mathcal{Q}^\delta](\Lambda(G))$ but a usual segment of the $\mathcal{S}^\delta - i\beta^2\mathcal{Q}^\delta$ plane. We also set its pre-image $L^\delta_t := [\mathcal{S}^\delta - i\beta^2\mathcal{Q}^\delta]^{-1}(\hat{L}^\delta_t)$ in the $\mathcal{S}^\delta$ plane (drawn in orange in 6.1.2). It is clear that L^δ_t contains the point it.

— $\tilde{L}^\delta_t := 3[-l_0; l_0] + it$ as a *straight segment* in the $\mathcal{S}^\delta$ plane (drawn in blue in 6.1.2). We claim that L^δ_t and $\tilde{L}^\delta_t$ are at most at a distance $O(l_0\varepsilon^2) + o_{\delta\to 0}(1)$ from each other in the $\mathcal{S}^\delta$ plane, where the constant O only depends on κ. In words, it means that L^δ_t is almost an horizontal segment in the $\mathcal{S}^\delta$ plane, up to $O(l_0\varepsilon^2) + o_{\delta\to 0}(1)$ vertical fluctuation. To prove this claim, we first show that the images of L^δ_t and $\tilde{L}^\delta_t$ by $\mathcal{S}^\delta - i\beta^2\mathcal{Q}^\delta$ are close in the $\mathcal{S}^\delta - i\beta^2\mathcal{Q}^\delta$ plane. As distances above scale δ are comparable (up to a constant factor only depending on κ) in the $\mathcal{S}^\delta$ and $\mathcal{S}^\delta - i\beta^2\mathcal{Q}^\delta$ planes, this

allows to conclude. This announced proximity between the cuts L_t^δ and $\tilde{L}_t^\delta$ is a consequence of the following facts :

1. The set $[\mathcal{S}^\delta - i\beta^2\mathcal{Q}^\delta](\tilde{L}_t^\delta)$ clearly contains the point $\hat{v}_t^\delta$.
2. Using the two different expansions of $\mathcal{Q}^\delta = \mathcal{Q}^\delta_{ext}$ above and below the axis $y = -2\varepsilon l_0$, one has for $|x_{1,2}| \leqslant 3l_0$:

$$\overline{\beta}^2\Big([\mathcal{S}^\delta - i\beta^2\mathcal{Q}^\delta](x_1+it) - [\mathcal{S}^\delta - i\beta^2\mathcal{Q}^\delta](x_2+it)\Big) = \overline{\beta}^2(x_1-x_2) - ia(x_1-x_2) + O(l_0\varepsilon^2) + o_{\delta\to 0}(1).$$

   As $\mathrm{Im}[\overline{\beta}^2 - ia] = -\sin(2\beta_0) - a = 0$, one can directly see that $\mathrm{Im}[\overline{\beta}^2(x_1 - x_2) - ia(x_1 - x_2)] = 0$ and thus deduce

$$[\mathcal{S}^\delta - i\beta^2\mathcal{Q}^\delta](x_1+it) - [\mathcal{S}^\delta - i\beta^2\mathcal{Q}^\delta](x_2+it) = \beta^2\cos(2\beta_0)(x_1-x_2) + O(l_0\varepsilon^2) + o_{\delta\to 0}(1).$$

   This implies that $[\mathcal{S}^\delta - i\beta^2\mathcal{Q}^\delta](\tilde{L}_t^\delta) = 3\beta^2\cos(2\beta_0)[-l_0; l_0] + \hat{v}_t^\delta + O(l_0\varepsilon^2) + o_{\delta\to 0}(1)$, i.e. with that specific choice of β, horizontal segments in the $\mathcal{S}^\delta$ plane are mapped in the $\mathcal{S}^\delta - i\beta^2\mathcal{Q}^\delta$ plane to *curves almost parallel* to $\beta^2\mathbb{R}$.
3. As a combination of the quasi-conformality of $\mathcal{S}^\delta - i\beta^2\mathcal{Q}^\delta$ above scale δ and the fact that the images of L_t^δ and $\tilde{L}_t^\delta$ are $O(l_0\varepsilon^2) + o_{\delta\to 0}(1)$ close in the $\mathcal{S}^\delta - i\beta^2\mathcal{Q}^\delta$ plane, one deduces that $\tilde{L}_t^\delta$ and L_t^δ are $O(l_0\varepsilon^2) + o_{\delta\to 0}(1)$ close in the $\mathcal{S}^\delta$ plane.

— One can now use Lemma 6.1.1 to construct at a *simple path formed by edges of* $[\mathcal{S}^\delta - i\beta^2\mathcal{Q}^\delta](\Lambda(G))$ at a distance smaller than 4δ from the segment $3\beta^2\cos(2\beta_0)[-l_0; l_0] + \hat{v}^\delta_{-3\varepsilon l_0}$ in the $\mathcal{S}^\delta - i\beta^2\mathcal{Q}^\delta$, coming from the discrete half-plane attached to the last mentionned segment. One denotes by $\hat{L}^{\partial,\delta}_{-3\varepsilon l_0}$ this simple path, as well as $L^{\partial,\delta}_{-3\varepsilon l_0} := [\mathcal{S}^\delta - i\beta^2\mathcal{Q}^\delta]^{-1}(\hat{L}^{\partial,\delta}_{-3\varepsilon l_0})$ its pre-image in the $\mathcal{S}^\delta$ plane, formed by consecutives edges of $\Lambda(G)$.

There is a geometrical observation on the path $L^{\partial,\delta}_{-3\varepsilon l_0}$ in the $\mathcal{S}^\delta$ plane, which has an important implication regarding boundary values of fermionic observables defined in what will be called later the comparison domain (see Section 6.1.4). One first labels the vertices of $L^{\partial,\delta}_{-3\varepsilon l_0} := (v_k)_{k\leqslant k_0^\delta}$ with the natural neighboring order, going (at macroscopic level) from left to right in $\mathcal{S}^\delta$ plane, assuming that vertices of G° correspond to even labels. As the kites have an *horizontal* symmetry axis, there are a priori four possible orientations (see Figure 6.1.3) for the vectors formed by consecutive vertices of $L^{\partial,\delta}_{-3\varepsilon l_0}$:

— Either $\overrightarrow{v^\circ_{2k}v^\circ_{2k+2}}$ is vertical, in the upper or the lower direction.

— Either $\overrightarrow{v^\circ_{2k}v^\circ_{2k+2}}$ is horizontal, from left to right or from right to left.

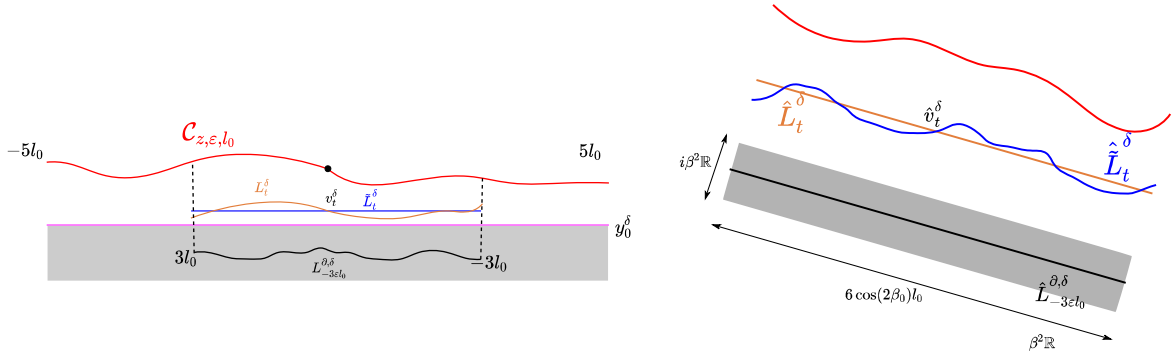

FIGURE 6.1.2 – (Left) Cuts used in the in $\mathcal{S}^\delta$ plane to define the boundary of the comparison domain. The lower boundary of the comparison domain is $L^{\partial,\delta}_{-3\varepsilon l_0}$. (Right) Image of the same cuts in $\mathcal{S}^\delta - i\beta^2\mathcal{Q}^\delta$ plane. The image of an horizontal segment in the $\mathcal{S}^\delta$ plane is sent close to a segment parallel to $\beta^2\mathbb{R}$ in the in $\mathcal{S}^\delta - i\beta^2\mathcal{Q}^\delta$ plane. The image of $L^{\partial,\delta}_{-3\varepsilon l_0}$ in the $\mathcal{S}^\delta - i\beta^2\mathcal{Q}^\delta$ plane is at a distance at most 4δ from a segment parallel to $\beta^2\mathbb{R}$.

We claim that the right to left case *is in fact not compatible with the construction of discrete half-planes*. To see that, recall that the kite region is a sucession of periodically (in the vertical direction) symmetrized kites. In particular, $\mathcal{Q}^\delta$ is *constant* along vertices belonging to the *same* vertical axis (whether it concerns two black or white vertices). Assume that $\overrightarrow{v^\circ_{2k}v^\circ_{2k+2}}$ is positively co-linear to (-1). Then we have the following facts.

— As the cut goes macroscopically from left to right in the $\mathcal{S}^\delta - i\beta^2\mathcal{Q}^\delta$ plane, there exist two consecutive vertices $v^\circ_{2r}, v^\circ_{2r+2}$ of $L^{\partial,\delta}_{-3\varepsilon l_0}$ (with $r > k$), belonging to the same kite, such that $\mathrm{Re}[v^\circ_{2r}] = \mathrm{Re}[v^\circ_{2k}]$ and $\mathrm{Re}[v^\circ_{2r+2}] = \mathrm{Re}[v^\circ_{2k+2}]$, but this time $\overrightarrow{v^\circ_{2r}v^\circ_{2r+2}}$ is positively colinear to 1. As $L^{\partial,\delta}_{-3\varepsilon l_0}$ is a simple path, one has $v^\circ_{2r} \neq v^\circ_{2k}$ and $v^\circ_{2r+2} \neq v^\circ_{2k+2}$.

— Let $v^\bullet_{1,2} \in G^\bullet$ be the vertices of the tangential quad containing $v^\circ_{2k}, v^\circ_{2k+2}$ (and also denote by $\tilde{v}^\bullet_{1,2}$ the two vertices of $G^\bullet$ belonging to the kite containing v°_{2r} and v°_{2r+2}). Those two vertices are vertically aligned in the $\mathcal{S}^\delta$ plane. As $\mathcal{Q}^\delta(v^\bullet_1) = \mathcal{Q}^\delta(v^\bullet_2)$, one directly sees that $[\mathcal{S}^\delta - i\beta^2\mathcal{Q}^\delta](v^\bullet_1) - [\mathcal{S}^\delta - i\beta^2\mathcal{Q}^\delta](v^\bullet_2) = \mathcal{S}^\delta(v^\bullet_1) - \mathcal{S}^\delta(v^\bullet_2) \in i\mathbb{R}$.

— There exist a line y in the $\mathcal{S}^\delta - i\beta^2\mathcal{Q}^\delta$ plane (used to construct $L^{\partial,\delta}_{-3\varepsilon l_0}$), parallel to $\beta^2\mathbb{R}$, such that $\hat{v}^\bullet_1$ is *above* y while $\hat{v}^\bullet_2$ is *below* y. This observation comes from the construction of discrete half-planes for general values of β (recalled in [33, Section 5.2]) and the fact that $|\arg(\beta^2)| \leqslant \frac{\pi}{2} - \mathsf{cst}(\kappa)$.

— In the case where v°_{2r} is strictly above v°_{2k} in the $\mathcal{S}^\delta$ plane, then the non-convex quad $(\hat{v}^\circ_{2r}\hat{\tilde{v}}^\bullet_1\hat{v}^\circ_{2r+2}\hat{\tilde{v}}^\bullet_2)$ in the $\mathcal{S}^\delta - i\beta^2\mathcal{Q}^\delta$ plane is a *translate in the upper vertical direction* of the non-convex quad $(\hat{v}^\circ_{2k}\hat{v}^\bullet_1\hat{v}^\circ_{2k+2}\hat{v}^\bullet_2)$. In particular, this implies that the vertices $\hat{\tilde{v}}^\bullet_{1,2}$ both lie *above* the axis y (as $\hat{\tilde{v}}^\bullet_{1,2}$ both lie *at or above* $\hat{v}^\bullet_1$). This is not compatible with the construction of the discrete half-planes via the line y. One can apply a similar reasoning in the case where v°_{2r} is strictly below v°_{2k} in the $\mathcal{S}^\delta$ plane to get a similar contradiction.

We are now in position to define the *discrete comparison domain* $\Omega^\delta_{z,\varepsilon,l_0}$ with Dobrushin boundary conditions near a wired arc of Ω^δ in the case where $z = 0$, $\vec{u} = 1$ and $\tau = -i$. Simple modifications allow to construct similars extension for other points of the wired arcs as well as points of the free arc $(ab)^\bullet$. In the following construction, $z \neq a, b$ and is assumed to belong to the approximation of the wired arc $(ba)^\circ$.

— The wired arc of $\Omega^\delta_{z=0,\varepsilon,l_0}$ is formed by

1. $L^{\partial,\delta}_{-3\varepsilon l_0}$
2. The approximations (up to $O(\delta)$) of two vertical segments (dashed in black in Figure 6.1.2) near $\pm 3l_0$, that link $L^{\partial,\delta}_{-3\varepsilon l_0}$ to the approximation of $\mathcal{C}_{z,\varepsilon,l_0}$ in $(\Omega_\delta, a^\delta, b^\delta)$. We denote respectively by $v^\circ_{\text{left,right}} \in \partial\Omega^\circ_\delta$ the points of juctions between the approximation of those vertical segments and $\partial\Omega^\circ_\delta$.
3. The two discrete arcs of $\partial\Omega^\circ_\delta$ that link respectively v°_{left} and v°_{right} to the axes $x = \mp 5l_0 + O(\delta)$ (each of those two discrete arc approximates a piece of $\mathcal{C}_{z,\varepsilon,l_0}$).

— The free arc of $\Omega^\delta_{z=0,\varepsilon,l_0}$ connects $\partial\Omega^\circ_\delta$ to itself *inside* Ω^δ from the axes $\mp 5l_0 + O(\delta)$, approximating the boundary of $\Omega^{l_0}_{z=0}$ that is above $\mathcal{C}_{z,\varepsilon,l_0}$. This free arc is drawn in green in Figure 6.1.1.

In the following proofs, we keep working in the case where $z = 0$ belongs to the wired arc, with $\vec{u} = 1$ and $\vec{\tau} = -i$, as a similar treatement can be done for any boundary point by rotating the picture accurately and swapping colors.

6.1.4 . Boundary arguments of fermionic observables in the extended domain

In this short subsection, we explain how the choice of special cuts for the extended domain near $z = 0$ allows to gain some information on the behavior near $L^{\partial,\delta}_{-3\varepsilon l_0}$ of the FK-Dobrushin observable defined in $\Omega^\delta_{z=0,\varepsilon,l_0}$. The main output of this discussion is the fact that one can compare the modulus of the s-holomorphic function associated to the FK correlator in $\Omega^\delta_{z=0,\varepsilon,l_0}$ to one of its projections, using basic random walks estimates. With the given construction, some of the projections of the observable defined in the extended domain are bounded from below near the wired boundary arc $L^{\partial,\delta}_{-3\varepsilon l_0}$, repeating a discussion made in [33, Lemma 5.3].

Let F_ε^δ be the s-holomorphic function associated to FK-Dobrushin observable defined by $(6.1.1)$ in the domain $\Omega^\delta_{z,\varepsilon,l_0}$ (the associated Dirac spinor is denoted by $\mathcal{X}_\varepsilon$), assuming once again that $z=0$ (still with $\vec{u}=1$ and $\tau=-i$) belongs to the wired arc and is away from its prime ends a,b. Recall that, by construction, the quads along the arc $L^{\partial,\delta}_{-3\varepsilon l_0}$ are kites with a horizontal symmetry axis. Up to a global choice of sign (which corresponds to a choice of sign for $\mathcal{X}_\varepsilon$), one has as in [33, eq (5.7)]

$$\arg F_\varepsilon^\delta(z) \;=\; \arg\left(i\varsigma(\overline{\mathcal{X}_\varepsilon(c_+)}-\overline{\mathcal{X}_\varepsilon(c_-)})\right), \tag{6.1.5}$$

for the boundary half-quads $(v^\bullet v^\circ_{2k} z v^\circ_{2k+2})$ on the wired part $L^{\partial,\delta}_{-3\varepsilon l_0}$ (see [33, Fig. 7] or Figure 6.1.3 for the notation). One can deduce that

— If $\overrightarrow{v^\circ_{2k}v^\circ_{2k+2}}$ is vertical, then $\arg F_\varepsilon^\delta(z)=\pm\frac{\pi}{4}$. Indeed, beyond the formula given by $(6.1.5)$, a way to check (at least up to π) this fact is based on the observation that $d\mathcal{Q}^\delta=0$ between v°_{2k} and v°_{2k+2}. As H^δ_ε vanishes identically at both v°_{2k} and v°_{2k+2}, this implies that $\mathrm{Im}[F^\delta_\varepsilon(z)^2\cdot i]=0$.

— If $\overrightarrow{v^\circ_{2k}v^\circ_{2k+2}}$ is horizontal, it is oriented in the positive direction by the previous discussion on the orientation of the path $L^{\partial,\delta}_{-3\varepsilon l_0}$. The formula $(6.1.5)$ ensures directly that $|\arg F^\delta_\varepsilon(z)|\leqslant\frac{\pi}{4}$. Once again, beyond the direct computation coming from the formula $(6.1.5)$, a way to check this fact (at least up to π) is based on the observation that H^δ_ε vanishes identically at both v°_{2k} and v°_{2k+2}, which implies that its increment between neighboring vertices of G° is proportional to $\mathrm{Im}[F^\delta_\varepsilon(z)^2+i|F^\delta_\varepsilon(z)|^2\frac{\mathcal{Q}^\delta(v^\circ_{2k+2})-\mathcal{Q}^\delta(v^\circ_{2k})}{\mathcal{S}^\delta(v^\circ_{2k+2})-\mathcal{S}^\delta(v^\circ_{2k})}]$ and vanishes, while it is clear that $|\mathcal{Q}^\delta(v^\circ_{2k+2})-\mathcal{Q}^\delta(v^\circ_{2k})|<\mathcal{S}^\delta(v^\circ_{2k+2})-\mathcal{S}^\delta(v^\circ_{2k})$.

In any case, the argument of F^δ_ε at any boundary half-quads is smaller than $\frac{\pi}{4}$. It is thus straightforward that it exists $\varphi_0(\kappa)>0$ small enough, only depending on κ, such that $\mathrm{Re}[\beta F^\delta_\varepsilon(z)e^{i\varphi}]\geqslant 0$ for all $|\varphi|\leqslant\varphi_0(\kappa)$ and all boundary half-quads of the wired arc $L^{\partial,\delta}_{-3\varepsilon l_0}$. An important output of that observation (coupled with the formula $(6.1.5)$) is that *redistribution coefficients* $k_\pm^{(\beta e^{i\varphi})}$ given in $(6.1.3)$ and $(6.1.4)$ *are positive* for all $|\varphi|\leqslant\varphi_0(\kappa)$ (choosing β accurately as in 6.1.3). Indeed, the boundary argument of the observable in the comparison domain is given by $(6.1.5)$ and is in $[-\frac{\pi}{4};\frac{\pi}{4}]$ along $L^{\partial,\delta}_{-3\varepsilon l_0}$. As long as $\arg(\beta e^{i\varphi})$ stays in $[-\frac{\pi}{4}+\mathsf{cst}(\kappa);\frac{\pi}{4}-\mathsf{cst}(\kappa)]$, one has $\mathrm{Re}[-i\overline{\varsigma}\beta e^{i\varphi}(\mathcal{X}(c_{++})-\mathcal{X}(c_{+-}))]>0$, which is (as explained at the end of Section 6.1.2) enough proves the positivity $k_+^{(\beta e^{i\varphi})}$. The treatement of $k_-^{(\beta e^{i\varphi})}$ is similar. It is in particular possible to apply the optional stopping theorem for backward walks stopped at the boundary of $\mathcal{S}^\delta-i\beta^2e^{2i\varphi}\mathcal{Q}^\delta$ for any value $|\varphi|\leqslant\varphi_0(\kappa)$, with the appropriate redistribution via $z_\pm$.

The combination of the aforementionned observations allows to prove the next proposition, which in words means that either $|F^\delta_\varepsilon|$ and $\mathrm{Re}[\beta F^\delta_\varepsilon]$ are *both bounded* or at least one can compare them at a bounded multiplicative factor (only depending on κ), not only at the boundary $L^{\partial,\delta}_{-3\varepsilon l_0}$ but also macroscopically close to $L^{\partial,\delta}_{-3\varepsilon l_0}$. This repeats a discussion made in [33, Lemma 5.14]. We

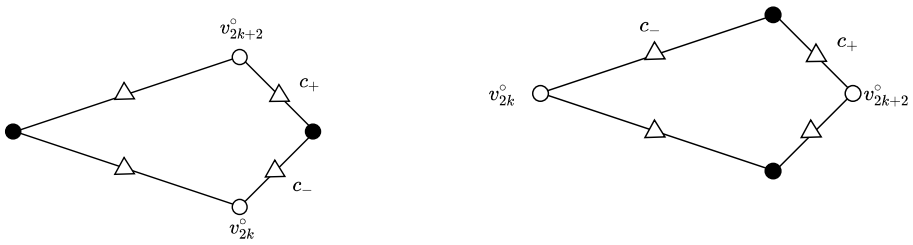

FIGURE 6.1.3 – Consecutive vertices of $L^{\partial,\delta}_{-3\varepsilon l_0}$ are either vertically aligned or horizontally aligned in the positive direction. The argument of the FK observable F^δ_ε defined in the comparison domain is in $[-\frac{\pi}{4};\frac{\pi}{4}]$.

note in what follows $\hat{s}_{min} = \mathrm{Im}[\overline{\beta}^2\hat{v}^\delta_{-3\varepsilon l_0}]$ as the coordinate along the $i\beta^2\mathbb{R}$ of the line used to construct $\hat{L}^{\partial,\delta}_{-3\varepsilon l_0}$ in the $\mathcal{S}^\delta - i\beta^2\mathcal{Q}^\delta$ plane. One can easily see that $\hat{s}_{min}$ is negative and its absolute value is comparable to $l_0\varepsilon$. We also define $\hat{s}_{mid} = \mathrm{Im}[\overline{\beta}^2\hat{v}^\delta_{l_0(-3\varepsilon+\varepsilon^{\frac{3}{2}})}]$

Proposition 6.1.2. *There exist positive constants $\hat{s}_0 = \hat{s}_0(\kappa)$, $\varphi_0 = \varphi_0(\kappa)$, $M_{1,2} = M_{1,2}(\kappa)$ and $\mathrm{cst}_{1,2} = \mathrm{cst}_{1,2}(\kappa)$ only depending on κ, and independent from $\varepsilon > 0$, l_0 and δ small enough, such that*

$$\mathrm{Proj}[F^\delta_\varepsilon(\hat{z}); \overline{\beta}e^{\pm i\varphi}\mathbb{R}] \geqslant -M_1(\kappa), \tag{6.1.6}$$

for any $\hat{z} = \hat{x}\beta^2 + i\hat{s}\beta^2$ of the $\mathcal{S}^\delta - i\beta^2\mathcal{Q}^\delta$ plane, as long as

- $\hat{x} \in \cos(2\beta_0)l_0[-1;1]$,
- $\hat{s} \in [\hat{s}_{mid}; \hat{s}_0 l_0]$,
- $\varphi \in \{0; \pm\varphi_0\}$.

In words, this means that $\mathrm{Re}[\beta F^\delta_\varepsilon e^{i\pm\varphi}]$ is bounded from below near $L^{\partial,\delta}_{-3\varepsilon l_0}$. As a consequence, for $\hat{z}$ in that region, one has $|F^\delta_\varepsilon(\hat{z})| \leqslant M_2 + \mathrm{cst}_2\,\mathrm{Re}[\beta F^\delta_\varepsilon(\hat{z})]$.

Proof. The proof adapts the arguments given in [33, Lemma 5.14], with the appropriate identifications between $\mathcal{S}^\delta$ and $\mathcal{S}^\delta - i\beta^2\mathcal{Q}^\delta$. The overall idea is to transfer the positivity of some projections of F^δ_ε at the boundary into the bulk, using random walks estimates on S-graphs. As recalled in Section 6.1.1, the quantity $\mathrm{Proj}[F^\delta_\varepsilon; \overline{\beta}\mathbb{R}]$ can be interpreted as a harmonic function for some random walk in the S-graph $\mathcal{S}^\delta - i\beta^2\mathcal{Q}^\delta$. Moreover (see [33, Section 5.4.1]), that random walk satisfies *uniform crossing estimates* above scale $\mathrm{cst}(\kappa)\delta$. This means that for $r \geqslant \mathrm{cst}(\kappa)\delta$, there is a positive and bounded from below probability (uniform in δ and only depending on κ) such that the backward walk associated to $\mathrm{Proj}[F^\delta_\varepsilon; \overline{\beta}\mathbb{R}]$ makes a full turn in any annulus formed by two concentric circles of radius r and $2r$ without leaving it.

We first treat the case $\varphi = 0$. For $k_0 > 0$ small enough, define the 'discrete' triangle $T^\delta(k_0)$ in the $\mathcal{S}^\delta - i\beta^2\mathcal{Q}^\delta$ plane, approximating up to $O(\delta)$ the triangle whose three corners are located at $i\beta^2(\hat{s}_{min} + 4k_0 l_0)$ and $i\beta^2\hat{s}_{min} \pm 2\cos(2\beta_0)l_0\beta^2$, assuming its 'bottom side' belongs to $\hat{L}^{\partial,\delta}_{-3\varepsilon l_0}$. This triangle is drawn in Figure 6.1.4.

Consider now the *backward* walk $\tilde{X}_t^{(-i\beta^2)}$ started at $\hat{z}$ associated to the harmonic function $\mathrm{Proj}[F^\delta_\varepsilon; \overline{\beta}\mathbb{R}]$ as in Proposition 6.1.3. One of the consequences of uniform crossing estimates above scale $\mathrm{cst}(\kappa)\delta$ is the following fact :

— Provided $k_0 = k_0(\kappa)$ is chosen small enough (but still macroscopic, i.e. larger than $\varepsilon^{\frac{1}{4}}$), there exist $\gamma > 0$, only depending on κ, such that the probability the backward walk associated to $\mathrm{Proj}[F^\delta_\varepsilon; \overline{\beta}\mathbb{R}]$ started at $\hat{z}$ visits the ball of radius 4ρ (drawn in red dashes in Figure 6.1.4) near one of the two lower corners of the triangle $T^\delta(k_0)$ is of order $O(\rho^{\frac{1}{2}+\gamma})$.

This fact is stated in [33, Section 5.4.1] and can be proved by recursive applications of crossing estimates at each scale, near a corner of the triangle, in the spirit of the proof of weak Beurling estimates (see e.g. [47, Proposition 2.11]). One can now apply the optional stopping theorem for the harmonic function $\mathrm{Proj}[F^\delta_\varepsilon; \overline{\beta}\mathbb{R}]$ at the time the backward walk started at $\hat{z}$ leaves $T^\delta(k_0)$.

— The previous discussion on the argument of F^δ_ε at the boundary ensures that $\mathrm{Re}[\beta F^\delta_\varepsilon]$ is positive along $\hat{L}^{\partial,\delta}_{-3\varepsilon l_0}$, thus the contribution of bottom side is positive. If the backward walk jumps above $\hat{L}^{\partial,\delta}_{-3\varepsilon l_0}$, one uses the redistribution procedure recalled at the end of Section 6.1.2, which is legitimate as the coefficients $k^{(\beta)}_\pm$ are positive

— The contribution of the two lateral sides of $T^\delta(k_0)$ at a distance larger than $\mathrm{cst}(\kappa)\delta$ from $\hat{L}^{\partial,\delta}_{-3\varepsilon l_0}$ is uniformly bounded. Indeed, one can use the fact that the probability that backward walk exits $T^\delta(k_0)$ from one of its vertical sides at distance $\rho \ll 1$ from $\hat{L}^{\partial,\delta}_{-3\varepsilon l_0}$ is of the order $\rho^{\frac{1}{2}+\gamma}$ together with $O(\rho^{-\frac{1}{2}})$ bound (coming from (5.2.18)) for $|F^\delta_\varepsilon|$ there.

— The contribution of the two lateral sides of $T^\delta(k_0)$ at a distance smaller than $\mathrm{cst}(\kappa)\delta$ from $\hat{L}^{\partial,\delta}_{-3\varepsilon l_0}$ is bounded from below by $-O(\delta^{-\frac{1}{2}})$, where O only depends on κ. To see that fact, fix a vertex $\hat{z_0} = \hat{x}\beta^2 + i\beta^2(\hat{s}_{min} + r_0)$ with $0 \leqslant r_0 \leqslant \mathrm{cst}(\kappa)\delta$. Once again, one can the compute $\mathrm{Re}[\beta F(\hat{z_0})]$ via the optional stopping theorem for the walk started at $\hat{z_0}$ and stopped when it leaves the square of witdh $5l_0\cos(2\beta_0)$ (symmetric with respect to the axis $i\beta^2$) whose bottom side is attached $\hat{L}^{\partial,\delta}_{-3\varepsilon l_0}$. The contribution ot the bottom side is again positive, while the bound (5.2.18) directly ensures that the contribution of the three other sides at a distance larger than $\mathrm{cst}(\kappa)\delta$ from $\hat{L}^{\partial,\delta}_{-3\varepsilon l_0}$ is $O(\delta^{-\frac{1}{2}})$ using. As stated in [47, Remark 3.18], the probability that the walk started at $\hat{z_0}$ leaves the square of width $5l_0\cos(2\beta_0)$ from one of its vertical sides at a distance smaller than $\mathrm{cst}(\kappa)\delta$ from $\hat{L}^{\partial,\delta}_{-3\varepsilon l_0}$ is exponentially small in $\frac{l_0}{\delta}$. As the kites have an

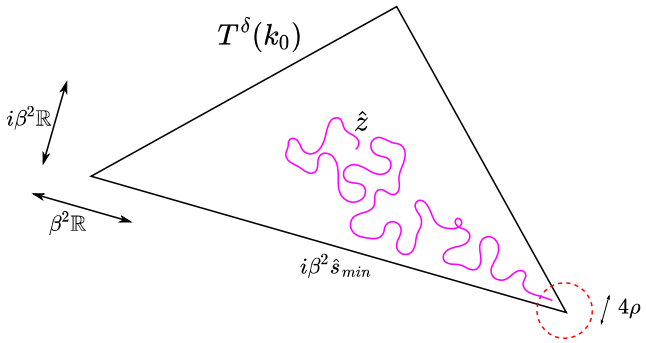

FIGURE 6.1.4 – Triangle $T^\delta(k_0)$ in the $\mathcal{S}^\delta - i\beta^2\mathcal{Q}^\delta$ plane near the straight cut $\hat{L}^{\partial,\delta}_{-3\varepsilon l_0}$. This triangle is used to apply the optional stopping theorem and prove that $\mathrm{Re}[\beta e^{i\pm\varphi_0}F^\delta_\varepsilon]$ is bounded from below near $\hat{L}^{\partial,\delta}_{-3\varepsilon l_0}$. The probability to visit the ball in red dashes, at a distance ρ from $\hat{L}^{\partial,\delta}_{-3\varepsilon l_0}$ is of order $\rho^{\frac{1}{2}+\gamma}$. The control of the values of $\mathrm{Re}[\beta F^\delta_\varepsilon]$ at a distance closer than $\mathrm{cst}(\kappa)\delta$ from $\hat{L}^{\partial,\delta}_{-3\varepsilon l_0}$ is obtained via a slightly more elaborated reasoning.

associated circle of radius larger than δ^{200}, $|F^\delta_\varepsilon|$ is bounded by δ^{-100} near $L^{\partial,\delta}_{-3\varepsilon l_0}$ and the contribution of those vicinities goes to 0 as δ goes to 0. One can then conclude as in the previous point.

This proves the result for $\varphi = 0$. Applying the same reasoning for the two backward walks on the $\mathcal{S}^\delta - ie^{i\mp\varphi_0}\beta^2\mathcal{Q}^\delta$ planes started close enough from the lower boundary and associated to $\mathrm{Proj}[F^\delta_\varepsilon; \overline{\beta}e^{i\pm\varphi_0}\mathbb{R}]$ leads to the same conclusion. Indeed, $\mathrm{Re}[\beta e^{i\mp\varphi_0}F^\delta_\varepsilon]$ is still non-negative along $\hat{L}^{\partial,\delta}_{-3\varepsilon l_0}$, thus one recovers that $\mathrm{Re}[\beta e^{i\mp\varphi_0}F^\delta_\varepsilon]$ is uniformly bounded from below as long as $\hat{z}$ is close enough to $\hat{L}^{\partial,\delta}_{-3\varepsilon l_0}$.

Packed together, the above conclusions prove the existence of absolute constants cst_2 and M_2, only depending on κ, such that $|F^\delta_\varepsilon(\hat{z})| \leqslant \mathrm{cst}_2 \cdot \mathrm{Re}[\beta F^\delta_\varepsilon(\hat{z})] + M_2$, provided $\hat{z}$ is close enough from the boundary $\hat{L}^{\partial,\delta}_{-3\varepsilon l_0}$. Note that this reasoning can be applied as long as $\hat{s} \leqslant k_0 l_0$ which proves this reasoning still holds *inside* Ω^δ. □

6.1.5 . Conclusion of the proof

We are now in position to state the key proposition that proves survival of boundary conditions near wired arcs when passing to the continuous limits for the functions H^δ. A similar idea, based on the control of area integrals of F^2 near the boundary was introduced in [33, Section 5.5] but the proof given there turns out to only apply in a fairly more restrictive setup (still it concerns a very particular case and is by huge means surpassed by the main result the same paper). More

importantly, the final argument used there to conclude is the Herglotz representation theorem for harmonic functions, which doesen't admit an extension for general functions ϑ. We bypass here such problem by using here the comparison principle in discrete with primitives of constant s-holomorphic functions. Let us emphasize that the next proposition doesn't require more than the differentiability of ϑ at the boundary point z (which holds almost everywhere as ϑ is a lipchitz function).

Proposition 6.1.3. *Fix $\varepsilon > 0$ a small positive number. Let H^δ be associated via (5.2.16) to the FK observable in Ω_δ given by (6.1.1), chosen with 0/1 discrete boundary conditions. Assume as above that the point $0 \in \partial\Omega$ (still with $\vec{u} = 1$, $\vec{\tau} = -i$) is away from the prime ends a and b and belongs to the approximation of the wired arc $(ba)^\circ$. Choosing $l_0 = l_0(z = 0)$ small enough to be able to apply the surgeries described in Section 6.1.3, one has $H^\delta(z') = O(\varepsilon^{\frac{1}{4}}) + o_{\delta\to 0}(1)$ for any $z' \in \big([-l_0; l_0] \times [-2\varepsilon l_0; 2\varepsilon l_0]\big) \cap \Omega_\delta$.*

Before proving Proposition 6.1.3, we first show that the function H^δ_ε associated to the FK-observable defined in the comparison domain $\Omega^\delta_{z,\varepsilon,l_0}$ *remains small* at a distance $O(l_0\varepsilon^{\frac{3}{2}})$ from the lower arc $L^{\partial,\delta}_{-3\varepsilon l_0}$. This is done to bypass the fact that at a distance $O(\delta)$ from $L^{\partial,\delta}_{-3\varepsilon l_0}$, one cannot use the bound (5.2.18) for F^δ_ε and has to stick with the trivial bound coming from radii of kites. The next proposition also allows to introduce in its proof the comparison with primitive of constant s-holomorphic functions, which is a powerfull tool to conclude in Proposition 6.1.3.

Proposition 6.1.4. *Let H^δ_ε be the FK-Dobrushin observable defined in the comparison domain $\Omega^\delta_{z,\varepsilon,l_0}$ near $z = 0$, with l_0 chosen small enough such that the surgeries of Section 6.1.3 can be done. Then for any $x \in [-l_0; l_0]$, one has the following upper bound $H^\delta_\varepsilon(x + il_0(-3\varepsilon + \varepsilon^{\frac{3}{2}})) = O(\varepsilon^{\frac{1}{2}}) + o_{\delta\to 0}(1)$, where O only depends on κ.*

Proof. Define via (5.2.17) the primitive of (a real valued multiple) of the *constant* s-holomorphic function $\beta \in \mathbb{T}$ by setting

$$H^\delta_{\mathrm{comp},\varepsilon} := \frac{\mathrm{Cst}(\kappa)}{l_0\varepsilon}\big(\mathrm{Im}[\beta^2\mathcal{S}^\delta + i\mathcal{Q}^\delta] + \mathrm{cst}'\big), \tag{6.1.7}$$

for some large enough constant $\mathrm{Cst}(\kappa)$ only depending on κ and some additive constant cst', that will both be fixed in the proof. One has the following facts :

A) $H^\delta_{\mathbf{comp},\varepsilon}$ is almost constant along horizontal segments

Given two points $x_{1,2} + it$ of the same horizontal segment $\tilde{L}^\delta_t$ in the $\mathcal{S}^\delta - i\beta^2\mathcal{Q}^\delta$ plane, a computation similar to the one made in the third step of Section 6.1.3 ensures that

$$[\mathcal{S}^\delta + i\overline{\beta}^2\mathcal{Q}^\delta](x_1+it) - [\mathcal{S}^\delta + i\overline{\beta}^2\mathcal{Q}^\delta](x_2+it) = (x_1-x_2) + i\overline{\beta}^2 a(x_1-x_2) + O(\varepsilon^2 l_0) + o_{\delta\to 0}(1),$$

which implies as $\mathrm{Im}[\beta^2 + ia] = 0$ that

$$\mathrm{Im}\,[\beta^2(\mathcal{S}^\delta + i\overline{\beta}^2\mathcal{Q}^\delta)](x_1+it) - \mathrm{Im}\,[\beta^2(\mathcal{S}^\delta + i\overline{\beta}^2\mathcal{Q}^\delta)](x_2+it) = O(\varepsilon^2 l_0) + o_{\delta\to 0}(1).$$

This means that $\mathrm{Im}[\beta^2\mathcal{S}^\delta + i\mathcal{Q}^\delta]$ varies at most by $O(\varepsilon^2 l_0) + o_{\delta\to 0}(1)$ along $\tilde{L}^\delta_t$. As $L^{\partial,\delta}_{-3\varepsilon l_0}$ and $\tilde{L}^\delta_{-3\varepsilon l_0}$ are $O(\varepsilon^2 l_0) + o_{\delta\to 0}(1)$ close from each other and $\mathrm{Im}[\beta^2\mathcal{S}^\delta + i\mathcal{Q}^\delta]$ is 2-lipchitz, one can fix the additive constant cst$'$ in the definition such that $H^\delta_{\mathrm{comp},\varepsilon}$ is $O(\varepsilon^2 l_0 \times \frac{\mathrm{Cst}(\kappa)}{\varepsilon l_0}) = O(\mathrm{Cst}(\kappa)\varepsilon) + o_{\delta\to 0}(1)$ along the bottom boundary arc $L^{\partial,\delta}_{-3\varepsilon l_0}$.

B) $H^\delta_{\mathbf{comp},\varepsilon}$ grows at positive linear speed in the upward direction

One can see that $\mathrm{Im}[\beta^2\mathcal{S}^\delta + i\mathcal{Q}^\delta]$ *grows linearly* at a positive and bounded from below speed (only depending on κ) when traveling in the upper direction inside the region $[-l_0; l_0] \times [-4\varepsilon l_0; l_0]$ of the $\mathcal{S}^\delta$ plane. Indeed recall that $a^2 + b^2 \leqslant \kappa^2$, $\cos(2\beta_0)^2 + \sin(2\beta_0)^2 = 1$ and $\sin(2\beta_0) = -a$. It is then straightforward to deduce that $\cos(2\beta_0)^2 \geqslant 1 - \kappa^2 + b^2$. In particular there exist $\mathrm{cst}(\kappa)$, only depending on κ, such that $\cos(2\beta_0) > |b| + \mathrm{cst}(\kappa)$. Separating the cases on whether $t_{1,2}$ belong or not to the kite region and using the associated expansions of $\mathcal{Q}^\delta_{ext}$ in $[-l_0; l_0] \times [-4\varepsilon l_0; l_0]$, one can see that for $t_1 > t_2$

$$\mathrm{Im}[\beta^2\mathcal{S}^\delta + i\mathcal{Q}^\delta](x + it_1) - \mathrm{Im}[\beta^2\mathcal{S}^\delta + i\mathcal{Q}^\delta](x + it_2) \geqslant \mathrm{cst}(\kappa)\cdot(t_1 - t_2) + O(l_0\varepsilon^2) + o_{\delta\to 0}(1) \tag{6.1.8}$$

In conclusion, choosing the constant $\mathrm{Cst}(\kappa)$ large enough ensures that the function $H^\delta_{\mathrm{comp},\varepsilon}$ is larger than 2 at the segment $\tilde{L}^\delta_{-\varepsilon l_0}$. One can now apply the comparison principle of Proposition 5.2.7 in the discrete topological rectangle (in $\Lambda(G)$) delimited by the boundary of $\Omega^\delta_{z,\varepsilon,l_0}$ and $\tilde{L}^\delta_{-\varepsilon l_0}$. The cost of the discretization to apply the comparison principle (i.e. including vertices of $G^\bullet$ separating nearby vertices of $\partial\Omega^\delta_{0,\varepsilon,l_0}$) is encapsulated in the $o_{\delta\to 0}(1)$ error term, as the increment of H^δ_ε between a vertex of G° in its wired arc and one of the neighboring vertices of $G^\bullet$ is the square of a disorder-disorder correlation. That disorder-disorder correlation vanishes in the limit $\delta \to 0$, using crossing estimates on general s-embeddings and the fact that that $z = 0$ is away from prime ends. One can then make the following simple observations

— On the lower arc $L^{\partial,\delta}_{-3\varepsilon l_0}$, $H^\delta_\varepsilon = o_{\delta\to 0}(1)$ while $H^\delta_{\mathrm{comp},\varepsilon}$ is $O(\varepsilon) + o_{\delta\to 0}(1)$.

— On the vertical sides of $\partial\Omega^\delta_{0,\varepsilon,l_0}$, $H^\delta_\varepsilon = o_{\delta\to 0}(1)$ while $H^\delta_{\mathrm{comp},\varepsilon}$ is larger than $O(\varepsilon) + o_{\delta\to 0}(1)$ (as the function grows $H^\delta_{\mathrm{comp},\varepsilon}$ when traveling in the upper direction and is $O(\varepsilon)$ at the bottom of those vertical segments).

— On the approximation of $\tilde{L}^\delta_{-\varepsilon l_0}$, $H^\delta_\varepsilon \leqslant 1$ (by the maximum principle for the FK-Dobrushin observable in $\Omega^\delta_{z=0,\varepsilon,l_0}$) while $H^\delta_{\mathrm{comp},\varepsilon}$ is larger than 2.

All together this implies that $H^\delta_\varepsilon - H^\delta_{\mathrm{comp},\varepsilon} \leqslant O(\varepsilon) + o_{\delta\to 0}(1)$ at the boundary of the discrete domain used to compare H^δ_ε and $H^\delta_{\mathrm{comp},\varepsilon}$, and is thus true in this entire discrete domain. Evaluating $H^\delta_{\mathrm{comp},\varepsilon}$ at the horizontal level $y = -(3\varepsilon + \varepsilon^{\frac{3}{2}})l_0$ gives the result. □

We are now in position to prove Proposition 6.1.3

Proof of Proposition 6.1.3. The proof is a combination of several simple observations and is now detailed step by step. We focus first on the control near $z = 0$ of the values of the function H^δ_ε (associated to the FK-Dobrushin correlator in the extended domain $\Omega^\delta_{z,\varepsilon,l_0}$) and conclude a similar control for H^δ using the comparison principle of Proposition 5.2.7. We keep identifying the points in $\mathcal{S}^\delta$ with their counterparts in $\mathcal{S}^\delta - i\beta^2\mathcal{Q}^\delta$. Before going into technical details, we explain briefly the different steps of our strategy.

1. First prove that one projection of the boundary integrals of F^δ_ε along segments of width $\asymp l_0$ in the $\mathcal{S}^\delta - i\beta^2\mathcal{Q}^\delta$ plane are $O(l_0^{\frac{1}{2}})$.
2. Deduce the same estimate for $|F^\delta_\varepsilon|$. Use then bound (5.2.18) to control an area integral estimate of $|F^\delta_\varepsilon|^2$ near $\hat{L}^{\partial,\delta}_{-3\varepsilon l_0}$. Recover a similar area integral estimate near $L^{\partial,\delta}_{-3\varepsilon l_0}$ in the $\mathcal{S}^\delta$ plane.
3. Find two vertical segments $x = x_{1,2}$ of lenght $l_0\varepsilon^{\frac{1}{2}}$ such that H^δ_ε remains small along those segments.
4. Use those two vertical segments and the comparison principle with the primitive of a constant s-holomorphic function to conclude for H^δ_ε.
5. Use the comparison principle between H^δ_ε and H^δ to conclude for H^δ.

Recall that $\hat{s}_{mid} = \mathrm{Im}[\overline{\beta}^2\hat{v}^\delta_{l_0(-3\varepsilon+\varepsilon^{\frac{3}{2}})}]$ and $\hat{s}_{top} = \mathrm{Im}[\overline{\beta}^2\hat{v}^\delta_{l_0\varepsilon^{\frac{1}{2}}}]$

Step 1 : Integrated horizontal estimates for one projection of F^δ_ε

Fix $\hat{s} \in [\hat{s}_{mid}; \hat{s}_0 l_0]$ and define as previously, in the $\mathcal{S}^\delta - i\beta^2\mathcal{Q}^\delta$ plane, the *straight segment* (drawn in orange in Figure 6.1.5) $\hat{\mathcal{L}}^\delta_{\hat{s}} := \cos(2\beta_0)\beta^2[-l_0; l_0] \times \{i\hat{s}\beta^2\}$, as well as $\hat{\mathcal{R}}^\delta_{\hat{s},l_0}$ the square of width $2l_0\cos(2\beta_0)$ whose bottom boundary is $\hat{\mathcal{L}}^\delta_s$ (also drawn in Figure 6.1.5). One denotes $\mathcal{L}^\delta_{\hat{s}}$ and $\mathcal{R}^\delta_{\hat{s},l_0}$ the preimages of $\hat{\mathcal{L}}^\delta_{\hat{s}}$ and $\hat{\mathcal{R}}^\delta_{\hat{s},l_0}$ in the $\mathcal{S}^\delta$ plane. The boundary of $\mathcal{R}^\delta_{\hat{s},l_0}$ is a continuous closed curve denoted $\mathcal{C}^\delta_{\hat{s},l_0}$ and is oriented in the counterclockwise direction.

Consider the integral $\mathbb{I}_{\mathbb{C}}[F^\delta_\varepsilon]$ along the closed contour $\mathcal{C}^\delta_{\hat{s},l_0}$, which vanishes. We are going to bound the different contributions of $\mathbb{I}_{\mathbb{C}}[F^\delta_\varepsilon]$ along three of the four arcs of $\mathcal{C}^\delta_{\hat{s},l_0}$.

— Combining the estimate $|F^\delta_\varepsilon|(z) \leqslant O(\mathrm{dist}(z, \partial\Omega^\delta_{z,\varepsilon,l_0})^{-\frac{1}{2}})$ coming from (5.2.18), an upper bound on the integral of $r \mapsto r^{-\frac{1}{2}}$ near 0, the fact that $|d\vartheta| \leqslant d|z|$ and the comparability between distances (above scale $\mathrm{cst}(\kappa)\delta$) in the $\mathcal{S}^\delta$ and $\mathcal{S}^\delta - i\beta^2\mathcal{Q}^\delta$ planes, one can see that the contribution of the lateral sides of $\mathcal{C}^\delta_{\hat{s},l_0}$ is of order $O(\int_0^{l_0} \mathrm{dist}(z, \partial\Omega^\delta_{z,\varepsilon,l_0})^{-\frac{1}{2}}|dz|) \leqslant O(\int_0^{l_0} r^{-\frac{1}{2}}dr) = O(l_0^{\frac{1}{2}})$, where O only depends on κ.

— Combining the a priori estimate $|F^\delta_\varepsilon(z)| \leqslant O(\mathrm{dist}(z, \partial\Omega^\delta_{z,\varepsilon,l_0})^{-\frac{1}{2}})$ coming from (5.2.18), the comparability between distances in $\mathcal{S}^\delta$ and $\mathcal{S}^\delta - i\beta^2\mathcal{Q}^\delta$ and the fact that the upper arc of $\mathcal{C}^\delta_{\hat{s},l_0}$ is of length $O(l_0)$, one concludes that the contribution of the upper arc is again $O(l_0 \times l_0^{-\frac{1}{2}}) = O(l_0^{\frac{1}{2}})$.

Taking the projection on $\beta\mathbb{R}$ allows to conclude that

$$\int_{\mathcal{L}_{\hat{s}}^{\delta}} \mathrm{Re}[\overline{\beta}(F_{\varepsilon}^{\delta} d\mathcal{S}^{\delta} + i\overline{F_{\varepsilon}^{\delta}} d\mathcal{Q}^{\delta})] = -\int_{\mathcal{C}_{\hat{s},l_0}^{\delta} \setminus \mathcal{L}_{\hat{s}}^{\delta}} \mathrm{Re}[\overline{\beta}(F_{\varepsilon}^{\delta} d\mathcal{S}^{\delta} + i\overline{F_{\varepsilon}^{\delta}} d\mathcal{Q}^{\delta})] = O(l_0^{\frac{1}{2}}). \tag{6.1.9}$$

Step 2 : Integrated area estimates for $|F_{\varepsilon}^{\delta}|^2$

One can always write $\mathrm{Re}[\overline{\beta}(F_{\varepsilon}^{\delta} d\mathcal{S}^{\delta} + i\overline{F_{\varepsilon}^{\delta}} d\mathcal{Q}^{\delta})] = \mathrm{Re}[\overline{\beta} F_{\varepsilon}^{\delta} (d\mathcal{S}^{\delta} - i\beta^2 d\mathcal{Q}^{\delta})]$. When traveling along $\mathcal{L}_{\hat{s}}^{\delta}$ from left to right, one has *by definition of the segment* $\hat{\mathcal{L}}_{\hat{s}}^{\delta}$ that $(d\mathcal{S}^{\delta} - i\beta^2 d\mathcal{Q}^{\delta}) \in \beta^2 \mathbb{R}^+$. Plugging this observation into (6.1.9), one recovers that

$$\int_{\hat{x} \in l_0 \cos(2\beta_0)[-1;1] \times \{\hat{s}\}} \mathrm{Re}[\beta F_{\varepsilon}^{\delta}(\hat{x}\beta^2 + i\hat{s}\beta^2)] d\hat{x} = O(l_0^{\frac{1}{2}}). \tag{6.1.10}$$

Using the inequality $|F_{\varepsilon}^{\delta}| \leqslant \mathrm{cst}_2 \,\mathrm{Re}[\beta F_{\varepsilon}^{\delta}] + M_2$ near $\hat{L}_{-3\varepsilon l_0}^{\partial,\delta}$ coming from Proposition 6.1.2, one deduces that for l_0 small enough

$$\int_{\hat{x} \in l_0 \cos(2\beta_0)[-1;1] \times \{\hat{s}\}} |F_{\varepsilon}^{\delta}(\hat{x}\beta^2 + i\hat{s}\beta^2]| d\hat{x} = O(l_0^{\frac{1}{2}}). \tag{6.1.11}$$

Using once again the upper bound $|F_{\varepsilon}^{\delta}| \leqslant O(\mathrm{dist}(z, \partial\Omega_{z,\varepsilon,l_0}^{\delta})^{-\frac{1}{2}})$ coming from (5.2.18), one deduces that

$$\int_{\hat{x} \in l_0 \cos(2\beta_0)[-1;1] \times \{\hat{s}\}} |F_{\varepsilon}^{\delta}(\hat{x}\beta^2 + i\hat{s}\beta^2)|^2 d\hat{x} = O(l_0^{\frac{1}{2}} (\hat{s} - \hat{s}_{min})^{-\frac{1}{2}}). \tag{6.1.12}$$

One can now *integrate* the estimate (6.1.12) in the $i\beta^2$ direction, from the level $\hat{\mathcal{L}}_{\hat{s}_{mid}}^{\delta}$ up to the level $i\beta^2 \hat{s}_{top}$ to deduce the area estimate (as $\int_0^y \hat{s}^{-\frac{1}{2}} d\hat{s} = O(y^{\frac{1}{2}})$)

$$\iint_{\substack{\hat{x} \in [-1;1] l_0 \cos(2\beta_0) \\ \hat{s} \in [\hat{s}_{mid}; \hat{s}_{top}]}} |F_{\varepsilon}^{\delta}(\hat{x}\beta^2 + i\hat{s}\beta^2)|^2 d\hat{x} d\hat{s} = O((l_0)^{\frac{1}{2}} \cdot (l_0 \varepsilon^{\frac{1}{2}})^{\frac{1}{2}}) = O(l_0 \varepsilon^{\frac{1}{4}}). \tag{6.1.13}$$

As areas in the $\mathcal{S}^{\delta}$ plane and in the $\mathcal{S}^{\delta} - i\beta^2 \mathcal{Q}^{\delta}$ are comparable above scale $\mathrm{cst}(\kappa)\delta$ while F_{ε}^{δ} is Hoelder above scale $\mathrm{cst}(\kappa)\delta$, one deduces that

$$\iint_{\substack{s \in l_0[-3\varepsilon + \varepsilon^{\frac{3}{2}}; \varepsilon^{\frac{1}{2}}] \\ x \in l_0[-1;1]}} |F_{\varepsilon}^{\delta}(x + is)|^2 dx ds = O(l_0 \varepsilon^{\frac{1}{4}}). \tag{6.1.14}$$

Step 3 : Smallness of H_{ε}^{δ} along some segments inside Ω_{δ}

Using the Fubini theorem, one can rewrite (6.1.14) as

$$\int_{x \in l_0[-1;1]} \Big(\int_{s \in l_0[-3\varepsilon + \varepsilon^{\frac{3}{2}}; \varepsilon^{\frac{1}{2}}]} |F_{\varepsilon}^{\delta}(x + is)|^2 ds \Big) dx = O(l_0 \varepsilon^{\frac{1}{4}}). \tag{6.1.15}$$

This implies the existence of $x_{1,2}$ near respectively $\pm l_0$ such that

$$\int_{s \in l_0[-3\varepsilon + \varepsilon^{\frac{3}{2}}; \varepsilon^{\frac{1}{2}}]} |F_{\varepsilon}^{\delta}(x_{1,2} + is)|^2 ds = O(\varepsilon^{\frac{1}{4}}) \tag{6.1.16}$$

Integrating (6.1.16) along the axes $x = x_{1,2}$ in the upward direction from the segment $\tilde{L}_{(-3\varepsilon+\varepsilon^{\frac{3}{2}})l_0}$ (where $H^\delta_\varepsilon = O(\varepsilon^{\frac{1}{2}}) + o_{\delta\to 0}(1)$ by Proposition 6.1.4), one deduces that $H^\delta_\varepsilon(x_{1,2}+is) = O(\varepsilon^{\frac{1}{4}}) + o_{\delta\to 0}(1)$ for any $(-3\varepsilon+\varepsilon^{\frac{3}{2}})l_0 \leqslant s \leqslant l_0\varepsilon^{\frac{1}{2}}$.

Step 4 : Concluding for H^δ_ε by comparing with the primitive of β^2

Define once again via (5.2.17) the primitive of (a real valued multiple) of the *constant* s-holomorphic function $\beta \in \mathbb{T}$ by

$$H^\delta_{\mathrm{comp},\varepsilon^{\frac{1}{2}}} := \frac{\mathrm{Cst}(\kappa)}{l_0\varepsilon^{\frac{1}{2}}}\big(\mathrm{Im}[\beta^2\mathcal{S}^\delta + i\mathcal{Q}^\delta] + \mathrm{cst}'\big). \tag{6.1.17}$$

Fixing cst' accurately and taking $\mathrm{Cst}(\kappa)$ large enough (only depending on κ), one has the following facts (as in the proof of Proposition 6.1.4 and still up to $o_{\delta\to 0}(1)$)

— $H^\delta_{\mathrm{comp},\varepsilon^{\frac{1}{2}}}$ is $O(\varepsilon)$ on the horizontal segment $\tilde{L}_{-3\varepsilon l_0+l_0\varepsilon^{\frac{3}{2}}}$ of the $\mathcal{S}^\delta$ plane.

— $H^\delta_{\mathrm{comp},\varepsilon^{\frac{1}{2}}}$ is $O(\varepsilon)$ on the vertical segments at the axes $x_{1,2}$, as it grows linearly (at a speed larger than $\mathrm{cst}(\kappa)(l_0\varepsilon^{\frac{1}{2}})^{-1}$) when traveling in the upward direction.

— The function $H^\delta_{\mathrm{comp},\varepsilon^{\frac{1}{2}}}$ is larger than 2 at the segment $\tilde{L}^\delta_{\varepsilon^{\frac{1}{2}}l_0}$.

One can now apply the comparison principle of Proposition 5.2.7 in an approximation of the rectangle $[x_1;x_2]\times[(-3\varepsilon+\varepsilon^{\frac{3}{2}})l_0; l_0\varepsilon^{\frac{1}{2}}]$ (drawn in blue in Figure 6.1.5). One has (up to $o_{\delta\to 0}(1)$) :

— On the lower arc that rectangle, $H^\delta_\varepsilon = O(\varepsilon^{\frac{1}{2}})$ while $H^\delta_{\mathrm{comp},\varepsilon^{\frac{1}{2}}}$ is $O(\varepsilon)$.

— On the vertical approximations of the axes $x = x_{1,2}$, $H^\delta_\varepsilon = O(\varepsilon^{\frac{1}{4}})$ while $H^\delta_{\mathrm{comp},\varepsilon^{\frac{1}{2}}}$ is larger than $O(\varepsilon)$ (as the function grows $H^\delta_{\mathrm{comp},\varepsilon^{\frac{1}{2}}}$ when traveling in the upper direction and has value $O(\varepsilon)$ at the lowest point of those arcs).

— On the approximation of $\tilde{L}^\delta_{\varepsilon^{\frac{1}{2}}l_0}$, $H^\delta_{\mathrm{comp},\varepsilon^{\frac{1}{2}}}$ is larger than 2, while $H^\delta_\varepsilon \leqslant 1$ by the maximum principle for FK-Dobrushin observable defined in the comparison domain.

All together this implies that $H^\delta_\varepsilon - H^\delta_{\mathrm{comp},\varepsilon^{\frac{1}{2}}} \leqslant o_{\delta\to 0}(1) + O(\varepsilon^{\frac{1}{4}})$ in the entire rectangle used to perform the discrete comparison principle. Evaluating $H^\delta_{\mathrm{comp},\varepsilon^{\frac{1}{2}}}$ in the region $[-\varepsilon l_0; 2\varepsilon l_0]\cap\Omega_\delta$ gives directly the upper bound $H^\delta_\varepsilon = O(\varepsilon^{\frac{1}{4}}) + o_{\delta\to 0}(1)$.

Step 5 : Concluding for H^δ by comparing with H^δ_ε

One can apply the comparison principle between H^δ and H^δ_ε in the discrete domain delimited in $\Lambda(G)$ by the wired arc $\partial\Omega^\circ_\delta$ and the free arc of $\Omega^\delta_{z,\varepsilon,l_0}$. One sees directly that $H^\delta \leqslant H^\delta_\varepsilon + o_{\delta\to 0}(1)$ in the entire domain Ω_δ. Once again,

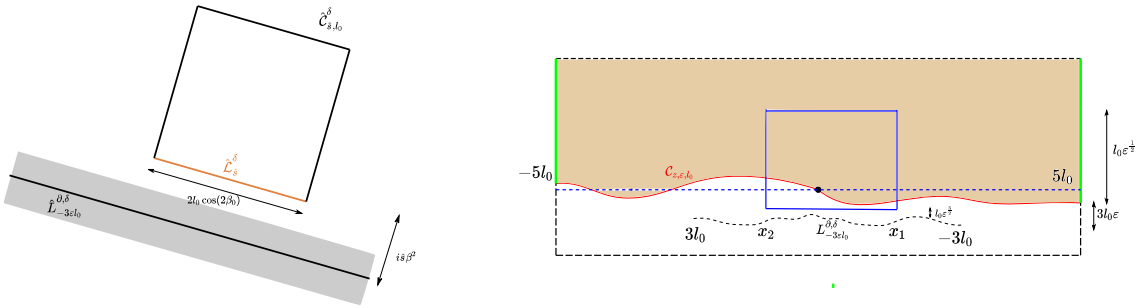

FIGURE 6.1.5 – (Left) Definition of the square $\hat{\mathcal{R}}^{\delta}_{\hat{s},l_0}$ in the $\mathcal{S}^{\delta} - i\beta^2\mathcal{Q}^{\delta}$ plane, whose bottom side is $\hat{\mathcal{L}}^{\delta}_{\hat{s}}$. (Right) Local picture to apply to comparison principle in Step 4 of the proof. We first use Proposition 6.1.4 to prove that at a distance $l_0\varepsilon^{\frac{3}{2}}$ from the lower arc of the comparison domain, the function H^{δ}_{ε} is bounded by $O(\varepsilon^{\frac{1}{2}})$. Then we prove that integrale along the axes $x_{1,2}$ to use the comparison principle in the blue rectangle.

the cost of including the vertices of $G^{\bullet}$ near the wired arc $\partial\Omega^{\circ}_{\delta}$ is encapsulated in the $o_{\delta\to 0}(1)$ term, as the increment of H^{δ} there is the square of disorder-disorder correlation, that vanishes in the limit $\delta \to 0$ as $z = 0$ is away from the prime ends. This concludes the proof. □

We are now in position to prove Theorem 6.1.1. The author is grateful to Sung-Chul Park for explaining how to prove the uniqueness statement in continuum, repeating an argument of [138, Proposition 5.8]

Proof of Theorem 6.1.1. Consider $f : \Omega \to \mathbb{C}$, obtained as a subsequential limit of the s-holomorphic functions $(F^{\delta})_{\delta>0}$, uniformly on compacts of Ω. Then the differential form $(f dz + i\overline{f} d\vartheta)$ is closed. The associated functions also $(H^{\delta})_{\delta>0}$ converge uniformly to $h = \frac{1}{2}\int\left(\mathrm{Im}[f^2 dz] + |f|^2 d\vartheta\right)$, which takes its values in $[0;1]$. Fix z a boundary point of the arc $(ba)^{\circ}$ (away from the prime ends) and $\varepsilon > 0$ small enough. Up to rotation and translation, we assume as previously that $z = 0$, $\vec{u}(z) = 1$ and $\tau(z) = -i$. Choosing l_0 small enough to perform the surgeries of Section 6.1.3, one deduces from Proposition 6.1.3 that $H^{\delta}(z') = O(\varepsilon^{\frac{1}{4}}) + o_{\delta\to 0}(1)$ for any $z' \in ([-l_0; l_0] \times [-2\varepsilon l_0; 2\varepsilon l_0]) \cap \Omega_{\delta}$. Let $(x_n)_{n\geqslant 0}$ a sequence of interior points of Ω converging to $z = 0$. Then $\limsup_n H^{\delta}(x_n) \leqslant O(\varepsilon^{\frac{1}{4}}) + o_{\delta\to 0}(1)$. Sending δ to 0 first, this ensures that $\limsup_n h(x_n) \leqslant O(\varepsilon^{\frac{1}{4}})$. As ε can be chosen arbitrarly small, one deduces that $\lim_n h(x_n) = 0$ and thus h extends continuously to 0 at $z = 0$. A similar reasoning (away from prime ends) on the free arc ensures that h extends

continuously to 1 on $(ab)^\bullet$ there. To conclude, one needs to prove there is only *one* function satisfying those conditions.

Consider $f_{1,2}$ as subsequential limits of functions F^δ, together with the naturally associated functions $h_{1,2}$. We have $|f_{1,2}(z)|^2 = O(\mathrm{dist}(z, \partial\Omega)^{-1})$. One first passes to the conformal parametrization used in (5.2.21). Since the second derivatives of ϑ are smooth, so does the function $\zeta \mapsto m(\zeta)$ defined below [33, eq (2.28)] (5.2.21), as well as $\zeta \mapsto z(\zeta)$. Recall that the function φ defined by $\varphi := \overline{\varsigma} f \cdot (z_\zeta)^{1/2} + \varsigma \overline{f} \cdot (\overline{z}_\zeta)^{1/2}$ satisfies the massive Dirac equation (as in [33, (2.28)]) given by

$$\varphi_{\bar{\zeta}} = im(\zeta) \cdot \overline{\varphi} \tag{6.1.18}$$

where $m = \frac{1}{2} H\ell$, with H the mean curvature of the surface (z, ϑ) at $z(\zeta)$ and ℓ the metric element at $z(\zeta)$. The metric element is bounded from above by some constant only depending on κ. It is also possible to see that $h = \int \mathrm{Im}[\varphi^2 d\zeta]$ in the ζ parametrization. Consider now the parametrization by $\mathbb{D}$ of $\tilde{\Omega}$ (the lift of Ω to (z, ϑ)) and let $\omega \in \mathbb{D}$. One can define as in [138, Proposition 5.8] the following function associated to φ

$$g(\omega) := \iint_{\mathbb{D}} G_{\mathbb{D}}(\zeta, \omega) 4m(\zeta) |\varphi(\zeta)|^2 dA(\zeta), \tag{6.1.19}$$

where $G_{\mathbb{D}}(\zeta, \omega)$ is the Green function in $\mathbb{D}$ associated to the Brownian motion started at ω. Standard arguments (see e.g. [77, Lemma 4.2]) ensure that $\Delta g = \Delta h = 8m(\zeta)|\partial_\zeta h|$, thus one has $\Delta h(\zeta) = 8m(\zeta)|\partial_\zeta h| = O(m(\zeta)\mathrm{dist}(\zeta, \partial\mathbb{D})^{-1})$. Since $m(\zeta)$ is smooth (and thus bounded in $\mathbb{D}$), one can repeat the computation of [33, Lemma A2] and prove that g extends continuously to 0 as ω goes to the unit circle.

Consider now two functions $g_{1,2}$ associated to $f_{1,2}$ via (6.1.19). Both functions $g_{1,2}$ extend continuously to 0 at the boundary of $\mathbb{D}$. This implies that $(h_1 - g_1) - (h_2 - g_2)$ is bounded, harmonic extends continuously to 0, except potentially at pre-images of the lifts of a and b. As there is no non-trivial functions with this property (see e.g. [74, Lemma 1.1]), this means that $h_1 - h_2$ continously extends to 0 up to the entire boundary of $\mathbb{D}$ (i.e. including at pre-images of the lifts of a and b). This means that $h_1 = h_2$ at the boundary of $\mathbb{D}$. The comparison principle stated in [138, Lemma 3.1] ensures $h_1 = h_2$ everywhere in $\mathbb{D}$ and concludes the proof. □

Bibliographie

[1] Michael Aizenman, David J Barsky et Roberto Fernández. "The phase transition in a general class of Ising-type models is sharp". In : *Journal of Statistical Physics* 47.3 (1987), p. 343-374.

[2] Michael Aizenman, A Klein et C Newman. "Percolation methods for disordered quantum Ising models". In : *Phase Transitions : Mathematics, Physics, Biology* (1993), p. 1-26.

[3] Kari Astala, Tadeusz Iwaniec et Gaven Martin. "Elliptic Partial Differential Equations and Quasiconformal Mappings in the Plane (PMS-48)". In : *Elliptic Partial Differential Equations and Quasiconformal Mappings in the Plane (PMS-48)*. Princeton University Press, 2008.

[4] Helen Au-Yang et Barry McCoy. "Theory of layered Ising models. II. Spin correlation functions parallel to the layering". In : *Phys. Rev. B* 10 (9 1974), p. 3885-3905. DOI : 10.1103/PhysRevB.10.3885. URL : https://link.aps.org/doi/10.1103/PhysRevB.10.3885.

[5] Helen Au-Yang et Barry M. McCoy. "Theory of layered Ising models : Thermodynamics". In : *Phys. Rev. B* 10 (3 1974), p. 886-891. DOI : 10.1103/PhysRevB.10.886. URL : https://link.aps.org/doi/10.1103/PhysRevB.10.886.

[6] Helen Au-Yang et Jacques HH Perk. "Critical correlations in a Z-invariant inhomogeneous Ising model". In : *Physica A : Statistical Mechanics and its Applications* 144.1 (1987), p. 44-104.

[7] Estelle L. Basor, Yang Chen et Nazmus S. Haq. "Asymptotics of determinants of Hankel matrices via non-linear difference equations". In : *J. Approx. Theory* 198 (2015), p. 63-110. ISSN : 0021-9045. DOI : 10.1016/j.jat.2015.05.002. URL : https://doi.org/10.1016/j.jat.2015.05.002.

[8] R. J. Baxter. "Free-fermion, checkerboard and Z-invariant lattice models in statistical mechanics". In : *Proc. Roy. Soc. London Ser. A* 404.1826 (1986), p. 1-33. ISSN : 0962-8444.

[9] R. J. Baxter. "Onsager and Kaufman's calculation of the spontaneous magnetization of the Ising model : II". In : *J. Stat. Phys.* 149.6 (2012), p. 1164-1167. ISSN : 0022-4715. DOI : 10.1007/s10955-012-0658-8. URL : https://doi.org/10.1007/s10955-012-0658-8.

[10] R. J. Baxter. “Solvable eight-vertex model on an arbitrary planar lattice”. In : *Philos. Trans. Roy. Soc. London Ser. A* 289.1359 (1978), p. 315-346. ISSN : 0080-4614. DOI : 10.1098/rsta.1978.0062. URL : https://doi.org/10.1098/rsta.1978.0062.

[11] RJ Baxter. “Onsager and Kaufman’s calculation of the spontaneous magnetization of the Ising model”. In : *Journal of Statistical Physics* 145.3 (2011), p. 518-548.

[12] Rodney J. Baxter. *Exactly solved models in statistical mechanics*. Reprint of the 1982 original. Academic Press, Inc. [Harcourt Brace Jovanovich, Publishers], London, 1989, p. xii+486. ISBN : 0-12-083182-1.

[13] Rodney J Baxter et Ian G Enting. “399th solution of the Ising model”. In : *Journal of Physics A : Mathematical and General* 11.12 (1978), p. 2463.

[14] V. Beffara et H. Duminil-Copin. “Smirnov’s fermionic observable away from criticality”. In : *Ann. Probab.* 40.6 (2012), p. 2667-2689. ISSN : 0091-1798. DOI : 10.1214/11-AOP689. URL : https://doi.org/10.1214/11-AOP689.

[15] Vincent Beffara et Hugo Duminil-Copin. “The self-dual point of the two-dimensional random-cluster model is critical for q greater than 1”. In : *Probability Theory and Related Fields* 153.3 (2012), p. 511-542.

[16] Alexander A Belavin, Alexander M Polyakov et Alexander B Zamolodchikov. “Infinite conformal symmetry in two-dimensional quantum field theory”. In : *Nuclear Physics B* 241.2 (1984), p. 333-380.

[17] Alexander A Belavin, Alexander M Polyakov et Alexander B Zamolodchikov. “Infinite conformal symmetry of critical fluctuations in two dimensions”. In : *Journal of Statistical Physics* 34.5 (1984), p. 763-774.

[18] Stéphane Benoist et Clément Hongler. “The scaling limit of critical Ising interfaces is CLE(3)”. In : *The Annals of Probability* 47.4 (2019), p. 2049-2086.

[19] Stéphane Benoist, Duminil-Copin Hugo et Clément Hongler. “Conformal invariance of crossing probabilities for the Ising model with free boundary conditions”. In : *Annales de l’Institut Henri Poincaré, Probabilités et Statistiques*. T. 52. 4. Institut Henri Poincaré. 2016, p. 1784-1798.

[20] J. E. Björnberg et G. R. Grimmett. “The phase transition of the quantum Ising model is sharp”. In : *J. Stat. Phys.* 136.2 (2009), p. 231-273. ISSN : 0022-4715. DOI : 10.1007/s10955-009-9788-z. URL : http://dx.doi.org/10.1007/s10955-009-9788-z.

[21] Jakob E. Björnberg. “Fermionic observables in the transverse Ising chain”. In : *J. Math. Phys.* 58.5 (2017), p. 053302, 24. ISSN : 0022-2488. DOI : 10.1063/1.4982637. URL : https://doi.org/10.1063/1.4982637.

[22] Jakob E. Björnberg. “Infrared bound and mean-field behaviour in the quantum Ising model”. In : *Comm. Math. Phys.* 323.1 (2013), p. 329-366. ISSN : 0010-3616. DOI : 10.1007/s00220-013-1772-4. URL : http://dx.doi.org/10.1007/s00220-013-1772-4.

[23] Niels Bohr. *Studier over metallernes elektrontheori*. Thaning & Appel in Komm., 1911.

[24] Cédric Boutillier et Béatrice De Tilière. “The critical Z-invariant Ising model via dimers : locality property”. In : *Communications in mathematical physics* 301.2 (2011), p. 473-516.

[25] Cédric Boutillier et Béatrice de Tilière. “Statistical mechanics on isoradial graphs”. In : *Probability in complex physical systems*. T. 11. Springer Proc. Math. Springer, Heidelberg, 2012, p. 491-512. DOI : 10.1007/978-3-642-23811-6_20. URL : https://doi.org/10.1007/978-3-642-23811-6_20.

[26] Cédric Boutillier et Béatrice de Tilière. “The critical Z-invariant Ising model via dimers : the periodic case”. In : *Probab. Theory Related Fields* 147.3-4 (2010), p. 379-413. ISSN : 0178-8051. DOI : 10.1007/s00440-009-0210-1. URL : https://doi.org/10.1007/s00440-009-0210-1.

[27] Cédric Boutillier, Béatrice de Tiliere et Kilian Raschel. “The Z-invariant massive Laplacian on isoradial graphs”. In : *Inventiones mathematicae* 208.1 (2017), p. 109-189.

[28] Cédric Boutillier, Béatrice de Tilière et Kilian Raschel. “The Z-invariant Ising model via dimers”. In : *Probability Theory and Related Fields* 174.1 (2019), p. 235-305.

[29] Stephen G Brush. “History of the Lenz-Ising model”. In : *Reviews of modern physics* 39.4 (1967), p. 883.

[30] Federico Camia et Charles M Newman. “Two-dimensional critical percolation : the full scaling limit”. In : *Communications in Mathematical Physics* 268.1 (2006), p. 1-38.

[31] John L Cardy. “Critical percolation in finite geometries”. In : *Journal of Physics A : Mathematical and General* 25.4 (1992), p. L201.

[32] Dmitry Chelkak. “2D Ising model : correlation functions at criticality via Riemann-type boundary value problems”. In : (2018), p. 235-256.

[33] Dmitry Chelkak. “Ising model and s-embeddings of planar graphs”. In : *arXiv preprint arXiv :2006.14559* (2020).

[34] Dmitry Chelkak. “Planar Ising model at criticality : state-of-the-art and perspectives”. In : *Proceedings of the International Congress of Mathematicians—Rio de Janeiro 2018. Vol. IV. Invited lectures*. World Sci. Publ., Hackensack, NJ, 2018, p. 2801-2828.

[35] Dmitry Chelkak. “Planar Ising model at criticality : state-of-the-art and perspectives”. In : *Proceedings of the International Congress of Mathematicians 2018 (ICM 2018), Vol. 3*. World Scientific Publishing Company Inc., 2019, p. 2789-2816.

[36] Dmitry Chelkak. “Robust discrete complex analysis : a toolbox”. In : *The Annals of Probability* 44.1 (2016), p. 628-683.

[37] Dmitry Chelkak, David Cimasoni et Adrien Kassel. “Revisiting the combinatorics of the 2D Ising model”. In : *Annales de l’Institut Henri Poincaré D* 4.3 (2017), p. 309-385.

[38] Dmitry Chelkak, Clément Hongler et Konstantin Izyurov. “Conformal invariance of spin correlations in the planar Ising model”. In : *Ann. of Math. (2)* 181.3 (2015), p. 1087-1138. issn : 0003-486X. doi : 10.4007/annals.2015.181.3.5. url : http://dx.doi.org/10.4007/annals.2015.181.3.5.

[39] Dmitry Chelkak, Clément Hongler et Konstantin Izyurov. “Correlations of primary fields in the critical Ising model”. In : *arXiv preprint arXiv :2103.10263* (2021).

[40] Dmitry Chelkak, Clément Hongler et Rémy Mahfouf. “Magnetization in the zig-zag layered Ising model and orthogonal polynomials”. In : *arXiv :1904.09168* (avr. 2019).

[41] Dmitry Chelkak et Konstantin Izyurov. “Holomorphic spinor observables in the critical Ising model”. In : *Communications in Mathematical Physics* 322.2 (2013), p. 303-332.

[42] Dmitry Chelkak, Konstantin Izyurov et Rémy Mahfouf. In preparation. 2019.

[43] Dmitry Chelkak, Konstantin Izyurov et Rémy Mahfouf. “Universality of spin correlations in the Ising model on isoradial graphs”. In : *arXiv preprint arXiv :2104.12858* (2021).

[44] Dmitry Chelkak, Benoît Laslier et Marianna Russkikh. “Bipartite dimer model : perfect t-embeddings and Lorentz-minimal surfaces”. In : *arXiv preprint arXiv :2109.06272* (2021).

[45] Dmitry Chelkak, Benoît Laslier et Marianna Russkikh. “Dimer model and holomorphic functions on t-embeddings of planar graphs”. In : *arXiv preprint arXiv :2001.11871* (2020).

[46] Dmitry Chelkak, Sung Chul Park et Yijun Wan. “Convergence of the massive energy density in the planar Ising model”. In : *In preparation* (2022).

[47] Dmitry Chelkak et Stanislav Smirnov. “Discrete complex analysis on isoradial graphs”. In : *Advances in Mathematics* 228.3 (2011), p. 1590-1630.

[48] Dmitry Chelkak et Stanislav Smirnov. “Universality in the 2D Ising model and conformal invariance of fermionic observables”. In : *Invent. Math.* 189.3 (2012), p. 515-580. issn : 0020-9910. doi : 10.1007/s00222-011-0371-2. url : http://dx.doi.org/10.1007/s00222-011-0371-2.

[49] Dmitry Chelkak et al. “Convergence of Ising interfaces to Schramm SLE”. In : *Comptes Rendus Mathematique* 352.2 (2014), p. 157-161.

[50] David Cimasoni. “Discrete Dirac operators on Riemann surfaces and Kasteleyn matrices”. In : *J. Eur. Math. Soc. (JEMS)* 14.4 (2012), p. 1209-1244. issn : 1435-9855. doi : 10.4171/JEMS/331. url : https://doi.org/10.4171/JEMS/331.

[51] David Cimasoni. “The critical Ising model via Kac-Ward matrices”. In : *Comm. Math. Phys.* 316.1 (2012), p. 99-126. issn : 0010-3616. doi : 10.1007/s00220-012-1575-z. url : https://doi.org/10.1007/s00220-012-1575-z.

[52] David Cimasoni et Hugo Duminil-Copin. “The critical temperature for the Ising model on planar doubly periodic graphs”. In : *Electron. J. Probab.* 18 (2013), no. 44, 18. issn : 1083-6489. doi : 10.1214/EJP.v18-2352. url : https://doi.org/10.1214/EJP.v18-2352.

[53] Pierre Curie. “Porprietes magnetiques des corps a diverses temperatures”. In : *Annales de Chimie et de Physique*. T. 7. 1895, p. 232-334.

[54] Percy Deift, Alexander Its et Igor Krasovsky. “Asymptotics of Toeplitz, Hankel, and Toeplitz+Hankel determinants with Fisher-Hartwig singularities”. In : *Ann. of Math. (2)* 174.2 (2011), p. 1243-1299. ISSN : 0003-486X. DOI : 10.4007/annals.2011.174.2.12. URL : https://doi.org/10.4007/annals.2011.174.2.12.

[55] Percy Deift, Alexander Its et Igor Krasovsky. “Toeplitz matrices and Toeplitz determinants under the impetus of the Ising model : some history and some recent results”. In : *Comm. Pure Appl. Math.* 66.9 (2013), p. 1360-1438. ISSN : 0010-3640. DOI : 10.1002/cpa.21467. URL : https://doi.org/10.1002/cpa.21467.

[56] Viktor S Dotsenko et Vladimir S Dotsenko. “Critical behaviour of the phase transition in the 2D Ising model with impurities”. In : *Advances in Physics* 32.2 (1983), p. 129-172.

[57] Julien Dubédat. “Dimers and families of Cauchy-Riemann operators I”. In : *J. Amer. Math. Soc.* 28.4 (2015), p. 1063-1167. ISSN : 0894-0347. DOI : 10.1090/jams/824. URL : https://doi.org/10.1090/jams/824.

[58] Julien Dubédat. “Exact bosonization of the Ising model”. In : *arXiv e-prints*, arXiv :1112.4399 (déc. 2011), arXiv :1112.4399. arXiv : 1112.4399 [math.PR].

[59] R. J. Duffin. “Potential theory on a rhombic lattice”. In : *J. Combinatorial Theory* 5 (1968), p. 258-272. ISSN : 0021-9800.

[60] Hugo Duminil-Copin. “Parafermionic observables and their applications to planar statistical physics models”. In : *Ensaios Matematicos* 25 (2013), p. 1-371.

[61] Hugo Duminil-Copin, Christophe Garban et Gábor Pete. “The near-critical planar FK-Ising model”. In : *Communications in Mathematical Physics* 326.1 (2014), p. 1-35.

[62] Hugo Duminil-Copin, Jhih-Huang Li et Ioan Manolescu. “Universality for the random-cluster model on isoradial graphs”. In : *Electron. J. Probab.* 23 (2018), Paper No. 96, 70. DOI : 10.1214/18-EJP223. URL : https://doi.org/10.1214/18-EJP223.

[63] Hugo Duminil-Copin, Jhih-Huang Li et Ioan Manolescu. “Universality for the random-cluster model on isoradial graphs”. In : *Electron. J. Probab.* 23 (2018), Paper No. 96, 70. DOI : 10.1214/18-EJP223. URL : https://doi.org/10.1214/18-EJP223.

[64] Hugo Duminil-Copin, Ioan Manolescu et Vincent Tassion. “Planar random-cluster model : fractal properties of the critical phase”. In : *Probability Theory and Related Fields* 181.1 (2021), p. 401-449.

[65] Hugo Duminil-Copin et Stanislav Smirnov. “Conformal invariance of lattice models”. In : *Probability and statistical physics in two and more dimensions*. T. 15. Clay Math. Proc. Amer. Math. Soc., Providence, RI, 2012, p. 213-276.

[66] Hugo Duminil-Copin et al. “Rotational invariance in critical planar lattice models”. In : *arXiv e-prints*, arXiv :2012.11672 (déc. 2020), arXiv :2012.11672. arXiv : 2012.11672 [math.PR].

[67] Bertrand Duplantier et Scott Sheffield. “Liouville quantum gravity and KPZ”. In : *Inventiones mathematicae* 185.2 (2011), p. 333-393.

[68] Robert G Edwards et Alan D Sokal. “Generalization of the fortuin-kasteleyn-swendsen-wang representation and monte carlo algorithm”. In : *Physical review D* 38.6 (1988), p. 2009.

[69] JA Ewing. “XXV. Contributions to the molecular theory of induced magnetism”. In : *The London, Edinburgh, and Dublin Philosophical Magazine and Journal of Science* 30.184 (1890), p. 205-222.

[70] Michael E Fisher. “Renormalization group theory : Its basis and formulation in statistical physics”. In : *Reviews of Modern Physics* 70.2 (1998), p. 653.

[71] Cornelius Marius Fortuin et Piet W Kasteleyn. “On the random-cluster model : I. Introduction and relation to other models”. In : *Physica* 57.4 (1972), p. 536-564.

[72] S. Friedli et Y. Velenik. *Statistical mechanics of lattice systems*. A concrete mathematical introduction. Cambridge University Press, Cambridge, 2018, p. xix+622. isbn : 978-1-107-18482-4.

[73] Jürg Fröhlich et Charles-Ed Pfister. “Semi-infinite Ising model”. In : *Communications in mathematical physics* 109.3 (1987), p. 493-523.

[74] JB Garnett et DE Marshall. *New Mathematical Monographs 2*. 2008.

[75] Giuseppe Genovese, Giambattista Giacomin et Rafael Leon Greenblatt. “Singular Behavior of the Leading Lyapunov Exponent of a Product of Random Matrices”. In : *Communications in Mathematical Physics* 351.3 (2017), p. 923-958.

[76] Reza Gheissari, Clément Hongler et SC Park. “Ising model : Local spin correlations and conformal invariance”. In : *Communications in Mathematical Physics* 367.3 (2019), p. 771-833.

[77] David Gilbarg et al. *Elliptic partial differential equations of second order*. T. 224. 2. Springer, 1977.

[78] Ulf Grenander et Gabor Szegö. *Toeplitz forms and their applications*. Univ of California Press, 1958.

[79] Ulf Grenander et Gabor Szego. *Toeplitz forms and their applications*. Second. Chelsea Publishing Co., New York, 1984, p. x+245. isbn : 0-8284-0321-X.

[80] Geoffrey R. Grimmett et Ioan Manolescu. “Universality for bond percolation in two dimensions”. In : *Ann. Probab.* 41.5 (2013), p. 3261-3283. issn : 0091-1798. doi : 10.1214/11-AOP740. url : https://doi.org/10.1214/11-AOP740.

[81] Geoffrey R. Grimmett, Tobias J. Osborne et Petra F. Scudo. “Entanglement in the quantum Ising model”. In : *J. Stat. Phys.* 131.2 (2008), p. 305-339. issn : 0022-4715. doi : 10.1007/s10955-008-9502-6. url : http://dx.doi.org/10.1007/s10955-008-9502-6.

[82] Werner Heisenberg. “Zur theorie des ferromagnetismus”. In : *Original Scientific Papers Wissenschaftliche Originalarbeiten*. Springer, 1985, p. 580-597.

[83] C. Hongler. “Conformal invariance of Ising model correlations”. In : *XVIIth International Congress on Mathematical Physics*. World Sci. Publ., Hackensack, NJ, 2014, p. 326-335.

[84] Clément Hongler. “Conformal invariance of Ising model correlations”. Thèse de doct. University of Geneva, 2010.

[85] Clément Hongler, Fredrik Johansson Viklund et Kalle Kytölä. “Conformal Field Theory at the Lattice Level : Discrete Complex Analysis and Virasoro Structure”. In : *arXiv e-prints*, arXiv :1307.4104v2 (mar. 2017), arXiv :1307.4104v2. arXiv : 1307.4104v2 [math-ph].

[86] Clément Hongler, Kalle Kytölä et Ali Zahabi. “Discrete holomorphicity and Ising model operator formalism”. In : *Analysis, complex geometry, and mathematical physics : in honor of Duong H. Phong*. T. 644. Contemp. Math. Amer. Math. Soc., Providence, RI, 2015, p. 79-115. doi : 10.1090/conm/644/12795. url : https://doi.org/10.1090/conm/644/12795.

[87] Clément Hongler et Stanislav Smirnov. “The energy density in the planar Ising model”. In : *Acta Math.* 211.2 (2013), p. 191-225. ISSN : 0001-5962. DOI : 10.1007/s11511-013-0102-1. URL : http://dx.doi.org/10.1007/s11511-013-0102-1.

[88] Clément Hongler, Fredrik Johansson Viklund et Kalle Kytölä. “Conformal Field Theory at the lattice level : discrete complex analysis and Virasoro structure”. In : *arXiv preprint arXiv :1307.4104* (2013).

[89] Dmitry Ioffe. “Stochastic geometry of classical and quantum Ising models”. In : *Methods of contemporary mathematical statistical physics*. T. 1970. Lecture Notes in Math. Springer, Berlin, 2009, p. 87-127. DOI : 10.1007/978-3-540-92796-9. URL : http://dx.doi.org/10.1007/978-3-540-92796-9.

[90] Ernst Ising. “Beitrag zur theorie des ferro-und paramagnetismus”. Thèse de doct. Grefe & Tiedemann, 1924.

[91] Thomas Ising et al. “The fate of Ernst Ising and the fate of his model”. In : *arXiv preprint arXiv :1706.01764* (2017).

[92] Konstantin Izyurov. “Holomorphic spinor observables and interfaces in the critical Ising mode Ph. D”. Thèse de doct. thesis, 2011.

[93] Leo P. Kadanoff et Horacio Ceva. “Determination of an operator algebra for the two-dimensional Ising model”. In : *Phys. Rev. B (3)* 3 (1971), p. 3918-3939. ISSN : 0163-1829.

[94] Leo P. Kadanoff et Mahito Kohmoto. “SMJ’s analysis of Ising model correlation functions”. In : *Ann. Physics* 126.2 (1980), p. 371-398. ISSN : 0003-4916. DOI : 10.1016/0003-4916(80)90181-5. URL : https://doi.org/10.1016/0003-4916(80)90181-5.

[95] Bruria Kaufman. “Crystal statistics. II. Partition function evaluated by spinor analysis”. In : *Physical Review* 76.8 (1949), p. 1232.

[96] Antti Kemppainen et Stanislav Smirnov. “Conformal invariance in random cluster models. II. Full scaling limit as a branching SLE”. In : *arXiv preprint arXiv :1609.08527* (2016).

[97] Antti Kemppainen et Stanislav Smirnov. “Random curves, scaling limits and Loewner evolutions”. In : *The Annals of Probability* 45.2 (2017), p. 698-779.

[98] R. Kenyon. “The Laplacian and Dirac operators on critical planar graphs”. In : *Invent. Math.* 150.2 (2002), p. 409-439. ISSN : 0020-9910. DOI : 10.1007/s00222-002-0249-4. URL : https://doi.org/10.1007/s00222-002-0249-4.

[99] R. Kenyon. “The Laplacian and Dirac operators on critical planar graphs”. In : *Invent. Math.* 150.2 (2002), p. 409-439. ISSN : 0020-9910. DOI : 10.1007/s00222-002-0249-4. URL : http://dx.doi.org/10.1007/s00222-002-0249-4.

[100] Richard Kenyon. “Conformal invariance of domino tiling”. In : *Annals of probability* (2000), p. 759-795.

[101] Richard Kenyon. “Dominos and the Gaussian free field”. In : *Annals of probability* (2001), p. 1128-1137.

[102] Richard Kenyon et Jean-Marc Schlenker. “Rhombic embeddings of planar quad-graphs”. In : *Transactions of the American Mathematical Society* 357.9 (2005), p. 3443-3458.

[103] Richard Kenyon et al. “Dimers and Circle patterns”. In : *arXiv e-prints*, arXiv :1810.05616 (2018), arXiv :1810.05616. arXiv : 1810.05616 [math-ph].

[104] Hendrik A Kramers et Gregory H Wannier. “Statistics of the two-dimensional ferromagnet. Part I”. In : *Physical Review* 60.3 (1941), p. 252.

[105] Hendrik A Kramers et Gregory H Wannier. “Statistics of the two-dimensional ferromagnet. Part II”. In : *Physical Review* 60.3 (1941), p. 263.

[106] Robert Langlands, Philippe Pouliot et Yvan Saint-Aubin. “Conformal invariance in two-dimensional percolation”. In : *arXiv preprint math/9401222* (1994).

[107] Robert P Langlands, Marc-André Lewis et Yvan Saint-Aubin. “Universality and conformal invariance for the Ising model in domains with boundary”. In : *arXiv preprint hep-th/9904088* (1999).

[108] Robert P Langlands et al. “On the universality of crossing probabilities in two-dimensional percolation”. In : *Journal of statistical physics* 67.3 (1992), p. 553-574.

[109] Jhih-Huang Li. “Conformal invariance in the FK-representation of the quantum Ising model and convergence of the interface to the $SLE_{16/3}$”. In : *Probab. Theory Related Fields* 173.1-2 (2019), p. 87-156. ISSN : 0178-8051. DOI : 10.1007/s00440-018-0831-3. URL : https://doi.org/10.1007/s00440-018-0831-3.

[110] Jhih-Huang Li et Rémy Mahfouf. “Conformal invariance in the quantum Ising model”. In : *arXiv preprint arXiv :2112.04811* (2021).

[111] Zhongyang Li. “Conformal invariance of dimer heights on isoradial double graphs”. In : *Ann. Inst. Henri Poincaré D* 4.3 (2017), p. 273-307. ISSN : 2308-5827. DOI : 10.4171/AIHPD/41. URL : https://doi.org/10.4171/AIHPD/41.

[112] Elliott H Lieb et Daniel C Mattis. *Mathematical physics in one dimension : exactly soluble models of interacting particles*. Academic Press, 2013.

[113] Marcin Lis. “Circle patterns and critical Ising models”. In : *Communications in Mathematical Physics* 370.2 (2019), p. 507-530.

[114] Marcin Lis. “Phase transition free regions in the Ising model via the Kac–Ward operator”. In : *Communications in Mathematical Physics* 331.3 (2014), p. 1071-1086.

[115] Russell Lyons et Yuval Peres. *Probability on trees and networks*. T. 42. Cambridge University Press, 2017.

[116] Remy Mahfouf. “Convergence of fermionic observable on general s-embeddings”. In : *In preparation* (2022).

[117] Remy Mahfouf. “Crossing estimates on general s-embeddings”. In : *Available at webpage of the author* (2022).

[118] Barry M. McCoy. “Integrable models in statistical mechanics : the hidden field with unsolved problems”. In : *Internat. J. Modern Phys. A* 14.25 (1999), p. 3921-3933. ISSN : 0217-751X. DOI : 10.1142/S0217751X99001834. URL : https://doi.org/10.1142/S0217751X99001834.

[119] Barry M. McCoy. “Theory of a two-dimensional Ising model with random impurities. III. Boundary effects”. In : *Phys. Rev. (2)* 188 (1969), p. 1014-1031.

[120] Barry M. McCoy et Jean-Marie Maillard. “The Importance of the Ising Model”. In : *Progress of Theoretical Physics* 127.5 (mai 2012), p. 791-817. ISSN : 0033-068X. DOI : 10.1143/PTP.127.791. eprint : http://oup.prod.sis.lan/ptp/article-pdf/127/5/791/5427363/127-5-791.pdf. URL : https://doi.org/10.1143/PTP.127.791.

[121] Barry M. McCoy, Jacques H. H. Perk et Tai Tsun Wu. “Ising field theory : quadratic difference equations for the n-point Green’s functions on the lattice”. In : *Phys. Rev. Lett.* 46.12 (1981), p. 757-760. ISSN : 0031-9007. DOI : 10.1103/PhysRevLett.46.757. URL : https://doi.org/10.1103/PhysRevLett.46.757.

[122] Barry M McCoy et Tai Tsun Wu. “The two-dimensional Ising model”. In : *The Two-Dimensional Ising Model*. Harvard University Press, 2013.

[123] Barry M. McCoy et Tai Tsun Wu. *The two-dimensional Ising model*. Second. Corrected reprint of [MR3618829], with a new preface and a new chapter (Chapter XVII). Dover Publications, Inc., Mineola, NY, 2014, p. xvi+454. ISBN : 978-0-486-49335-0 ; 0-486-49335-0.

[124] Barry M McCoy et Tai Tsun Wu. *The two-dimensional Ising model*. Courier Corporation, 2014.

[125] Barry M. McCoy et Tai Tsun Wu. “Theory of a two-dimensional Ising model with random impurities. I. Thermodynamics”. In : *Phys. Rev. (2)* 176 (1968), p. 631-643.

[126] Barry M. McCoy et Tai Tsun Wu. “Theory of a two-dimensional Ising model with random impurities. II. Spin correlation functions”. In : *Phys. Rev. (2)* 188 (1969), p. 982-1013.

[127] Paul Melotti. “Modèles intégrables de spins, vertex et boucles”. Thèse de doct. Sorbonne université, 2019.

[128] Paul Melotti, Sanjay Ramassamy et Paul Thévenin. “Cube moves for s-embeddings and alpha-realizations”. In : *arXiv preprint arXiv :2003.08941* (2020).

[129] Christian Mercat. “Discrete Riemann surfaces and the Ising model”. In : *Comm. Math. Phys.* 218.1 (2001), p. 177-216. ISSN : 0010-3616. DOI : 10.1007/s002200000348. URL : http://dx.doi.org/10.1007/s002200000348.

[130] RJ Messikh. “The surface tension near criticality of the 2d-Ising model”. In : *arXiv preprint math/0610636* (2006).

[131] Martin Niss. “History of the Lenz–Ising Model 1950–1965 : from irrelevance to relevance”. In : *Archive for history of exact sciences* 63.3 (2009), p. 243-287.

[132] Martin Niss. “History of the Lenz–Ising Model 1965–1971 : the role of a simple model in understanding critical phenomena”. In : *Archive for History of Exact Sciences* 65.6 (2011), p. 625-658.

[133] Martin Niss. “History of the Lenz-Ising model 1920–1950 : from ferromagnetic to cooperative phenomena”. In : *Archive for history of exact sciences* 59.3 (2005), p. 267-318.

[134] *NIST Digital Library of Mathematical Functions*. F. W. J. Olver, A. B. Olde Daalhuis, D. W. Lozier, B. I. Schneider, R. F. Boisvert, C. W. Clark, B. R. Miller, B. V. Saunders, H. S. Cohl, and M. A. McClain, eds. URL : http://dlmf.nist.gov/.

[135] Lars ONSAGER. "Crystal statistics. I. A two-dimensional model with an order-disorder transition". In : *Physical Review* 65.3-4 (1944), p. 117.

[136] John PALMER. *Planar Ising Correlations*. T. 49. Springer Science & Business Media, 2007.

[137] S. C. PARK. "Massive Scaling Limit of the Ising Model : Subcritical Analysis and Isomonodromy". In : *arXiv e-prints*, arXiv :1811.06636 (nov. 2018), arXiv :1811.06636. arXiv : 1811.06636 [math.PR].

[138] SC PARK. "Convergence of fermionic observables in the massive planar FK-Ising model". In : *arXiv preprint arXiv :2103.04649* (2021).

[139] Rudolf PEIERLS. "Statistical theory of adsorption with interaction between the adsorbed atoms". In : *Mathematical Proceedings of the Cambridge Philosophical Society*. T. 32. 3. Cambridge University Press. 1936, p. 471-476.

[140] A. PELIZZOLA. "Boundary critical behaviour of two-dimensional layered Ising models". In : *Internat. J. Modern Phys. B* 11.11 (1997), p. 1363-1388. URL : https://doi.org/10.1142/S0217979297000708.

[141] Jacques HH PERK. "Nonlinear partial difference equations for Ising model n-point Green's functions". In : *Proc. II International Symposium on Selected Topics in Statistical Mechanics, Dubna*. 1981, p. 138-151.

[142] Jacques HH PERK. "Quadratic identities for Ising model correlations". In : *Physics Letters A* 79.1 (1980), p. 3-5.

[143] Jacques HH PERK et Helen AU-YANG. *Ising models and soliton equations*. Rapp. tech. 1985.

[144] Jacques HH PERK et Helen AU-YANG. "New results for the correlation functions of the Ising model and the transverse Ising chain". In : *Journal of Statistical Physics* 135.4 (2009), p. 599-619.

[145] Pierre PFEUTY. "The one-dimensional Ising model with a transverse field". In : *Annals of Physics* 57.1 (1970), p. 79-90.

[146] Charles-Edouard PFISTER et Yvan VELENIK. "Mathematical theory of the wetting phenomenon in the 2D Ising model". In : *arXiv preprint cond-mat/9701161* (1997).

[147] Instituts Solvay. Conseil de PHYSIQUE et Institut international de physique SOLVAY. *Le magnétisme : Rapports et discussions du sixième Conseil de physique, tenu à Bruxelles du 20 au 25 octobre 1930*. Gauthier-Villars et cie, 1932.

[148] Haru PINSON. "Rotational invariance of the 2d spin-spin correlation function". In : *Comm. Math. Phys.* 314.3 (2012), p. 807-816. ISSN : 0010-3616. DOI : 10.1007/s00220-012-1545-5. URL : https://doi.org/10.1007/s00220-012-1545-5.

[149] Aran RAOUFI. "Translation-invariant Gibbs states of the Ising model : general setting". In : *The Annals of Probability* 48.2 (2020), p. 760-777.

[150] Karin REICH. "Der erste Professor für Theoretische Physik an der Universität Hamburg : Wilhelm Lenz". In : (2011).

[151] Larissa RICHARDS. "Convergence Rates of Random Discrete Model Curves Approaching SLE Curves in the Scaling Limit". Thèse de doct. University of Toronto, 2021.

[152] Dalton AR SAKTHIVADIVEL. "Magnetisation and mean field theory in the Ising model". In : *SciPost Physics Lecture Notes* (2022), p. 035.

[153] Mikio SATO, Tetsuji MIWA et Michio JIMBO. "Studies on holonomic quantum fields. I–IV". In : *Proc. Japan Acad. Ser. A Math. Sci.* 53 (1977), p. 6-10,147-152,153-158,183-185. ISSN : 0386-2194. URL : http://projecteuclid.org/euclid.pja/1195518148.

[154] Oded SCHRAMM. "Scaling limits of loop-erased random walks and uniform spanning trees". In : *Israel Journal of Mathematics* 118.1 (2000), p. 221-288.

[155] Theodore D SCHULTZ, Daniel C MATTIS et Elliott H LIEB. "Two-dimensional Ising model as a soluble problem of many fermions". In : *Reviews of Modern Physics* 36.3 (1964), p. 856.

[156] Scott SHEFFIELD. "Exploration trees and conformal loop ensembles". In : *Duke Mathematical Journal* 147.1 (2009), p. 79-129.

[157] Scott SHEFFIELD et Wendelin WERNER. "Conformal loop ensembles : the Markovian characterization and the loop-soup construction". In : *Annals of Mathematics* (2012), p. 1827-1917.

[158] Barry SIMON. "OPUC on one foot". In : *Bull. Amer. Math. Soc. (N.S.)* 42.4 (2005), p. 431-460. ISSN : 0273-0979. DOI : 10.1090/S0273-0979-05-01075-X. URL : https://doi.org/10.1090/S0273-0979-05-01075-X.

[159] Barry Simon. “OPUC on one foot”. In : *Bull. Amer. Math. Soc. (N.S.)* 42.4 (2005), p. 431-460. ISSN : 0273-0979. DOI : 10.1090/S0273-0979-05-01075-X. URL : https://doi.org/10.1090/S0273-0979-05-01075-X.

[160] Stanislav Smirnov. “Conformal invariance in random cluster models. I. Holomorphic fermions in the Ising model”. In : *Ann. of Math. (2)* 172.2 (2010), p. 1435-1467. ISSN : 0003-486X. DOI : 10.4007/annals.2010.172.1441. URL : https://doi.org/10.4007/annals.2010.172.1441.

[161] Stanislav Smirnov. “Critical percolation in the plane : conformal invariance, Cardy’s formula, scaling limits”. In : *Comptes Rendus de l’Académie des Sciences-Series I-Mathematics* 333.3 (2001), p. 239-244.

[162] Stanislav Smirnov. “Towards conformal invariance of 2D lattice models”. In : *In* International Congress of Mathematicians. Vol. II*, pages 1421–1451. Eur. Math. Soc., Zürich* (2006).

[163] Stanislav Smirnov et Wendelin Werner. “Critical exponents for two-dimensional percolation”. In : *arXiv preprint math/0109120* (2001).

[164] Béatrice de Tilière. “The Z-Dirac and massive Laplacian operators in the Z-invariant Ising model”. In : *Electronic Journal of Probability* 26 (2021), p. 1-86.

[165] Kenneth G Wilson. “The renormalization group and critical phenomena”. In : *Reviews of Modern Physics* 55.3 (1983), p. 583.

[166] Tai Tsun Wu et al. “Spin-spin correlation functions for the two-dimensional Ising model : Exact theory in the scaling region”. In : *Phys. Rev. B* 13 (1 1976), p. 316-374. DOI : 10.1103/PhysRevB.13.316. URL : https://link.aps.org/doi/10.1103/PhysRevB.13.316.

[167] C. N. Yang. “The Spontaneous Magnetization of a Two-Dimensional Ising Model”. In : *Phys. Rev.* 85 (5 1952), p. 808-816. DOI : 10.1103/PhysRev.85.808. URL : https://link.aps.org/doi/10.1103/PhysRev.85.808.